

Reconfiguring the Ship Environment for Damage Stability Enhancement

By

Donald Paterson

PhD Thesis

Maritime Safety Research Centre

Department of Naval Architecture, Ocean and Marine Engineering

University of Strathclyde

Glasgow, 2020

Copyright statement

This thesis is the result of the author's original research. It has been composed by the author and has not been previously submitted for examination which has led to the award of a degree.

The copyright of this thesis belongs to the author under the terms of the United Kingdom Copyright Acts as qualified by University of Strathclyde Regulation 3.50. Due acknowledgement must always be made of the use of any material contained in, or derived from, this thesis.

Signed:

Date: xx.xx.xxxx

Acknowledgements

There are a number of people to whom I wish to extend my deepest gratitude for their contribution and support in the completion of this thesis.

Firstly, I wish to thank my supervisor Professor Dracos Vassalos for his mentorship, guidance, commitment, friendship and continued belief in me over the duration of this thesis. It is a very rare opportunity for one to get to work with someone of such high esteem and I count myself amongst a lucky few. Sir Isaac Newton was once quoted as having said “If I have seen further it is by standing on the shoulders of Giants” and I can certainly say, if indeed I have been able to see any further it is because I have stood upon his shoulders.

I would also like to thank my second supervisor, Dr Evangelos Boulougouris, who initially introduced me to the subject of damage stability and always made time to answer my many questions and point me in the right direction. For this I am truly thankful.

In addition, I would like to thank the many amazing people I have worked with at Strathclyde University over the years, including Kristian Karolius with whom I have had many insightful exchanges over the years and has become a close and dear friend. Furthermore, I would like to thank Georgios Atzamos who I have worked very closely with over the duration of my research and I am very grateful for his friendship.

Last and by no means least, I would like to thank my friends and family who have supported me over the years, particularly my mother whom without her encouragement I would most probably have never attended university.

Abstract

It has often been said that, from a fundamental Naval Architecture perspective, the primary design objective to be achieved is for a ship to remain afloat and upright (safety-related objectives). This is particularly true in case of vessel flooding, where this objective becomes harder still. The traditional risk control option adopted in Naval Architecture to meet safety-related objectives is by rules and regulations, targeting damage limitation, nominally instigated in the wake of maritime accidents claiming heavy loss of life. The first Merchant Shipping Act of 1854 is the earliest known legal requirement addressing safety at sea and concerning watertight bulkheads, i.e., permanent (passive) reconfiguration of the internal ship environment to enhance safety. This has been the most common measure, manifesting itself in the wake of every serious flooding accident since the beginning, back in the 19th century. Notably, with accidents providing the main motivation, emphasis has primarily been placed on reducing consequences, i.e., on cure rather than prevention. The key reason for this, derives from the fact that the residual risk post flooding accidents is unacceptably high, meaning that the most-cost-effective way to reduce flooding risk is to target the residual risk. This being the case, the prevailing situation can be drastically improved through understanding of the underlying mechanisms leading to vessel loss and to identification of governing design and operational parameters to target flooding risk reduction more cost-effectively. On one hand, this necessitates the development of appropriate methods, tools and techniques capable of meaningfully addressing the physical phenomena involved. On the other hand, this nurtures wider understanding and wisdom. Safety is normally a compromise to vessel earning potential and, as public demand for higher safety standards grows, industry is forced to choose between viability of business and safety of customers. Unfortunately, in any such compromise, safety loses. However, the key reason for this is strongly linked to the traditional myopic focus on only permanent, designed-related safety measures, pertaining in particular to flooding incidents. Traditional flooding protection through watertight subdivision is largely dictated by IMO regulations and has a physical limit which, if exceeded, a safety plateau is reached. This is currently the case and with damage stability standards progressively increasing, the safety gap between existing and new ships is dangerously widening. Adding to the problem is the progressive erosion of design stability margins, making stability management unsustainable and leading to loss of earnings at best. The need for monitoring and managing the residual risk through active intervention/protection over the life-cycle of the vessel drives the industry in searching to adopt a new normal. This new normal is the innovation being explored in this thesis, by addressing safety enchantment through a systematic reconfiguration of the ship environment for passive and active protection in flooding (and to some extent fire) accidents. In

this respect, the “design-optimal” internal arrangement of a vessel, is adapted and reconfigured, using passive and active containment systems for flooding/fire incidents, in the form of high-expansion foam products. Several case studies are being presented to explain and explore the safety-enhancement potential. This demonstrates transformational reduction in flooding/fire risk, in the most cost-effective way available.

Table of Contents

Copyright statement.....	1
Acknowledgements	2
Abstract.....	3
Table of Contents	5
List of Figures	10
List of Tables.....	14
Abbreviations	16
Chapter 1: Introduction.....	18
1.1 Problem Definition, Innovation and Impact.....	18
1.1.1 The Problem.....	18
1.1.2 The Innovation.....	18
1.1.3 The Impact.....	19
1.2 Background.....	19
1.2.1 The First Steps	19
1.2.2 The Birth & Reign of Subdivision – A Record of Disasters	20
1.2.3 Forces Driving Regulatory Development.....	23
1.2.4 Reconfiguration Going into Overdrive	24
1.2.5 Making Sense of Reconfiguration	26
1.2.6 A New wave of Reconfiguration – Safe Return to Port.....	28
1.2.7 RoPax Vs Cruise Ships: Hitting a “Wall”	30
1.2.8 Widening the Reconfiguration Perspective: Passive and Active Protection	31
1.2.9 Life-cycle Risk Management	31
1.2.10 Fuelling Technological Innovation in Solving the Damage Stability Problem	33
1.3 The Way forward: Technological Innovation is the Key.....	34
1.3.1 Damage Stability: Still the Highest Risk Contributor in the Maritime Industry.....	34
1.3.2 Damage Stability Research at Strathclyde as an Enabler	35
1.3.3 The PROTEUS Software Suite.....	35
1.3.4 Loss Modalities of a Damaged Ship.....	36
1.4 Adaptive Reconfigurable Environment Safety Technology (AREST) Systems.....	40
1.4.1 The Concept	40
1.4.2 AREST Systems	40
1.5 Structure of Thesis.....	44
Chapter 2: Thesis Aim & Objectives.....	47

Chapter 3: Critical Review on Passive & Active Reconfiguration for Damage Stability Protection	48
3.1 Opening Remarks	48
3.2 Rules & Regulations as the Prime Mover	49
3.2.1 General Concept of Stability Measurement & Subdivision	49
3.2.2 General Outlook on Damage Stability Evolution	52
3.2.3 Rules and Regulations as RCOs for Damage Protection	55
3.3 Ship Design Impact on Reconfiguration of the Internal Ship Space	56
3.3.1 Design Vulnerability	56
3.3.2 Design Vulnerability by Ship Type	57
3.3.3 Life-Cycle Considerations - Design Phase	59
3.3.4 The Design Optimisation Problem (Subdivision) – Multi-Objective Optimisation	61
3.3.5 Structural Design Influences	64
3.3.6 Structural Crashworthiness	69
3.4 Impact of Operation on Reconfiguration of the Internal Ship Space	71
3.4.1 Overview	71
3.4.2 Vulnerability in Ship Operation	71
3.4.2 Life-Cycle Considerations – Operational Phase	72
3.4.3 Conflict in Configuration between Operation and Safety	73
3.5 Ship Emergencies Impact on Reconfiguration of the Internal Ship Space	76
3.5.1 Overview	76
3.5.2 Life-Cycle Considerations – Operational Phase	77
3.5.3 Configuring the Ship Environment for Emergency Response	78
3.6 Closing Remarks	80
Chapter 4: Research Methodology Adopted	82
4.1 General Remarks	82
4.2 Overview of Methodology	83
Chapter 5: Ship Damage Stability and Survivability Assessment Process	90
5.1 Opening Remarks	90
5.2 Limitations in Hydrostatics & the Need for Numerical Simulations	90
5.3 Background on the Development of Simulation Tools	93
5.4 Survivability Assessment Process	95
5.4.1 Preparation of the Simulation Model	95
5.4.2 Damage Scenario Definition	97
5.4.3 Impact of sample size on error	99
5.4.4 Simulation Strategies	101
5.4.5 Initial Conditions	103

5.4.6 Survivability Estimation	109
5.4.7 Forensic Analysis of Vulnerability Sources	110
5.5 Closing Remarks	114
Chapter 6: Passive & Active Reconfiguration for Damage Stability Protection	116
6.1 Opening Remarks	116
6.2 Targeted Solutions for Transient Flooding Protection	117
6.2.1 Transient Flooding Overview & Pertinent RCO Considerations	117
6.2.2 AREST P1 System Description	119
6.2.3 AREST P1 Impact Example	122
6.3 Targeted Solutions for Progressive Flooding Protection	124
6.3.1 Progressive Flooding Overview & Pertinent RCO Considerations	124
6.3.2 AREST A1 System Description	126
6.3.3 AREST A2 System Description	129
6.3.4 AREST A2 Impact Example	134
6.4 Verification of Vital Foam Properties for Class and Administration Approvals	136
6.4.1 Permeability Verification	140
6.4.2 Verification of Foam Adhesion & Cohesion	147
6.4.3 Verification of Foam Compressibility	149
6.5 Summary	150
Chapter 7: Passive & Active Damage Control Example - Permeant Foam Application & Progressive Flooding Suppression	151
7.1 Opening Remarks	151
7.2 Part A: Static Stability Assessment	153
7.2.1 Vessel Main Particulars	153
7.2.2 Vessel Stability Model	153
7.2.3 Vessel Subdivision	154
7.2.4 Required Subdivision Index – R	154
7.2.5 Calculation Drafts	155
7.2.6 Permeabilities	155
7.2.7 Damage Stability Assessment – as built	156
7.2.8 Existing Vessel GM limit Curve	156
7.2.9 Vulnerability Assessment	158
7.2.10 Solution Impact Assessment	161
7.2.11 Conclusions – Part A	164
7.3 Part B: Dynamic Survivability Assessment	165
7.3.1 Modelling of the Ship Environment and External Conditions	165
7.3.2 Simulation Properties & Damage Generation	169

7.3.3 Simulation Results – As built.....	171
7.3.4 Simulation Results – With AREST A1 & P1 Systems	184
7.3.5 Conclusions – Part B.....	186
Chapter 8: Passive Flooding Control Application Example – (AREST P1 System).....	187
8.1 Opening Remarks.....	187
8.2 Part A: Static Stability Assessment.....	188
8.2.1 Scope of Work	188
8.2.2 Case Study – Large Cruise Vessel C1	190
8.3 Part B: Dynamic Survivability Assessment.....	200
8.3.1 Scope of Work	200
8.3.2 Modelling of the Ship Environment and External Conditions	202
8.3.3 Simulation Properties & Damage Generation	205
8.3.4 Simulation Results – As built.....	206
8.3.5 Simulation Results –Static Foam Installations in Place	211
8.3.6 Consideration of the AREST A2 system for progressive flooding prevention	213
8.3.7 Conclusions – Part B.....	217
Chapter 9: Active Damage Control Application Example – Controlling Progressive Flooding (AREST A2) 218	
9.1 Opening Remarks.....	218
9.2 Modelling of the Ship Environment and External Conditions.....	219
9.2.1 Ship Principle Particulars	219
9.2.2 Simulation model and Arrangement.....	219
9.2.3 Verification of internal geometry	221
9.2.4 Opening Definition	222
9.3 Numerical time-domain simulations (SOLAS 2009 assumptions).....	222
9.3.1 Overview	222
9.3.2 Collision Damage Sample.....	223
9.4 Numerical time-domain simulations – Stress Test.....	224
9.4.1 Overview	224
9.4.2 Damage Generation	224
9.4.3 Overview of simulation results.....	225
9.5 Numerical Time-domain simulations – Calm Water.....	230
9.6 Progressive Flooding Critical Design features and Solutions	232
9.6.1 Identification of critical openings.....	232
9.6.2 Progressive Flooding - AREST A2 Solution	235
9.7 Transient Flooding – Proposed Solutions	237
9.7.1 Inadequate Cross-flooding	237

9.7.2 Areas with insufficient reserve buoyancy	240
9.8 Numerical time-domain simulations – Impact of solutions	243
9.9 Conclusions	246
Chapter 10: Discussion & Recommendations	247
10.1 Opening remarks	247
10.2 Innovation & Impact.....	247
10.3 Prevention Vs. Mitigation.....	248
10.4 Old Ships Vs New Ships.....	248
10.5 Active Measures Vs Passive Measures for Damage Protection	249
10.6 Life-Cycle Risk Management and Safety Culture	250
10.7 Recommendations for Future Research.....	250
10.7.1 Life-Cycle Flooding Risk-Based Regulatory Framework.....	250
10.7.2 Formalisation of the Process for Damage Stability Assessment, Protection and control.....	251
10.7.3 Institutionalisation of the Method, Process, Tools and RCOs.....	251
Chapter 11: Concluding Remarks	252
Chapter 12: Bibliography	254
Appendix A: Interpretation of Results.....	262
Appendix B: R1 Simulation Results	264
Appendix C: CS1 Simulation Results	277
Appendix D: CS2 simulation results (SOLAS 2009 assumptions)	290
Appendix E: CS2 Simulation results (Stress-Test)	305

List of Figures

Figure 1-1 - Damage stability evolutionary changes, based on diagram shown in (Hutchinson & Scott, 2016)	23
Figure 1-2: The IMO Framework for Passenger Ship Safety (IMO SLF 47/48).....	29
Figure 1-3: Research outcome suggested level of R for passenger vessels (EMSA II, 2009-2012) left, (EMSA III, 2013-2015) right.....	30
Figure 1-4: Barrier Management (“Bow-Tie”) (Vassalos, Atzampos, Cichowicz, & Paterson, 2018)	32
Figure 1-5: Illustrative example of vessel lightweight and KG variation.....	32
Figure 1-6: Casualty events for ships in the period 2011-2019.....	34
Figure 1-7: Capacities of largest passenger ships by year (Clarkson, 2020).....	34
Figure 1-8: PROTEUS Software capabilities	36
Figure 1-9: Overview of flooding stages – based on diagram shown in (Ruponen P. , 2007).....	37
Figure 1-10: Typical transient loss modality distribution for a SOLAS'90 cruise ship, model experiment and numerical simulation results (Vassalos et al., 2005)	38
Figure 1-11: Loss modality distribution for a SOLAS '90 cruise vessel	38
Figure 1-12: Time History of Floodwater Accumulation on Deck	39
Figure 1-13: Filling void Spaces in the wing spaces of a cruise ship.....	41
Figure 1-14: AREST A1 systems, large-scale system with pumps (right), small-scale system with compressed gas release (right)	41
Figure 1-15: Flow paths and critical progressive flooding sources	42
Figure 1-16: Example of shutter closing arrangements	43
Figure 3-1: Design Vulnerability Distribution for a RoPax (left) and Cruise vessel (right).....	57
Figure 3-2: High freeboard ship	58
Figure 3-3: Low-freeboard ship	58
Figure 3-4: Multi-free-surface effect.....	59
Figure 3-5: Three vessel life-cycle design phases (Vassalos, Atzampos, Cichowicz, & Paterson, 2018).....	60
Figure 3-6: Relative frequency of occurrence of fire incidents; 20% of space “uses” contribute to 80% of all fire occurrences (Guarin, Majumder, R. Pusia, & Vassalos, 2007)	66
Figure 3-7: Depiction of SEM parameters with water elevation in the vehicle deck at the Point of No Return (PNR) - case of RoPax (left), conventional method considering the floodwater volume as a total water on the vehicle deck inside an undamaged tank (right). (HARDER, 2003)	68
Figure 3-8: Concepts of crashworthy structures: (a) Longitudinal structure on-board an inland waterway gas carrier (Ludolph & Boon, 2000); b) Transverse structure on board a RoPax vessel (Ehlers, Broekhuijsen, Alsos, Biehl, & Tabri, 2008); (c) Corrugated structure on board an inland waterway	70
Figure 3-9: MV Estonia – As Operated at the Time of her Loss, based on diagram in (Jasionowski A. , 2011).....	72
Figure 3-10: Operational Phase (Vassalos, Atzampos, Cichowicz, & Paterson, 2018).....	73
Figure 3-11: Cruise Vessel Growth Trend.....	74
Figure 3-12: Catering spaces and flows for a typical cruise ship, based on diagram shown in (Vie, 2014).....	76
Figure 3-13: Emergency Response Phase (Vassalos, Atzampos, Cichowicz, & Paterson, 2018)..	77
Figure 3-14: Damage Control Actions List.....	80
Figure 4-1: Overview of vessels considered	82

Figure 4-2: Methodology Adopted	83
Figure 5-1: Comparison in level of detail captured, static model left, simulation model right.....	95
Figure 5-2: Example Opening Arrangement- from case study not included within thesis.....	96
Figure 5-3: Example damage & sea state sample taken from HARDER distributions (HARDER, 1999-2003)	98
Figure 5-4: Typical collision damage sample for small cruise vessel, sourced from case study not included within thesis	98
Figure 5-5: Standard Error relative to sample size for Hs.....	100
Figure 5-6: Confidence Intervals, 100 samples left, 1,500 samples right.....	101
Figure 5-7: Basis Ship Overview	104
Figure 5-8: Example ND draft distribution	105
Figure 5-9: Draft distribution relative to SOLAS range for all ships	106
Figure 5-10: Draft distribution relative to SOLAS range for RoPax vessels only	106
Figure 5-11: Draft distribution relative to SOLAS for cruise ships only.....	106
Figure 5-12: Comparison of SOLAS and operational draft ranges with respect to ship age	107
Figure 5-13: Large cruise vessel - variations in PoB over one year	108
Figure 5-14: CDF for Time to Capsize.....	109
Figure 5-15: Transient Capsize Roll Time-History	110
Figure 5-16: Progressive Flooding Capsize Roll Time-History	110
Figure 5-17: Floodwater accumulation and opening immersion time-history.....	112
Figure 5-18: Example of Floodwater Progression Mapping.....	113
Figure 5-19: Example of opening ranking by frequency and flooding severity.....	114
Figure 6-1: Example of foam cutaway for access to systems	121
Figure 6-2: Example application site within large cruise vessel double hull.....	121
Figure 6-3: Example foam installation	122
Figure 6-4: Example foam installation, vessel fore shoulder	122
Figure 6-5: Floodwater & roll time history comparison, with and without AREST P1	123
Figure 6-6: Example AREST A1 Tank/pump arrangement for medium size RoPax.....	127
Figure 6-7: Example shutter assembly, top and bottom rails, vertical section (side view).....	131
Figure 6-8: Example shutter assembly, right & left sides, Horizontal section (top view)	131
Figure 6-9: Example shutter assembly, top and bottom rails, vertical section (side view).....	132
Figure 6-10: Foam Delivery System	133
Figure 6-11: Typical example of major progressive flooding conduits on cruise vessel BH Deck	134
Figure 6-12: Comparison of floodwater evolutions, as-built (above), with AREST A2 (below).	136
Figure 6-13: Foam sample dimensions, atmospheric pressure test (left), added pressure test (right).....	140
Figure 6-14: Atmospheric pressure water absorption test overview.....	141
Figure 6-15: Atmospheric pressure water absorption test apparatus	141
Figure 6-16: Foam water absorption with respect to exposure time.....	142
Figure 6-17: Overpressure water absorption test	142
Figure 6-18: Foam specimen and pressure vessel.....	143
Figure 6-19: Foam water absorption relative to external water pressure	144
Figure 6-20: Development of compressed foam skin at high water pressures.....	144
Figure 6-21: Foam water absorption as a function of specimen size	145
Figure 6-22: Effect of Sample Size on Permeability Determination.....	145
Figure 6-23: Sample shielded foam water absorption.....	146
Figure 6-24: Pull-test Diagram	148
Figure 6-25: Stud fixed to foam/plate assembly (left), foam separated from steel plate (right)	148

Figure 6-26: Compression-cycle press/hold/release (10% deformation left, 50% deformation right)	149
Figure 6-27: Foam stress strain curve under compression	150
Figure 7-1: Stability Model Calculation Sections	153
Figure 7-2: R1 Subdivision Arrangement	154
Figure 7-3: Permeability distribution assumption with foam in place.....	156
Figure 7-4: R1 as-built GM damage stability related limit curves.....	157
Figure 7-5: R1 as-built Risk Profile.....	159
Figure 7-6: Vulnerable space locations.....	160
Figure 7-7: Foam volume optimisation, aft shoulder (left), fore shoulder (right).....	161
Figure 7-8: Comparison of vessel Risk Profiles, with (right) and without (left) AREST solutions	162
Figure 7-9: GM limit comparison before and after AREST solutions.....	163
Figure 7-10: Simulation model calculation sections	166
Figure 7-11: Simulation model arrangement.....	166
Figure 7-12: Comparison of hydrostatic & simulation model properties	167
Figure 7-13: Simulation model opening arrangement.....	168
Figure 7-14: SOLAS 2009 CDF of Hs encountered during accidents, as obtained in (HARDER, 1999-2003).	169
Figure 7-15: JONSWAP wave spectrum for Hs=4m	169
Figure 7-16: Collision damage sample	171
Figure 7-17: Cumulative probability distribution of Time to Capsize for all collision damages. Indication of Survivability Index=0.89, with 30 minutes exposure.	172
Figure 7-18: Location and extent of capsized cases.....	173
Figure 7-19: Risk Profile resulting from static assessment	173
Figure 7-20: Source of fore shoulder vulnerability, area of floodwater accumulation.....	182
Figure 7-21: Source of aft shoulder vulnerability, area of floodwater accumulation.....	182
Figure 7-22: Typical fore shoulder damage case demonstrating progressive flooding of ro-ro deck.....	182
Figure 7-23: Sources of asymmetry surrounding vessel aft shoulder	183
Figure 7-24: Sources of asymmetry surrounding vessel fore shoulder	183
Figure 7-25: AREST Cumulative probability distribution of Time to Capsize for all collision damages. Indication of Survivability Index=0.951, with 30 minutes exposure.	185
Figure 7-26: Comparison of TTC with/without static foam solution	185
Figure 7-27: Comparison of loss scenarios location & extent, as built (left) and with AREST (right).....	186
Figure 8-1: Evolution of Stability Requirements as Mandated by IMO.....	189
Figure 8-2: Cruise Vessel C1 Stability Model.....	191
Figure 8-3: Cruise Vessel C1 Subdivision.....	191
Figure 8-4: Example static foam installation (right), space modelling (left)	193
Figure 8-5: as-operated vessel risk profile.....	194
Figure 8-6: Current vessel GM limit and margins	195
Figure 8-7: AREST P1 installation locations	197
Figure 8-8: Risk Profile with modifications	198
Figure 8-9: Updated GM Limit Curve	199
Figure 8-10: Comparison between hydrostatic and simulation model arrangements.....	203
Figure 8-11: Comparison of hydrostatic & simulation model properties	204
Figure 8-12: Simulation model opening arrangement.....	204
Figure 8-13: Collision damage sample	206

Figure 8-14: Cumulative probability distribution of Time to Capsize for all collision damages. Indication of Survivability Index=0.987.....	207
Figure 8-15: Location and extent of capsize cases.....	208
Figure 8-16: Risk Profile resulting from static assessment	208
Figure 8-17: Cross-flooding restriction sources FR160-264, Deck 1	210
Figure 8-18: Cross-flooding restriction sources FR136-224, Tank Top Deck	211
Figure 8-19: Cumulative probability distribution of Time to Capsize for all collision damages. Indication of Survivability Index=0.992.....	212
Figure 8-20: Comparison of TTC with/without static foam solution	212
Figure 8-21: Residual Loss Scenarios	213
Figure 8-22: Critical stairwell openings, ST02.2 & ST03, Deck02.....	215
Figure 8-23: Critical fire door, PB07, Deck02	215
Figure 8-24: Critical fire door, PB15, Deck02	215
Figure 8-25: GM limit curve enhancement with AREST A2 & P1 systems	216
Figure 9-1: CS2 simulation hull form sections.....	219
Figure 9-2: CS2 simulation model arrangement.....	220
Figure 9-3: Comparison of hydrostatic & simulation model properties	221
Figure 9-4: Simulation model opening arrangement	222
Figure 9-5: Collision damage sample, breach extent and location	223
Figure 9-6: SOLAS collision damage sample CDF, damage length and centre	224
Figure 9-7: SOLAS collision damage sample vertical extents.....	224
Figure 9-8: Stress Test damage sample, breach extent and location.....	225
Figure 9-9: Cumulative distribution of the Time to Capsize for all physical capsizes with an indication of the Survivability Index of 0.966.....	226
Figure 9-10: Longitudinal damage extent centre and breach volume (XLYLZL) of progressive and transient capsizes.	228
Figure 9-11: Longitudinal damage extent centre (m) and Time To Capsize (seconds) of progressive and transient capsizes.	229
Figure 9-12: Opening Vulnerability Ranking by Frequency	232
Figure 9-13: Opening Vulnerability Ranking by Net FW Mass Transfer	232
Figure 9-14: Opening Vulnerability Ranking by High FW Mass Transfer Frequency	233
Figure 9-15: critical openings (left) and foam barrier solution example (right)	235
Figure 9-16: Representative transient loss scenario – resulting from collision.....	237
Figure 9-17: Sources of asymmetrical flooding, COMP 2&3, Deck 01 and Deck 0.....	238
Figure 9-18: Cold-rooms resulting in asymmetry, COMP 2-4, Deck 02	239
Figure 9-19: Representative transient loss case (Fore) – resulting from collision	239
Figure 9-20: Sources of asymmetry within compartments 11 & 12, Deck 01 and Tween Deck respectively.	240
Figure 9-21: Proposed Partial Bulkheads, Deck 02	241
Figure 9-22: Proposed Partial Bulkheads, Deck 03	241
Figure 9-23: Proposed partial bulkheads within Compartments 10 and 12, Deck 02.....	242
Figure 9-24: Proposed partial bulkheads within Compartments 10 and 12, Deck 03.....	242
Figure 9-25: Cumulative distribution function of the Time to Capsize for all physical capsize cases relating to simulations in waves and calm water following implementation of proposed solutions.	243
Figure 9-26: Longitudinal damage extent centre (m) and Time To Capsize (seconds) of cases with solutions implemented in calm water simulations.....	245
Figure 9-27: Longitudinal damage extent centre (m) and Time To Capsize (seconds) of cases with solutions implemented in Hs=7m simulations.....	246

List of Tables

Table 1-1: A Record of Disasters and Related Legislation/Reconfiguration.....	20
Table 1-2: Reconfiguration of the ship environment adopted by the sample of retrofitted Ro-Ro passenger ships for Stockholm Agreement compliance, (Vassalos & Papanikolaou, 2002).....	25
Table 1-3: Survivability & Critical Hs formulation developments	27
Table 1-4: PROTEUS history of development	35
Table 3-1: Passenger Vessel KPIs considered in (SAFEDOR, 2005-2009)	63
Table 3-2: Strength and Operational Utility of Various Structural Parts and Components, (Misra, 2016).....	64
Table 3-3: Historical perspective on the improvements in the minimum requirements of safety, (Klanac, 2011).....	65
Table 5-1: Opening characteristics employed in modelling, based on FLOODSTAND (Ruponen & Routi, 2011)	96
Table 6-1: HAZID Participants	136
Table 6-2: Risk category, frequencies and consequence scales	138
Table 6-3: HAZID table excerpt	139
Table 6-4: Foam water absorption with respect to exposure time	141
Table 6-5: Foam water absorption with respect to pressure (3 hours exposure).....	143
Table 6-6: RCO-specific Adhesion and Cohesion requirements.....	147
Table 6-7: Pull-test results	148
Table 7-1: RoPax R1 principle particulars.....	153
Table 7-2: Loading condition summary.....	155
Table 7-3: Generalised compartment permeabilities.....	155
Table 7-4: Permeabilities for Ro-Ro spaces.....	155
Table 7-5: as-operated Attained Index calculation.....	156
Table 7-6: R1 statutory loading conditions & existing GM margins.....	157
Table 7-7: Vulnerable space properties.....	159
Table 7-8: Foam volume optimisation C1.....	160
Table 7-9: Foam volume optimisation DT6 & DT20	160
Table 7-10: Attained Index calculation with AREST solutions.....	161
Table 7-11: GM limit comparison before and after AREST solutions.....	162
Table 7-12: GM limit comparison before and after AREST solutions for statutory loading conditions.....	163
Table 7-13: Loading condition summary	165
Table 7-14: Model correlation summary	168
Table 7-15: Transient capsizing case damage dimensions	174
Table 7-16: Progressive flooding capsizing case damage dimensions.....	176
Table 7-17: Transient capsizing case results summary.....	177
Table 7-18: Progressive flooding capsizing case results summary	180
Table 8-1: Case Study Vessel Particulars	190
Table 8-2: Loading Conditions Considered	192
Table 8-3: SOLAS 2009 space permeability assumptions	193
Table 8-4: as-operated Attained Index calculation.....	193
Table 8-5: Loading condition overview & GM margins with projected growth.....	195
Table 8-6: AREST P1 Installation sites.....	196
Table 8-7: Installation volumes & weights.....	197

Table 8-8: Attained Index Calculation with modifications & reduced GM	197
Table 8-9: Comparison of GM margins.....	199
Table 8-10: Loading condition summary	202
Table 8-11: Model correlation summary	204
Table 8-12: Capsize Case Damage Dimensions – Collison.....	209
Table 8-13: Capsize Case Simulation Result Summary.....	209
Table 8-14: Ranking of critical openings.....	214
Table 8-15: Summary of solution specific GM margin benefits	216
Table 9-1: CS2 Principle Particulars.....	219
Table 9-2: Model correlation summary	221
Table 9-3: Stress-test results breakdown	226
Table 9-4: Comparison of progressive flooding cases Hs=0m & Hs=7m	230
Table 9-5: Comparison of transient flooding cases Hs=0m & Hs=7m.....	231
Table 9-6: Critical Opening Summary.....	234
Table 9-7: AREST A2 - solution summary.....	236
Table 9-8: Summary of all assessment results	244
Table 9-9: Summary of progressive cases with indication of their TTC.....	244
Table 9-10: Summary of transient capsizes cases, with indication of their TTC.....	245

Abbreviations

FLOODSTAND	Integrated FLOODing control and STANDard for stability
SOLAS	Safety Of Life At Sea
WoD	Water on Deck
TTC	Time to Capsize
IMO	International Maritime Organisation
GT	Gross Tonnage
GZ	Righting lever
GM	Metacentric Height
MSC	Maritime Safety Committee
Ro-Ro	Roll-on/Roll-off Vessel
RoPax	Roll-on/Roll-off Passenger Vessel
DG-MOVE	Directorate-General for Mobility and Transport
SRtP	Safe Return to Port
RBD	Risk-Based Design
GBS	Goal-Based Standards
ADA	Alternative Design and Arrangements
SLF	Sub-Committee on Stability and Load Lines and on Fishing Vessels' Safety
LSA	Life Saving Appliances
GOALDS	GOAL based Damage Stability
FLARE	FLooding Accident REsponse
eSAFE	enhanced Stability After Flooding Event
EMSA	European Maritime Safety Agency
R	Required Subdivision Index
A	Attained Subdivision Index
EC	European Commission
Hs	Significant Wave Height
Hs_Crit	Critical Significant Wave height
AREST	Adaptive, Reconfigurable Environment Safety Technology
SMS	Safety Management System
DSS	Decision Support System
DCP	Damage Control Plan
GRP	Glass Reinforced Plastic
RCO	Risk Control Option
TRL	Technology Readiness Level
JONSWAP	Joint North Sea Wave Project
HARDER	HARmonisation of DEsign Rationale
SAFEDOR	Design, Operation and Regulation for SAFETy
ITTC	the International Towing Tank Conference
SDC	The Sub-Committee on Ship Design and Construction
SA	The Stockholm Agreement
KPI	Key Performance Indicator
VCG	Vertical Centre of Gravity

MARPOL	The International Convention for the Prevention of Pollution from Ships
NTQ	Novel Technology Qualification
PoB	People on Board
FSA	Formal Safety Assessment
PLL	Potential Loss of Life
DoF	Degree of Freedom
LPP	Length between Perpendiculars
SE	Standard Error
CDF	Cumulative Distribution Function
IACS	International Association of Classification Societies
WT	Watertight
SWT	Semi-Watertight
PU	Polyurethane
ROV	Remote Operated Valve
HAZID	Hazard Identification
TVF	Transverse Flooding Opening ID

Chapter 1: Introduction

1.1 Problem Definition, Innovation and Impact

1.1.1 The Problem

Ships are fundamentally designed to carry payload from one location to another, supported by the provision of buoyancy, dictated by hull shape, internal volume and superstructure (permeable volume). In case of flooding accidents, depending on the amount and distribution of permeable volume, a ship may sink from inadequate buoyancy or capsize from inadequate stability in a manner that is either fast/transient loss or slow/progressive flooding loss. Traditional flooding protection in the maritime industry entails watertight subdivision to an extent dictated by IMO regulations BUT this has a physical limit which, if exceeded, a safety plateau is reached. This is currently the case with most ships in the maritime industry. Moreover, with damage stability standards progressively increasing, the safety gap between existing and new ships is dangerously widening. Furthermore, with design stability margins progressively eroding, stability management is unsustainable, leading to loss of earnings and, more importantly, life.

1.1.2 The Innovation

The idea of an “Unsinkable” ship is treated as a misnomer in the vocabulary of the maritime industry, particularly after the Titanic disaster, which tainted the idea for ever. However, Titanic was designed with consideration of just a single damage scenario, whilst the design of modern megaships today necessitates consideration of tens of thousands of scenarios. This leads to a wealth of additional knowledge, ranging from general arrangements to forensic detail of the ship internal environment. This, combined with recent technological developments derived from five years of research and application at the Department of Naval Architecture, Ocean and Marine Engineering, enables a systematic consideration of all loss modalities in a damaged ship and restoration of loss buoyancy post-flooding casualties. This is made feasible either through the deployment of high expansion foam in selected vulnerable spaces as a means of passive/active protection or in the form of deployable barriers to curtail and control the process of flooding. Both approaches have been tested in a number of feasibility studies with industry, involving new designs and existing ships and are currently undergoing approvals with class and administration. The latter is ship-type and ship-design specific, but the process is generic and therefore, widely applicable. Moreover, the same concept being used to address design of newbuildings can also

be used to attend to existing ships, which are currently operating at inferior stability standards, resulting from a hiccup in maritime legislation known as the “Grandfather Clause”.

1.1.3 The Impact

Being able to solve the damage stability problem for ships will lead to a transformational change in ship design and operation with immeasurable impact on the whole maritime industry. Given that damage stability failure represents 90% of the risk to human lives in maritime accidents (Papanikolaou, Zaraphonitis, & Vassalos, 2010), this affects over 2 billion people who travel on passenger ships each year and around 100,000 commercial vessels, operated by 1.5 million crew (UNCTAD, 2017). Inadequate damage stability has been the cause of 53% of all vessel losses over the past decade and was the primary cause of 65% of losses in 2018 (Allianz, 2019). For passenger ships, the maximum number of passengers carried by the largest cruise ships each year has risen dramatically, almost doubling to 6,800 in 2019 compared to 1999 (Clarkson, 2020). This means that there is now a far greater risk of passenger fatality from any given single accident. Similarly, passenger ferries are responsible for approximately 1,000 damage stability-linked fatalities per year, with 163 reported passenger ferry accidents occurring between 2002-2016, resulting in over 17,000 deaths (Lloyds Register Foundation, 2018). Moreover, raising the bar on maritime safety has a direct benefit to the UK insurance sector with reductions in claims and economic loss to the industry. The UK has a 35% share of global marine insurance premiums and 60% of protection and indemnity insurance, with 26% of total global shipbroking being undertaken in the UK (Maritime UK, 2016). Analysis of 230,000 marine insurance industry claims, with a value of almost \$10bn between July 2013 and July 2018, shows that ship flooding incidents are the most expensive cause of loss for insurers, accounting for 16% of the value of all claims – equivalent to more than \$1.5bn over this period (Allianz, 2019).

1.2 Background

1.2.1 The First Steps

Notwithstanding the paramount importance of ship stability and safety today, theoretical treatment of these essential properties for ship design and operation are less than three centuries old. The mathematical properties of the metacentre, GM, one of the essential ship stability parameters, was explained for the first time by Pierre Bouger (Bouger, 1746), whilst Leonhard Euler (Euler, 1749) introduced the restoring moment for small angles of heel. In the UK, George Atwood developed a formula in 1796 for the calculation of the righting lever GZ for the whole range and in 1850, Canon Moseley introduced the concept of dynamical stability referring to the area under the GZ curve. It is interesting to note, however, that the great majority of ship designers and shipbuilders at the beginning of the 19th Century regarded these developments as

highly theoretical and, hence, they were initially ignored. In fact, the first criteria involving Moseley’s concept were adopted by the American Navy in the latter part of the 19th Century. Any criteria in use were based on experience and it was clear that experiential knowledge was a poor guide, since, in severe storms of 1821-1822 some 2,000 vessels perished with the loss of about 20,000 lives in the North Sea alone. Following this, the value of GM was increasingly used as a criterion and for many years it was assumed (in some circles, this is still true today) that adequate metacentric height could be used as the sole measure of stability (intact and damage). Furthermore, it was thought that this was sufficient for all angles of heel and for all conditions of loading, even though GM is an indicator of only static upright stability. Indeed, the first specific criterion on residual stability standards at the 1960 SOLAS Convention did not deviate from this, imposing a requirement for a minimum residual GM of 0.05m.

1.2.2 The Birth & Reign of Subdivision – A Record of Disasters

Focus did not broaden from metacentre and static stability considerations until the introduction of the first merchant shipping act in 1854. Here, it was sought to mitigate flooding risk through mandatory reconfiguration of the internal ship environment by way of watertight bulkheads. Hence, the first legal requirements for subdivision were born, with ships covered by the standard required to possess a collision bulkhead along with transverse bulkheads around the engine room. The placement of these was predominantly intuitive and not based on calculations of any kind, but it could certainly be said this was a step in the right direction. Unfortunately, however, what followed was a series of many hard-learned lessons as safety standards improved in a reactive and accident driven manner, lending credence to the saying “safety regulations are written in blood”. Eventually this led to the adoption of the first internationally agreed system of subdivision in SOLAS 1929, amidst other key developments listed within Table 1-1.

Table 1-1: A Record of Disasters and Related Legislation/Reconfiguration

Date	Disaster
1854	The first Merchant Shipping Act of 1854 is the first known legal requirement addressing safety at sea and concerning <u>watertight bulkheads</u> . It was enacted as a direct result of the rapid foundering of the Birkenhead in 1852 after striking a rock off South Africa drowning some 500 women and children. The loss was rapid because the cavalry officers on board had holes cut in the transverse bulkheads in order to exercise their horses, (Lancaster, 1997).
1862	Pressure in Parliament by the ship owners succeeded in repelling the Act because it was simply based on “mischievous” behaviour. Within three years the London and the Amelia both sank in the same storm because of inadequate subdivision with 233 people drowning in the London alone. It is frightening that from 1876-1892, 10,381 vessels belonging to the UK were totally lost with 27,010 seamen and 3,543 passengers drowning, with losses attributed to “Acts of God”. It is also worth noting that in 1878 HMS “Eurydice” was lost with nearly 400 lives lost as the ship was caught by a strong squall unprepared with some of her upper half-ports on the main deck open for ventilation and as she heeled under the force of the wind, water entered the open ports causing a sudden and complete loss of the ship.

- 1883** The Daphne capsized with the loss of 124 lives immediately after being launched in the Clyde. Sir Edward Reed, the Commissioner of inquiry into the accident recommended that consideration should be given of the extent to which stability entered into design, construction, stowage, load line and freeboard of ships.
- 1891** The Bulkhead Committee of the British Board of Trade recommended a 2-compartment standard for passenger ships but the recommendations were not adopted. Unbelievably, in many parts of the world, one-compartment ships still exist, in spite of clear understanding today that the risk is completely “off the scale”.
- 1895** Germany introduced a 2-compartment standard, following the rapid loss of the Elbe with the death of 340 people.
- 1913** Following the Titanic catastrophe in April 1912 with a loss of 1,430 lives, the first International Conference on the Safety of Life at Sea (SOLAS) takes place in London to consider proposals by UK, Germany and France. The regulations formulated did not come into effect due to World War I.
- 1914** The Empress of Ireland capsized in the Gulf of St. Lawrence, sinking in 14 minutes, with 1,012 lives lost. The need for subdivision, it was stated “gathers momentum” but it was not until 1929 when a full International Conference was convened to consider this matter. However, the system of subdivision devised, falls short of that agreed in 1913, evidence that IMO regulations reflect not experiential knowledge as it is widely believed but the compromise reached in each convention.
- 1928** Loss of the Vestris inspired proposals at the SOLAS Conference in 1930 for more secure engine room deck openings.
- 1929** United States ratifies the 1929 SOLAS Convention but only after the loss of the Mohawk by collision and of Morro Castle by fire.
- 1948** Loss of the Sankey with all hands and the Flying Enterprise in 1952 inspired legislation to prevent shifting cargoes.
- 1948** SOLAS Convention and the first specific criterion on residual stability standards with the requirement for a minimum residual GM of 0.05m. This represented an attempt to introduce a margin to compensate for the upsetting environmental forces.
- 1954** Princess Victoria capsized and sank when large waves burst open the stern door in rough weather with the car deck and starboard engine room flooding (134 died).
- 1955** Fire in the engine room of the Empire Windrush, with large loss of life, inspired the dispersal of fire pump controls.
- 1956** The Andrea Doria built under SOLAS 1948 requirements, which were a slight improvement of the 1929 Conference capsizes in heavy seas and this alerts the profession to the fact that the effect of waves on safety ought to be considered. This accident strongly influences proposals made to SOLAS 1960.
- 1974** Straitsman capsized and sank whilst approaching its berth with its vehicle door partly open as a result of squat, flooding the vehicle deck.
- 1974** IMO published Resolution A.265 (VIII) - regulations dealing with subdivision and damage stability on a probabilistic basis - as equivalent to SOLAS deterministic rules.
- 1987** Herald of Free Enterprise capsized when the bow wave and bow-trim combined to bring the open bow door underwater, flooding the vehicle deck.
- 1987** Santa Margarita Dos capsized in port in Venezuela due to heeling while loading vehicles as a result of flooding of the vehicle deck.

- 1987/1988** Following the Herald of Free Enterprise accident in 1987 with the loss of 193 lives and a public outcry, SOLAS '90 came into effect for new ships build after 1990, introducing a considerable increase in damage stability standards, (Spouge J. , 1989). Proposals by UK to phase-in upgrading of existing ships to SOLAS '90 is rejected by IMO but a regional Agreement is reached by the North West European Nations.
- 1991** 1991: After a madman set fire on the Scandinavian Star causing the death of 169 people, retrospective legislation was introduced for the first time in respect of enhanced "Structural Fire Protection".
- 1994** The Estonia is lost involving the loss of 852 lives. IMO rejects proposals for capability of withstanding water on deck of Ro-Ro Passenger Ships. Regional agreement is reached ("Stockholm Agreement") by the North West European Nations and later by the whole EU, Australia and Canada, (T. E. Svensen, 1998)
- 1995** In the 1995 SOLAS Diplomatic Conference SOLAS '90 is adopted as a global safety standard of damage stability. A proposal to IMO of a new damage stability framework based on probabilistic methods by the North West European Nations, following intensive research in the wake of Estonia was tabled as an item for long term discussion. The proposal considers explicitly the effect of waves and water on deck (performance-based criteria) deriving from the work undertaken by the Strathclyde Stability Research Group and allows for various safety nets aiming to ensure that the Estonia disaster will never happen again. A probabilistic framework was also developed and proposed (Rusaas, 1996), which formed the foundation for the EU Project HARDER (HARDER, 2003), where the foundation of the probabilistic regulations for damage stability was developed and brought to IMO, leading eventually to SOLAS 2009.
- 2000** Express Samina: Flooding of the engine room and spreading of floodwater through open watertight doors, leading to 81 fatalities.
- 2006** Al Salam Boccaccio '98: Following fire on the car deck, sprinklers were activated, which led to floodwater being accumulated on the vehicle deck because of blocked freeing ports, leading to the vessel capsizing with 1,002 dead.
- 2012** Costa Concordia: Side grounding damage, leading to up-flooding and capsize with 32 casualties.
- 2014** MV Sewol: Overloading and inadequate stability, leading to vessel listing heavily following a turn and eventually capsizing with 295 casualties, mostly children.
-

Most of the accidents referred to above have led to improved legislation only in regards to subdivision, which is evidence not only of the disaster-triggered mode of regulation but also of the incident-specific approach religiously adopted. That is to say, focus was very often placed on fixing what had gone wrong as opposed to what could go wrong. Obviously, subdivision did work to a point and the maritime industry norm of "If something works, don't fixed it" prevailed. Perhaps another reason for bulkheads having lasted so long uncontested was that they were never employed very effectively in the first instance, which left a lot of room for improvement. Consequently, over a century has been spent in this direction, squeezing every last drop out of bulkheads, which are still to this day being pursued as the primary risk control option for flooding risk mitigation and control. It is interesting however, to delve into the detail of its development and evolution in an effort to discern learning outcomes.

1.2.3 Forces Driving Regulatory Development

As mentioned previously, evolutionary safety developments have undoubtedly been accident-driven and such incidents have fuelled a process of gradual improvement over the years, Figure 1-1.

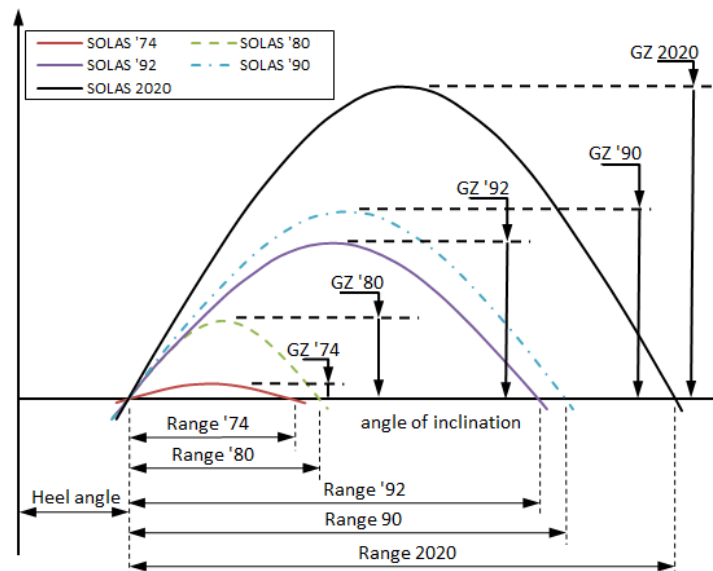


Figure 1-1 - Damage stability evolutionary changes, based on diagram shown in (Hutchinson & Scott, 2016)

However, there are undoubtedly other forces at play in shaping regulatory development and science can often lose to political dictate or industrial pressures. This stems from the prevailing opinion that safety lies in antithesis to profitability, which generates strong resistance to legislative change and limits the degree to which standards may be raised at any given time. Consequently, it can take a multitude of accidents of similar profile before significant changes are made, as demonstrated by the following series of RoPax vessel casualties due to the effects of water on deck:

- 1953 Princess Victoria capsized and sank when large waves burst open the stern door in rough weather with the car deck and starboard engine room flooded (134 died).
- 1974 Straitsman capsized and sank whilst approaching its berth with its vehicle door partly open as a result of squat, flooding the vehicle deck.
- 1987 Herald of Free Enterprise capsized when the bow wave and bow-trim combined to bring the open bow door underwater, flooding the vehicle deck.
- 1987 Santa Margarita Dos capsized in port in Venezuela due to heeling while loading vehicles as a result of flooding of the vehicle deck.
- 1994 Estonia capsized and sank due to flooding of the vehicle deck.

The fact of the matter is that, whilst accidents with water on deck as a common loss mechanism have contributed to the evolutionary change of legislation, recurrence of such accidents clearly

demonstrated that lessons learned did not go far enough. The Ro-Ro concept in RoPax ship designs provides perhaps one of the clearest examples of safety objectives clashing with functional/operational objectives. These spaces are fundamental to the economic viability of such concepts, thus triggering a struggle in this evolution between safety of passengers and viability of business. Therefore, whilst large open spaces in RoPax vessels are an obvious design vulnerability, reconfiguring this space to enhance safety is not favoured and often resisted. The key reasons for this inertia stem primarily from the shortcomings of reconfiguration in the form of watertight partitioning, which:

- Consume deck and hull space, affecting ergonomics
- Erode earning potential (cargo space, internal logistics, deadweight, turn-around times)
- lead to loss of income

Ultimately, regulations should act to provide the operator with a safety net and not a noose from which he can hang his business. As such, it is important that as we strive to improve safety, we also seek cost-effective means to do so. Otherwise, any attempt to raise safety standards will inevitably be met with resistance, in which instance we may once again end up awaiting the next disaster to awaken us.

1.2.4 Reconfiguration Going into Overdrive

Building on the previous section, it has taken one of the largest modern-day catastrophes, namely the Estonia disaster, claiming 853 lives, to shake the foundations of the industry. Such was the scale of the disaster; it had the effect of bringing economic and other barriers down, leading to an onslaught of hull space reconfiguration, both external and internal to the ship hull. Driving this process was a new regulatory instrument known as the Stockholm Agreement, which was reached in 1996 and required that EU RoPax vessels be assessed considering the accumulation of 500mm of water on the vehicle deck. Relaxations to this value could be made depending on the vessel area of operation and if a residual freeboard of 2m could be demonstrated, no water on deck effects needed to be assumed, thus encouraging the design of higher freeboard ships (global reconfiguration). As an alternative route to compliance, the Stockholm Agreement also allowed for model testing to be conducted with consideration of the worst damage case defined for SOLAS '90 compliance. Additionally, a level keel midship damage had also to be considered, if the worst damage location according to SOLAS 90 lay outside the range $\pm 10\%$ Lpp from the vessel midship. This represented the first performance-based standard, accounting for water on deck and environmental conditions in the area of operation, as well as the dynamic behaviour of the vessel, the environment and their interaction. Perhaps most significantly the Stockholm Agreement was the first regulation pertaining to damage stability that has been applied retrospectively. In the

maritime industry, this was highly unprecedented as new legislation generally applies only to newbuildings, thus leaving the majority of ships (90% of all the ships are already in operation) operating at inferior standards. This is known as the Grandfather Clause, a serious drawback in maritime safety and its evolution (Grandfather Clause is the legal term used to describe a situation whereby an old rule continues to apply to some existing situations, while a new rule will apply to all future situations). In any case, the effect of the regulation was to fuel an extensive process of vessel reconfiguration in order to bring old and new vessels up to standard. Examples of the various solutions adopted are outlined in Table 1-2, pertaining to the North West European Nations Ro-Ro fleet, (Vassalos & Papanikolaou, 2002).

Table 1-2: Reconfiguration of the ship environment adopted by the sample of retrofitted Ro-Ro passenger ships for Stockholm Agreement compliance, (Vassalos & Papanikolaou, 2002).

Modification (RCO)	Design Impact
Transverse Doors on the Car Deck	Major modification as it effects the overall cost, survivability and operation significantly
Ducktail	Major modification as it effects the overall cost, survivability and operation significantly
Ducktail Sponsons	Major modification as it effects the overall cost, survivability and operation significantly
Side Sponsons	Major modification as it effects the overall cost, survivability and operation significantly
Side Casings	It could be major or minor conversion depending on cost and effect on cargo capacity
Making existing rooms watertight on the Car Deck	Minor
Internal Tank – Re-arrangement	Minor
Buoyancy Tanks	Minor
Additional Subdivision	Minor or major, depending on the location and size of the conversion
Making existing rooms watertight below the Car Deck	Minor
B/5 Longitudinal Bulkheads	Minor or major depending on the location and size of the conversion
Cross-flooding Arrangement	Minor or major depending on the location and size of the conversion
Heeling Tanks	Minor
FW tanks	Minor
Ballast Tanks	Minor
Stabilising Tanks	Minor
Scupper Arrangements	Minor
Additional Centre Casing on Car deck	Minor
Stern Boxes	Minor
In Flooding Valves	Minor
New Bulbous bow	Major
Foam Fillings in void tanks	Major

Observing the various risk control options used, the tendency to clutter the internal ship spaces becomes obvious. This stems primarily from the fact that most of these solutions were to be applied in retrospect, which is always sub-optimal and particularly difficult to do with subdivision. It is, however, interesting to note that no RoPax vessel has been lost due to water on deck problems since the introduction of this legislation, though one must be careful when making such observations. In fact, the Stockholm Agreement has remained in parallel with probabilistic regulations for damage stability. However, a recent European Commission project titled “Assessment of specific EU stability requirements for ro-ro passenger ships” (EU-DGMOVE, 2019), has demonstrated that the requirements of SOLAS 2020 now make this standard redundant.

1.2.5 Making Sense of Reconfiguration

Decluttering of internal configuration through structural changes was assisted significantly by the introduction of the SOLAS 2009 probabilistic rules for damage stability, which represented two key changes in direction. Firstly, moving from a deterministic to a probabilistic framework, and secondly, from design towards performance-based standards. Traditional deterministic instruments based on a prescriptive regime represented a major roadblock that threatened to inhibit progress. Shaped by existing technology and with an inherent but not explicitly stated safety level, the deterministic requirements were by nature extremely hard to challenge. In this respect, the level of innovation that was feasible in design and reconfiguration was severely restrained. In contrast, SOLAS 2009 as a risk-based standard was far better suited to cater for innovation and could in theory cater for all credible means of damage stability enhancement, provided that their impact on risk could be quantified and validated by some appropriate means.

In relation to internal configuration, the deterministic requirements according to SOLAS 90 placed a great deal of constraint on what was possible within design. Key examples of this include “floodable length” and “permissible length of compartments” criteria, which dictated bulkhead arrangements. SOLAS 2009, in contrast, allowed any arrangement to be used provided the vessel could meet requirements, thus broadening the design space. In addition, margin line criteria in SOLAS 90 had the effect of directing focus primarily below the bulkhead deck, as no credit could be gained in the equilibrium floating position for any watertight configuration above the margin line. However, this was amended in SOLAS 2009 where credit could be gained for any buoyant volume so long as unprotected openings are not immersed. A final important example of how the regulations influenced vessel configuration was the consideration of B/2 damage penetrations and much greater damage lengths than the deterministic B/5, 2-compartment standard. This was highly significant, as many design configurations had hitherto taken advantage of this limited

damage size, meaning configuration was designed to satisfy the letter of the rules but not the intent.

However, being able to follow a rational approach to subdivision and flooding protection brought new problems of its own. Namely, with probabilistic damage stability rules having originally been developed on the basis of cargo ship damage statistics, serious concerns have been raised regarding the adopted s-factor formulation and the associated Required Subdivision Indices, particularly for RoPax and large cruise ships (Vassalos & Jasionowski, 2011) (Vassalos, 2016).

The current s-factor formulation has also fallen into question in relation to its capacity to cater for the diversity and complexity of modern passenger vessels. Rahola's proposal to use GZ curve properties to measure stability, (Rahola, 1939), cast the die for future regulatory developments and hence focus was placed on global ship stability parameters (i.e. Range, Freeboard, GM, Beam). However, as the scale and complexity of ships has changed dramatically since Rahola's proposals, a great deal of uncertainty surrounds the ability of generalised global stability parameters to provide an accurate measure of survivability. Furthermore, there are additional concerns surrounding the degree to which formulations based on such parameters guide the designer in the right direction, particularly in relation to internal configuration which is dealt with in a very indirect and reductive manner at present. Some efforts have been made over the years in order to help amend this, as summarised in Table 1-3, where for example Cichowicz et al. included residual internal volume within the formulation. This was then followed by Atzampos who proposed a scaling factor, λ , to account for vessel size. Unfortunately, the conclusions in most cases were that, despite significant improvements being possible, a "one-size-fits-all" formulation is unlikely to be able to cater for all vessels and as such Direct Approaches are often favoured.

Table 1-3: Survivability & Critical Hs formulation developments

Formulation	Proposed by	Year
$s = 4.9 \sqrt{\frac{F_E \cdot GM}{B}}$	Bird & Brown	1974
$H_{S_{crit}} = 4 \frac{GZ_{max}}{0.12} \cdot \frac{Range}{16}$	Tuzcu and Tagg (HARDER project)	2002
$H_{S_{crit}} = \frac{\frac{1}{2} GZ_{max} \cdot Range}{\frac{1}{2} GM_f \cdot Range} V_R^{\frac{1}{3}}$	J. Cichowicz et al. (GOALDS)	2016
$H_{S_{crit}} = 7 \cdot \left[\frac{MIN(\lambda \cdot Range, TRange)}{TRange} \cdot \frac{MIN(\lambda \cdot GZ_{max}, TGZ_{max})}{TGZ_{max}} \right]^{1.05}$	G. Atzampos (eSAFE)	2019

Such concerns have led to a certain degree of disquiet in industry and academia, along with apprehensions deriving from the escalation of passenger ships to megaships. Consequently, research focus on damage stability has shifted towards large passenger ships and to a more holistic approach to flooding and fire incidents, known as “Safe Return to Port”.

1.2.6 A New wave of Reconfiguration – Safe Return to Port

In May 2000, the IMO Secretary-General called for a critical review of the safety of large passenger ships noting that "what merits due consideration is whether SOLAS requirements, several of which were drafted before some of these large ships were built, duly address all the safety aspects of their operation – in particular, in emergency situations". This visionary prompt led the IMO Maritime Safety Committee (MSC) to adopt a new “philosophy” and a working approach for developing safety standards for passenger ships. In this approach, illustrated in Figure 1-2 (SLF 47/48), modern safety expectations are expressed as a set of specific safety goals and objectives. These address design (prevention), operation (mitigation) and decision making in emergency situations (emergency response), with an overarching safety goal commensurate with no loss of human life due to ship-related accidents. This quest, which is in principle a life-cycle risk management framework, has climaxed to the “zero tolerance” concept of Safe Return to Port, introduced in July 2009 and the ensuing developments pertaining to “Safety Level”, “Alternative Design and Arrangements”, “Risk-Based Design” and “Goal-Based Standards”. This prompted an open proclamation by the then (April 2012) Secretary General of the International Maritime Organisation Koji Sekimizou, in addressing guests in the annual dinner of the Royal institution of Naval Architects, that deterministic requirements have no future. The term “Safe Return to Port (SRtP)” has been widely adopted in discussing this framework, which addresses all the basic elements pre-requisite to quantifying the safety level (life-cycle risk) of a ship at sea and providing an approach for de-risking fire and flooding casualties, as outlined in the following.

IMO (SLF 47/48) *Passenger Ship Safety*

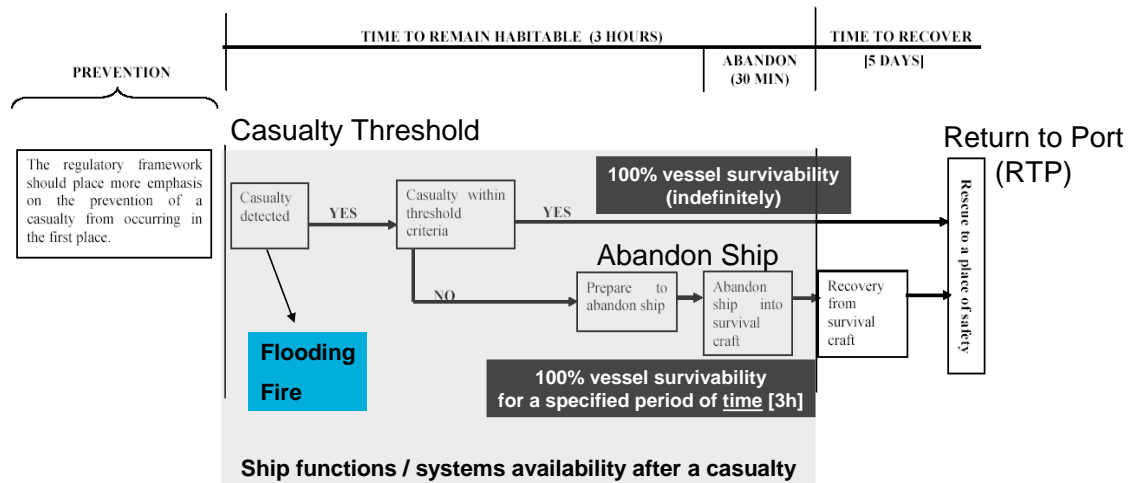


Figure 1-2: The IMO Framework for Passenger Ship Safety (IMO SLF 47/48)

Casualty Threshold: This supports the goal that the ship should be designed for improved survivability so that, in the event of a casualty, persons can stay safely on board as the ship proceeds to port. In this respect and for design purposes (only), a casualty threshold needs to be defined whereby a ship suffering a casualty below the established threshold is expected to stay upright and afloat and be habitable for as long as necessary in order to return to port under its own power or wait for assistance. It constitutes part of the design work to determine this threshold value rationally, as it greatly influences the design arrangements (ship environment re-configuration). This, in turn, has introduced a new wave of internal ship space reconfiguration by way of protecting vital machinery with longitudinal B/10 bulkheads around engine spaces, as well as internal reconfiguration for redundancy provision, including partitioning in the engine room itself or other redundancy arrangements aimed at segregating essential systems.

Emergency Systems Availability / Evacuation and Rescue: Should the casualty threshold be exceeded, the ship must remain stable and afloat for sufficiently long time (3 hours recommended) to allow safe and orderly evacuation (assembly, disembarkation and abandoning) of passengers and crew. Availability of emergency systems to perform all requisite functions in any of the scenarios considered is, therefore, implicit in the framework. In addition, the ship should be crewed, equipped and have arrangements in place to ensure the health, safety, medical care and security of persons on-board in the area of operation. This includes consideration of climatic conditions and the availability of SAR functions until more specialised assistance is available. Consequently, an array of changes in the internal ship environment have been introduced as well as new spaces (safety areas) to enhance requisite functionality post-casualty,

including: safety centres, redundant safety systems, new evacuation routes, muster stations, new LSA, many of the latter within the internal ship envelop.

1.2.7 RoPax Vs Cruise Ships: Hitting a “Wall”

In support of the aforementioned developments and in the pursuit to de-risk large passenger ships, a series of projects have investigated this problem and laid down the foundation for a passenger ship-specific damage stability framework, process and criteria, (GOALDS, 2009-2012), (EMSA II, 2009-2012), (EMSA III, 2013-2015), (eSAFE, 2017-2019), (EU-DGMOVE, 2019) and (FLARE, 2019-2022). The outcome of two of these projects, EMSA II and EMSA III, are shown in Figure 1-3, which demonstrates the cost-effective level to which the Required Subdivision Index could be raised for RoPax and cruise vessels.

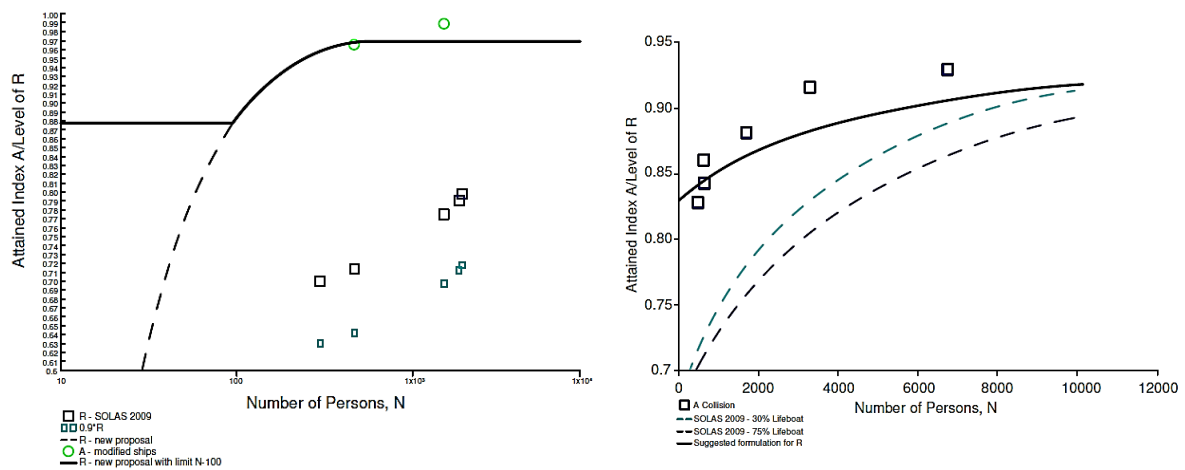


Figure 1-3: Research outcome suggested level of R for passenger vessels (EMSA II, 2009-2012) left, (EMSA III, 2013-2015) right

However, the strong suggestion by these research projects on increasing the damage stability standards, specifically for small RoPax vessels and for passenger ships in general, has been met with strong resistance by industry. Ultimately ending in a compromise at IMO for much more modest damage stability standards. Key reasons for this relate to the industry becoming increasingly aware that design measures to improve damage stability standards, primarily through further reconfiguration of the internal environment, are reaching saturation. Consequently, we stand at a crucial point where viability of business must be compromised more than ever in favour of passenger safety. For this reason, something has to change, as sacrificing business viability will never be the route leading to a solution. Hence, the shift to a new perspective was an inevitability.

1.2.8 Widening the Reconfiguration Perspective: Passive and Active Protection

The dogma “Innovation is born out of necessity” has once again offered a way forward. Namely, in the quest for damage stability improvement, design (passive) protection has traditionally been the only means to achieve this in a measurable/auditable way (SOLAS 2009, Ch. II-1). However, in principle, the consequences from inadequate damage stability can also be reduced by operational (active) measures, which may be highly effective in reducing loss of life (the residual risk). However, the present lack of measurement and verification of the risk reduction potential of any active measures poses a problem. In simple terms, what is needed is the means to account for risk reduction by operational (interventional) RCOs as well as measures that may be taken during emergencies. Such risk reduction may then be considered alongside that deriving from design measures. What needs to be demonstrated and justified is the level of risk reduction and a way to account for it, the latter by adopting a formal process and taking requisite steps to institutionalise it. Efforts in this direction are the focus of an ongoing large-scale EC-funded research Project, (FLARE, 2019-2022). The key facilitator in this respect is the regulation for Alternative Design and Arrangements, (IMO, 2013), (IMO, 2006), which opens the door to innovation and is key to this thesis.

1.2.9 Life-cycle Risk Management

Ship flooding risk is by no means a static measurement and, in fact, is almost constantly varying over the day-to-day operation of the vessel. The reasons for this stem from a multifarious array of influential factors such as the opening of WTDs, variations in loading condition, changes in weather etc. Further still, greater variations in flooding risk have a tendency to occur gradually, over longer durations of the vessel life cycle. In order to illustrate this point, it is helpful to view this in the form of a bowtie diagram as shown in Figure 1-4. Here, one can observe causal events of the left, the risk event in the centre (flooding accident) and the consequences on the right-hand side. In addition, for each potential threat and consequence several barriers in the form of Risk Control Options are in place.

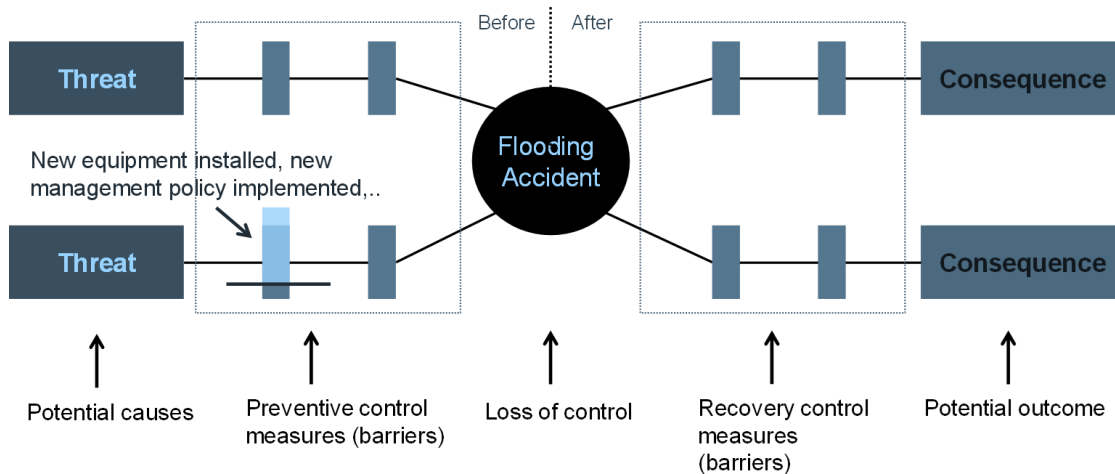


Figure 1-4: Barrier Management (“Bow-Tie”) (Vassalos, Atzampos, Cichowicz, & Paterson, 2018)

The need for life-cycle risk management derives from the fact the effectiveness of these barriers tends to change over time, either as new threats present themselves or due to degradation of the barriers themselves. As previously mentioned, this can occur in a somewhat subtle way during the general operation of the vessel, or in a more significant way throughout the vessel life cycle. A typical example of this relates to growth in vessel lightweight, which has the effect of increasing KG and draft, both of which have negative effects on vessel resilience to flooding. This is demonstrated within Figure 1-5, where an illustrative example of the variation in lightweight and KG for a large cruise vessel is shown at incremental steps. Here, for a single loading condition, the impact of vessel growth is demonstrated and plotted relative to the vessel limiting GM curve. Though rather extreme variations are depicted here, this clearly demonstrates how a vessel can fall out of compliance given sufficient growth, thus highlighting one of many reasons it is important to manage flooding risk over the vessel life cycle.

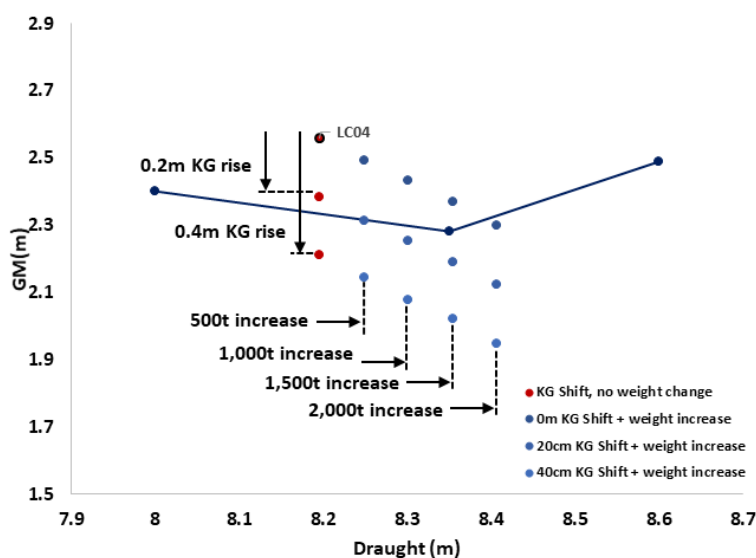


Figure 1-5: Illustrative example of vessel lightweight and KG variation

Barriers can and do come in the form of both preventative measures and recovery or control measures. Furthermore, these barriers can exist in the form of design (passive protection) or interventional (active) RCOs. Unfortunately, to date focus has largely been placed solely on design measures and predominantly on control as opposed to prevention. There are several reasons for this, primarily relating to the difficulty in quantifying the impact of preventative measures such as crew training or the installation of a new navigation system, which makes this hard to regulate for. However, in the understanding that safety affects everything in the life-cycle of a ship and is, in turn, affected by everything, focussing entirely on design measures and ignoring any interventional measures is becoming harder to justify. Ideally focus would broaden to accept risk control options pertaining to all influential factors, such as:

- Process, people, technology, organisation, environment, science and engineering.
- Rules, regulations, codes and internal practices (safety culture).
- Passive, active, removable, non-removable, endogenous, exogenous.

1.2.10 Fuelling Technological Innovation in Solving the Damage Stability Problem

Notwithstanding the lack of a life-cycle regulatory framework complete with passive and active measures of damage stability protection, the regulation for “Alternatives” provides the requisite platform for the first important steps. As indicated in the foregoing, with accidents providing the primary motivation, emphasis has largely been placed on reducing consequences, i.e., on cure rather than prevention. The key reason for this, derives from the fact that the residual risk post flooding accidents is unacceptably high, meaning that the most-cost-effective way to reduce flooding risk is to focus on the residual risk, namely on technological innovation, targeting cost-effective solutions to damage stability problem.

In this respect, the prevailing situation can be drastically improved through an understanding of the underlying mechanisms leading to vessel loss and through the identification of governing design and operational parameters to target flooding risk reduction cost-effectively. This, in turn, necessitates the development of appropriate methods, tools and techniques, capable of meaningfully addressing the physical phenomena involved.

1.3 The Way forward: Technological Innovation is the Key

1.3.1 Damage Stability: Still the Highest Risk Contributor in the Maritime Industry

Within half a century, the subject of damage stability of ships has climaxed to the “zero tolerance” concept of Safe Return to Port, introduced in July 2009 and the ensuing developments pertaining to “Safety Level”, “Alternative Design and Arrangements”, “Risk-Based Design” and “Goal-Based Standards”. This has put ship safety in perspective and with flooding post collision and grounding accidents continuing to be the key risk contributor for passenger ships, resolving this problem remains a priority, Figure 1-6. In particular, for cruise ships, Figure 1-7 shows that the maximum numbers of passengers carried by the largest cruise ships each year has risen dramatically, almost doubling to 6,800 in 2019 compared to 1999 (Clarkson, 2020). This means that there is now a far greater risk of passenger fatality from any given single accident.

Moreover, the realisation that risk is inextricably linked to operation and a derivative of exposure has driven the industry to life-cycle considerations for effective risk management. This, in turn, has provided the motivation and the platform for wider industry inculcation.

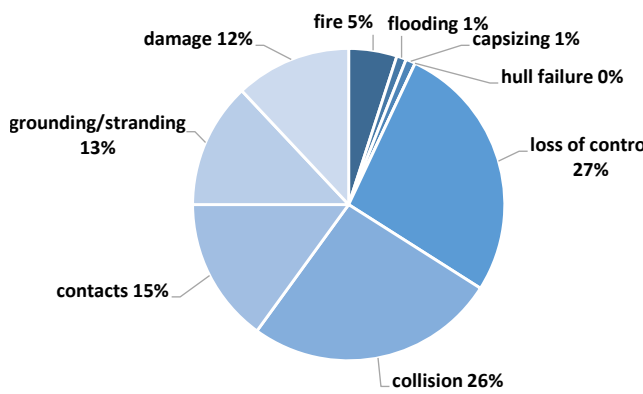


Figure 1-6: Casualty events for ships in the period 2011-2019

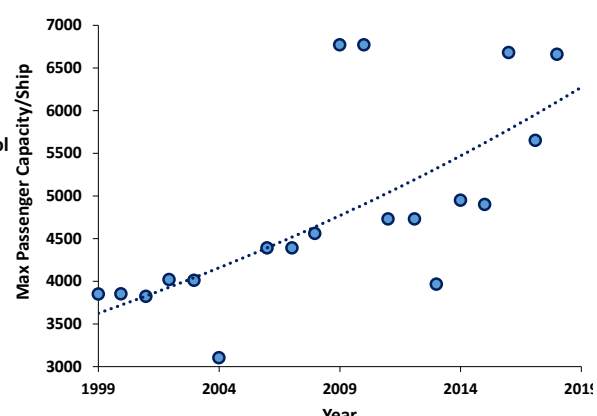


Figure 1-7: Capacities of largest passenger ships by year (Clarkson, 2020)

1.3.2 Damage Stability Research at Strathclyde as an Enabler

Damage stability research at Strathclyde has been leading the way internationally for over 5 decades, helping to raise the subject from embryonic existence to a scientific subject at par with other performance requirements in ship dynamics and hydrodynamics, such as resistance, propulsion, seakeeping and manoeuvring. In this process, unabated research at Strathclyde in damage stability from the Herald of Free Enterprise accident to date, funded initially by the UK Government and subsequently by the EU, (Turan & Vassalos, 1994) (Letizia, 1996), has raised capability in addressing the damage stability problem in ships to forensic level detail, which in turn nurtured and encouraged the novelty presented in this thesis. A great deal of this development has been translated into a software suite under the name of PROTEUS, as described in the following section.

1.3.3 The PROTEUS Software Suite

1.3.3.1 General Capabilities and Overview of Historical Development

PROTEUS is a ship hydrodynamics and dynamics software suite, developed by the University of Strathclyde along with Brookes Bell Safety at Sea Ltd and marketed by the latter as a seakeeping and stability software with routes going back four decades. The software is capable of modelling the dynamic behaviour of intact and damaged vessels in the time-domain when exposed to wind and wave effects, in addition to performing several other functions, Figure 1-8. Over the years, the software has undergone a series of developments and versions, briefly summarised within Table 1-4. In addition, the software has been validated against numerous model experiments and benchmark tests on various vessel types.

Table 1-4: PROTEUS history of development

Developer	Year	Version
G. Konstantopoulos	1987	PROTEUS
O. Turan	1992	PROTEUS1
L. Letizia	1996	PROTEUS2
A. Jasionowski*	2001	PROTEUS3
A. Jasionowski*	2004	PROTEUS3.1

*Primary Developer

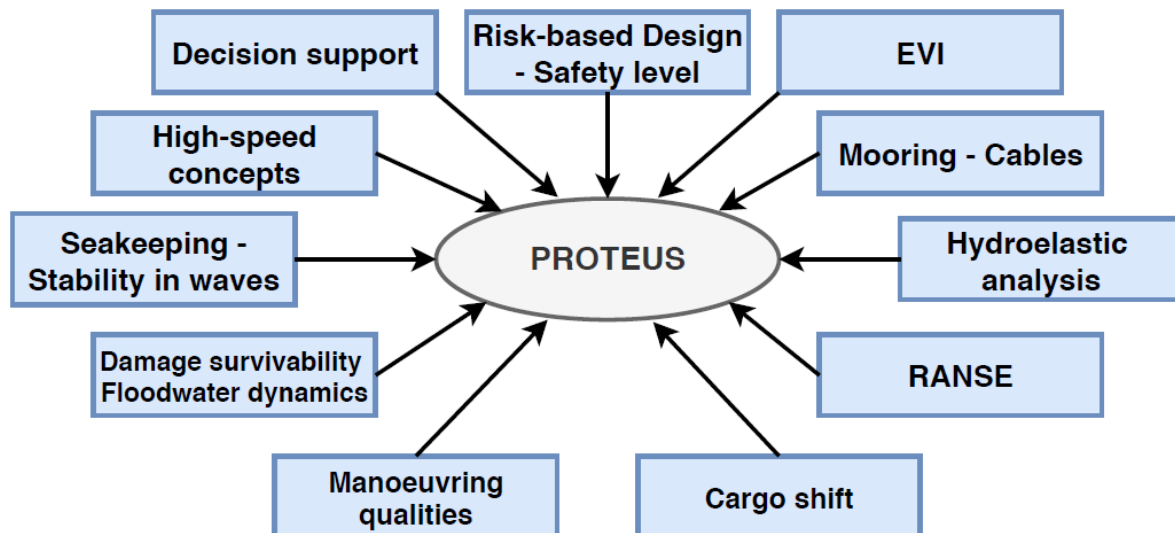


Figure 1-8: PROTEUS Software capabilities

1.3.3.2 Research Contribution to PROTEUS

In the undertaking of this research, the PROTEUS software suite has been used extensively as a means of conducting dynamic assessment of ship damage survivability in a wave environment. The vessels considered have highly complex internal environments, which calls for assessment of the flooding process in forensic detail. The necessity for this comes from the recognition that, while global ship parameters (e.g. beam, freeboard) may act to set the stage for flooding, it is in fact localised details within the vessel internal geometry such as openings and their distribution that hold the greatest impact on the floodwater evolution. It is this latter area where the present research has sought to contribute, by providing a number of techniques by which such features can be analysed and assessed as regards their criticality. The result is a system that allows targeted solutions to be developed in order to affect the flooding outcome by containing and controlling floodwater within the ship environment. This provides the foundation for identifying the location, type and magnitude of re-configuration required within the ship environment for the most cost-effective passive or active damage protection and control. In principle, the level of protection has no limit and thus, theoretically speaking, any ship could be rendered unsinkable. Of course, in reality there will always be economic considerations, which in the case of only marginal safety improvements will always take president.

1.3.4 Loss Modalities of a Damaged Ship

As indicated in the foregoing, in order to contain and control the outcome of a ship hull breach in the event of collision or grounding, it is important to be able to understand whether the ship will survive the damage or not and in the latter case, how long it will take. In any event, it will be

prudent to have all this knowledge a priori (e.g., during the design phase) by exploring all feasible scenarios, identifying loss scenarios and taking measures to either contain and control all such scenarios or allow for safe evacuation of all the people on-board. This, in turn, entails understanding of loss modalities and the nature of floodwater progression at forensic level. The latter will be explained in detail in the thesis, but a brief explanation of the former is warranted here to allow for an educated presentation of the various flooding risk control options being introduced in the next section.

Following hull breach of a ship in a seaway that leads to flooding of internal ship spaces, the ship will first undergo a transient response as a result of the inrush of floodwater, which can lead to capsize without equilibrium being restored (transient asymmetric flooding). Such response normally results with the ship heeling towards the oncoming waves but depending on the latter and the ship response, the vessel may heel towards the leeside. This, in turn, may be beneficial depending on the size of the breach and the internal ship arrangement. As a general conclusion, there are so many parameters in large passenger ships affecting this initial response, the floodwater evolution and the ship behaviour that one cannot address these prescriptively. Here a generalised description is presented in Figure 1-9 to facilitate better understanding of the detail in the thesis.

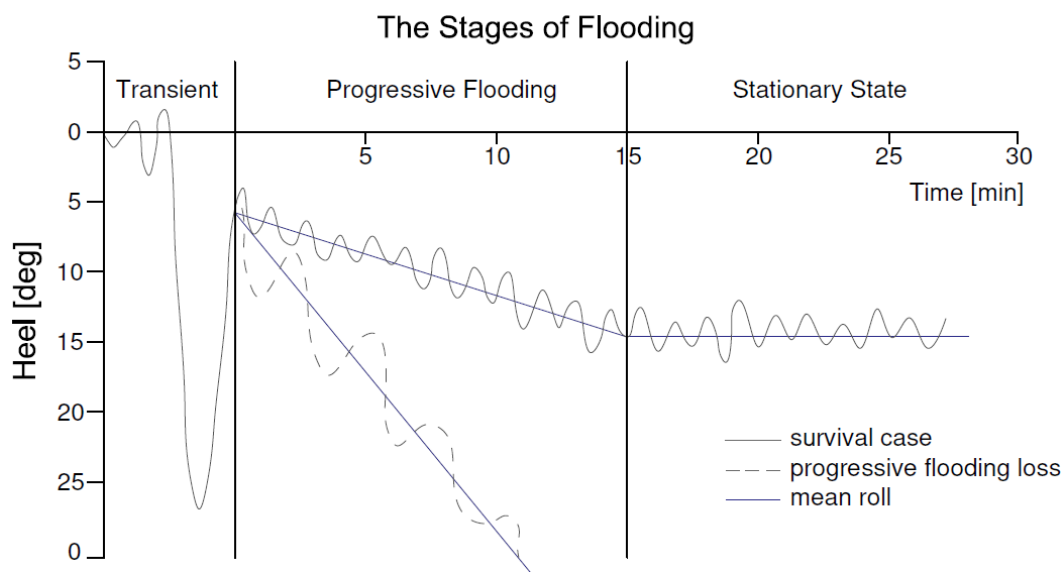


Figure 1-9: Overview of flooding stages – based on diagram shown in (Ruponen P., 2007)

This transient capsizing phenomenon was first noticed and studied in (Spouge J. R., 1986) and (Vassalos, Jasionowski, & Guarin, 2005) for RoPax and Cruise vessels respectively, but the observations and derived results did not make any significant inroads into the regulation-making process. This is rather unfortunate, as time limitations relating to transient flooding capsizing, render this the most dangerous loss modality. Some attempts have been made to consider the

effect of transient flooding on stability by focusing on different stages of this process in a quasi-static manner and, in this respect, an intermediate stage s-factor has been adopted at IMO (SOLAS 2009 Regulations). Figure 1-10, shows the roll response time-history relating to a large-scale model experiment and numerical simulation results of the same (Vassalos, Jasionowski, & Guarin, 2005). Here, a typical large cruise vessel design ($\approx 240\text{m}$) was subjected to a 2-compartment SOLAS damage amidships, demonstrating that transient capsizes could take place for a ship in full compliance with statutory damage stability regulations.

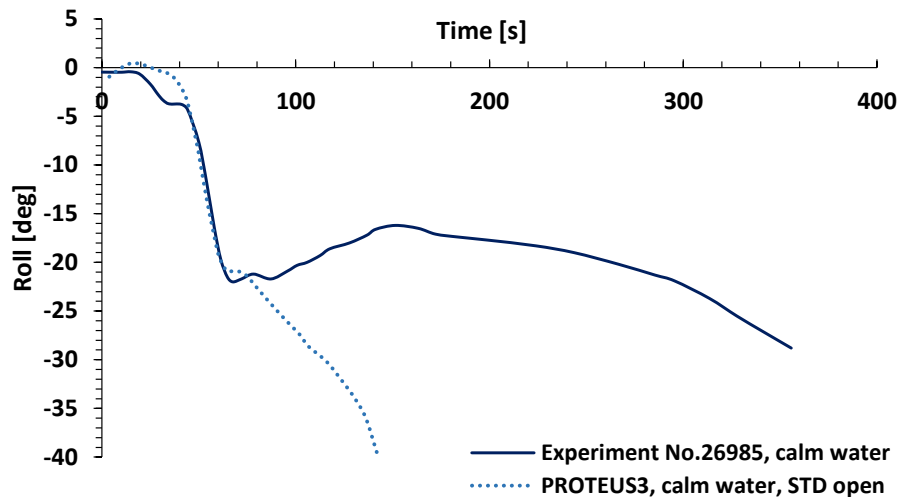


Figure 1-10: Typical transient loss modality distribution for a SOLAS'90 cruise ship, model experiment and numerical simulation results (Vassalos et al., 2005)

Similarly, Figure 1-11, where the PROTEUS time-domain simulation software is used to identify different loss modalities, demonstrates that transient capsizes for 2-compartment damages of a very good SOLAS '90 cruise ship design is quite common.

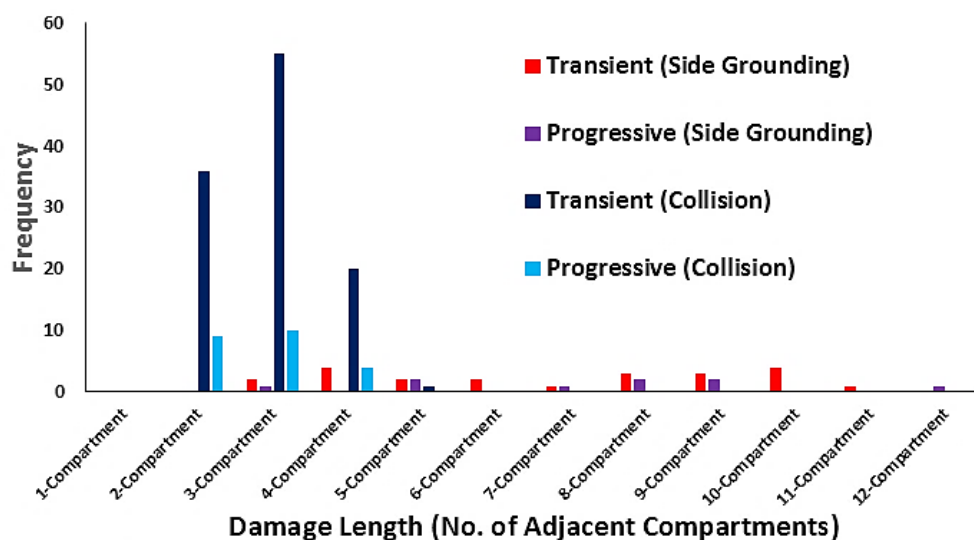


Figure 1-11: Loss modality distribution for a SOLAS '90 cruise vessel

Progressive flooding capsizes have been studied more systematically in the various EC-funded projects, amongst others mentioned in the foregoing, and have formed the basis for the current SOLAS requirements (SOLAS 2009 and SOLAS 2020). However, even in these regulations, this loss modality is considered primarily on the basis of experimental results pertaining to RoPax vessels in waves up to $H_s=4\text{m}$. The effect of the latter has then been considered as an average influence on survivability, captured by correlating GZ-curve properties (GZ_{max} and Range) to H_s . In general, the primary loss modality witnessed was progressive flooding of the vehicle deck as demonstrated in Figure 1-12. This is the mode of capsizing that made the basis for all contemporary developments, particularly pertaining to probabilistic regulations adopted at IMO. The rapidly escalating trace of water on deck in Figure 1-12 designates the time instant, referred to in the literature as the “point of no return”, at which the mass of floodwater on the car deck increases exponentially and the vessel capsizes very rapidly.

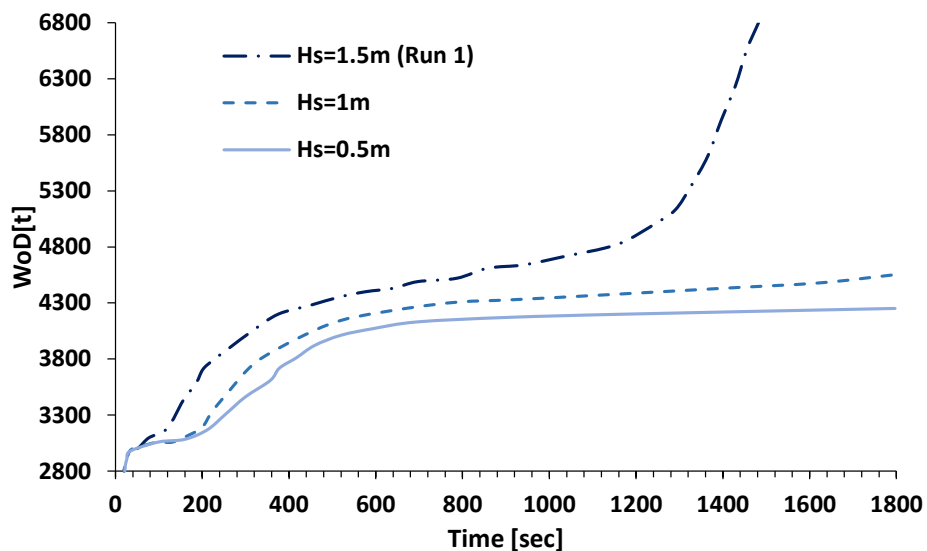


Figure 1-12: Time History of Floodwater Accumulation on Deck

Of course, the presence of superstructure may considerably delay the process, as in the case of the RoPax vessel Estonia where it has taken 50 minutes for the vessel to capsize and eventually sink. Moreover, water accumulation on the car deck is not entirely deterministic as it depends on many stochastic influences. Hence, it is rather difficult to estimate the amount of water on deck leading to vessel capsizing. In cruise ships, a similar mechanism may lead to vessel loss, in this case related to the service corridor on the main deck and other large open spaces, which provide the conduit for water to spread longitudinally in the vessel and up-flooding via the vertical service trunks and stairwells.

1.4 Adaptive Reconfigurable Environment Safety Technology (AREST) Systems

1.4.1 The Concept

As presented within the opening sections, safety is normally a compromise to vessel earning potential and, as public demand for higher safety standards grows, industry is progressively forced to choose between business viability and customer safety. To address this for flooding risk (the kernel of the research presented in this thesis), the “in operation” optimal internal arrangement of the vessel is adapted and reconfigured, using passive (in-built) and active (controlled) containment systems. This is another way of stating that the vessel is rendered more resilient (designing the ship to adapt in the event of failure). Each of these systems, employs the use of high expansion foam to restrict and contain the amount of floodwater entering the ship hull following a flooding incident. The resultant solutions are aimed at being entirely non-intrusive and provide a highly effective means of protection when in crisis from any flooding event. Consequently, with passive/active foam protection in place, flooding risk is all but eradicated. This leads to a transformational reduction in flooding risk in the most cost-effective way available.

1.4.2 AREST Systems

This relates to a University of Strathclyde Patent (Patent No.PCT/ GB2017/050681, jointly owned by the author) pertaining to a series of active and passive systems, comprising the use of high expansion foam to restrict and contain the floodwater entering the hull following a flooding accident. The deployable systems also offer fire protection as per SOLAS II-2. An illustration and brief description for the various systems is provided in the following.

1.4.2.1 AREST P1: Passive Foam Installation – Permanent Void Filling

This is a passive flooding protection system involving the Installation of permanent foam in void spaces to provide additional reserve buoyancy when these spaces are damaged following a flooding incident, thus increasing GM and restoration forces. Such installations act much like buoyancy tanks with the added benefit of being impermeable, thus providing buoyancy within the immediate damaged area. Upon installation, the foam adheres to the vessel steel structure and acts as a protective/anti-corrosive coating, prohibiting build-up of moisture between the foam and ship structure whilst offering effective insulation. The foam is resilient and will last, without degradation, for the vessel life span (>50 years). Figure 1-13, shows a typical application site behind the cabin linings of a cruise vessel.

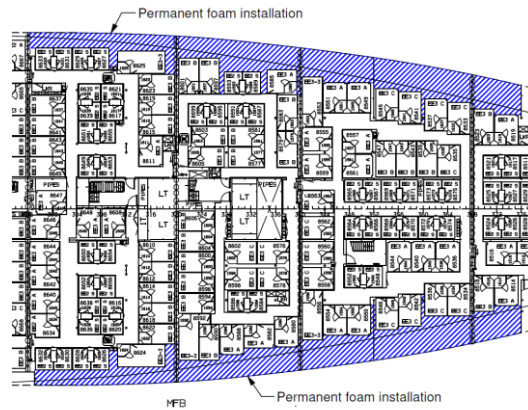


Figure 1-13: Filling void Spaces in the wing spaces of a cruise ship

1.4.2.2 AREST A1: Active Foam Application – Filling Voids in Flooded Compartments

This is an active foam deployment system comprising a modular, standard “kit of parts” in the form of foaming agents stored in bottles or IBC containers, with a dedicated pump or compressed gas system for deployment and a centralised piping network for distribution. The system is located in a non-intrusive location within the vessel and is fully integrated into the ship Safety Management System (SMS) with dedicated Decision Support. Foam is deployed in high-risk ship compartments on top of the floodwater entering the ship to suppress, contain and control its progression and potentially to push floodwater out. The result in a reduction in lost buoyancy, leading to enhanced damage stability and floatability. The foam being used is closed cell with 1-2% permeability, 1:50 expansion ratio, 1 bar expanding pressure and 2 bar compressive strength. Typical examples of such systems are provided within Figure 1-14 below.



Figure 1-14: AREST A1 systems, large-scale system with pumps (right), small-scale system with compressed gas release (left)

intermediate supports and can be deployed within minutes to curtail and control previously identified critical floodwater pathways. In this respect, drawing on the results of time-domain flooding simulations, an effective Damage Control Plan (DCP) could be set up and suitably executed with the aid, for example, of a suitable Decision Support System (DSS) linked to the ship SMS. Through doing so, this process can be guided in the most effective way and the vessel damage response team can be granted the ability to actively suppress floodwater propagation. This is achieved by isolating the damage area following any foreseeable critical flooding event for which progressive flooding is responsible for loss. This offers a distinct advantage over existing Damage Control Plans, which are limited in that they rely entirely on fixed design measures in order to contain the spread of floodwater, or else bulkier more restrictive watertight doors need be used. As such, they have limited flexibility and cannot effectively deal with all probable loss scenarios. In addition, there are a number of areas within any vessel in which watertight integrity must be sacrificed in order to allow for effective operation of the vessel i.e. lift trunks, service corridors and ro-ro decks.

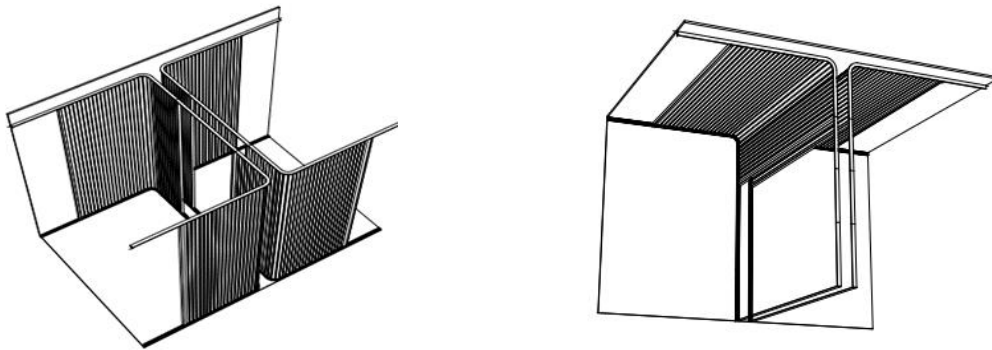


Figure 1-16: Example of shutter closing arrangements

1.5 Structure of Thesis

The thesis is constructed into eleven chapters and five Appendices as outlined within the following:

Chapter 1: Introduction

The introductory chapter begins by outlining the damage stability problem we still face today and moves into the area of innovation being explored within this research and potential impact this could have. Following this, a brief background is provided on the development of damage stability both as a subject and from the regulatory perspective, with due consideration given to the forces and events that have driven these developments. The chapter then moves on to discuss more contemporary developments, citing technological innovation as a key component in our endeavours to further improve ship damage stability performance. In closing, a brief overview is provided of the novel damage stability Risk Control Options that have been developed as part of this research.

Chapter 2: Thesis Aim & Objectives

In this chapter, the primary aim of the thesis is described along with the various objectives that have been set in the hope of achieving this aim.

Chapter 3: Critical Review on Passive & Active Reconfiguration for Damage Stability Protection

Chapter 3 outlines the key findings and observations made, having conducted an extensive critical review on the manner in which vessels have been and are currently reconfigured for damage stability protection. The chapter begins by firstly considering the influence rules and regulations have had on driving and shaping the way we design for damage stability, ranging from the earliest developments to where we currently stand today. The impact of this reconfiguration is then explored with regards to three key stages within the vessel life-cycle, namely design, operation and emergency response. In each instance the effectiveness of current Risk Control Options is explored and competing design objectives are examined, revealing gaps and shortcomings within existing approaches and thus highlighting areas in which improvements can be made.

Chapter 4: Research Methodology Adopted

Chapter 4 serves to provide an overview of the methodology that has been employed in the undertaking of this research. Here, the approach adopted is described in the form of eight distinct stages, each of which is elaborated upon in detail as regards the activities that are conducted and also the value and purpose of each stage within the wider methodology.

Chapter 5: Ship Damage Stability and Survivability Assessment Process

This chapter provides a detailed overview of the ship damage stability and survivability assessment process that has been adopted in the completion of this research. In the opening section, the limitations that exist within the current statutory calculation methodology, namely hydrostatic assessment, are explored along with the value of numerical time-domain simulations as a means of compensating for some of these shortcomings. Following this, an in-depth description of the survivability assessment process is provided ranging from the preparation of the simulation model, definition of input parameters and calculation approaches. The chapter then closes by describing the way simulation results can be used in order to conduct a forensic level examination of the flooding process, determining sources of vulnerability and informing the process of deriving appropriate RCOs.

Chapter 6: Reconfiguring the Ship Environment to Enhance Safety

Chapter 6 serves to outline how the information provided through completing the survivability assessment process outline within Chapter 5 has been used in order to generate a number of novel Risk Control Options. Detailed descriptions of each RCO and their function are then provided. Finally, the chapter closes by touching upon the Class and Administration approval process for such RCOs, providing some examples of the steps that must be taken in this direction.

Chapter 7: Passive & Active Flooding Control Example - Permeant Foam Application & Progressive Flooding Suppression

Within this chapter the first application example is described in relation to a medium-sized RoPax vessel, currently operating today. In line with the thesis methodology, both static and dynamic damage stability assessments are conducted. The results of these assessments are used to inform the implementation of two of the RCOs developed as part of this research. Both assessments are then reevaluated in order to determine the impact of the RCOs on vessel survivability.

Chapter 8: Passive Flooding Control Application Example - (AREST P1 System)

Chapter 8 outlines a further application example, this time in relation to a large cruise vessel, thus providing a different perspective from the initial RoPax application example. Again, in this example the vessel is assessed according to the methodology developed within this research in order to identify areas of vulnerability within the vessel design. RCOs are then implemented and their impact on ship survivability is measured.

Chapter 9: Active Flooding Control Application Example – Controlling Progressive Flooding (AREST A2)

Within this chapter a third and final application example is described, in this instance relating to a new build cruise vessel design of unprecedented size. This provides an interesting example as this particular vessel design represents upper limits of modern passenger vessel design. Here, as in the other examples, the vessel is subjected to damage stability assessment in line with the thesis methodology, following which a number of RCOs are employed in order to reduce flooding risk.

Chapter 10: Discussion & Recommendations

Chapter 10 reflects on the work presented within the thesis, starting firstly by focusing on the level of innovation offered and the potential impact of the work conducted. Discussion then continues in relation to the nature of the maritime industry, its history and peculiarities, which are expanded upon in the light of this research. Finally, the chapter closes by making a number of recommendations on the way forward with a view to consolidating the research findings.

Chapter 11: Conclusions

In this final chapter, the overarching conclusions that may be drawn from the work presented within this thesis are described in addition to contributions that have been made.

Chapter 2: Thesis Aim & Objectives

The primary aim in the undertaking of this research has been to develop and present a methodological process by which ships may be reconfigured in order to provide a level of damage stability resilience, for which it would not be hyperbolic to state, approaches unsinkable. Furthermore, it is aimed to provide such resilience in a cost-effective, practical and feasible manner. Of course, it is well understood that such a goal may appear, on the surface at least, overly ambitious, perhaps even naïve or worse still a demonstration of hubris. As such, the following objectives have been set forth in the qualification of this notion in the hope that this research, at the very least, may bring us a step closer to this aim.

Objectives:

- To critically review the subject of damage stability and survivability with particular focus placed upon the historical development of Risk Control Options (RCOs) aimed to mitigate, contain and control flooding risk by reconfiguring the internal ship architecture. Through doing so it is hoped to identifying gaps, pitfalls and opportunities to improve upon.
- To present a methodological treatment of damage stability and survivability where, by using state of the art tools and knowledge, the design and implementation of RCOs can be done in the most effective manner. It is hoped to achieve this by exhaustively and systematically exploring all design vulnerabilities in the event of flooding, thus allowing for targeted solutions during design in addition to operation with focus on emergencies.
- Set upon the foundation of sound and extensive analysis, it is then intended to seek out new and innovative Risk Control Options for damage stability enhancement, taking a step away from conventional norms in order to broaden the design space and provide solutions of greater utility than those currently established.
- To devise and present any such solutions to high TRL, thus enabling feasible applications to targeted safety-critical ship types and enumeration of the ensuing results.
- On the basis of the results achieved and any identified gaps, draw conclusions to guide future developments and applications, offering recommendations on the way forward.

Chapter 3: Critical Review on Passive & Active Reconfiguration for Damage Stability Protection

3.1 Opening Remarks

The idea of subdividing the internal volume of a ship into compartments in order to mitigate the effects of hull breach and flooding is by no means a recent one. In fact, the importance of doing so, intuitive as it is, was established some 38 centuries ago by the Babylonians and sanctioned within the Code of Hammurbi (Francescutto & Papanikolaou, 2010). However, despite this early development, the question of flooding protection slept for many years until awoken once again in the 19th century, during which vessel designs were undergoing transformative changes. Firstly, moving from wood to iron construction and secondly, growing much larger in size and capacity. Concerning the latter, more people were now at risk than ever before and unfortunately the development of flooding protection did not come fast enough. Instead, a number of major accidents and great loss of life drove development, as was discussed within the introduction.

Having said this, there have always been people of practice with great vision and intuition, who have paved the way to reconfiguring the ship internal space for safety in ways that we still struggle to master today. The design of the 'Great Eastern' is one such example of this and was a vessel that stretched the limits of Victorian technology. She was built at an unprecedented scale for her time, with a length of 207m, displacement of 22,000 tons and a speed of 14 knots. During regular service, the vessel could accommodate 4,000 passengers, which could be further increased to 10,000 soldiers when acting as a troop ship. Incorporated into the design were the very latest technological achievements in Naval Architecture and Marine Engineering including riveted iron construction, steam power, and propulsion in the form of paddle wheels and a stern screw propeller. Perhaps most remarkably, the Great Eastern had not only watertight subdivision but also a 'double hull', which acted to improve crashworthiness and prevent minor damage penetrations leading to large scale flooding. These are concepts only recently being adopted in modern passenger vessel design under the provisions of Safe Return to Port.

However, what may appear obvious or ingenious, needs to be contrasted against other design requirements pertaining to performance, functionality and cost. In fact, despite the many great advances described, the Great Eastern was never a commercial success and there is a lesson in

that. Internal reconfiguration impedes functionality (reduces ergonomics and space), performance (flow of people and goods) and comes at a cost (construction and maintenance). Further still, structural strength and reliability as well as the basic need for structures to be crashworthy, add more constraints on top of those pertaining purely to safety, leading to a complex design optimisation problem. Vectorisation (turning constraints into objectives – Design for X) has been a vehicle to facilitate design optimisation and, as such, design for safety and risk-based design. This, in turn, has facilitated rational decision-making in the design process, particularly concerning reconfiguration of the internal ship space.

In this respect, this chapter will address the various requisite ingredients leading to cost-effective reconfiguration of the ship internal environment for damage stability protection/enhancement. This is achieved by considering ship design and operation (including emergencies) as well as pertinent design constraints/objectives in the form of rules, regulations, performance, functionality and cost. Too often, safety-minded practitioners in the maritime industry feel that compliance and evasion cover the whole safety spectrum. However, this critical review will demonstrate that safety has been the largest single factor affecting the evolution of ship design and operation, with reconfiguration of the internal ship environment representing the most treaded avenue to enhancing maritime safety with respect to damage stability.

3.2 Rules & Regulations as the Prime Mover

3.2.1 General Concept of Stability Measurement & Subdivision

This section discusses how rules and regulations for damage stability protection (as Risk Control Options) have been developed and how these rules, as key determining factors, have influenced ship internal configuration, namely subdivision at the design stage. It should be noted, the term reconfiguration is meant to imply the evolutionary process involved as well as the concept of active intervention in reconfiguring the internal space of a ship. This, in turn, is linked inextricably with ship stability quantification and provision, particularly when the ship hull is damaged as a result of collision or grounding.

The question as how to quantify ship stability is a long-standing one and was first addressed in the period around 250 B.C. by Archimedes, (Heath, 2002) and (Horst, 2007). However, it was not until the 17th/18th century before the first attempts to crystallise these principles were made. Notably, in 1698, Paul Hoste introduced the concept of metacentric height as a measure of ship stability, or GM as it is commonly known today (Hoste, 1697), (Vassalos, 1999) , (King, 1998). Pierre Bouguer, who introduced in 1746 the actual term “metacentre”, later elaborated this

concept further in a more widely acknowledged exposition (Bouger, 1746). In 1749, Leonhard Euler focused on the righting moment at a particular angle of heel as a better measure of stability (Euler, 1749). However, it was George Atwood who eventually demonstrated in 1798 that such measure can be derived for any angle, inventing thereby the GZ curve (G. Atwood, 1798). Other milestones on stability quantification, achieved thereafter, include Canon Moseley's concept of using the area under the GZ curve as a better measure of ship stability in 1850, (Vassalos, 1999). Further still, in 1939, Jaakko Rahola made propositions to use a function of GZ curve to express the ability of a ship to stay in functional equilibrium after flooding (Rahola, 1939). This is a development of particular significance to this research as it is one of the earliest examples of informed reconfiguration of the ship environment for flooding protection. The emphasis, however, was on global ship parameters rather than the details of the internal ship environment, which is highly influential in the case of large passenger ships. Regardless, his approach influenced subsequent regulatory developments for all ship types, an issue, which Rahola could not possibly have conceived of at the time.

As advances in identifying "stability" parameters progressed, the legislation process for implementation of any such "technicalities" has surprisingly been slow, even though the need for some "legal" safety instrument was realised for many centuries. First attempts to introduce governmental intervention have been in place since ancient times, such as a ban on sailing in winter (15th September to 26th May) in Rome during the Roman Empire (27 BC – AD 476 / 1453), which remained in force in some places until as late as the 18th century. Other examples include the first recorded regulations on load line during middle ages in Venice in 1255 (cross marked on each ship), or the first system of survey inspections imposed by The Recesses of the Diet of the Hanseatic League of 1412.

However, it was not until the Industrial Revolution of the 19th century that the true face of risk encountered by shipping started to show, with the introduction of steam-powered engines, steel hulls and the rapid escalation of sea trade to the dimensions of an "industry". During the winter of 1820 alone, more than two thousand ships were wrecked in the North Sea, causing the death of twenty thousand people in just a single year, with some 700-800 ships being lost annually in the UK on average. Such loss toll has prompted the main maritime nations of the time, France and UK, to exercise their policy-making powers to introduce accident-preventive regulations, to great opposition from the industry. Of note are Colbert's Naval Ordinance, instituted by a Royal Declaration of 17th August 1779 in France, which introduced again the office of huissier-visiteur, a surveyor. In addition, the Merchant Shipping Act of 1850 (reinforced by the Government in 1854 and amended by the Act of 21 December 1906) in the United Kingdom, obliged the Board of Trade to monitor, regulate and control all aspects of safety and working conditions of seamen. The latter

also saw the implementation of load line requirements, which were applied to all vessels, including foreign ships visiting UK ports.

However, the catalyst for significant change did not come until the sinking of the Titanic in 1912, after having struck an iceberg on her maiden transatlantic voyage to New York. In this single incident 1,500 people lost their lives, leading to the adoption of the first International Convention for the Safety of Life at Sea (SOLAS) on January 21st, 1914, gaining international recognition. The SOLAS Convention has been subsequently revised and adopted four times since then, specifically in 1929, 1948, 1960 and 1974, with the latter still in force today. This is supported by the provision of a flexible process of revisions through amendment procedures included in Article VIII. It is worth noting that, although the provisions of SOLAS 1914 prescribed requirements on margin line and the factor of subdivision in addressing the state of a damaged ship, the Convention did not even mention the concept of stability at all. Instead, all focus was on intuitive/empirical internal volume reconfiguration (i.e. subdivision) as opposed to informed reconfiguration by stability calculations. It was the third Convention of 1948, which finally referred to stability explicitly in Chapter II-B, Regulation 7, and subsequently SOLAS 1960, which actually prescribed specific stability requirements. Unfortunately, only one parameter of stability after flooding was considered, with the regulations calling for a residual GM of 1 cm. Finally, SOLAS 1974, adopted Rahola's proposals of using properties of the GZ curve as a measure of stability. In principle, Rahola's approach has formed the basis for amendments of technical requirements on stability ever since (Womack, 2002), applied in various frameworks for adherence to the SOLAS '74 goal "The subdivision of passenger ships into watertight compartments must be such that after an assumed damage to the ship's hull, the vessel will remain afloat and stable". Further still, Rahola's use of GZ curve properties to guide subdivision and to quantify stability are at the core of even the most modern amendments to SOLAS 1974 criteria of ship stability in the damaged condition, (IMO, 2006), (Tuzcu C. , 2003). This can easily escape attention, since the overall damage stability assessment framework, based on Kurt Wendel's concepts of the probabilistic index of subdivision A, (Wendel, 1960), (Wendel, 1968), is rather a complex mathematical construct, with the basic details not easily discernible. The framework is also a major step-change in the philosophy of stability standardisation or indeed internal ship space configuration.

As indicated above, it seems that such implicit reliance on Rahola's measures is a major obstacle for practical disclosure of the meaning of stability standards, as no common-sense interpretations are possible, regardless of the acclaimed rationality of the overall framework. Rahola himself has stressed: "When beginning to study the stability arm curve material ... in detail, one immediately observes that the quality of the curves varies very much. One can, therefore, not apply any

systematic method of comparison but must be content with the endeavour to determine for certain stability factors such values as have been judged to be sufficient or not in investigations of accidents that have occurred". This then leads one to ask, "what is sufficient?" and unfortunately today's standards do not offer an explicit answer. The profession seems to be content with an implicit comparative criterion, whereby a Required Index R is put forward as an acceptance instrument (ultimately as "a" stability measure). However, this is offered without clear explanation as to what is implied if the criterion is met or in what sense the goal of keeping the vessel upright and afloat is catered for. In essence, the question "what does $A=R$ mean?", had not been explicitly disclosed until the early 2000s. Here, the adoption of Design for Safety and the ensuing design methodology "Risk-Based Design" provided the means to design ships with a known safety level and, in the case of damage stability, known flooding risk, (Vassalos, 2008), (Vassalos, 2012).

3.2.2 General Outlook on Damage Stability Evolution

Against the background of a system where everything is principally empirical and statistical, it was widely believed that the prevailing situation could be drastically improved through better understanding of the underlying mechanisms leading to vessel loss. This, in turn, could enable the identification of governing design and operational parameters to target risk reduction in the most cost-effective manner, whilst also reducing uncertainty. Such aims necessitated the development of appropriate methods, tools and techniques capable of meaningfully addressing the physical phenomena involved. Having said this, it was not until the 1990s when simplified, yet highly innovative, numerical models addressing damage survivability were proposed, pertaining to damaged ship dynamics in a seaway (Vassalos & Turan, 1992) (Zaraphonitis, Papanikolaou, & Spanos, 1997).

The subject of damage survivability in waves (with the ship hull breached), received particular attention following the tragic accident of Estonia, to the extent that this led to a step change in the way damage stability and survivability are being addressed. Specifically, conventional hydrostatic calculation techniques were supplemented by assessment methods based on first principles, allowing vessel performance to be measured in a given environment and loading condition. In parallel, other major developments were brewing and an in-depth evaluation and re-engineering of the entire probabilistic framework was launched through the EC-funded project HARDER (HARDER, 1999-2003). The motivations behind this derived from the compelling need to understand the impact of the then imminent introduction of probabilistic damage stability regulations for cargo and passenger ships. At the same time, there was a growing appreciation of the deeply embedded problems in both the rules and the harmonisation process itself. Consequently, the HARDER project became an IMO vehicle carrying the major load of the

regulatory development process, fostering international collaboration at its best. This was a key factor, contributing to the eventual success in achieving harmonisation and in proposing a workable framework for damage stability calculations in IMO SLF 47. Deriving from developments at fundamental and applied levels in this project as well as other EC-funded projects, including (NEREUS, 1999-2002), (ROROPROB, 1999-2002), (Jasionowski A., 2005). This was further supported by other international collaborative efforts such as the work by the Stability in Waves Committee at the International Towing Tank Conference from 1996 onwards, e.g. (Jasionowski & Vassalos, 2001), following which a clearer understanding of damage stability and survivability started to emerge. Application and verification of the developing numerical tools helped raise confidence in the available knowledge to address the subject matter effectively and with sufficient engineering accuracy. All this effort provided the inspiration and the foundation for the EC-funded large-scale Integrated Project (SAFEDOR, 2005-2009). This offered the opportunity to consolidate contemporary developments on damage stability and survivability, thus rendering implementation possible even with severe time limitations. The knowledge gained has been used to critically address contemporary regulatory instruments and to foster new and better methodologies, primarily to safeguard against known design deficiencies in respect to passive damage protection. This facilitated the evolution of safer designs, reflecting this knowledge, (Vassalos, York, Jasionowski, Kanerva, & Scott, 2006). However, the cultural “shock” of adopting probabilistic rules in the maritime industry has had a more profound effect. Surprisingly, the biggest influence has been seen at the birthplace of prescription, namely IMO as indicated earlier, with goal-setting performance-based approaches becoming the new face of safety. What is known as Safe Return to Port (SRtP) within SOLAS 2009, enforceable on every newbuild passenger vessel and on special purpose ships over 120m in length, has paved the way for holistic approaches to risk, specifically concerning fire and flooding. Both developments, represent a step change from the deterministic methods of assessing subdivision and damage stability. The old concepts of floodable length, criterion numeral, margin line, 1 and 2 compartment standards and the B/5 line have disappeared from newbuilding projects, which now adopt a more holistic approach to addressing damage stability and survivability. This has led to safer and more ergonomic designs (for the first time in the history of hull configuration for fire protection). With some safety-minded ship owners the possibility now exists, and is being exploited, to address and undertake design and operational measures to managing flooding risk in all conceivable events (statistical, experiential, judgemental). This involves consideration of all pertinent damage scenarios, loading conditions and environments to deal with subdivision, damage survivability in waves and residual functionality of essential systems post-damage. Furthermore, evacuation and rescue along with decision support systems onboard are also being addressed, targeting cost-effective safety as a key design objective, alongside other conventional

design objectives, (Vassalos, 2012). Furthermore, the use of numerical time-domain simulation tools for survivability estimation in passenger vessel newbuilding projects, particularly cruise vessels, has indicated considerable (positive) differences in comparison with SOLAS II-1, based on static assessment (Atzampos, 2019). The reason for this comes from the fact that the Direct Method (use of time-domain numerical simulations of damage survivability in waves) removes the need for conservative assumptions and irrational generalisations being made in the assessment process. Furthermore, this provides a large amount of additional and highly useful information that can be used in order to inform ship design and operation for damage protection (especially in extreme cases - emergencies).

Notwithstanding the above, with probabilistic damage stability rules having originally been developed on the basis of cargo ship damage statistics, serious concerns have been raised. Specifically, the adopted formulation for the calculation of the survival probability of passenger ships and the associated required subdivision indices have fallen into question, particularly for RoPax and large cruise ships, (Vassalos, Jasionowski, York, & Tsakslakis, 2008). Disquiet in industry and academia, along with concern deriving from the escalation of passenger ships to megaships, has seen research focus on damage stability shift towards large passenger ships, (Vassalos & Jasionowski, 2011) and (Vassalos, 2016). Resultantly, a series of projects investigated this problem and laid down the foundation for a passenger ship-specific damage stability framework, process and criteria, (Papanikolaou, et al., 2013), (EMSA III, 2013-2015). Becoming more actively involved with passenger ships has also brought to light another important and material problem. Namely, in the quest for damage stability improvement, design (passive protection, i.e., internal volume configuration) measures have traditionally been the only means to achieve this in a measurable/auditable way (SOLAS 2009, Ch. II-1). However, in principle, the consequences from inadequate damage stability can also be reduced by operational measures (active protection), which may be highly effective in reducing loss of life (the residual risk). There are two reasons for this. The first relates to the traditional understanding that operational measures safeguard against erosion of the design safety envelop (increase of residual risk over time). The second derives from lack of measurement and verification of the risk reduction potential of any active measures. This includes things we know to have an impact on safety such as crew training, navigation systems, frequency of drills etc., but have not yet found a way to quantify that impact. In simple terms, what is required, is the ability to account for risk reduction by any means and this includes operational (active protection) measures as well as any steps that may be taken during emergencies (again active protection). Such risk reduction may then be considered alongside that deriving from design measures. Therefore, new approaches for risk reduction (operational and in emergencies) should be considered in addition to design measures.

What then needs to be demonstrated and justified is the level of risk reduction and a way to account for it, the latter by adopting a formal process and taking requisite steps to institutionalise it. Efforts in this direction has led to setting up the large-scale EC-funded research project, FLARE, (FLARE, 2019-2022).

3.2.3 Rules and Regulations as RCOs for Damage Protection

Before reviewing the design impact of reconfiguration of the internal ship space, it will be of interest to consider the regulations influencing and driving this process. Here, an indication is provided, based on the research outline in the foregoing, as to how relevant or effective available regulatory instruments are in being able to prevent or mitigate disasters:

- SOLAS '74: 1-compartment standard (prevents ship from sinking / capsizing if one compartment is breached; resistance to capsize in waves unknown).
- SOLAS '90: 2-compartment standard (prevents ship from sinking / capsizing if any two compartments are breached; resist capsize of 2-compartment worst damage in sea states with Hs approximately 2.5m – Ro-Ro vessels).
- Stockholm Agreement (Ro-Ro Passenger ships): as in SOLAS '90 but with a pre-defined level of water on deck varying on the basis of freeboard and in operational sea states of up to 4m Hs.
- Harmonised SOLAS Chapter II-1: SOLAS 2009 – intended as an equivalent to SOLAS '90; though such equivalence has not yet been fully established.
- SOLAS2020: This is the new SOLAS regulation with provisions catering specifically for ships with ro-ro spaces, along with generally enhanced safety requirements. Regarding the former, this has been addressed in a recent EC research project titled “Assessment of specific EU stability requirements for ro-ro passenger ships” (EU-DGMOVE, 2019) where it was concluded that the requirements of the directive 2009/45/EC and 2003/25/EC (Stockholm Agreement) could be replaced by the damage stability framework as per SOLAS 2020. However, the Required Index level should be set as per SDC3 proposal (equivalent to SOLAS2020 R for ships of capacity exceeding 1,350).

Concerning the latter two, a major revision to the subdivision and damage stability sections of SOLAS Chapter II-1, based on a probabilistic approach, entered into force for new vessels with keels laid on or after 1st January 2009 and 1st January 2020, respectively. However, whilst development of the probabilistic regulations included extensive calculations on existing ships, which had been designed to meet deterministic SOLAS regulations, little or no effort has been expended into implementing these regulations to such ships (Grandfather Clause).

3.3 Ship Design Impact on Reconfiguration of the Internal Ship Space

In his keynote speech in the 2012 IDDC Conference being held in Glasgow, Professor Vassalos gave the following definition of design: "I see design both as the conduit and the water, the art and the science, the analysis and the synthesis, the means and the end, the God and the mountain". In simpler terms, damage protection for the whole life-cycle of the vessels is a design concern. With this in mind, this section will start by defining design vulnerabilities for damage stability and how this has evolved in different ship types. The section then proceeds to focus on the design phase of the life cycle, before embarking on contrasting configuration against other design objectives, including structural strength. Particular attention with the latter will be paid on crashworthiness and the impact and potential that this might have on passive damage stability protection.

3.3.1 Design Vulnerability

"Vulnerability" is a word that is extensively used within the naval sector (R. Ball, 1994) but not as frequently within merchant shipping in so far as damage stability is concerned. Vulnerability is also used in the second generation intact stability criteria with specific definition provided in SDC 5, par. 1.2, (IMO, 2006). However, the way in which this term has been used by the University of Strathclyde relates to "the probability that a ship may capsize or sink within a certain time when subjected to any feasible flooding scenario". As such, vulnerability contains (and provides) information on every parameter that affects ship damage stability, (D. Vassalos, 2012). The vulnerability to flooding of passenger ships is well documented through a number of accidents claiming many lives (e.g. MS Estonia). Such vulnerability relates in many cases to Water on Deck (WoD), involving flooding into large undivided cargo spaces, often leading to rapid capsize of the ship. However whilst for RoPax vessels this design vulnerability is well understood, cruise ships also suffer from a similar loss modality which has been brought to light as recently as the early 2000s, (Vassalos, Ikeda, Jasionowski, & Kuroda, 2004). The latter case relates to flooding of the service corridor on the subdivision deck, along with larger dining and entertainment spaces, all of which act as conduit for floodwater to spread along the ship, giving rise to large free surfaces and propagating through stairwells and lift trunks. Figure 3-1 provides typical results demonstrating such vulnerability in the design of RoPax and Cruise vessels, respectively.

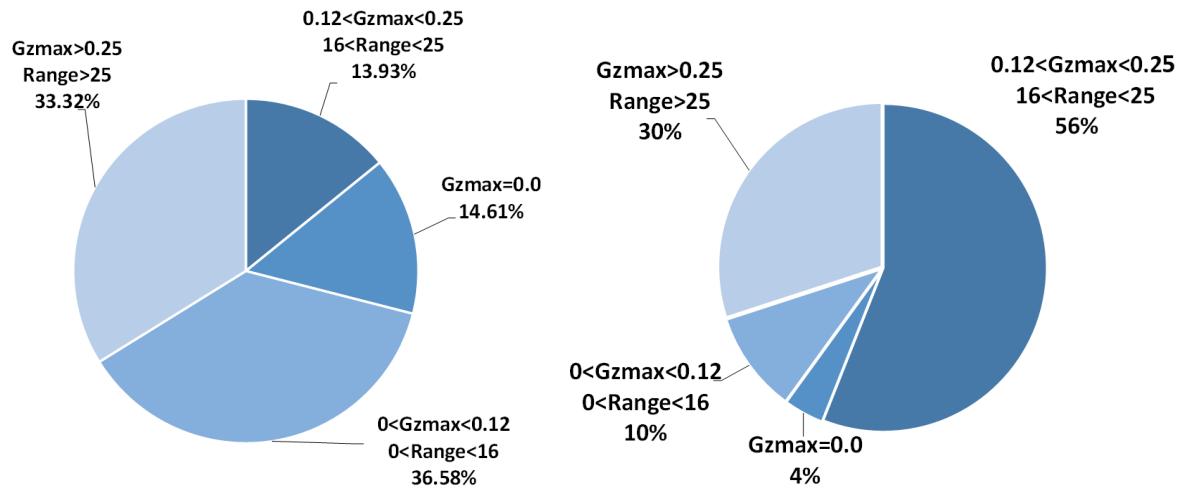


Figure 3-1: Design Vulnerability Distribution for a RoPax (left) and Cruise vessel (right)

3.3.2 Design Vulnerability by Ship Type

In the Introduction chapter, a description of loss modalities is presented pertaining to the dynamic behaviour of the ship and its interaction with the sea and the floodwater, which are general modes of loss common to most ship types. There are, however, certain ship types with greater propensity to experience certain loss modalities and these can occur in different manners depending on the vessel design. In particular, this relates to open spaces on the main and upper decks, leading to design vulnerabilities that require particular attention to the configuration of the internal ship space, (Vassalos & Guarin, 2009), as briefly described within the following.

High Freeboard Ships:

For ships with high freeboard, typically only vessels with a limited positive righting lever will capsize within a moderate sea state. The oncoming wave train will induce significant rolling only in marginally stable cases, which could lead to eventual capsizing in larger sea states. It is often the case that such vessels are more vulnerable in case of damage to the leeward side, since restoration levers are generally lower towards the damaged side, thus inducing larger dynamic roll. Furthermore, the vessel will often heel towards the side of damage and therefore, wind effects will work to overturn the vessel in case of damage to the leeward side.

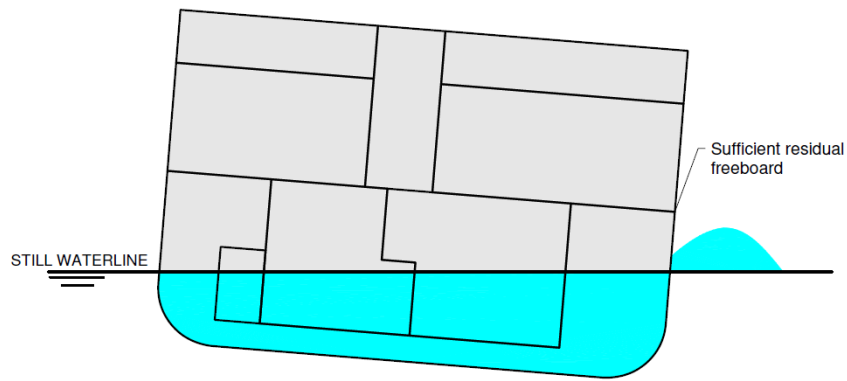


Figure 3-2: High freeboard ship

Low Freeboard RoPax Ships:

This is the classification of ships that were predominantly tested in model basins in Project HARDER (HARDER, 2003). The results from these tests were then used in order to inform the derivation of the SOLAS 2009 s-factor formulation. The mode of loss in such cases stems from steep waves boarding the deck, leading to rapid water accumulation until the vessel reaches a stage, named in literature as the “point of no return”, at which the vessel capsizes very rapidly.

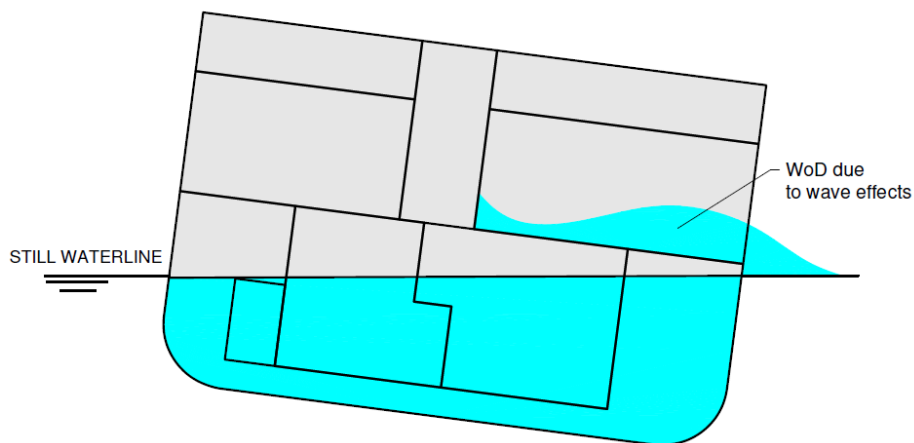


Figure 3-3: Low-freeboard ship

Multi-Free-Surface Effect:

This mechanism of capsize is relevant to ships with complex watertight subdivision such as cruise ships. As the hull is breached, water rushes through various compartments at different levels, substantially reducing stability even when the floodwater amount is relatively small. As a result the ship can heel to large angles, even for small damage openings, letting water into the upper decks that spreads swiftly through these spaces and may lead to rapid capsize at any stage of the flooding, (Vassalos, Jasionowski, & Guarin, 2005).

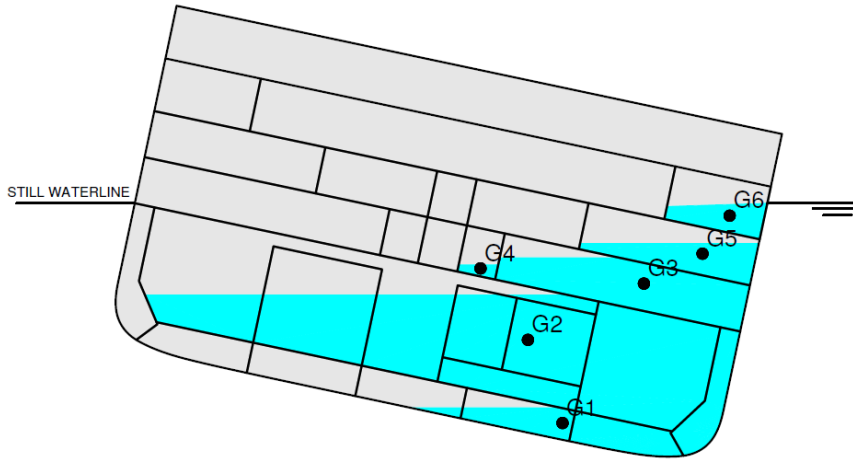


Figure 3-4: Multi-free-surface effect

3.3.3 Life-Cycle Considerations - Design Phase¹

Traditionally, regulations focus on built-in solutions, identified normally during the design phase. Whereas, active/interventional measures considered during operation or emergency response phases, whilst fuelling debates on their risk reduction potential, have never actually been measured or verified, as explained in the foregoing. In this respect, a framework that facilitates assignment of risk merit to every risk control measure is key to life-cycle risk management. A life-cycle perspective facilitates a holistic approach to damage stability, encompassing risk control options for all three phases and accounting for each by using, for example, IMO cost-effectiveness criteria. This, however, assumes that the risk reduction potential of all such measures is known and, as explained earlier, this is where there is a big gap in this approach that needs to be overcome before such a process can be formalised and adopted. This constitutes the kernel of the work yet to be undertaken. With this perspective in mind, Figure 3-5 presents, in a form of flowchart, a “pipeline” comprising different phases and levels of a life-cycle vulnerability assessment approach. The levels referred to in this figure relate to the fidelity of the tools being used to address specific requirements during the life-cycle, namely static or quasi-static, time-domain numerical simulation tools and high-fidelity tools such as Computational or Experimental Fluid Dynamics. Such approach is justified as different design stages (concept, preliminary, detail), require different tools that best satisfy the constraints and objectives in the design process. For example, watertight subdivision, general dimensioning of internal arrangements, initial positioning of ship systems, evacuation routes and arrangements would require low-fidelity, fast and accurate tools.

¹ This section is based primarily on the work outlined within the paper “Life-Cycle Flooding Risk Management of Passenger Ships” of which the author was a co-author

On the other hand, modelling transient, progressive and cross- flooding processes in extreme sea states with the view to identify loss-scenarios post-casualty, demands robust and versatile tools (e.g., time-domain simulation tools). At the extreme, in cases where the detail offered by the most advanced Computational Fluid Dynamic and Experimental Fluid Dynamic tools will make a difference, use of these (Level 3 tools) is justified. In fact, use of Level 2 and 3 tools will also be required for verification purposes (for example approval of Alternative Design and Arrangements); this would apply to all three life-cycle phases.



Figure 3-5: Three vessel life-cycle design phases (Vassalos, Atzampos, Cichowicz, & Paterson, 2018)

Decisions made during the design phase, shape safety over the whole life cycle and very much set the stage in this manner. In this respect, use of advanced tools and exploiting knowledge in all forms at the design stage is most effective and, hence, highly desirable. Particularly as it is often extremely hard to undo or reverse any of the decisions that are made during this stage. The derived knowledge could be used in further design iterations or indeed stored in a knowledge base for use over the life cycle of the vessel, including emergencies. Key to life cycle risk management is the understanding that both the operational phase (monitoring and management of residual risk) as well as emergencies (emergency response) depend crucially on information gained during the design phase. Specifically, this would include the identification of pertinent design vulnerabilities that lead to critical accident scenarios in pre-specified loading and environmental conditions. Then, on the basis of this, it is prudent that appropriate measures have been taken during the design stage to ensure:

- a) Design vulnerabilities have been identified and design measures taken to reduce these
- b) Evaluation of residual risk, including KPIs for monitoring purposes during the operational phase
- c) Preparedness in addressing all identified critical scenarios in case of an emergency (emergency response), (Vassalos & Paterson, 2020).

3.3.4 The Design Optimisation Problem (Subdivision) – Multi-Objective Optimisation

Ship design is inherently multi-disciplinary, and consequently any design modification is accepted or rejected on the basis of its impact across a wide array of performance criteria, rather than dealing with any single performance quality in isolation, i.e. life-cycle cost. The debate over sequential or parallel processes and design vectorisation no longer resides solely in the academic sphere and is instead very much a problem being faced and addressed by the industry. The SOLAS '90 approach for bulkhead spacing imposed limitations on the basis of ship floodable length criteria under Regulation 6, which restricted the degree of flexibility afforded to the designer in optimising the vessel subdivision arrangement. Even after the adoption of probabilistic rules in which the decision on the number of bulkheads is part of the overall goal-based approach, the internal architecture still has the tendency to become overly cluttered and expensive, with diminishing returns being realised as the number of bulkheads increases. The EU-funded project (ROROPROB, 1999-2002) focussed exactly on this problem and provided valuable input to the industry in this respect. Typically, one of the cruise ships being assessed in this research (C1), was initially designed with 25 bulkheads, which following optimisation of the subdivision arrangement was subsequently reduced to 16. This resulted from the fact that it was demonstrated to the yard that the difference in the A-Index was negligible, whilst the cost of adding additional bulkheads and the subsequent requirement for additional systems (heeling tanks, pumps, etc.), was completely unjustified. However, the push for continuously increasing standards for new buildings, and with attention spreading above the bulkhead deck (two additional decks), brought the need for additional subdivision above the bulkhead deck, this time with A60 bulkheads. More importantly, however, it brought competition through interference with ship functionality (for example with evacuation routes), so the problem became not only multi-disciplinary optimisation, but also multi-objective (Vassalos & Papanikolaou, 2018) (R. Pusia, 2012).

In (Vassalos & Papanikolaou, 2018), the suggestion was made that such a problem is covered by a Risk-Based Ship Design framework, where optimisation is inherent to the concept and safety is one of the quantifiable objectives. In this respect, life-cycle Assessment of ship safety,

performance and return on investment are inherently integrated. In (R. Pusia, 2012), this approach, as a design and decision support tool, is proposed to be used in the conceptual design stage to quickly arrive at design alternatives that both satisfy requirements (owner and regulatory) and have maximised commercial performance. As ship design is inherently multi-disciplinary, a proposed design modification is accepted or rejected based on its multi-disciplinary performance rather than on a single performance metric such as life-cycle cost. To assess the performance of each such function (discipline) and thus the feasibility of the entire design, dedicated instruments and measures must be applied. Conventionally, these have been applied sequentially (Gale, 2013), as during the past neither computers nor software tools were powerful enough and there was an absence of relevant numerical techniques to facilitate parallel assessment. The need for a parallel assessment or design evaluation is essential for multi-disciplinary design, for it seeks to identify trade-offs between different performance measures. As such, parallel design evaluation dramatically reduces the number of iterations towards a ship design, whilst satisfying all constraints and providing the best performance achievable. Furthermore, as virtually any new build ship is a variation of some past design, any such design may serve as a prototype for future designs. This practice is common amongst all shipyards and design offices, where new designs are often an evolution from older designs. However, regardless of the amount of deviation from the baseline design, we still face the design customisation problem. The baseline design must be customised to new owner requirements and further modifications can be required within a limited timeframe, especially if such design changes occur later within the process or even after construction has commenced. Additionally, regulatory requirements (e.g., stability, fire safety) have to be fulfilled and these might already be different to those used for the baseline design, particularly as damage stability regulations constantly evolve, thus featuring so-called SOLAS'90, SOLAS 2009, SOLAS2020 and in the future SOLAS 20XX ships. It is also the case that satisfaction of various regulatory requirements, though essential, is not always a sufficient condition to maintain competitiveness. For example, there exist other marketing objectives such as low life-cycle cost (i.e., capital, operational, maintenance etc.) and high earning capacity that must also be addressed. To this end, the design customisation problem becomes a rather complex one and designers are faced with the challenge of producing a design solution that is not only feasible and safe, but also competitive.

During the SAFEDOR Project (SAFEDOR, 2005-2009), a number of steps were taken towards multi-objective and multi-disciplinary optimisation of passenger ships, with safety (risk) presenting a key design objective whilst accounting for performance and functionality through a number of key performance indicators as shown in Table 3-1.

Table 3-1: Passenger Vessel KPIs considered in (SAFEDOR, 2005-2009)

Design Driver	KPI
Functionality	Loading/unloading time Lane metres Volume efficiency of spaces Luggage flow efficiency Deadweight
Performance	Hull resistance Structures Propulsion Energy Efficiency Build Cost Modularity and standardisation levels (variety and use of standardised components)
Safety (SOLAS)	Stability (lightweight, VCG) Damage stability (A-Index) Fire safety (risk screening Fire Index) Systems vulnerability index (compliance with SRtP) Evacuability Index (compliance with MSC.1/Circ.1238)

At the tail end of SAFEDOR, with mega ships being designed to SOLAS 2009 probabilistic regulations, the goal-based approach encouraged by the nature of the regulations brought to surface more questions, more requirements, hence more objectives, leading to problems that were not always warranted (the “swinging of the pendulum” phenomenon). The list in the following is indicative of the optimisation problem addressed, with requirements pertaining to safety objectives and, in particular, reconfiguration of the internal ship space:

Subdivision and layout (Platform Optimisation):

This entails optimisation of ship subdivision and layout by considering concurrently the following:

- Intact stability (new IS code with emphasis on dynamic stability in waves) → impact on GM
- Damage stability and survivability using performance-based probabilistic rules. Normally defining minimum number of bulkheads and tanks
- Fire safety (A-60 bulkheads)
- Systems availability for Safe Return to Port, aiming for optimal routing and minimum redundancy
- Placement of openings / doors, escape routes and evacuation plan (muster list)
- Service / people flows (functionality)

- LSA Alternative Design and Arrangements: Address novel LSA arrangements under IMO Circular 1212.

3.3.5 Structural Design Influences

The internal space in a ship could vary from a single space like the launches of the river Meghna of Bangladesh (zero reconfiguration) to modern megaships with 8,236 spaces, 717 compartments, 1,160 openings (Oasis of the Seas, RCCL – extreme reconfiguration). Hydrodynamic performance dictates the ship shape whilst structural strength and reliability requirements dictate the ship frame (decks, girders, plating, bulkheads – longitudinal and transverse, outer shell); a good summary being provided in Table 3-2, (Misra, 2016). Whereas, Table 3-3, (Klanac, 2011), adds to this by providing a direct connection between various accidents and the reconfiguration measures taken.

Table 3-2: Strength and Operational Utility of Various Structural Parts and Components, (Misra, 2016)

Item	Function
Strength deck, side shell and bottom plating	Form a box girder resisting bending and other loads.
Freeboard deck, side shell and bottom plating	Function as a watertight envelop providing buoyancy.
Bottom plating	Withstands hydrostatic pressure.
Forward bottom plating	Withstands slamming; plating thickness is increased; intermediate frames are provided. Breast hooks and stringers are fitted. Minimum forward draught is recommended.
Inner bottom, bottom plating DB floors and girders	Act as a double-plated panel to distribute the secondary bending effects due to hydrostatics loads and cargo loads to main supporting boundaries such as bulkheads and side shell. Resist docking loads.
Inner bottom	Acts as tank boundary for bottom tanks and withstands local loading due to cargo. Contributes to longitudinal strength.
Strength deck, upper deck	Withstands cargo handling equipment loading and cargo loading in some case as that of the container ship. Withstands loading due to shipping of green seas.
Remaining decks	Mainly withstand cargo loading, depending on extent and distance from neutral axis; contribute to longitudinal bending strength.
Side shell	Withstands hydrostatic pressure, dynamic effects due to pitching heaving rolling and wave loads.
Transverse bulkheads	Act as internal stiffening diaphragms for the hull girder and resist in plane torsion. Do not contribute to longitudinal strength. Generate watertight longitudinal subdivisions.
Longitudinal bulkheads, Bulkheads in General	Contribute to longitudinal strength. From tank boundaries support decks and loads generating equipment such as king posts and add rigidity. Serve as watertight partitions.

Stiffening of Plates		
Corrugations on bulkheads		Stiffen the bulkheads in place of vertical horizontal stiffeners.
Deck beams		Stiffen the deck.
Deck girders		Support the beams, deck transverses and transfer the load to pillars and bulkheads.
Transverse framing		Stiffens the side shell; supports the longitudinal stiffening. Supported in turn, by the decks, stringers and the longitudinal girders.
Longitudinal framing		Stiffens the shell, decks, tank top etc. Is supported by the deep transverses.
Side shell framing (general)		The web size is an important factor as regards a. Cargo stowage b. Panelling and insulation c. Running of wiring, vents, piping etc.
Vertical plates in double bottom (side and centre girders)		Stiffen the bottom panel as tank boundaries.

Table 3-3: Historical perspective on the improvements in the minimum requirements of safety, (Klanac, 2011)

Incident	Type of Accident	Convention instated/updated	Measures instigated
Titanic (1912)	Collision with iceberg and loss of 1517 lives as a result of poor organisation of disembarkation and lack of lifeboats.	SOLAS (1914)	Watertight subdivision
Torrey Canyon (1967)	Grounding and spillage of 120,000t of crude	CLC (1969) MARPOL (1973)	Compulsory liability for damage imposed on the owner/Segregated ballast tanks for all new tankers w/t 70,000+ DWT
Amoco Cadiz (1978)	Grounding and spillage of 250,000t with claims of \$2bn. presented by the French government	MARPOL (1978)	Segregated ballast tanks for all new tankers w/t 20,000+ DWT with protective arrangement
Herald of Free Enterprise (1987)	Flooding and capsizing with the loss of 193 lives	ISM / SOLAS Ch. II-1 (1990)	Operational safety management/Watertight subdivision of garage decks
Exxon Valdez (1989)	Grounding and spillage of 40,000t with damage of \$3bn.	OPA (1990)/ MARPOL (1992)	All ships entering US waters to have double hulls/Double hull or risk-equivalent alternative arrangement for all newly-built ships
Scandinavian Star (1990)	Fire with the loss of 158 lives	SOLAS Ch. II-2	Requirements for fire zone subdivision

Bulk carrier lost in the early '90s.	Flooding and breaking	SOLAS Ch. XII (1997)	Bulk carriers to have sufficient strength to undergo partial flooding of compartments
Estonia (1994)	Flooding and capsizing with the loss of 852 lives	SOLAS Ch. II-1 (1995)	Requirements for flooding tolerance, instigated in SOLAS (1990), to be applied to existing ships and also newly-built ships
Erika (1999)	Breaking of hull and spillage of 20,000t with some €840 mil. worth of damage	EU EMSA (2002)	Accelerated phase-out of single-hull tankers
Prestige (2002)	Breaking of hull and spillage of approximately 60,000t of crude with total damage claimed of more than \$2.5bn	Resolution on places of refuge (2003)	Ship in distress should be accepted to a harbour providing a controlled environment

Fire safety has been ahead of the reconfiguration “game” in comparison to damage stability by having specific spaces being addressed as origin of fire, e.g. Figure 3-6 (Guarin, Majumder, R. Pusia, & Vassalos, 2007), with 10 space categories being responsible for 80% of all fire incidents on-board passenger ships.

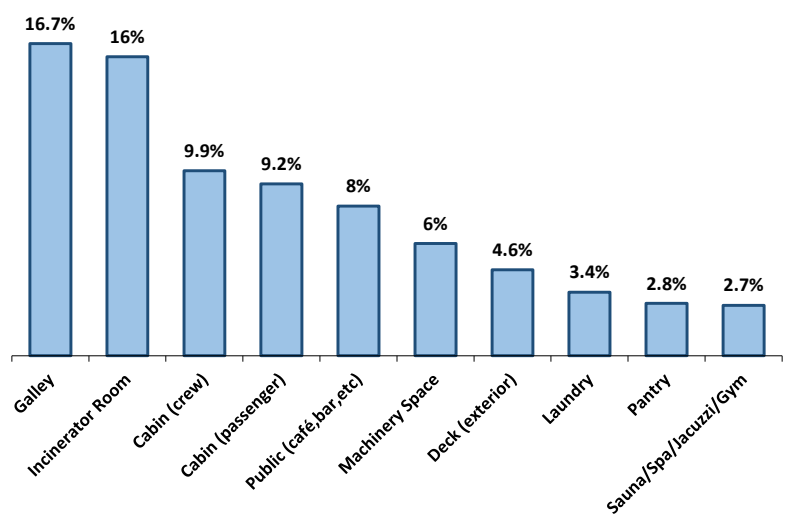


Figure 3-6: Relative frequency of occurrence of fire incidents; 20% of space “uses” contribute to 80% of all fire occurrences (Guarin, Majumder, R. Pusia, & Vassalos, 2007)

However, the vast majority of damage stability regulatory developments have failed to deal with internal space reconfiguration in a direct manner. Instead, regulations tend to implicitly but not explicitly deal within internal configuration, despite this being such an obvious, predominantly influencing feature, particularly for large passenger ships. A key reason for this stems from the

fact that the original damage stability criteria, derived from model tests by Bird and Browne (Bird & Browne, 1973), used global parameters to define survivability in waves, as shown below, and everybody subsequently followed their lead. Of course, damaged GM and freeboard, as Bird used, are influenced by internal configuration, but the nature of the formulation is such that it does not clearly provide much feedback to the designer in this direction.

$$s = 4.9 \sqrt{\frac{F_E \cdot GM}{B}} \quad \text{Eq. 3-1}$$

Where, F_E = effective freeboard (m), GM = Metacentric Height (m) and B = Beam (m)

In a similar manner, Tuzcu and Tagg (Tuzcu & Tagg, 2002), in project HARDER, derived a survivability factor that formed the basis for the SOLAS 2009 damage stability probabilistic rules, linking sea state (H_{s_crit}) to parameters of the residual stability curve, namely GZ_{max} and Range, as given in (Eq. 3-2).

$$H_{s_crit} = 4 \frac{GZ_{max}}{0.12} \cdot \frac{Range}{16} = 4s^4 \leftrightarrow s = \left(\frac{H_{s_crit}}{4} \right)^{0.25} \quad \text{Eq. 3-2}$$

Again, despite damaged GZ_{max} and Range being heavily influenced by internal configuration and truncated as regards unprotected openings, there is no direct feedback granted to the designer as regards internal configuration and this is an important missing link.

The first attempt to escape from this regulatory “trap” is evident in the work of (Vassalos, Turan, & Pawlowski, 1997) in their proposal of the Static Equivalent Method targeting the reconfiguration of the vehicle deck in RoPax ships, as shown in (Eq. 3-3).

$$H_{s_crit} = \left(\frac{h}{0.085} \right)^{\frac{1}{1.3}} \quad \text{Eq. 3-3}$$

Here, both the H_{s_crit} and h are taken as median values of the respective random quantities. The critical significant wave height can be then used in the s -factor formulation adopting the cumulative distribution of waves from IMO. In project HARDER (HARDER, 2003), the formulation was updated following a statistical relationship between dynamic water head (h), the freeboard (f) and the critical heel angle and the mean significant survival wave height.

only way forward in determining the damage survivability of cruise ships is by using the direct method of assessment, as explained in Chapter 5, which is also being adopted in EU-Project FLARE, (FLARE, 2019-2022). However, the strong suggestion by these research projects on increasing damage stability standards, specifically for RoPax vessels and in general for passenger ships, has been met with strong resistance by industry. This has ultimately led to a compromise being reached at IMO for much more modest damage stability standards. Key reasons for this relates to the industry having reached a conclusion that design measures to improve damage stability standards, primarily through further reconfiguration of the internal environment has reaching saturation and a crucial point where viability of business has to be compromised in favour of passenger safety. Something must change and sacrificing viability of the business will never be the route leading to a solution. Hence, the shift to a new perspective became inevitable.

3.3.6 Structural Crashworthiness

Structural design has already been exploited as a means of managing safety, related to accidental loads and breaches of hulls. In the 20th century, nuclear-powered ships faced a clear danger if the reactor were to be physically damaged, e.g. by a ship-to-ship collision. This led to Woisin (Woisin, 1979) describing some reconfiguration of the hull that would result in a higher tolerance in the collision energy of the side structures prior to undergoing breaching. These first investigations served the purpose of, not only of creating more crashworthy side structure designs, but also in capturing the mechanics of ship-to-ship collisions. From that period, the work of Minorsky (Minorsky, 1959) should be noted, which established the proportional relationship between the capacity to absorb collision energy and the volume of the structure involved in deformation. McDermott et al. (McDermott & R. G. Kline, 1974) showed that the key element for ship structures to have an extended capacity to absorb energy is to allow the structure to undergo large membrane tension. Based on his conclusions, substantial work followed with Pedersen and Zhang, (Pedersen & Zhang, 2000), attempting to estimate collision energy and loads based on the Minorsky empirical formula, while Amdahl (Amdahl, 1982), Lützen (Lützen, 2001), Wierzbicki and Abramowicz, (Wierzbicki & Abramowicz, 1983), and Kitamura (Kitamura, 1997), (Kitamura, 2001), developed analytical methods using an upper-bound theorem, referred to as super-element solutions, the latter addressing both collisions and groundings. Deriving from these findings, a series of novel designs of both side and bottom structures have been and are still being investigated, (Lehmann & Peschmann, 2002), (Ludolph & Boon, 2000), (Graaf, Vredevelde, & Broekhuijsen, 2004), (Naar, Kujala, Simonsen, & Ludolph, 2002) and (Klanac, Ehlers, Tabri, Rudan, & Broekhuijsen, 2005). What all these studies have in common is that their conceptual developments are focused on the definition of the topology of a novel crashworthy structure, such as shown here in Figure 3-8.

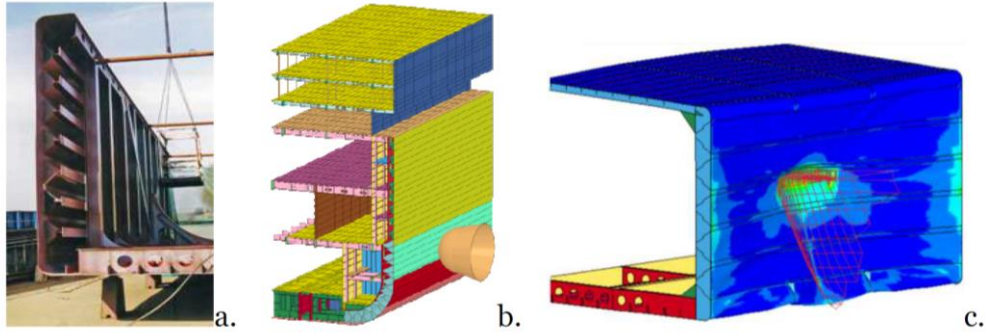


Figure 3-8: Concepts of crashworthy structures: (a) Longitudinal structure on-board an inland waterway gas carrier (Ludolph & Boon, 2000); (b) Transverse structure on board a RoPax vessel (Ehlers, Broekhuijsen, Alsos, Biehl, & Tabri, 2008); (c) Corrugated structure on board an inland waterway

Based on these estimation methodologies, many studies have been conducted focusing on protecting certain regions of interest against external forces, such as offshore structures in (Storheim & Amdahl, 2014), an LNG tanker in (Wang & H. C. Yu, 2008), etc. More recently, Paik (Paik, 2007), (Paik, 2020) and Wilson (Wilson, 2018), proposed advanced techniques for finite element modelling to simulate structural crashworthiness with increased accuracy in collisions and groundings. Most of these studies conclude that crashworthiness of ships can be controlled effectively with conventional double-bottom and double-sided structures.

3.3.6.1 Impact on Damage Stability Protection

There are two basic approaches of considering the impact of crashworthiness as a means of internal ship space reconfiguration on damage protection. An easy way of describing this effect is by using two approaches:

The Direct Approach (using Finite Element Techniques), (Vassalos, 2004)

$$R_f = P_f \cdot P(b|f) \cdot P(sc|b) \cdot P(loss|sc) \quad \text{Eq. 3-5}$$

Where,

R_f = flooding risk

P_f = flooding event probability

$P(b|f)$ = hull breach probability conditional on the flooding event

$P(sc|b)$ = probability of sinking of capsizing, conditional on hull breach

$P(loss|sc)$ = probability of loss of human life, conditional on ship sinking or capsizing

Therefore, in simple terms, a crashworthy structure, conditional on the flooding event, will lead in reducing the probability of hull breach or lead to a distribution of breaches in any given zone that will be weighted towards shallow penetrations, and hence reduce the flooding risk.

The Statistical Approach (using the SOLAS2009 probabilistic framework), (Bae, Vassalos, & Boulougouris, 2020)

The assumption in the SOLAS probabilistic framework in calculating the A-Index is that a flooding event has already taken place and we evaluate the conditional probability of survival. The local index pertains to calculating the average survivability in each zone (local Index). Therefore, a crashworthy structure would render the zone in question impermeable (with high probability); hence by reducing the local permeability in the zone in question, a benefit to the index is gained.

This idea had led to considering, the AREST P2 system, described briefly in the Introduction Chapter with more detail given in Chapter 6.

3.4 Impact of Operation on Reconfiguration of the Internal Ship Space

3.4.1 Overview

Ship operation is not only the longest phase in the ship life cycle but is the only phase that justifies (more often than not) return on investment. As such, reconfiguring the internal ship environment for any reason that may impact upon this will meet strong opposition. This is, of course, why safety comes into rules and regulations, which if not met the ship could not operate. Therefore, trying to raise the safety level beyond the rules takes a great deal of time, effort and inculcation. This interaction between operational and safety objectives will be considered in this section from the point of view of the manner in which this influences internal environment reconfiguration and how this, in turn, affects damage stability and safety. However, even if operation were restricted to the design envelop, it is during this phase where design assumptions and other limitations, leading to the residual risk, need to be managed. This means that that the flooding risk needs to be monitored and controlled to ensure that risk remains tolerable throughout the life of the ship. Such control may be achieved by passive and active means and this will be explored in this section.

3.4.2 Vulnerability in Ship Operation

A threat that exacerbates further the design vulnerability to flooding of passenger ships, probably at the heart of many catastrophes, is vulnerability in operation. This is an issue that has been attracting serious attention at IMO over many years and legislation is now in place (IMO, June 2006). It aims to address the fact that passenger ships are operated with a number of Watertight (WT) doors open, thus considerably worsening the design vulnerability of these ships, SOLAS II-1/15. Figure 3-9 demonstrates this rather emphatically, by considering the well-known Estonia

case as she was designed and as operated at the time of her loss, (Jasionowski A. , 2011). In this case, because of open WT doors, the vulnerability of the vessel was at 68%; 3.5 times higher than her design vulnerability of 19%.

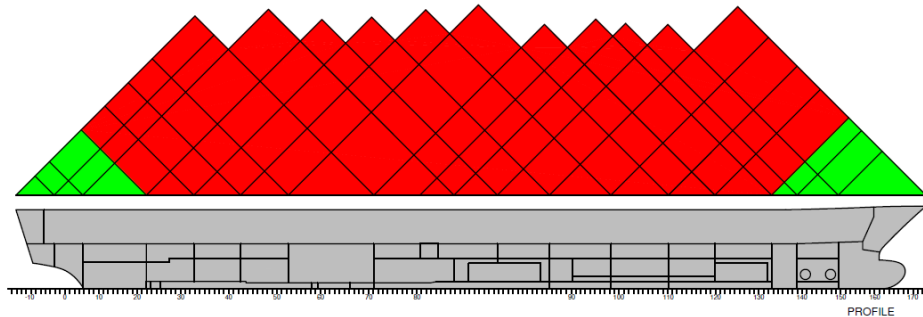


Figure 3-9: MV Estonia – As operated at the time of her loss, based on diagram in (Jasionowski A. , 2011)

3.4.2 Life-Cycle Considerations – Operational Phase²

In the preamble of this section it is mentioned that flooding risk must be monitored and reviewed to ensure changes in design and operation are reflected in the way risk is managed. This sounds straightforward in so far as changes take place in tangible, hence measurable, ship and environmental parameters, e.g., draft levels, loading condition, fluid tank levels, watertight door status, as well as prevailing wind and wave conditions. However, there are many other significant parameters and conditions, for example ship management, improving navigational equipment, training, safety culture and so on, which unarguably affect safety significantly. Unfortunately, the impact of the majority of these factors on safety cannot, at present, be measured and hence monitored, as there is not a system yet in place to assign risk credit/value to such influences. This will be one of the significant outcomes of EU Project SAFEMODE, (SAFEMODE, 2019-2022)

Notwithstanding this, monitoring what can be measured and are known to be KPIs for flooding risk in real time is a step in the right direction to facilitating effective flooding risk monitoring, management and control, as depicted in Figure 3-10.

² This section is based primarily on the work outlined within the paper “Life-Cycle Flooding Risk Management of Passenger Ships” of which the author was a co-author



Figure 3-10: Operational Phase (Vassalos, Atzamos, Cichowicz, & Paterson, 2018)

3.4.3 Conflict in Configuration between Operation and Safety

Large passenger vessels, like most ships, are operated with the primary intention of making money, whilst at the same time aiming to do so in a safe manner. Unfortunately, when it comes to ship internal configuration and architecture, what is good for safety is often bad for business. Hence, satisfying both objectives becomes somewhat of a delicate balancing act and inevitably, conflicts manifest themselves in various forms within the internal arrangement. Passenger ships and particularly cruise vessels, generate money through two primary channels, namely ticket sales and on-board purchases. The former is linked closely, though not exclusively, to passenger capacity and the latter to the provision of on-board services and entertainment. In both instances, transformational changes have been taking place and over recent decades economies of scale have driven developments towards increasingly large vessels at unprecedented rates, see Figure 3-11.

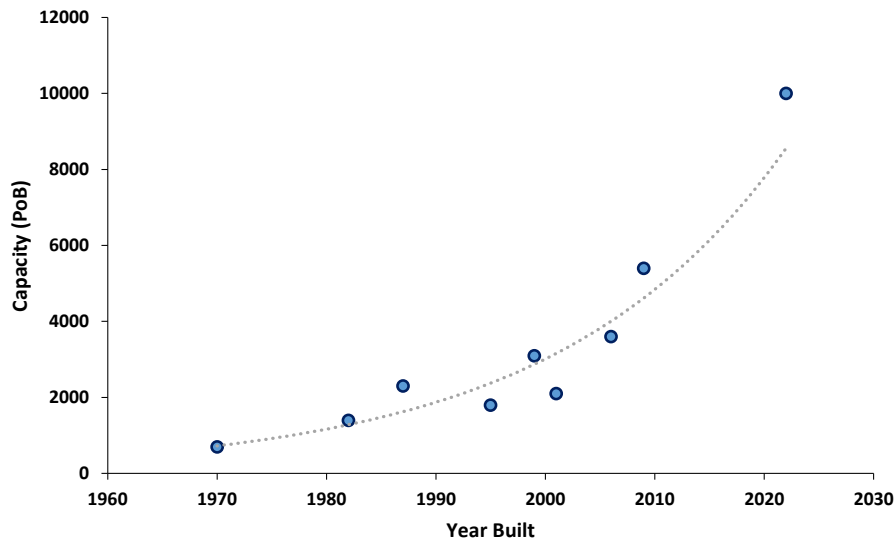


Figure 3-11: Cruise Vessel Growth Trend

A secondary effect of this growth, has been the provision of a far greater platform from which the operator can offer increasingly diverse and elaborate forms of on-board entertainment, with it now being possible to “open up” the vessel more than ever before (Kulovaara, 2015). Modern cruise ships must cater for many cultures, demographics and interests, all of which must be achieved on a mass scale. In so doing, they tend to offer a multifarious array of features including, but by no means limited to, restaurants, bars, casinos, spas, theatres and even ice rinks. Consequently, ship internal configuration is primarily aimed at accommodating all these features within limited real estate. Furthermore, flowing and uninterrupted spaces are often favoured in order to create an unconfined atmosphere, whilst also ensuring a continuous passenger flux along the ship (S McCartan, 2015).

This is where the first notable conflict arises between configuration for operation and that for safety. Most of the aforementioned features are normally situated across the two decks located above the vessel bulkhead deck, which is favoured given that the boat deck would otherwise obstruct cabin views and balconies should accommodation be situated here. However, having these spaces located relatively low within the vessel superstructure also leaves them vulnerable to flooding and this is where problems arise. Large flowing spaces, while favourable from an operational and aesthetic perspective, can give rise to rapid floodwater accumulation and propagation. Firstly, when damaged, such spaces offer no reserve buoyancy, which is crucial during the transient roll cycle. For this reason, damages with large vertical extents are particularly vulnerable to transient capsizing, in fact, almost invariably transient losses involve at least one of these decks. Further still, should the vessel survive the transient flooding stage, in certain damage scenarios, these open spaces have the tendency to act much like a ro-ro space and fall prey to the effects of water on deck. This phenomenon, as witnessed in many of the

assessments conducted as part of this research, occurs predominantly in high sea states, where wave-induced pumping effects cause progressive flooding on the upper decks. Floodwater then rapidly spreads, giving rise to large free-surfaces and often leading to vessel capsizing. As such, the prevalence of open spaces within large passenger vessels presents somewhat of a design paradox, whereby the safer a vessel is, the more open spaces it can have. However, the more open spaces it has, the less safe it becomes.

Such spaces also pose a risk regarding the propagation of fire but, in contrast to flooding, a great deal of progress has been made in this area through the alternative design and arrangements process. In 1986, the cruise vessel "Sovereign of the Seas" was designed with an atrium extending over three decks within one fire zone, which was approved under equivalent arrangements according to SOLAS I/5. Later, in 1999, "Voyager of the Seas" pushed the boundaries further still, with an atrium spanning three fire zones, again approved using equivalency design. Such developments then ushered in SOLAS II.2/17 on "Alternative Design and Arrangements for Fire Safety" and the second-generation Voyager-class vessels have atria spanning over four fire zones (Sames, 2009). In each instance, novel means were adopted in order to mitigate fire risk, either in the form of advanced analysis techniques, technology or both. Perhaps there is a lesson to be learned here as regards flooding, where unfortunately no such regulatory system exists in order to facilitate the implementation of alternative designs concerning flooding specifically. Perhaps SOLAS Ch. II-1, Regulation 4 (Damage Stability /Equivalence) offers such a possibility but this, as far as it is known, has not yet been taken up. Consequently, there has been little innovation in this respect, despite great potential, and recognition of this has fuelled many of the developments made within this research.

In addition to the prevalence of open spaces, there is another key example in which internal configuration for operation and safety lie in opposition. This relates not to spaces, but instead, the channels of communication between them. Effective vessel operation relies on the ability to transport people and goods throughout the vessel in an efficient manner. An example of this is provided in Figure 3-12, showing catering spaces and flows for a typical cruise ship. This is just one of many processes that require such movements throughout the vessel, but even in this isolated case, one can observe the widespread pathways that exist. Such pathways, though essential, impair safety by providing conduits through which progressive flooding may occur. These exist as corridors in the case of longitudinal flooding progression and in the form of service elevators and stairwells, where up/down flooding may occur. Unfortunately, to date there is little that can be implemented in the protection of such openings without greatly impairing operability.

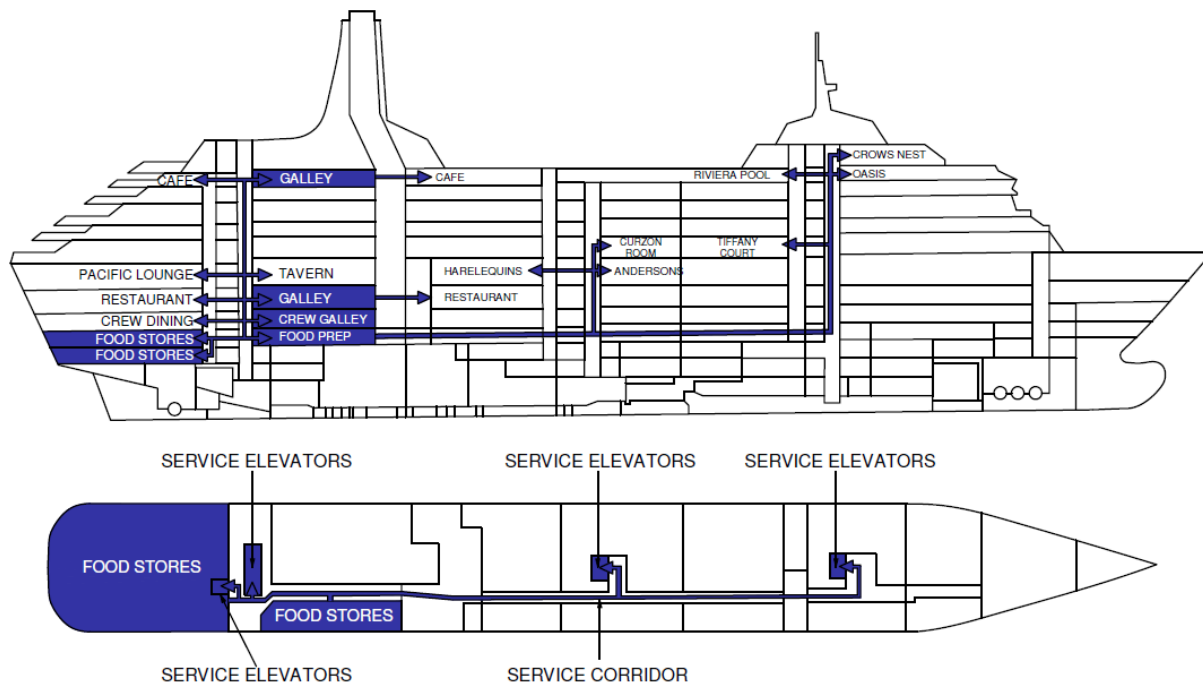


Figure 3-12: Catering spaces and flows for a typical cruise ship, based on diagram shown in (Vie, 2014)

3.5 Ship Emergencies Impact on Reconfiguration of the Internal Ship Space

3.5.1 Overview

Flooding emergencies and the ensuing risk are still dominant in the maritime industry as explained in the introduction Chapter. Hence, emergency response, as the last line of defence is of paramount importance. However, what this section is delving into is impact that addressing this need has on internal ship space configuration. Like the operational phase, most of the key elements affecting emergency response are not measurable/auditable and, therefore, do not provide any guidance to the operator in his strive to adopt cost-effective means to mitigate and control flooding risk in this vital last phase. However, new technologies have been explored to enhance situational awareness and guidance of evacuees during emergencies, e.g., EC-funded Project SAFEPASS (SAFEPASS, 2018-2020), and also interventional measures to restore stability post damage, (Vassalos, Paterson, & Boulougouris, 2019). Every one of these, provide a platform for transformational changes in the way in which emergencies on-board are currently being addressed and this section will look into how these affect the internal ship environment and, in turn, interact and conflict with safety-related changes and, hence, how they influence one another.

3.5.2 Life-Cycle Considerations – Operational Phase³

The emphasis in this phase is on ensuring that in any of the critical scenarios where ship stability is compromised, the ship will remain upright and afloat, with all safety systems available, for sufficient time to ensure safe evacuation of all the people on-board. However, similar to the operational phase most of the key elements affecting emergency response are not measurable/auditable, thus not providing any guidance to the operator in his strive to adopt cost-effective means to mitigate and control flooding risk in this vital last phase. This, in turn, affects decision making, particularly when competing objectives are considered, which may influence how effective damage protection and control might be. Recent developments in this area as well as the conflict between damage stability protection, in terms of how reconfiguration of ship space, competes with these other objectives are being addressed in the following section. Figure 3-13 presents a schematic of what this phase entails.

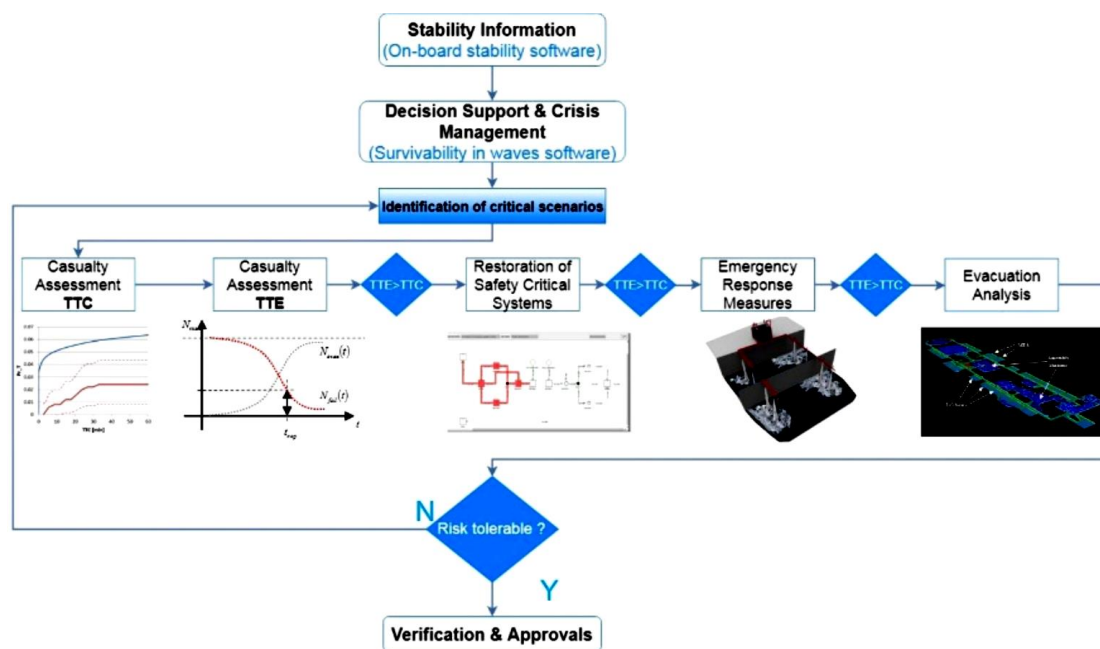


Figure 3-13: Emergency Response Phase (Vassalos, Atzampos, Cichowicz, & Paterson, 2018)

³ This section is based primarily on the work outlined within the paper “Life-Cycle Flooding Risk Management of Passenger Ships” of which the author was a co-author

3.5.3 Configuring the Ship Environment for Emergency Response

The internal environment of a vessel and its configuration are heavily influenced by emergency response considerations. Perhaps most notably, provisions relating to means of escape and evacuation have a significant bearing on the internal layout. SOLAS ChII-2, Reg.3, pertains to means of escape and governs the design and designation of doors, corridors, and stairwells. This is further supported by evacuation principles, which are concerned with emergency routing and the safe and timely transport of passengers and crew in an emergency (Champion, Ahola, & Kujala, 2015). In order to inform the internal configuration in this respect, evacuation analysis is often conducted in line with MSC.1/Circ.1033 (IMO, 2007). Through doing so, optimal evacuation routes can be identified, along with their appropriate dimensions. This is a highly important characteristic of the internal configuration as evacuation routes, though undoubtedly an essential safety feature, can themselves exacerbate flooding by providing conduits for floodwater progression. These come predominantly in the form of corridors, escape trunks and stairwells that penetrate both horizontally and vertically through watertight structure. Furthermore, evacuation considerations can also impose on the operational functionality of the vessel, especially where there are multiple corridors within accommodation spaces, which remove from the footprint available for cabin space.

Emergency response considerations also affect the vessel internal configuration in accordance with SOLAS Chapter III, relating to lifesaving appliances and arrangements. Here, stipulations are made regarding the design and location of muster stations which, in accordance with Regulation 11, should be located as close as possible to embarkation spaces, whilst being readily accessible from accommodation and workspaces. Furthermore, each person assigned to a given muster station should have at least 0.35 m² area available to them and this is where large open spaces within cruise vessel designs have their advantage and are, as such, often used for this purpose. SOLAS Chapter III also mandates, in accordance with Reg.13, that lifeboats and survival craft should be located on both port and starboard sides of the vessel, positioned as close to the waterline and as far forward from the propellers as practical. For this reason, most cruise vessels are configured with lifeboats situated two decks above the bulkhead deck, where the vertical travel required for deployment is minimal, whilst ensuring the lifeboats are clear from green water effects or indeed immersion in the damaged floating position.

Another highly influential factor over the vessel internal arrangement are the requirements of Safe Return to Port (SRtP), as outlined within MSC. 216(82). The aim here is to provide a safe and habitable environment for both crew and passengers, while the damaged vessel returns to safe

harbour. This entails that certain vital systems remain functional post damage such as propulsion, portable water system, HVAC system, galley systems, lighting etc. Unfortunately, to date the degree of damage considered for flooding under SRtP is rather limited, with just one-compartment flooding scenarios considered, meaning that residual functionality is not assessed for a large percentage of probable damage scenarios. This is, however, more comprehensive for fire scenarios. In any case, the effect of these requirements on internal configuration comes in the form of compartment segregation in order to protect vital systems, or otherwise, systems are replicated in order to ensure availability. This can add a great deal of complexity to the vessel internal arrangement and in some cases can introduce asymmetries within the flooding process, where longitudinal subdivision is employed. Further to the above, and much like the designation of muster stations, vessels are also allocated safe zones. These provide safe locations where passengers can gather in order to have access to the benefits of retaining such systems, including heating, food, sanitation, lighting, ventilation and so on. Again, for this purpose larger public spaces are often utilised, such as restaurants and bars.

Emergency response considerations also affect the vessel internal arrangement in the form of damage control. In accordance with SOLAS II-1, Reg.19, each vessel must have a damage control plan and manual onboard, containing the information specified within MSC/Circ. 919 and MSC.1/Circ. 1245. This generally comprises a series of actions to be taken in the immediate wake of an accident in order to identify damage extents and subsequently minimise and localise the spread of floodwater. An example of the general damage control process is provided within Figure 3-14, with items relating specifically to space configuration shown in green. Here, the first of these items concerns the preservation of the vessel watertight envelope by closing all watertight doors and hatches, along with weathertight appliances. In addition, all valves on pipe runs passing through watertight structure are also to be closed. All such features exist within the vessel arrangement specifically to prevent the propagation of floodwater and essentially work to reduce the permeable volume available to a given damage breach. Following this stage, a more informed process of space reconfiguration takes place in the form of actively redistributing mass within the vessel. This generally occurs in two ways, firstly by activating the bilge pumps within the damaged space in order to lessen floodwater accumulation and secondly through the process of counter ballasting, using ballast and heel/trimming tanks. The aim here is to improve the vessel floating position to either facilitate a more timely and orderly evacuation or indeed to enable the vessel to safely return to port. This comes, however, without due consideration of the dynamic behaviour of the ship and the effect that this might have on counter-ballasting and any other actions being considered by the simplistic approach that currently prevails.

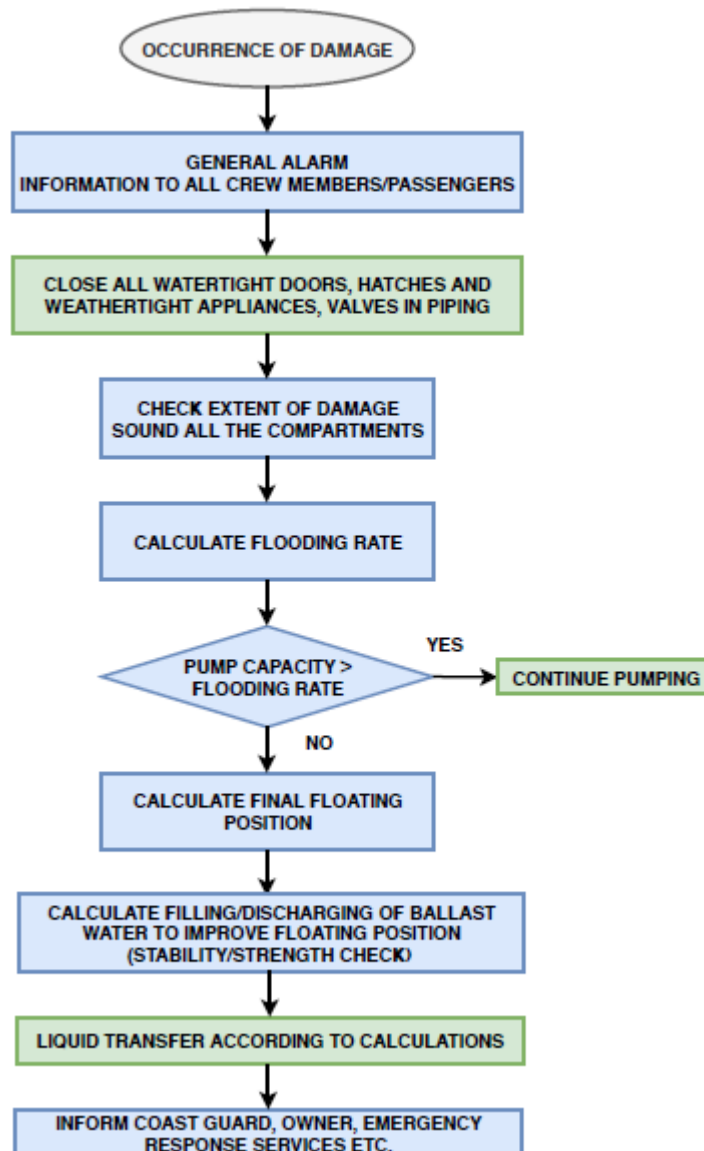


Figure 3-14: Damage Control Actions List

3.6 Closing Remarks

Based on the research presented within the foregoing, the following conclusions can be drawn in summary:

- Historically speaking, the primary driving force behind vessel reconfiguration has come in the form of rules and regulations pertaining to flooding and to a lesser extent fire. In such instances, change has occurred slowly, often in a reactive manner in the wake of accidents.
- Gradually, however, an increasingly proactive approach to the problem of damage stability is emerging with, for example, IMO instruments such as Safe Return to Port making significant strides in this direction.

- The nature of internal configuration that is favourable for operation is often in conflict with that for safety and hence objectives pertaining to each generally lie in antithesis. For this reason, the rate of safety progression has often been slowed due to industry resistance on the grounds that their ability to operate a viable business would be impaired. This, in turn, is indicative of a greater problem relating to the efficiency and variety of existing RCOs for flooding risk. It would appear that there is an urgent need to start seeking alternative and more effective solutions, rather than continued sole reliance on conventional measures such as watertight subdivision.
- Further exacerbating this problem is the tendency towards building progressively larger passenger ships, which places an ever-growing number of people at risk, leading to a policy of zero-risk tolerance.
- In order to achieve this aim, one must consider the vessel throughout its entire life-cycle (design, operation, emergency response) and understand the requirements within each stage. This would involve consideration of the constraints and conflicting requirements that each stage brings to the decision-making process in relation to the optimal configuration of the internal ship space. Only then, can one hope to provide solutions capable of achieving this aim.

Chapter 4: Research Methodology Adopted

4.1 General Remarks

The present chapter serves to provide an overview of the approach adopted in the undertaking of this thesis. As expressed within Chapter 2, the overarching research aim has been to demonstrate that in this age, it is not only possible, but indeed practical to protect a vessel against all manner of conceivable flooding risks. Naturally, in order to substantiate such a notion, one must first adopt a methodology that employs a rigorous and comprehensive assessment of vessel damage stability and survivability. This is essential, firstly as a means of informing the design and implementation of appropriate RCOs, and secondly, in order to provide the right platform for testing and verification. The latter being of particular importance as the solutions that have been sought in this undertaking fall outside the boundaries of conventional norms and this demands that due diligence be paid. In light of this, the process shown in Figure 4-2 has been developed in order to evaluate vessel damage stability performance from all pertinent perspectives. Furthermore, as a means of demonstrating broad applicability, this methodology has been applied to a comprehensive range of vessel types, as outlined in Figure 4-1. Of these studies, the results of three cases have been included within this thesis, comprising two cruise vessels and one RoPax.

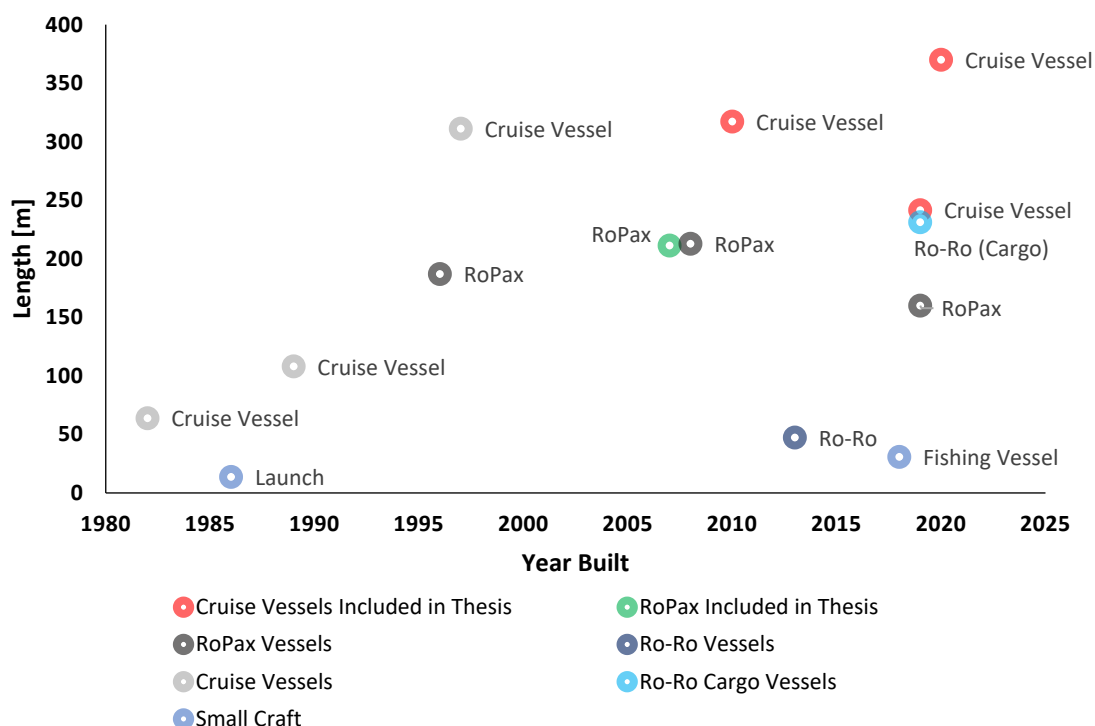


Figure 4-1: Overview of vessels considered

4.2 Overview of Methodology

The methodology adopted has been tailored to cater for the design and implementation of the RCOs developed as part of this research and is comprised of eight distinct stages, as elaborated within the following.

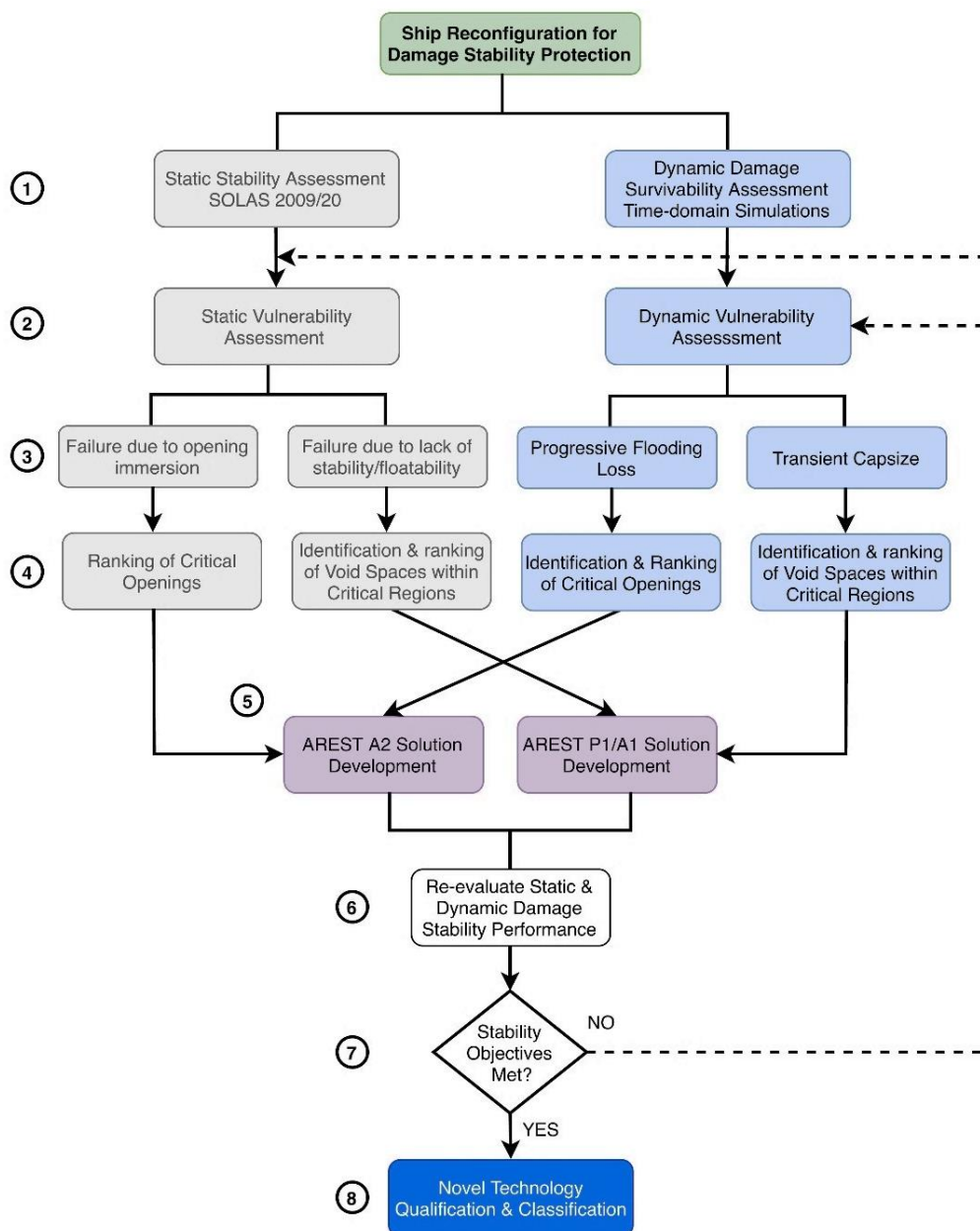


Figure 4-2: Methodology Adopted

Stage 1: Static & Dynamic Damage Stability Assessments

The process begins by conducting two forms of damage stability assessment in parallel, one based upon conventional hydrostatic assessment techniques and the other using advanced numerical time-domain flooding simulations, herein distinguished as static and dynamic approaches, respectively.

The static component of this damage stability assessment is conducted in accordance with applicable IMO statutory instruments, which vary depending on vessel age, type and size. When assessing new build vessels engaged in international voyage, this relates to the requirements of either SOLAS 2009 or SOLAS 2020 as applicable. Both these forms of assessment offer a distinct advantage over deterministic instruments in that they are, for the most part, performance based in nature. This enables a quantifiable baseline risk level to be established, from which the impact of RCOs can later be measured and compared. Unfortunately, a great many existing ships and domestic vessels are regulated on the basis of older prescriptive regimes, with an implicit but not explicitly quantifiable safety level. For this reason, vessels falling within this category have been subjected to the probabilistic damage stability assessment process and the resultant solution has been derived on this basis.

A secondary and complimentary assessment is also conducted at this stage utilising numerical time-domain simulations as a means of assessing vessel survivability. This form of assessment, as in the case of SOLAS 2009/20, is also performance based and thus well suited for assessing RCOs. However, the manner in which vessel performance is measured differs greatly between the two approaches. Numerical simulations draw upon first principles and have a greater capacity to capture the underlying physics of the flooding process. This means they do not suffer to the same extent from elements of assumption, generalisation and simplification that are commonplace within technical standards. Consequently, the results from numerical simulations work to not only support and verify the results of the static assessment, but also offer a wealth of additional information and insight into important flooding processes and components of survivability that simply cannot be captured using statics.

Stage 2: Static & Dynamic Vulnerability Assessments

The second stage in the process involves the execution of two complimentary vulnerability assessments. Here, the results generated within the previous stage, stemming from both static and dynamic assessment techniques, are called upon in order to establish the degree of vulnerability present and its sources. With respect to static assessment, this firstly involves calculation of the Attained Subdivision Index, which provides a measure of ship safety as regards collision damage. The compliment of this value (1-A) can then be used in order to establish a

baseline risk level from which the impact of RCOs implemented later within the process can be gauged.

With regards to dynamic assessment, overall vessel survivability is measured in a different manner, using the Survivability Index. This is calculated according to the direct approach to damage stability analysis rather than statistical approaches, as is the case in determining the vessel Attained Index. For this reason, among others relating to differences in the geometric modelling of the vessel, openings, damages etc., the Attained Index and Survivability Index cannot be directly compared. However, both Indices provide an indication of a baseline safety level from which further improvements can be measured. The Survivability Index is determined quite simply as the ratio between the number of cases survived within a given sample and the total sample population, conditional on a certain exposure time. The compliment of this value, representing the probability of vessel capsize or sinking, can then be used in order to provide a measure of vessel vulnerability to flooding.

Stages 3: Loss Modality Determination

Having previously quantified vessel vulnerability, the third stage in the methodology proceeds to identify the nature of vulnerability through the assessment of failure modes. Gaining such understanding is crucial in deriving RCOs, as any effective treatment must be founded upon accurate diagnosis. Generally speaking, there are two primary modes in which a vessel may be lost to flooding, namely transient capsize and progressive flooding loss. Transient flooding occurs in the immediate wake of a damage event and can induce rapid capsize. This comes as a result of floodwater rushing into the damaged compartment in an asymmetric fashion, which has the effect of inducing a large heel response that can overcome the vessel. In contrast, progressive flooding occurs over a much longer duration and results from the immersion of non-watertight openings forming a channel of communication between intact and damaged spaces. This causes floodwater to propagate throughout the vessel, gradually reducing reserve buoyancy and eroding stability to the point at which the vessel may capsize.

Both statics and dynamics offer different information and a different degree of accuracy with which to determine loss modality. With reference to statics, the results of the probabilistic damage stability assessment can be used in order to provide an indication of which loss modality may be realised. However, an explicit determination cannot be made using this approach for reasons elaborated upon further within Chapter 5. Instead, cases prone to transient capsize have been identified by isolating damage scenarios in which the intermediate s -factor was dominant or where an excessive angle of heel at equilibrium was found. These form effective criteria for predicting transient capsize potential as the intermediate s -factor deals with flooding stages prior

equilibrium and is therefore reflective of the transient flooding stage. Furthermore, a large angle of heel at equilibrium indicates either asymmetrical flooding or limited residual GM, both of which are known to be leading causes of transient capsizing. With regards to the identification of cases liable to progressive flooding loss, static assessment enables this to be done by isolating cases in which unprotected openings were found to be immersed at the final stage of flooding. In addition, cases with marginal residual range are also identified here, since such cases are prone to wave induced progressive flooding.

In contrast to static assessment, the results stemming from dynamics allow the loss modality to be identified explicitly. This is possible as numerical flooding simulation tools can capture the physics of the flooding process, in addition to providing an overview of the full time-evolving flooding event. Here, transient capsizing cases are firstly distinguished by assessing the TTC relating to each loss scenario. As previously stated, transient capsizing occurs abruptly following the initial hull breach, which enables such loss scenarios to be identified by filtering cases according to TTC. This is then further supported through observation of the case specific roll time histories, which can reveal if the vessel was indeed lost during the transient roll response. Inversely, progressive flooding loss scenarios are identified as those with longer flooding durations, often characterised by a roll time history that displays a gradual increase in average roll over the flooding sequence. In addition, average floodwater mass accumulation is assessed in the same manner to establish if the vessel is taking on water, thus indicating progressive flooding. Finally, information pertaining to openings is analysed in order to assess if any openings have allowed floodwater to progress from a damaged to intact space.

Following the processes outlined above, all loss scenarios are then categorised into progressive flooding losses and transient capsizing cases, with each category then subjected to specific forms of additional analysis as outlined within stage 4. As will become apparent, it is greatly important to make this distinction, as each loss modality has differing design constraints and requires a different form of treatment in terms of RCOs.

Stage 4: Identification & Ranking of Critical Openings and Spaces

In the previous two stages both the level of vulnerability and its nature in terms of loss modality are determined. Building on this, stage 4 within the process seeks to identify and rank the sources of vulnerability in relation to safety critical spaces and openings within the vessel internal geometry. This provides valuable information that can be used to underpin the implementation of RCOs within the subsequent stage, allowing those spaces and openings that constitute the greatest risk to be targeted. This enables maximum risk reduction to be realised with the least degree of reconfiguration, thus leading to the most cost-effective solution. Once again, the results

from both the static and dynamic assessments are used to inform this process and are handled in different manners.

Static assessment affords a way in which to identify and rank critical openings by isolating damage cases in which either opening immersion within the final floating position or limited range to opening immersion are responsible for failure. The resultant loss in Attained Index contribution for damage cases limited in this way can then be calculated, providing an indication of opening-specific flooding risk. Where a given opening is responsible for failure across multiple damage cases, the flooding risk relating to each case is summed to provide a total risk value. Having followed this process, critical openings can be identified as those leading to the greatest loss in Attained Index and can therefore be targeted for protection.

In contrast to statics, the results stemming from dynamic assessment allow critical openings to be identified and ranked in a much more comprehensive manner. Firstly, dynamic simulation models contain all pertinent openings within the vessel internal geometry, ranging across the entire weathertight envelope. Static models on the other hand, contain only a limited number of all openings within a simplified geometry, which are used in order to truncate the GZ curve upon immersion. This only captures a fraction of the internal geometry and does not allow for the full flooding chain to be assessed. Another important distinction between the two approaches, is the ability within dynamics to capture the actual opening geometry and assign physical characteristics in relation to watertight integrity/resistance. This means that the results stemming from dynamic assessment are far more reflective of reality. When ranking openings following dynamic assessment, three primary parameters are used. Firstly, the frequency in which each opening is involved within a progressive flooding loss is calculated. This is then followed by an assessment of the mass of floodwater that has passed through each opening. Finally, by combining the previous two measurements, opening risk can be identified as the frequency in which a given opening is involved in major progressive flooding. These values can then be used in order to identify and rank critical openings, which are then targeted for protection if feasible.

With regards to the identification of critical spaces, the results stemming from the static assessment are used in order to identify local vulnerabilities within the vessel design. This is accomplished through examination of case-specific Index losses in the form of $p*(1-s)$. For a given damage case, this value represents the difference between the maximum potential Attained Index contribution and that which was achieved, thus providing a measure of flooding risk contribution. By observing the results in this way, critical spaces within the design can be identified where peak risk values occur or where there is a high concentration of cases contributing to the flooding risk.

The results from dynamic assessment are used in a similar manner in order to identify critical spaces, in this case focusing on spaces within the vessel found to have a high frequency of involvement in loss scenarios. In particular, those spaces that are frequently involved in loss scenarios with smaller damage dimensions are targeted, as these represent the most probable damage events.

Stages 5: Solution Development

This stage of the process involves targeted application of RCOs, specifically those developed as part of this research. Here, depending on the loss modalities identified within stage 3, different RCOs are employed. With regards to transient flooding, systems that are built into the vessel design are favoured as there is no time to enact any active measures following such events. Furthermore, RCOs in such cases are aimed at providing the vessel with a greater damaged GM whilst also offsetting any asymmetries within the flooding process, both of which are highly influential parameters in relation to transient capsizes. The areas targeted for such solutions are those identified within stage 4 as being safety critical. When protecting against progressive flooding, active in addition to passive RCOs are considered in the protection of spaces and openings. This is possible due to the longer flooding duration attributed to progressive flooding cases, which enables time for actuated systems to be utilised. In such cases, RCOs are aimed at either uprating the watertight integrity of critical openings such as to be able to contain floodwater, or alternatively, at increasing vessel reserve buoyancy and preventing the immersion of openings. Again, information stemming from stage 4 is used in order to target the highest risk openings and spaces.

Stages 6: Re-evaluation of Static and Dynamic Damage Stability

Having implemented RCOs, the vessel damage stability performance is re-evaluated in order to gauge the impact on vessel survivability. As part of this process, both the static and dynamic calculation models are modified in order to account for the effects of each RCO being employed, following which the assessments conducted across stages 2-4 are repeated. Information from this updated assessment is then fed into stage 7.

Stages 7: Determination if Stability Objectives are Met

Within this stage a determination is made as to whether stability objectives have been reached. The exact nature of these objectives can vary across different applications of the methodology and there is flexibility in this sense. For example, the goal could be to uprate a SOLAS 2009 vessel to 2020 compliance, and this would set the constraints. Alternatively, if an existing ship had suffered significant lightweight growth, then stability objectives could relate to expanding GM

margins by some value. However, the desired stability objective to be employed in the execution of this methodology would be to seek the optimum level of risk reduction based on all credible RCOs. In this case, an iterative process would ensue until such point that diminishing returns in risk reduction are realised, i.e. when the application of further solutions is no longer cost-effective.

Stage 8: Novel Technology Qualification & Classification

The final stage in the methodology is to undergo a Novel Technology Qualification (NTQ) process, which is the route offered by most classification societies towards the approval of new and innovative technologies. This is important, as currently established codes and procedures tend to be empirical by nature, and thus, solutions without prior precedent are ill covered, if at all. The overriding objective behind this process is to ensure that any RCO proposed is “fit for purpose” and this relates to not only safety but also performance, functionality and availability. In addition, this stage acts to test the practicality of the solution, which is a highly important consideration as one does not want to solve one problem by introducing another. Furthermore, what can look very attractive on the page can often fail to stand up to practical scrutiny and for any research in this direction to have true value; it must be applicable in practice.

Chapter 5: Ship Damage Stability and Survivability Assessment Process

5.1 Opening Remarks

This chapter serves to provide an overview of the survivability assessment process that has been adopted in the undertaking of this research. Here, particular emphasis has been placed on the use of numerical time-domain simulation tools, even though traditional static assessment techniques have also been employed. The chapter starts by providing a justification for the use of flooding simulations, citing the areas in which such tools can be used in order to account for some of the limitations of hydrostatics. This is followed by an overview of the development of such tools and their various applications to date. Finally, a comprehensive overview of the process by which vessel survivability has been determined is provided, along with several processes that have been developed in order to extract maximum utility from the process and the ensuing results.

5.2 Limitations in Hydrostatics & the Need for Numerical Simulations

Flooding simulations allow for a more refined assessment of vessel damage survivability in comparison to the conventional hydrostatic calculation techniques found within current IMO regulatory instruments (SOLAS 2009/2020). This is particularly true in the case of large passenger vessels, where the ability of hydrostatics to accurately assess and quantify ship survivability remains a highly contentious point. Vassalos addresses this specific issue in detail within (Vassalos, 2016). Here, he calls attention to a number of areas in which the current static-based regulatory scheme fails to cater for cruise vessels in an appropriate manner, as summarised within the following:

- The classification of all vessels carrying more than 12 persons as “passenger vessels” is highly reductive and fails to account for the diversity of vessels falling within this category, each of which can possess widely different sources of vulnerability stemming from entirely different flooding mechanisms.
- Cruise vessels have not been represented in the development of the current s-factor and there has been a lack of consideration of large vessels in general.
- The exposure time of 30 minutes used in the development of the current s-factor does not account for the longer flooding durations cruise vessels can undergo (>3 hours), nor does it account for the far greater evacuation time required for such vessels.

- Cruise vessels have vastly different levels of complexity in internal geometry, leading to greater uncertainty in the flooding process and outcome.
- With some vessels now being designed to carry >10,000 persons, there can be a huge disparity in the people at risk in comparison to smaller passenger vessels.

Put plainly, there is a clear and observable difference between cruise vessels and RoPax vessels, which needs to be accounted for by some means. The introduction of SOLAS 2020 made some progress in this direction by introducing a more stringent s-factor for RoPax vessels in case of damage to the ro-ro deck. However, this alone represents the sole distinguishing element between these two ship types and is one that serves only to differentiate RoPax vessels from cruise vessels and not the other way round. That is to say, it acts only to cater for flooding mechanisms relating specifically to RoPax ships and there are no such provisions designed to cater for cruise vessels and their own specific flooding mechanisms. As such, it would appear that some effort is required in order to bring the regulations back into harmony with reality as regards cruise vessels. This can only be achieved by addressing the areas within the current regulatory system in which cruise vessels are poorly accounted for, as listed within the previous. If not, other tools must be sought in order to fill this gap and it is here where numerical simulations could hold the answer.

Further to the above, there are also a number of limitations inherent to the static assessment process itself as opposed to any regulatory shortcomings or mistreatments. These relate primarily to the inability of hydrostatics to accurately account for and capture different loss modalities. This is highly important, not only in determining risk, but also in identifying appropriate RCOs. Traditionally, the Attained Subdivision Index has been used in order to gauge the effectiveness of RCOs, either by measuring improvement in the Attained Index itself or as an input to a Formal Safety Assessment (FSA) for the determination of ΔPLL and RCO cost effectiveness. This process allows for a relatively fair and time-efficient means of ranking RCOs but fails to account for the whole picture. One of the fundamental philosophies behind the probabilistic approach to damage stability assessment is that two vessels with the same Attained Subdivision Index are considered equally safe (IMO, 2017). This is, however, not necessarily the case as the element of time is removed from the question. If we considered two vessels, each having an Index of 0.8, there is no indication of the severity of the twenty percent of cases in which each vessel is lost. That is to say, one vessel could be prone to transient capsizing and the other to progressive flooding loss, in which case the casualty rate would vary dramatically and so too the risk level. Some effort was made to account for this in the collision risk model developed within GOALDS and more recently the EMSA III project (EMSA, 2014). Here, the risk model accounted for “fast” and “slow” flooding probabilities within the event tree, but this determination was made

independently of the Attained Subdivision Index and therefore was not based on the actual damage stability behaviour of the vessel. Furthermore, there is some ambiguity surrounding what constitutes “fast” flooding in comparison to “slow”, leading one to ask, “how fast is fast?” and inversely “how slow is slow?”.

Notwithstanding the above, static assessment techniques, even though unable to directly distinguish between loss modalities, do provide some indication. Firstly, in order to account for transient asymmetric flooding, the current regulations apply an intermediate s-factor in cases where flooding is not considered instantaneous (within 60 seconds). Here, a quasi-static approach is adopted whereby the flooding process is broken down into various stages and phases, providing snapshots of the flooding process, but not the full time-dependant flooding progression. This, in turn, can be used to determine if the vessel possesses a higher risk of capsize within intermediate stages of flooding, thus allowing cases that could be prone to transient capsize to be identified. However, this quasi-static treatment of intermediate flooding has long fallen into question due to the highly violent and dynamic nature of the initial flooding stages (Dafermos & Papanikolaou, 2016). It was, in fact, this recognition that fuelled a lot of the early development of numerical flooding simulation tools as described later within this chapter.

In the consideration of the potential for progressive flooding, the regulations work by truncating the vessel damaged GZ-curve at the point of immersion of unprotected openings or by considering the vessel as lost if such openings were immersed at equilibrium. This, in turn, allows cases prone to progressive flooding to be identified if limited in this way and the underlying logic here is clear as to the prevention of progressive flooding. Where the limitations of this approach appear is in the fact that, by truncating the GZ curve in this way, we focus on only a small portion of the flooding chain. Should the entire floodwater evolution have been allowed to unfold, we learn nothing of what may have happened nor the consequences. Important questions relating to the actual extent of flooding that would be realised, the openings through which this would occur and the time that this would take are all left unanswered. This limited scope through which the flooding process is viewed also has potential repercussions as regards the implementation of RCOs. For example, if we only focus on the initially immersed opening in the flooding sequence and if this opening for operational reasons could not be protected, the designer may reside themselves to the fact that this is an unavoidable risk. However, there is every possibility that if the flooding chain could not be broken here, it may very well be broken a little further within the flooding evolution and this information is all lost within the current regulatory scheme.

To summarise, static assessment techniques provide a somewhat opaque and limited view of flooding risk and its sources. Consequently, it is important that where possible and appropriate we support these calculations with other tools. For this reason, in the undertaking of this research

numerical time-domain simulations have been used as part of a systematic approach to assessing vessel survivability in the case of cruise vessels, where the greatest uncertainty lies and also in the case of a RoPax vessel. This is in line with evolving trends within the industry where, given the potential severity of a major accident involving a large passenger vessel, simply ensuring compliance is no longer considered sufficient (Tobias King, 2016). Instead, there has been a turn towards the use of first principle tools coupled with a more proactive approach that promotes continuous safety improvement over simply ensuring compliance. After all, one has only to look into past accident statistics to find many examples of where compliance was not good enough, following which it will soon be understood that it is not a question of whether, but a question of when.

5.3 Background on the Development of Simulation Tools

Since their inception in the mid-1980s, time-domain flooding simulations have been used in order to gain a better understanding of complex flooding processes that cannot be captured accurately using static assessment techniques. Early forms of such tools were used predominantly to assess the damage survivability of RoPax vessels, with a focus on cross-flooding and the accumulation of water on deck. Such research was fuelled by a number of major accidents that occurred around this time, including the loss of “Herald of Free Enterprise” in 1987 and the sinking of “Estonia” in 1994, both of which acted as catalysts for development in the understanding that something had to change. One of the earliest examples of such work was the investigation conducted by Spouge when assessing the sinking of the Ro-Ro ferry European Gateway (Spouge J. R., 1986). Here, he employed a quasi-static simulation approach, with flooding rates determined by a simple hydraulic model, leading to one of the earliest reports on the effects of transient asymmetric flooding. Unfortunately, however, it became clear that the abrupt and highly dynamic nature of transient flooding could not be captured accurately using quasi-statics, leading to the development of an improved model by Vredeveldt & Journee (Vredeveldt & Journee, 1991). In contrast, their approach relied on a hybrid simulation model whereby roll motion was captured using dynamics whilst other, less critical, degrees of freedom were dealt with in a quasi-static manner. Journee, Vermeer, & Vredeveldt then later expanded this to account for dynamic motion in all six degrees of freedom (Journee, Vermeer, & Vredeveldt, 1997). In parallel with such developments, Vassalos & Turan (Turan & Vassalos, 1994) developed a 3DoF dynamic flooding model, capable of accounting for the effects of irregular seas as opposed to the calm water assumption made by the majority of other models at the time. This was an important development given that $\approx 70\%$ of accidents occur in waves and shortly after this model was further expanded in order to account for all 6DoF by Vassalos & Letizia (Vassalos & Letizia, 1995). In the years that followed, such tools were further advanced and refined, with Papanikalaou

(Papanikolaou, Zaraphonitis, Spanos, Boulougouris, & Eliopoulou, 2000) applying the “lumped mass concept” in order to better account for internal floodwater dynamics and sloshing effects; a concept which was further developed by Jasionowski and Vassalos (Jasionowski & Vassalos, 2001). Not long after these developments, the first application of numerical simulations to cruise vessels were conducted, perhaps most notably recorded in the works by Vassalos (Vassalos, Ikeda, Jasionowski, & Kuroda, 2004) and Van’t Veer (R. Van't Veer, 2004). In both cases simulations were conducted on large cruise vessels, accounting for motion in all six DoF. The breach sizes examined were in line with that used in the HARDER model tests, namely a two-compartment damage scenario about amidships of 0.033%LPP in length, B/5 in penetration and spanning from the tank top to one deck above the vessel bulkhead deck. In each case, the vessel internal geometry was modelled in detail, both in terms of compartmentation and in terms of openings. Interestingly, despite the similarities between these assessments, two very different sets of conclusions were drawn. On the one hand, Van’t Veer concluded that cruise vessels were predominantly prone to loss of residual stability through progressive flooding rather than transient capsizing. In contrast, Vassalos alerted to the fact that cruise vessels were indeed vulnerable to transient capsizing, citing multiple free-surface effects formed in the early stages of flooding as the causal factor. This should have been particularly alarming given the modest damage size and penetration examined, but instead, the conclusions drawn by Van’t Veer became more widely accepted, fostering the notion that cruise vessels are vulnerable only to progressive flooding. Consequently, the question of transient flooding as regards cruise vessels had been left to sleep for many years until awoken recently in such research projects as eSAFE and FLARE. The results in each case would suggest that both sets of conclusions were in fact correct, having demonstrated that the loss modality experienced by cruise vessels is highly sensitive to input conditions such as GM, breach size and the degree of asymmetry present within the vessel subdivision.

In conclusion, it could be said that time-domain flooding simulations have proven to be a vital asset in assessing vessel survivability, particularly in areas where there is uncertainty over the results yielded by static assessment. Of course, flooding simulations are by no means perfect and are themselves subject to certain simplifications and assumptions. Nevertheless, they enable us to take one-step closer to the reality of the situation.

5.4 Survivability Assessment Process

5.4.1 Preparation of the Simulation Model

Flooding simulations allow for a far greater level of detail within the vessel internal geometry to be captured in comparison to hydrostatic models. Here, all features liable to inhibit or facilitate the flooding process are modelled with consideration of the vessel's entire weathertight envelope, usually spanning two or three decks above the bulkhead deck. This includes the consideration of spaces such as cold rooms, lift trunks, ventilation trunks, escape trunks, stairwells, A-class fire rated structure and watertight divisions. The result is something far more representative of the actual vessel geometry in comparison to static models, which for a medium-sized cruise vessel would comprise some 700 spaces as opposed to the 250 spaces one would expect to find within the static equivalent. The ability to capture geometric details in this way is of particular importance concerning cruise vessels, as the simplifications made within statics often lead to a very reductive representation of the vessel internal arrangement. This is in contrast to RoPax vessels, where the internal geometry is rather simple to begin with and so the level of detail lost is significantly less. Figure 5-1 below provides a comparison between the static and simulation models of a medium size cruise vessel, which has been used in a case study not included within this thesis.

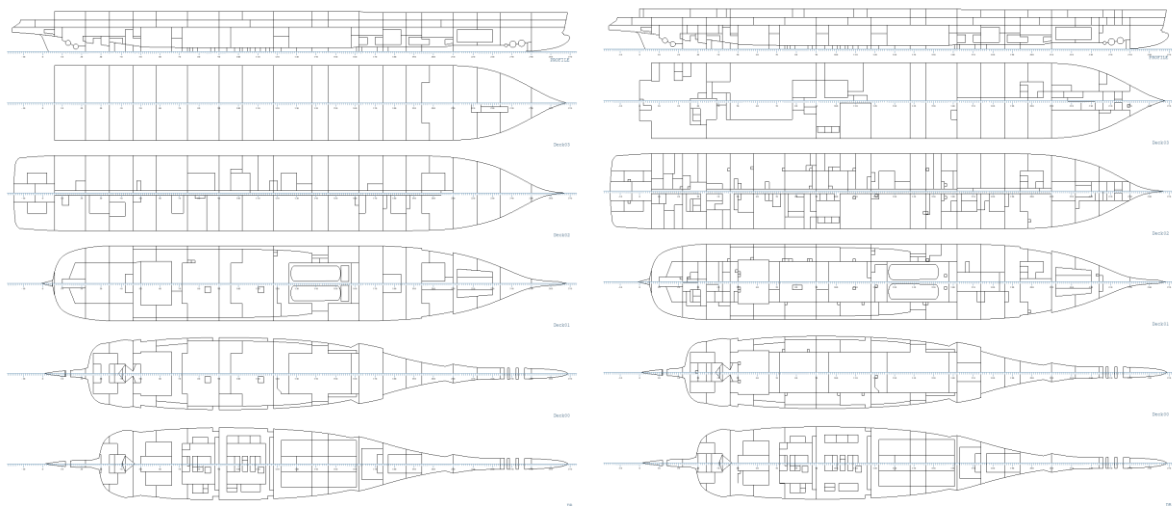


Figure 5-1: Comparison in level of detail captured, static model left, simulation model right

In addition to modelling internal spaces in far greater detail, simulation models also account for internal openings in a manner far more reflective of reality. In general, all openings linking the modelled rooms are accounted for and represented by their physical geometries. Doors are also assigned leakage and collapse properties in accordance with the findings of the EU project FLOODSTAND (Ruponen & Routi, 2011). Here, full-scale tests coupled with FEA analysis were conducted on a number of typical passenger vessel door types in order to determine their

resistance to floodwater, see Table 5-1. Each opening is also assigned a uniform discharge coefficient of $C_d=0.6$, which represents the industry standard for this property. At the time of flooding, all doors are assumed to have a closed status such as to assess vessel survivability in its “best state”, which provides a fair baseline risk level from which to gauge the benefits of additional RCOs. Otherwise, improvements would pertain to vessel operational risk according to its existing design, i.e. recommending certain existing doors be closed in case of damage. Having followed this process, the simulation model of a medium to large cruise vessel would generally contain around 1,000-1,500 openings as shown in Figure 5-2.

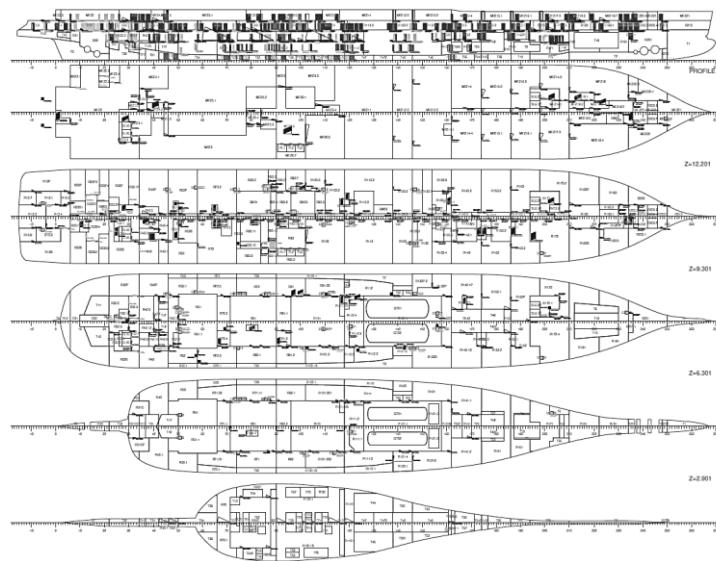


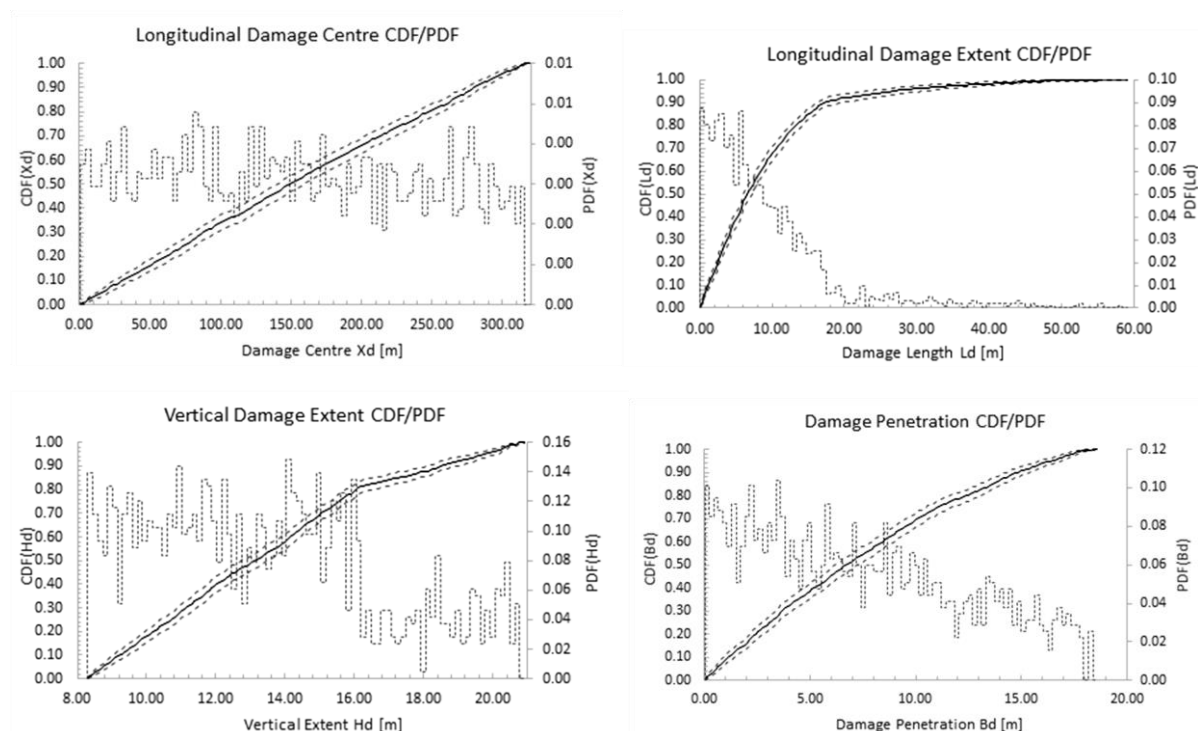
Figure 5-2: Example Opening Arrangement- from case study not included within thesis

Table 5-1: Opening characteristics employed in modelling, based on FLOODSTAND (Ruponen & Routi, 2011)

Type	Direction	H Leak (m)	A ratio	Hcoll (m)
LWT	into	-	-	8
	out	-	-	8
A-class sliding	into	0	0.025	1
	out	0	0.025	1
A-class hinged	into	0	0.02Heff	2.5
	out	0	0.03Heff	2.5
A-class double leaf	into	0	0.025	2
	out	0	0.025	2
Cold room sliding door	into	0	0.01Heff	3.5
	out	0	0.01Heff	3.5
B-class joiner door	into	0	0.03Heff	1.5
	out	0	0.03	1.5
Windows	-	-	-	>18

5.4.2 Damage Scenario Definition

Damage scenarios have been defined by applying Monte Carlo sampling techniques to pertinent damage and sea state probability distributions, producing a multitude of damage breaches characterised by size, location and environmental conditions. The sample size considered varies across the assessments conducted within this research, but no less than 1,500 cases have been considered for any given damage type for reasons explained in greater detail later within this section. A number of different probability distributions have been used in order to inform the sampling process. Firstly, collision damages have been defined according to the distributions generated within the EU project (HARDER, 1999-2003), which form the basis of the current s-factor applicable to all passenger ships, see Figure 5-3. In such cases, the existing distributions have been further expanded in order to account for variation in the lower extent of damage based on the work outlined in (Bulian, Cardinale, Francescutto, & Zaraphonitis, 2019). Though not presented within this thesis, other damage types may also be considered in the application of the methodology described within Chapter 4. Specifically, side and bottom groundings could be accounted for utilising the distributions developed following the extensive work conducted in GOLADS (Papanikolaou, et al., 2013) and later EMSA III (EMSA, 2015). An example of a typical collision breach sample is provided in Figure 5-4.



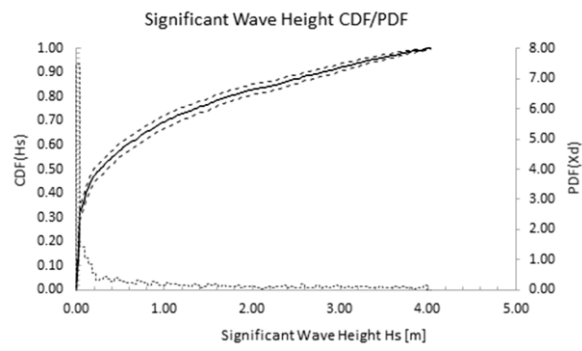


Figure 5-3: Example damage & sea state sample taken from HARDER distributions (HARDER, 1999-2003)

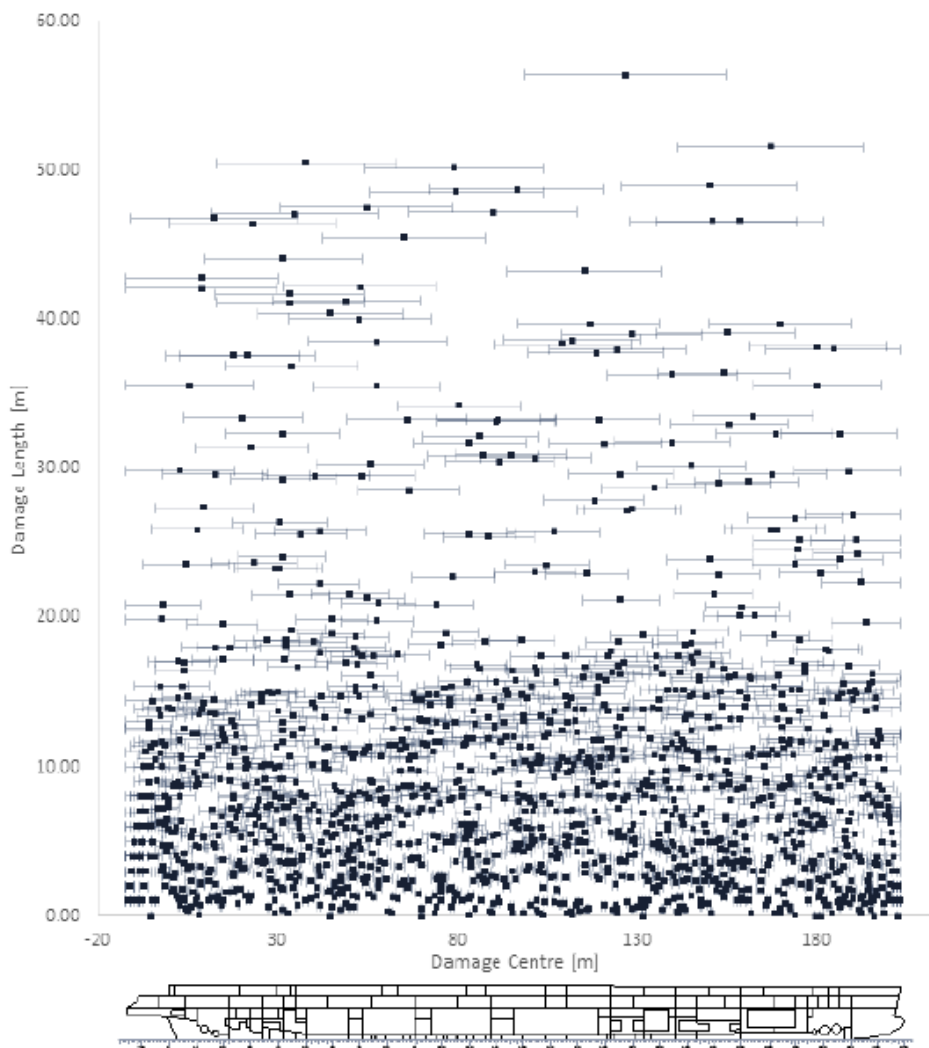


Figure 5-4: Typical collision damage sample for small cruise vessel, sourced from case study not included within thesis

5.4.3 Impact of sample size on error

When generating scenarios by sampling probability distributions, it is important to ensure that the sample is a fair and accurate representation of the underlying distributions. The magnitude of the error incurred here is predominantly a function of the sample size and as such, it is of great importance to ensure that a statistically valid sample is considered. However, as the sample size increases, so too does the calculation time and computational cost, so one must seek to strike a balance between these two competing objectives. In order to make this determination, the Standard Error of the mean has been used to ascertain sample quality and is a measure of the accuracy in which the sample mean \bar{x} reflects the actual distribution mean μ , calculated in accordance with Equation 5-1.

By assessing the magnitude of the Standard Error as a function of sample size, the relationship between these two parameters can be derived, as shown in Figure 5-5 for Hs. Here, it can be observed that there are diminishing returns in error reduction for sample sizes greater than 750 samples. Similar tendencies were identified when assessing other parameters in this way, with a variation ± 50 samples found across all cases. This would indicate an optimal sample size of 700-800 samples, though as indicated previously, no less than 1,500 samples have been considered in this research. The reason a greater sample quantity has been considered stems from the nature of the sampling process itself, which provides a subset of all probable cases with proportional representation of various extents but fails to capture all possible scenarios. This is particularly true in the case of low probability events, which are often poorly represented within small samples. To provide an example, if one were to compare a random damage sample to zonal damages, the ratio of 2-compartment to 4-compartment damages would most likely be the same in each case, however, the sample would only consider a fraction of all probable 2 and 4-compartment cases. As such, by increasing our sample size we capture a greater number of these “black swan” events, even though our error may remain for the most part unchanged.

$$SE = \frac{\sigma}{\sqrt{n}} \quad \text{Eq. 5-1}$$

Where,

σ = sample standard deviation

n = number of samples

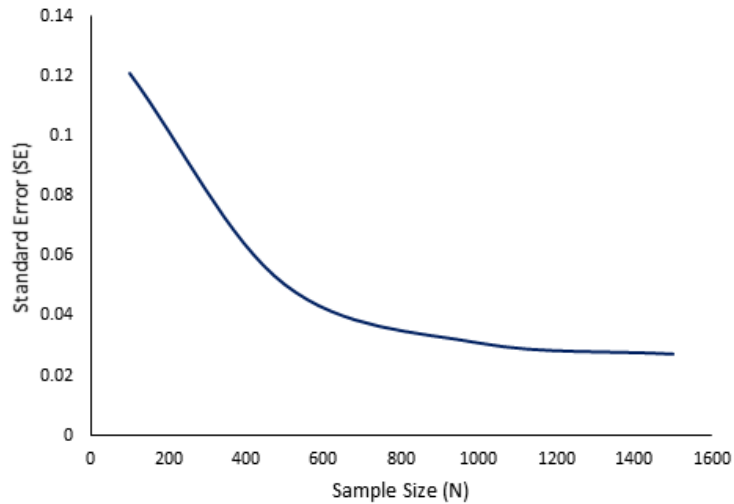


Figure 5-5: Standard Error relative to sample size for H_s

In addition to considering the Standard Error, confidence intervals have also been derived for each sample in order to illustrate the range of confidence across the sample CDF. For this purpose the Dvoretzky–Kiefer–Wolfowitz inequality (Dvoretzky, Kiefer, & Wolfowitz, 1956) has been utilised, which allows different rates in violation to be identified across the range of the distribution, see Equations 5-2 and 5-3. An example of how this error varies relative to sample size is also provided in Figure 5-6, though within the application examples provided later within this thesis, these confidence intervals are featured in the cumulative distribution functions for TTC.

$$F_n(x) - \varepsilon \leq F(x) \leq F_n(x) + \varepsilon \quad \text{Eq. 5-2}$$

$$\varepsilon = \sqrt{\frac{\ln \frac{2}{\alpha}}{2n}} \quad \text{Eq. 5-3}$$

Where,

$F(x)$ = the true sample CDF

$F_n(x)$ = lower and upper bounds

$1 - \alpha$ = Level of confidence, i.e. $\alpha = 0.05$ for 95% confidence

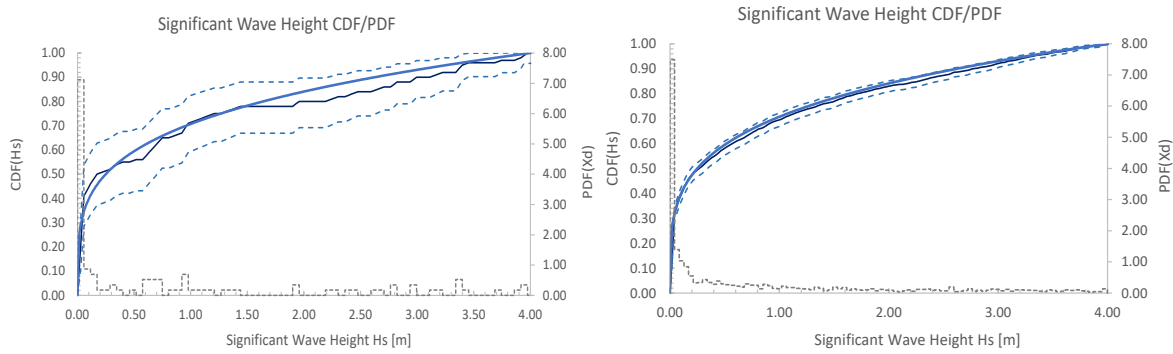


Figure 5-6: Confidence Intervals, 100 samples left, 1,500 samples right

5.4.4 Simulation Strategies

Within the following section, a number of simulation strategies that have been adopted in the undertaking of this research are described. These strategies have been developed in order to act as a means of improving the time efficiency of the process and also to facilitate various forms of analysis, as described in the following. The overarching ethos of the approaches described has been to ensure that effort is not expended in vain, which has been achieved by filtering out cases deemed superfluous to given forms of assessment.

Assessment-base case isolation:

The first simulation strategy that has been employed is founded upon the principle of assessment-based case isolation. Here, information from prior hydrostatic damage stability assessment has been used in order to inform the scenario selection process for subsequent dynamic assessment. There are a number of ways in which this can be done, such as isolating potential transient capsizing cases where intermediate stages are critical or by isolating potential progressive flooding cases where openings are immersed. However, in general these results have been used in order to filter-out “certain survival” cases from the sample. To elaborate further, if it is found during static assessment that certain cases possess residual stability properties far in excess of the requirements, there is nothing to be gained by further subjecting these cases to dynamic assessment. Care, of course, must be taken here such as not to isolate any marginal cases from the sample, where subjection to dynamic simulation could capture phenomena not accounted for during static assessment. As such, only those cases where there is no question as to the outcome should be negated, a typical example of which would be one-compartment damage scenarios pertaining to a large modern cruise vessel. This has the effect of reducing the calculation time without jeopardising the accuracy of the assessment and allows focus to be placed on marginal to severe cases, where a greater wealth of knowledge and information could be gained and where there is greater potential impact from any improvement.

Accounting for the impact of Hs on survivability:

When assigning environmental properties to the scenario sample it has, in some cases, been deemed appropriate to examine the effect of variations in Hs on ship survivability. In such instances, a pragmatic approach has been adopted to this form of assessment whereby the subject vessel has firstly been assessed under the most adverse conditions. This usually entails the consideration of either a constant Hs of 4m relating to the maximum SOLAS sea state, or Hs=7m to be in line with maximum of the IACS global wave distribution (ICAS, 2001). Of course, theoretically any value of Hs could be specified here in order to be in line with the vessel area of operation. Through doing so, one can ensure the vessel is assessed and designed according to the environment to which it will be exposed. Following such assessment, the impact of lower constant or alternatively random sea states can be conducted in a more time-efficient manner. Specifically, those cases found to survive the wave conditions relating to either of the extremities previously described, could be safely assumed to survive in a lesser sea state. As such, these cases can be negated going forward, meaning only a subset of marginal cases within the initial sample need be subjected to further assessment.

Stress Test:

As outlined within the previous section, sampling serves to capture a subset of all probable damages in a manner that is proportionately reflective of the underlying probability distributions. However, such a process can often fail to capture low probability events in any great number, meaning extreme scenarios can be left unassessed. In response to this issue, a modified sampling scheme has been developed in what is referred to as a vessel “stress test”. Here, the most adverse damage length (60m) and significant wave height (Hs=7m) are considered, whilst randomly sampling all other variables. The reason for the latter stems from the fact that shallower damage penetrations or limited damage heights in many cases can give rise to worse conditions than maximum extents. In contrast, there is a clear correlation between damage length and flooding severity, so consideration of maximum length is justified here. The results of such an assessment serve to identify vessel resilience to flooding in the worst foreseeable conditions and this is conducted in the knowledge that these events, improbable as they may be, can occur. After all, if risk assessment predicts the occurrence of major accident once in a hundred years, one can never tell whether this will occur tomorrow, within fifty years or a hundred years from now (Tobias King, 2016).

5.4.5 Initial Conditions

5.4.5.1 Introduction

The probabilistic damage stability concept calculates the Attained Subdivision Index with respect to three loading conditions, which combine to form a theoretical draft range for a given vessel. At each of these loading conditions, a partial index is calculated, and weighting factors are applied in order to account for the likelihood that the vessel will be operating at or near any of these drafts at the time of collision. In this respect, these weighting factors can be viewed as a representation of the vessel operational profile. Currently, the same weighting factors are applied to all vessels covered by the standard in a “one-size-fits-all” manner, with no differentiation made on the basis of ship type. This assumes, in essence, that vessels such as cruise ships, dry cargo ships and RoPax share the same operational profile. However, this is clearly not the case as these ship types are known to have vastly different tendencies in the nature of their operation. Furthermore, there are several other operational factors liable to affect a given vessel's draft range and operational profile that are presently unaccounted for and their influence on flooding risk remains unclear. This includes, but is not limited to, factors such as the vessel area of operation, age, seasonal variations, route, etc.

In light of the above, the following section provides information on the true operational loading behaviour of passenger vessels as a means of determining which initial condition(s) would be most appropriate to consider in the assessment of vessel survivability.

5.4.5.2 Methodology

In the undertaking of this task, historical loading condition data has been sourced from 36 vessels, comprising 27 cruise ships, 6 RoPax vessels and 3 cruise ferries which range between 2 and 38 years in age and 19,800 GT - 227,000 GT in size, see Figure 5-7.

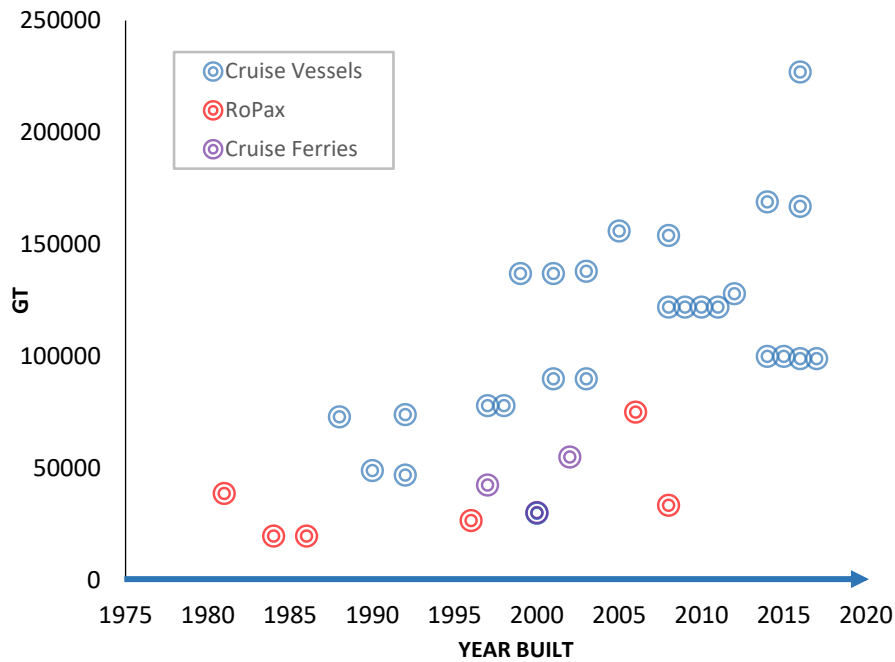


Figure 5-7: Basis Ship Overview

The data sourced includes ship-specific loading condition histories, recorded over a timespan ranging from 1-2 years of operation. By extracting draft readings from this data, draft probability distributions are derived for each vessel and then combined to generate a number of global distributions, accounting for all vessels and specific vessel types. These distributions have been derived with respect to each vessel's assumed SOLAS draft range (ds-dl), which serves to provide a picture of how the vessel is operated relative to the assumptions made in SOLAS.

Due to the large variance in size between the vessels contained within the test group, it was necessary to firstly non-dimensionalise the draft data. Here, the data has been normalised with respect to each vessel's assumed SOLAS 2009 draft range (maximum and minimum draft values according to ds and dl), as outlined within Eq.5-4.

$$T_{ND} = \frac{\bar{T}_i - \min(\bar{T}_i)}{\max(\bar{T}_i) - \min(\bar{T}_i)} \quad \text{Eq. 5-4}$$

Where,

- $\max(\bar{T}_i), \min(\bar{T}_i)$ are the lower and upper limits of the draft range (m)
- \bar{T}_i is a given mean draft reading sourced from the data
- T_{ND} is the resultant non-dimensional draft value

In order to derive a given draft distribution, the non-dimensional draft range is discretised across the range [0, 1] in increments of 0.1 and the frequency in which each vessel has operated within each interval is calculated in accordance with the operational data, as demonstrated within Figure

5-8. This is a similar process to that adopted in the cases of (Meng, Weng, & Suyi, 2014) and (Hollenbach, Klug, & Mewis, 2007), where draft probability distributions have been derived in this manner for various types of cargo vessels along with Ro-Ro passenger vessels.

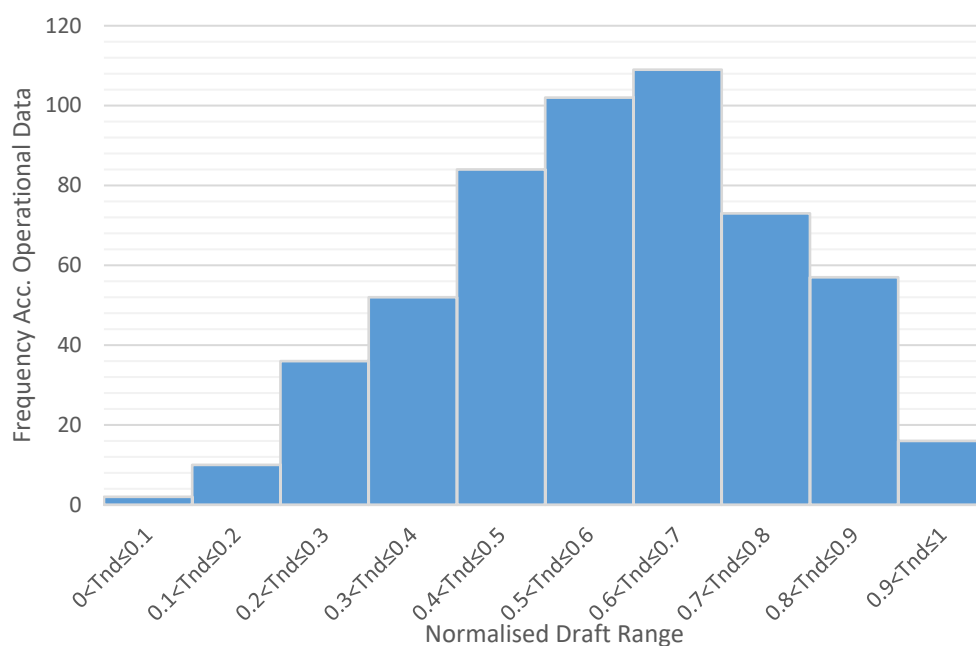


Figure 5-8: Example ND draft distribution

5.4.5.3 Results

In accordance with the process outlined in the previous section, ship specific draft distributions have been derived and subsequently combined in order to yield generalised distributions relating to:

- All vessel data, Figure 5-9
- Cruise vessel data only, Figure 5-11
- RoPax vessel data only, Figure 5-10

Through doing so, it has been possible to assess the manner in which passenger vessels operate relative to SOLAS assumptions. Furthermore, by considering ship types independently, it has been possible to identify any ship-specific operational tendencies and traits. The resultant distributions show, in all cases, a tendency for passenger vessels to operate predominantly within the upper region of their draft range, with this tendency being more pronounced for cruise vessels. However, RoPax vessels were found to operate at the upper extremity of their draft range more frequently than cruise vessels. It should be noted, however, that the average age of the cruise vessels within the sample is 14 years in comparison to the RoPax average of 24 years, so it is reasonable to assume that the cruise vessels within the sample have a considerable growth margin yet to be utilised.

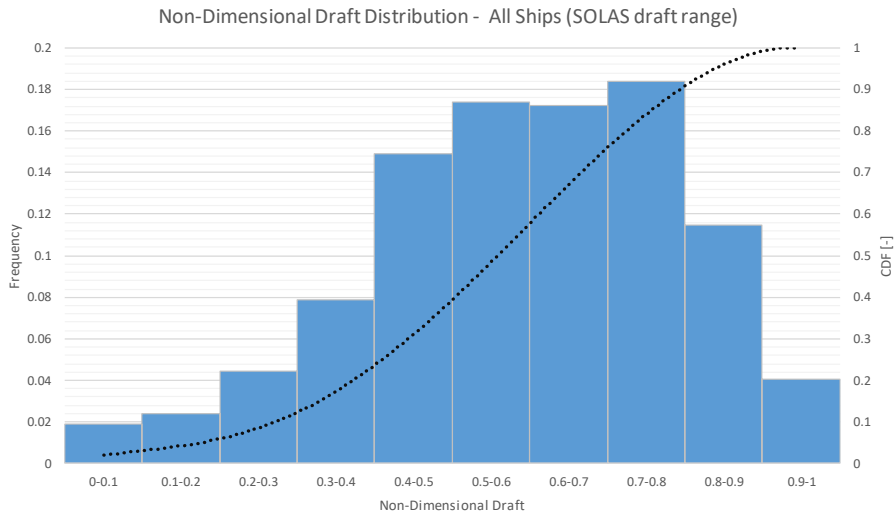


Figure 5-9: Draft distribution relative to SOLAS range for all ships

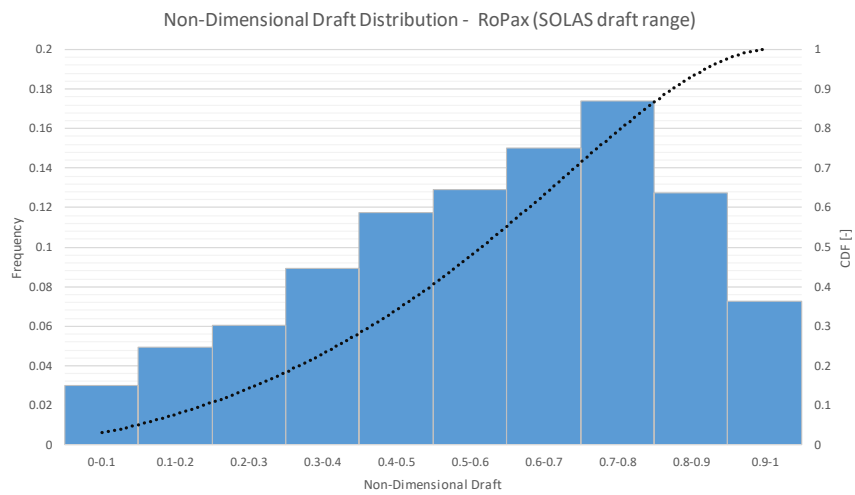


Figure 5-10: Draft distribution relative to SOLAS range for RoPax vessels only

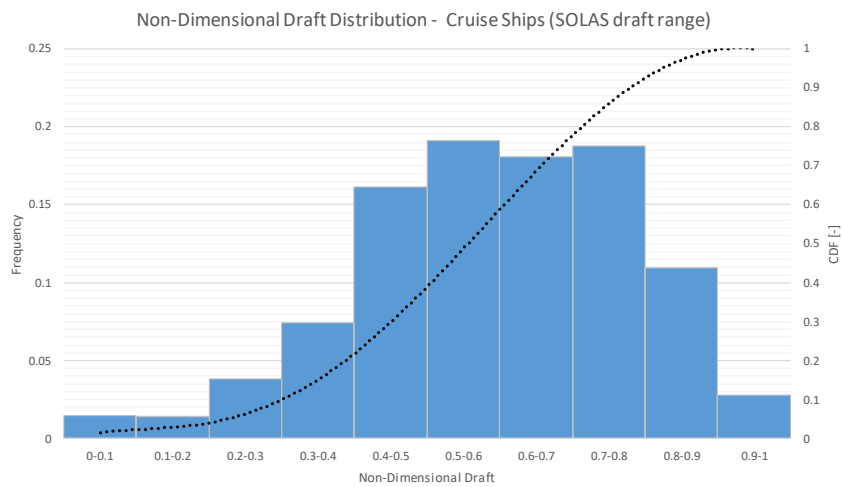


Figure 5-11: Draft distribution relative to SOLAS for cruise ships only

Further to the above, the size of each vessel’s operational draft range (max and min recorded drafts) has been assessed relative to that assumed by SOLAS(ds-dl), as shown in Figure 5-12. Here, the ratio between these two draft ranges is presented for each vessel in relation to the year of their launch, with a ratio greater than one indicating that the operational draft range was found to be smaller than that assumed by SOLAS. The results of this process indicated that majority of the sample vessels, 62.5%, were found to operate within narrower draft ranges than those assumed by SOLAS, of which 50% were found to operate in draft ranges under half the size of their SOLAS equivalent. This was found to be particularly true for younger vessels, where there is a more pronounced disparity between SOLAS assumptions and actual operation.

In such cases where the SOLAS draft range was found to be narrower than the operational draft range, the reason for this was often due to the SOLAS definition of the “Light service draft”, which entails that a full complement of passengers be on-board. In contrast, the operational data for a number of vessels contained loading conditions in which much fewer passengers were on-board, yielding shallower drafts. It is also important to note that despite the draft range being wider in these cases, the frequency in which a given vessel was found to visit the lower end of this range was minimal (4.8% average operational time). This does, however, raise interesting questions with regards to flooding risk and current SOLAS regulations, where the Required Index, evacuation times and passenger-induced heeling moments are based on a full complement of passengers. This is demonstrated for a cruise vessel in Figure 5-13, where variations by as much as 1,300 passengers have occurred. Theoretically speaking, similar ND distributions to those derived in this section for drafts could be generated in relation to PoB. By doing so, it would be possible to identify the operational behaviour of different ship-types with regards to variations in the passenger capacity being utilised. This, in turn, could provide valuable input to risk models for calculating PLL, both with regards to flooding risk in addition to other risk sources.

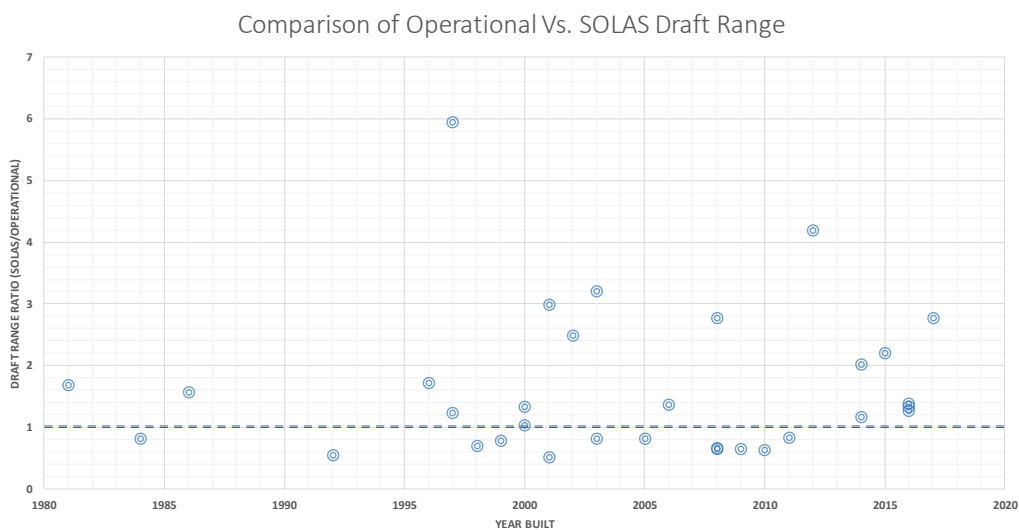


Figure 5-12: Comparison of SOLAS and operational draft ranges with respect to ship age

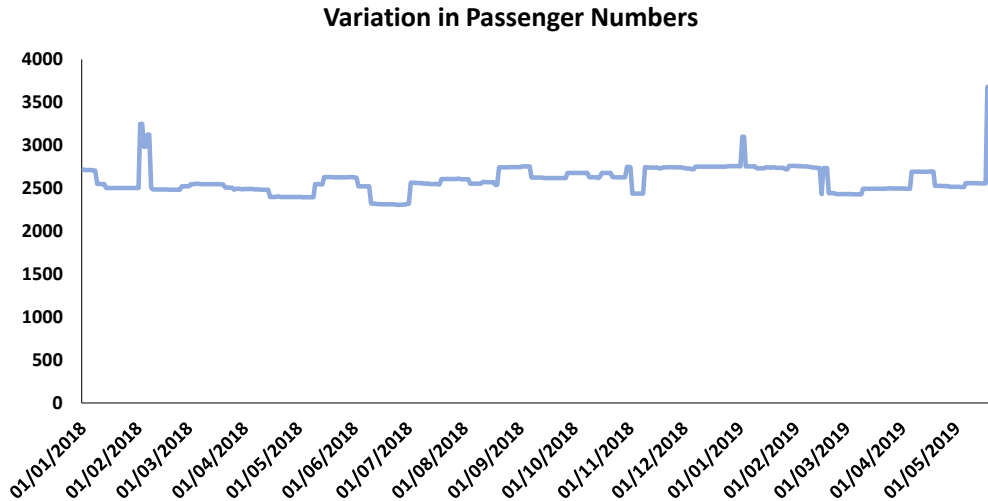


Figure 5-13: Large cruise vessel - variations in PoB over one year

5.4.5.4 Summary

Based on the findings outlined within the foregoing, it has been identified that passenger vessels generally operate within a much narrower draft range than that presently assumed within SOLAS. Furthermore, the evidence would suggest that passenger vessels and particularly cruise vessels operate predominantly within the upper region of their draft range. For this reason, in the undertaking of the survivability assessments conducted within this thesis, a single draft has been considered relating to the vessel design draft at limiting GM, calculated in accordance with statutory requirements. This has a number of benefits, firstly regarding calculation time, which would be much greater if one were to assess a multitude of drafts. Secondly, several of the damage distributions are draft dependant and would entail the generation of draft specific damage scenarios. These simplifications are of course justified, as the sensitivity in outcome across the narrow operational draft range of cruise vessels would likely be negligible.

Further to the above, dry tank conditions have been assumed in accordance with conventional SOLAS calculations. Here, tanks are considered empty and as such may be flooded, although the liquid load is accounted for in the initial condition.

5.4.6 Survivability Estimation

The results of the flooding simulations allow the vessel Survivability Index to be determined, which simply represents the ratio of cases survived to cases lost. This is a time-conditional value, often depicted as the cumulative distribution function of Time to Capsize (TTC), shown in Figure 5-14 for a cruise vessel. Here, the probability of vessel capsizing can be observed with respect to time. The complement of this value then represents the vessel probability of survival, or Survivability Index, conditional on exposure time. In addition, through observation of the shape of the CDF, one can learn a great deal about the modality of the loss scenarios giving rise to the capsizing risk. The CDF of a vessel with a higher propensity for transient capsizing will demonstrate a sharp increase within the lower time range, after which only a gradual increase in capsizing probability will be observed. Alternatively, a vessel with a higher propensity for progressive flooding will possess a CDF with only a slight increase within the lower time range, following which the curve will take on a much sharper incline towards longer exposure times. In addition, the CDF is also shown with 95% confidence intervals, determined in accordance with Eq.5-1. This accounts for statistical uncertainty and provides an upper and lower bound for the Survivability Index.

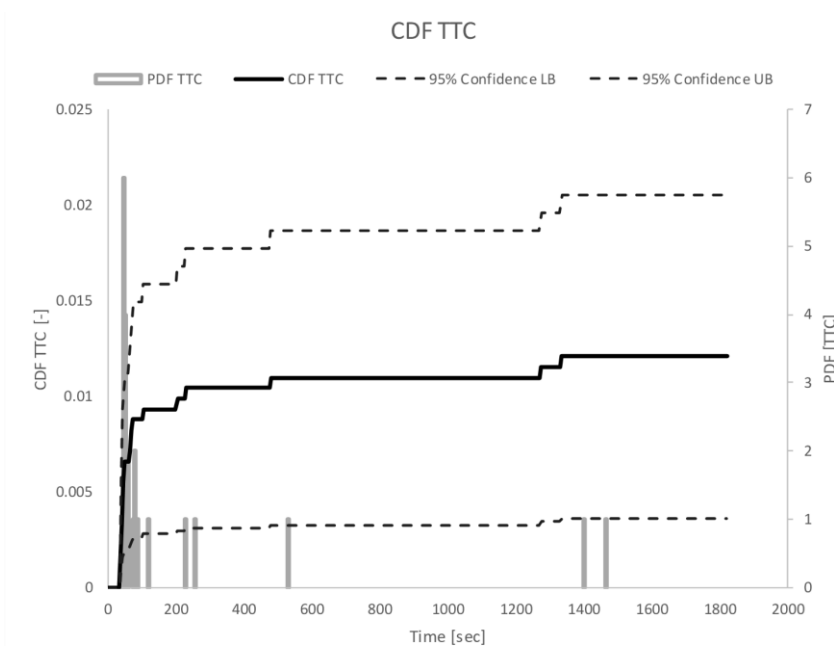


Figure 5-14: CDF for Time to Capsize

5.4.7 Forensic Analysis of Vulnerability Sources

5.4.7.1 Determining Loss Modality

Having conducted the vessel survivability assessment described in the foregoing, there will be a subset of the initial scenario sample identified as capsized cases. These scenarios have then been subjected to a process of detailed forensic investigation, which starts at the highest level with the determination of the modality of loss. This is achieved through consideration of the TTC and roll time-history relating to each scenario, which illustrates clearly if the vessel is lost as a result of transient effects or indeed flooding progression over a greater period time. Figure 5-15 & Figure 5-16 provide examples pertaining to transient and progressive flooding capsized cases, both resulting from an assessment conducted on a cruise vessel.

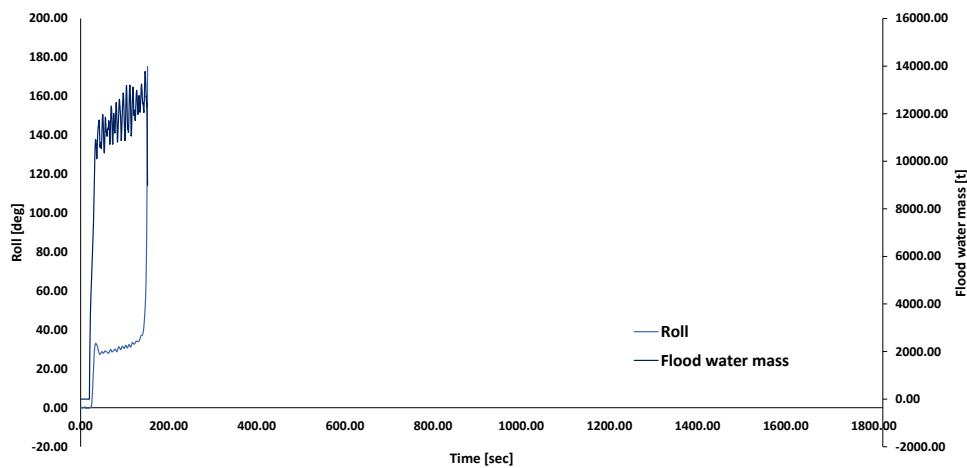


Figure 5-15: Transient Capsize Roll Time-History

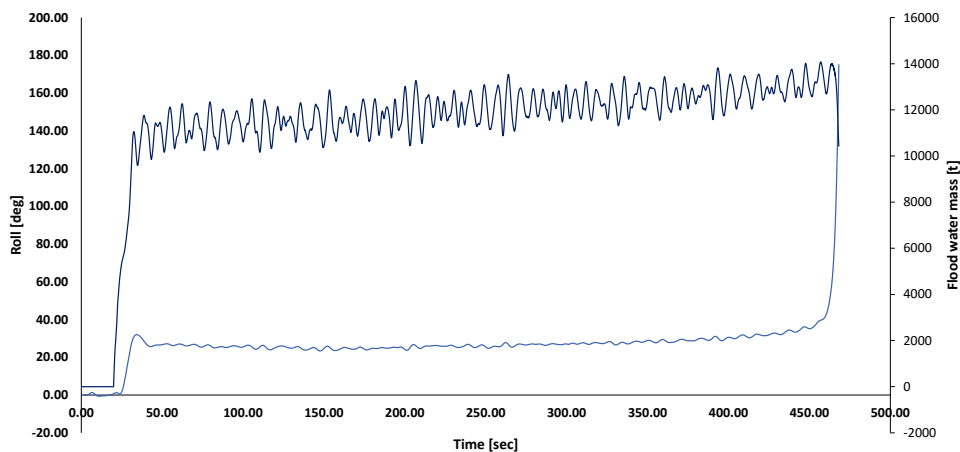


Figure 5-16: Progressive Flooding Capsize Roll Time-History

This is an important first step not only in identifying the root cause of ship vulnerability but also in the development of appropriate RCOs. The determination of whether the vessel is lost because of transient capsized or progressive flooding has a large impact on the nature of the RCO that

should be employed. Firstly, there is the element of time, which in the case of transient capsizing would not allow a system requiring actuation to be used, thus shifting the focus to built-in stability solutions. Alternatively, if progressive flooding were the underlying cause of loss, then the designer would best focus on the openings that facilitate such flooding, as described in the next section.

5.4.7.2 Identification of Critical Openings

The second stage in the forensic investigation relates to the consideration of progressive flooding loss scenarios and the openings through which this flooding occurs. The nature and severity of progressive flooding is dependent on the internal geometry of the vessel, which is a complex environment and one in which attention to detail is of great importance. At the highest level, the susceptibility of a given vessel to progressive flooding can be viewed as a function of the following characteristics of its internal geometry:

- Ability to inhibit flooding progression (WT door, SWT doors, A-class Fire doors...)
- Ability to distribute floodwater favourably (i.e. cross-flooding, up-flooding, down-flooding...)
- Predominance of features that facilitate progressive flooding (Lift trunks, vents, service corridors, undivided spaces...)

Given the above, vulnerabilities in such cases tend to stem from local as opposed to global design features, which calls for a detailed assessment of all such aforementioned features. The results yielded from the numerical simulations provide a lot of information on the flooding process, however, the difficulty comes when managing and processing this information in order to identify vulnerabilities and subsequently effective Risk Control Options.

One of the first ways in which this problem has been approached concerns the evaluation of case-specific floodwater evolutions and the sequence of opening immersion, as illustrated in Figure 5-17. In this example, the time-history of floodwater mass has been superimposed with the openings that are immersed throughout the flooding progression. Here, one can observe an initial rapid accumulation of floodwater within the early stages of the flooding process, in addition to a swift succession of openings becoming involved. This occurs as the initially effected spaces begin to flood and many of the openings involved during early stages are within the immediately breached compartment(s) as equalisation takes place. Following this transient stage, a more gradual accumulation of floodwater unfolds, and this is characteristic of progressive flooding to neighbouring spaces. Here is where focus should be placed in the endeavour to contain flooding and by observing each case in this way, such critical openings can be identified and selected as candidates for protection. In addition, by assessing the flooding chain in this manner, one can attempt to break the chain at the earliest feasible stage, thus limiting the extent of flooding to the

greatest degree possible. It should be noted, however, that a certain degree of care needs to be taken in interpreting this information, as there are both positive and negative forms of progressive flooding, meaning this information cannot be viewed in isolation. Instead, the roll response time-history is often viewed in the same manner in order to determine if the immersed openings are acting to disperse floodwater favourably, i.e. cross-flooding/equalisation, or are generating further asymmetry.

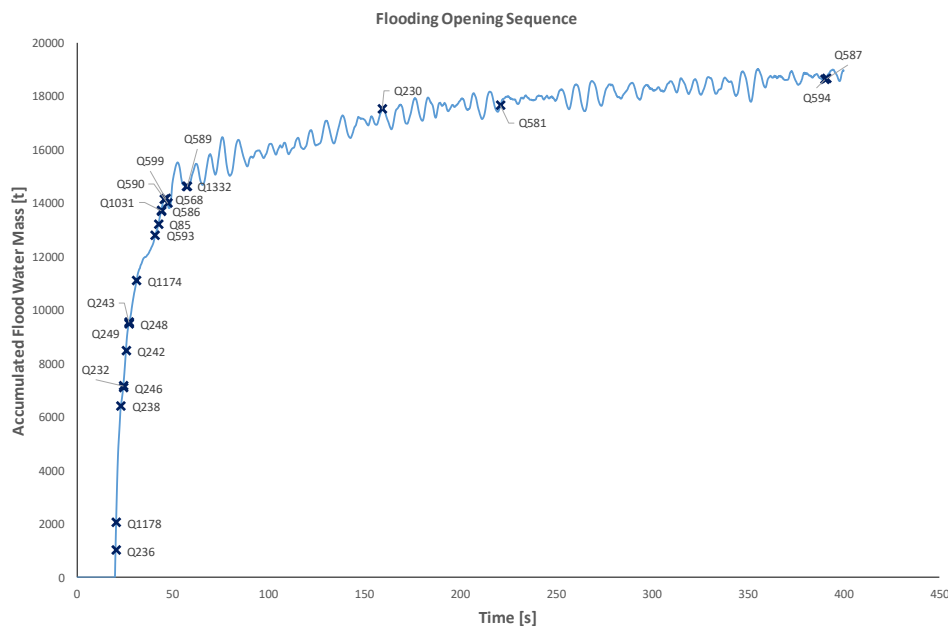


Figure 5-17: Floodwater accumulation and opening immersion time-history

Alternatively, the sequence of space involvement can be called upon, firstly as a means of ascertaining which spaces are involved within the flooding evolution and, secondly, as an indicator of positive or negative progressive flooding occurrence. This is demonstrated in Figure 5-18, where one can observe that the initially damaged compartments form a highly asymmetric distribution of floodwater. This is then followed by those spaces involved in positive progressive flooding in the form of cross-flooding, which works to equalise the vessel and offset the initial asymmetry. The flooding sequence then moves towards gradual progressive flooding and eventual down flooding, both of which represent negative forms of progressive flooding as they work to erode reserve buoyancy and increase asymmetry within the flooding process. As such, through observing the results in this manner, one can deduce which spaces involved within the flooding sequence are involved in negative progressive flooding, following which the openings that form the channels of communication between these spaces and the damage space can be targeted for protection.

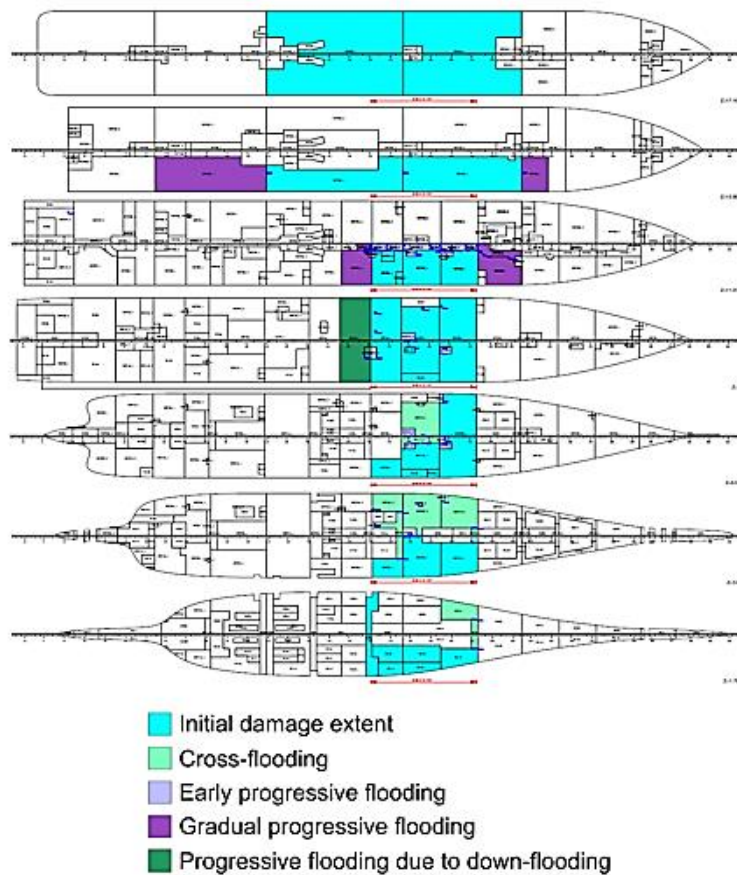


Figure 5-18: Example of Floodwater Progression Mapping

Building on the above, a more general approach has been developed in order to allow for a timely means of ranking openings based on their criticality. This involves a three-stage approach, each of which focuses on a different measure of opening criticality in order to ensure all pertinent vulnerability metrics are accounted for, including:

Stage 1 - Frequency of Occurrence: In this stage, all progressive flooding cases that have led to capsizes have been analysed in order to identify those openings that facilitate flooding progression in each case. The openings identified have then been assessed with regards to their frequency of involvement, thus allowing their vulnerability to be ranked in this respect.

Stage 2 - Net Floodwater Mass Transfer: In recognition of the fact that those openings identified in stage 1 as vulnerable may be of high frequency but low consequence, a second and complimentary assessment has been conducted in which the net mass of floodwater transferred through each opening has been evaluated. This provides a secondary measure of criticality by focusing on severity as opposed to probability of involvement.

Stage 3 - High Floodwater Mass Transfer Frequency: The third and final assessment is a hybrid of the two previously outlined stages. Here, those openings that possess both high floodwater

mass transfer and frequency of involvement are considered, allowing openings to be ranked based on both probability and consequence.

The results of this process produce a ranking of opening criticality as shown within the example in Figure 5-19. Here, openings shown to have a high frequency of involvement in major progressive flooding can then be targeted first for protection, in a top down approach.

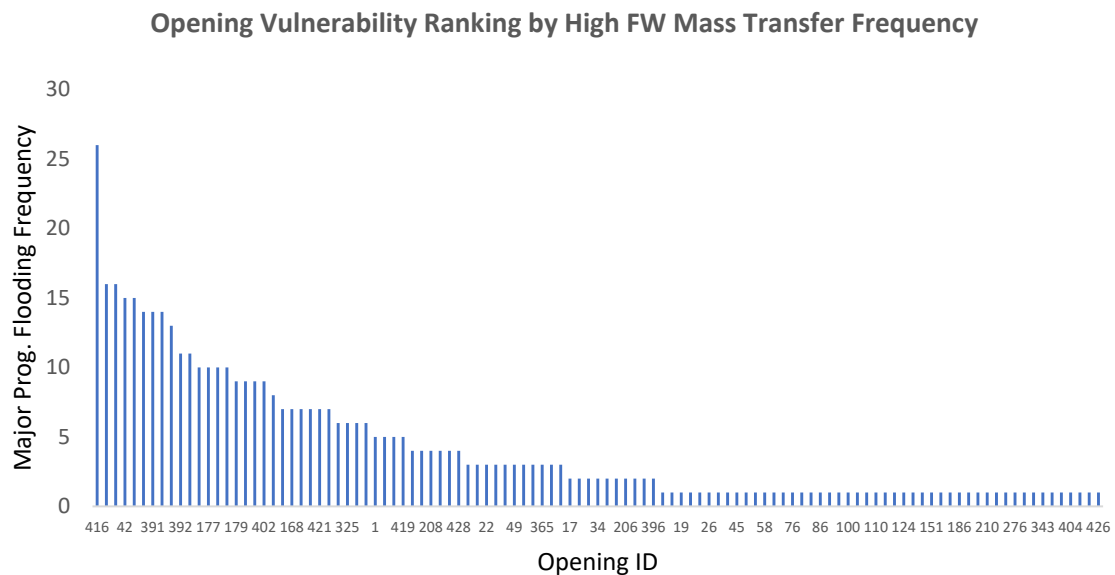


Figure 5-19: Example of opening ranking by frequency and flooding severity

5.5 Closing Remarks

Based on the research presented within this chapter, the following remarks can be made in summary:

- Both the benefits and limitations of damage stability analysis by way of hydrostatic assessment have been elaborated, particularly in relation to cruise vessel damage survivability assessment.
- A solution, or at the very least, mitigating measure for such drawbacks has been described in the form of numerical time-domain flooding simulations, citing prior examples where such tools have been used for exactly this purpose.
- The means by which the scenarios are defined for such assessment have been specified, outlining the uncertainty within this process and also a number of steps that have been taken in order to reduce errors.
- In particular, an extensive study has been conducted looking into the operational loading condition behaviour of cruise vessels, resulting in the consideration of appropriate initial conditions in the survivability assessments conducted as part of this research.

- Furthermore, a number of simulation strategies that have been developed are described, which act to improve time efficiency and also allow for focused forms of analysis to be conducted. Such processes are essential, not only in the undertaking of research, but also in practice, if these tools were ever to be institutionalised within industry.
- Finally, the means by which vessel survivability has been gauged, following flooding simulations, is described in addition to the detailed forensic analysis processes that have been undertaken. This provides the ideal basis from which to progress into the development stage of appropriate RCOs, as described within the next chapter.

Chapter 6: Passive & Active Reconfiguration for Damage Stability Protection

6.1 Opening Remarks

Within the previous chapter, the process by which vessel loss modalities and their root causes may be identified was elaborated. Building upon this, the present chapter serves to outline how this information has been utilised to its fullest for the design and development of a number of novel RCOs intended to cater for specific loss mechanisms. This contrasts with conventional approaches based upon static assessment, whereby the actual mode of loss is only accounted for in an unstructured way, if indeed at all. As touched upon in Chapter 5, this derives from the fact that current SOLAS regulations do not accommodate transient capsizes in an appropriate manner as they rely on a quasi-static treatment of a highly dynamic event. In addition, progressive flooding is also dealt with in a simplistic manner, through truncating the GZ curve at the earliest immersion of unprotected openings, thus telling us nothing of the wider floodwater evolution. This, in turn, drapes a shroud of uncertainty over the efficacy of RCOs founded upon such analysis and questions soon arise as to their performance in more realistic scenarios. Risk Control Options are designed with the sole intention of “mitigating and controlling” risk and as such, there is great importance surrounding the method by which risk is determined/calculated. Alarmingly, depending on which method is adopted, very different RCOs may appear favourable, which naturally evokes questions as to which risk metric is the correct one to go by. For this reason, where there is uncertainty, it is important to employ various forms of assessment in the determination of RCOs and to understand the limitations of each. If there are disagreements in outcome, it is then important to determine why this may be the case in order to make an informed choice. After all, without the right information underpinning the design process, any resultant RCO would be equivalent to a house built on sand. For this reason, there is a strong link between the assessment process outlined within the previous chapter and the means by which the RCOs proposed in the following have been developed. Furthermore, the RCOs proposed seek to venture into what has hitherto been somewhat uncharted and underutilised territory, namely the use of active forms of damage stability protection in conjunction with passive forms. The aim here has been to bestow upon the designer the gift of choice between active and passive measures, thus broadening the design space and providing them with some much-needed breathing room in an increasingly demanding regulatory system fuelled by rising societal expectations. A similar choice is being offered to the operator in addressing life-cycle damage stability management problems as well as in real emergencies on board. The intention here is not to espouse active measures over

passive ones, but instead to encourage the development of alternative measures to be used in harmony with existing passive measures. As is described later within this chapter, both have their strengths and weaknesses depending on the loss modality being addressed and guidance is presented on how to determine suitability in this respect. In total, three systems are proposed as outlined briefly within Chapter 1, which are extensively described within the following. In each case, foam technology is used as the working medium for either flooding containment, suppression or both and each system shares in common the effect of reconfiguring the ship environment to improve damage stability. The name that has been allocated to such solutions is Adaptive Reconfigurable Environment Safety Technology (AREST) and each system is categorised depending on the loss modality they best cater for as reflected through the nature of reconfiguration they offer. Furthermore, system-specific applications are provided in order to demonstrate their effect and the chapter closes by considering some of the important steps that must be taken in the approval of such systems.

6.2 Targeted Solutions for Transient Flooding Protection

6.2.1 Transient Flooding Overview & Pertinent RCO Considerations

The transient stage of flooding occurs in the period immediately following the damage breach, as explained in Chapter 1. During this stage, floodwater begins to rush into the vessel, inducing a rapidly increasing heeling moment generated by the floodwater mass (the name given to this phenomenon by John Spouge is “transient asymmetric flooding”, though such asymmetry could be bimodal). This, in turn, has the tendency to incite a large heeling response, which has been found in some cases to immerse the vessel up to two decks above the bulkhead deck (Khaddaj-Mallat, Rousset, & Ferrant, 2009) (Vassalos, Jasionowski, & Guarin, 2005). If these decks lie within the damage extent, they are liable to experience rapid flooding, accumulating substantial floodwater with free surfaces across a multitude of decks and spaces. The above effects can be exacerbated further depending on the degree of asymmetry present within the vessel internal architecture/space configuration. Where compartments are subdivided by even marginally watertight partitioning, such as A-class firewalls and insulated cold room walls, this can retard the flow of floodwater transversely within the compartment, thus inhibiting effective equalisation. The combination of all the aforementioned effects then has the potential to give rise to rapid capsize and alarmingly this is true even in the case of large passenger vessels (Vassalos, Ikeda, Jasionowski, & Kuroda, 2004). For this reason, transient capsize represents the most

dangerous form of flooding, as it leaves neither time for damage control actions to be executed nor time for evacuation. As a result, any form of transient loss will likely invoke a high cost in terms of human life.

With the abrupt nature of such events rendering any operational damage response activities ineffective RCOs aimed at reducing transient flooding risk must be built into the design, such that they are immediately effective following damage in the form of a residual up righting moment. In addition, when designing in order to avoid transient loss, one must first consider the elements that give rise to such incidents, the primary sources of which are as follows:

- Inadequate initial stability, GM.
- Ineffective subdivision, especially in large undivided spaces above the bulkhead deck
- Sources of asymmetry within the vessel subdivision or inadequate systems in place to offset asymmetries.
- Insufficient reserve buoyancy and inappropriate distribution of such.

In respect to the above causal factors, perhaps the most difficult to amend is lack of adequate initial stability. This is particularly true in the case of cruise vessels, where tight weight restrictions and the delicate balancing of weights makes any reduction in KG an incredibly difficult task. This leaves only global design changes as a means of increasing stability, such as increased beam and freeboard, which would be highly costly and impractical within the latter stages of the design process. Given the above, the most efficient means of avoiding transient loss is to focus on mitigating asymmetries within the vessel subdivision and, in some cases, increasing reserve buoyancy by reducing permeable volume within the hull envelop (reconfiguration of the internal ship space). The former can be achieved by improving vessel cross-flooding in order to reduce the effects of floodwater-induced heeling, either by employing cross-flooding ducts or by focusing on openings and partitions that inhibit transverse equalisation. However, this is by no means an easy task. The effectiveness of cross-flooding arrangements can have limitations concerning the damage size they can cope with, or else, extremely large cross-flooding ducts are required in order to provide ample capacity. Furthermore, longitudinal partitions are in some cases essential in order to segregate and protect vital systems/machinery and, therefore, cannot be removed without jeopardising such systems. More important still, is the fact that any equalisation by means of transfer moment suffers from the fact that untimely action could exacerbate the very problem it was meant to solve, namely the induced heeling moment could add to the floodwater moment if the two actions were in phase.

Alternatively, reserve buoyancy can be provided to the vessel by means of partial bulkheads located within the upper decks, which act to provide reserve buoyancy high within the vessel,

yielding large restoration forces when immersed during the transient roll cycle. However, the problem with such solutions is that they normally encroach on hotel and entertainment areas, where open spaces are favoured, and aesthetics are crucially important.

6.2.2 AREST P1 System Description

6.2.2.1 System Overview

In recognition of the previously described limitations relating to existing transient flooding RCOs, the “AREST P1” system has been developed as part of this research, offering operators a highly effective means of enhancing stability margins whilst also being simple, non-intrusive, lightweight and easily installed.

The system utilises strategically located fixed foam installations as a means of providing buoyancy and, more importantly, stability within vulnerable vessel areas. These are identified in accordance with the process outlined within Chapter 4, targeting preferably un-utilised void spaces within such vulnerable areas. These often exist as wing tanks situated on the outer perimeter of accommodation and machinery spaces, the nature and location of which offers two key benefits. Firstly, as these spaces are generally waste volume, the application of permanent foam does not affect the utility of any spaces currently in use and, as such, the day-to-day operation of the ship is not impaired in any way. Secondly, as these spaces are located high and wide within the vessel, the restoration moments generated by the fixed foam installations are maximised, thus greatly improving system efficiency (high stability, low foam volume). Another, very important, service of such an application relates to ship damage survivability in waves where scenarios pertaining to transient flooding are primarily linked to low GM. As such, increased GM is the only manner in which such scenarios can be avoided, presenting an added advantage in that damage survivability is considerably improved also. This is an extremely innovative way of tackling such a major problem, experienced by most ships.

The system can be applied to both new builds and existing vessels. In the first case, offering an effective means of widening stability margins and futureproofing the vessel against inevitable weight growth high within the vessel throughout its service life, and in the second case, offering a simple, yet highly effective, means of restoring GM margins within existing ships.

6.2.2.2 System Functional Description

The system working principle is simple and concerns the provision of additional reserve buoyancy and stability to a vessel within the damaged condition. This is achieved through the application of permanent foam installations in vulnerable areas, in particular targeting un-utilised void spaces. As mentioned previously, the nature of these spaces is such that they are

often located along the inner edge of the hull, meaning maximum restoration moments can be realised where foam installations are fitted. Inversely, it is important to consider that in the absence of these foam installations, floodwater occupying these spaces would lead to maximum overturning moments and asymmetries and thus the benefits are twofold. When in place, such installations act much like buoyancy tanks, with the added benefit that they are an impermeable volume and, as such, can provide buoyancy within the immediate damaged area. Furthermore, this buoyancy is directly available following flooding as it is built into the ship voids and does not require actuation of any kind. This is particularly beneficial in cases where the vessel loss modality is transient capsizing, which does not permit any time in which to enact active means of damage control. Such a system, though novel in the application to large vessels and the location sites chosen, is not entirely without precedent. A number of administrations currently allow for such applications in small craft vessels as outlined within (AMSA, 2011) and (USCG, 2012).

Installation of the system is achieved with portable foam generators, which pump foam resin and hardener compounds to a static mixing nozzle located within the application site. Upon mixing the two compounds, an exothermic reaction takes place that leads to polymerisation and foam generation. The foam initially takes on a liquid form that will follow the path of least resistance, thus ensuring a homogenous distribution within the space. In areas where there are large volumes of foam required, this process may have to be conducted in several stages, filling the space layer by layer in order to maximise the foam expansion ratio. Application of the system is also highly flexible and can be conducted even where there is minimal to no existing access. This is achieved by boring entry holes in the existing bulkheads large enough to insert the foam-mixing nozzle (\approx DN10/17.15mm), following which foam can be pumped into the target space from an adjacent location while being monitored via umbilical camera. In cases where the application site has connectivity to neighbouring spaces, through openings or penetrations, shielding can be erected in order to prevent foam migration. Where existing systems are present within the application site that may require access such as pipe routing and cable trays, provisions are made in order to ensure such systems are accessible following foam installation. Generally, such spaces are avoided but if necessary foam material can be cut away or protective screening can be erected in order to allow access to vital components, as shown in Figure 6-1.

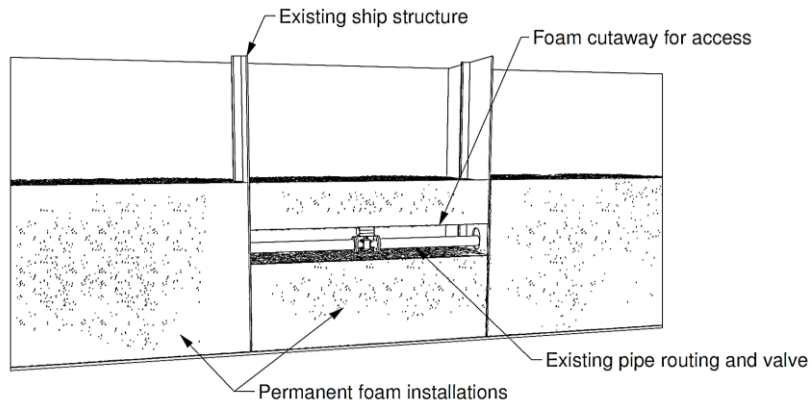


Figure 6-1: Example of foam cutaway for access to systems

During application of the foam components, the exothermic reaction that ensues can give rise to temperatures of the order of 100°C. As such, any heat sensitive materials or equipment are to be shielded during application, which is ensured using foam panels of the same composition as the system foam, which act as an insulating body. Upon installation, the foam will adhere to the vessel steel structure, where it acts as a protective/anti-corrosive coating that prohibits the build-up of moisture between the foam and the ship structure as well as shielding the structure from air, Figure 6-2 & Figure 6-3. Once in place, the foam acts as a dormant body, which will last without degradation for a period of 50-100 years.

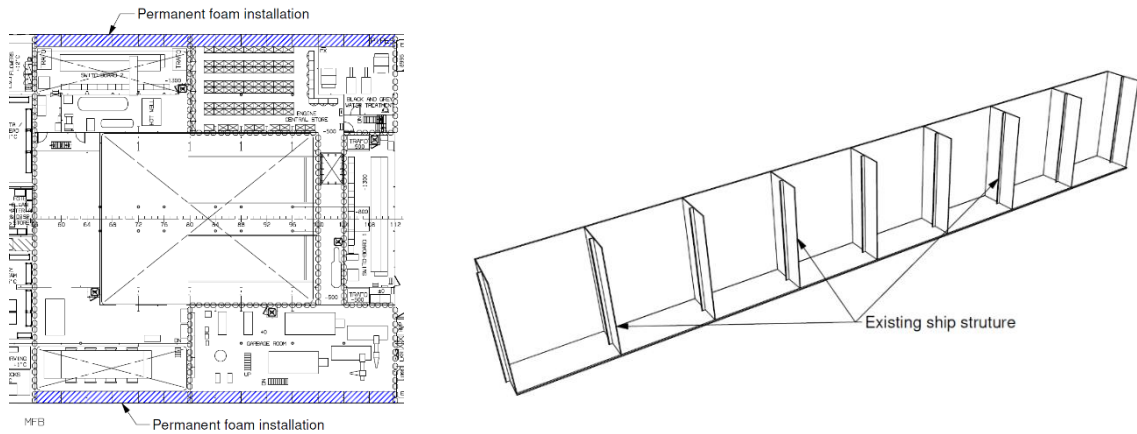


Figure 6-2: Example application site within large cruise vessel double hull

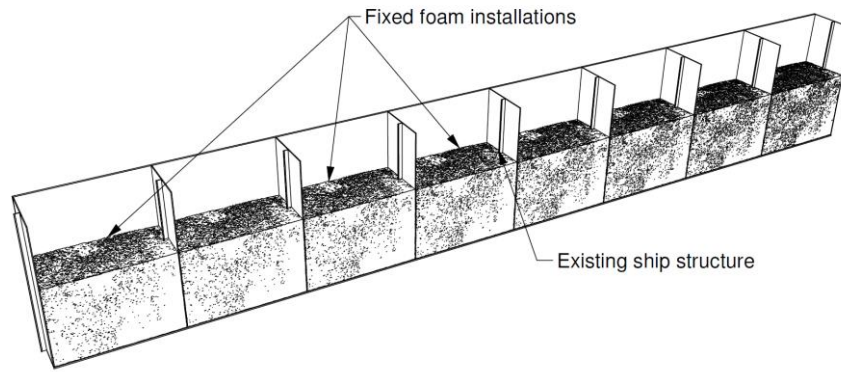


Figure 6-3: Example foam installation

6.2.3 AREST P1 Impact Example

In order to illustrate the effect of the AREST P1 system, the details of a typical application are provided within the following. Here, a large cruise vessel has been examined, having demonstrated vulnerability to transient capsizing in damages surrounding the vessel fore shoulder. For this reason, unutilised void spaces within this region have been targeted for application of the AREST P1 system and an example of such installations is provided in Figure 6-4, shown in blue. In this example, cavities behind cabin linings have been selected that are situated just below the vessel bulkhead deck and above the intact waterline, meaning that the buoyancy reserves gained act with immediate effect during the transient response.

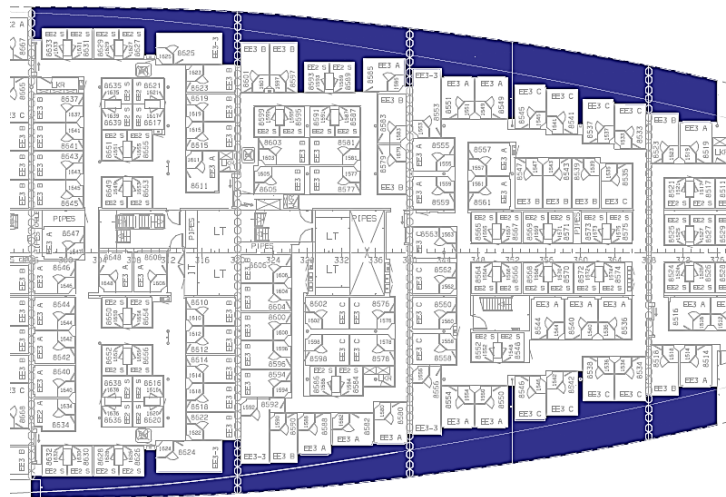


Figure 6-4: Example foam installation, vessel fore shoulder

In order to demonstrate the impact of this solution, the vessel has been subjected to numerical time-domain simulations, considering one of many transient capsizing cases identified within this area as an example. For the purposes of comparison, the vessel has firstly been assessed in the as-built condition and subsequently with the AREST P1 system installed (more details are

provided in Chapter 8). A representative result stemming from this process is shown in Figure 6-5 below, where the floodwater mass and roll time histories are presented for each case. In the as-built condition, the vessel undergoes a sharp increase in floodwater mass, generating a transient roll angle of 20 degrees. The vessel then hangs at this angle for a short period before abruptly capsizing following some 250 seconds. In contrast, with the AREST P1 system installed, the vessel transient response is vastly diminished, reaching only 6 degrees before promptly recovering to a stationary state of approximately 2 degrees average roll. This is a remarkable difference in outcome and stems from the far greater damaged GM afforded to the vessel by the passive foam installations.

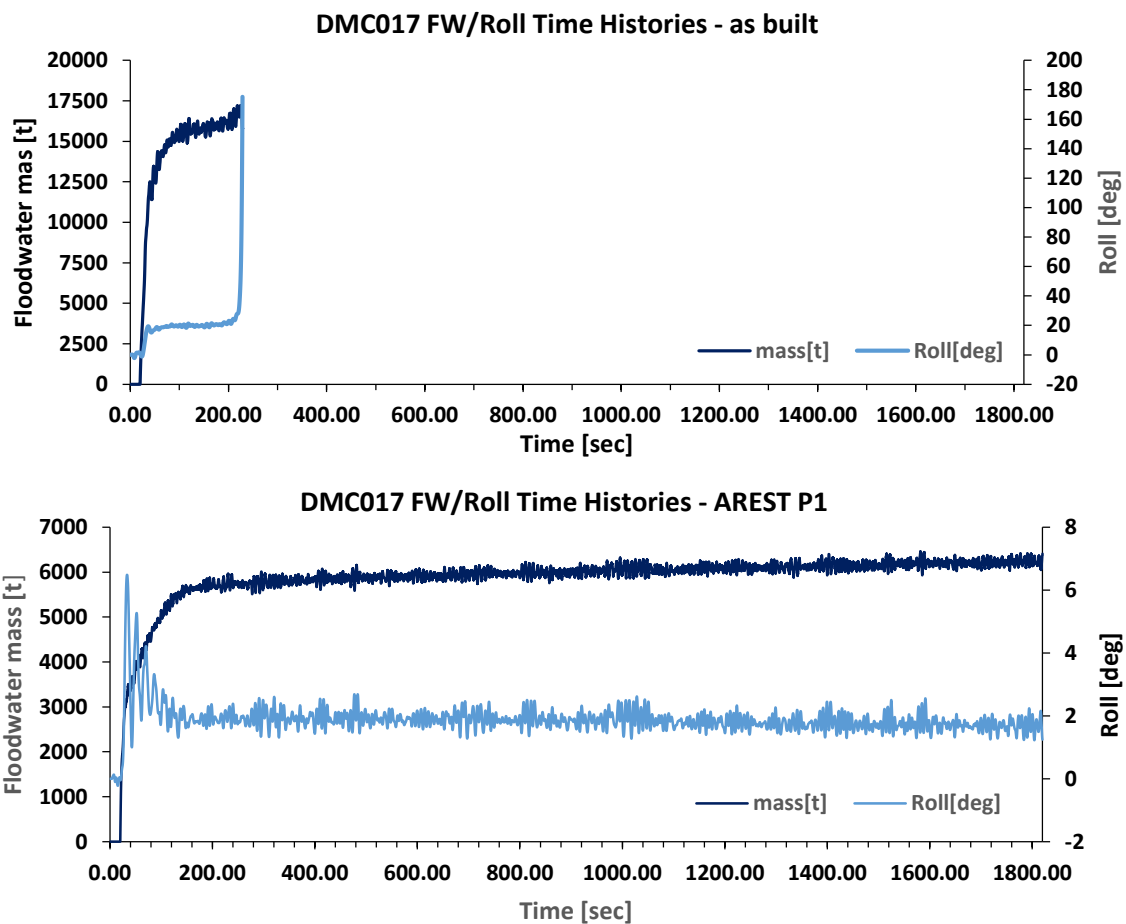


Figure 6-5: Floodwater & roll time history comparison, with and without AREST P1

6.3 Targeted Solutions for Progressive Flooding Protection

6.3.1 Progressive Flooding Overview & Pertinent RCO Considerations

The progressive flooding stage follows survival of the transient stage and occurs in such cases where there is active communication between the initially damaged compartment(s) and adjacent spaces. This communication can exist as either non-watertight openings or partitions and provided such features have become immersed, whether as a result of the vessel floating position or in a wave-induced manner, progressive flooding will inevitably occur. As this takes place, floodwater begins to propagate throughout the vessel into undamaged spaces, which has the effect of eroding vessel reserve buoyancy and stability. If left unabated, this can gradually cause sufficient stability/buoyancy loss, such that the vessel will either capsize or founder. The rate and manner in which progressive flooding occurs depends greatly on the internal geometry of the vessel and, in contrast with transient loss, can take from several minutes to hours.

When considering Risk Control Options intended to reduce the risk stemming from progressive flooding, there are two important distinctions to be made in comparison with transient loss, the first of which relates to time. While transient loss occurs over a very short period, progressive flooding loss occurs over a much longer duration. Importantly, this means time is afforded to the crew in order to enact damage control measures, meaning RCOs can come in the form of either design measures or alternatively active/operational measures. The second important distinction relates to the condition of the vessel following damage. When a vessel experiences transient loss, this is due to the vessel having insufficient stability to survive the very immediate damage extent. In contrast, when a vessel endures a damage leading to progressive flooding loss, it starts from a position of sufficient stability with which to survive the damage, following which its stability is gradually diminished over time due to floodwater propagating into intact spaces. In realisation of this fact, one can deduce that the most effective way of mitigating progressive flooding risk is to provide the vessel with the means to cut off the channels of communication between damaged and intact compartments. To date, this has primarily been achieved through the implementation of fixed partitioning, most commonly in the form of watertight and semi-watertight bulkheads accompanied by doors of equal watertight rating, providing a solution that is effective to a certain point. However, it is becoming ever more apparent that the use of bulkheads and watertight partitioning alone is no longer capable of meeting modern safety demands. One illustration of this point is in the progressive manner in which more is being demanded of the service deck in terms

of the provision of residual stability. This, in turn, has led to such areas being heavily subdivided with partial bulkheads, SWT doors and other such features, all of which add complexity to the arrangement, affect operability and are only rendered partially effective due to the requirement for service corridors to span this deck, which act as a conduit for progressive flooding.

Such problems arise in the attempt to satisfy what are in fact two conflicting objectives, namely, to design a vessel with high levels of ergonomics and operability whilst also being safe with regards to damage stability. The former relies heavily on the ease of ingress and egress between spaces, which is counter intuitive in relation to the prevention of floodwater propagation, where the opposite is favourable. The answer to this problem could lie in more effective utilisation of damage control and there is a tendency in this direction. When SOLAS 2020 came into force on January 1st, 2020, a new regulation within Chapter II-1, Regulation 19-1, was introduced and mandates that damage control drills are conducted on board at least once every 3 months. Damage control holds great potential for damage stability risk reduction, but at present is limited. Damage control is, after all, only ever going to be as effective as the means by which the crew are afforded in order to “control” the damage. Currently, there is very little that can be done other than closing watertight and weathertight openings along with other pertinent valves, all of which have limited flexibility and fail to provide a truly active/effective means of controlling damage. The closest form of active damage control is counter ballasting, which differs from other measures in two primary ways. Firstly, some form of informed/intelligent actuation is required and secondly it can be tailored to the given scenario in relation to both the amount and location of ballasting to be employed to alter the vessel floating position. However, there is limited flexibility here concerning the capacity of ballast water that can be employed and there is uncertainty surrounding the availability of such systems post flooding. Furthermore, depending on the location of the damage, counter ballasting may be rendered ineffective or indeed counterproductive, given that when the vessel is rolling in waves, an induced moment needs to be suitably timed. Ultimately, counter ballasting offers only a symptomatic treatment and not a cure in that it does not deal with the cause of excessive heel but instead works to mitigate the effects of the cause.

In recognition of the aforementioned limitations in existing active forms of damage control, two further RCOs have been developed within this research. This has been conducted with a focus on active space reconfiguration, with such solutions herein referred to as Adaptive, Reconfigurable Environment Safety Technology (AREST), as explained in the foregoing. Reconfiguration in each case is achieved by different means, firstly through in-situ foam deployment within vulnerable spaces (AREST A1) and secondly by active partitioning of internal spaces/volumes (AREST A2), both of which are described in detail within the following sections.

6.3.2 AREST A1 System Description

6.3.2.1 System Overview

The AREST A1 system has been designed as a means of active intervention in the event of loss of hull integrity and therefore the buoyancy within critical damaged compartment(s). This is achieved by deploying high expansion foam to vulnerable ship compartments when damaged in order to suppress, contain and control floodwater progression, thus enhancing vessel damage stability performance. The most noticeable effect of this is a reduction in lost buoyancy stemming from the prevention of progressive flooding, further complemented by the potential to displace floodwater from the compartment in some cases. In addition, free surface effects are also mitigated by restricting the movement and volume of mobile floodwater within the compartment. Improved survivability in this case is ascertained by modifying compartment permeability, which in turn has a positive effect on the vessel Attained Index. It is envisaged that this system is best utilised by targeting vulnerable spaces, including those which, although normally accessible during vessel operations, have a large effect on vessel damage stability performance. In this respect, the system operates in a similar manner as a fixed fire suppression system introduces CO₂ into a space to extinguish a fire.

The improved damage stability performance provides a significantly increased range of safe operation for the vessel, without affecting the use of the protected spaces during their normal service and other activities. This system can be applied to both void spaces and normally manned spaces, having a warning and evacuation system in place, which is equivalent to, for example, the alarms for a fixed fire suppression system. Where machinery spaces are protected by the system, consideration needs to be given on a case-by-case basis for the criticality of the systems within the compartment and whether any of their functionality is required by remote control after deploying the system. The main action of the system is to enhance the residual damage stability characteristics and not to protect the equipment within the spaces. It may be that after deployment the vessel will remain upright but with reduced functionality, in which case there may be a loss of power or certain machinery systems. However, this is considered secondary to the extended evacuation time and ease of egress afforded by the vessel being maintained in a favourable floating position for longer, if evacuation is in fact needed at all. After deployment, the resins will set to a solid foam mass, effectively becoming fixed foam buoyancy as in the case of the AREST P1 system. As such, this foam body will then need to be removed by external mechanical means and specialised cleaning methods in order to access into the compartment and the items within it.

6.3.2.2 System Functional Description

AREST A1 system consists of a fixed supply of both foam resin and hardener agents; each stored within an individual tank. The tanks are made of steel or plastic (see Figure 6-6), with both tanks connected to dedicated-piping networks for distribution of each foam component to the protected compartment(s). A gauging and sampling pipe on each tank allows the tanks to be sounded and for periodical samples of each component to be extracted for testing. Tank ventilation and vacuum relief is provided by a solenoid actuated valve that opens when the system is energized. This is also backed up by secondary vent line with a manual valve for maintenance along with filling and draining when not powered up.

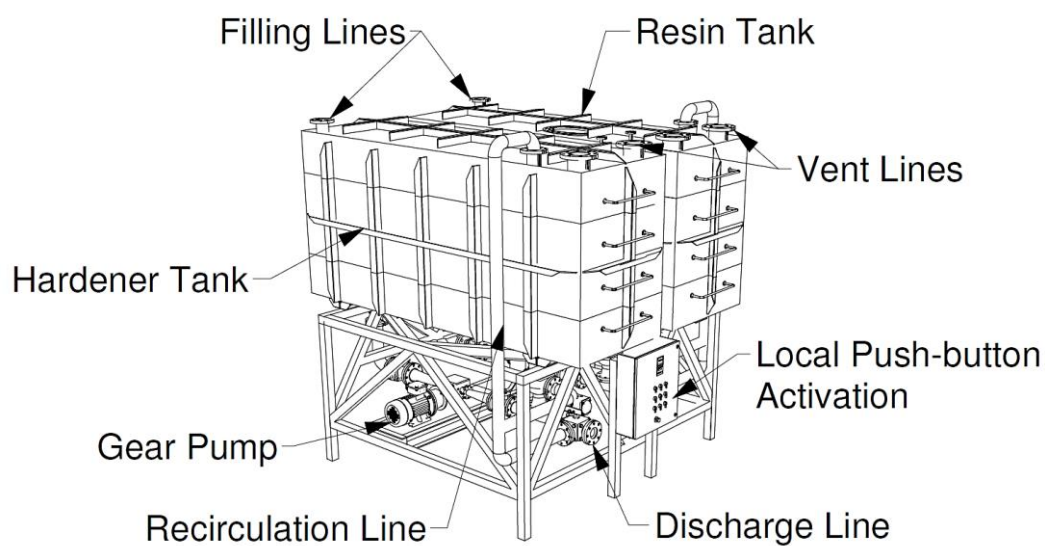


Figure 6-6: Example AREST A1 Tank/pump arrangement for medium size RoPax

Two electrically driven and synchronised gear pumps, located on the resin and hardener lines respectively, are used to deliver both foam components to a number of mixing nozzles located within the protected compartment(s). Both resin and hardener lines have re-circulation loops whereby the pumps can be used to circulate each component periodically. This enables faster foam deployment as it removes the requirement for pump-priming while also allowing the pumps to be tested when necessary. A control panel/starter is used to start the pumps and open the hardener and resin remote operated valves (ROV). The control panel is redundantly supplied from two separate incoming power supplies (main and backup) and is located near to the pumps but not within the vulnerable compartment. Activation of the system is a combination of two pushbuttons on the starter panel. Pushbutton 1 'circulation' will start both pumps and begin circulating the system; Pushbutton 2 'activation' will open both the hardener and resin ROV simultaneously and begin a timer for self-deactivation. When the pre-set timer has finished counting the system will automatically stop i.e. both pumps stop and ROV close. Pushbutton 2

shall have no effect unless Pushbutton 1 is activated, reducing the chances of false activation. These switches can be located in situ and remotely (Bridge) and are operated independently from each other.

Stopping of the system, as mentioned previously, is initiated when the timer count is complete or alternatively, via an emergency stop circuit to allow the system to be halted at any time. A pressure relief valve is provided on each line to allow automatic recirculation and pump running at system pressures when the distribution valve is either closed or at a dead point in rotation from recirculation to delivery.

Manually operated Isolating valves located throughout the system will have a clearly identified position and are only operated during tank draining or component maintenance. Those fitted with solenoid actuators are also to remain closed until system activation or such time that recirculation of the foam components is taking place or the tanks are being filled.

Within the protected compartment, both the resin and hardener lines divide into port and starboard side branches for uniform filling of the space. Each branch contains a number of static mixing nozzles where resin and hardener components are mixed to form a homogeneous solution. The interaction of the two components produces a chemical reaction (polymerisation) that enables the in-situ production of foam. The system operating panel and control unit are located in an electrical locker on the bridge, with bulkier equipment such as pump starters located in a convenient position closer to the main foam storage tanks. The system is interfaced and can be controlled from the Safety Management System (SMS). The system is also equipped with a decision support system, which in the event of collision or grounding will provide the master with an advised course of action based on the extent and location of flooding. This is facilitated by a water ingress detection system with sensors located in the protected compartments. The system is activated manually and ultimately this decision lies with the master of the vessel.

To aid in the decision process there will be CCTVs located within the protected space, or briefed watch keepers available to check the space, in conjunction with the water detection and alarm system. This allows the final decision on deployment to be an informed one, based on water detection and visual camera views to allow cross confirmation of a water indication. Furthermore, in case of manned spaces, confirmation can be obtained that evacuation has been completed. The entire process of distributing foam into the protected compartment can be monitored in real-time using video cameras within the compartment, until the foam fill is sufficient to block the camera. Within the protected compartment, there may be systems which are considered to be critical to the survival and subsequent navigation of the vessel (for example, Safe Return to Port). These are to be provided with protection from the foam to allow them to maintain their function and

operation. Such systems will generally include compartment vents, cross-flooding arrangements and cross-flooding valves along with bilge and pumping arrangements. In general, these protective devices come in the form of local enclosures that allow the normal passage of air but have sufficient impermeability with which to resist the passage of the curing foam. These will need to be customised for each individual arrangement and installation on each vessel, with the minimum volume that is practical and clear observation panels on normally monitored items.

6.3.3 AREST A2 System Description

6.3.3.1 System Overview

As touched upon within Chapter 1, the internal arrangement of a vessel is a highly complex environment, containing a multifarious array of potential propagation paths for both flooding and fire. This, in turn, can make it very difficult not only to predict the outcome of a given flooding/fire incident, but also in the determination of effective RCOs for such risks. However, amidst this complexity, it is possible to identify the primary conduits through which the spread of floodwater and fire may occur, which if suitably protected can arrest propagation altogether. In case of flooding, the process by which such critical propagation paths can be identified is outlined within Chapter 5. In the majority of cases, these exist as unprotected openings on the bulkhead deck, where the watertight integrity of the vessel has to be compromised for the sake of functionality and operability (i.e. lift trunks, stairwells, service corridors). The difficulty then comes in finding a form of protection for such openings that does not inhibit the latter. In contrast, fire has existing forms of protection that are less detrimental to operation than those relating to flooding, predominantly comprising fire-rated doors and insulated bulkheads. However, vast numbers of such features are required in fire protection, which greatly contributes to the overall complexity and cost within the vessel design, occasionally with great impact on ergonomics.

In recognition of this problem and the huge potential for safety improvement in this area, the AREST A2 system has been developed. This is a dual-purpose system that works to contain both flooding and fire, making it distinct from a number of risk control options in that it protects against two risk sources, instead of just one. The system is a form of opening protection with two modes of operation, depending on whether propagation of fire or floodwater is to be prevented. The system is comprised of two fire shutters, situated apart from one another in order to form a cavity in between. When acting in the protection of fire, these shutters are used in the conventional sense (like fire doors) and can be opened and closed as desired for fire drills or any other purpose. However, in case of flooding, the shutter assembly is actively converted from a fire-rated to watertight closure through the introduction of expanding foam to the cavity formed between the two shutters.

Such a system presents a number of benefits, the primary of which is its ability to protect against both flooding and fire without impeding the operability of the vessel. Roller or sliding shutters provide a virtually unobstructed passageway and when open, the shutter and mechanism are hidden above or alongside the doorway. In relation to cruise vessels, this means that the flow of persons and goods are entirely unobstructed. This is also true in the case of RoPax vessels, with the additional benefit that the system is clear of any risk of damage from vehicles moving through the opening. Furthermore, the system is highly flexible and can protect large openings where it would otherwise be infeasible to protect with doors or, if possible, would require a large number of doors to do so. Instead, one shutter system can span distances of up to 10m uninterrupted, with the capability to further extended this to 30m with the provision of intermediate supports. This means the system can be used as a substitute in areas where there would otherwise be a number of fire doors or additionally where there are large open spaces, such as Ro-Ro decks. In such cases, the result would be an internal geometry that possesses a greater level of utility through enhanced ergonomics, whilst also having a far greater level of safety.

6.3.3.2 System Functional Description

The AREST A2 system is comprised of two A-60 rated fire shutters, situated 0.3m apart in order to form a cavity. The shutter curtains are constructed from continuously interlocked galvanised steel or GRP laths, securely held in place by end locks mounted on rails recessed into the deck, Figure 6-7. The shutter thicknesses and lath profiles vary depending on the required watertight rating and the distance to be spanned by the system, though the shutters themselves are not watertight and instead foam is introduced to the system for this purpose, allowing for a lightweight construction. Side rails are constructed of galvanised steel and roll-formed into a tee section, with a rubber weather seal to prevent foam leakage. The shutters are fixed to the existing vessel structure using mild steel plate of appropriate thickness relative to the opening size and strength requirements, Figure 6-8.

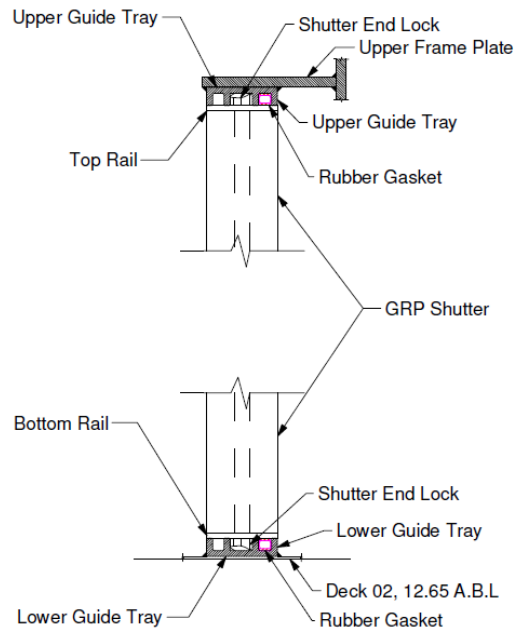


Figure 6-7: Example shutter assembly, top and bottom rails, vertical section (side view)

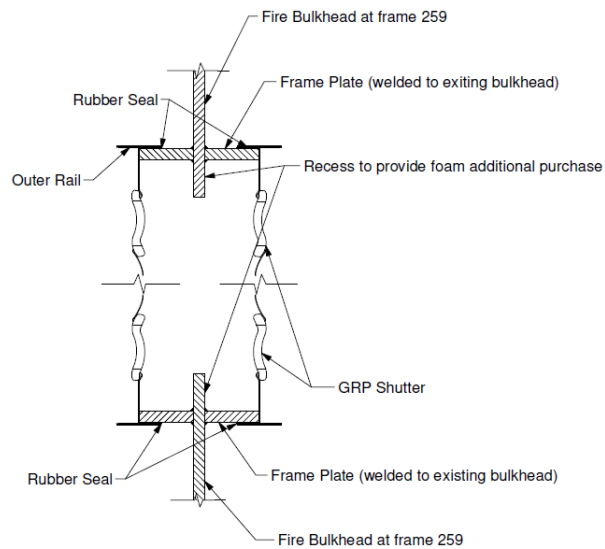
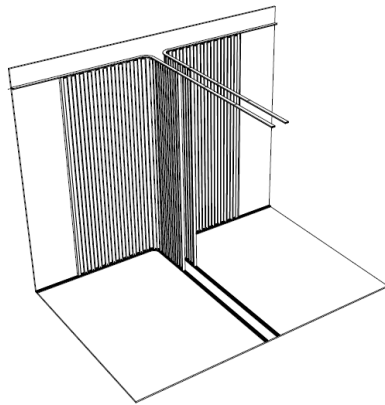


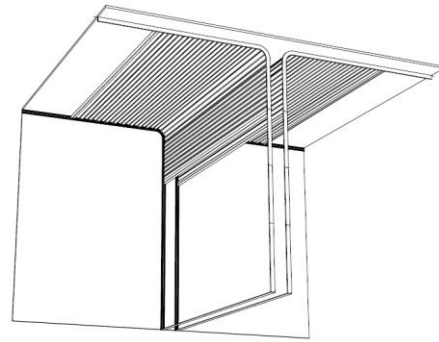
Figure 6-8: Example shutter assembly, right & left sides, Horizontal section (top view)

The shutter orientation and direction of opening is highly flexible,

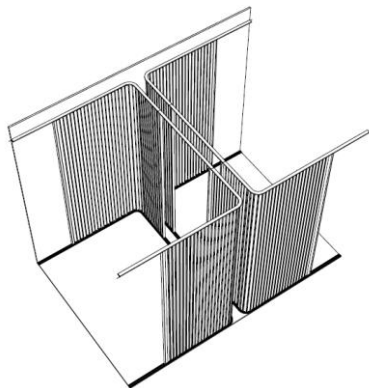
Figure 6-9, meaning that the system can be introduced even where there are tight space constraints, such as areas with limited free height or narrow corridors. Where penetrations exist within the existing vessel free height, provisions will have to be made in order to up-rate these to watertight rating using for example doubler plates, slipsils or bulkhead packing glands.



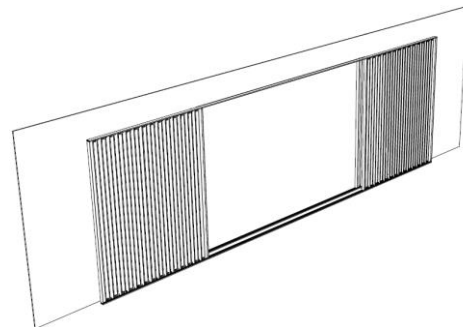
Transverse Folding Barriers



Vertically Descending Barriers



Transverse Folding Half Barriers



Transverse Closing Barriers

Figure 6-9: Example shutter assembly, top and bottom rails, vertical section (side view)

Opening and closing of the shutter is achieved via a 3-phase geared motor, mounted on one of the shutter endplates. This electrically operates the shutters and adjustable limit switches are incorporated to stop the shutter at the end of each travel. Local controls include open, close and stop buttons along with mirrored remote operation from the bridge/safety centre. Both the control panel and motor are redundantly supplied from two separate incoming power supplies (main and emergency) to enhance system availability.

In the event of flooding, high expansion foam is injected into the cavity formed between the shutters by a foam delivery unit located in close proximity to the shutter arrangement. This system is comprised of two vessels ($\approx 60\text{dm}^3$ in volume) containing foam resin and hardener components, respectively. During regular service, these are kept under Nitrogen blanket at atmospheric pressure. In addition, the system has a third vessel containing nitrogen gas under pressure for pumping purposes as shown in Figure 6-10.

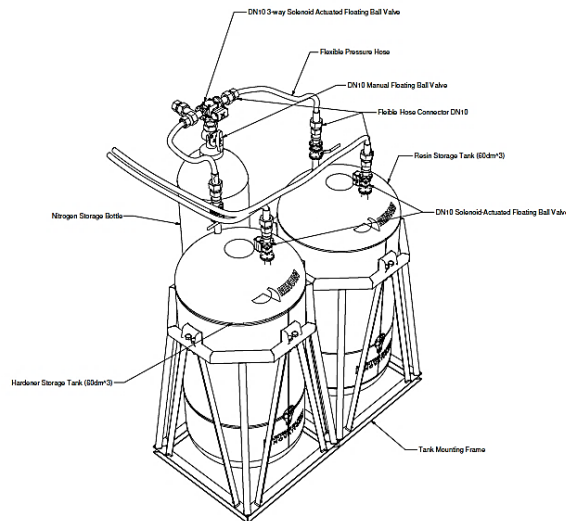


Figure 6-10: Foam Delivery System

Once activated, a solenoid-actuated ball valve is opened on the Nitrogen tank, which pressurises the resin vessels. This has the effect of displacing the resins from their respective tanks, where they are carried via flexible hosing to a common static mixing nozzle. This nozzle is situated within the upper centre fire shutter assembly and serves to mix both resin and hardener components before delivering them into the shutter system. A third line leading from the nitrogen tank is also used in order to deliver a small quantity nitrogen to the static mixer which has the effect of enhancing foam expansion ratio.

Once introduced, the foam resins undergo rapid polymerisation and expand to fill the cavity. Simultaneously, the foam begins to set and adhere to all surrounding surfaces, forming a watertight seal. This process occurs over a period of approximately 5 minutes, following which the AREST A2 system will achieve a watertight rating of approximately 1 bar or 10m water head. Furthermore, this process can take place even in the presence of floodwater, in which case the expansion force of the foam will displace water from within the barrier before setting. The foam delivery system, as in the case of the shutters, also has local and remote means of activation via dual push buttons and has dual power supplies for redundancy.

For maintenance purposes, manually operated ball valves are located on all three vessels allowing resin and Nitrogen tanks to be replaced periodically, for the system to be tested and parts replaced if required.

The system is interfaced and can be controlled from the Safety Management System (SMS). The system is also equipped with a decision support system, which in the event of collision or grounding will provide the master with an advised course of action based on the extent and location of flooding.

6.3.4 AREST A2 Impact Example

Within this section, a typical application of the AREST A2 system is described as a means of demonstrating the potential positive impact such a system can have on flooding process. The example provided concerns a large cruise vessel suffering from a 3-compartment damage scenario located towards the vessel aft shoulder. This is a case that demonstrated extensive progressive flooding in the as-built condition, culminating in eventual capsizes. In accordance with the process outlined in Section 5.4.7 of Chapter 5, this case has been subjected to detailed forensic examination of the flooding process, allowing the primary conduits for progressive flooding to be identified. This is illustrated in Figure 6-10, where red and green markers denote vertical and transverse progressive flooding sources respectively. The example shown here focuses only on the immediately damage area and, in particular, the vessel bulkhead deck, which typically forms the stage for flooding escalation. However, using this approach it is also possible to identify all primary progressive flooding sources for every compartment within the vessel. Through doing so, one can also identify the openings that must be protected in order to isolate any given compartment, thus containing floodwater progression following any given event. In practical terms however, it would be infeasible and furthermore superfluous to protect each one of these openings. As such, the process of forensic examination does not simply assess the openings through which progressive flooding occurs, but instead goes further by focusing on the openings through which critical progressive flooding occurs i.e. progressive flooding leading to vessel loss. This is also highlighted within Figure 6-11 where, despite several openings having been identified as progressive flooding sources, in fact only two openings have been identified as leading to a critical form of flooding progression. This includes openings TVF1 and TVF4 both of which are double A-class fire doors.

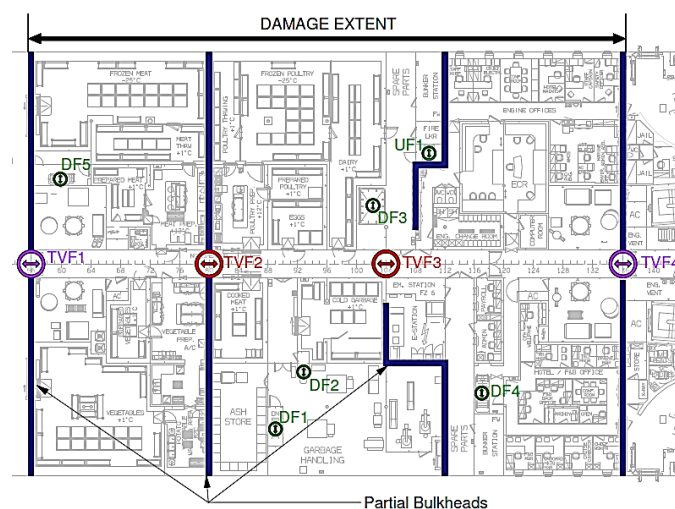


Figure 6-11: Typical example of major progressive flooding conduits on cruise vessel BH Deck

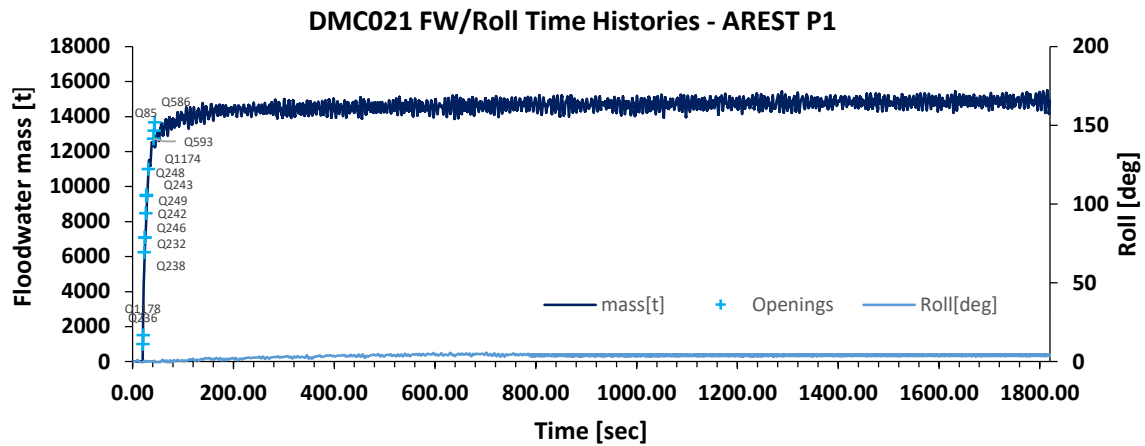


Figure 6-12: Comparison of floodwater evolutions, as-built (above), with AREST A2 (below)

6.4 Verification of Vital Foam Properties for Class and Administration Approvals

This section aims to provide some insight into the approvals process for systems such as those described within the foregoing. Over the duration of this research, two of the aforementioned RCOs, namely the AREST A1 and P1 systems, have been subjected to the process of Novel Technology Qualification. This is a system afforded by Classification Societies through which new technologies may be approved, thus granting confidence that such systems will perform safely and reliably. The process is risk-based in nature and largely centres around a HAZID process through which systems are de-risked and functional/design requirements are set forth. An example of this is provided within the following in relation to the HAZID process that has been conducted on the AREST P1 system. Here the process specified within (DNVGL, 2015) has been followed, though this approach is largely based on IMO FSA guidelines (IMO, 2018). The HAZID session was conducted over two days, involving 16 participants as listed in Table 6-1.

Table 6-1: HAZID Participants

Name	Affiliation	Role
Clayton Van Welter	RCCL	AVP, Maritime Safety
Georgios Atzamos	RCCL	Naval Architect, Newbuild & Innovation
Greg Chronopoulos	RCCL	Director, Marine Operations Celebrity
Joey Goulas	RCCL	Assistant Project Manager, space manager
Joseph Miorelli	RCCL	AVP, Newbuild and technical projects
Justin Epstein	RCCL	Sr. Naval Architect, Newbuild fleet modernisation
Justin Palermo	RCCL	Port Captain, Marine nautical manager
Leonardo Carmona	RCCL	Manager, stability and naval architecture
Oceane King	RCCL	Associate project manager, newbuild processes
Rami Nurminen	RCCL	Director, Technical assurance

Stavros Zannikos	RCCL	Chief Engineer Celebrity Sr. Manager, tech. projects and newbuild
Thomas McKenney	RCCL	development
Adam Janicek	Minova	Product Manager
Peter Assinder	Minova	Global head of sales
Dracos Vassalos	UoS/MSI	Professor of Maritime Safety
Donald Paterson	UoS/MSI	Naval Architect

In total nine hazard categories, as listed within the following, have been considered leading to the identification of 46 individual hazards.

- Categories and number of hazards considered
- Installation - System integration
- Guest experience
- Environment
- Compliance to rules and regulations
- Occupational health and working conditions – Safety
- Operability
- Maintainability
- Stability and performance

Details on risk categories, frequencies and consequence scales are provided within Table 6-2, on the following page.

Table 6-2: Risk category, frequencies and consequence scales

							Probability					
							1	2	3	4	5	
							Remote	Unlikely	Occasional	Probable	Frequent	
							Expected to occur only in exceptional circumstances	Expected to occur at least once during design life	Expected to occur a few times during design life	Expected to occur at least once per 5 years per vessel	Expected to occur at least once per year per vessel	
		People	Downtime	Environment	Reputation	Cost (USD)	T > 30 years	T < 30 years	T < 15 years	T < 5 years	T < 1 years	
Consequence	5	Major	Fatality/s and/or permanent disability/s	Major damage/loss of the system (> 2 months)	Massive impact on owners environmental KPIs	Extensive global negative attention	> 5M or total system cost increase 100%	M	S	H	H	H
	4	Substantial	Major injury, long term absence	System breakdown, disabled for a longer period (< 2 months)	Major impact on owners environmental KPIs	Negative attention in international/s ocial media	1M - 5M or total system cost increase <100%	M	M	S	H	H
	3	Moderate	Slight injuries, <5 working days lost	System breakdown, temporarily disabled (< 2 weeks)	Moderate impact on owners environmental KPIs	Regional public and slight national media attention	100k-1M or total system cost increase <50%	L	M	M	S	H
	2	Minor	Superficial injuries	Failure can be rectified within <1 day	Minor impact on owners environmental KPIs	Limited impact. Local public concern, may include media	10k-100k or total system cost increase <25%	L	L	M	M	S
	1	Insignificant	No injuries	Failure can be rectified within <2 hours	Insignificant impact on owners environmental KPIs	Slight impact. Local public awareness, but no public concern	<10k or total system cost <10%	L	L	L	M	M

To provide an indication of what this process entails, an excerpt from the HAZID results is provided within Table 6-3 below, outlining hazards identified in relation to stability. Observation of the table contents indicates a number of hazards pertaining to foam properties, which yields certain functional requirements relating to permeability, compressibility and adhesion. The burden of proof then lies upon the system designer in order to ensure these requirements are met and it is this process that is elaborated within the following sections.

Table 6-3: HAZID table excerpt

HAZID ID#	HAZARD GROUP	HAZARD	CAUSES	EFFECT	DETECTION	EXISTING SAFEGUARD	Risk category	Consequence	Likelihood	Criticality
7.1	Stability	Insufficient GM margins	The system fails to provide sufficient stability enhancement	Vessel operation impaired by limited stability margins	Prior stability calculations to determine benefit	System performance verified through both dynamic and static assessments	C	5	1	M
7.2	Stability	Degradation of foam over vessel life-cycle	System properties are deteriorated over the period of time	Insufficient stability performance from insufficient buoyancy		The foam is inert and will last for >50 years	C	5	1	S
7.3	Stability	Foam installation fails to withstand pressure head of water.	Insufficient compressive strength.	Foam collapse and water ingress.	Foam compressive strength test	Foam determined to have sufficient strength.	C	4	1	M
7.4	Stability	Foam permeability is too high.	Insufficient closed cell structure within foam mass.	Foam absorbs floodwater leading to buoyancy reduction.	Foam water absorption tests	Foam determined to have sufficient permeability.	C	3	1	L
7.5	Stability	Foam installation will break free or apart under buoyant force.	Insufficient foam adhesion and cohesion	Water enters protected space, system ineffective.	Foam adhesion and cohesion tests	Foam determined to have sufficient adhesive and cohesive properties.	C	4	1	M

6.4.1 Permeability Verification

6.4.1.1 Overview

In order to determine the permeability of foam utilised within the previously described RCOs, it was deemed necessary to conduct a water absorption test on the proposed foam technology. By doing so, the mass of water absorbed by the foam can be quantified as a function of time and varying external water pressure. From these results, a determination can be made as regards an appropriate foam permeability value, with due consideration given to the anticipated exposure time of the foam to water and the pressures under which this might occur. To this end, two water absorption tests have been conducted, the first under atmospheric pressure conditions and the second with incrementally increasing overpressure. The foam specimens used within these experiments are formed of the same foam material that is to be used for marine installations and are of the dimensions specified within Figure 6-13. Furthermore, the foam samples have been cut from the internal volume of a greater foam mass and thus does not benefit from the effects of any outer skin formed within the foam moulding process.

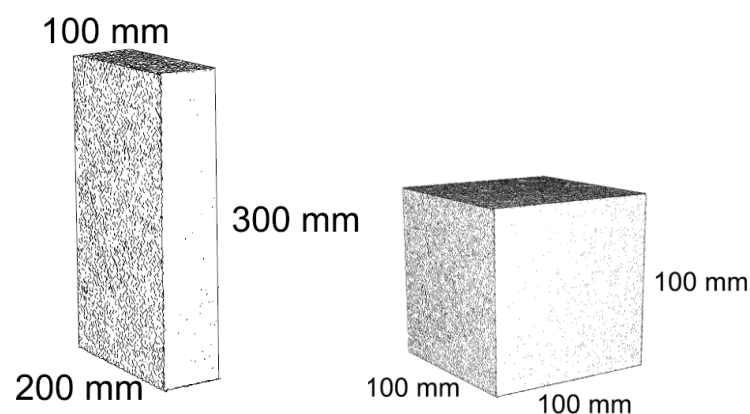


Figure 6-13: Foam sample dimensions, atmospheric pressure test (left), added pressure test (right)

6.4.1.2 Atmospheric Pressure Test

The first water absorption test has been conducted at atmospheric pressure, with the foam specimen anchored fully immersed in water for a period of 28 days. The intention here has been to observe and monitor the magnitude of water absorbed over time. As such, following the 28-day period and at several intermediate stages, the foam block has been removed from the water and weighed, allowing the wetted mass of the specimen to be assessed relative to its dry weight. By following this process, it is possible to determine the volume of water absorbed by the foam relative to its total volume, thus providing an exposure time varying permeability value.

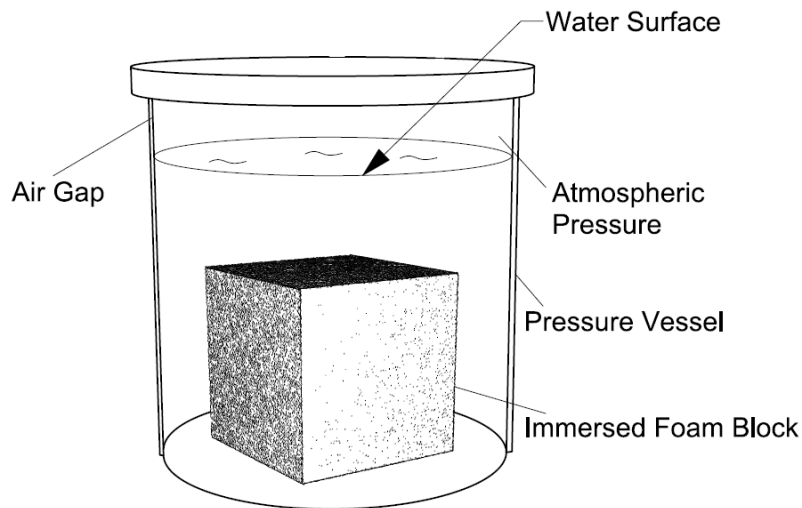


Figure 6-14: Atmospheric pressure water absorption test overview



Figure 6-15: Atmospheric pressure water absorption test apparatus

The results of the experiment have shown that the foam has a water absorption ranging from 2%, following 24 hours, up to 2.7% after 28 days exposure. If the relationship between exposure time and water absorption is observed, as shown in Figure 6-16, it is clear that the rate of water uptake is decreasing with time and tends towards a maximum of approximately 3%. This yields a permeability value for the foam of 0.03, conditioned on 28 days exposure at atmospheric pressure.

Table 6-4: Foam water absorption with respect to exposure time

Foam exposure Time [days]	Water absorption [%]
1	2.1
2	2.1
3	2.2
14	2.5
28	2.7

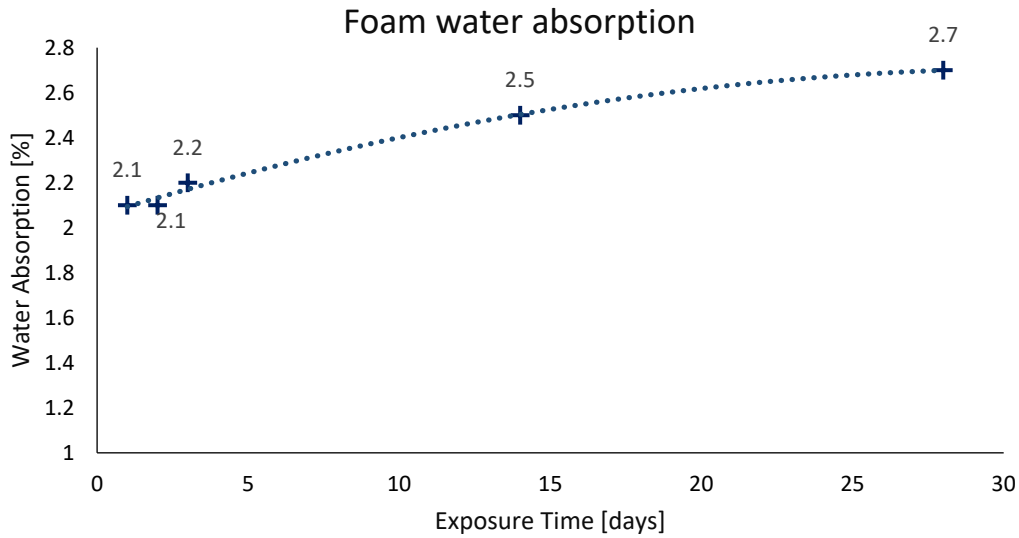


Figure 6-16: Foam water absorption with respect to exposure time

6.4.1.3 Over-Pressure Test

In the understanding that in practice the passive foam installations will likely be subjected to pressures greater than atmospheric, a secondary water absorption test has been conducted at varying degrees of overpressure. Here, foam sample specimens have been fully immersed in water within a pressure vessel, see Figure 6-17. Compressed air has then been injected into the vessel in a controlled manner, generating water pressures acting on the foam of 0.5, 1 and 3 bars overpressure. At each pressure increment, a given foam specimen has been subjected to three hours exposure time. Here, 3 hours was deemed appropriate as it is in line with the requirements of Safe Return to Port. Following this time, the foam has been weighed in order to calculate the wetted weight of the specimen and thus permeability as a function of water pressure.

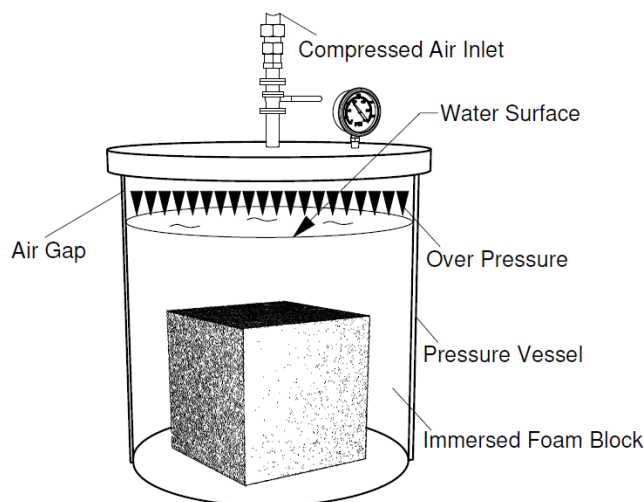


Figure 6-17: Overpressure water absorption test

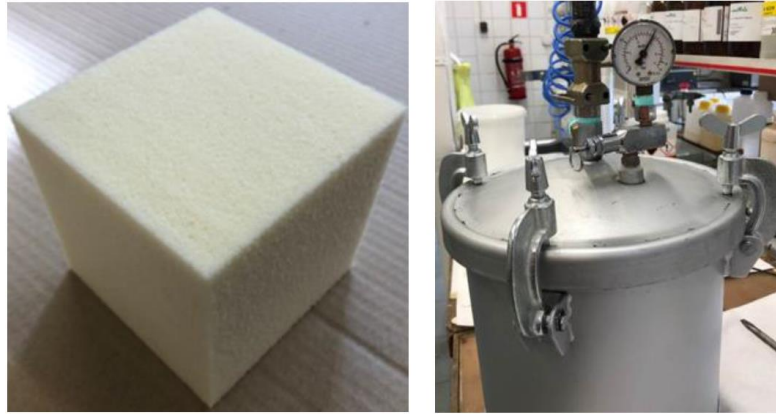


Figure 6-18: Foam specimen and pressure vessel

The results of this experiment are summarised in Table 6-5 and Figure 6-19 below, where an increase in foam permeability can be observed at water pressures ranging up to 0.5 bar, moving from 1% to 2% permeability. Interestingly, at pressures beyond this point it was found that the foam permeability is insensitive to increasing pressure, remaining at a constant value of approximately 2%. The fact that greater amounts of water are not absorbed with higher water pressures may appear counter intuitive, but this can be explained by a favourable phenomenon that takes place when the foam is exposed to large water pressures. In such cases, the outer layer of the foam specimen, when acted upon by the pressurised water, undergoes a mild compression as shown in Figure 6-20. This, in turn, has the effect of forming an outer skin of lesser permeability than the foam interior, which shields the foam against further water uptake. As such, the results would suggest that the foam possess a 2% permeability value, even whilst exposed to the worst conceivable conditions with respect to water pressure head.

Table 6-5: Foam water absorption with respect to pressure (3 hours exposure)

Overpressure (bar)	Water absorption [%]
0	1
0.5	2
1.0	2
1.5	2

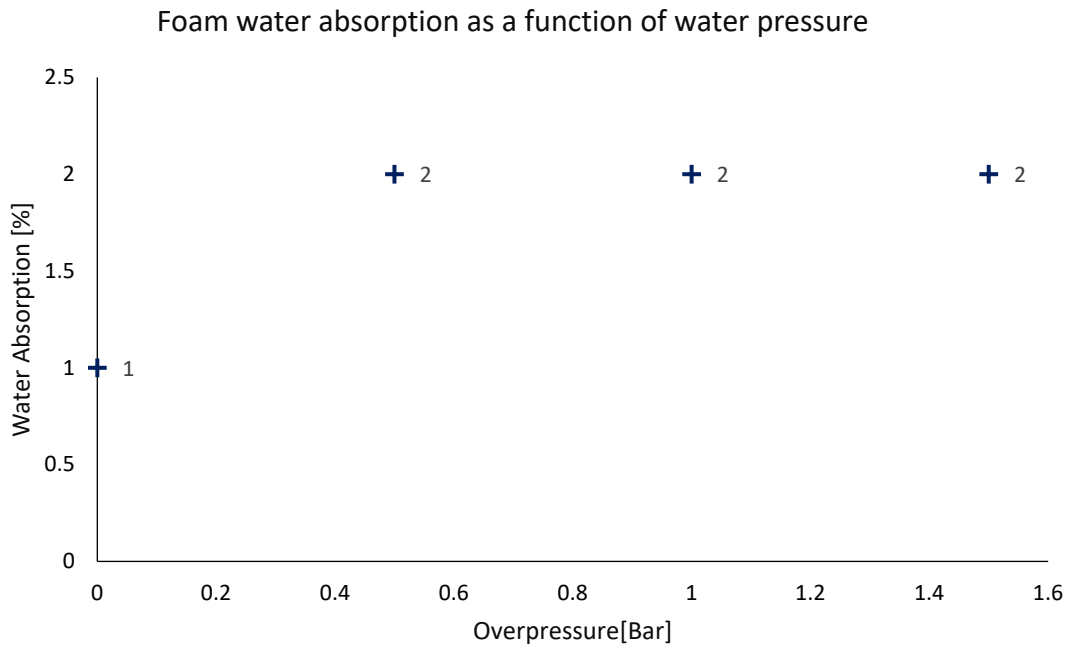


Figure 6-19: Foam water absorption relative to external water pressure

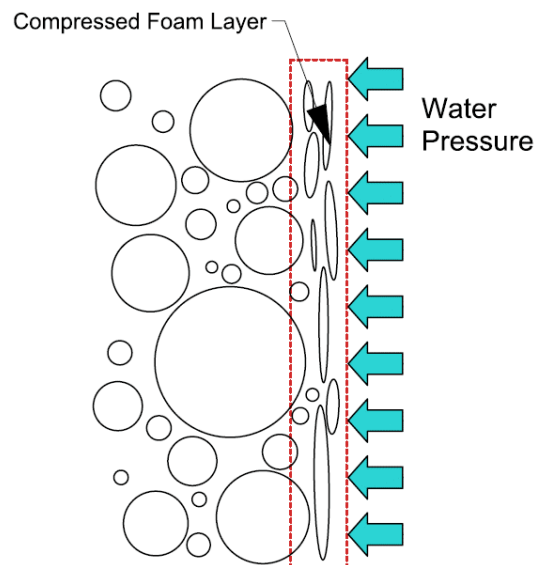


Figure 6-20: Development of compressed foam skin at high water pressures

6.4.1.4 Additional Considerations

With respect to the results outlined within the foregoing, it is important to consider the effects of scale and their impact on the permeability value calculated. The sample sizes used within the experiments are of the order of 0.001m^3 in comparison to the static foam installations which are of the order of $200\text{-}300\text{m}^3$ in size. This is important, as the manner in which the foam absorbs water is such that smaller sample sizes will demonstrate higher permeability than large ones. Consequently, the experiments are inherently conservative due to the scale at which they have

been conducted. The reason for this stems from the fact that the “wetted depth” or “distance travelled” by the water from the foam exterior to the foam interior is not affected by scale, as shown in Figure 6-21. This, in turn, means that the wetted volume of foam relative to the specimen size will decrease with increasing foam volume. This effect is further described in Figure 6-22, where an example of general relationship between sample size and value of permeability determined is illustrated.

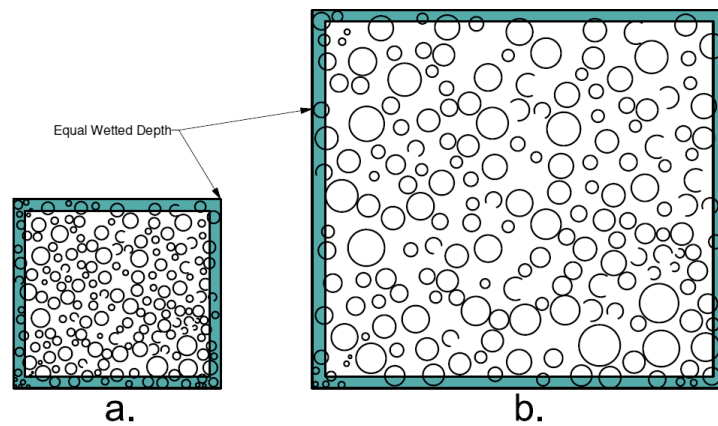


Figure 6-21: Foam water absorption as a function of specimen size

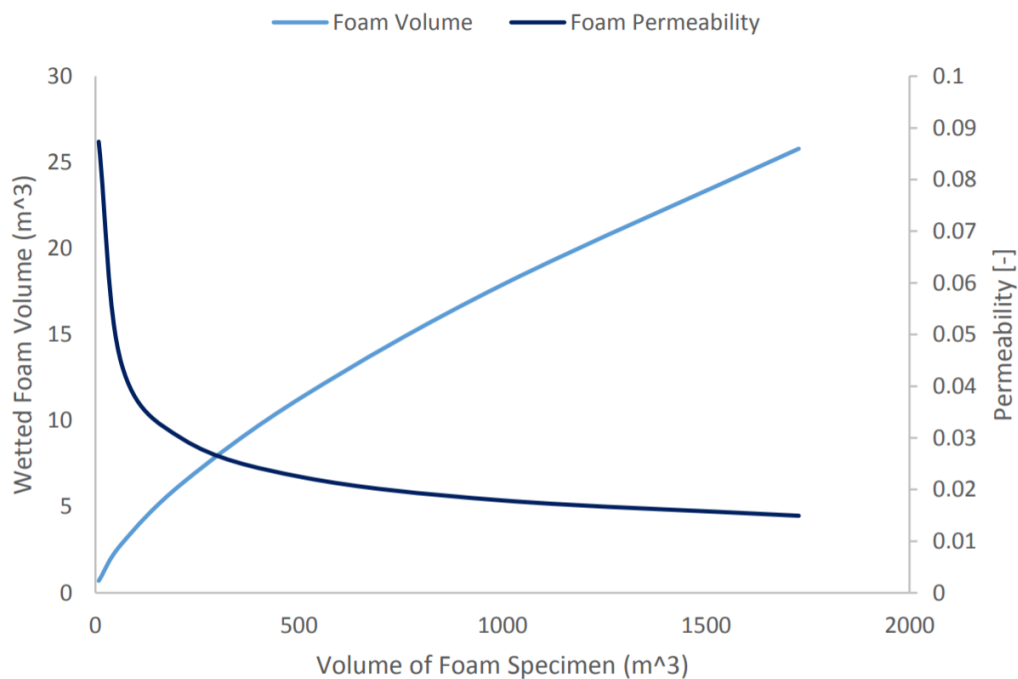


Figure 6-22: Effect of Specimen Size on Permeability Determination

Furthermore, the experiments conducted have assumed the entirety of the foam surface area to be in contact with water, thus increasing water uptake. However, in practice, it is more than likely that only a portion of the foam surface will be in contact with water and thus the water absorption in reality will be much less, as demonstrated in Figure 6-23.

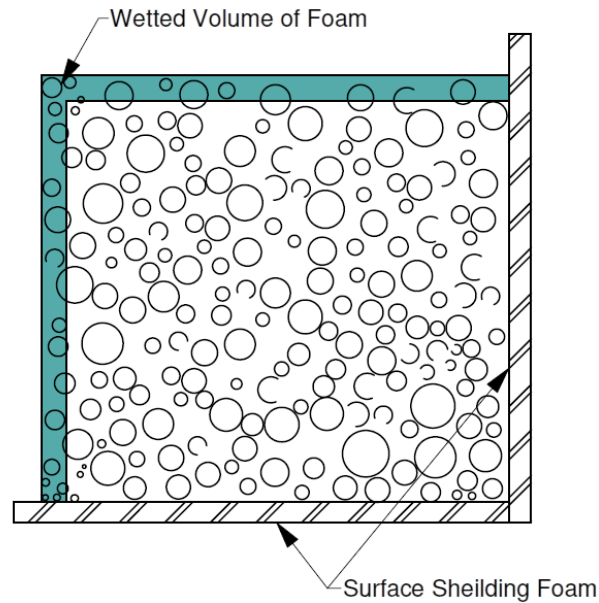


Figure 6-23: Sample shielded foam water absorption

6.4.1.5 Summary

Based upon the results outlined within the foregoing, the following conclusions can be drawn:

- At atmospheric pressure, the foam possesses a maximum permeability of 3% following 28 days exposure time.
- When assessed up to 1.5 bars overpressure, the foam was identified as having a permeability value of 2%, given 3 hours exposure time.
- In both experiments, the results were highly conservative due to the sample size utilised.
- A permeability value for the foam of 5% has been considered, allowing for a 3% safety margin.

6.4.2 Verification of Foam Adhesion & Cohesion

6.4.2.1 Overview

Other parameters deemed significant during the HAZID process include the adhesive and cohesive properties of the foam technology which has varying significance depending on which of the proposed RCOs is being considered, as detailed within Table 6-6.

Table 6-6: RCO-specific Adhesion and Cohesion requirements

RCO	Adhesion	Cohesion
AREST P1	Installations must remain in place during their service life and following a flooding incident, where they must withstand buoyant forces.	Foam must possess sufficient cohesion to ensure the installation does not break apart when acted upon by buoyant forces.
AREST A1	Foam must have sufficient adhesion such that it bonds to surface within the compartment rather than flowing out of the damage opening.	Foam cohesion should be sufficient in order to prevent break-up of the foam mass under the action of ship and floodwater motions along with buoyant forces.
AREST A2	Foam must have sufficient adhesion in order to create a watertight seal within the shutter arrangement.	non-critical.

Given the above, it was undertaken to determine the adhesive and cohesive properties of the foam by conducting what is referred to as a “pull-off” test. This works by measuring the force required in order to separate the foam from a given bonded surface (adhesion) or alternatively the force necessary to separate the foam body itself (cohesion). Following this process, these parameters can then be used as input in the RCO design process, where the expected buoyant force or loads acting upon a given foam installation can be measured relative to these terms.

6.4.2.2 Pull-off Test for Adhesion and Cohesion Determination

Adhesion is a property that varies depending on the nature of the bonding surface and increases when moving from smoother to coarser surfaces. However, in this case steel was considered appropriate given that the targeted spaces for such installations (voids) have predominantly steel surfaces. The pull-off test, also referred to as a stud-pull test, works by firstly applying a layer of foam to a steel plate and allowing it to cure. Following this process, an adhesive connection is made between a metal stud and the foam surface, using an epoxy resin of a stronger bond than that expected by foam adhesion, see Figure 6-24. An incision is then made in the foam around the

perimeter of the stud, see Figure 6-25, such that foam adhesion to the plate is the only force resisting separation. An apparatus is then used in order to pull the stud/foam assembly from the steel plate and the force required to do so is recorded, thus providing a measure of foam adhesion.

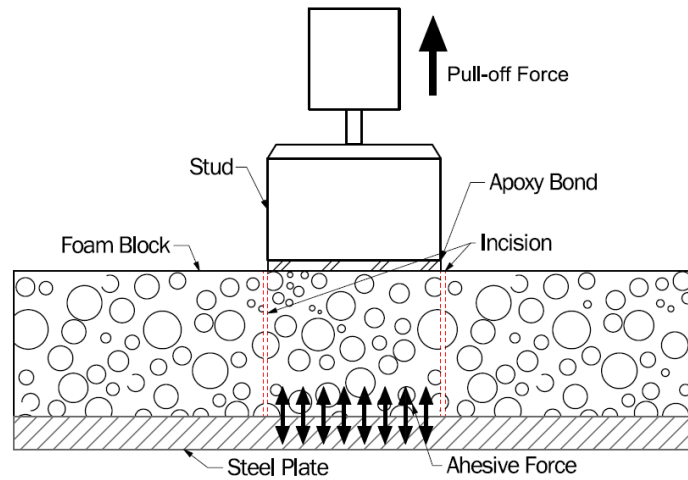


Figure 6-24: Pull-test Diagram



Figure 6-25: Stud fixed to foam/plate assembly (left), foam separated from steel plate (right)

The foam cohesive properties have also been measured in a similar way (same process, without the steel plate) and the results in each case are provided within Table 6-7: Pull-test results. Here it can be observed that the foam possesses an extremely high level of adhesion and cohesion. In fact, a tear force of 13 tonnes per square metre would be required in order to break the bond of foam to the steel surface. As a result, and given the contact area of the foam installation to the surrounding ship structure, it is highly unlikely that the foam body would break free from its bonds even when fully immersed.

Table 6-7: Pull-test results

Adhesion to steel [Mpa]	Cohesion at foam surface [Mpa]
0.13	0.19

6.4.3 Verification of Foam Compressibility

6.4.3.1 Overview

The last critical system property that will be elaborate upon within this chapter relates to the behaviour of the foam under compression. Again, this is a property of varying significance across each RCO but, in general, the foam requires sufficient compressive strength with which to resist expected water pressures whilst at the same time being sufficiently elastic in order to absorb vibrations and sustain hydroelastic effects. In order to make this determination, the foam stress-strain curve has been calculated using a compression-testing machine. The results of this process then provide a basis from which expected loads on the foam mass can be gauged relative to its compressive strength properties.

6.4.3.2 Compressive Strength Analysis

In determining the foam compressive strength characteristics, two experiments have been conducted on a foam specimen of 100mm x 100mm x 50mm in size. In each case, the foam samples have been placed within a compression-testing machine where they have undergone 10% and 50% deformation respectively, see Figure 6-26.



Figure 6-26: Compression-cycle press/hold/release (10% deformation left, 50% deformation right)

The results of this process are presented in Figure 6-27, where the foam stress-strain curve is presented. Here, the foam displays linear elasticity under compressive pressure up to ≈ 0.22 MPa (22m water head), in which the foam cell walls compress and bend. Past this point, the foam cell walls begin to buckle, fracture and yield, resulting in permanent deformation (plastic behaviour). This represents significant compressive strength and far exceeds expected water pressure heads, which are of the order of 10m. Furthermore, though the degree of deformation that takes place within the elastic region is slight, $<5\%$, this is more than enough to absorb any vibrations and hydroelastic loads that may be expected.

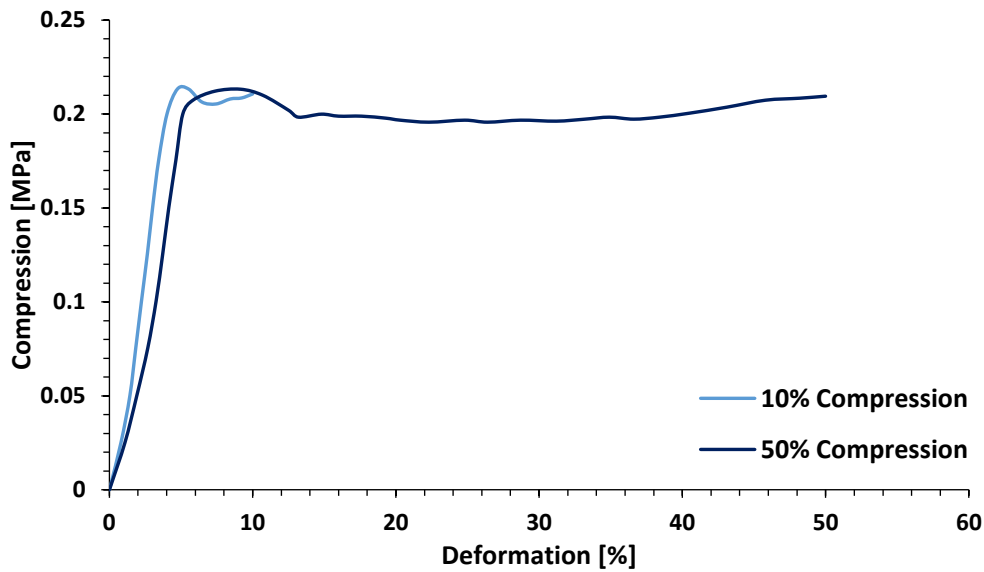


Figure 6-27: Foam stress strain curve under compression

6.5 Summary

- Several new forms of RCO have been introduced with a view to providing readily adaptable ship internal configurations for damage stability enhancement, referred to as Adaptive Reconfigurable Environment Safety Technology.
- It is stressed that the nature of internal reconfiguration required in the treatment of different loss modalities differs greatly. For this reason, it is important to identify vessel loss modalities prior to determining appropriate RCOs.
- Furthermore, it has been shown that is possible to develop effective RCOs that do not inhibit vessel functionality and operability, thus removing the burden of having to choose between safety and these other attributes.
- Depending on vessel size and age along with whether the vessel is a new-build or undergoing retrofitting, the constraints surrounding the implementation of RCOs differs. As such, a designer needs flexibility and variety in their choice. For this reason, three unique solutions have been presented, each of which have given strengths and weaknesses but combine to provide a strong arsenal with which to combat flooding risk.
- Any new technology being introduced into the maritime industry must undergo a process of “de-risking” and approvals, which has been demonstrated in the case of the proposed solutions under the Novel Technology Qualification scheme. Several examples are provided in order to give a flavour of what this process entails.

Chapter 7: Passive & Active Damage Control

Example - Permeant Foam Application & Progressive Flooding Suppression

7.1 Opening Remarks

This chapter serves to present an example of the implementation of AREST A1 system. As described within the previous chapter, this system works by deploying expanding foam into high-risk ship compartments, which forms on top of the floodwater entering the ship to suppress, contain and control its progression. Furthermore, in this particular example, it was found that certain spaces within the given vessel arrangement were found to be vulnerable to flooding while also being unutilised void spaces. For this reason, application of the AREST P1 system is also considered within this example using permanent foam installations, thus generating a hybrid solution. This is itself an indication that when it comes to dealing with flooding risk, or indeed risk in general, there is seldom a “one-size-fits-all” solution. Different RCOs have their own unique advantages or disadvantages depending on the nature of the risk source and as such, it is necessary to try and identify a case-optimal solution from a wider pool of solutions.

The vessel chosen for this study is a medium size RoPax vessel designed and built according to SOLAS 2009, with properties as described within the following sections. At present, RoPax vessels are a category of ship that lie in a somewhat precarious situation, with SOLAS 2020 having just come into effect and its true impact yet to be realised. Specifically, SOLAS 2020 ushered in a revised and more stringent s-factor formulation for damage cases involving Ro-Ro spaces. Adding to this, the general increase in the required safety level for this vessel type brings uncertainty regarding the degree to which vessel design and operability will be affected. Furthermore, as mentioned within Chapter 3, a recent EC research project, summarised in (Cichowicz, Olufsen, & Vassalos, 2019), has demonstrated that the requirements of the Stockholm Agreement have been made redundant for newbuild vessels in the advent of SOLAS 2020. This is a particularly significant finding due to the potential that SOLAS 2020 could be applied in retrospect as the Stockholm Agreement was, thus presenting a significant challenge in bringing older vessels up to standard. The conventional RCOs employed when enhancing RoPax safety include the addition of sponsons, ducktails or bulkheads on the vessel Ro-Ro deck. Neither of these represent a particularly attractive solution, with the former adding weight and increasing resistance and the latter affecting operability in terms of turn-around times, available lane metres and loading flexibility. In recognition of these limitations, it was undertaken in this case study to demonstrate

that the AREST systems could be utilised in answer to this problem and as a means of enhancing vessel survivability in a simple yet highly efficient and cost-effective way.

In assessing vessel vulnerability to flooding and as a means of informing the implementation and evaluation of RCOs, the methodology outlined within Chapter 4 has been adopted. In line with this process, two forms of survivability assessment have been conducted including static and dynamic approaches, as outlined below.

Part A: Static stability assessment, using statutory SOLAS 2009 regulations: Vessel vulnerability has been determined in accordance with statutory calculation techniques (probabilistic damage stability assessment), using the Attained Subdivision Index A as a global measure of ship safety and $P^*(1-s)$ as a measure of local vulnerability to flooding. Reconfiguration stemming from the implementation of RCOs is then accounted for as a reduction in space permeability, which has a positive and measurable impact on both the Attained Index and local risk values. As such, the impact of RCOs can be measured and the solution can be optimised.

Part B: Dynamic survivability assessment, using time-domain simulations in a seaway: In this secondary assessment, vessel survivability is evaluated using numerical time-domain simulations. This affords a means of verifying the results of the static assessment, in addition to offering the ability to capture the flooding process in far greater detail. This, in turn, provides a wealth of additional information that can be utilised in assessing vulnerability sources and the impact of the proposed RCOs. In this respect, the simulation results are used in order to evaluate specific loss scenarios at the forensic level in order to gain a greater understanding of local vulnerabilities and the impact of the proposed reconfiguration on specific cases. The overall impact on vessel vulnerability is then ascertained through calculation of the vessel Survivability Index, both with and without the systems in place.

7.2 Part A: Static Stability Assessment

7.2.1 Vessel Main Particulars

The following table outlines the main particulars of the test case vessel:

Table 7-1: RoPax R1 principle particulars

Principle Particulars	
Ship's name	RoPax R1
Length OA	212.80 m
Length BP	195.3 m
Length WL	203.75 m
Breadth, moulded	25.8 m
Draught, design	6.55 m
Draught, scantling	6.70 m
Draught, subdivision	6.70 m

7.2.2 Vessel Stability Model

The ship model used in the damage stability calculations consists of the following buoyant volumes:

- Hull from base line up to Deck 5 (14.8m above base)
- Two propeller shafts including bossings
- Two propellers
- Two rudders
- Two fins

The following volumes are deducted from the buoyant volume:

- Two bow thruster tunnels
- One anti-suction tunnel
- Two stern thruster tunnels
- Three sea chests
- Two fin stabiliser recesses

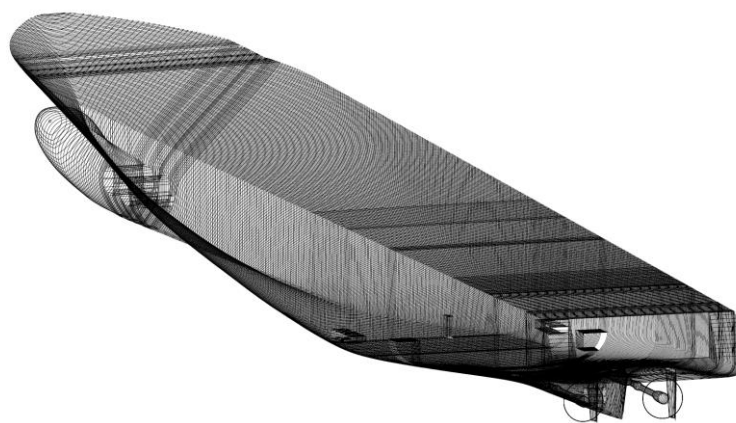


Figure 7-1: Stability Model Calculation Sections

7.2.3 Vessel Subdivision

Figure 7-2 below provides an overview of the vessel subdivision arrangement that has been used in order to inform damage generation.

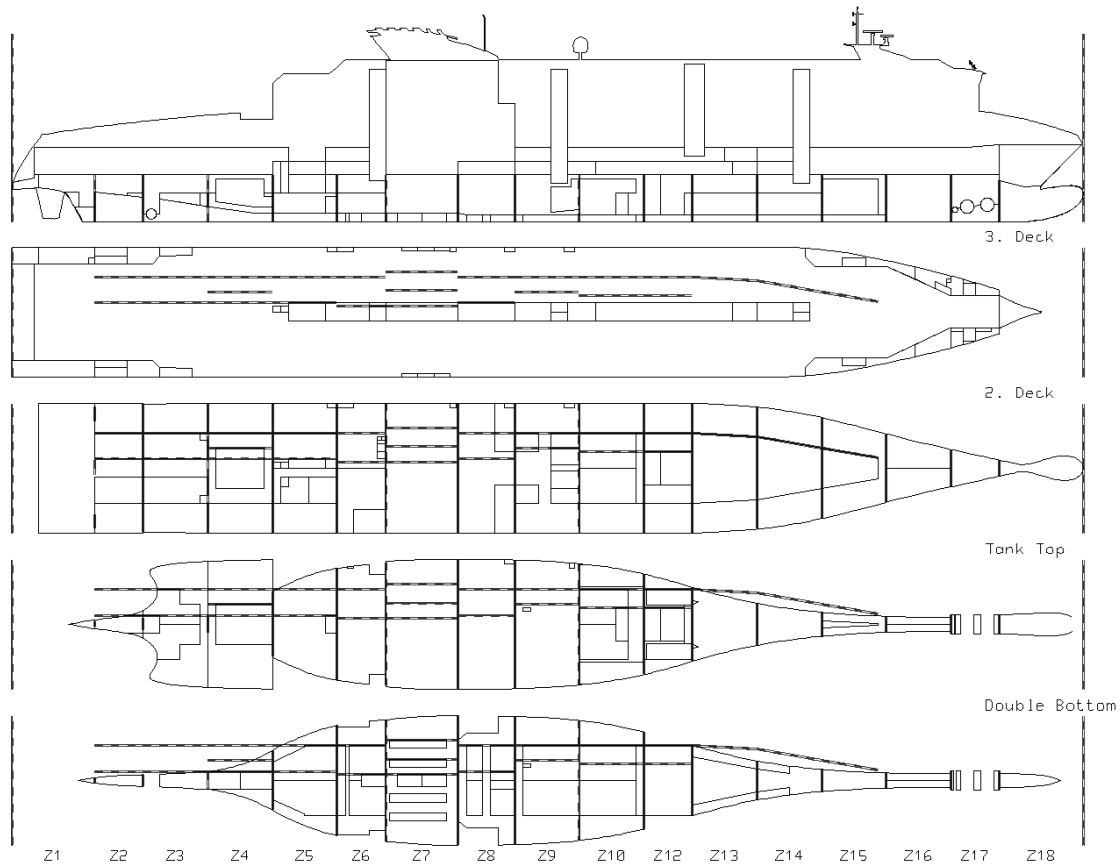


Figure 7-2: R1 Subdivision Arrangement

7.2.4 Required Subdivision Index - R

The vessel has been assessed such the Attained Subdivision Index is not less than the Required Subdivision Index as calculated according to the following formula:

$$R = 1 - \frac{5000}{L_S + 2.5N + 15225} \quad \text{Eq. 8-1}$$

Where,

N_1 - number of persons for whom lifeboats are provided

$N_1 = 600$

N_2 - number of persons that the ship is permitted to carry in excess of N_1

$N_2 = 1400$

$N = N_1 + 2 \cdot N_2$

$N = 3400$

$L_S = 212.25 \text{ m}$

7.2.5 Calculation Drafts

The initial conditions have been defined in accordance with SOLAS II-1, Regulation 7, whereby three draughts corresponding to the deepest subdivision draught d_s (6.7m), the lightest service draught d_l (5.807m) and for the partial subdivision draught d_p calculated according to the following formula:

$$d_p = d_l + 0.6 \cdot (d_s - d_l) \quad \text{Eq. 8-2}$$

A typical aft trim of 0.35 m has been applied to the light service draught along with zero trim (even keel) conditions assumed for partial and deepest subdivision draughts. The resultant loading conditions are summarised within Table below.

Table 7-2: Loading condition summary

Condition	Des.	T (m)	TR (m)	GM (m)	KG (m)	Disp. (t)
dl	Light service draught	5.807	-0.35	1.78	13.75	17093
dp	Partial subdivision draught	6.343	0.00	1.905	13.25	19302
ds	Deepest subdivision draught	6.700	0.00	2.26	12.89	20884

7.2.6 Permeabilities

In allocating space permeabilities, two approaches have been taken. Firstly, for those spaces unaffected by either the AREST A1 or P1 systems, permeability values have been defined in accordance with SOLAS assumptions as outlined within Table 7-3 and Table 7-4.

Table 7-3: Generalised compartment permeabilities

Spaces	Permeability
Appropriated to stores	0.6
Occupied by accommodation	0.95
Occupied by machinery	0.85
Intended for liquids	0.95
Void spaces	0.95

Table 7-4: Permeabilities for Ro-Ro spaces

Spaces	Permeability at draught d_s	Permeability at draught d_p	Permeability at draught d_l
Ro-Ro spaces	0.90	0.90	0.95

However, in such cases that the AREST system was assumed to be in effect, the permeability of the protected space has been defined as that of the intact space less the volume of expanded foam delivered to the space. Furthermore, contrary to the general assumption of a homogeneous distribution of permeability, it has instead been assumed that the foam forms a volume spanning from the upper limit of the compartment downwards with a permeability of 0.05, as substantiated within Chapter 6. This assumption has been made as a result of the foam’s ability to form on top of the water surface. The remainder of the protected compartment, unaffected by the foam, has been assumed to have permeability in line with conventional assumptions. This is further demonstrated within Figure 7-3 below.

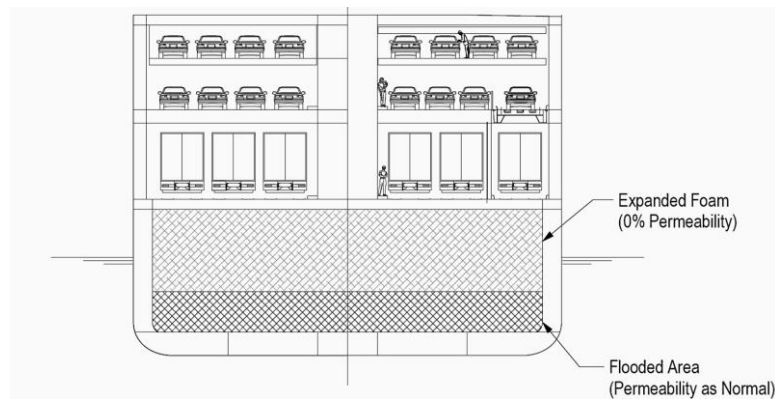


Figure 7-3: Permeability distribution assumption with foam in place

7.2.7 Damage Stability Assessment – as built

The vessel has first been subjected to damage stability assessment under her present GM limit curve conditions, which have proven to be optimal with the vessel achieving an Attained Index of 0.7911 with a Required Index of 0.7943, as shown in Table 7-5.

Table 7-5: as-operated Attained Index calculation

	Draught	Intact GM (m)	Trim (m)	Partial Indices		Attained Index	
DI	5.807 m	1.78	-0.35	AI	0.793	0.2	0.1586
Dp	6.343 m	1.905	0.00	Ap	0.796	0.4	0.3184
Ds	6.700 m	2.26	0.00	As	0.792	0.4	0.3171
				Required Subdivision Index R			0.7911
				Attained Subdivision Index A			0.7943

7.2.8 Existing Vessel GM limit Curve

Based on the Attained Index results presented within the foregoing, the vessel GM limit curve has also been calculated in order to form a baseline from which the impact the proposed solutions can later be measured. This is presented within Figure 7-4 along with the limiting GM curve relating to Stockholm Agreement compliance, both of which are shown relative to the vessel’s

statutory loading conditions. Here, it can firstly be observed that the vessel damage stability requirements are marginally dominated by those relating to SOLAS 2009 as opposed to the Stockholm Agreement. This is not typical for most RoPax designs, which are normally limited by the requirements of the SA. However, this particular design has substantial freeboard, measuring 2.7m at subdivision draught, which works to mitigate vessel vulnerability to water on deck. Furthermore, it can be observed that the vessel currently possesses significant GM margins, ranging from 0.23m to 1.977m, see Table 7-6.

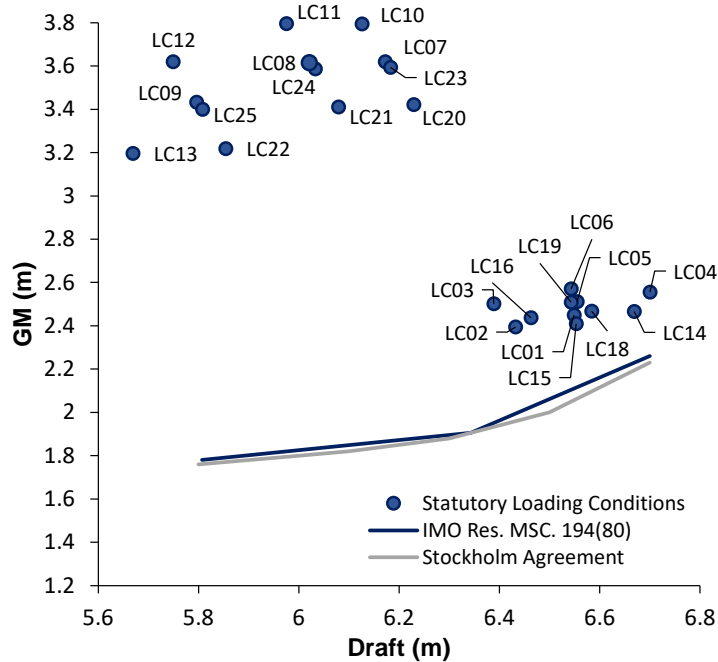


Figure 7-4: R1 as-built GM damage stability related limit curves

Table 7-6: R1 statutory loading conditions & existing GM margins

CASE	DISP (t)	T (m)	TR (m)	GM (m)	GM Req. (m)	GM Margin (m)
LC01	20208	6.549	-0.000	2.449	2.110	0.339
LC02	19710	6.432	-0.081	2.395	1.993	0.402
LC03	19507.5	6.389	-0.006	2.501	1.951	0.550
LC04	20886.1	6.7	-0.002	2.555	2.260	0.295
LC05	20263.6	6.555	-0.108	2.511	2.116	0.395
LC06	20185.6	6.543	-0.027	2.57	2.104	0.466
LC07	18570.4	6.172	-0.018	3.62	1.865	1.755
LC08	17947.9	6.021	-0.098	3.615	1.830	1.785
LC09	17029.9	5.796	-0.247	3.433	1.777	1.656
LC10	18390.4	6.126	-0.094	3.794	1.854	1.940
LC11	17767.9	5.975	-0.175	3.796	1.819	1.977
LC12	16849.9	5.749	-0.326	3.62	1.766	1.854
LC13	16470	5.669	0.001	3.196	1.748	1.448
LC14	20745.6	6.669	0.006	2.466	2.229	0.237
LC15	20247.6	6.553	-0.083	2.409	2.114	0.295

LC16	19845.1	6.463	-0.075	2.437	2.024	0.413
LC18	20387.7	6.584	-0.089	2.467	2.145	0.322
LC19	20185.2	6.543	-0.024	2.508	2.104	0.404
LC20	18808	6.229	0.019	3.422	1.878	1.544
LC21	18185.5	6.079	-0.062	3.411	1.843	1.568
LC22	17267.5	5.854	-0.212	3.218	1.791	1.427
LC23	18628	6.183	-0.057	3.593	1.868	1.725
LC24	18005.5	6.033	-0.139	3.587	1.833	1.754
LC25	17087.5	5.808	-0.290	3.399	1.780	1.619

7.2.9 Vulnerability Assessment

7.2.9.1 Critical Space Identification

In order to inform the process of determining which spaces would be best served by protection from the AREST A1 and P1 systems, the results of the probabilistic damage stability assessment have been used in order to derive the vessel Risk Profile. This particular diagram provides what could be thought of as a “risk mapping” across the vessel in the form of $p^*(1-s)$ according to varying damage lengths. This metric is of course not a “true” risk quantification but is indicative and serves to highlight regions of vulnerability. The resultant Risk Profile is provided within Figure 7-5 and demonstrates vessel vulnerability in both the fore and aft shoulders, highlighted in blue circles. The reasons for this stemmed from stability problems, such as capsizing or excessive heel, as opposed to criteria fails relating to opening immersion etc. Specifically, the vessel displayed a tendency to take on an unfavourable floating position in damages within these regions, resulting in a diminished waterplane area and thus damage GM. Peak flooding risk was identified towards the vessel aft shoulder, stemming from damages of 3-compartment length. The fore shoulder, though demonstrating a lower peak flooding risk value, was found to possess a higher density of loss scenarios, again primarily resulting from 3-compartment damages. In addition, several smaller damage cases of 2-compartment length were identified here as having an s-factor ranging between $0 < s < 1$. Considering these results, spaces within these regions were targeted for protection by the AREST systems.

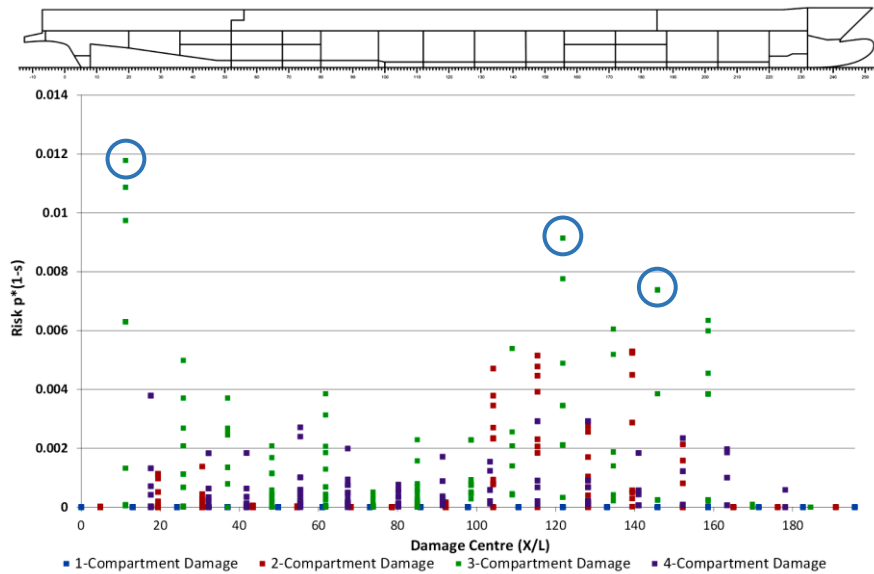


Figure 7-5: R1 as-built Risk Profile

Within the vessel fore shoulder region, two dry tanks (DT6 & DT20) were selected for protection by the AREST P1 system. This decision was made after having determined through ship survey that these spaces were unutilised “dead space” and could, therefore, be filled with foam permanently without affecting the operation of the vessel. In contrast, the high-risk area identified around the vessel aft shoulder was found to stem from a compartment C1, which was used daily within the vessel operation. As such, in order to maintain the utility of this space, the AREST A1 system was considered suitable as foam would only be introduced into the space at the time of collision. An overview of the space volumes is provided within Table 7-7 along with an indication of their location within the vessel within Figure 7-6.

Table 7-7: Vulnerable space properties

Compartment ID	Compartment Volume (m ³)	RCO
Compartment C1	799.3	AREST A1
Dry Tank No 6	1690.6	AREST P1
Dry Tank No 20	578.8	AREST P1

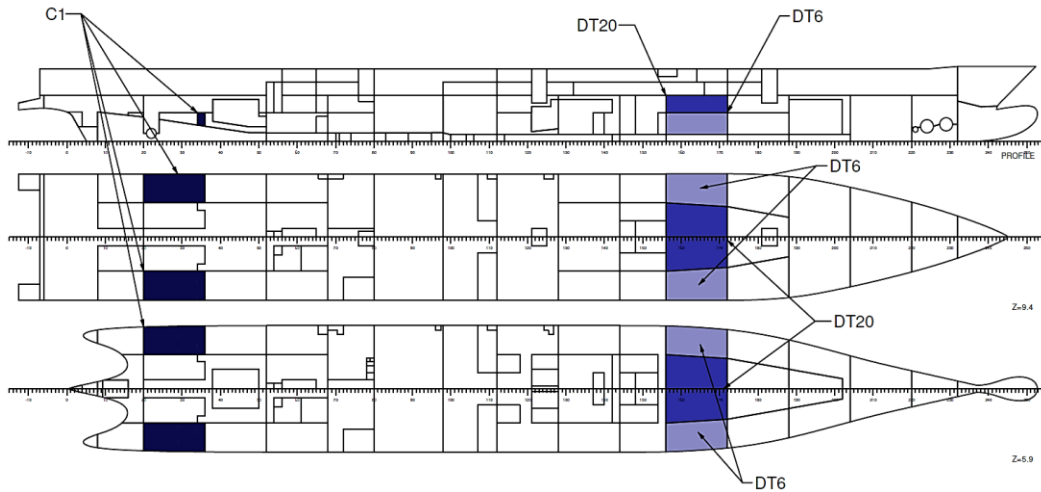


Figure 7-6: Vulnerable space locations

7.2.9.2 Determination of Optimum Foam Volume

In order to identify the optimal volume of foam to deliver to each of the protected spaces, a sensitivity analysis has been conducted in which each space has been filled at incremental foam volumes (space permeability reductions) and the resultant Attained Index value has been calculated. Following this, collision risk in the form of 1-A has been calculated for each iteration. The results of this process have then been used in order to plot risk as a function of foam volume. From this, a point of diminishing returns can be identified, thus providing the optimum volume of foam to be introduced with respect to risk reduction. The results of this process are outlined within Table 7-8 and Table 7-9, Table 9-10 along with a depiction in Figure 7-7.

Table 7-8: Foam volume optimisation C1

Fill (%)	Permeability (μ)	Foam Volume (m^3)	Index A	Risk (1-A)
90	0.1	719.37	0.82545	0.17455
70	0.285	559.51	0.825	0.175
40	0.57	319.72	0.81346	0.18654
10	0.855	79.93	0.79859	0.20141
0	0.95	0	0.7943	0.2062

Table 7-9: Foam volume optimisation DT6 & DT20

Fill (%)	Permeability (μ)	Foam Volume (m^3)	Index A	Risk (1-A)
90	0.1	1940.337	0.827	0.173
70	0.285	1509.151	0.8217	0.1783
40	0.57	862.372	0.81198	0.18802
10	0.855	215.593	0.7999	0.2001
0	0.95	0	0.7943	0.2057

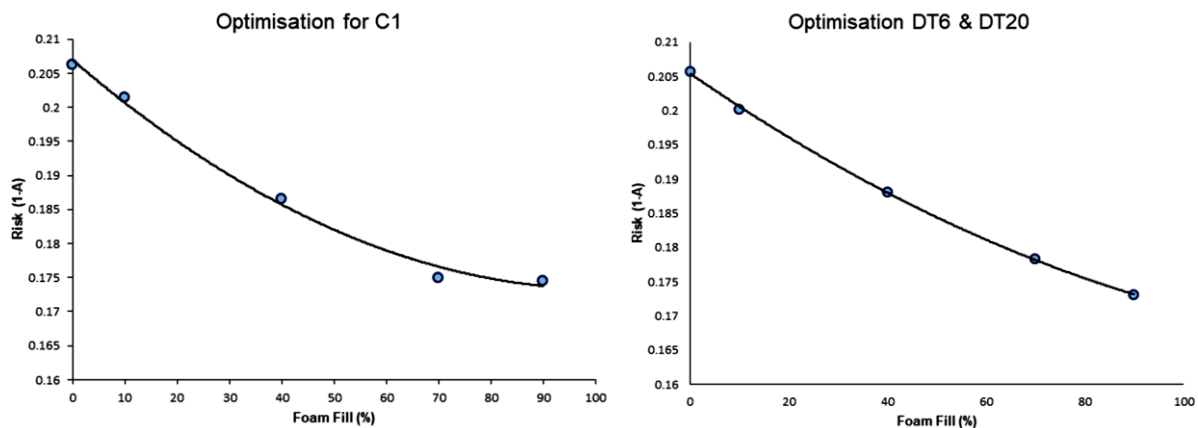


Figure 7-7: Foam volume optimisation, aft shoulder (left), fore shoulder (right)

On the basis of the above results, an optimum fill percentage of 70% is identified for both DT20 and DT6, yielding a foam volume of 385 m³ and 1124 m³ for each space respectively. In addition, an optimum foam volume of 559.51m³ has been determined for space C1, representing a 70% reduction in space permeability.

7.2.10 Solution Impact Assessment

7.2.10.1 Recalculation of Vessel Attained Index

The impact of the proposed solutions has first been gauged from the perspective of increased Attained Index. In this respect, the damage stability performance of the vessel has been reassessed with the aforementioned solutions in place, leading to the results provided within Table 7-10. Here, a significant increase in Attained Index can be observed, increasing from 0.794 to 0.865 in comparison to the existing design. This represents a substantial improvement and would be hard to match with any conventional RCOs that exist today, let alone in a manner that does not impact vessel operation. However, simply looking at the vessel Attained Index does not provide a full picture of the solution impact and so the vessel Risk Profiles are compared within the next section.

Table 7-10: Attained Index calculation with AREST solutions

	Draft	Intact GM (m)	Trim (m)		Partial Index	Attained Index	
dl	5.818 m	1.78	-0.35	Al	0.882	0.2	0.176
dp	6.347 m	1.905	0	Ap	0.871	0.4	0.348
ds	6.700 m	2.26	0	As	0.852	0.4	0.341
					Required Subdivision Index R		0.791
					Attained Subdivision Index A		0.865

7.2.10.2 Comparison of vessel Risk Profiles

Figure 7-8 below illustrates a comparison between the vessel Risk Profiles both before and after implementation of the AREST solutions. Here it can be observed that the solutions have been successful in greatly mitigating the risk within both the fore and aft shoulders regions. By doing so, the solutions have also had the effect of bringing the Risk Profile of the vessel into balance, with greater uniformity now existing across the vessel profile, meaning there are no longer any particular points of marked weakness within the vessel design.

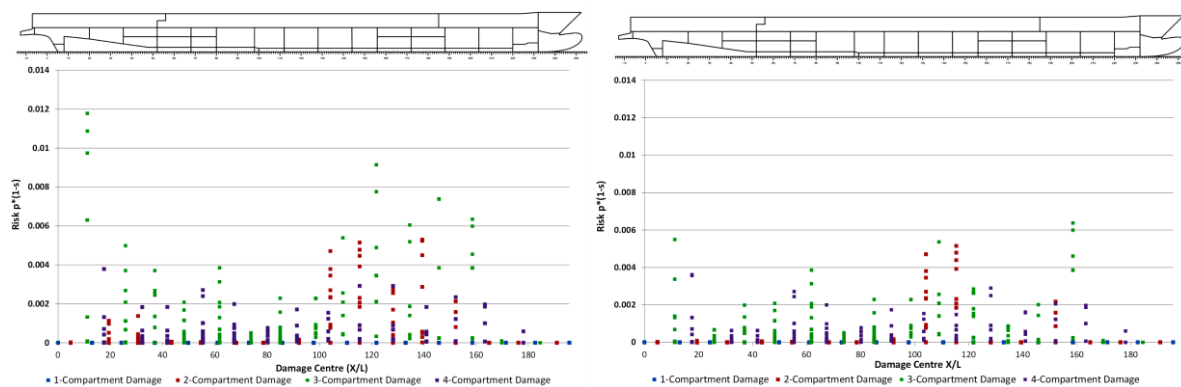


Figure 7-8: Comparison of vessel Risk Profiles, with (right) and without (left) AREST solutions

7.2.10.3 Impact on Vessel GM limits

The final metric considered in demonstrating the impact of the AREST solutions, is the variation in vessel statutory GM limits. This is an important parameter to consider as this directly affects the operation of the vessel, loading capacity and ultimately business viability/profitability. Table 7-11 and Figure 7-9 in the following, shows a comparison between these values, demonstrating an average reduction in GM requirements of 26cm. For a RoPax vessel of this size, this represents a significant reduction and would provide the operator with a far greater range of safe operation. Furthermore, improvement in GM margins of this scale would indicate that such solutions could be highly effective in future-proofing vessel designs and also acting as a means of enhancing the safety of older vessel designs in retrospect, such as to close the ever growing safety gap that is emerging between new and existing vessels, see Table 7-12.

Table 7-11: GM limit comparison before and after AREST solutions

	Draft (m)	Existing GM limit (m)	AREST GM limit (m)	ΔGM (m)
dl	5.81	1.78	1.52	0.26
dp	6.34	1.905	1.64	0.265
ds	6.7	2.26	1.99	0.27

Table 7-12: GM limit comparison before and after AREST solutions for statutory loading conditions

CASE	T (m)	GM (m)	GM Req. as-built (m)	GM Margin as-built (m)	GM Req. AREST (m)	GM Margin AREST (m)	ΔGM Margin (m)
LC01	6.549	2.449	2.110	0.339	1.842	0.607	0.268
LC02	6.432	2.395	1.993	0.402	1.727	0.668	0.266
LC03	6.389	2.501	1.951	0.550	1.685	0.816	0.266
LC04	6.7	2.555	2.260	0.295	1.990	0.565	0.270
LC05	6.555	2.511	2.116	0.395	1.848	0.663	0.268
LC06	6.543	2.57	2.104	0.466	1.836	0.734	0.268
LC07	6.172	3.62	1.865	1.755	1.602	2.018	0.263
LC08	6.021	3.615	1.830	1.785	1.568	2.047	0.262
LC09	5.796	3.433	1.777	1.656	1.518	1.915	0.260
LC10	6.126	3.794	1.854	1.940	1.592	2.202	0.263
LC11	5.975	3.796	1.819	1.977	1.558	2.238	0.261
LC12	5.749	3.62	1.766	1.854	1.507	2.113	0.259
LC13	5.669	3.196	1.748	1.448	1.489	1.707	0.259
LC14	6.669	2.466	2.229	0.237	1.960	0.506	0.269
LC15	6.553	2.409	2.114	0.295	1.846	0.563	0.268
LC16	6.463	2.437	2.024	0.413	1.758	0.679	0.267
LC18	6.584	2.467	2.145	0.322	1.876	0.591	0.268
LC19	6.543	2.508	2.104	0.404	1.836	0.672	0.268
LC20	6.229	3.422	1.878	1.544	1.615	1.807	0.264
LC21	6.079	3.411	1.843	1.568	1.581	1.830	0.262
LC22	5.854	3.218	1.791	1.427	1.531	1.687	0.260
LC23	6.183	3.593	1.868	1.725	1.604	1.989	0.263
LC24	6.033	3.587	1.833	1.754	1.571	2.016	0.262
LC25	5.808	3.399	1.780	1.619	1.520	1.879	0.260

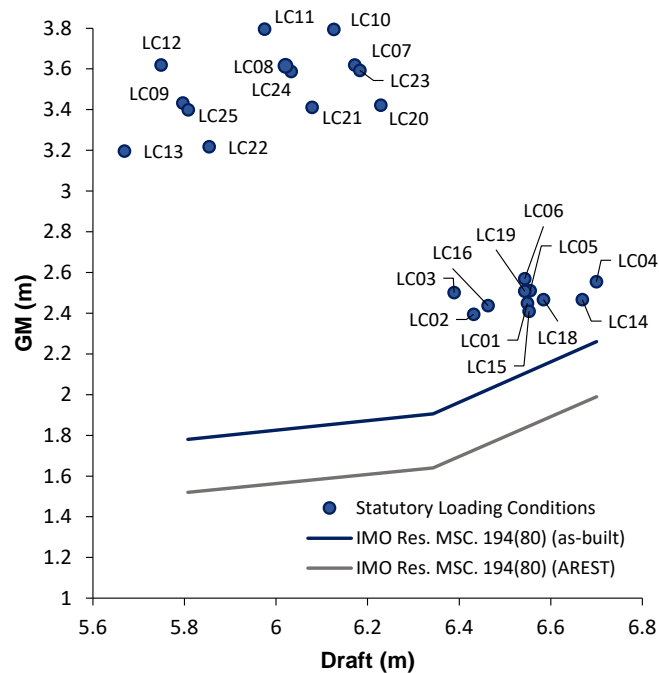


Figure 7-9: GM limit comparison before and after AREST solutions

7.2.11 Conclusions – Part A

Based on the findings outlined within this Chapter, the following concluding remarks can be made:

- AREST systems have shown to be non-intrusive reconfiguration measures, capable of protection post-damage in a highly cost-effective manner.
- The active protection system presented is, by nature of its design, highly flexible and can be easily applied to both new-builds and existing vessels.
- Though not included within the presentation of this thesis, this system has been applied across a range of RoPax vessels both SOLAS '90 and SOLAS 2009 compliant and has in each case demonstrated similar levels of improvement, demonstrating a wide range of applicability.
- The systems employed, through enhancing ship survivability to nearly the point of rendering a ship a lifeboat, fits the Safe Return to Port principle.

7.3 Part B: Dynamic Survivability Assessment

7.3.1 Modelling of the Ship Environment and External Conditions

7.3.1.1 Initial Condition

In assessing vessel survivability, consideration has been given to a single loading condition relating to the vessel deepest subdivision draught, under limiting GM conditions dictated by SOLAS 2009 compliance. This specific condition has been chosen as analysis of operational data within Chapter 5 demonstrated a tendency for RoPax vessels to operate predominantly towards the upper end of their draft range, with highest frequency recorded at approximately 0.8 of the non-dimensional draft range. Furthermore, consideration of the deepest subdivision draught also provides the grounds for a more rigorous evaluation of vessel survivability as residual freeboard is at its lowest, which subsequently increases the propensity for water accumulation on deck.

Table 7-13: Loading condition summary

Property	Value
Displacement [tonnes]	20,874
Trim [m]	0.00
GM [m]	2.26
KG [m]	12.89
Draft [m]	6.7

7.3.1.2 Simulation Model

As outlined within Chapter 5, the use of numerical time-domain simulations allows for details to be captured that would otherwise be ignored by static assessment and this is particularly true with regards to the level of detail accounted for when modelling the vessel internal geometry. For this reason, the existing static model of the vessel has been modified such to include all spaces liable to have a significant influence on the flooding process. This has involved the addition of all spaces partitioned by 'A' class fire rated walls, cold rooms, lift trunks, stairwells and escape trunks. In total, 36 spaces have been added to the stability model, now totalling 329 spaces ranging from the vessel baseline to the upper extremity of the Ro-Ro deck, Deck 05 (14.8m from B.L.). In contrast with examples later provided within Chapters 8 and 9, both of which concern cruise vessels, the level of additional detail required in this RoPax example is significantly less. The reason for this stems from the comparatively simple internal geometry of RoPax vessels coupled with the fact that static models for these ship types are modelled up to and inclusive of the Ro-Ro deck. This means that no additional decks must be included for the purposes of

numerical simulations, whereas cruise vessel models often require further definition to include one if not two decks more than the static model.

The resultant simulation model calculation sections are shown in Figure 7-10 along with the vessel arrangement in Figure 7-11.

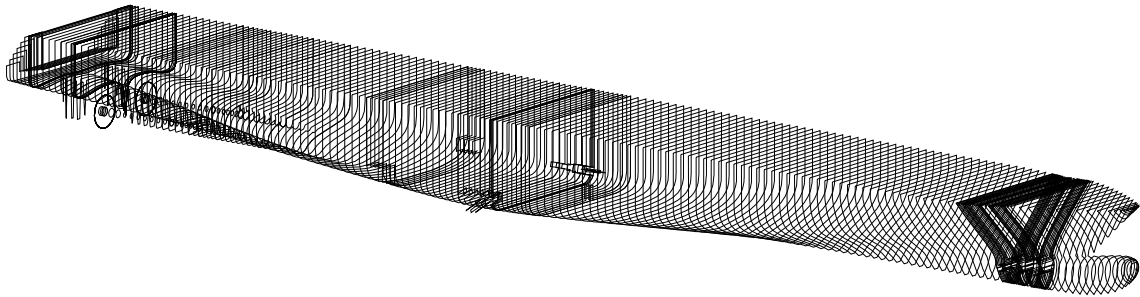


Figure 7-10: Simulation model calculation sections

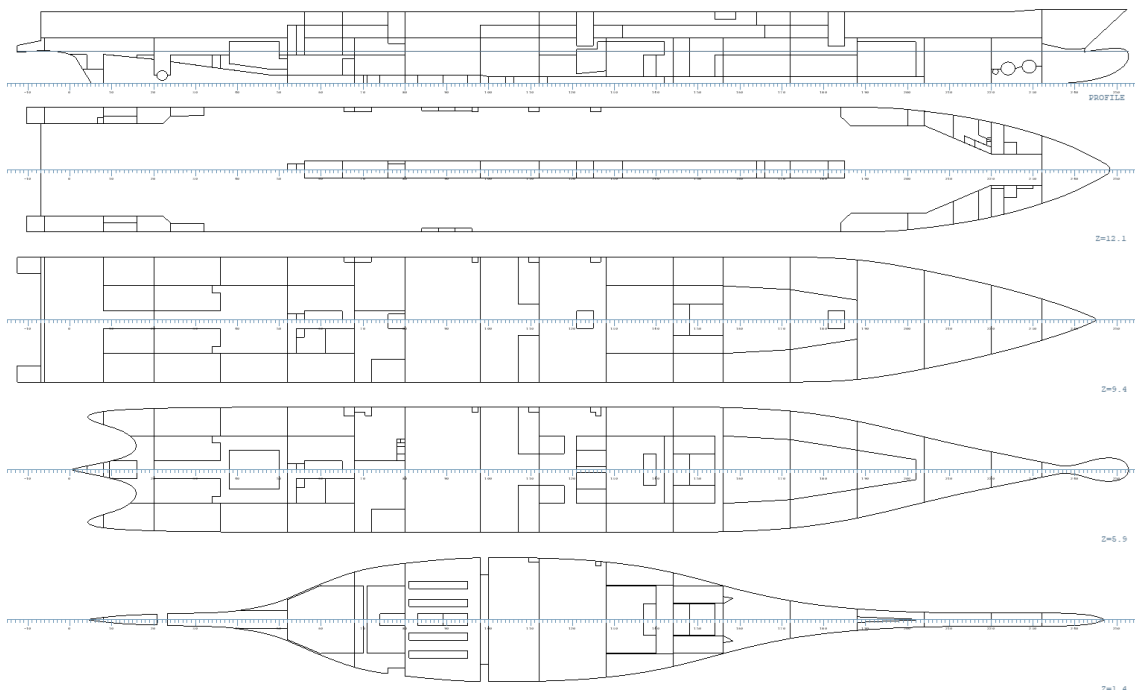


Figure 7-11: Simulation model arrangement

7.3.1.3 Verification of Internal Geometry

As the simulation model is exported from static stability software to dynamic simulation software, it is important to ensure continuity across the models. For this reason, a comparison has been performed between key model parameters. This includes properties such as compartment and tank volumes, centres of gravity and permeabilities. The results of this process are provided in Figure 7-12 below, where it can be observed that there is good correlation between the two models. This is an important step in order to ensure that no inaccuracies are introduced into the simulation model that could distort the results yielded.

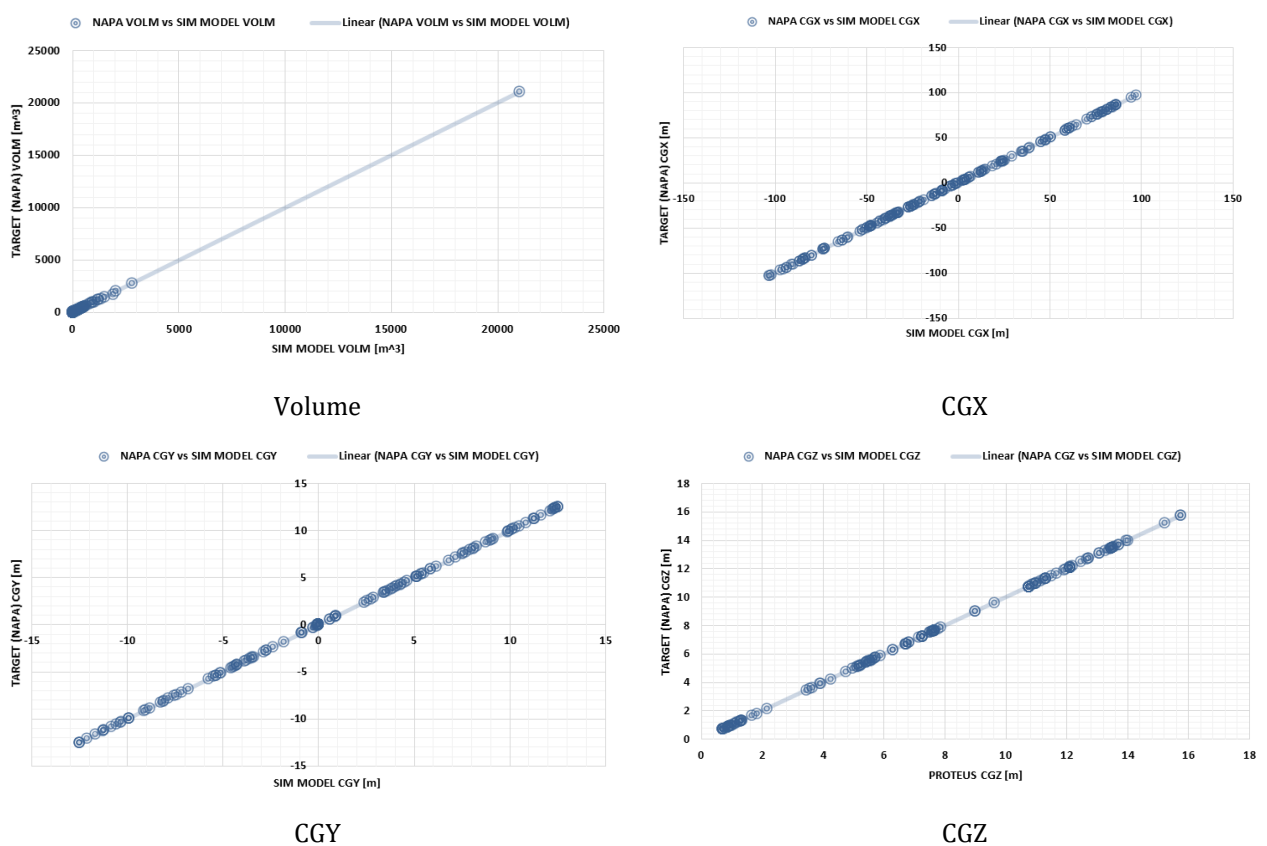


Figure 7-12: Comparison of hydrostatic & simulation model properties

A summary of the results above is provided within Table 7-14, where maximum deviations in values are listed. From the results presented here it is clear that there is no significant disparity between the two models.

Table 7-14: Model correlation summary

Property	Maximum difference [%]	Value
Volume	0.875	0.265 m ³
CGX	0.075	0.052 m
CGY	0.81	0.003 m
CGZ	0.42	0.08 m
Permeability	0.00	0.00

7.3.1.4 Opening Definition

In addition to enhancing the detail within the vessel internal geometry, the opening definition has also been modified for dynamic assessment. Here, all primary openings linking internal spaces have been modelled in their physical form and assigned flooding resistance properties in line with the process outlined within Chapter 5. In total, 204 openings have been modelled as shown in the opening arrangement within Figure 7-13 below.

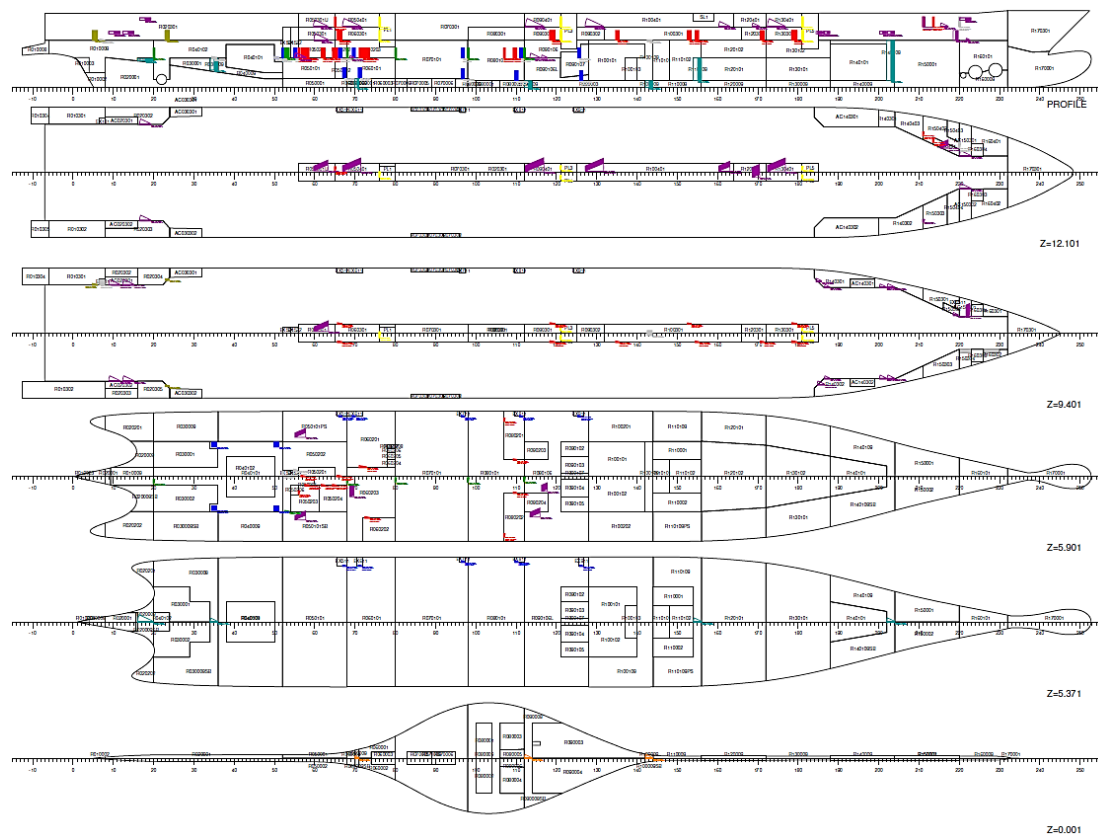


Figure 7-13: Simulation model opening arrangement

7.3.2 Simulation Properties & Damage Generation

7.3.2.1 Simulation Environment

The significant wave height utilised in the simulations has been fixed to $H_s=4\text{m}$ which represents the upper limit of the SOLAS sea state distribution, shown in Figure 7-14. This rather conservative assumption was made, as the intention of this assessment is to identify areas of vulnerability within the vessel design and this is better served by considering the most adverse conditions.

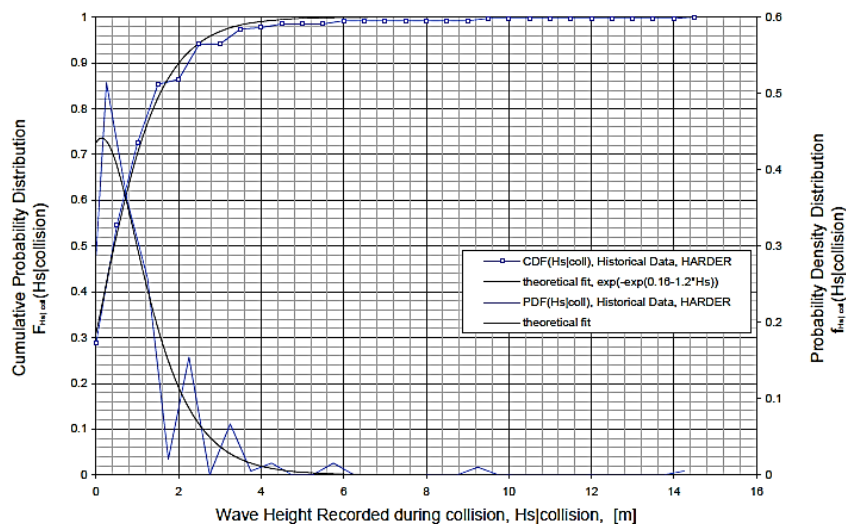


Figure 7-14: SOLAS 2009 CDF of H_s encountered during accidents, as obtained in (HARDER, 1999-2003).

The simulations are conducted in random waves generated with consideration of the JONSWAP wave spectrum, with the spectral density relative to circular wave frequency provided in Figure 7-15.

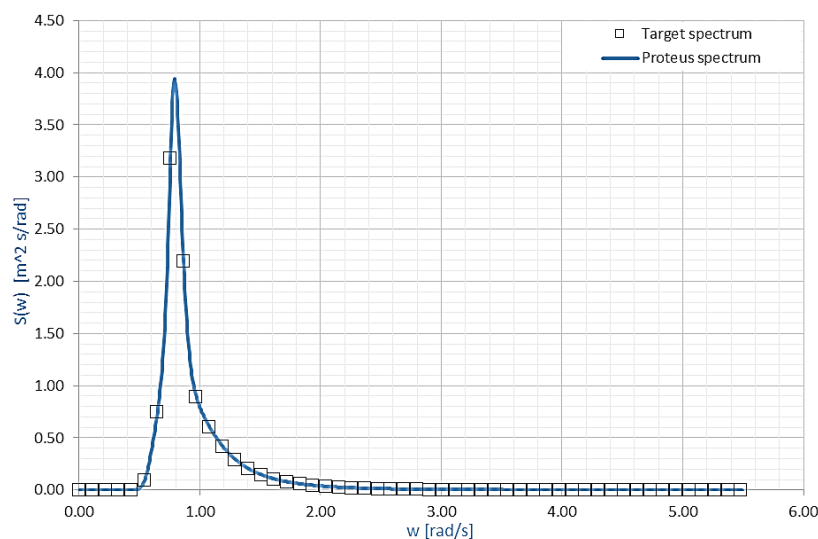


Figure 7-15: JONSWAP wave spectrum for $H_s=4\text{m}$

7.3.2.2 Exposure Time

The total exposure time for each simulation is 1,800 seconds (30 minutes), which is in line with the exposure time upon which the SOLAS s-factor is based. An extra 20 seconds is added to this time to allow the vessel to settle into the wave environment prior to the damage breach being activated at t=20s.

7.3.2.3 Damage Generation

In total 1,500 collision damages, shown in Figure 7-16, have been generated using Monte Carlo sampling techniques and with respect to the SOLAS damage distributions, comprising:

- Damage side, $ind_{side} \in \{-1,1\}$
- Longitudinal position of damage centre, X_c [m], $X_f \in [0, L_{ship}]$
- Longitudinal extent of potential damage, $L_{x,p}$ [m], $L_{x,p} \in [0,60]$
- Transversal extent of potential damage, $L_{y,p}$ [m], $L_{y,p} \in [0,0.5 \cdot B_{ship}]$
- Vertical position of lower limit of potential damage, $Z_{LL,p}$ [m], $Z_{LL,p} \in [0,6.7]$
- Vertical extent of potential damage, H_d [m], $H_d \in [0, H_{d,max}]$

An overview of the damage scenarios generated is provided in Figure 8-13 and a summary of the sample properties is provided within the following:

- Maximum damage length =55.2 m
- Average damage length =8.94 m
- Maximum transverse extent (measured from side shell at W.L.) =12.9m
- Average transverse extent =4.75 m
- Maximum vertical extent =18.65 m
- Average vertical extent = 8.81 m

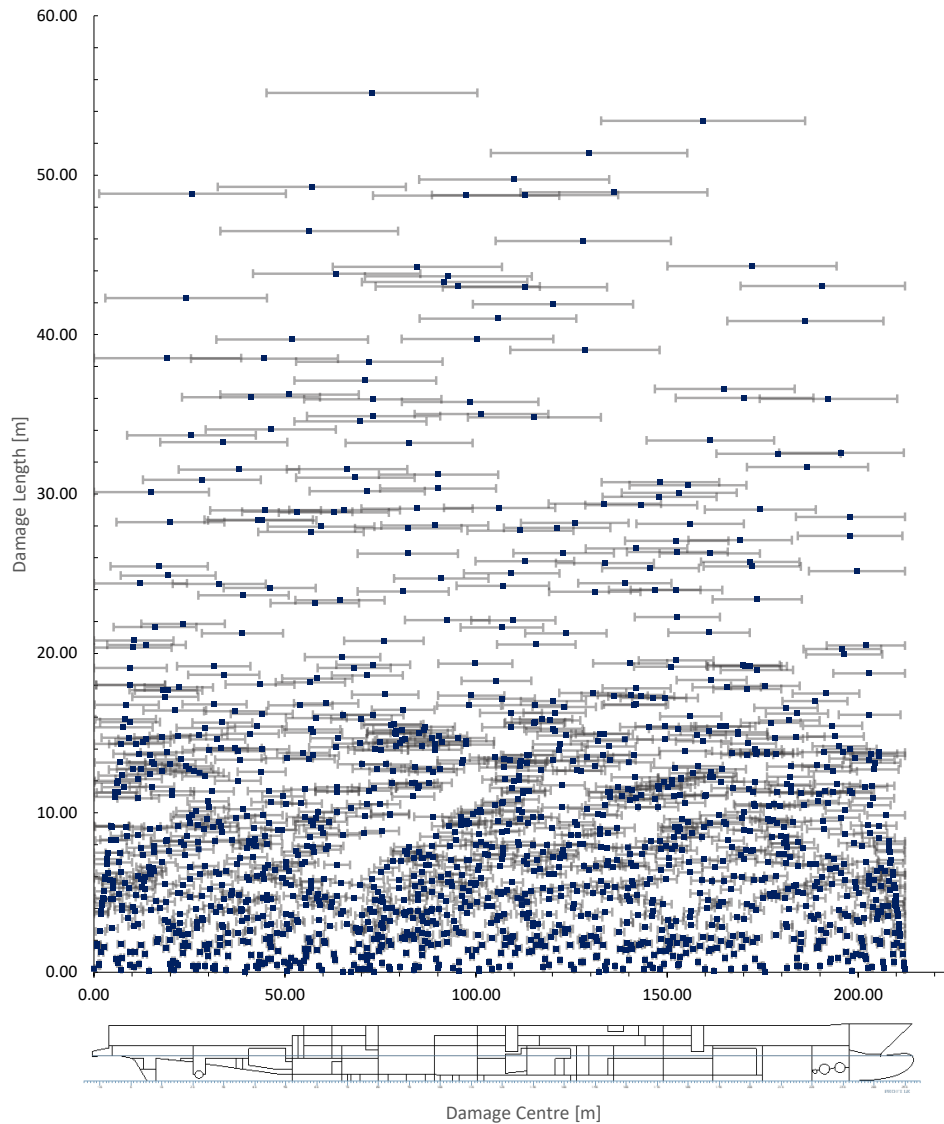


Figure 7-16: Collision damage sample

7.3.3 Simulation Results – As built

The results of the numerical simulations have demonstrated a total of 164 capsizes cases, which form the Cumulative Distribution Function for Time to Capsize provided in Figure 7-17. By viewing the results in this form, one can observe the time varying probability of capsizing, the complement of which is the time varying Survivability Index. Furthermore, observation of the shape of the CDF provides some insight into the nature of the loss scenarios being witnessed. In this example, of the 164 capsizes cases identified, 116 were found to result from transient capsizing and 48 due to progressive flooding. This demonstrates a propensity for transient loss, which is characterised by the sharp increase in the CDF below 300 seconds. Beyond this point, the CDF increases gradually as a result of a range of progressive flooding losses occurring at various stages

up until 26 minutes, after which no capsizing cases were recorded. Based on these findings, the vessel Survivability Index for 30 minutes exposure time was found to be 0.89 with 95% confidence intervals included, determined in accordance with Eq.5-1 in Chapter 5.

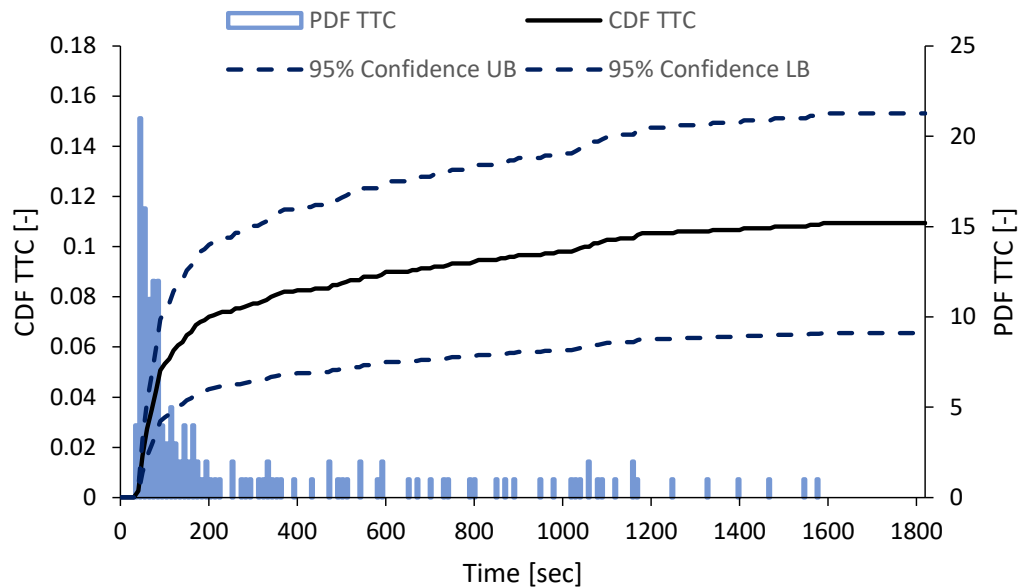


Figure 7-17: Cumulative probability distribution of Time to Capsize for all collision damages. Indication of Survivability Index=0.89, with 30 minutes exposure.

In addition to the above, detailed simulations results may be found within Appendix B which are to be interpreted according to Appendix A.

7.3.3.1 Loss Scenario Overview & Comparison

A summary of the location and extent of all capsizing cases is provided in Figure 7-18, with progressive flooding losses depicted with light blue markers and transient capsizing cases shown in dark blue. From these results, one can observe areas of heightened vulnerability towards the vessel fore and aft shoulders, where there are concentrations of capsizing cases and where the shortest damage lengths have given rise to vessel loss. In all cases no fewer than two compartments have been compromised, though the smallest damage length attributed to a loss scenario was just 2.79m. In general, the majority of capsizing cases with smaller damage lengths have succumbed to progressive flooding loss, with greater damage extents often resulting in transient capsizing (all cases of >25m in length). Progressive flooding losses also appear to occur exclusively towards the vessel fore and aft shoulders, whereas transient capsizing cases were identified across the entire vessel length, with exception of the bow portion. When comparing the simulation results to those stemming from the static assessment, shown in Figure 7-19, it is clear that there is good agreement between the results both in terms of the location of vulnerable areas identified and also the damage lengths giving rise to this vulnerability. However, the static results

fail to provide detailed feedback on the exact nature of this vulnerability and the mechanisms driving it, which is explored within the next section using the simulation results.

An overview of all capsizes case damage dimensions is provided in Table 7-15 and Table 7-16 below, along with a brief summary of the loss modality specific simulation results in Table 7-17 and Table 7-18.

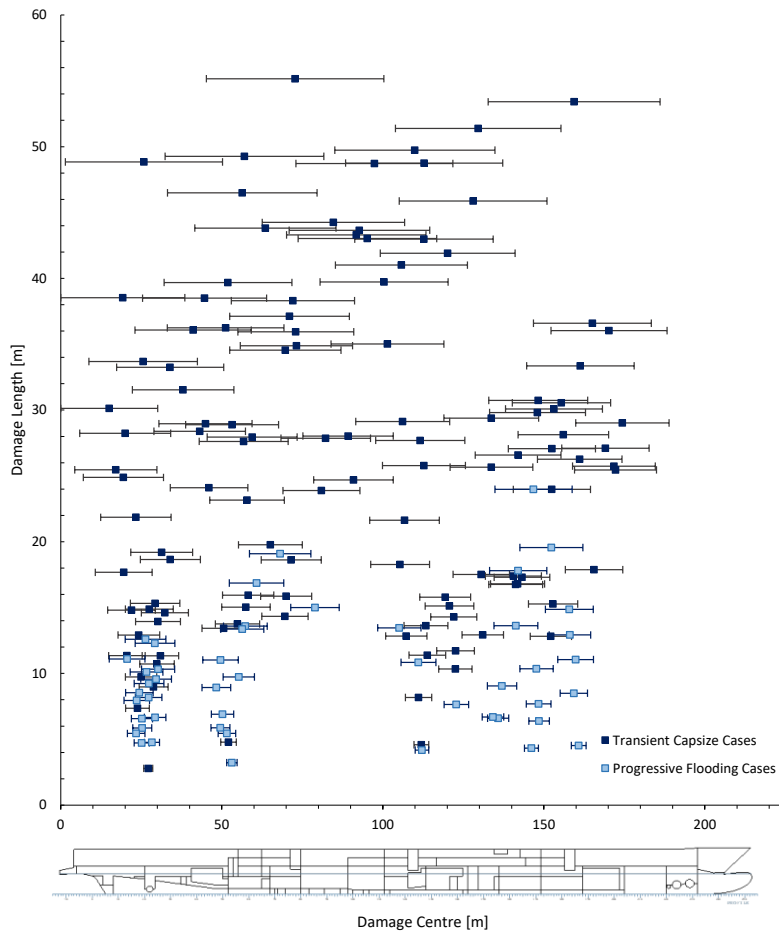


Figure 7-18: Location and extent of capsizes cases

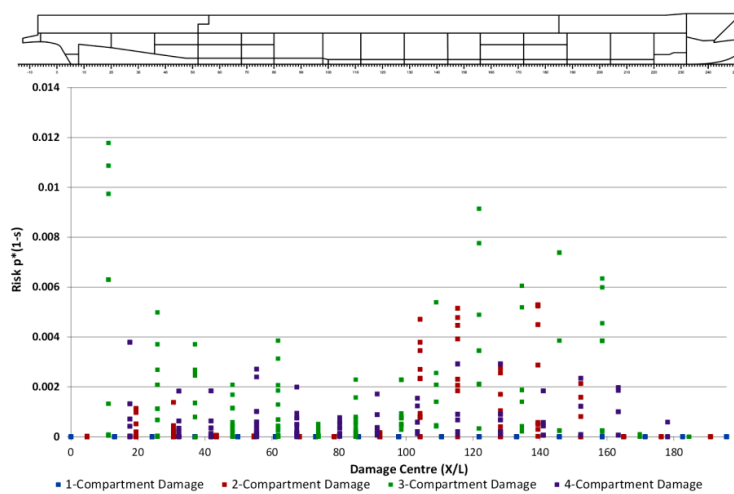


Figure 7-19: Risk Profile resulting from static assessment

Table 7-15: Transient capsizes case damage dimensions

Transient Capsizes Cases									
Case ID	X1 [m]	X2 [m]	Xc [m]	Lx [m]	Y1 [m]	Y2 [m]	Z1 [m]	Z2 [m]	Hs [m]
DMC19	91.31	134.29	112.80	42.98	-500.00	-6.87	5.17	12.66	4.00
DMC10	33.11	79.61	56.36	46.50	-500.00	-8.11	2.16	18.63	4.00
DMC05	32.41	81.68	57.04	49.27	-500.00	-10.01	1.61	14.64	4.00
DMC11	105.12	150.99	128.06	45.88	5.06	500.00	1.30	13.23	4.00
DMC51	22.20	53.74	37.97	31.54	8.94	500.00	2.77	17.09	4.00
DMC43	8.72	42.40	25.56	33.68	-500.00	-3.13	4.11	11.01	4.00
DMC04	85.09	134.82	109.96	49.73	6.77	500.00	6.25	12.47	4.00
DMC38	83.93	118.94	101.43	35.01	-500.00	-5.14	2.27	13.70	4.00
DMC41	52.45	87.01	69.73	34.55	-500.00	-5.71	5.62	12.99	4.00
DMC21	99.20	141.11	120.15	41.91	9.10	500.00	1.71	12.02	4.00
DMC45	17.34	50.59	33.97	33.25	0.64	500.00	2.03	13.14	4.00
DMC14	41.62	85.44	63.53	43.82	-500.00	-6.45	3.78	16.05	4.00
DMC15	70.91	114.57	92.74	43.66	-500.00	-9.13	1.88	13.57	4.00
DMC62	119.00	148.39	133.69	29.39	-500.00	-4.40	4.34	15.62	4.00
DMC99	7.00	31.89	19.45	24.88	-500.00	-6.35	2.43	18.49	4.00
DMC09	73.04	121.76	97.40	48.72	12.15	500.00	3.33	17.17	4.00
DMC22	85.26	126.27	105.77	41.01	9.86	500.00	4.43	10.46	4.00
DMC74	5.90	34.13	20.02	28.24	-500.00	-2.93	1.02	12.15	4.00
DMC03	103.91	155.30	129.60	51.39	0.55	500.00	0.95	11.66	4.00
DMC16	70.11	113.40	91.75	43.30	-500.00	-7.01	3.51	13.00	4.00
DMC18	73.70	116.73	95.21	43.02	8.98	500.00	6.05	14.53	4.00
DMC28	25.41	63.90	44.66	38.50	11.73	500.00	3.32	13.18	4.00
DMC24	80.51	120.24	100.38	39.73	-500.00	-12.13	6.45	10.31	4.00
DMC29	52.93	91.24	72.08	38.31	12.01	500.00	0.88	18.17	4.00
DMC61	133.14	162.95	148.05	29.82	6.76	500.00	3.53	12.67	4.00
DMC138	21.75	40.95	31.35	19.19	-500.00	-3.05	3.38	12.27	4.00
DMC36	55.01	90.95	72.98	35.94	-500.00	-2.59	1.27	17.38	4.00
DMC27	0.00	38.53	19.26	38.53	-1.21	500.00	3.51	15.24	4.00
DMC39	55.74	90.63	73.18	34.89	11.69	500.00	0.94	13.72	4.00
DMC145	24.68	43.33	34.01	18.65	6.63	500.00	0.22	11.54	4.00
DMC160	10.72	28.39	19.56	17.68	-500.00	-5.48	3.47	17.82	4.00
DMC93	120.90	146.56	133.73	25.66	6.72	500.00	1.13	13.42	4.00
DMC30	52.47	89.59	71.03	37.12	2.97	500.00	2.93	14.04	4.00
DMC25	32.07	71.76	51.91	39.69	-500.00	-12.40	4.85	10.29	4.00
DMC82	42.99	70.61	56.80	27.62	-500.00	-2.47	0.35	13.28	4.00
DMC59	0.00	30.12	15.06	30.12	-6.56	500.00	3.88	16.35	4.00
DMC64	91.62	120.75	106.18	29.13	-500.00	-6.73	0.94	13.23	4.00
DMC100	78.54	103.24	90.89	24.70	-500.00	-10.11	5.78	15.47	4.00
DMC119	95.93	117.56	106.74	21.63	6.80	500.00	1.28	17.12	4.00
DMC72	28.95	57.33	43.14	28.39	-500.00	-12.45	0.60	18.30	4.00
DMC02	132.72	186.13	159.43	53.41	-500.00	4.14	6.39	11.25	4.00
DMC78	45.47	73.42	59.44	27.95	3.10	500.00	4.49	12.25	4.00
DMC32	33.09	69.32	51.21	36.24	7.74	500.00	4.17	10.20	4.00

DMC161	121.80	139.32	130.56	17.52	-500.00	-7.40	2.85	13.01	4.00
DMC113	46.25	69.41	57.83	23.16	9.92	500.00	5.82	11.78	4.00
DMC91	99.89	125.67	112.78	25.79	4.02	500.00	1.73	11.27	4.00
DMC85	139.00	166.06	152.53	27.06	-500.00	-6.37	4.85	13.99	4.00
DMC44	144.66	178.02	161.34	33.36	-1.77	500.00	2.62	13.50	4.00
DMC149	96.23	114.50	105.36	18.28	12.50	500.00	4.03	14.34	4.00
DMC200	111.50	127.29	119.39	15.80	4.31	500.00	0.25	10.90	4.00
DMC235	20.06	34.94	27.50	14.88	6.22	500.00	3.34	10.77	4.00
DMC60	138.13	168.21	153.17	30.08	-500.00	2.34	0.09	13.22	4.00
DMC86	128.71	155.29	142.00	26.58	2.45	500.00	2.06	13.68	4.00
DMC117	12.42	34.27	23.35	21.86	-500.00	-1.37	6.53	12.20	4.00
DMC217	21.62	36.95	29.29	15.33	1.16	500.00	0.56	14.03	4.00
DMC302	106.56	120.19	113.38	13.63	-500.00	-3.91	4.08	12.09	4.00
DMC262	62.45	76.78	69.61	14.33	-500.00	-6.56	4.30	13.34	4.00
DMC33	23.07	59.14	41.11	36.07	10.75	500.00	1.63	9.71	4.00
DMC198	62.06	77.92	69.99	15.86	-500.00	-10.67	5.82	11.74	4.00
DMC84	155.58	182.69	169.14	27.11	1.86	500.00	1.82	12.37	4.00
DMC224	113.16	128.28	120.72	15.12	-500.00	-4.76	5.33	11.47	4.00
DMC105	33.98	58.08	46.03	24.10	-500.00	-9.41	6.50	18.95	4.00
DMC176	133.47	150.27	141.87	16.80	-500.00	-4.53	1.58	12.21	4.00
DMC131	55.21	74.98	65.09	19.77	-500.00	-12.14	2.58	13.31	4.00
DMC451	24.52	35.23	29.87	10.72	-500.00	-3.59	2.00	11.50	4.00
DMC76	141.98	170.11	156.05	28.13	3.40	500.00	0.08	17.94	4.00
DMC411	108.14	119.53	113.84	11.39	3.44	500.00	5.44	18.24	4.00
DMC683	20.15	27.50	23.82	7.36	-500.00	-3.87	0.19	18.25	4.00
DMC340	100.87	113.72	107.29	12.84	-500.00	-2.61	3.09	16.96	4.00
DMC336	17.79	30.70	24.25	12.92	4.40	500.00	6.13	11.24	4.00
DMC333	124.58	137.51	131.05	12.93	-500.00	-11.99	2.27	17.01	4.00
DMC501	20.09	29.82	24.95	9.73	2.76	500.00	1.81	10.85	4.00
DMC34	152.24	188.27	170.25	36.03	-500.00	1.76	1.02	10.16	4.00
DMC390	116.75	128.47	122.61	11.72	-500.00	-2.00	4.24	15.98	4.00
DMC13	62.54	106.79	84.66	44.25	-500.00	-2.47	0.62	9.99	4.00
DMC01	45.19	100.36	72.78	55.16	11.22	500.00	0.89	9.67	4.00
DMC92	158.89	184.64	171.77	25.74	-500.00	-0.53	1.44	18.87	4.00
DMC249	25.01	39.62	32.32	14.61	-500.00	-1.21	4.33	10.57	4.00
DMC07	1.41	50.25	25.83	48.84	-9.98	500.00	6.19	9.89	4.00
DMC280	23.20	37.14	30.17	13.94	0.57	500.00	2.22	18.88	4.00
DMC56	140.20	170.75	155.47	30.55	-500.00	0.46	0.39	10.09	4.00
DMC179	132.90	149.65	141.28	16.75	-500.00	-2.02	5.08	11.56	4.00
DMC417	25.26	36.61	30.94	11.34	-500.00	-2.61	5.16	13.25	4.00
DMC66	159.89	188.91	174.40	29.02	-1.46	500.00	2.14	16.27	4.00
DMC94	4.36	29.83	17.09	25.46	-3.99	500.00	2.56	9.71	4.00
DMC81	97.77	125.47	111.62	27.70	9.46	500.00	3.06	15.61	4.00
DMC561	24.33	33.31	28.82	8.98	2.74	500.00	3.63	10.73	4.00
DMC195	50.22	66.17	58.19	15.95	5.33	500.00	3.47	13.60	4.00
DMC146	62.23	80.86	71.54	18.62	3.67	500.00	3.88	10.55	4.00
DMC69	38.77	67.66	53.21	28.89	8.13	500.00	0.15	12.12	4.00
DMC77	75.20	103.23	89.22	28.03	-500.00	-6.75	0.41	11.02	4.00

DMC612	107.04	115.22	111.13	8.18	2.80	500.00	5.96	12.37	4.00
DMC239	14.55	29.36	21.96	14.81	-500.00	-8.85	0.49	13.65	4.00
DMC472	117.37	127.70	122.54	10.33	-500.00	-3.13	0.13	11.06	4.00
DMC416	14.87	26.21	20.54	11.35	-500.00	-1.14	0.86	17.09	4.00
DMC89	148.02	174.29	161.16	26.27	2.46	500.00	0.77	13.84	4.00
DMC167	134.58	151.87	143.23	17.30	-500.00	-0.48	5.08	18.06	4.00
DMC08	88.47	137.23	112.85	48.76	-500.00	-6.64	1.76	9.52	4.00
DMC950	109.70	114.29	112.00	4.59	-500.00	-10.51	5.45	14.29	4.00
DMC107	140.50	164.47	152.48	23.97	6.00	500.00	5.67	15.28	4.00
DMC155	156.67	174.54	165.61	17.88	1.31	500.00	4.10	15.21	4.00
DMC308	43.86	57.29	50.58	13.42	-500.00	-5.21	0.44	11.64	4.00
DMC108	68.99	92.88	80.94	23.89	-500.00	-2.52	0.49	18.50	4.00
DMC164	131.86	149.26	140.56	17.40	-500.00	1.93	2.83	12.73	4.00
DMC55	132.88	163.62	148.25	30.74	-500.00	1.02	2.15	9.59	4.00
DMC68	30.45	59.42	44.94	28.97	-500.00	-10.13	4.97	9.89	4.00
DMC265	114.91	129.20	122.05	14.29	-500.00	-2.64	2.46	9.89	4.00
DMC31	146.81	183.40	165.10	36.59	-7.44	500.00	5.39	9.73	4.00
DMC227	49.96	65.00	57.48	15.04	10.39	500.00	5.20	16.47	4.00
DMC95	159.56	185.01	172.28	25.46	-500.00	2.87	5.68	16.62	4.00
DMC80	68.35	96.20	82.27	27.85	-500.00	-6.88	0.94	10.97	4.00
DMC219	145.22	160.49	152.86	15.27	-500.00	-6.73	5.01	12.45	4.00
DMC924	49.69	54.47	52.08	4.78	-500.00	-2.38	6.28	16.60	4.00
DMC1142	25.77	28.56	27.16	2.79	5.76	500.00	1.12	13.11	4.00
DMC341	145.77	158.59	152.18	12.82	-500.00	1.05	4.25	11.17	4.00
DMC291	47.98	61.74	54.86	13.75	-500.00	-4.73	3.29	10.11	4.00

Table 7-16: Progressive flooding capsized case damage dimensions

Progressive Flooding Losses									
Case ID	X1 [m]	X2 [m]	Xc [m]	Lx [m]	Y1 [m]	Y2 [m]	Z1 [m]	Z2 [m]	Hs [m]
DMC565	43.84	52.77	48.30	8.93	6.08	500.00	0.98	10.60	4.00
DMC807	46.64	52.51	49.57	5.87	-500.00	-5.85	5.39	13.64	4.00
DMC157	133.13	150.93	142.03	17.80	4.69	500.00	6.63	9.77	4.00
DMC304	50.52	64.11	57.31	13.59	-500.00	-6.55	1.74	10.13	4.00
DMC300	134.51	148.14	141.32	13.63	-500.00	-7.01	2.85	10.79	4.00
DMC364	23.11	35.40	29.25	12.29	-500.00	-8.13	2.46	10.28	4.00
DMC743	25.96	32.62	29.29	6.66	-500.00	-4.14	0.90	11.53	4.00
DMC141	58.57	77.66	68.12	19.09	-500.00	-10.67	1.12	10.71	4.00
DMC589	20.16	28.70	24.43	8.54	-500.00	-11.03	2.03	12.64	4.00
DMC810	22.36	28.22	25.29	5.86	-500.00	-11.76	1.13	16.84	4.00
DMC106	134.80	158.78	146.79	23.98	-500.00	2.37	5.43	9.60	4.00
DMC857	20.69	26.14	23.42	5.44	-500.00	-5.15	4.14	15.56	4.00
DMC439	44.07	55.10	49.59	11.03	2.02	500.00	3.01	17.04	4.00
DMC752	132.53	139.13	135.83	6.60	-500.00	-2.10	1.39	15.01	4.00
DMC554	132.49	141.55	137.02	9.05	-500.00	-0.61	3.26	11.72	4.00
DMC470	142.54	152.90	147.72	10.36	-500.00	0.02	3.64	11.71	4.00
DMC657	144.53	152.22	148.38	7.68	-500.00	1.77	6.11	14.71	4.00

DMC719	46.77	53.67	50.22	6.91	-500.00	-12.79	1.83	12.35	4.00
DMC132	142.58	162.14	152.36	19.56	7.21	500.00	2.98	15.32	4.00
DMC989	110.08	114.26	112.17	4.18	-500.00	-3.45	5.04	9.92	4.00
DMC661	119.01	126.65	122.83	7.64	-500.00	-3.62	0.55	9.70	4.00
DMC856	48.88	54.32	51.60	5.44	6.23	500.00	1.98	17.83	4.00
DMC755	21.92	28.49	25.20	6.57	11.83	500.00	1.14	14.53	4.00
DMC500	50.43	60.17	55.30	9.73	-500.00	-7.52	4.50	18.49	4.00
DMC928	25.92	30.68	28.30	4.76	-500.00	-12.61	0.30	15.25	4.00
DMC739	130.87	137.56	134.22	6.70	-500.00	-5.14	2.58	11.25	4.00
DMC766	145.34	151.73	148.53	6.39	-500.00	-3.63	1.73	18.95	4.00
DMC630	19.63	27.58	23.60	7.95	-500.00	-12.26	0.98	9.95	4.00
DMC538	22.78	32.01	27.39	9.23	12.67	500.00	2.38	11.77	4.00
DMC480	21.58	31.69	26.64	10.11	10.19	500.00	3.16	10.95	4.00
DMC511	24.82	34.39	29.60	9.57	9.30	500.00	3.68	17.80	4.00
DMC356	20.02	32.61	26.31	12.59	12.12	500.00	2.59	13.16	4.00
DMC448	105.63	116.47	111.05	10.84	-500.00	-9.57	1.14	13.75	4.00
DMC335	151.64	164.57	158.10	12.92	-500.00	-0.61	0.80	12.55	4.00
DMC611	23.19	31.37	27.28	8.18	-500.00	-10.53	6.58	9.51	4.00
DMC236	150.48	165.35	157.92	14.87	-500.00	3.06	4.49	18.06	4.00
DMC473	25.06	35.39	30.22	10.32	11.90	500.00	5.34	17.86	4.00
DMC174	52.36	69.22	60.79	16.86	-500.00	-0.29	2.83	12.15	4.00
DMC933	22.79	27.52	25.15	4.73	8.11	500.00	0.65	11.46	4.00
DMC307	98.38	111.84	105.11	13.46	-500.00	-1.64	2.43	13.59	4.00
DMC981	144.02	148.34	146.18	4.32	-500.00	0.35	5.00	17.03	4.00
DMC591	155.08	163.58	159.33	8.50	-500.00	2.71	0.76	11.95	4.00
DMC228	71.43	86.44	78.94	15.01	-500.00	-2.75	0.53	14.35	4.00
DMC436	15.05	26.15	20.60	11.10	-500.00	-11.99	4.31	15.82	4.00
DMC437	154.36	165.41	159.89	11.06	-500.00	5.60	3.61	14.09	4.00
DMC1098	51.54	54.77	53.16	3.23	-500.00	-8.68	2.61	13.03	4.00
DMC957	158.57	163.10	160.83	4.53	-500.00	2.13	3.92	10.96	4.00
DMC311	49.65	63.02	56.34	13.37	5.54	500.00	2.54	11.45	4.00

Table 7-17: Transient capsize case results summary

Transient Capsize Cases						
Case ID	Time to Capsize [s]	Final fw. mass rate [t/h]	Final avg. fw. mass [t]	Max fw. mass [t]	Max roll [deg]	Final avg. heel [deg]
DMC19	36.35	1860601	4376	7633	176	35
DMC10	38.91	2389256	8656	13315	175	26
DMC05	39.01	2286079	9817	12520	175	42
DMC11	39.35	1912464	9568	12305	-175	-41
DMC51	41.70	1536274	5213	8704	-175	-37
DMC43	42.34	928150	4376	5828	176	32
DMC04	42.50	1727915	4871	8654	-175	-30
DMC38	43.07	1453984	7271	10169	175	40
DMC41	43.18	1361703	4108	7983	175	28
DMC21	43.77	1054545	6161	8737	-175	-27
DMC45	43.91	1083138	6019	8424	-176	-32
DMC14	44.15	2235769	10353	14825	175	37

DMC15	44.36	1571872	8773	11950	175	39
DMC62	44.45	1572492	5215	10242	175	27
DMC99	44.59	1173658	4438	7465	175	40
DMC09	44.78	1566971	8558	11969	-175	-31
DMC22	46.19	927953	4823	7182	-175	-28
DMC74	46.19	822174	3749	5827	176	33
DMC03	46.31	1545852	12015	15303	-175	-34
DMC16	46.73	1512368	7825	11894	175	30
DMC18	46.75	1414164	4328	9726	-175	-27
DMC28	48.07	1105764	5656	8736	-175	-31
DMC24	48.17	814333	3013	5236	175	34
DMC29	48.36	1478469	9472	13942	-175	-38
DMC61	48.37	998119	6043	8147	-175	-36
DMC138	50.76	768196	4012	6121	175	37
DMC36	51.54	1456579	11575	16254	175	42
DMC27	51.70	795106	4823	8983	-175	-31
DMC39	52.02	1159366	8604	12205	-175	-35
DMC145	53.44	564681	3010	5389	-175	-28
DMC160	54.14	798667	3277	6891	175	31
DMC93	54.20	664364	6459	8284	-175	-43
DMC30	54.63	933453	7707	11311	-175	-31
DMC25	54.87	572093	4806	6478	175	39
DMC82	55.63	680225	6822	9813	175	27
DMC59	56.18	476810	3896	6660	-175	-23
DMC64	56.21	642281	6548	8945	175	26
DMC100	56.48	950576	3773	9247	175	25
DMC119	56.96	665163	6854	9317	-175	-42
DMC72	58.21	724655	4510	9109	175	29
DMC02	58.89	1365899	7791	12599	175	26
DMC78	60.60	673412	6143	8411	-175	-29
DMC32	60.60	384448	4791	6088	-175	-41
DMC161	61.36	458854	3790	5841	175	25
DMC113	62.43	543451	2863	6148	-175	-26
DMC91	62.74	315239	4552	6183	-175	-34
DMC85	63.43	618165	4903	8212	175	22
DMC44	66.03	749450	7635	11702	-175	-18
DMC149	66.08	546314	4049	7490	-175	-30
DMC200	67.19	340483	4464	6219	-175	-36
DMC235	67.65	276336	2473	4154	-175	-30
DMC60	68.40	322738	6125	8161	175	20
DMC86	70.33	364298	6169	8197	-175	-36
DMC117	71.63	385098	2632	4923	176	31
DMC217	72.75	329521	3300	5833	-175	-23
DMC302	73.26	245671	3663	5112	175	31
DMC262	73.45	513683	4617	7317	175	32
DMC33	73.47	167237	4059	5076	-176	-27
DMC198	73.75	392533	2483	5476	175	23
DMC84	76.66	280247	4256	6422	-175	-29
DMC224	77.00	223686	2505	4297	175	26
DMC105	77.34	429928	2317	7280	175	24
DMC176	78.94	298492	5214	7275	175	25

DMC131	79.69	328207	3975	7114	175	22
DMC451	80.03	226123	2144	4212	175	20
DMC76	80.22	357618	6790	9286	-175	-24
DMC411	81.53	302062	3336	5574	-175	-34
DMC683	81.72	253099	2539	4724	175	27
DMC340	83.06	260055	3407	5965	175	25
DMC336	84.22	231691	2417	4188	-175	-26
DMC333	84.81	325546	2999	6350	175	21
DMC501	86.73	167578	2424	3892	-175	-29
DMC34	88.65	165310	5570	7063	175	23
DMC390	89.31	168416	3065	5261	175	24
DMC13	89.36	284392	11208	14478	175	23
DMC01	89.45	150889	10865	13620	-175	-32
DMC92	90.05	320568	3911	8507	175	17
DMC249	91.85	235714	3230	5349	175	23
DMC07	92.76	209008	4749	6407	-175	-13
DMC280	98.70	190477	3438	5822	-175	-31
DMC56	104.35	70712	6257	7709	175	24
DMC179	107.11	234003	4806	6970	175	22
DMC417	109.40	154781	2067	4686	175	20
DMC66	110.98	263634	4415	9979	-175	-14
DMC94	113.46	95690	3462	4731	-175	-24
DMC81	114.53	203532	5023	9177	-175	-18
DMC561	116.36	117102	2307	3854	-175	-25
DMC195	118.51	226335	4975	8160	-176	-22
DMC146	122.78	138532	5613	6961	-176	-23
DMC69	125.54	140104	4745	7578	-175	-20
DMC77	127.57	119263	7323	9208	175	16
DMC612	134.71	132910	2744	4747	-175	-25
DMC239	135.04	89812	1598	4898	175	16
DMC472	144.77	57870	3499	4895	175	22
DMC416	145.33	118070	2354	5461	175	21
DMC89	146.45	93534	4046	7182	-176	-17
DMC167	147.05	149394	4511	7888	175	18
DMC08	152.96	44581	8771	10404	175	23
DMC950	159.73	104661	1651	4303	175	18
DMC107	160.98	152512	5059	8723	-176	-14
DMC155	161.07	102631	3800	6997	-175	-19
DMC308	163.18	75931	4008	5684	175	16
DMC108	163.32	97295	7034	10184	175	13
DMC164	176.53	58303	5226	6730	175	17
DMC55	179.09	22257	7453	8696	176	17
DMC68	185.88	67404	3510	4825	175	21
DMC265	195.75	32380	3059	4043	175	24
DMC31	196.92	79754	5943	7184	175	20
DMC227	202.76	116046	3661	8651	-175	-15
DMC95	216.56	93436	3734	8816	175	11
DMC80	224.35	27501	7172	9390	175	17
DMC219	257.45	42415	3821	5938	175	13
DMC924	258.60	96318	3474	6570	175	19
DMC1142	273.00	50793	2063	3964	-175	-19

DMC341	283.57	27016	4235	5420	175	14
DMC291	297.84	18038	4279	5048	175	23

Table 7-18: Progressive flooding capsize case results summary

Progressive Flooding Losses						
Case ID	Time to Capsize [s]	Final fw. mass rate [t/h]	Final avg. fw. mass [t]	Max fw. mass [t]	Max roll [deg]	Final avg. heel [deg]
DMC565	313.27	26459	4289	5118	-175	-20
DMC807	320.54	74500	3645	5889	175	16
DMC157	330.97	6572	5278	5878	-175	-26
DMC304	333.14	30048	4243	5172	175	18
DMC300	347.12	25925	4176	5295	175	18
DMC364	359.44	31095	1582	3133	175	17
DMC743	369.13	40451	1703	3777	175	15
DMC141	398.35	17440	6574	7806	175	19
DMC589	437.65	30008	1596	3730	175	16
DMC810	471.34	27867	1660	3949	175	16
DMC106	478.90	17683	5074	5997	175	27
DMC857	498.12	38235	1722	3890	175	20
DMC439	502.11	28971	5196	6994	-175	-16
DMC752	511.69	25515	3995	5342	175	20
DMC554	543.34	17064	3627	4607	175	22
DMC470	549.12	17329	4348	5265	176	20
DMC657	588.19	22148	4393	5488	176	19
DMC719	590.90	37497	3716	5370	175	16
DMC132	598.11	31031	4446	7273	-175	-12
DMC989	651.34	8537	3800	4167	175	31
DMC661	679.07	10891	3700	4170	175	32
DMC856	704.45	22332	4425	5578	-176	-22
DMC755	733.04	38807	1923	4359	-175	-21
DMC500	741.24	37041	4186	6817	175	19
DMC928	799.38	31511	1588	3837	176	18
DMC739	808.39	19021	3334	4223	175	22
DMC766	856.24	19794	4284	5579	175	16
DMC630	875.44	29609	1918	2977	175	22
DMC538	892.36	29623	1699	3650	-175	-18
DMC480	956.36	34315	1749	3723	-175	-17
DMC511	980.30	37340	1745	4819	-175	-16
DMC356	1026.32	33340	1779	4682	-175	-16
DMC448	1033.86	27826	3256	5007	175	15
DMC335	1044.80	31944	3460	5093	175	15
DMC611	1067.60	14721	2967	3412	175	34
DMC236	1067.87	25573	3380	4691	175	18
DMC473	1083.35	33432	1807	4914	-175	-17
DMC174	1098.78	16601	3936	4831	175	24

DMC933	1129.85	28713	1830	3246	-175	-20
DMC307	1162.81	20362	4036	5115	175	22
DMC981	1168.54	17316	4531	5174	175	27
DMC591	1172.21	23796	3571	4626	176	20
DMC228	1254.89	26078	5077	6973	175	19
DMC436	1336.48	37779	1434	4536	175	16
DMC437	1402.53	25363	3393	4514	175	18
DMC1098	1475.95	32404	3719	4943	175	23
DMC957	1556.49	21376	3541	4473	175	23
DMC311	1589.46	15526	4610	5466	-175	-21

7.3.3.2 Diagnostics

In order to determine the source of vessel vulnerability to both progressive flooding and transient capsizing, the flooding process for each loss scenario has been examined in detail. Starting firstly with progressive flooding, the simulation results have demonstrated particular vulnerability to this loss modality around the vessel fore and aft shoulders. Following forensic examination of such cases, the reason for this was found to stem from progressive flooding to the ro-ro deck under the action of waves. In both the fore and aft regions of the vessel subdivision, there are several U-shaped voids connected by cross-flooding ducts in addition to asymmetrical tank arrangements split along the vessel centre line. When damaged, such spaces have the effect of inducing a heightened transient roll response, resulting in water accumulation on deck. This effect is then exacerbated further due to the attitude of the vessel when damaged towards the fore and aft shoulders, where significant trim is generated. Depending on the damage location (fore or aft shoulder), water entering the ro-ro deck begins to gather towards either the fore or aft extremes, as depicted within Figure 7-20 and Figure 7-21. Here, the presence of partial side-casings coupled with trim, traps floodwater and inhibits drainage out of the damage opening under the wave induced roll response. Accumulating floodwater within these areas then gradually increases vessel trim, resulting in a greater amount of water accumulation on deck and an intensification of the angle of heel. Eventually, the vessel reaches a critical level of immersion and heel, after which floodwater begins to propagate along the damaged side of the ro-ro space, generating a large free surface and resulting in eventual capsizing. This is demonstrated in Figure 7-22, depicting floodwater progression on the ro-ro deck following a fore shoulder damage case.

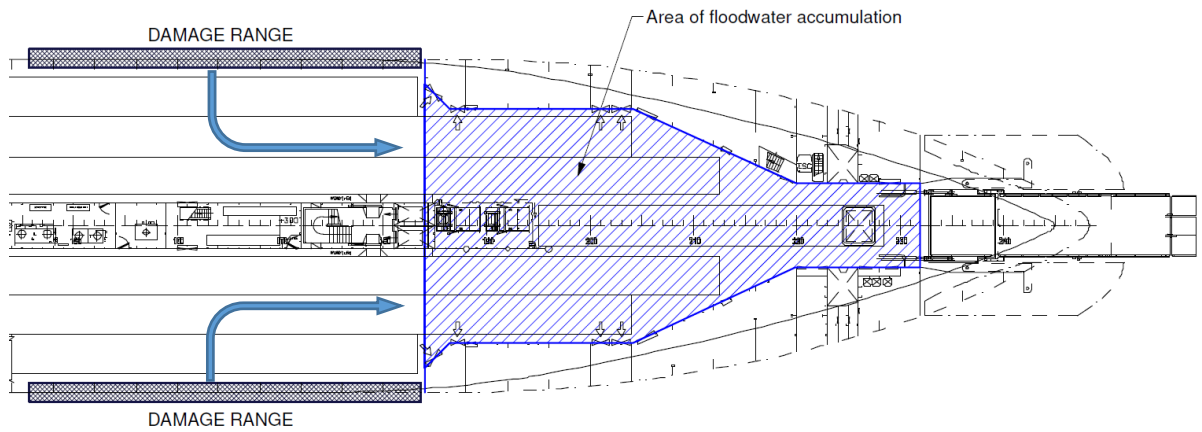


Figure 7-20: Source of fore shoulder vulnerability, area of floodwater accumulation

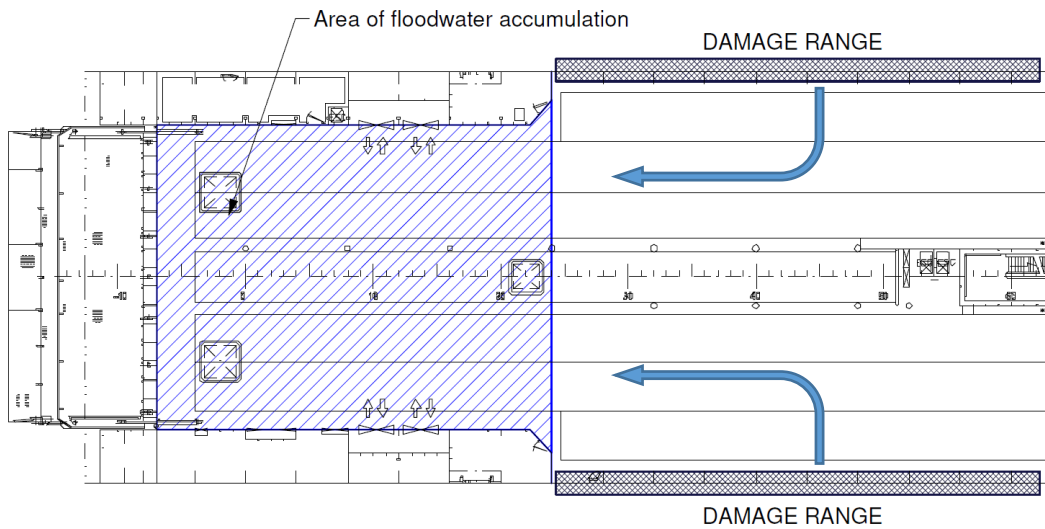
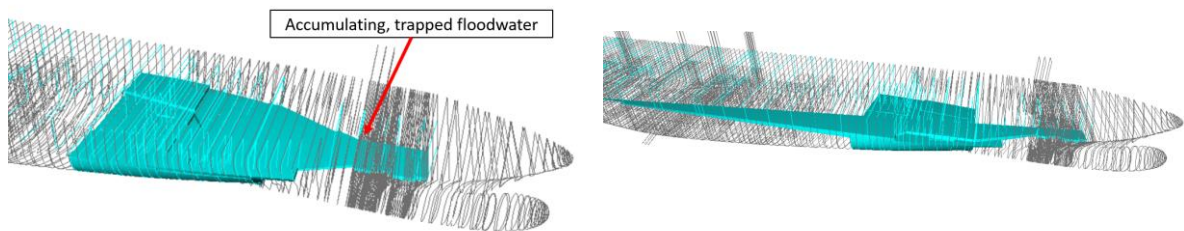


Figure 7-21: Source of aft shoulder vulnerability, area of floodwater accumulation



t=6 minutes, initial FW accumulation fore

t=15 minutes, Gradual FW progression aft

Figure 7-22: Typical fore shoulder damage case demonstrating progressive flooding of ro-ro deck

Vulnerability to transient capsizes was also identified as stemming primarily from the vessel fore and aft shoulders, where the shortest damage lengths have given rise to this loss modality. However, with increasing damage length, transient capsizes cases have also been experienced at number of locations situated along the length of the vessel. The underlying cause of such losses

can in many cases be attributed to areas of asymmetry within the vessel subdivision, particularly within fore and aft regions. Figure 7-23 below, highlights some of these features that exist around the aft shoulder. Here, areas within the vessel tank arrangement that are prone to asymmetrical flooding when damaged are shown hatched in blue (depicted in relation to starboard side damage). In addition, a cross-flooding duct attributed to a U-shaped void within this area is highlighted in red, where significant retardation in floodwater equalisation was experienced across several cases.

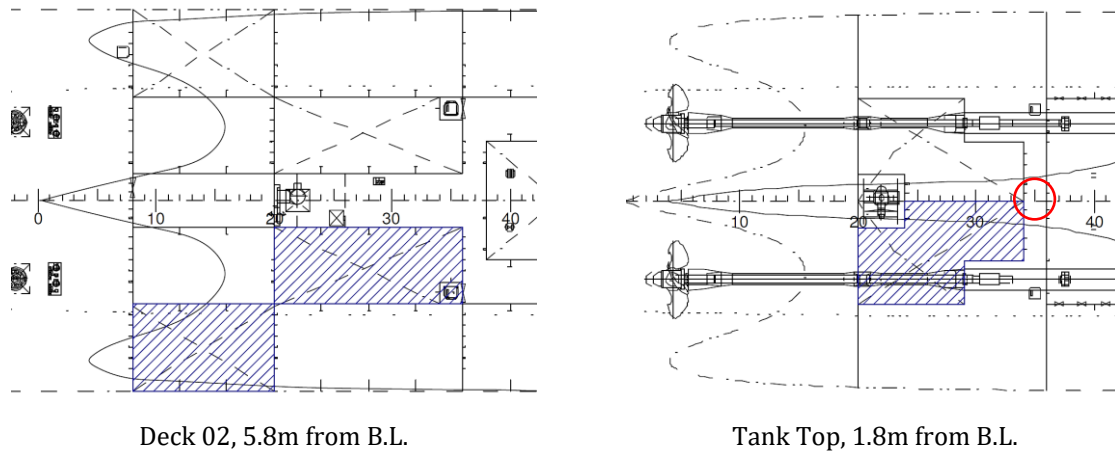


Figure 7-23: Sources of asymmetry surrounding vessel aft shoulder

With regards to the vessel fore shoulder, similar features were identified as increasing vulnerability to transient capsizing, shown in Figure 7-24. Here again, areas within the vessel tank arrangement liable to induce asymmetric flooding were identified, presented within blue hatching. Further to this, perforated bulkheads and narrow cross-flooding ducts within this area were found to inhibit effective equalisation, shown in red.

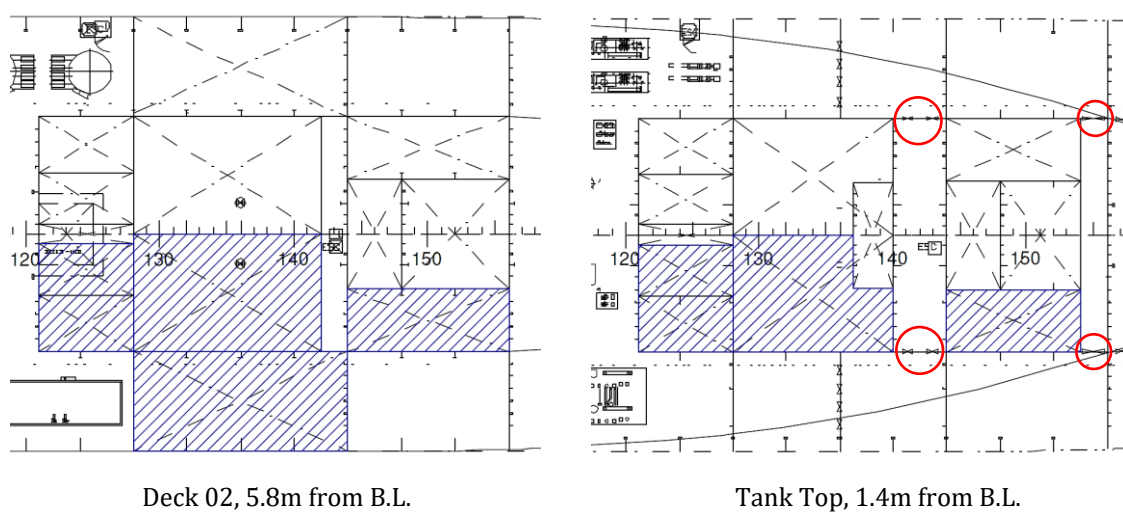


Figure 7-24: Sources of asymmetry surrounding vessel fore shoulder

Adding to above, the absence of side casing on the ro-ro deck has also proven to have a significant bearing on the propensity for transient capsizing. When the ro-ro deck becomes immersed during

the transient roll response, the absence of side casing means that this space offers little to no additional reserve buoyancy and restoration with which to resist the overturning moment generated by the intruding floodwater. Instead, floodwater rapidly enters the ro-ro deck through the damage opening where it spreads and collects towards the damaged side, inducing rapid capsize in a multitude of cases.

7.3.4 Simulation Results – With AREST A1 & P1 Systems

In order to gauge the impact on vessel survivability resulting from the solution derived within Section 7.8.9, all loss scenarios identified within the initial assessment have been reevaluated with the AREST A1 and P1 systems in place. As specified previously within Section 7.2.6, the impact of these systems has been accounted for through modification of the space permeability attributed to protected spaces within the simulation model. The results of this assessment have demonstrated that the proposed solutions have been highly effective enhancing vessel survivability, particularly with regards to progressive flooding. In total, progressive flooding losses were found to reduce from 48 capsize cases in the as-built condition to just 9 cases following implementation of the AREST systems ($\approx 80\%$ reduction). Transient capsize cases were improved to a lesser, yet still significant extent, reducing from 116 to 80 cases ($\approx 30\%$ reduction). This is reflected in the shape of the updated CDF of TTC for the vessel, shown in Figure 7-26, where, though reduced, a sharp increase can still be observed below 300 seconds indicating a particular vulnerability to transient capsize. A far greater improvement can be observed beyond 300 seconds where, in contrast to the as-built case, the shape of the CDF flattens indicating limited risk as regards progressive flooding. In summary, the vessel Survivability Index for 30 minutes exposure time was found increase significantly from 0.89 to 0.951, with 95% confidence intervals depicted on the CDF in accordance with Eq.5-1 in Chapter 5. This improvement is further demonstrated in Figure 7-26, where the as-built TTC values for each loss scenario are contrasted against those calculated within the AREST solutions in place. Here, in addition to observing the numerous cases in which the systems were successful in ensuring vessel survivability, one can also observe several cases in which the TTC was extended, thus granting the vessel more time to execute damage control measures and evacuate.

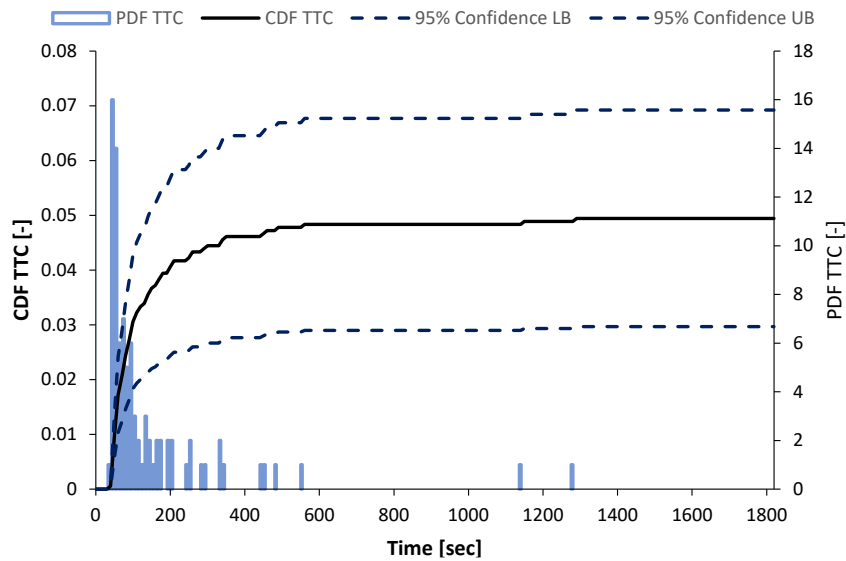


Figure 7-25: AREST Cumulative probability distribution of Time to Capsize for all collision damages. Indication of Survivability Index=0.951, with 30 minutes exposure.

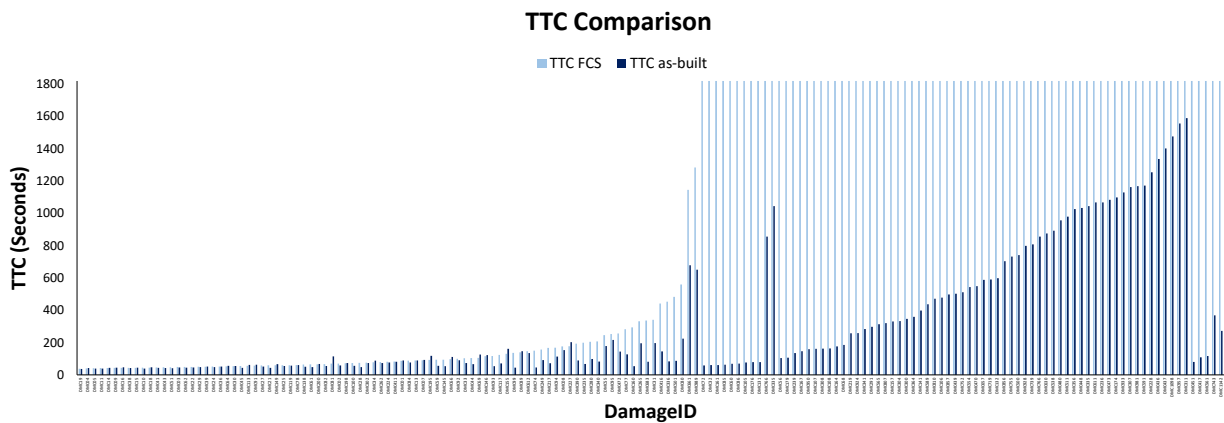


Figure 7-26: Comparison of TTC with/without static foam solution

In addition to the above, it is also interesting to contrast the location and extents of the residual loss scenarios identified following implementation of the solutions to the as-built case, shown in Figure 7-27. Here, the first significant observation that can be made relates to the reduction in loss scenario concentration within the areas surrounding the protected compartments. This is most prominently witnessed for those cases with shorter damages lengths, generally falling below 25m. Whereas larger damage cases that exist within these areas, spanning 3-compartments or more, remain prone to transient capsizing. There are also several cases of shorter damage length that continue to give rise to both transient and progressive flooding losses. However, such scenarios do not involve the protected spaces and therefore should not be expected to benefit from protection by the systems. Instead, further protection would be required in order to mitigate this risk.

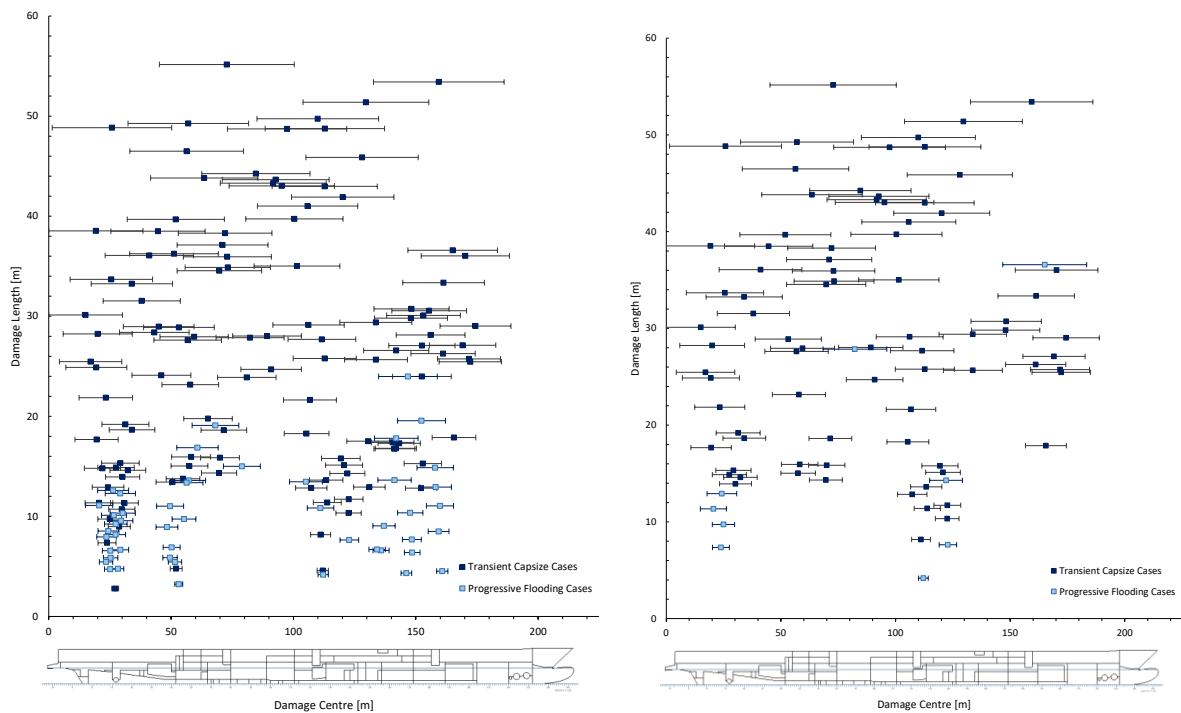


Figure 7-27: Comparison of loss scenarios location & extent, as built (left) and with AREST (right)

7.3.5 Conclusions – Part B

Based on the results presented within the foregoing, the following conclusions can be drawn in summary:

- The results from the time-domain simulations have demonstrated good agreement with those stemming from static assessment. In particular, both assessments highlighted vulnerability within the same regions of the vessel, though simulations have provided greater insight into the nature of these vulnerabilities.
- The primary cause of vessel loss to progressive flooding has been identified as wave induced water accumulation on the ro-ro deck, with is typical for RoPax vessels.
- With regards to transient capsizes, the primary causal factor was identified as asymmetry within the vessel subdivision coupled with inadequate cross-flooding. Furthermore, the absence of side casing along the ro-ro deck was identified as another significant factor.
- Implementation of the AREST A1 and P1 systems has been shown to significantly improve vessel survivability, particularly in cases succumbing to progressive flooding of the vehicle deck.
- Unfortunately, a number of capsizes cases resulting from modest damage lengths still remain and for this reason further protection would be recommended in order to combat these cases.
- In total, application of the two solutions has demonstrated an increase in vessel Survivability Index from 0.89 to an impressive 0.951.

Chapter 8: Passive Flooding Control Application Example – (AREST P1 System)

8.1 Opening Remarks

As indicated in Chapters 1 and 6, the passive flooding protection system addressed in this research pertains to the Installation of permanent foam in void spaces within the ship envelop. This implemented with the aim to provide additional reserve buoyancy when these spaces are damaged, following a flooding incident. Pursuing this idea, it was interesting to discover that there are traditionally sufficient void spaces in the area of interest (in the periphery of the ship and at an elevation near the ship Centre of Gravity (KG)), to offer significant passive protection to flooding incidents for most passenger ships, existing and newbuildings. Such installations act much like buoyancy tanks with impermeable volume to provide buoyancy within the immediate damaged area. Interestingly, a direct consequence of limiting the ship permeable volume is to improve the damage stability margins of the ship (GM margins), which in turn offers considerable financial benefits to the operator as statutory non-compliance directly implies less cargo or worse an unsafe ship. Therefore, life-cycle stability management of all existing passenger ships necessitates close attention to the erosion of these margins, relative to statutory requirements. In this respect, every effort in this direction is being expended by the operator but in the majority of cases concerning passenger ships, this leads to drastic and expensive solutions being considered, using for example, ducktails or external sponsons, permanent ballast and so on. Hence, providing a cost-effective solution for damage stability protection whilst at the same time offering a means for life-cycle damage stability management is, clearly a very attractive innovation.

The methodology employed to assess the impact of this reconfiguration as a flooding protection system (and as a means of life-cycle damage stability management) is in line with the process described within Chapter 4 and as applied in Chapter 7. This includes assessment of vessel survivability with use of both static and dynamic assessment techniques forming two stages of assessment, as described within the following.

Part A: Static stability assessment, using statutory SOLAS 2009 regulations: In this, reduction in permeable volume will lead to an increase in Index A, hence to enhanced damage stability protection as well as an increase in GM.

Part B: Dynamic survivability assessment, using time-domain simulations in a seaway: In this secondary assessment, the premise of flooding protection through this reconfiguration and

subsequent enhanced survivability will be ascertained, using a performance-based approach. Here, the impact on eradicating specific loss scenarios will be examined as well as the overall reduction in vulnerability to flooding, the latter being known to be different from that through using statics, as elaborated upon in Chapter 5.

8.2 Part A: Static Stability Assessment

8.2.1 Scope of Work

This passive flooding protection control application example provided here is aimed at assessing the feasibility of utilising fixed foam installations within a cruise vessel. As the vessel considered is currently in operation, the additional ensuing objective is to assess whether this solution offers a means of providing damage stability enhancement and assisting in ship stability management.

Passenger vessel safety is one of the most important challenges facing the maritime industry today and flooding remains the highest risk source. Consequently, much of what exists within naval architecture discourse revolves around how best to assess vessel damage stability performance and to what level the safety requirement should be set. However, from a design perspective, emphasis is too often placed on how best to utilise what we already have, instead of focusing on what else could be done in order to improve safety. As a result, the majority of vessels built today continue to rely on a combination of traditional passive protection measures, most of which have existed for over a century and are starting to show their age. Bulkheads and other forms of fixed partitioning, in particular, place safety in conflict with functionality, inevitably resulting in compromise. The difficulty, therefore, comes not in designing a safe ship, but instead, designing a ship that is both safe, functional and viable. As safety standards continue to rise at an increasing rate, Figure 8-1, this problem is amplified further and it is becoming progressively more difficult to strike a balance between these two objectives. At the same time, there is an ever-growing safety gap between existing vessels and new-buildings, with passive protection measures and their difficulty of application in retrospect again stifling safety enhancement and leaving older vessels behind in the process.

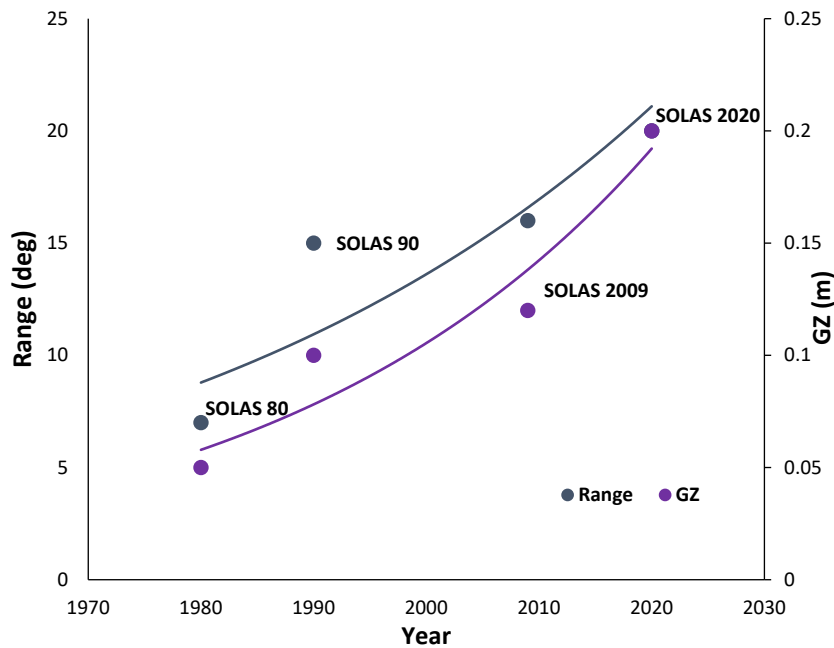


Figure 8-1: Evolution of Stability Requirements as Mandated by IMO

The primary problem that faces existing ships is erosion of their stability margins over the vessel life cycle. This comes as a result of growth in lightweight which, more often than not, occurs above the vessel KG, resulting in a gradual reduction in vessel GM. Predominantly, it is this reduction in GM that ultimately inhibits the vessel range of safe operation as opposed to the added weight itself. That is to say, the problem is generally one of stability as opposed to floatability. At present, operators seeking to improve the stability margins of their existing ships have little at their disposal with which to do so, and those options that do exist are far from favourable. Typical examples include the addition of ducktails and sponsons, both of which are highly expensive and only marginally effective. They also introduce problems of their own by adding weight and increasing resistance, which, in turn, drives up operating costs. Put plainly, any operator who elects to install such features will never stop paying for them. Unfortunately, “desperate times, call for desperate measures” and at present operators are forced into the position where such steps must be taken simply because they have little to no other options made available to them; this, however, need not be the case.

In response to this problem, research effort over the past few years has identified a novel and very effective solution to this problem, the “AREST P1” system as described in detail within Chapter 4.

8.2.2 Case Study – Large Cruise Vessel C1

The following section provides an overview of the methodology adopted and supporting calculations in the assessment of the effectiveness of the proposed system as a means of passive damage stability protection through internal reconfiguration. For this purpose, the cruise vessel C1 has been utilised and subjected to a probabilistic damage stability assessment in accordance with IMO MSC.216(82) (SOLAS 2009) as a first step. This will ensure that Class and Administration will readily accept any benefits gained through this form of reconfiguration as it refers to a permanent (passive) change of the vessel permeability in specific spaces and hence passive flooding protection. The improvement afforded by the fixed foam installations has been measured in terms of increased GM margins as opposed to other metrics such as ΔPLL or ΔA -Index. The reason for this is simply due to the fact that, from the operators perspective, the former is the most important and familiar measurement with direct impact on the operability of their vessels.

8.2.2.1 Vessel Main Particulars

Table 8-1: Case Study Vessel Particulars

Cruise Ship C1 – Principle Particulars	
Ship's name	C1
Length OA	317.2 m
Length BP	293.7 m
Breadth, moulded	36.8 m
Draught, subdivision	8.6 m
Draught, design	7.3 m
No. Passengers	3,148 persons
No. Crew	1,252 persons

8.2.2.2 Vessel Stability Model

The ship model used in the damage stability calculations consists of the following buoyant volumes:

- Hull from base line to DK6 (Deck 4, 17.3m above base)
- Two pods
- Two foils

The following volumes are deducted from the buoyant volume:

- Three bow thruster tunnels
- One anti-suction tunnel
- Six sea chests
- Aft mooring space

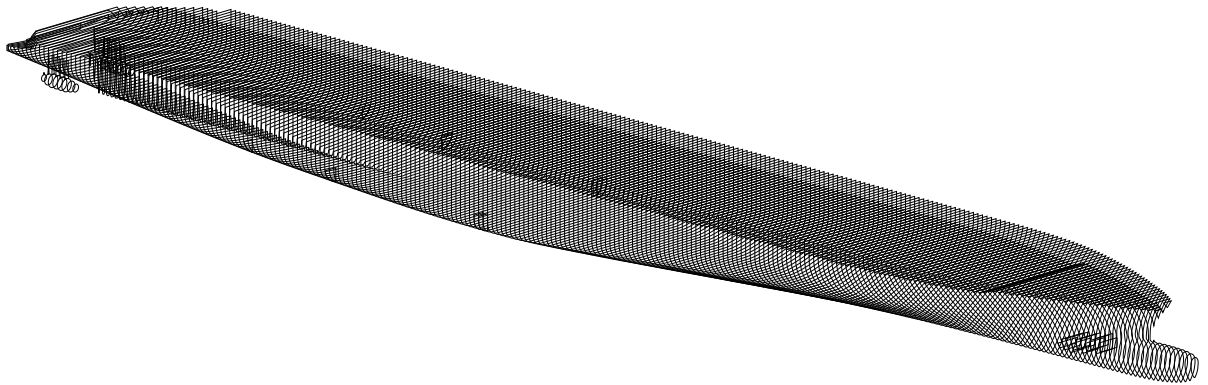


Figure 8-2: Cruise Vessel C1 Stability Model

8.2.2.3 Vessel Subdivision

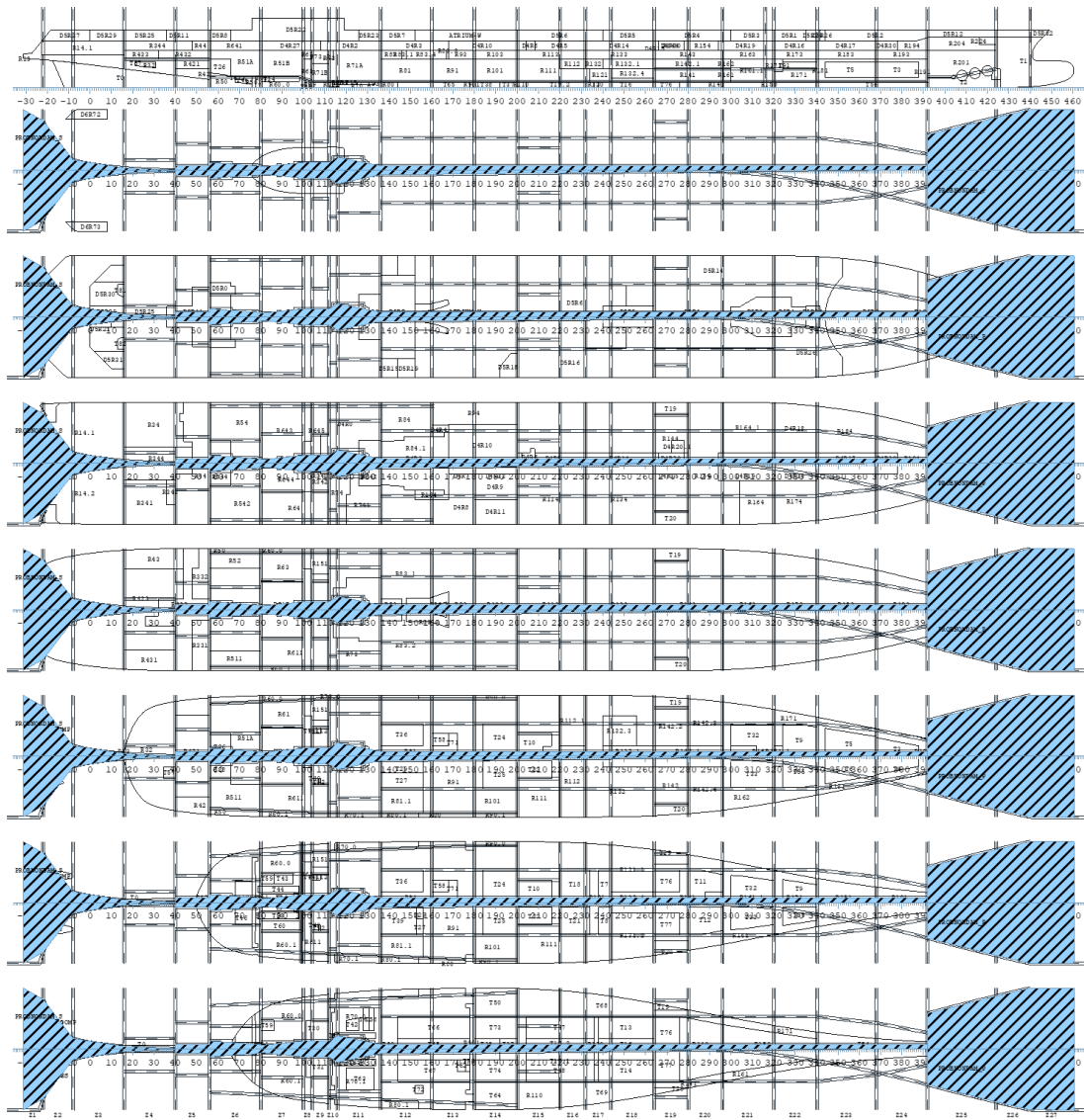


Figure 8-3: Cruise Vessel C1 Subdivision

8.2.2.4 Required Subdivision Index - R

The vessel has been assessed such that the Attained Subdivision Index is not less than the Required Subdivision Index as calculated according to the following formula:

$$R = 1 - \frac{5000}{L_s + 2.5N + 15225} \quad \text{Eq. 8-1}$$

Where,

N_1 – number of persons for whom lifeboats are provided

$N_1 = 3,300$

N_2 – number of persons that the ship is permitted to carry in excess of N_1

$N_2 = 1,101$

$N = N_1 + 2 \cdot N_2$

$N = 5,502$

$L_s = 316.19 \text{ m}$

8.2.2.5 Calculation Drafts

Vessel calculation drafts have been defined in accordance with statutory requirements as described within Chapter 7, section 7.2.5, resulting in the loading conditions specified within Table 8-2.

Table 8-2: Loading Conditions Considered

INIT		DS	DP	DL
T0	m	8	8.36	8.6
TR0	m	0	0	0.3
GM0	m	2.64	2.49	2.57
KG	m	17.92	18.29	18.61
DISP	t	61,520	59,234	56,023

8.2.2.6 Permeabilities

The permeability values used within the assessment have been defined in one of two ways. Firstly, those spaces not influenced by the AREST P1 system have been assigned permeability values in line with conventional SOLAS assumptions, Table 8-3. However, in such cases that fixed foam installations have been assumed to be in effect, the permeability of the protected space has been altered not in the traditional sense (i.e. homogenous reduction), but instead by modelling the foam installation as a separate volume of permeability 0.05 as shown in Figure 8-4 and justified in Chapter 6, Section 6.4.

In general, the assumptions made in assessing the impact of the permanent foam installations as a permeability reduction are in line with MSC Res.216(82) (SOLAS 2009),

Regulation 7-3.3, where it is stated that “Other figures for permeability may be used if substantiated by calculations”.

Table 8-3: SOLAS 2009 space permeability assumptions

Spaces	Permeability
Appropriated to stores	0.60
Occupied by accommodation	0.95
Occupied by machinery	0.85
Intended for liquids	0.95
Void spaces	0.95
Permanent Foam Installations	0.00

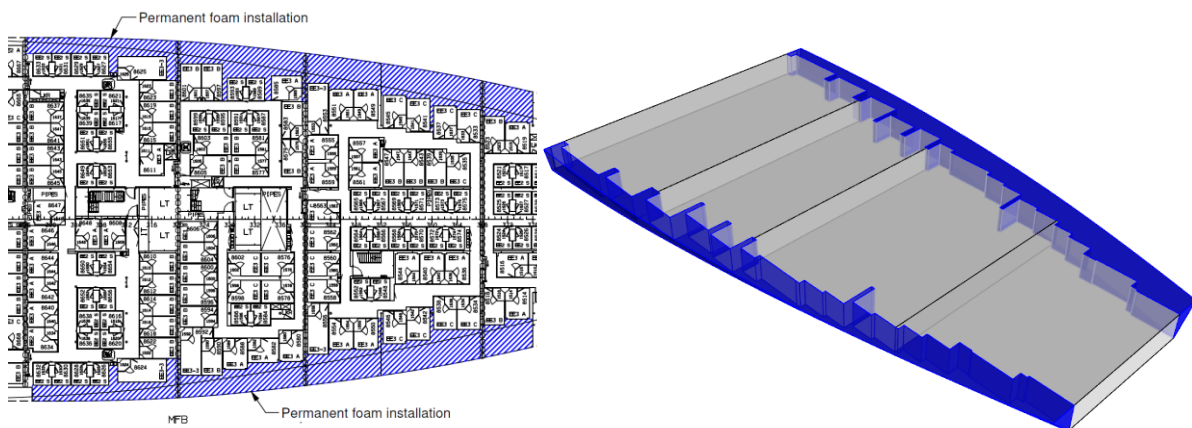


Figure 8-4: Example static foam installation (right), space modelling (left)

8.2.2.7 Damage Stability Assessment – as operated

The vessel has first been subjected to damage stability assessment under her present GM limit curve conditions, which have proven to be optimal with the vessel achieving an Attained Index of 0.8296 with a Required Index of 0.830, as shown in Table 8-4.

Table 8-4: as-operated Attained Index calculation

Loading Condition	T (m)	TR (m)	GM (m)	A	W	A*W
DL	8.00	0.30	2.57	0.846	0.2	0.1692
DP	8.36	0.00	2.49	0.829	0.4	0.3315
DS	8.60	0.00	2.64	0.822	0.4	0.3289
					Attained Index	0.830
					Required Index	0.829

The vessel risk profile, shown in Figure 8-5, demonstrates vulnerability around the fore and aft shoulders, which is typical of cruise vessels. This risk can be attributed to a combination of both

lack of reserve buoyancy and residual GM, in addition to having insufficient range to the immersion of unprotected openings.

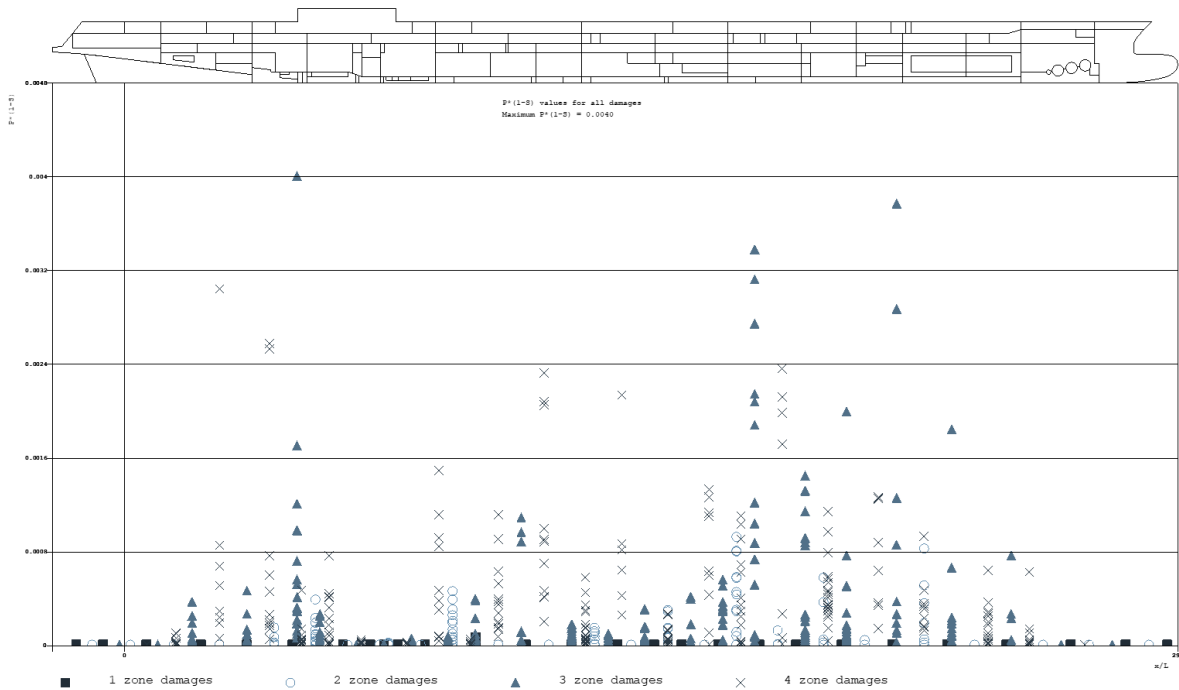


Figure 8-5: as-operated vessel risk profile

8.2.2.8 Assessment of Existing Vessel GM Margins

The presented limiting curve and loading conditions are based on the cruise ship C1 stability booklet. Observation of the vessel GM limit curve highlights that GM margins in some 40% of cases lie below 10cm. By predicting an annual increase in vessel Lightweight KG by 2cm (in line with previous growth trends), additional GM margins of approximately 35cm for all loading cases are required in order to remain compliant in 20-years' time. This has been estimated using a constant lightweight value but having altered the vertical centre of gravity by 40cm for each statutory loading condition.

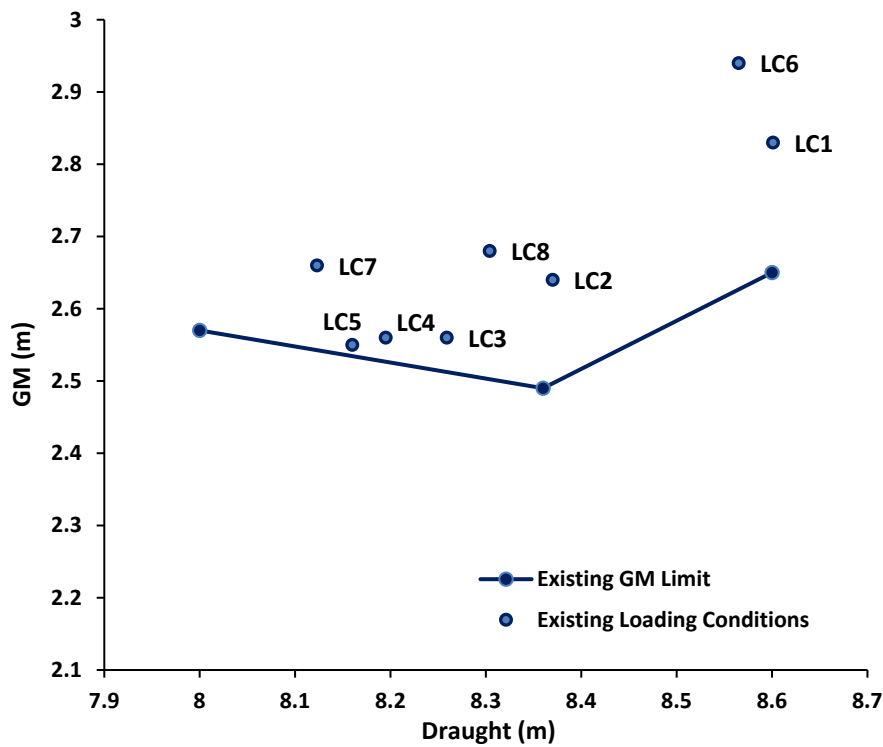


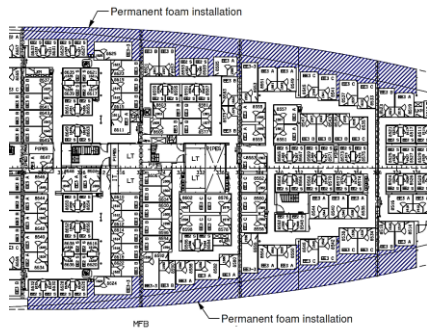
Figure 8-6: Current vessel GM limit and margins

Table 8-5: Loading condition overview & GM margins with projected growth

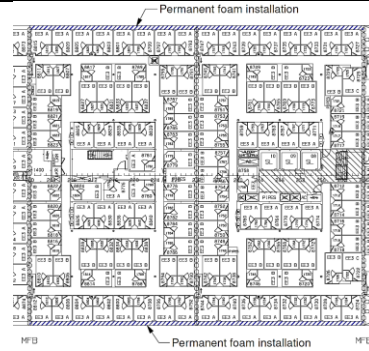
ID	Description	T(m)	GM(m)	GM Req. (m)	GM Margin (m)	ΔGM (20 yrs. growth)
LC1	100% Cons Max. Draught	8.601	2.83	2.65	0.18	0.337
LC2	75% Bunkers and stores	8.370	2.64	2.50	0.14	0.339
LC3	50% Bunkers and stores	8.259	2.56	2.51	0.05	0.360
LC4	25% Bunkers and stores	8.195	2.56	2.53	0.03	0.358
LC5	Arrival Condition	8.160	2.55	2.54	0.01	0.355
LC6	Ballast Departure Condition	8.565	2.94	2.62	0.32	0.337
LC7	Ballast Arrival Condition	8.123	2.66	2.55	0.11	0.356
LC8	Docking Condition	8.304	2.68	2.51	0.17	0.347

8.2.2.9 Proposed Modifications

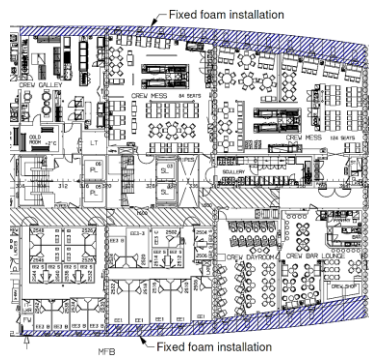
Table 8-6: AREST P1 Installation sites



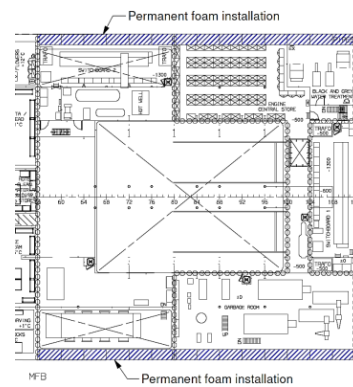
Foam Volume = 650.5m^3 , Weight = 8.13 tonnes



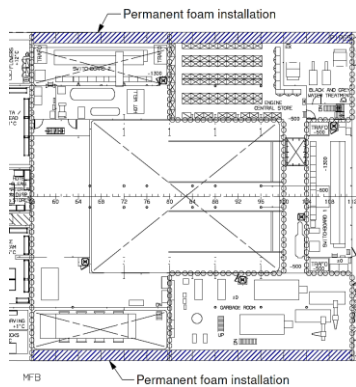
Total Volume = 112m^3 , Weight = 1.4 tonnes



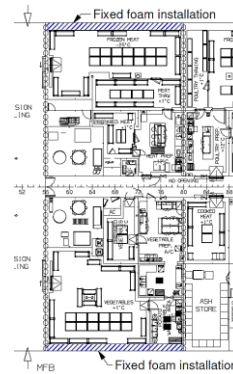
Volume = 383m^3 , Weight = 4.788 tonnes



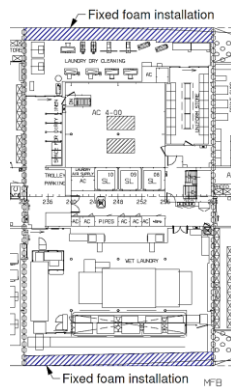
Total Volume = 112m^3 , Weight = 1.4 tonnes



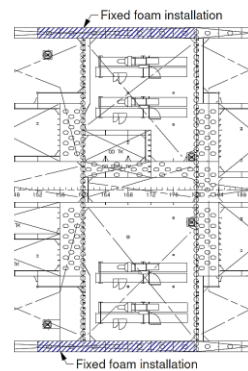
Volume = 237m^3 , Weight = 2.963 tonnes



Total Volume = 67m^3 , Weight = 0.838 tonnes



Total Volume = 93m^3 , Weight = 1.16 tonnes



Total Volume = 59m^3 , Weight = 0.74 tonnes

8.2.2.10 Reconfiguration Summary

The following provides a summary of all proposed permanent foam installation locations as shown in Figure 8-7. In addition, a breakdown of all foam volumes and installation weights is provided within Table 8-7. The location of the foam installations has been focused within areas found to possess the highest flooding risk. The foam has also been located predominantly around Decks 1 & 2, which lie within the region of the damaged waterline and above, thus providing both buoyancy and stability at equilibrium and as the vessel is heeled from this position.

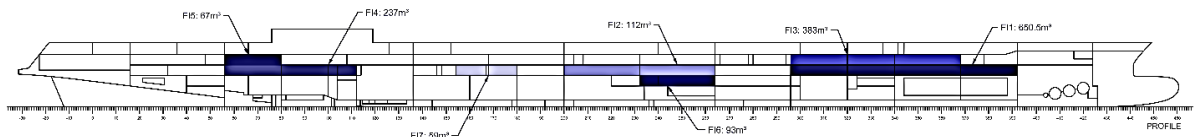


Figure 8-7: AREST P1 installation locations

Table 8-7: Installation volumes & weights

Foam Application	Foam Volume (m ³)	Weight (Tonnes)
1	651	8.131
2	112	1.400
3	383	4.788
4	237	2.963
5	67	0.838
6	93	1.163
7	59	0.738
Total	1601.5	20.019

8.2.2.11 Damage Stability Assessment – With Reconfiguration

Following re-modelling of the vessel internal geometry such as to account for the aforementioned modifications, the vessel damage stability performance has been re-assessed in order to ascertain the new GM limiting values. The results of this process are outlined within Table 9.

Table 8-8: Attained Index Calculation with modifications & reduced GM

Loading Condition	T (m)	TR (m)	GM (m)	A	W	A*W
DL	8.00	0.30	2.400	0.8401	0.2	0.1680
DP	8.36	0.00	2.280	0.8216	0.4	0.3286
DS	8.60	0.00	2.490	0.8309	0.4	0.3323
					Attained Index	0.829
					Required Index	0.829

Observation of the updated vessel risk profile, shown in Figure 11, again shows vulnerability within the fore and aft shoulder regions of the ship and reflects closely that of the unmodified vessel. The reason for this stems from the fact that the calculation GM has been reduced as far as possible in order to achieve compliance and produce new limiting GM values. As such, improved safety has been substituted for a greater range of safe operation.

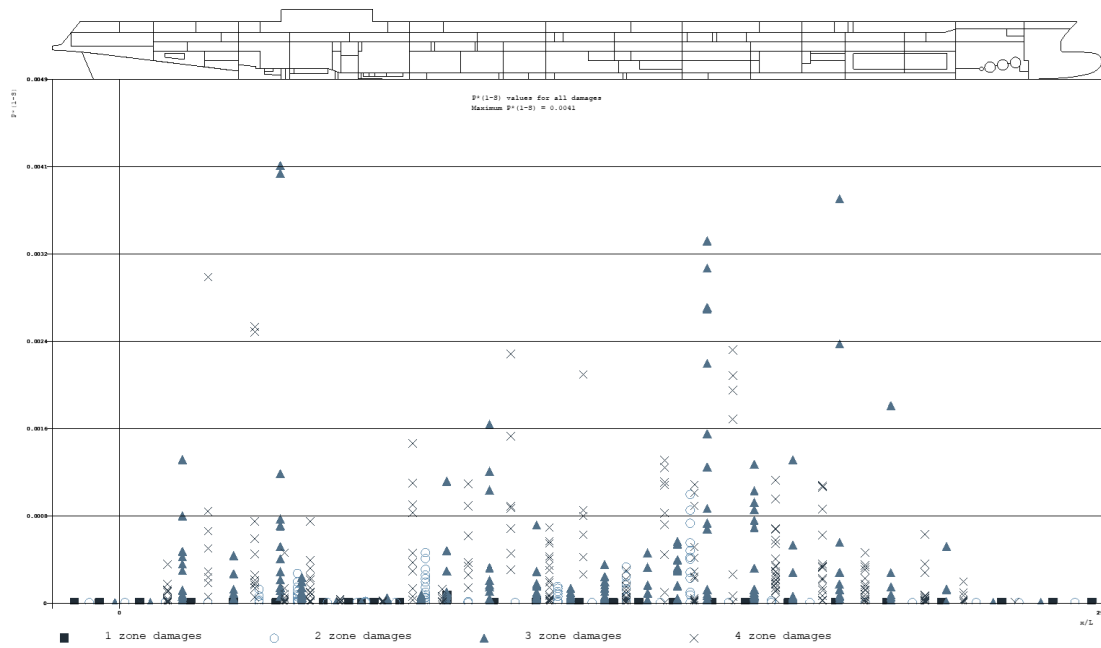


Figure 8-8: Risk Profile with modifications

8.2.2.12 Loading Condition & GM Margin Overview- With Modifications

Following the proposed modifications, GM Margins have been increased between 16cm - 21cm, with the resultant margins now ranging between 20cm - 48cm. With consideration of the projected growth in vessel lightweight KG of 2cm/year, 50% of statutory loading conditions can now survive this growth without jeopardising compliance.

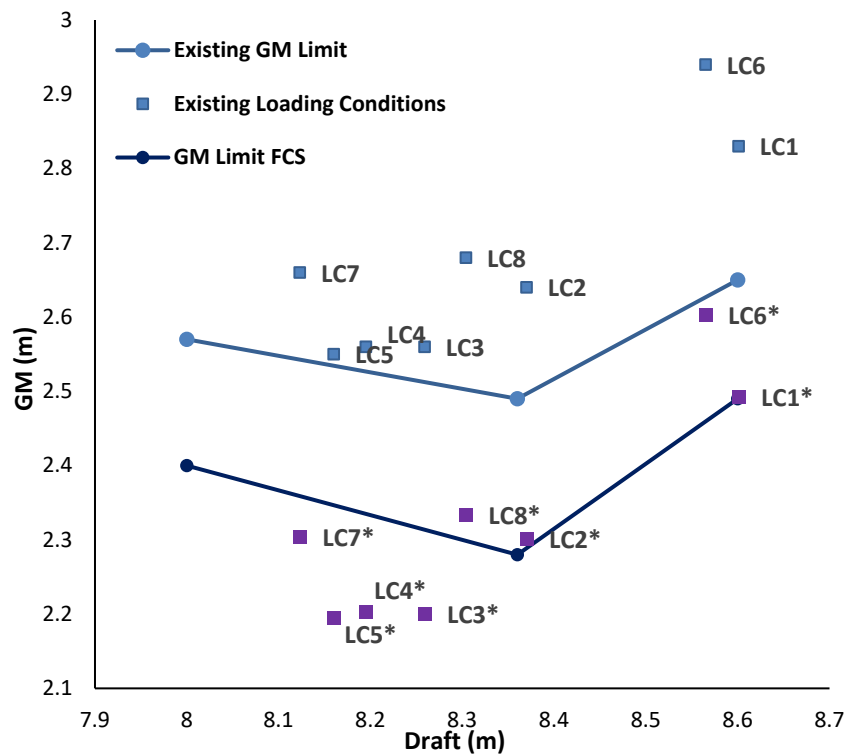


Figure 8-9: Updated GM Limit Curve

Table 8-9: Comparison of GM margins

ID	Existing			With AREST	
	GM (m)	GM Req. (m)	GM Margin (m)	GM Req. (m)	GM Margin (m)
LC1	2.83	2.65	0.18	2.491	0.339
LC2	2.64	2.5	0.14	2.289	0.351
LC3	2.56	2.51	0.05	2.314	0.246
LC4	2.56	2.53	0.03	2.335	0.225
LC5	2.55	2.54	0.01	2.347	0.203
LC6	2.94	2.62	0.32	2.459	0.481
LC7	2.66	2.55	0.11	2.359	0.301
LC8	2.68	2.51	0.17	2.299	0.381

8.2.2.13 Conclusions – Part A

Deriving from the study presented in the foregoing, the following specific conclusions may be drawn:

- Weight growth high up on the ship and the ensuing erosion of design stability margins may lead to serious stability problems at sea, in particular propensity to transient flooding and ensuing rapid loss of the vessel in case of flooding accidents.

- A continuous quest to address and solve this problem led to an innovative solution that is likely to eradicate centuries-old problems and provide a platform for cost-effective stability management over the life-cycle of the vessel. This entails a risk-informed reduction in permeable volume in selected void spaces within the ship construction.
- Interestingly, the majority of ships are being designed and built in a way that leads to considerable void spaces, which when flooded following a collision incident, cause asymmetric flooding, potentially during the transient phase and hence to rapid loss of the vessel.
- The aforementioned design vulnerability could turn into a very effective passive flooding protection system with permanent foam installation in high-risk void spaces.
- What remains to be examined is the impact on damage survivability in waves by using performance assessment tools, which is examined in Part II next.

8.3 Part B: Dynamic Survivability Assessment

8.3.1 Scope of Work

This section presents the work undertaken to further look into stability management and enhanced survivability solutions for Cruise1 through passive protection using fixed foam in targeted ship void spaces. This assessment is a continuation of the study outlined in Part A” and has been conducted in accordance with three primary objectives, namely:

- To address vessel survivability using numerical time-domain flooding simulations as a means of performing a physical experiment numerically.
- To gauge the impact of the passive foam solution, designed according to static assessment, on the survivability of the vessel when considering damaged ship dynamics.
- To seek additional means of widening the impact of this or other reconfiguration measures on the basis of the additional forensic information provided by numerical simulations.

As touched upon in Chapter 5, static assessment techniques cannot see, or are indeed blind to, a number of key characteristics of the flooding process. This includes, but is not limited to, the identification and distinction of loss modalities (transient or progressive flooding capsizes), the impact of wave induced effects and the ability to measure Time to Capsize. This allows vessel survivability to be viewed from a different, more physics-based and more detailed perspective, enabling us to identify aspects that may have been “missed” within the static assessment. In this respect, it is comparable to obtaining a “second opinion”. Given the above, numerical time-domain simulations have been conducted in order to verify and substantiate the results of the static assessment and the passive foam solution founded upon these results. Moreover, this

assessment has been conducted in order to identify additional vulnerabilities from the point of view of dynamics, which could be catered for by using passive foam in the areas where these vulnerabilities have been identified. Furthermore, floodwater progression in various loss modalities enables us to seek additional means of enhancing vessel GM margins, this time by focusing on the risk of progressive flooding and the use of other AREST systems, such as deployable foam barriers, to curtail such progression. This has been conducted in the understanding that a combination of different solutions (reconfigurations), each of which caters for different forms of flooding protection, would provide the most optimal solution, leading to enhanced survivability and higher GM margins.

On the basis of the aforementioned considerations, the vessel has been assessed at a single loading condition corresponding to the deepest subdivision draft and associated limiting GM. The simulations have been performed in irregular waves (JONSWAP spectrum) with a fixed significant wave height of $H_s=4\text{m}$, representing the upper limit of the SOLAS wave distribution (stress testing of the vessel). In total, 1,500 collision damage simulations have been conducted with an exposure time of 30 minutes. Each damage scenario has been sampled from the SOLAS damage distributions, characterised by random location, length, height and penetration. Upon completion of the simulations, the Time to Capsize (TTC) has been evaluated for each damage case, providing an indication of the vessel Survivability Index for collision damages. The results produced for the vessel in the “as-built” condition have highlighted 22 capsized cases (3 progressive flooding cases/19 transient capsized cases), which translates to a Survivability Index of 0.987. Following this initial assessment, the results have been scrutinised further in order to identify vulnerable design features within the vessel design and, more specifically, the sources of this vulnerability. Finally, the previously developed passive foam solution for damage protection has been implemented, demonstrating a rise in Survivability Index from 0.987 to 0.991.

Subsequently, the additional study outlined above has been conducted with a focus on critical openings and the employment of protection by way of deployable foam barriers (AREST A2 system). As damage stability enhancements (hence GM margins) are determined on the basis of statutory requirements, this assessment has been conducted using hydrostatic damage stability calculations in line with SOLAS. The approach adopted has been to calculate the degree in which the influence of each unprotected opening affects the potential A Index contribution belonging to each damage case. By doing so, openings can be ranked in order of criticality measured by lost A-Index. This, in turn, has been used in order to inform which openings deployable barriers would best protect from a risk reduction perspective. The results of this process have shown that, with the protection of only four openings, the vessel GM margins have increased by 10cm,

which when combined with the passive foam solution, yields a net improvement ranging from 30-56 cm.

8.3.2 Modelling of the Ship Environment and External Conditions

8.3.2.1 Initial Condition

The loading condition defined within the model is summarised in Table 8-10 and represents the vessel “Deepest Subdivision Draft”, as defined within SOLAS 2009, at the respective GM limiting value for this case. The reason for loading condition having been chosen is due to the fact that firstly, as demonstrated within Chapter 5, most cruise vessels operate towards the upper region of their draft range. Secondly, the subdivision draft often represents the most safety critical loading condition due to reduced freeboard and reserve buoyancy.

Table 8-10: Loading condition summary

Property	Value
Displacement [tonnes]	61,520
Trim [m]	0.00
GM [m]	2.640
KG [m]	17.92
Draft [m]	8.60

8.3.2.2 Simulation Model

In line with the process outlined within Chapter 5 and as in the application example presented within Chapter 7, the existing definition of the vessel internal geometry has been modified to include a higher level of detail within the arrangement. This has entailed consideration of all spaces capable of inhibiting or facilitating floodwater propagation across all decks up to and including Deck 05 (14.1m A.B.L). The result of this process has led to the definition of a further 331 spaces within the model, now comprising some 585 spaces. It is interesting to note here the contrast in the level of additional detail required between static and dynamic models in the case of this cruise vessel as opposed to the RoPax that was outlined within the previous chapter. Whereas the modelling of an additional 36 spaces was necessary within the RoPax example, an additional 331 spaces were required in this case, demonstrating the significant level of simplification that occurs when assessing cruise vessels by hydrostatic calculation.

A comparison between the hydrostatic and simulation model arrangements is provided within Figure 8-10.

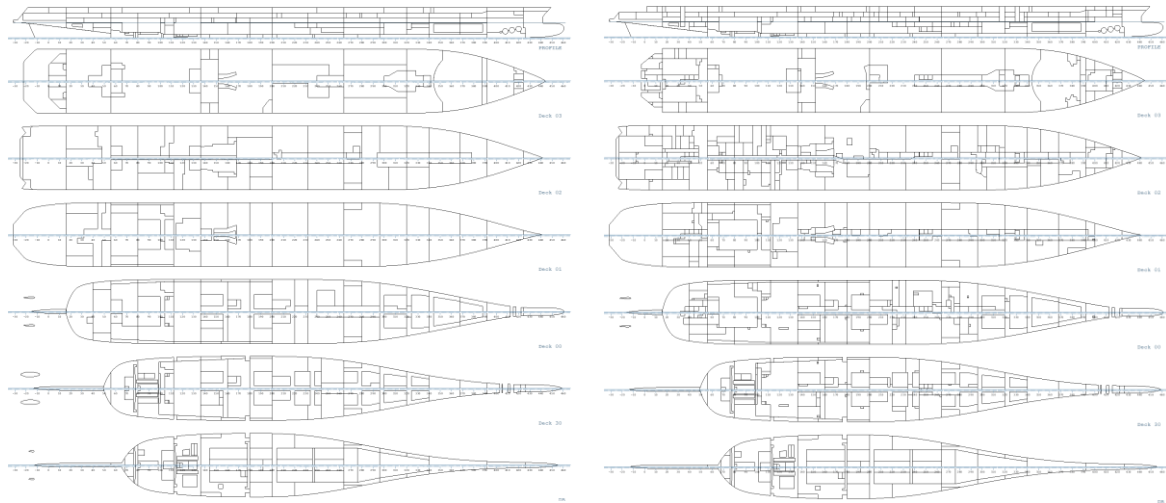
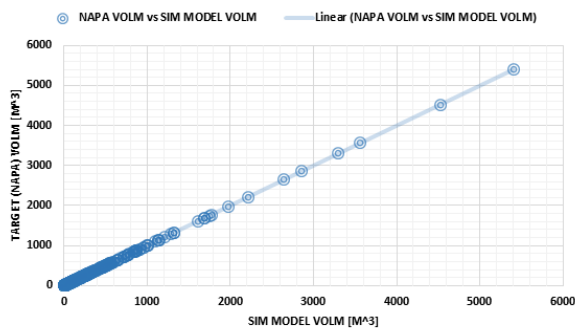


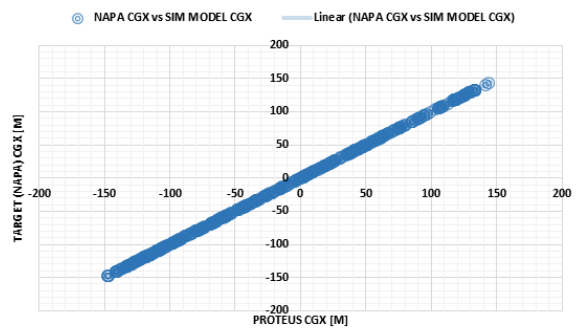
Figure 8-10: Comparison between hydrostatic and simulation model arrangements

8.3.2.3 Verification of Internal Geometry

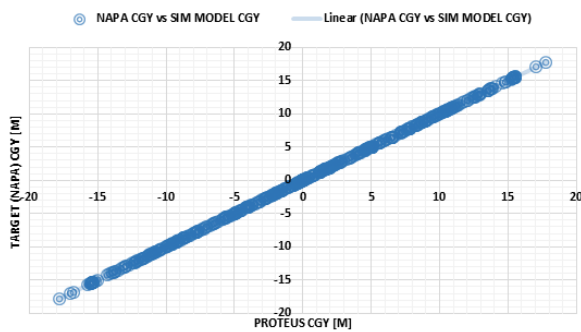
In order to ensure that the simulation model accurately reflects the hydrostatic model used for statutory compliance, a comparison has been performed between key model parameters. This includes properties such as compartment and tank volumes, centres of gravity and permeabilities. The results of this process are provided in Figures 3-6 below, where it can be observed that there is good correlation between the two models. This is an important step in order to ensure that no inaccuracies are introduced into the simulation model that could distort the results yielded.



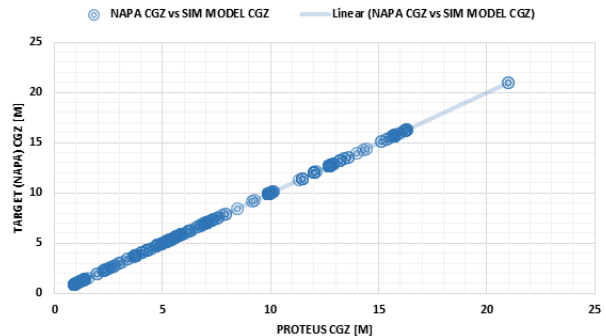
Volume



CGX



CGY



CGZ

Figure 8-11: Comparison of hydrostatic & simulation model properties

Table 8-11 below provides a summary of the above comparison, highlighting the maximum differences observed for each property in terms of both percentage and actual value. From these figures it can be observed that no significant disparity between the models exists.

Table 8-11: Model correlation summary

Property	Maximum difference [%]	Value
Volume	0.18	1.76 m ³
CGX	0.09	0.034 m
CGY	2.04	0.011 m
CGZ	0.09	0.010 m
Permeability	0.00	0.000

8.3.2.4 Opening Definition

The vessel opening definition has been conducted in accordance with the process described within Chapter 5, leading to the definition of 1,336 openings as shown within Figure 8-12.

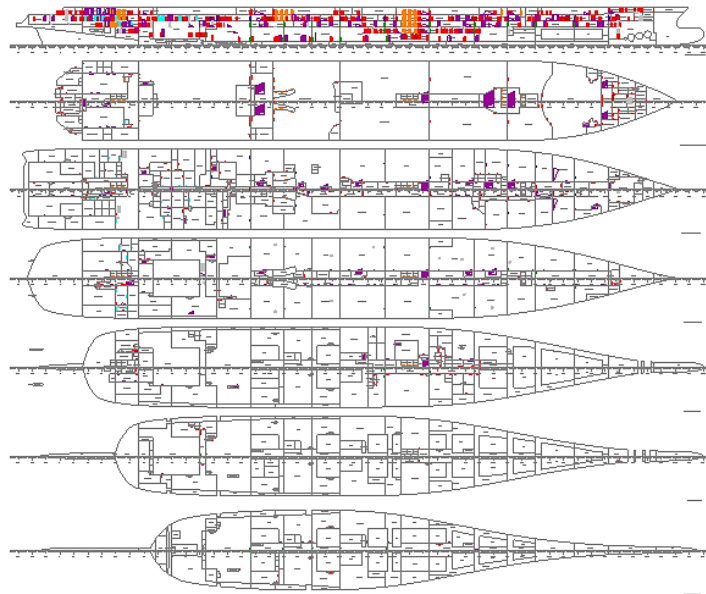


Figure 8-12: Simulation model opening arrangement

8.3.3 Simulation Properties & Damage Generation

8.3.3.1 Simulation Environment

As in the case of the RoPax example outlined within Chapter 7, the simulation wave environment has been fixed to $H_s=4\text{m}$ in all cases, with random waves generated with consideration of the JONSWAP wave spectrum. Once again, the decision for this resulted from the desire to test the vessel within the most adverse conditions according to SOLAS assumptions.

8.3.3.2 Exposure time

The total exposure time for each simulation is 1,800 seconds (30 minutes), which is in line with the exposure time upon which the SOLAS s-factor is based. An extra 20 seconds is added to this time to allow the vessel to settle into the wave environment prior to the damage breach being activated at $t=20\text{s}$.

8.3.3.3 Damage Generation

In total 1,500 collision damages have been generated using Monte Carlo sampling techniques and with respect to the SOLAS damage distributions, comprising:

- Damage side, $ind_{side} \in \{-1,1\}$
- Longitudinal position of damage centre, $X_c[\text{m}], X_f \in [0, L_{ship}]$
- Longitudinal extent of potential damage, $L_{x,p}[\text{m}], L_{x,p} \in [0,60]$
- Transversal extent of potential damage, $L_{y,p}[\text{m}], L_{y,p} \in [0,0.5 \cdot B_{ship}]$
- Vertical position of lower limit of potential damage, $Z_{LL,p}[\text{m}], Z_{LL,p} \in [0,8.6]$
- Vertical extent of potential damage, $H_d[\text{m}], H_d \in [0, H_{d,max}]$

An overview of the damage scenarios generated is provided in Figure 8-13 and a summary of the sample properties is provided within the following:

- | | |
|--|----------|
| • Maximum damage length | =58.4 m |
| • Average damage length | =19.9 m |
| • Maximum transverse extent (measured from side shell at W.L.) | =18.6 m |
| • Average transverse extent | =9.27 m |
| • Maximum vertical extent | =20.92 m |
| • Average vertical extent | =14.59 m |

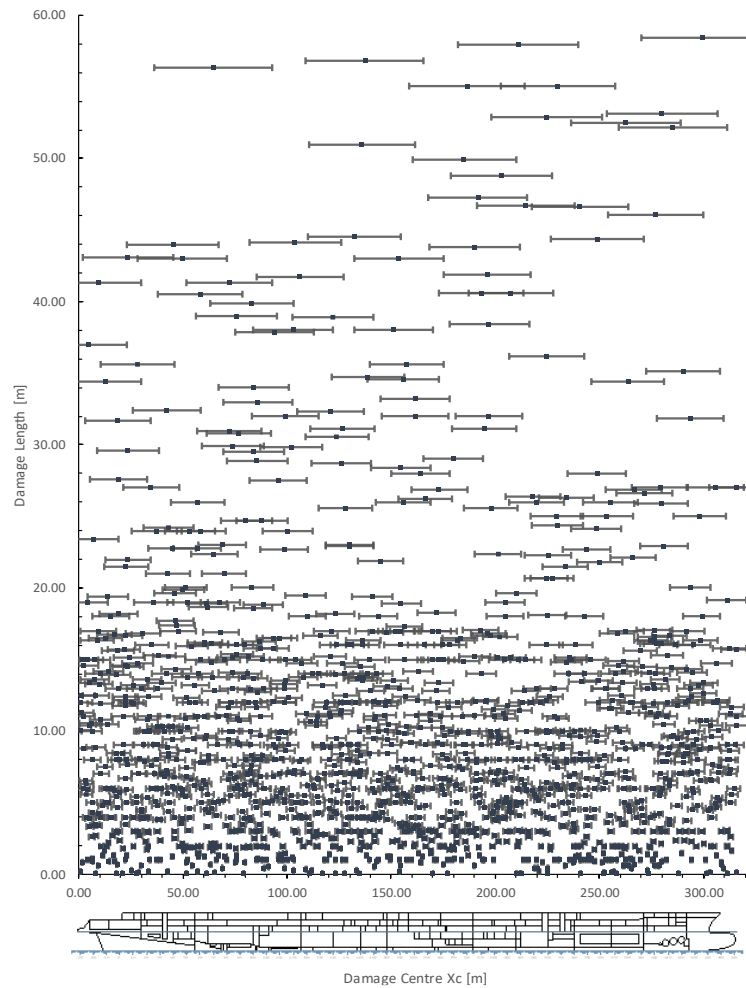


Figure 8-13: Collision damage sample

8.3.4 Simulation Results – As built

8.3.4.1 Summary

The results of the numerical simulations have identified a total of 22 capsizes cases, yielding the cumulative distribution function for Time to Capsize shown in Figure 8-14, with 95% confidence intervals calculated in accordance with Eq5-3. Here it can be observed that the majority of capsizes cases occur below five minutes, indicating transient capsizes as the primary loss modality. Only three cases leading to progressive flooding capsizes have been identified, ranging from 8-22 minutes in TTC. Based on these findings, the vessel Survivability Index for 30 minutes exposure time has been found to be 0.987.

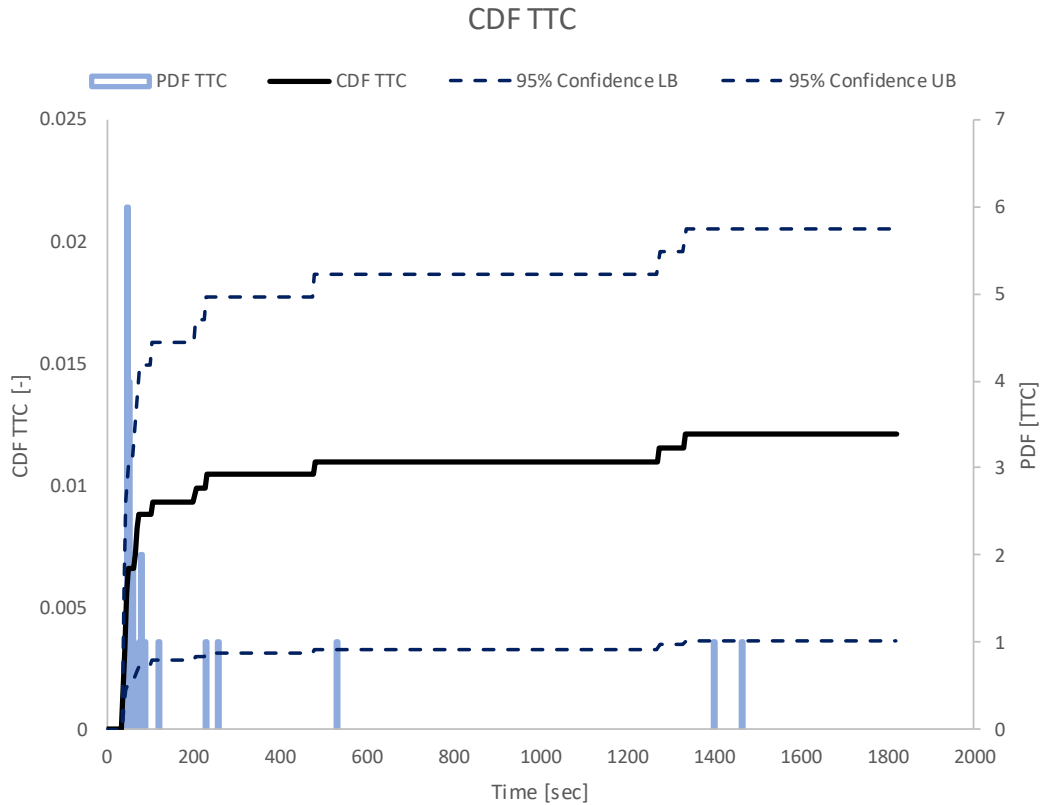


Figure 8-14: Cumulative probability distribution of Time to Capsize for all collision damages. Indication of Survivability Index=0.987.

Detailed results for all collision damage simulations are provided in Appendix C.

8.3.4.2 Loss Scenario Overview & Comparison

Figure 8-15 below demonstrates the location and magnitude of all loss scenarios identified, which have been marked with the respective TTC calculated in each case. Here, it can be clearly observed that there is a concentration in capsized case occurrence towards amidships, demonstrating vulnerability within this area. This is an important finding as the results from the static assessment, summarised in the risk profile presented in Figure 8-16, demonstrate areas of high risk surrounding the fore and aft shoulders of the vessel. Furthermore, it can be observed that the vessel suffers from a particular vulnerability to transient loss, with only three progressive flooding capsized cases identified in contrast to 19 transient capsized cases. This indicates a prevalence of asymmetrical flooding coupled with inadequate damaged GM, the reasons for which are explored further in the following section. Generally speaking, all loss scenarios found could be considered extreme cases, with the majority of cases being over 35m in damage length and all exposed to $H_s=4m$.

An overview of all capsized case damage dimensions is provided in Table 8-12 below along with a brief summary of the simulation results in Table 8-13.

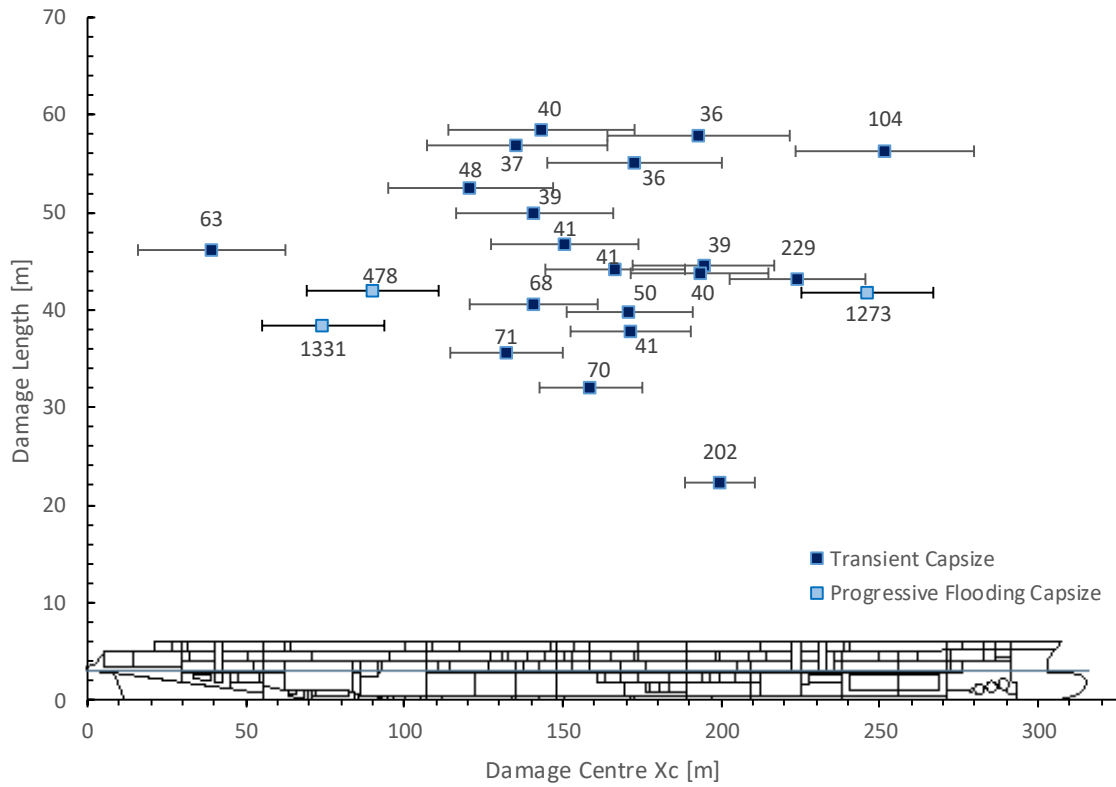


Figure 8-15: Location and extent of capsizing cases.

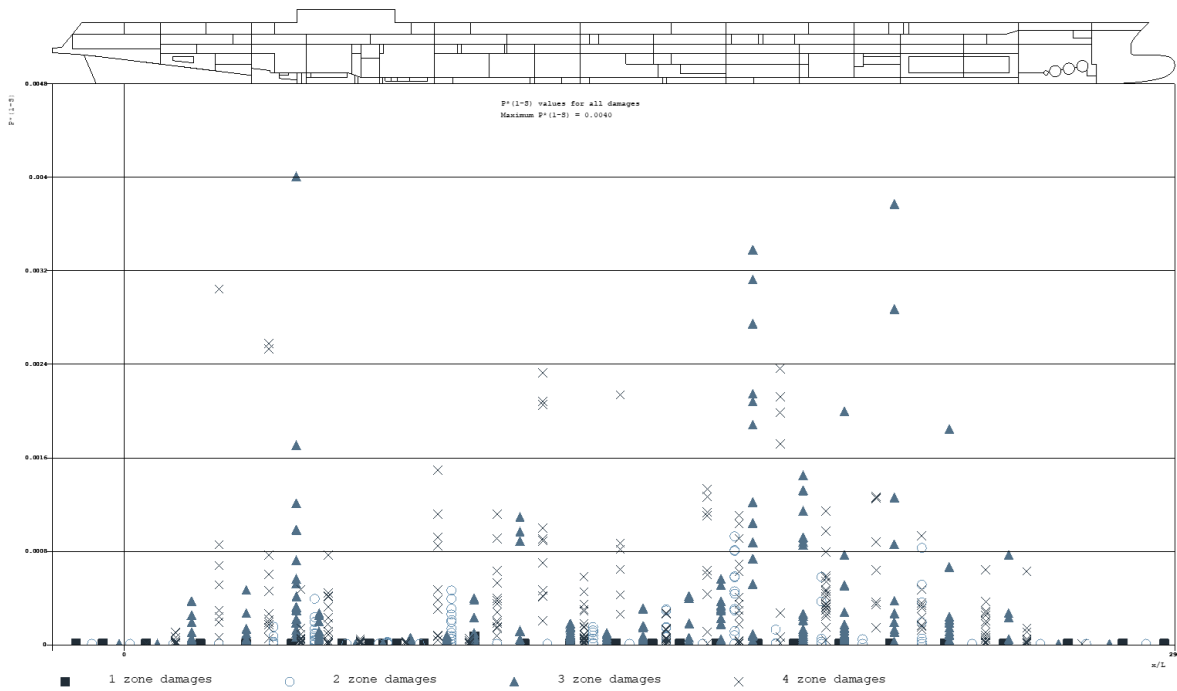


Figure 8-16: Risk Profile resulting from static assessment

Table 8-12: Capsize Case Damage Dimensions – Collision

Case ID	X1 [m]	X2 [m]	Xc [m]	Lx [m]	Y1 [m]	Y2 [m]	Z1 [m]	Z2 [m]	Hs [m]
DMC01_Hs400_01	114	173	143	58	15.9	500.0	5.9	10.2	4
DMC02_Hs400_01	145	200	173	55	16.6	500.0	1.1	14.7	4
DMC03_Hs400_01	164	222	193	58	7.9	500.0	1.2	13.5	4
DMC04_Hs400_01	107	164	136	57	14.6	500.0	1.6	13.1	4
					-				
DMC05_Hs400_01	223	280	252	56	500.0	2.7	2.6	16.5	4
DMC06_Hs400_01	95	147	121	53	6.9	500.0	4.7	14.9	4
DMC08_Hs400_01	116	166	141	50	7.2	500.0	5.2	14.5	4
					-				
DMC09_Hs400_01	127	174	151	47	500.0	-3.8	2.5	10.3	4
DMC11_Hs400_01	16	62	39	46	12.0	500.0	1.6	15.1	4
DMC12_Hs400_01	172	217	194	45	12.9	500.0	2.6	20.2	4
					-				
DMC14_Hs400_01	145	189	167	44	500.0	-2.8	4.7	15.8	4
					-				
DMC16_Hs400_01	171	215	193	44	500.0	-12.6	1.3	15.4	4
DMC17_Hs400_01	203	246	224	43	1.9	500.0	5.1	17.2	4
DMC24_Hs400_01	120	161	141	41	6.0	500.0	7.3	14.3	4
					-				
DMC27_Hs400_01	151	191	171	40	500.0	-1.9	0.9	12.3	4
DMC33_Hs400_01	153	190	172	38	14.5	500.0	1.4	20.1	4
DMC36_Hs400_01	114	150	132	36	15.7	500.0	3.0	19.0	4
					-				
DMC49_Hs400_01	143	175	159	32	500.0	-18.3	4.2	19.1	4
					-				
DMC110_Hs400_01	188	211	200	22	500.0	-15.3	2.3	19.0	4
DMC30_Hs400_01	55	94	74	38	12.4	500.0	2.6	13.6	4
DMC20_Hs400_01	69	111	90	42	9.4	500.0	2.4	12.2	4
DMC21_Hs400_01	225	267	246	42	-7.7	500.0	0.9	20.3	4

Table 8-13: Capsize Case Simulation Result Summary

Case ID	Time to Capsize [s]	Final fw. mass rate [t/h]	Final avg. fw. mass [t]	Max fw. mass [t]	Max roll [deg]	Final avg. heel [deg]
DMC01_Hs400_01	40.49838	933089	7485	9140	-175	-50.8
DMC02_Hs400_01	36.23699	2192092	9831	12461	-175	-49.8
DMC03_Hs400_01	36.17362	1753071	11059	14115	-175	-58.5
DMC04_Hs400_01	37.03188	1455011	9183	11357	-175	-54.1
DMC05_Hs400_01	104.1698	417172	18794	22520	176	37.1
DMC06_Hs400_01	48.23249	1169854	10451	12867	-175	-52.3
DMC08_Hs400_01	38.84195	1731801	10311	12567	-175	-59.2
DMC09_Hs400_01	41.36105	852949	7709	10638	175	38.6
DMC11_Hs400_01	62.6855	613544	11808	14298	-175	-51.8
DMC12_Hs400_01	39.49442	1944643	9759	11834	-175	-50.4

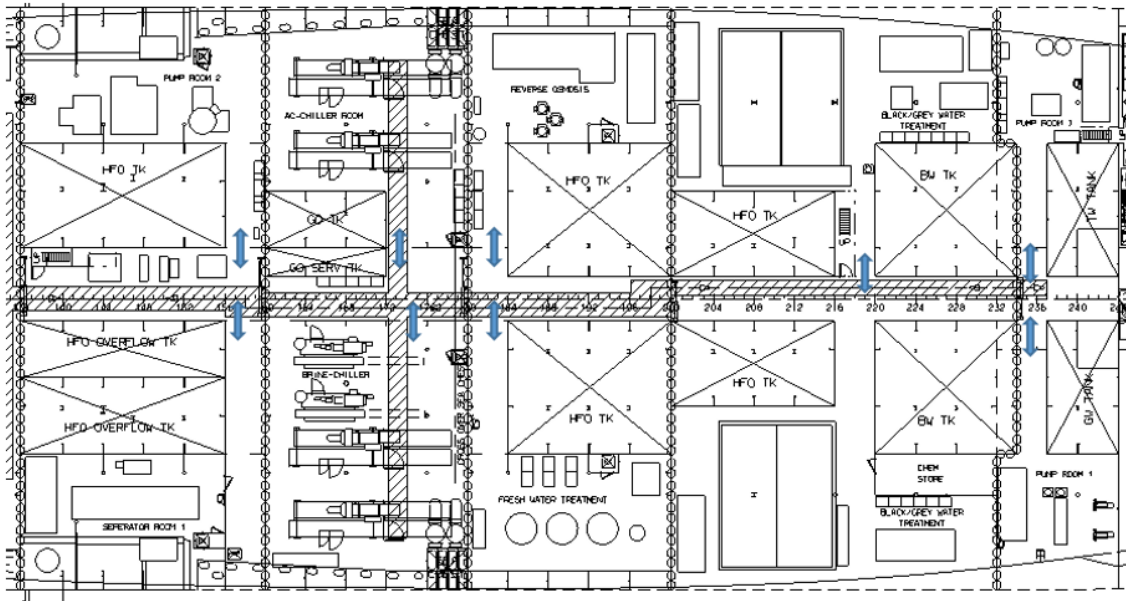


Figure 8-18: Cross-flooding restriction sources FR136-224, Tank Top Deck

8.3.5 Simulation Results –Static Foam Installations in Place

8.3.5.1 Summary

A secondary assessment has been conducted in order to measure the impact of damage protection previously specified within Part I. Here, all loss scenarios identified within the initial assessment have been re-assessed with the static foam solution incorporated within the simulation model. The results of this process demonstrated a reduction in capsized cases from 22 to 15, producing the CDF of TTC presented in Figure 8-19 below. Here it can be observed that the static foam solution has been successful in eradicating all progressive flooding losses, hence the Plateau that can be observed within the CDF past approximately 200 seconds. The solution has also been successful in eliminating four transient loss cases located within the fore and aft shoulder regions and where there are passive foam installations present. This improvement is also summarised in Figure 8-20, where the “as-built” TTC is contrasted against the TTC values calculated with passive foam in place.

Based on the updated results, the vessel Survivability Index for 30 minutes exposure time and with 95% confidence has increased from 0.987 to 0.992.

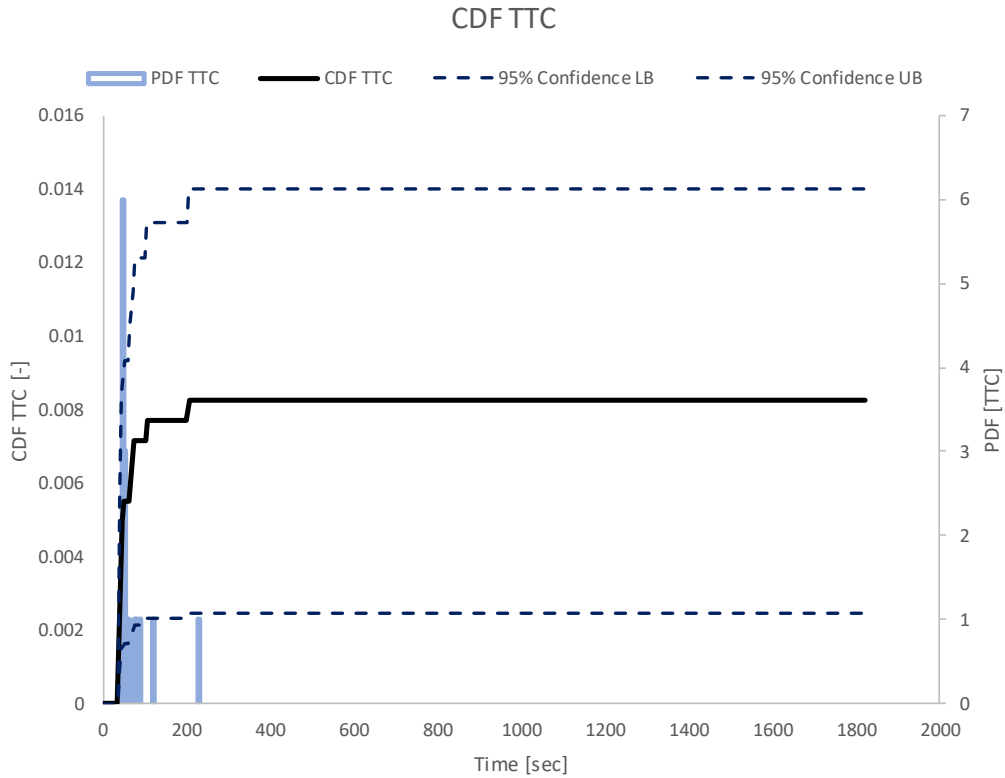


Figure 8-19: Cumulative probability distribution of Time to Capsize for all collision damages. Indication of Survivability Index=0.992.

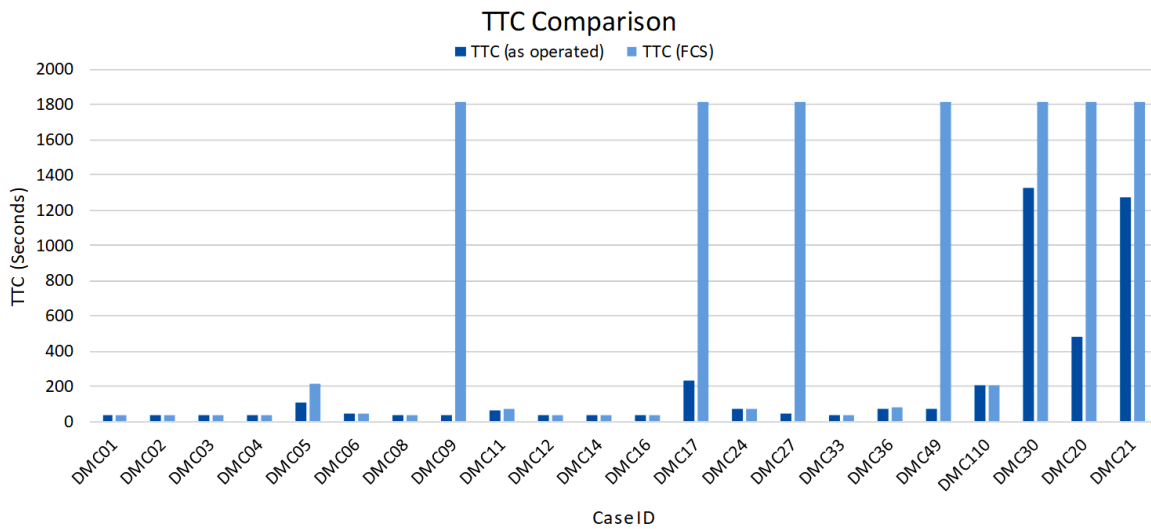


Figure 8-20: Comparison of TTC with/without static foam solution

The locations of the residual loss scenarios show a concentration of transient capsizes cases still exists towards amidships, Figure 8-21. The reason for the fixed-foam protection not having catered for these cases, as touched upon earlier, stems from the fact that there is a contrast between static and dynamic assessment with regards to those areas found to be vulnerable. Consequently, as the passive foam installations are located towards those regions found to be vulnerable through static assessment they fail to cater for the high risk areas identified through

dynamic assessment. However, there are a number of candidate spaces located towards the vessel mid third that could be used in order to deal with the remaining loss scenarios and this would have an additional positive impact on the static assessment, which can be exploited.

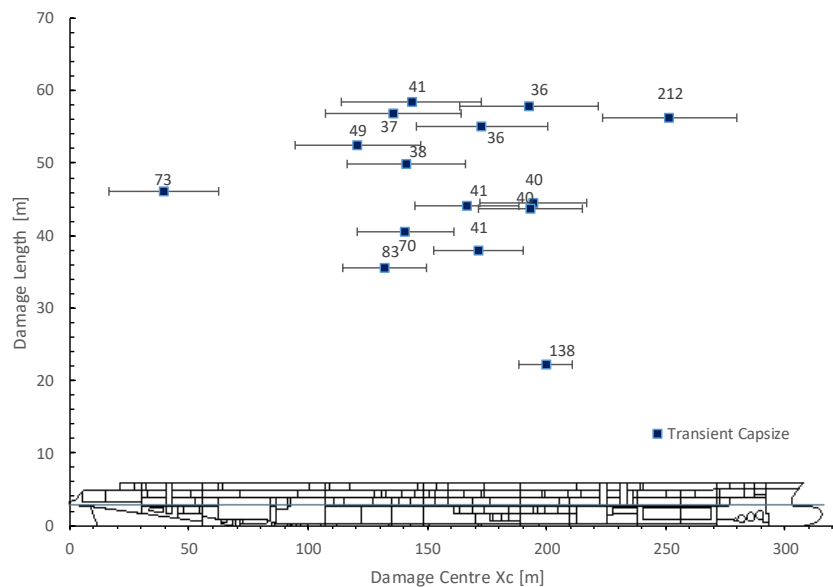


Figure 8-21: Residual Loss Scenarios

8.3.6 Consideration of the AREST A2 system for progressive flooding prevention

As a continuation of the static assessment conducted within part A and using the results from part B as input, a further study has been conducted in order to explore additional means of providing the vessel with increased GM margins. This assessment has been conducted with a specific focus on critical openings, which are proposed to be protected by the AREST A2 system. As GM margins are determined on the basis of statutory requirements, this assessment has been conducted using hydrostatic damage stability calculations. Unfortunately, this form of damage stability assessment cannot model the effects of progressive flooding in the physical sense and instead the potential for progressive flooding is captured through the modelling of unprotected openings. These have the effect of truncating the damaged GZ curve, which in turn reduces the Range and GZmax values that may be used in the determination of the s-factor. As such, the modelling of such openings accounts for the risk of progressive flooding, albeit in an indirect sense. Given this, the approach adopted has been to calculate the degree in which the influence of each unprotected opening affects the potential A-Index contribution belonging to each damage case and verifying this with the simulation results. By doing so, openings can be ranked in order of criticality measured by lost Index, see Table 3 below. This, in turn, can be used to inform which openings deployable barriers would best protect from a risk reduction perspective.

Table 8-14: Ranking of critical openings

Rank	Affected Damage Case	Opening ID	A Index Contribution	Max potential A Index Contribution	Lost A Index Contribution
1	DS/SDSS3-5.1.0	ST02.2	0	0.00112	0.00112
2	DP/SDSP18-20.5.0	PB15P	0	0.00062	0.00062
3	DP/SDSS18-20.1.0-2	PB15S	0	0.00055	0.00055
4	DP/SDSP18-20.2.0-2	PB15P	0	0.00055	0.00055
5	DS/SDSS18-20.2.0-2	PB15S	0	0.00055	0.00055
6	DP/SDSS3-5.1.0	ST02.2	0.00058	0.00112	0.00053
7	DS/SDSS19-21.5.0	PB15S	0.00034	0.00075	0.00041
8	DL/SDSS18-20.5.0	PB15S	0	0.00034	0.00034
9	DP/SDSS19-21.5.0	PB15S	0.00041	0.00075	0.00033
10	DL/SDSS18-20.2.0	PB15S	0	0.00027	0.00027
11	DS/SDSP19-21.5.0	PB15P	0.0004	0.00067	0.00027
12	DP/SDSP19-21.5.0	PB15P	0.0004	0.00067	0.00027
13	DS/SDSP20-22.4.0	PB17P	0.00013	0.0004	0.00027
14	DP/SDSP12-14.3.0	PB07PT	0.00048	0.00074	0.00026
15	DS/SDSP12-14.3.0	PB07PT	0.00055	0.00074	0.00019

Having followed the process above, a total of four critical openings have been identified as highlighted in Figures 16-18. Here, it can be observed that two stairwells along with two double-leaf fire doors constitute the highest risk openings. In the case of stairwells, a horizontally closing dual-shutter system is recommended which, when the cavity formed between the shutters is foamed, would form a watertight seal. As regards the double-leaf fire doors, a transverse closing, dual fire-shutter system is proposed. This would allow the existing fire doors to be removed and instead the fire shutters would take their place. These shutters could then be used in the same manner as any regular fire shutter system during regular service and fire drills. Only when the vessel is involved in a flooding incident would the foam component of the barrier be used in order to create a watertight seal.

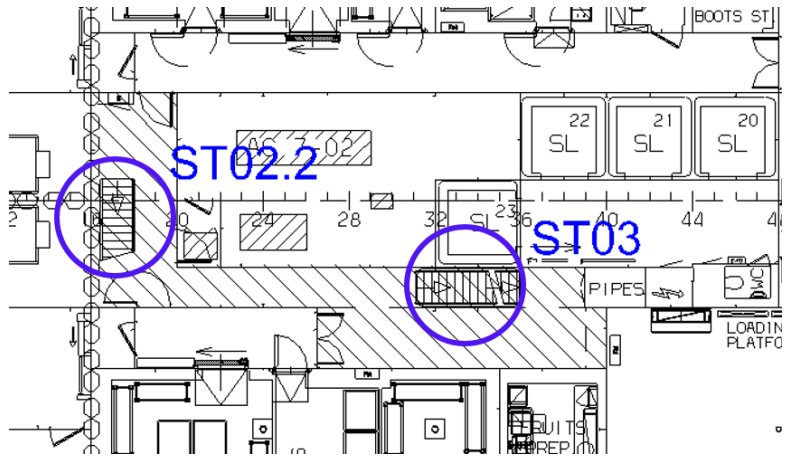


Figure 8-22: Critical stairwell openings, ST02.2 & ST03, Deck02

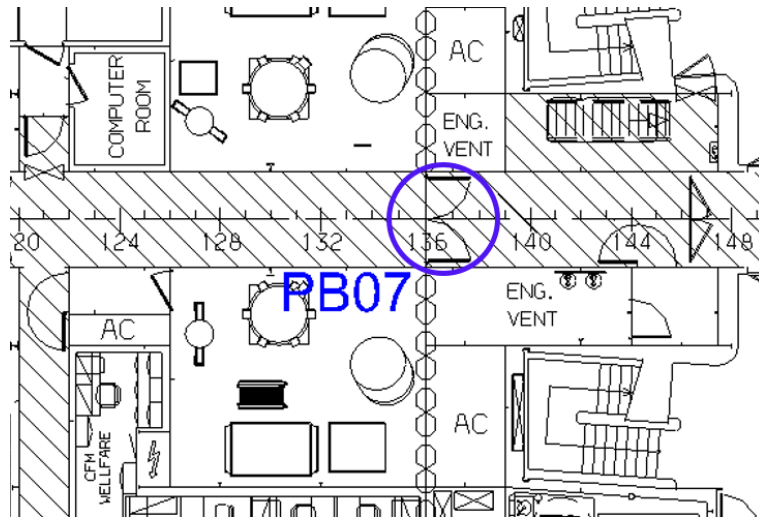


Figure 8-23: Critical fire door, PB07, Deck02

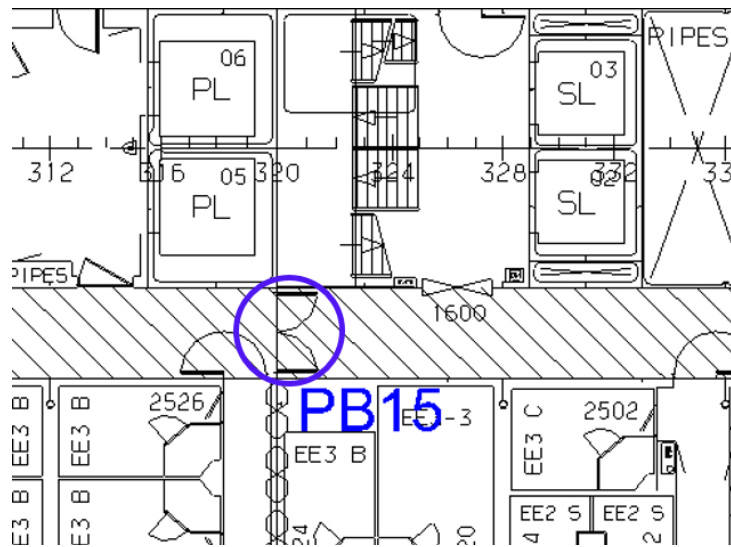


Figure 8-24: Critical fire door, PB15, Deck02

Having targeted the openings described in the previous, the vessel damage stability performance has been re-evaluated with these openings assumed watertight and the existing passive foam solution in place. The vessel GM limit curve has then been derived on the basis of the condition A=R, shown in Figure 19, and the updated GM margins have been calculated. The results show that in protecting just the four openings specified, the vessel GM margins can be increased by an additional 10cm across the entire draft range. This then yields a net benefit, in respect to both solutions, of 30-56cm as summarised within Table 4.

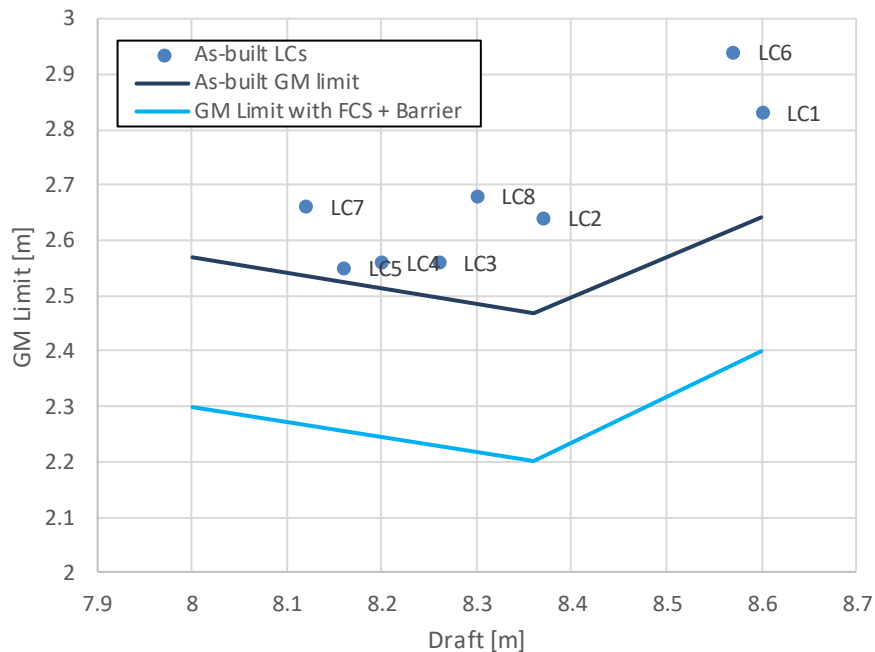


Figure 8-25: GM limit curve enhancement with AREST A2 & P1 systems

Table 8-15: Summary of solution specific GM margin benefits

T[m]	ID	Existing			With FCS		With Barriers + FCS	
		GM (m)	GM Req. (m)	GM Margin (m)	GM Req. (m)	GM Margin (m)	GM Req. (m)	GM Margin (m)
8.12	LC7	2.66	2.55	0.11	2.359	0.301	2.266	0.394
8.16	LC5	2.55	2.54	0.01	2.347	0.203	2.255	0.295
8.2	LC4	2.56	2.53	0.03	2.335	0.225	2.244	0.316
8.26	LC3	2.56	2.51	0.05	2.314	0.246	2.228	0.332
8.3	LC8	2.68	2.51	0.17	2.299	0.381	2.216	0.464
8.37	LC2	2.64	2.5	0.14	2.289	0.351	2.208	0.432
8.57	LC6	2.94	2.62	0.32	2.459	0.481	2.375	0.565
8.6	LC1	2.83	2.65	0.18	2.491	0.339	2.400	0.430

8.3.7 Conclusions – Part B

Deriving from the study presented in the foregoing, the following specific conclusions may be drawn:

- Time domain simulations have clearly demonstrated that passive foam installations in ship void spaces is a very effective reconfiguration solution for flooding protection, as was also clearly indicated through static assessment.
- The additional information afforded by dynamic assessment relates to the impact of this benefit, in particular the elimination of progressive flooding loss scenarios and the significant reduction in transient loss scenarios.
- In addition, focussing on the different mechanics of the loss, afforded by time-domain simulations, it was possible to identify additional vulnerabilities in the middle-section of the ship for further passive protection.
- Finally, the forensic detail of the flooding evolution within the ship, provided requisite additional information for critical openings protection by using an ARESTA2 system (deployable foam barriers), which in turn led to increasing further the GM margins and hence further facilitating life cycle damage stability management for the ship in question.

Chapter 9: Active Damage Control Application Example – Controlling Progressive Flooding (AREST A2)

9.1 Opening Remarks

This chapter focuses on the application of active flooding control technology (AREST2 and AREST2F), namely deployable barriers for flooding and fire protection, on a 10,500 POB cruise ship C2, the largest ship ever, currently being constructed. The methodological treatment of flooding protection through reconfiguration of the internal ship environment is described in this chapter in forensic detail, complete with the implementation and impact of flooding control by targeted reconfiguration of the internal ship space. Designing and operating a 10,500 POB cruise ship carries with it a great responsibility and, as such, demands a safety platform that goes beyond that which is currently required by regulations. For this reason, it was endeavoured to undertake a form of damage stability assessment that would subject the vessel to the most adverse scenarios statistics have to offer. The intention here being that, should any of these unlikely though plausible events ever occurred, life on-board will not be compromised. Furthermore, and as has often been said, “you learn more from a failure than you do from success” and this holds true when assessing vessel survivability. That is to say, the designer gains information of far greater utility through the identification of loss scenarios and mechanisms revealed therein, than he does from a survival case. For this reason, it is of crucial importance that we identify, or indeed, actively seek out any and all failure modes we can within the design stage, lest they be revealed to us at a later time and at a far greater cost. After all, when it is a question of safety it is only prudent to plan for the worst whilst working for the best and it is with this in mind that the present investigation has sought to adopt a systematic, in-depth approach to identify credible solutions to any realisable problem. The assessment follows the methodology and process described in Chapter 4 and Chapter 5, starting first by accounting for the current regulatory requirements and culminates in a vessel “stress test”. The latter has seen the vessel subjected to most extreme scenarios from all conceivable perspectives, namely: (a) design loading condition at limiting GM; (b) maximum significant wave height (7 m) from IACS Global wave statistics and (c) maximum probable damage length with randomly defined damage location, penetration and height.

As expected, CS2 survived all damages reflected in current regulations with considerable margins and failed only in 34 out of 1,000 cases in the extreme scenarios outlined in the foregoing (9 progressive flooding and 25 transient losses). This demonstrates an exceptional level of damage survivability by any measure and means but, given the project in question, it was thought

appropriate to adopt a zero-tolerance philosophy and to strive to achieve this in a feasible and economically viable way. To this end, 5 foam-based barriers have been introduced on deck 2, which can be deployed in situ to curtail all progressive flooding scenarios. Furthermore, six semi-watertight bulkheads on decks 3 and 4 have been explored in order to curtail a number of the transient capsize scenarios; thus leaving only a few extreme transient losses where the limitation comes from physics and, presently, there is nothing we can do about it.

9.2 Modelling of the Ship Environment and External Conditions

9.2.1 Ship Principle Particulars

The main particulars of the vessel are provided in the following table.

Table 9-1: CS2 Principle Particulars

Parameter	Value
Length overall (LOA)	370.07 m
Length between perpendiculars	351.57 m
Beam (B)	48.5 m
Design draft	9.10 m
Subdivision draft (HSD)	9.40 m
Height of the main deck	22.5 m
Displacement (DS)	114488 ton
People on Board	10,500

9.2.2 Simulation model and Arrangement

As covered within Chapter 5 and previously executed within Chapter 8, a detailed representation of the vessel internal geometry has been created within the simulation model. This includes definition of all relevant spaces within the vessel weathertight envelop, with the resultant model containing some 825 spaces as opposed to the static model, which comprised just 367 spaces. This is indicative of the reductive representation of the vessel one can expect to find in hydrostatic calculations. In any case, a depiction of the resultant vessel arrangement and hull form considered is provided within Figure 9-1 and Figure 9-2.

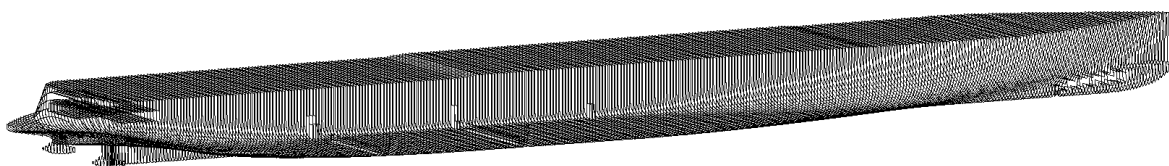


Figure 9-1: CS2 simulation hull form sections

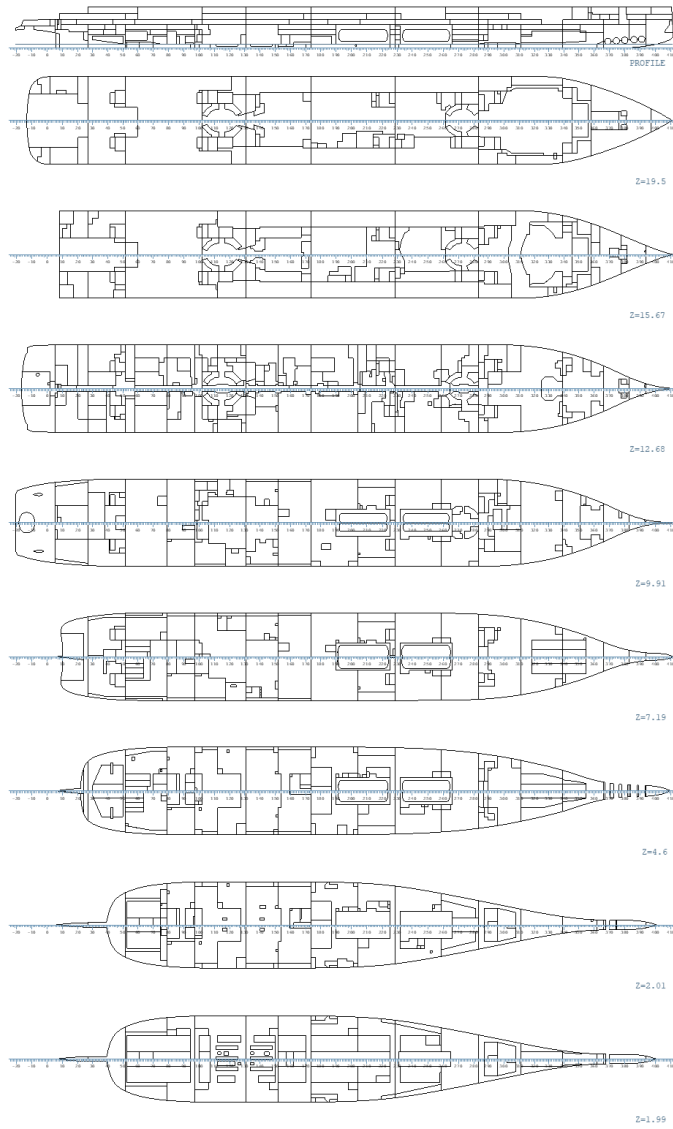


Figure 9-2: CS2 simulation model arrangement

9.2.3 Verification of internal geometry

As described in Chapter 8, the vessel has also undergone an assessment of correlation between the static model and the simulation model in order to ensure no inaccuracies have been introduced as a results of the conversion process. The results of this process are summarised within Figure 9-3.

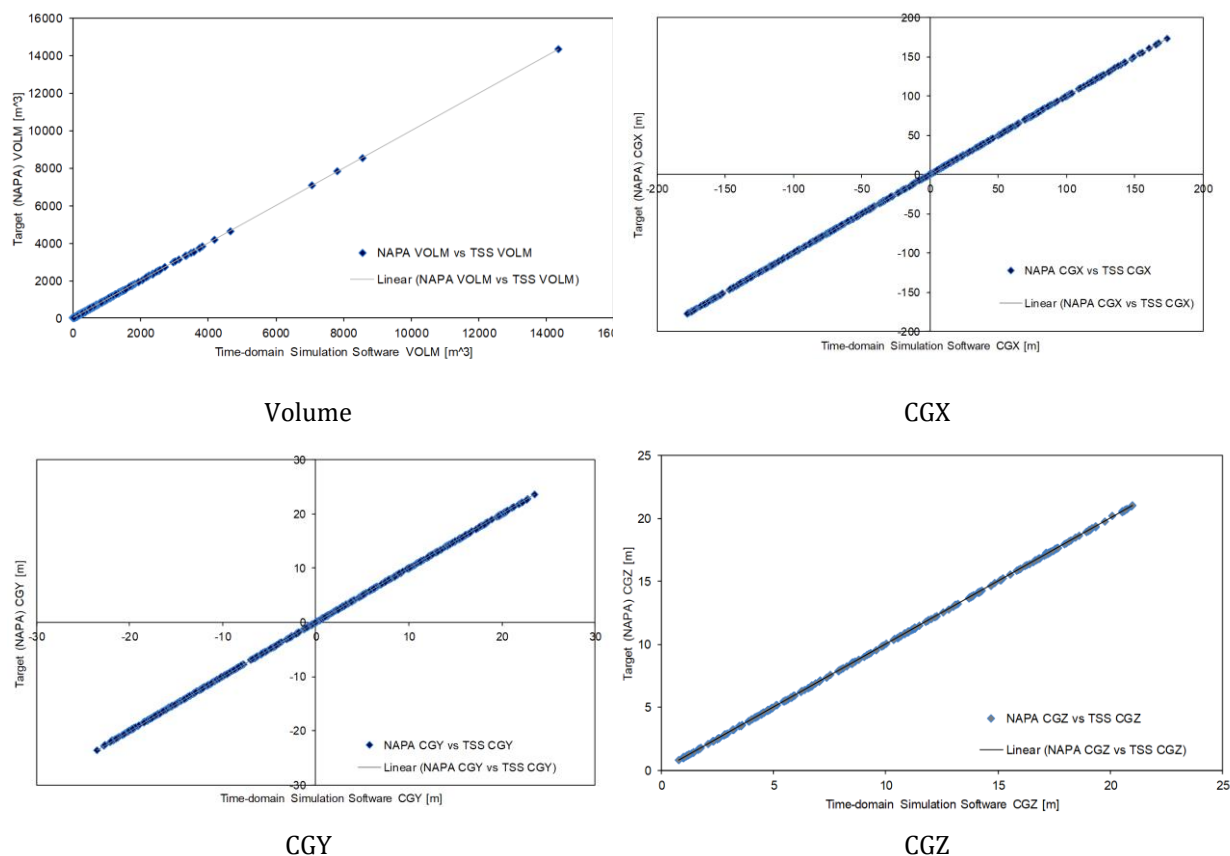


Figure 9-3: Comparison of hydrostatic & simulation model properties

Table 9-2 below provides a summary of the above comparison, highlighting the maximum differences observed for each property in terms of both percentage and actual value. From these figures it can be observed that no significant disparity between the models exists.

Table 9-2: Model correlation summary

Parameter	Maximum difference [%]	Value
Volume	1.4	5.127 m ³
CGX	0.09	-0.148 m
CGY	20.1	0.005 m
CGZ	-0.75	-0.130m
Permeability	0	0

9.2.4 Opening Definition

The vessel opening definition has been conducted in accordance with the process described within Chapter 5, leading to the definition of 1,526 openings as shown within Figure 9-4 Figure 8-12.

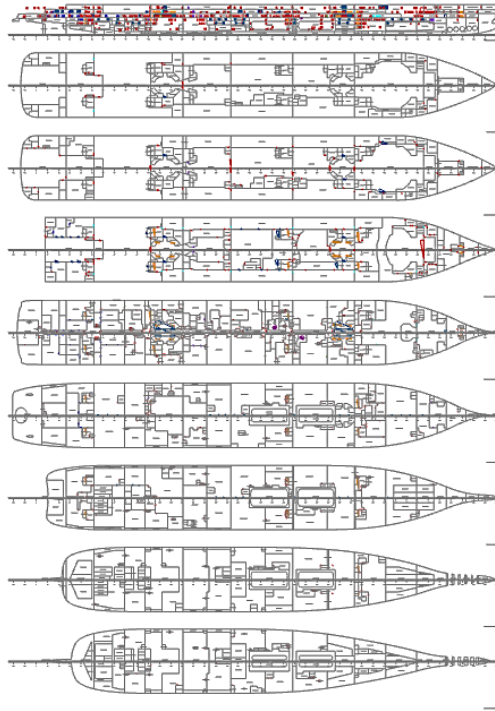


Figure 9-4: Simulation model opening arrangement

9.3 Numerical time-domain simulations (SOLAS 2009 assumptions)

9.3.1 Overview

At first instance, time-domain numerical simulations are performed in line with SOLAS 2009 assumptions, sampling from pertinent damage and wave distributions as described within Chapter 5. A total of 1,000 collision damage simulations are performed for a single loading condition, namely the deepest subdivision draft (ds), in irregular waves (JONSWAP spectrum) sampled from the SOLAS distribution with 4 metre maximum significant wave height.

The numerical simulation results have indicated that zero cases will capsize within the given simulation time (30 minutes). The cumulative distribution function for Time To Capsize (TTC), based on actual capsizes, translates to an equivalent Attained Subdivision Index of 1.0. This demonstrates a significant level of survivability within the as-designed condition, but one must

remember that when sampling damages, you only capture a subset of all probable scenarios, leading to the vessel stress-test described later within this chapter.

Detailed results for all numerical simulations are provided in Appendix D consisting of comprehensive summaries.

9.3.2 Collision Damage Sample

Figure 9-5 below, provides an illustration of the collision damage sample. Here it can be observed that even those damages possessing the greater damage length are not liable to give rise to extensive flooding in terms of the number of compartments breached. This comes by virtue of the vessel size and there are seldom more than three compartments comprised within the damage sample.

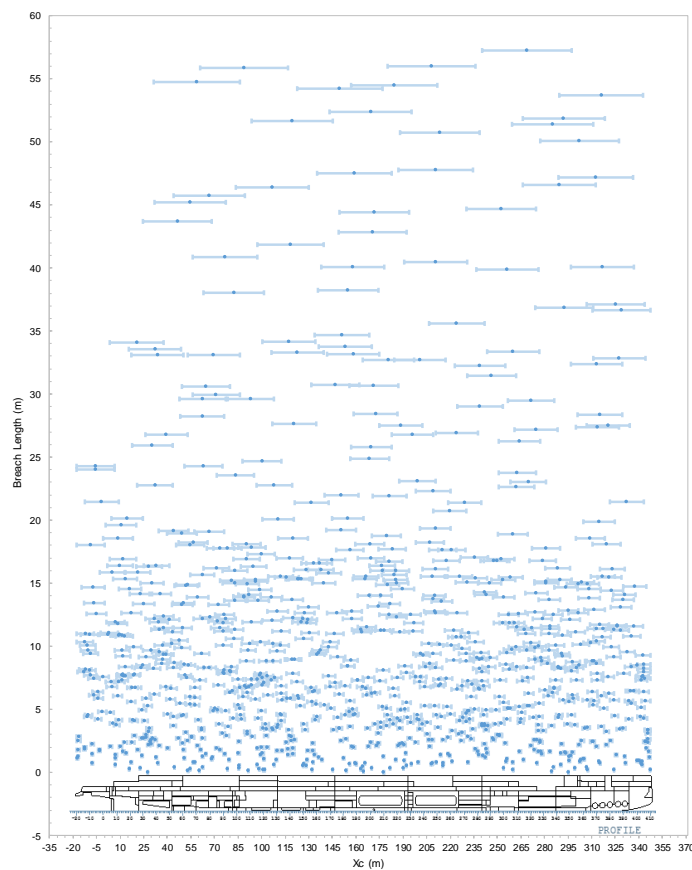


Figure 9-5: Collision damage sample, breach extent and location

The previous point is further illustrated with consideration of the damage sample CDF, Figure 9-6, which indicates some 90% of damages have lengths below 25m, with only 1.3% having length greater than 50m (3-compartment equivalent).

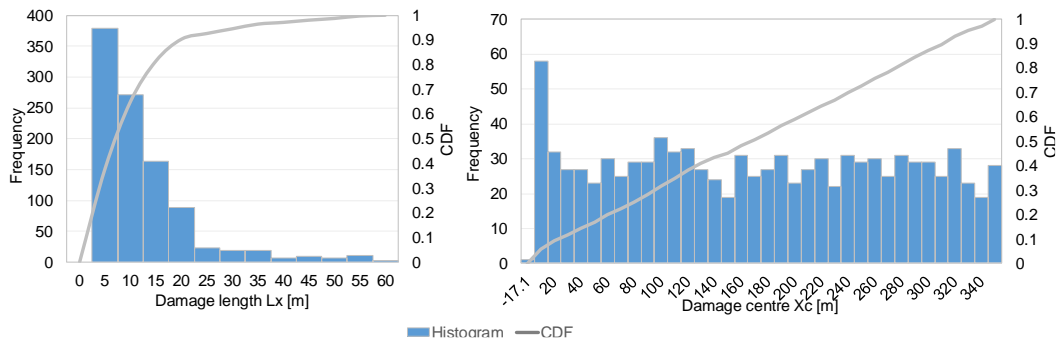


Figure 9-6: SOLAS collision damage sample CDF, damage length and centre

Furthermore, it was also found that only approximately 50% of damage cases extended above the vessel bulkhead deck, which is a damage characteristic that greater affects the propensity of a given case to succumb to transient capsizing.

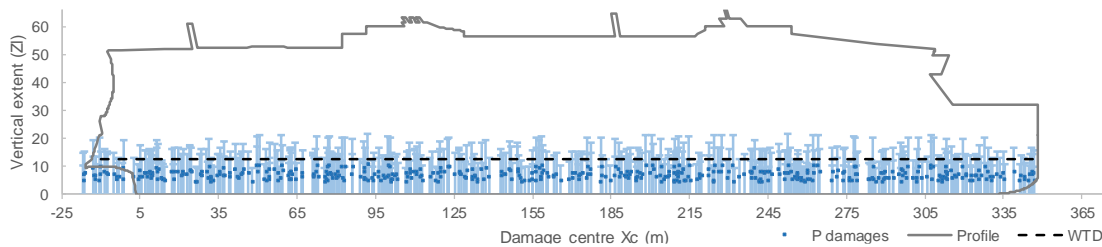


Figure 9-7: SOLAS collision damage sample vertical extents

9.4 Numerical time-domain simulations – Stress Test

9.4.1 Overview

As was mentioned within the introduction to this chapter, it has been undertaken to conduct a form of assessment that will truly test the extremities of vessel survivability. This is of course not a fair measure of vessel survivability, but it is a measure nevertheless, and has been conducted in the spirit of assessing what could go wrong regardless of event probability. In this respect, a single sea state of 7 metres wave height (IACS global maximum) is utilised in the simulations with an irregular wave environment in accordance with the JONSWAP spectrum. The exposure time has been set at 30 minutes duration, as in previous the previous studies.

9.4.2 Damage Generation

A total of 1,000 collision damages have been sampled for numerical simulations with a fixed damage length, representing the maximum possible longitudinal breach based on SOLAS damage statistics (60 metres), with all other damage characteristics having been sampled randomly. The reason for this stems from the strong correlation between damage length and severity, whereas

other damage properties have a greater tendency to lead to more adverse outcomes at lesser extents. In addition and deviating from general SOLAS assumptions, random values for the damage extent below the water line have been sampled from the distribution proposed in eSAFE (Bulian et al., 2018). An illustration of the resultant damage sample is provided within Figure 9-8.

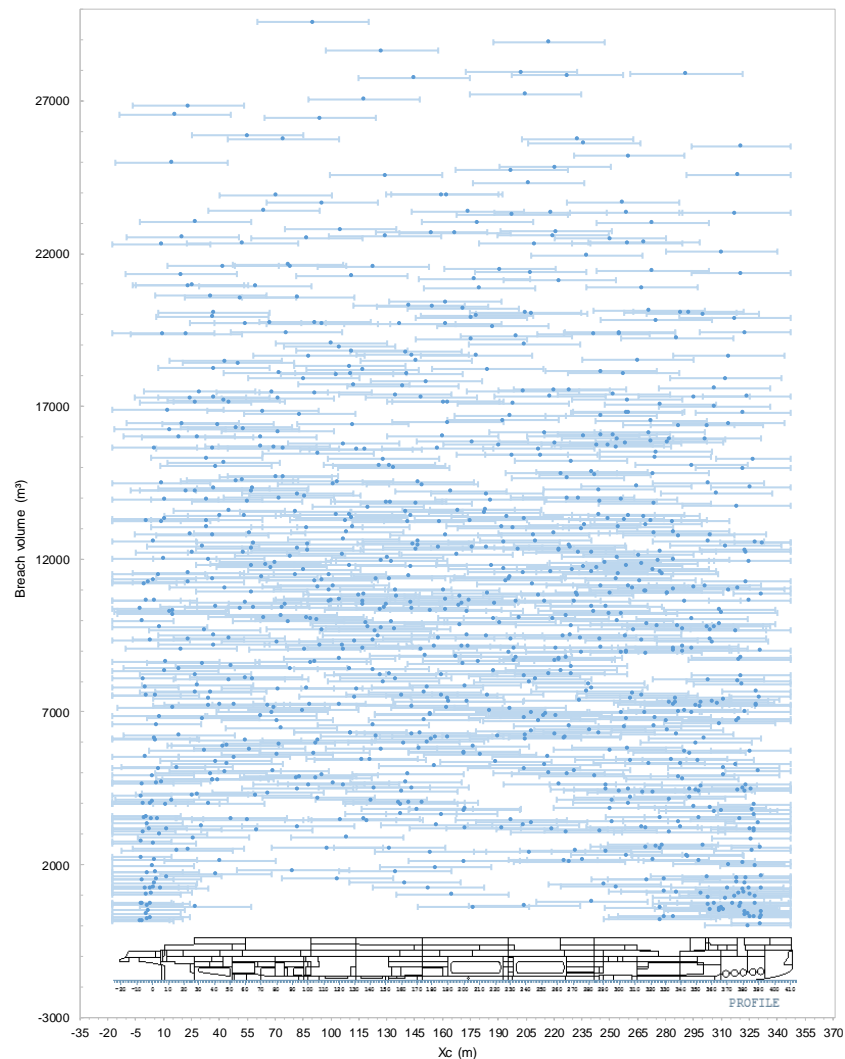


Figure 9-8: Stress Test damage sample, breach extent and location

9.4.3 Overview of simulation results

The numerical simulation results have indicated that 34 cases will capsize within the given simulation time. The cumulative distribution function for Time to Capsize (TTC) based on actual capsizes shows that the vessel achieves an equivalent Survivability Index of 96.6% (see Figure 9-9). By analysing the mode of loss across all loss scenarios, 25 transient and 9 progressive flooding cases have been observed. Table 9-3 provides information on each of these cases relating

to time to capsize, maximum 3-minute average heel, sinkage, maximum floodwater mass and the final floodwater mass rate of the floodwater envelope.

Detailed results for all numerical simulations are provided in Appendix E, consisting of comprehensive summaries.

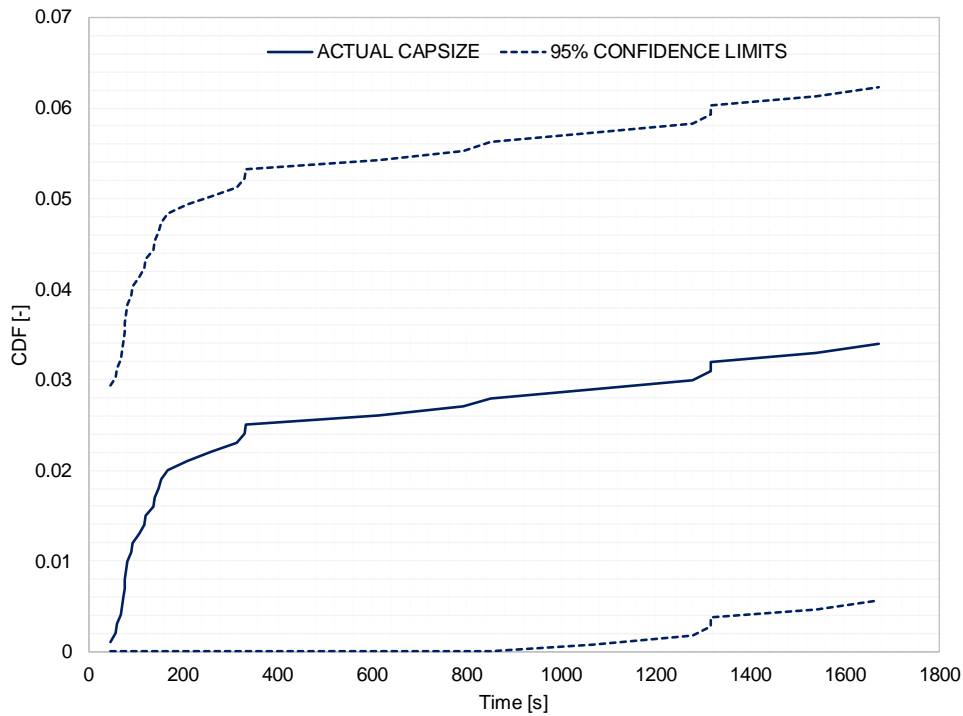


Figure 9-9: Cumulative distribution of the Time to Capsize for all physical capsizes with an indication of the Survivability Index of 0.966

Table 9-3: Stress-test results breakdown

Damage case	TTC [s]	Max 3-min average heel [deg]	Final sinkage [m]	Max fl. mass [t]	Final fl. mass rate (env) [t/h]
Progressive capsizes					
DMC156	1317.5	-36.8	-3.2	26873.0	16828.6
DMC181	1279.1	33.2	-4.3	40975.5	21723.1
DMC234	1064.9	-32.7	-3.8	35073.0	0.0
DMC275	1671.3	36.0	-2.8	23074.0	40422.8
DMC307	1538.8	-32.0	-4.5	44689.3	1807.9
DMC493	1316.1	34.2	-5.3	51316.9	0.0
DMC625	850.8	34.2	-5.0	48819.6	14895.1
DMC815	614.5	-32.2	-4.7	44730.3	950.6
DMC980	793.6	-33.4	-4.4	40045.5	1722.8
Transient capsizes					
DMC02	117.2	-37.3	-3.3	33499.0	811805.4
DMC35	135.7	-33.8	-4.4	46070.7	421019.8

DMC77	77.7	41.9	-4.1	42732.8	2206297.1
DMC79	257.2	37.1	-3.9	36025.9	33706.4
DMC130	208.4	-28.4	-4.4	45339.5	193015.9
DMC423	69.0	-55.5	-4.4	27855.5	1760997.6
DMC465	106.4	-42.9	-3.5	28872.4	778642.5
DMC515	56.1	57.8	-5.2	41008.5	2964449.8
DMC521	76.7	53.6	-5.8	38748.2	1497550.9
DMC533	146.5	32.1	-3.8	37970.5	538236.1
DMC606	314.1	33.2	-4.1	42097.2	52674.6
DMC607	75.0	45.5	-4.0	33230.3	1669617.2
DMC616	81.5	48.8	-5.4	44901.9	1491403.6
DMC619	89.4	36.4	-4.7	47866.0	1213666.6
DMC659	119.1	31.4	-4.0	44463.8	735063.1
DMC697	140.1	-34.7	-4.1	45935.6	418818.3
DMC713	46.7	-56.4	-5.6	31102.2	2691813.8
DMC733	91.9	-44.8	-5.0	47090.7	1113827.0
DMC778	331.7	-32.8	-4.4	42942.2	19390.6
DMC791	329.4	-38.6	-4.6	41155.2	25997.2
DMC794	71.2	48.3	-4.5	29457.5	1039163.1
DMC798	152.8	-34.4	-3.5	30632.8	427462.2
DMC843	74.4	61.5	-3.6	28173.7	1331749.7
DMC857	168.5	-27.0	-3.2	33914.1	389954.7
DMC924	59.2	58.7	-5.0	34268.8	2731221.7

In addition, Figure 9-10 and Figure 9-11 provide an indication of each capsized case, the breach location and the respective loss modality realised, relative to breach volume and TTC.

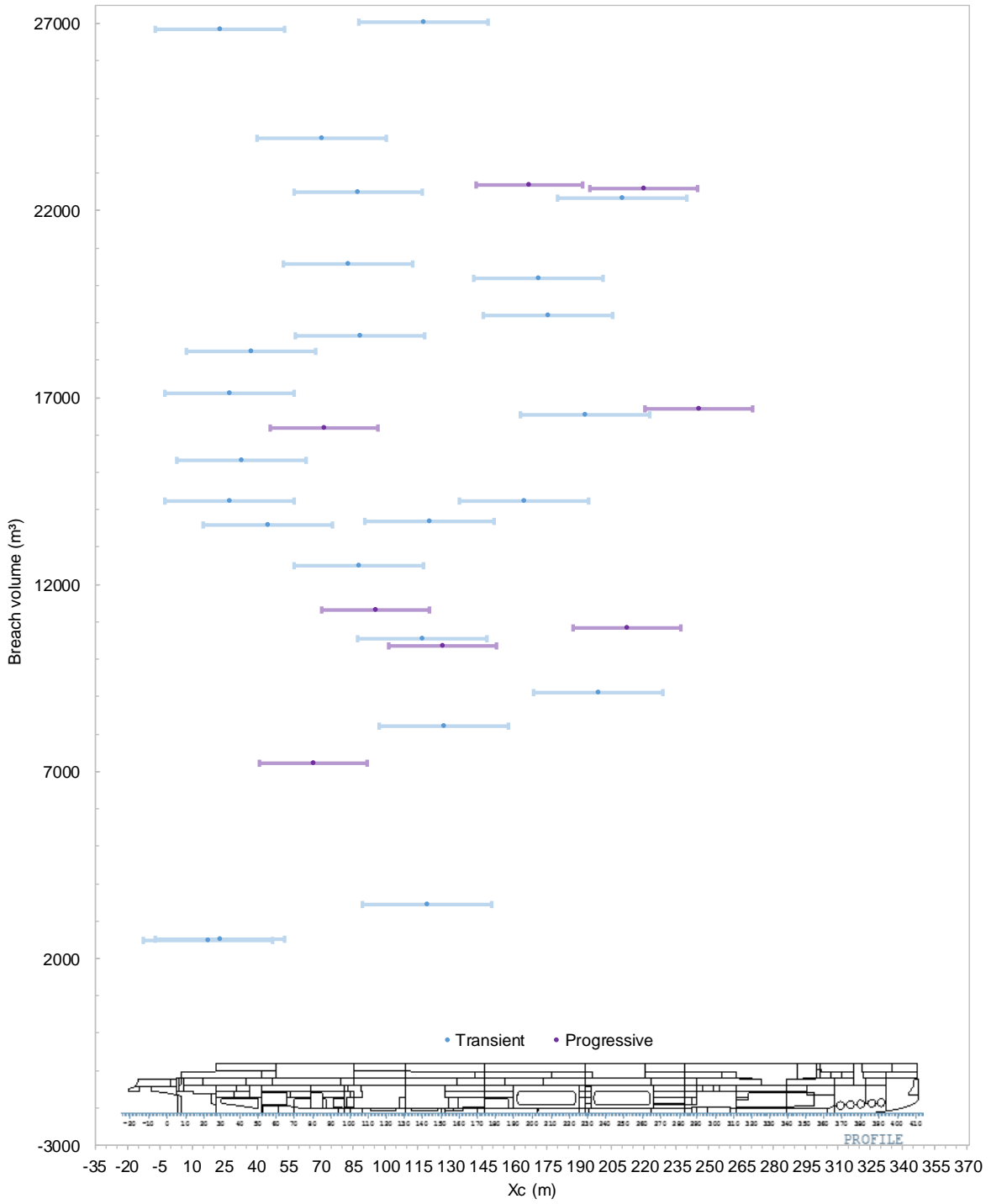


Figure 9-10: Longitudinal damage extent centre and breach volume (XLYLZL) of progressive and transient capsizes.

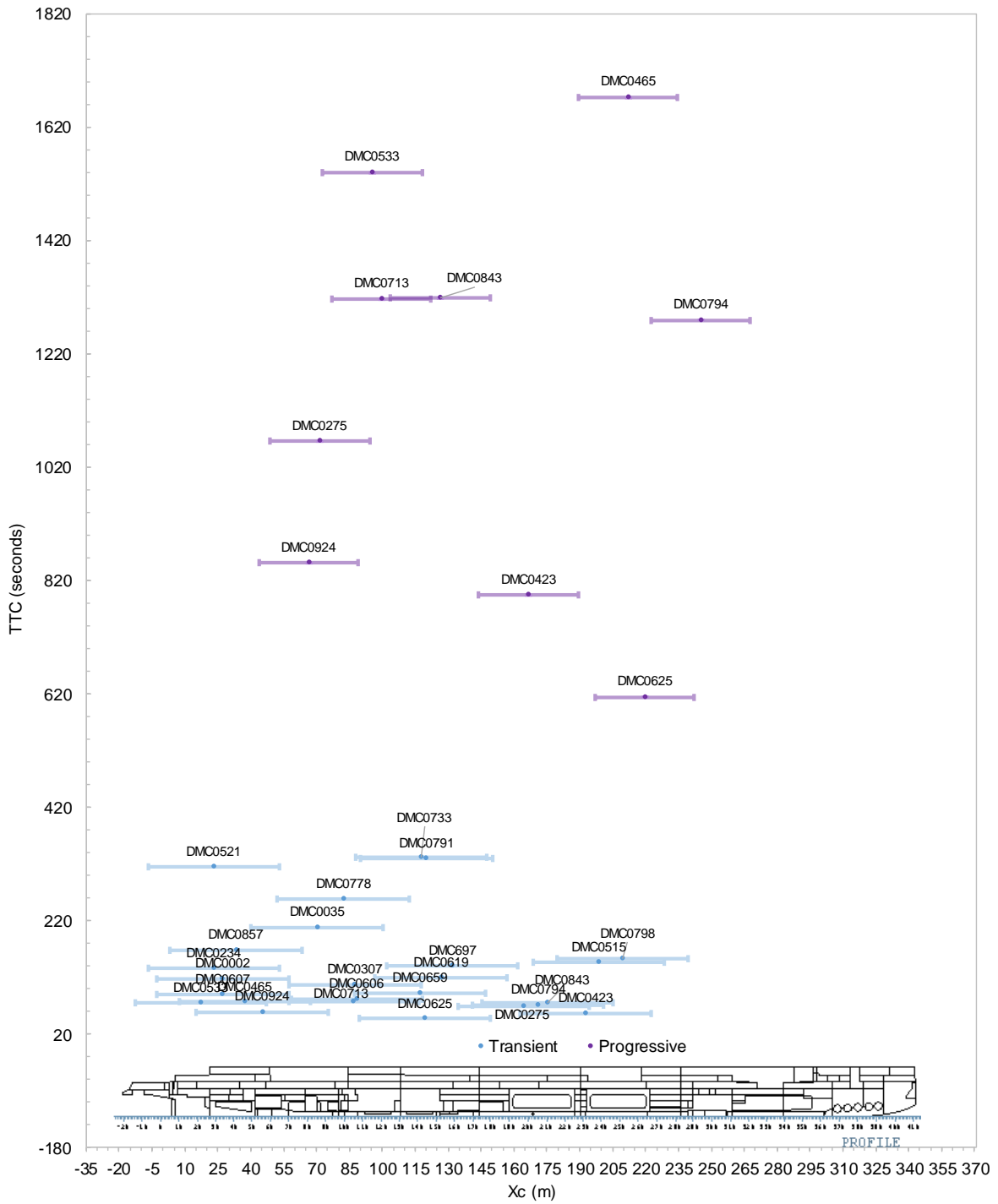


Figure 9-11: Longitudinal damage extent centre (m) and Time To Capsize (seconds) of progressive and transient capsizes.

9.5 Numerical Time-domain simulations – Calm Water

In order to ascertain the degree to which the wave environment examined within the vessel stress test has impacted vessel survivability, a complimentary assessment in calm water has been conducted considering the same collision damages, Table 9-4. Firstly, concerning progressive flooding, the results have shown this mode of loss to be sensitive to wave effects with all cases surviving within calm water conditions. This would indicate that in each of these cases the vessel possesses enough residual freeboard with which to ensure either unprotected openings are not immersed or, at the very least, to slow the flooding process. Regarding the latter it is interesting to note that many cases demonstrated a high level of floodwater mass accumulation still ongoing when the simulation time elapsed, so there is every reason to assume that given longer exposure time many of these cases may capsize. In addition, and as was touched upon in Chapter 3, progressive flooding can be greatly influence by wave induced pumping effects, resulting in floodwater progression across upper decks. As such, when assessed in calm water, the vessel is not susceptible to this dangerous phenomenon.

Table 9-4: Comparison of progressive flooding cases $H_s=0m$ & $H_s=7m$

9 Progressive capsizes	TTC [s]	
	7 metres	Calm water
DMC156	1317.47	1820
DMC181	1279.09	1820
DMC234	1064.94	1820
DMC275	1671.26	1820
DMC307	1538.76	1820
DMC493	1316.135	1820
DMC625	850.77	1820
DMC815	614.49	1820
DMC980	793.60	1820

With regards to transient capsize, in contrast with progressive flooding, this loss modality showed little sensitivity to wave effects with just 4 out of 25 cases surviving by comparison, Table 9-5. This stands to reason given the scale of the damages explored in which the floodwater induced moment far outweighs the wave induced excitations.

Table 9-5: Comparison of transient flooding cases $H_s=0m$ & $H_s=7m$

25 Transient capsizes	TTC [s]	
	7 metres	Calm water
DMC02	117.23	124.2
DMC35	135.69	115.45
DMC77	77.67	87.69
DMC79	257.19	1820
DMC130	208.45	179.07
DMC423	68.97	98.27
DMC465	106.44	99.41
DMC515	56.07	1820
DMC521	76.65	78.59
DMC533	146.53	152.9
DMC606	314.10	1820
DMC607	74.96	76.57
DMC616	81.49	80.15
DMC619	89.44	135.58
DMC659	119.09	131
DMC697	140.07	160.23
DMC713	46.74	1820
DMC733	91.87	107.4
DMC778	331.72	480.93
DMC791	329.41	131.8
DMC794	71.20	65.69
DMC798	152.84	1820
DMC843	74.40	78
DMC857	168.51	192.95
DMC924	59.24	60.92

The resultant vessel Survivability Index in calm water was calculated as 0.979, marking a 1.3% improvement over that calculated within the stress-test. The reason for only a marginal change being witnessed here stems simply from the fact that the primary loss modality experienced by the vessel is transient capsize, which was found to be insensitive to wave effects.

9.6 Progressive Flooding Critical Design features and Solutions

9.6.1 Identification of critical openings

In alignment with the process outlined within Chapter 5, the simulation results pertaining to progressive flooding loss have been subjected to forensic analysis in order to identify and rank critical openings. In accordance with this approach, openings have been ranked in terms of frequency of involvement, floodwater mass transferred and a combination of the latter two. The results of this process are provided within Figure 9-12, Figure 9-13, and Figure 9-14 along with a summary in Table 9-6.

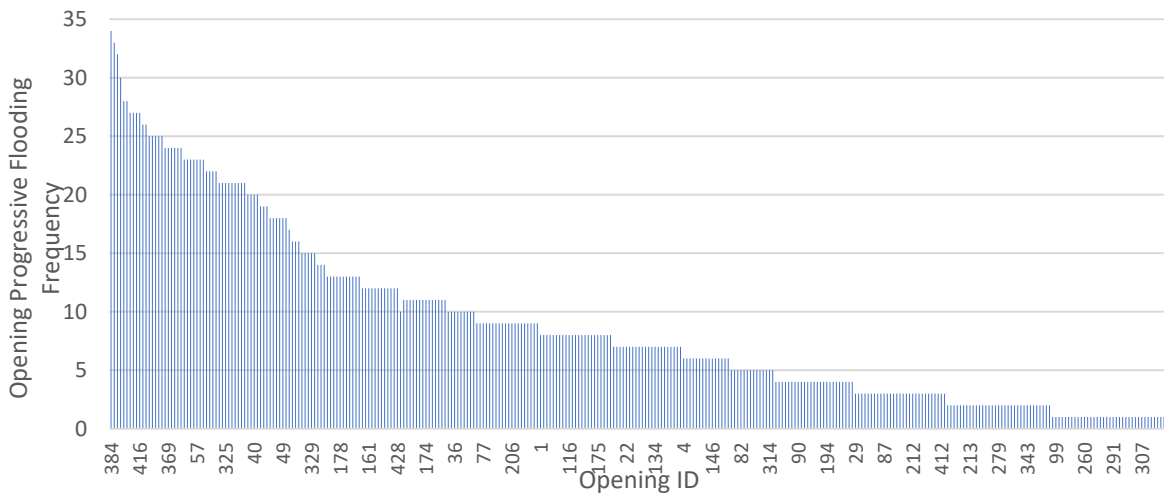


Figure 9-12: Opening Vulnerability Ranking by Frequency

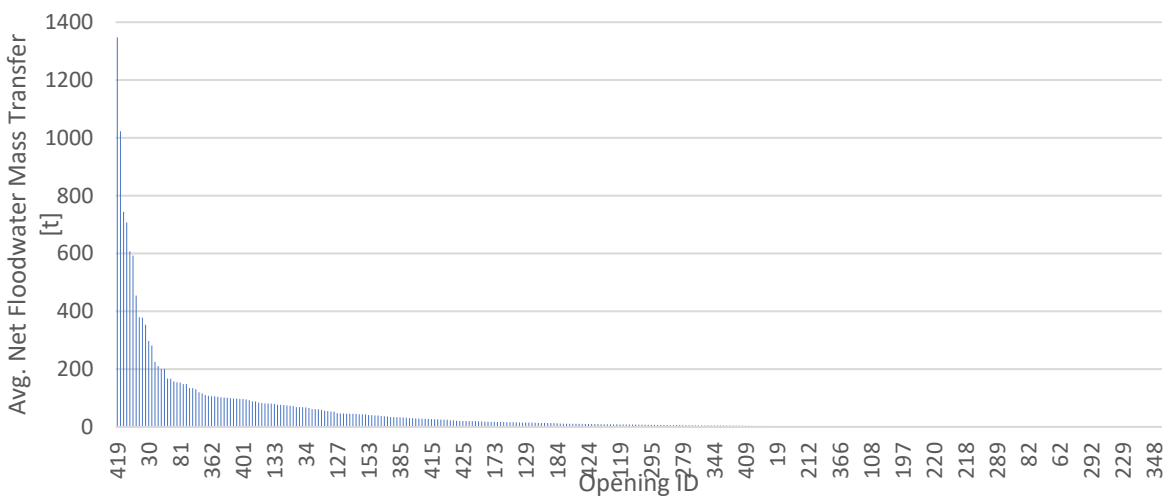


Figure 9-13: Opening Vulnerability Ranking by Net FW Mass Transfer

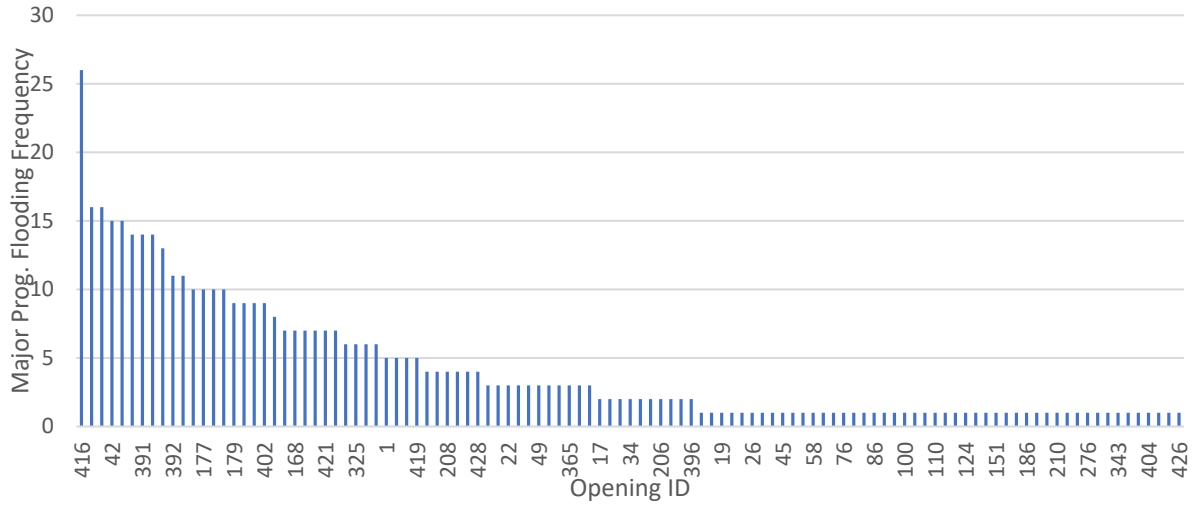


Figure 9-14: Opening Vulnerability Ranking by High FW Mass Transfer Frequency

Table 9-6: Critical Opening Summary

Compartment connection	Model ID	Opening Type	X (m)	Y (m)	Z (m)	Width (m)	Height (m)	Area (m ²)	Collapse Pressure (m)	Leak Height (m)
3 <-> 4	OPE0223	Double Leaf Hinged Fire Door	45.643	-3.9	12.66	2.7	2	5.4	2	0
3 <-> 4	OPE0227	Double Leaf Hinged Fire Door	48.579	-0.058	12.66	2.6	2	5.2	2	0
3 <-> 4	OPE0222	Double Leaf Hinged Fire Door	45.877	3.9	12.66	2.7	2	5.4	2	0
4 <-> 5	FB001	Open Corridor	-105.002	0	12.66	3	3	9	0	0
5 <-> 6	OPE0238	Hinged Fire Door	81.138	-2.6	12.66	0.85	2	1.7	2.5	0
5 <-> 6	OPE0239	Hinged Fire Door	80.983	2.6	12.66	0.95	2	1.9	2.5	0
5 <-> 6	OPE0237	Double Leaf Hinged Fire Door	80.177	-0.001	12.66	2.6	2	5.2	2	0
7 <-> 8	OPE0284	Hinged Fire Door	129.015	-2.6	12.66	0.95	2	1.9	2.5	0
7 <-> 8	OPE0285	Double Leaf Hinged Fire Door	134.274	0.371	12.66	2.6	2	5.2	2	0
7 <-> 8	OPE0362	Unprotected Connection	131.763	1.5	12.66	1.35	2.5	3.375	0	0
9 <-> 10	OPE0299	Hinged Fire Door	173.68	0.29	12.66	2.6	2	5.2	2.5	0
9 <-> 10	OPE0300	Hinged Fire Door	172.865	2.6	12.66	0.85	2	1.7	2.5	0
11 <-> 12	OPE0330	Hinged Fire Door	223.469	1.997	12.66	0.95	2	1.9	2.5	0
11 <-> 12	OPE0328	Double Leaf Hinged Fire Door	223.469	0.143	12.66	2.6	2	5.2	2	0
11 <-> 12	OPE0331	Hinged Fire Door	223.469	-1.71	12.66	0.95	2	1.9	2.5	0
13 <-> 14	OPE0336	Double Leaf Hinged Fire Door	244.786	0.231	12.66	2.7	2	5.4	2	0

9.6.2 Progressive Flooding - AREST A2 Solution

In order to eradicate the risk stemming from progressive flooding, each of the openings outlined within Table 9-6 will require some form of protection to provide a watertight barrier in case of flooding. One means of achieving this would be to uprate the watertight properties of each opening, though such a solution would have a hugely negative impact on the functionality of the vessel, particularly as these openings lie on the vessel service corridor. Instead, it is proposed to utilise foam barriers situated in line with the bulkheads located in proximity to these openings. By using such an approach, multiple progressive flooding openings for which a particular bulkhead opening is the source can be dealt with together, reducing the number of barriers required from 16 to just 5. This is further illustrated in the Figure below, where critical openings are highlighted within the blue circles and the proposed foam barrier is illustrated within the right hand Figure 23.

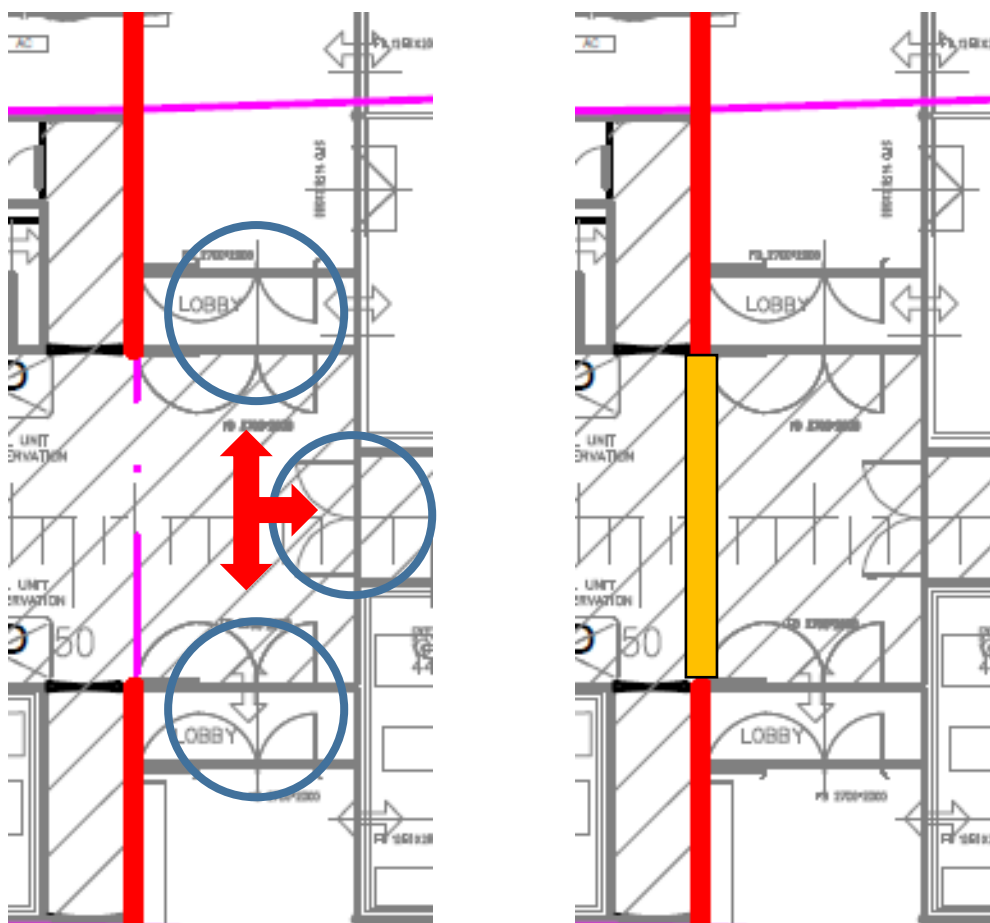
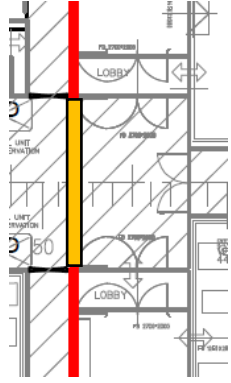
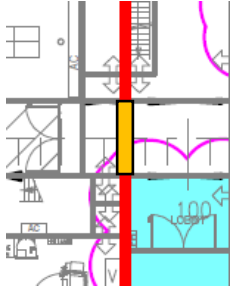
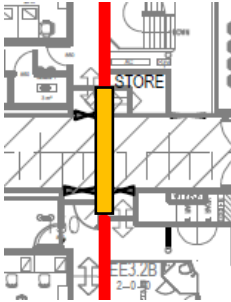
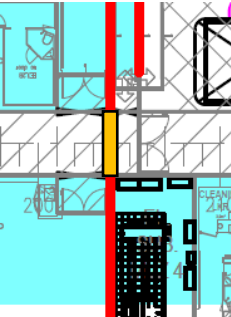


Figure 9-15: critical openings (left) and foam barrier solution example (right)

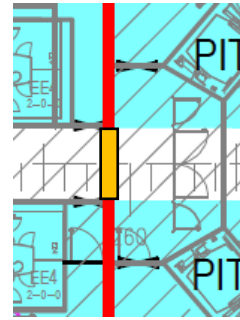
The dimensions of the openings in those bulkheads linked to progressive flooding were found to span from 4.1m up to 7.8m, thus the use of conventional semi-watertight doors would be ineffective here. In this respect, the use of foam barriers was deemed most appropriate as they can span up to 10 in width. Furthermore, the foam barriers are lightweight, non-intrusive, easily

installed and rapidly deployable. Critically, they can withstand pressures up to 1.5 bar (15 metres head), which in case of flooding of the upper decks, it is vital for any barriers used (such as fire doors) to be able to withstand such pressures, which is not currently not the case). To this end, Table 9-7 below provides an overview of all critical progressive flooding sources along with the proposed foam barrier solution.

Table 9-7: AREST A2 - solution summary

Properties	Illustration
Compartment Connection: 3 <-> 4 Frame: 52 Deck: Deck 02, 12.65m A.B.L. Breadth: 7.8m Height: 3m Openings served: 3	
Compartment Connection: 5 <-> 6 Frame: 97 Deck: Deck 02, 12.65m A.B.L. Breadth: 5.2m Height: 3m Openings served: 3	
Compartment Connection: 7 <-> 8 Frame: 152 Deck: Deck 02, 12.65m A.B.L. Breadth: 4.1m Height: 3m Openings served: 3	
Compartment Connection: 9 <-> 10 Frame: 204 Deck: Deck 02, 12.65m A.B.L. Breadth: 4.1m Height: 3m Openings served: 2	

Compartment Connection: 11 <-> 12
 Frame: 259
 Deck: Deck 02, 12.65m A.B.L.
 Breadth: 7.8m
 Height: 3m
 Openings served: 3



9.7 Transient Flooding – Proposed Solutions

The results of the numerical time-domain simulations demonstrate that the majority of loss scenarios witnessed came as a result of transient flooding. In the same manner as before, these cases were subjected to detailed flooding analysis enabling several vulnerability sources to be identified along with potential solutions, as outlined within the following.

9.7.1 Inadequate Cross-flooding

A number of areas within the vessel have been found to have insufficient cross-flooding in place, which leads to asymmetric flooding and worsens the effects of transient flooding. Such areas have been identified around the vessel aft shoulder and amidships. Figure 9-16, below shows a representative transient loss scenario within the vessel aft. Here it can be observed that the initial breach forms a highly asymmetrical damage and subsequently significant cross-flooding is required.

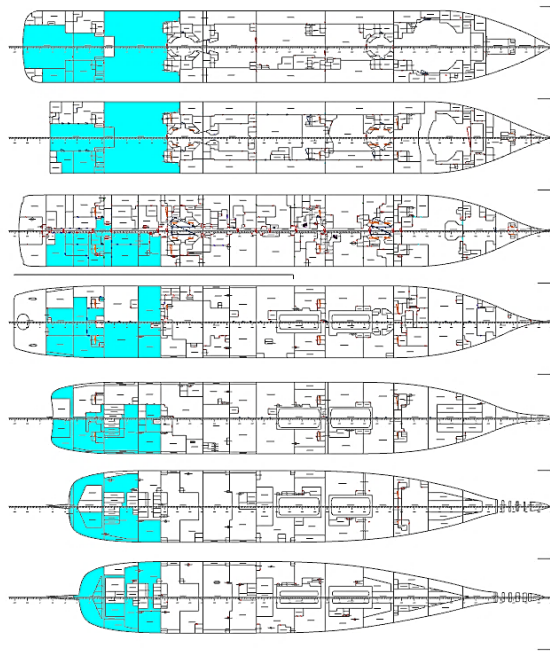


Figure 9-16: Representative transient loss scenario – resulting from collision

However, a number of features within this area have been found to prevent effective equalization as listed below:

- Lack of cross-flooding within Compartment 2, Deck 01, which can be amended by introducing openings to allow communication between these spaces as shown in Figure 9-17. Such a solution would, however, have to be weighted against the requirements of Safe Return to Port.
- Abundance of insulated cold rooms within compartment 3, Deck 0 & Deck 01. Cold room doors have a collapse height of 3.5m and as such this partitioning acts similarly to SWT structure preventing transverse flooding (shown in blue). One potential solution to this problem would be to have a system in place whereby such openings could be automatically opened following damage, thus allowing cross-flooding to take place (Figure 9-17).
- Abundance of insulated cold rooms spanning compartments 2-4 on Deck 02, once again acting to prevent transverse flooding. As, described above, a means to automatically open certain critical openings, following damage, could provide a solution.

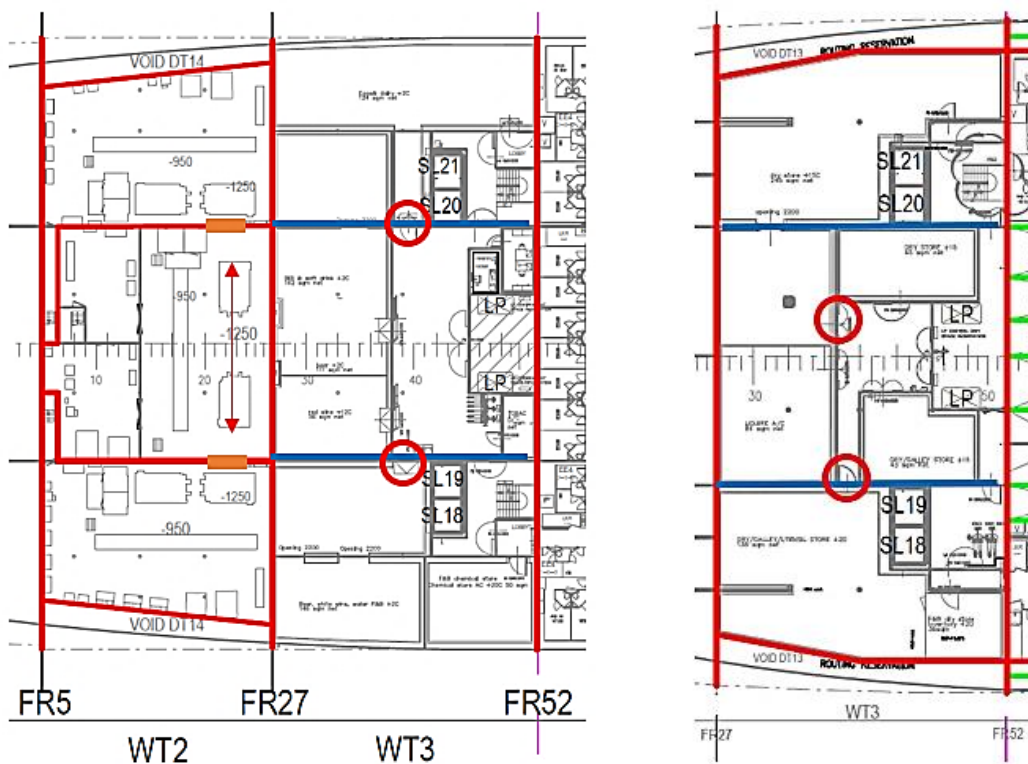


Figure 9-17: Sources of asymmetrical flooding, COMP 2&3, Deck 01 and Deck 0

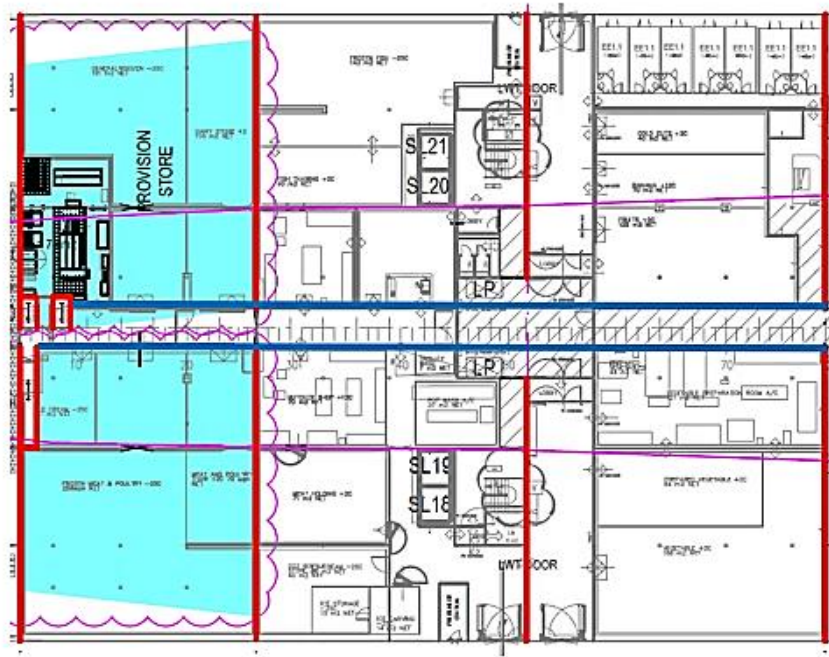


Figure 9-18: Cold-rooms resulting in asymmetry, COMP 2-4, Deck 02

Sources of asymmetrical flooding were also found around the vessel mid-ship. Figure 27 below shows the initial damage extent of a typical transient loss scenario within this area. Observation of the initially breached compartments highlights a large degree of cross flooding is required in order to compensate for this initial asymmetry.

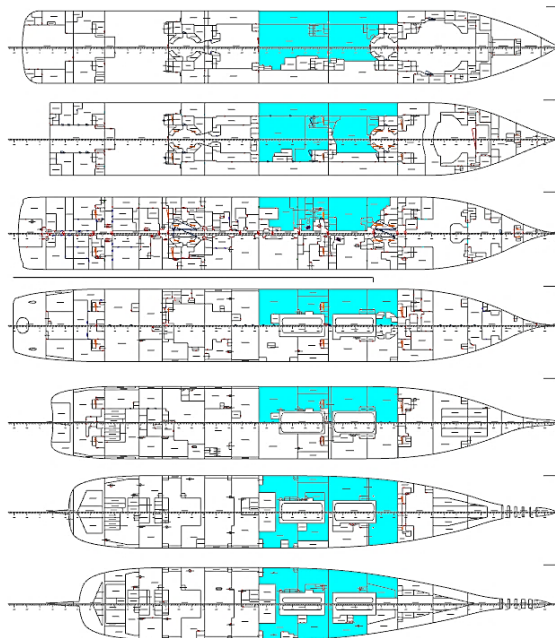


Figure 9-19: Representative transient loss case (Fore) – resulting from collision

However, a number of design features were found to inhibit this process including:

- Lack of communication between the port and starboard side compartments within Compartment 12, Tween Deck, which generates asymmetric flooding. This can be amended by introducing openings between these spaces as highlighted in Figure 9-20 in orange.
- A-class fire doors retarding floodwater equalisation within compartment 11 on Deck 0, shown in Figure 9-20 within orange circles. This can be solved by providing these openings with a means of automatically opening, following a flooding event within this area.



Figure 9-20: Sources of asymmetry within compartments 11 & 12, Deck 01 and Tween Deck respectively.

9.7.2 Areas with insufficient reserve buoyancy

In addition to certain design features that give rise to asymmetries, a number of areas have been identified that would benefit from additional reserve buoyancy high within the vessel in order to provide the vessel with the ability to withstand the transient roll cycle. The first of these areas relates to the main restaurant spanning from compartment 4 -7 and across decks 2 & 3. This is a large open space, which that when damaged can accumulate a large volume of floodwater that can spread unabated. In order to combat this effect, it is recommended to install four partial bulkheads within the restaurant area, shown in Figure 9-21 & Figure 9-22. These are to be located

near frame 80, which has been identified as the location where most loss scenarios would benefit from the solution. Unfortunately, the installation of permanent bulkheads here would obstruct the flow of passengers within this area and negatively impact the aesthetic of the space. In this respect, this problem serves to highlight a typical example of safety objectives clashing with business/operability objectives. However, this could potentially be overcome through utilisation of the AREST A2 system, in which the bulkheads would only be deployed when needed and as such would not affect regular service. Of course, due consideration would have to be given as regards the feasibility of deploying these bulkheads in time, particularly for transient capsized cases.

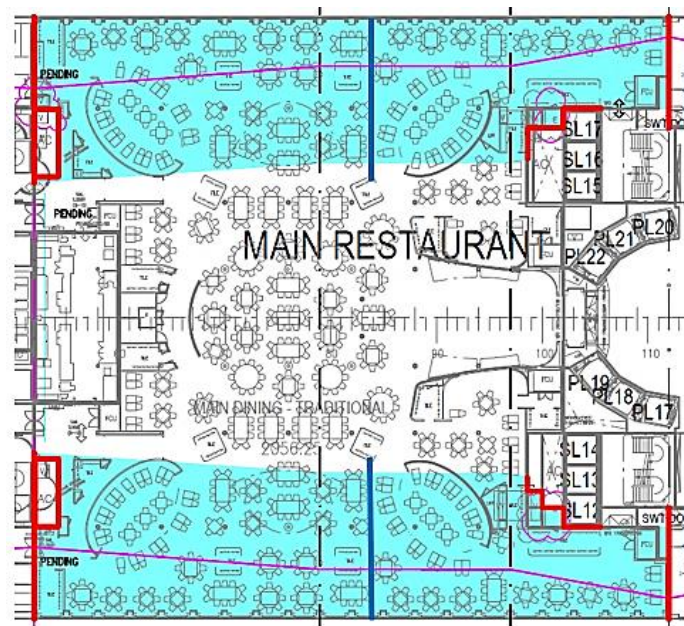


Figure 9-21: Proposed Partial Bulkheads, Deck 02

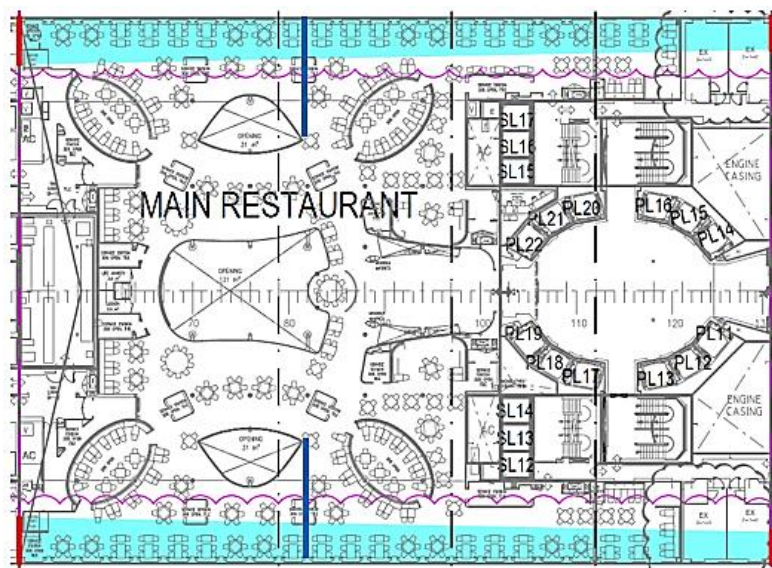


Figure 9-22: Proposed Partial Bulkheads, Deck 03

In addition to the restaurant area, the accommodation spaces within compartments 10 & 12, located on Deck 02 and Deck 03, were found to benefit from the installation of 4 partial bulkheads that would help to provide additional reserve buoyancy capable of resisting transient flooding effects. These have been located as shown in blue within Figure 9-23 and Figure 9-24 below, where they lie between the cabin lining of separate cabin spaces and do not encroach on the corridor.

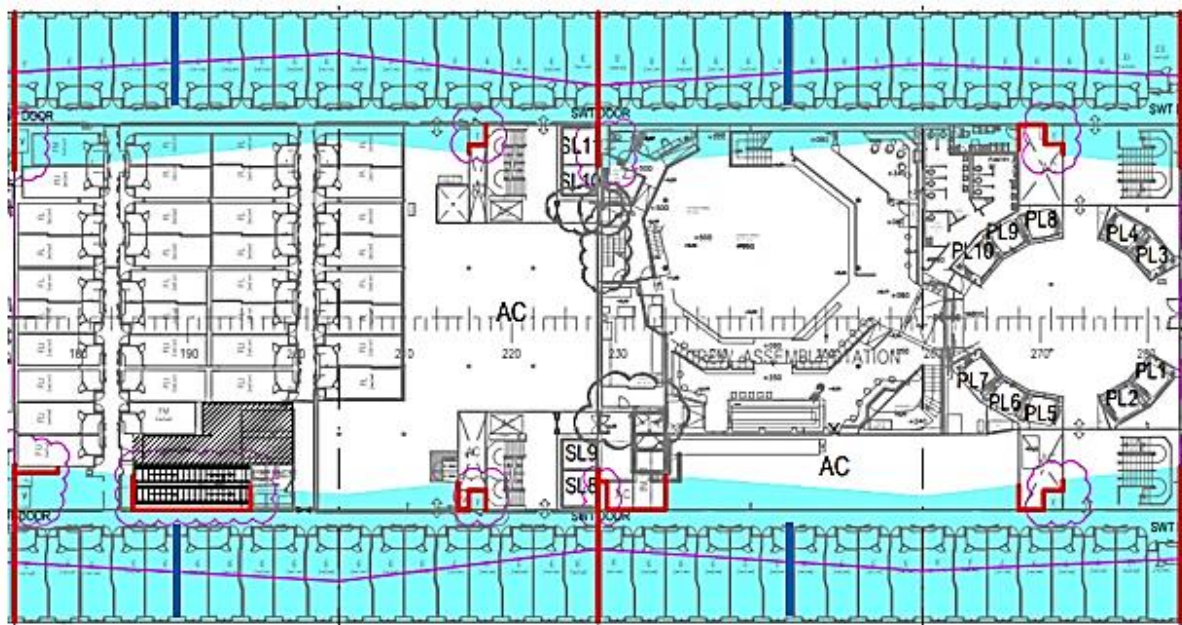


Figure 9-23: Proposed partial bulkheads within Compartments 10 and 12, Deck 02.

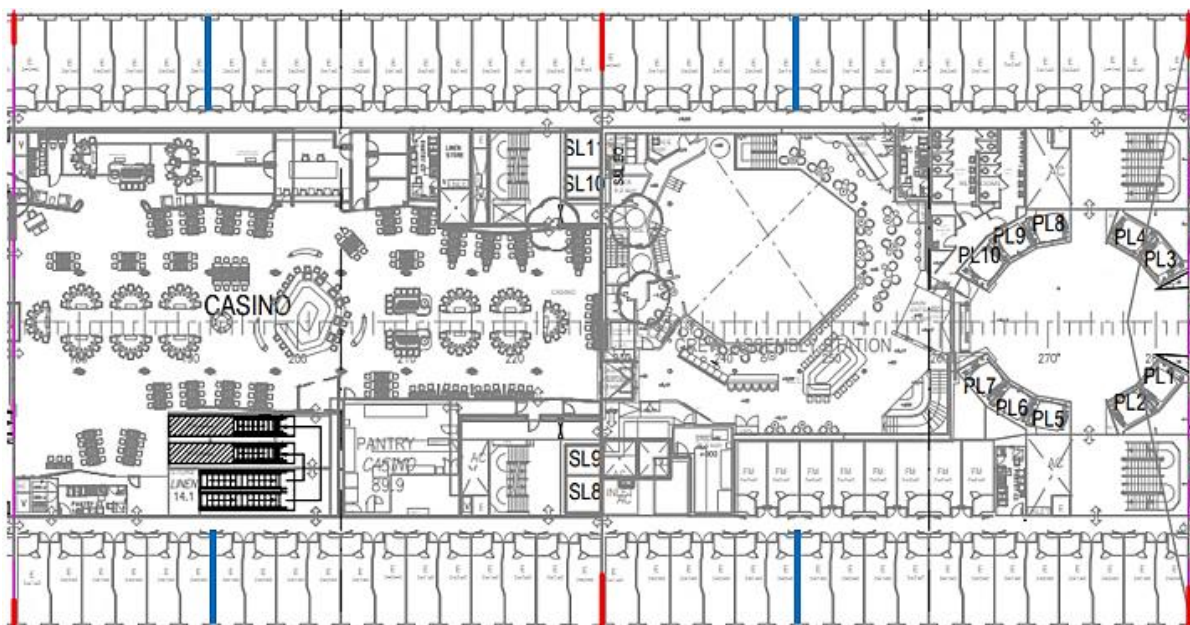


Figure 9-24: Proposed partial bulkheads within Compartments 10 and 12, Deck 03.

9.8 Numerical time-domain simulations – Impact of solutions

Having implemented the solutions outlined within the foregoing, both stress-test and calm water assessments have been repeated in order to gauge survivability benefit. In the first instance, the results of this process have demonstrated a reduction in total capsize cases from 34 to 20 cases. Under calm water assessment, this is further reduced from 25 to 13 capsize cases. Figure 9-25 shows the cumulative distribution functions for Time to Capsize (TTC) for both assessments shown relative to the results of the as-built stress test. Here it can be observed the vessel Survivability Index has increased from 0.966 in the as built case, to 0.98(Hs=7m) and 0.987(Hs=0). Table 9-8 provides an overview of the results stemming from each assessment conducted and provides a breakdown in relation to the modes of loss realised.

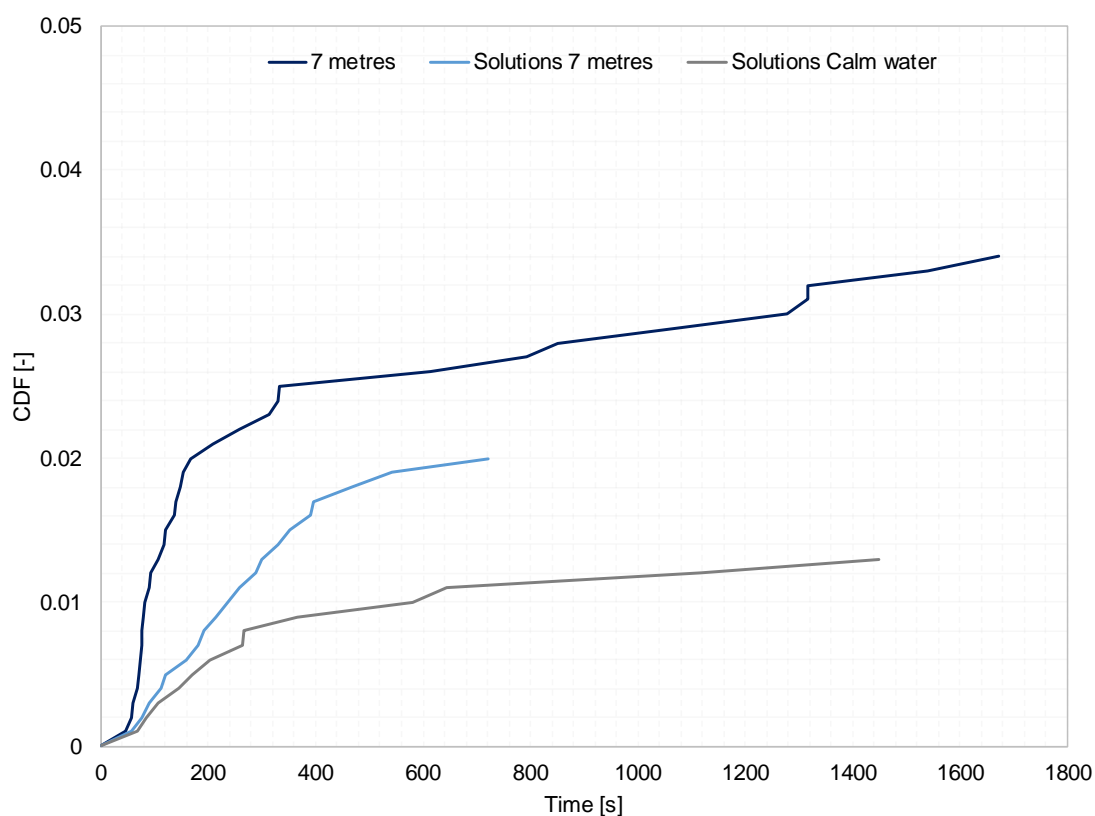


Figure 9-25: Cumulative distribution function of the Time to Capsize for all physical capsize cases relating to simulations in waves and calm water following implementation of proposed solutions.

Table 9-8: Summary of all assessment results

Assessment	Hs(m)	Survivability Index	Number of capsizes	Progressive cases	Transient cases
Stress-Test (as-built)	7 metres	0.966	34	9	25
	Calm water	0.980	20	0	20
Stress-Test (with solutions)	7 metres	0.980	20	0	20
	Calm water	0.987	13	0	13
SOLAS 2009 assumptions (as-built)	Random up to 4 metres	1	0	0	0

Further to the above, Table 9-9 and Table 9-10 provide a summary of the loss modality specific results in terms of TTC. Here, some interesting observations can be made. Firstly, the AREST A2 barrier system has proven effective at eradicating all progressive flooding scenarios, even under the most adverse conditions conceivable. The implementation of more traditional risk control options in the attempt to improve vessel reliance to transient capsizes, has shown a 30% reduction in the number of cases witnessed and worked to transition a further 25% of cases into progressive flooding loss scenarios. The latter cases are highlighted within the table in blue and there is every reason to assume that these scenarios could be effectively dealt with by implementing further progressive flooding protection in the form of foam barriers.

Table 9-9: Summary of progressive cases with indication of their TTC

9 Progressive capsizes	TTC [s]		Solutions TTC [s]	
	7 metres	Calm water	7 metres	Calm water
DMC156	1317.47	1820	1820	1820
DMC181	1279.09	1820	1820	1820
DMC234	1064.94	1820	1820	1820
DMC275	1671.26	1820	1820	1820
DMC307	1538.76	1820	1820	1820
DMC493	1316.135	1820	1820	1820
DMC625	850.77	1820	1820	1820
DMC815	614.49	1820	1820	1820
DMC980	793.60	1820	1820	1820

Table 9-10: Summary of transient capsize cases, with indication of their TTC

25 Transient capsizes	TTC [s]		Solutions TTC [s]	
	7 metres	Calm water	7 metres	Calm water
DMC02	117.23	124.2	353.2	1820
DMC35	135.69	115.45	119.6	107
DMC77	77.67	87.69	541.2	1820
DMC79	257.19	1820	289.6	1820
DMC130	208.45	179.07	181.4	144
DMC423	68.97	98.27	89.5	265
DMC465	106.44	99.41	192.1	267
DMC515	56.07	1820	1820	1820
DMC521	76.65	78.59	160.3	204
DMC533	146.53	152.9	391.5	1450
DMC606	314.1	1820	720.5	1820
DMC607	74.96	76.57	214.1	1820
DMC616	81.49	80.15	77	84
DMC619	89.44	135.58	257.3	1820
DMC659	119.09	131	329.5	645
DMC697	140.07	160.23	396.8	365
DMC713	46.74	1820	1820	1820
DMC733	91.87	107.4	1820	580
DMC778	331.72	480.93	1820	1820
DMC791	329.41	131.8	235.9	1820
DMC794	71.2	65.69	299.7	1118
DMC798	152.84	1820	1820	1820
DMC843	74.4	78	111.5	169
DMC857	168.51	192.95	468.2	1820
DMC924	59.24	60.92	56.9	67

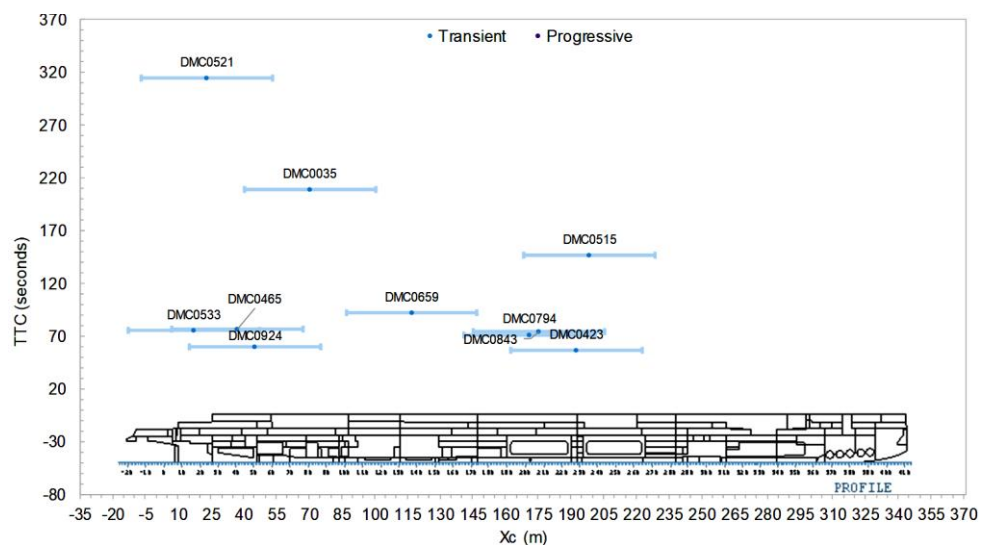


Figure 9-26: Longitudinal damage extent centre (m) and Time To Capsize (seconds) of cases with solutions implemented in calm water simulations.

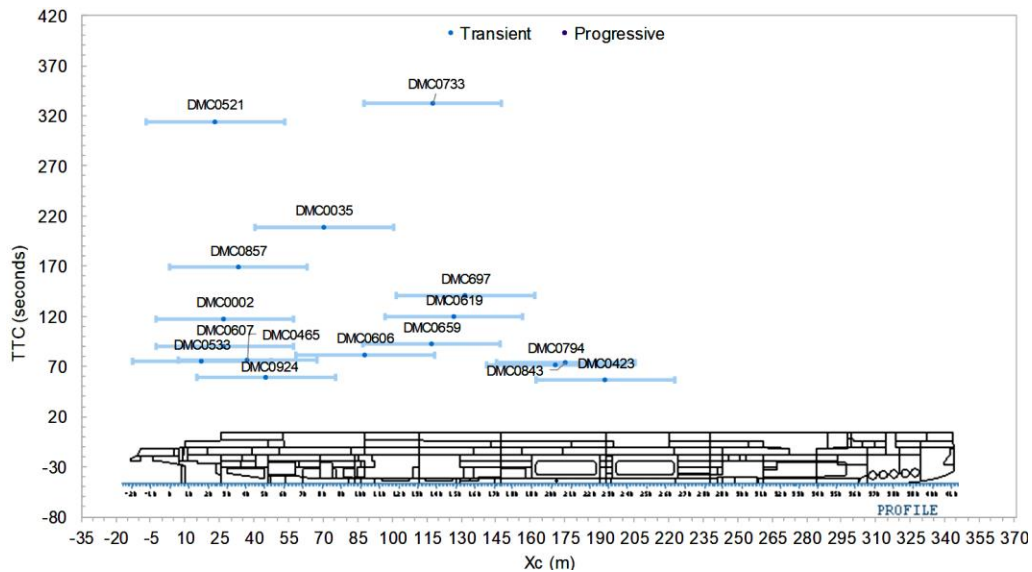


Figure 9-27: Longitudinal damage extent centre (m) and Time To Capsize (seconds) of cases with solutions implemented in $H_s=7m$ simulations.

9.9 Conclusions

In light of the study presented within this Chapter the following conclusions can be drawn:

- When designing and operating a 10,500 PoB cruise vessel it is important to employ a safety platform that goes beyond that which is required by currently in force regulations in order to ensure safety is not compromised.
- This has been achieved by conducting a multi-level assessment of C2, starting firstly with numerical time-domain simulations having been conducted in accordance with statutory assumptions, followed by a progressively more rigorous examination considering the most extreme foreseeable damage scenarios.
- In both assessments, the vessel has proved to have extremely high resilience to the effects of flooding, achieving an Attained Index of 1 according to SOLAS 2009 assumptions and an Attained Index of 0.966 when assessed in accordance with the most arduous assumptions.
- This demonstrates an exceptional level of damage survivability but, given the project in question, it was thought appropriate to adopt a zero-tolerance philosophy and strive to achieve this in a feasible and economically viable way.
- To this end, five foam barriers have been introduced in order to curtail progressive flooding, eradicating all progressive flooding losses even in the most extreme cases.
- In addition, a total of 8 partial bulkheads in combination with the addition of 4 openings to facilitate cross flooding has been shown to mitigate the effects of transient flooding.
- The combination of the aforementioned Risk Control Options for active damage control has seen the vessel Survivability Index rise from 0.966 to 0.987.

Chapter 10: Discussion & Recommendations

10.1 Opening remarks

Based on the work presented in the foregoing and on the research undertaken to develop, present and apply a new methodology for damage stability protection, applicable to all ships, a stage has been reached where feasibility studies on a number of varying ship types and sizes have demonstrated great potential for raising the bar on damage stability protection significantly. In this respect, having delved into this subject for a number of years, it would be of interest to consider again, at the end of the journey, Innovation and Impact of the proposed reconfiguration of the ship environment for damage stability protection, as a starting point for discussion. Both aspects, in turn, depend on the target industry and its history and peculiarities, which will be expanded upon in the light of this research. This will then lead to recommendations on the way forward with the view to consolidating the research findings and institutionalising the developed process, potentially leading to a regulatory framework where the current innovation will form the basis for de-risking ships. These will be considered under a number of headings as outlined next.

10.2 Innovation & Impact

The innovation developed and presented in this research is founded on many years of research at the Department of NAOME at Strathclyde. As such, even though it is difficult to claim that one day I was watching on TV a foam company filling sub-terrain tunnels in the USA, which were used by youth for drug abuse, and I stood up shouting EUREKA, this is not far from the truth. The only difference being that it was my supervisor Professor Vassalos who was running and shouting when he linked the foaming of tunnels to the foaming of ship voids. It was also him who set up a 5-year research project to develop this idea to fruition. In this process, I have taken this idea and developed it into a damage stability protection system, complete with approvals and wide range application. The novelty of the idea in its various AREST systems is unique and its impact immeasurable. Being able to offer cost-effective damage protection for all types of ships is only the beginning and the “small change”. The real benefit will only be realised once a regulatory framework has been set in place that gives credit to active solutions for damage control alongside passive solutions. Indeed, one day we may question the need of bulkheads all together if ship spaces could be protected posteriori. Similarly, we might ask why we are taxing the ship beam to

gain initial stability and paying for this choice over the entire ship life. If all that is needed is good intact stability and marginal damage stability with adequate damage control, subdivision may then be down-rated and ergonomics will take its place with active protection systems on-guard. Ships will look sleek, fuel efficient – hence environmentally friendly, of enhanced functionality because of high ergonomics and unparalleled safety. All the boxes will have been ticked.

10.3 Prevention Vs. Mitigation

Benjamin Franklin once said, “An ounce of prevention is worth a pound of cure” and this has become almost a dogma in most fields of science and engineering. There are, however, two aspects worth considering from a different perspective. The first is residual risk, which for large passenger ships is so excessive that reducing this must be first priority. For example, consider ship C2 in this research, which is a 10,500 People On Board (POB) ship. In the IMO FSA for cruise ships (IMO, 2009), it has been proposed that Risk Control Options for ship safety enhancement will be costed against the propensity of society to spend towards saving one life, which for the western world relates to an upper limit of \$8M. With the A-Index of this ship being approximately 0.9, according to IMO SOLAS 2009 and assuming that collision has taken place, the residual risk is worth €8.4B, a few times over the worth of the ship. The second relates to the feasibility of preventive Vs mitigating measures. For effective preventive measures, we should be searching far into the left of the fault tree, where the emphasis lies on sociotechnical, organisational and cultural matters, which will require long term investment and effort to identify and bring to fruition effective RCOs. Mitigation measures, on the other hand, are linked strongly to technological innovation, where the strength currently lies. Hence, solutions are likely to be of shorter term and, more than likely, cost-effective. Therefore, mitigation still remains a key target.

10.4 Old Ships Vs New Ships

The shipping industry is very old and, consequentially, very traditional. As discussed in the Introduction chapter, damage protection in the form of reconfiguration of the internal ship environment (watertight bulkheads) was the first risk control option proposed in 1854 but it has taken many more accidents and significant loss of life, including the Titanic, for it to be internationally adopted as SOLAS 1929. It is more than likely that the delay was primarily due to the fact that the industry was keenly aware that serving safety will compromise functionality and earnings, ultimately viability of business and this contrast and conflict continues to this day. This is clearly obvious in that new regulations for damage stability apply only to new buildings (Grandfathers Clause). Hence, assuming a 5% constant growth of the industry over the years, this leaves the majority of ships (existing ships) with an inferior damage stability standard and

damage protection, a gap that widens progressively to the extent that SOLAS becomes less and less relevant. The only way that this “landslide” will be arrested is if cost-effective active damage control measures were made available, thus incentivising the industry to adopt these for life-cycle risk management of damage stability. This is what is being offered with the AREST systems covered in this research, which will serve as portals to a transformational change in maritime safety.

10.5 Active Measures Vs Passive Measures for Damage Protection

Active and passive measures for damage control have co-existed almost from the outset. One could imagine that in the absence of decks, old seamen would have had to use buckets, later on pumps and other means to empty floodwater from ship hulls, plug holes with any matter of means, adjust sails and so on. More latterly, safety equipment, LSA, drill teams, Safety Centres, Safety Masters, all active damage protection measures have been progressively introduced, most in the wake of accidents. However, the exact contribution of these measures to safety was never considered, even as a discussion topic, irrespective of how effective these might be as damage protection control options. The dogma that “if it cannot be measured, it cannot be improved” has gone a step further in the maritime industry to become “if it cannot be measured, it cannot be regulated”. Hence, all these options, however cost-effective and safety-effective these might be, are not being considered as a means of damage protection in the same way that passive measures are. For example, for passive protection we have indices of subdivision, indices for damages, indices for survival, indices for everything and for active protection we have nothing. There is some refreshing new ground on passenger evacuation metrics but this is still highly general (some say arbitrary) and incomplete. Novel Technology Qualification (risk assessing and de-risking the novelty), offers a portal for introducing active means of damage protection and modern tools offer enhanced capability to estimate flooding risk over the life cycle, even live on-board ships, as indicated in the foregoing. This is the requisite platform to facilitate change and as discussed in the Introduction Chapter, project FLARE will facilitate a systematic and structured way to account for such developments. This, in turn, will change the maritime safety agenda and its evolution.

10.6 Life-Cycle Risk Management and Safety Culture

Decisions made during the design phase, shape safety over the whole life cycle. In this respect, use of advanced tools and exploiting knowledge in all forms at the design stage is most effective and, hence, highly desirable. As such, the methodology, tools and processes described in the foregoing provide the right platform to achieve this for effective damage protection and control. Key to life-cycle flooding risk management is the understanding that both the operational phase (monitoring and management of residual risk) as well as emergencies (emergency response) depend crucially on having identified during the design phase pertinent design vulnerabilities. This then leads to the identification of critical accident scenarios in pre-specified loading and environmental conditions and, on the basis of this, having taken appropriate measures to ensure damage protection and control to adopted tolerable levels. The AREST systems presented in this thesis have been developed with this in mind and on the basis of understanding the forensic detail of design vulnerabilities for damage stability and the ensuing behaviour of ships in extreme damage conditions, pertinent to the ships being built and operated today. In addition, offering the industry a cost-effective means for flooding risk reduction and control will incentivise adoption of higher safety standards, thus providing a mechanism to fuel continuous improvement.

10.7 Recommendations for Future Research

Plato's "circle of knowledge" was built on Socrates idea, which loosely translated, means that only with knowledge can one appreciate ignorance. In this respect, it is almost dogmatic that at the end of a research cycle, more research should be envisioned. I am glad to realise that the same applies to my research. Key among these include the following:

10.7.1 Life-Cycle Flooding Risk-Based Regulatory Framework

Utilising the IMO probabilistic damage stability framework, the provisions for AD&A and Goal-Based Standards and the Safety-Level Approach, a Life-Cycle Flooding Risk-Based Regulatory Framework will enable and support a continuous evolution of regulations. This, in turn, will ensure that the risk level is ALARP (As Low As Reasonably Practicable) whilst providing a sound platform for benchmarking alternative/novel ship and system designs and operating procedures for new and existing ships. To this end, a fundamental prerequisite is that pertinent risks need to be quantified, in many cases almost in real time throughout the life cycle of the ship, from design and daily operation to crisis situations. To this end, there is a clear need for more holistic consideration of measures mitigating flooding risk, namely active as well as passive measures of

flooding protection, in a way that every measure is assigned a risk metric and is accounted for in such risk assessment. This will provide maritime industry with more flexibility to achieve compliance with IMO safety requirements, and hence the mechanism for continuous safety improvement.

10.7.2 Formalisation of the Process for Damage Stability Assessment, Protection and control

Much of what has been presented in this thesis, pertaining to damage stability and survivability assessment and control is linked to research performed, almost exclusively, at Strathclyde University over the past few decades. As such, changing the safety agenda of the maritime industry would necessitate steps to formalise this process following the normal channels of class and administration approvals and subsequent submission to IMO. This could then render the proposed solutions for damage stability protection and control IMO and Administration-approved RCOs, whilst promoting and facilitating the introduction of such measures to the wider maritime industry.

10.7.3 Institutionalisation of the Method, Process, Tools and RCOs

Similar effort needs to be expended towards validation and verification of the requisite methodology, process, tools and RCOs to facilitate progressive institutionalisation in the maritime industry and ultimately integration on daily design work and in operation. A rigorous attempt in this direction is being led and supported by the EU Project FLARE, where most of these elements are being tackled. However, continuous effort in this direction is still warranted, particularly as rapid technological change will render any existing gaps wider and more difficult to fill.

Chapter 11: Concluding Remarks

Based on the work presented in this thesis, the first overarching conclusion will have to refer to the unsinkable ship aspiration. While sceptics will always occupy a corner of the human normality spectrum and some will argue that if there is enough knowledge and wisdom to engineer an unsinkable ship, by definition, the same ingenuity and wisdom will find ways to sink it, hence negate this concept. However, in most engineering problems that have been approached methodologically, we lay down a claim (unsinkable ship), we develop an argument (reconfiguration-based flooding protection; resilience) and we produce evidence (feasibility studies and implementation examples). It can be concluded, therefore, that in principle and in so far as damage stability is concerned, we can design and operate ships within a defined tolerable risk level, commensurable with modern societal expectations, however high these might be.

In pursuing the development, execution and validation of the aforementioned argument, considerable in-depth work has been undertaken, mostly innovative, with potential for immeasurable impact that is yet to be delivered, leading to the following specific conclusions:

- Damage stability continues to be the highest risk contributor with serious implications, particularly for the giants of passenger ships being currently designed and built. This serious limitation is the product of traditional myopia in the maritime industry where emphasis on passive damage protection and control has deprived the industry of technological innovation and capability for active measures and intervention, thus stifling any real improvement on raising damage stability standards, commensurate with expectations of modern society.
- This necessitates and nurtures the development of innovative solutions based on technological advances but also a shakeup of the shackles of tradition in the maritime industry where the regulatory environment encourages and supports only passive damage stability protection (mainly reconfiguration of the internal ship space through subdivision), which can offer no more gains.
- Deviating from tradition by embracing a completely novel solution to reconfiguring the ship environment, namely the use of high expansion foam products to offer a combination of passive and active damage protection, delivers a pragmatic way to address the gaps identified through the critical review, thus offering a way forward for de-risking ships from damage stability problems, embedded in any ship design.
- A methodological approach has been developed and presented, enabling forensic examination of any ship in any conceivable scenario and by addressing flooding evolution and impact on ship stability systematically, targeted active and passive flooding protection

and control measures have been developed and implemented, demonstrating capability for de-risking ships in any probable flooding scenario in a cost-effective and safety efficient manner.

- Implantation of specifically designed flooding protection systems to a high TRL level, on a number of cruise ships and RoPax has demonstrated impressive capability for flooding protection, raising damage stability standards to unparalleled levels, destined to create a stair in the maritime industry but also to incentivise all stakeholders for a new beginning and an open-minded approach to improving maritime safety, accounting for all passive and active means of damage protection and control.
- In the maritime industry, everything starts with the ship owner and this is where the onus lies for any significant change in the status quo. Then comes IMO, Flag States and Port-State Control. Accounting for this, large-scale research projects are in place with all the key stakeholders actively engaged to create a new normal in maritime safety with safety being addressed by all manner of means and with credit being assigned to all such contributions.

Bibliography

- Allianz. (2019). *Safety and Shipping*. Munich, Germany: Allianz.
- Allianz. (2020). *Safety and Shipping Review*. Munich, Germany: Allianz.
- Amdahl, J. (1982). Energy absorption in ship-platform impacts, Doctoral thesis. *Norwegian Institute of Technology*.
- AMSA. (2011). *National Standard for Commercial Vessels, Part C Design & Construction, Section 6B, Buoyancy and Stability After Flooding*. Canberra: Australian Maritime Safety Authority.
- Atzampos, G. (2019). Atzampos, G: "A Holistic Approach to Damage Survivability Assessment of Large Passenger Ships", PhD Thesis. *University of Strathclyde, Department of Naval Architecture, Ocean and Marine Engineering*.
- Bae, E., Vassalos, D., & Boulougouris, E. (2020). Methodology in Risk-Based Crashworthiness to improve Ship Survivability in a Seaway. *5th International Conference on Ships and Offshore Structures, ICSOS*. Glasgow, UK.
- Bird, H., & Browne, R. (1973). Damage Stability Model Experiments. *Transactions of the Royal Institute of Naval Architects, Vol. 116*, 69-91.
- Bouger, P. (1746). *Traité du Navire, de sa Construction et de ses Mouvements*. Paris.
- Bulian, G., Cardinale, M., Francescutto, A., & Zaraphonitis, G. (2019). Complementing SOLAS damage ship stability framework with a probabilistic description for the extent of collision damage below the waterline. *Ocean Engineering, Vol 186*.
- Champion, J., Ahola, M., & Kujala, P. (2015). Outlining a Provident Initial Design Approach with regard to Cruise Ship Conversions. *12th International Marine Design Conference*, (pp. 235-246). Tokyo, Japan.
- Cichowicz, J., Olufsen, O., & Vassalos, D. (2019). Ro-Ro passenger ships – from Stockholm Agreement to SOLAS2020. *Proceedings of the 17th International Ship Stability Workshop* (pp. 199-207). Helsinki, Finland: STAB.
- Cichowicz, J., Tsakalakis, N., Vassalos, D., & Jasionowski, A. (2016). Damage survivability of passenger ships - Re-engineering the safety factor. *MDPI*.
- D. Vassalos. (2012). Damage Stability of Passenger Ships- Notions and Truths. *Proceedings of the 11th International Conference on the Stability of Ships and Ocean Vehicles*. Athens, Greece.
- Dafermos, G., & Papanikolaou, A. (2016). On the Survivability of RoPax and Cruise Ships a new approach to differences in design. *Proceedings of the 6th Int. Conference on Design for Safety, Hamburg*.
- DNVGL. (2015). *Technology Qualification Management and Verification - DNVGL-SE-0160*. DNVGL.
- Dvoretzky, A., Kiefer, J., & Wolfowitz, J. (1956). Asymptotic Minimax Character of the Sample Distribution Function and of the Classical Multinomial Estimator. *Annals of Mathematical Statistics*, 642-669.

- Ehlers, S., Broekhuijsen, J., Alsos, H., Biehl, F., & Tabri, K. (2008). Simulating the collision response of ship side structures: a failure criteria benchmark study. *International Shipbuilding Progress*, 55(1/2), 127–144.
- EMSA. (2014). *Risk Level and Acceptance Criteria for Passenger Ships. First interim report, part 1: Risk Level of current fleet*. European Maritime Safety Agency.
- EMSA. (2015). *Evaluation of risk from raking damage due to grounding, Report No.2015-0168, Rev. 2*.
- EMSA II. (2009-2012). Study of the specific damage stability parameters of Ro-Ro passenger vessels according to SOLAS 2009, including water on deck calculation. EC.
- EMSA III. (2013-2015). Study to Assess Acceptable and Practicable Risk Levels for Damage Stability of Passenger Ships. EC.
- eSAFE. (2017-2019). *Damage Stability of Cruise Ships, Joint Industry Project*. Cruise Ship Safety Forum.
- EU-DGMOVE. (2019). *Assessment of Specific EU Stability Requirements for Ro-Ro Passenger Ships*.
- Euler, L. (1749). *Scientia Navalis seu Tractatus de Construendis ac Dirigendis Navibus*. St. Petersburg, Russia.
- FLARE. (2019-2022). *Flooding Accident Response*. EU H2020 – MG2.2 .
- Francescutto, A., & Papanikolaou, A. (2010). Babylonian. *Proceedings of the Institution of Mechanical Engineers, Vol.255, Part M*, 17-32.
- G. Atwood, M. d. (1798). *Scientia Navalis seu Tractatus de Construendis ac Dirigendis Navibus*. In RINA, *Philosophical Transactions of the Royal Society of London, Vol.88* (pp. 6-310). London.
- Gale, P. (2013). The Ship Design Process. In T. Lamb, *Ship Design and Construction*. SNAME.
- GOALDS. (2009-2012). Goal-Based Damage Stability of Passenger Ships. *DG Research, EU*.
- Graaf, B. V., Vredeveltdt, J., & Broekhuijsen, J. (2004). Construction aspects for the Schelde Y-shape crashworthy hull structure. *Proceedings of the Third International Conference on Collision and Grounding of Ships*, (pp. 229-233). Izu, Japan.
- Guarin, L., Majumder, J., R. Pusia, A. J., & Vassalos, D. (2007). Design for Fire Safety. *Proceedings of the 3rd International Conference on Design for Safety*. San Francisco, USA.
- HARDER. (1999-2003). *Harmonisation of Rules and Design Rationale*. European Commission, DG XII-BRITE.
- HARDER. (2003). *"Harmonisation of Rules and Design Rationale": Final Technical Report*. EC Contract No. GDRB-CT-1998-00028.
- Heath, T. (2002). *"The Works of Archimedes"*. New York, USA: Dover Publications.
- Hollenbach, U., Klug, H., & Mewis, F. (2007). Container Vessels - Potential for Improvements in Hydrodynamic Performance. *Proc. 10th International Symposium on Practical Design of Ships and Other Floating Structures*. Houston, Texas, USA.

- Horst, N. (2007). *Leonard Euler And The Theory Of Ships*. Michigan, USA: Michigan College of Engineering, Department of Naval Architecture and Marine Engineering.
- Hoste, P. (1697). *Théorie de la construction des vaisseaux ("Theory of Ship Construction")*. Lyon, France: Arisson & Posule.
- Hutchinson, K. W., & Scott, A. L. (2016). Passenger Ro-Ro Ferry Damage Stability: Status and Development of International Regulations. *Design & Operation of Ferries & Ro-Pax Vessels* (pp. 67-78). London, UK: RINA.
- ICAS. (2001). *No.34 Standard Wave Data, Corr. Nov 2001*.
- IMO. (2006). *Guidelines on Alternative Designs and Arrangements for SOLAS, Chapter II-1 & III, MSC/Circ.1212*. London: IMO.
- IMO. (2006). *MSC 82/24/Add.1, Adoption of amendments to the International Convention for the safety of life at sea, 1974, Res MSC.216(82)*.
- IMO. (2007). *MSC.1/Circ.1238, Guidelines for Evacuation Analysis for New and Existing Passenger Ships*. London: IMO.
- IMO. (2009). *FSA Cruise Ships, IMO MSC.85. Denmark*.
- IMO. (2013). *Guidelines for the Approval of Alternatives and Equivalent for SOLAS Chapters II-1 and III, MSC.1/Circ. 1455*.
- IMO. (2017). *Resolution MSC.429(98) Revised Explanatory Notes to the SOLAS Chapter II-1 Subdivision and Damage Stability Regulations*. Maritime Safety Committee.
- IMO. (2018). *Revised Guidelines for Formal Safety Assessment for the use in the IMO Rule-making Process - MSC-MEPC.2/Circ, 12/Rev.2*. London: IMO.
- IMO. (June 2006). *Resolution MSC.216(82), Amendments to the international convention for the Safety Of Life At Sea 1974*. London: International Maritime Organisation.
- Jasionowski, A. (2005). "Survival Criteria for Large Passenger Ships", Final Report, Safety at Sea Ltd. *SAFENVSHIP Project*.
- Jasionowski, A. (2011). Decision support for ship flooding crisis management. *Ocean engineering*, 38, 1568-1581.
- Jasionowski, A., & Vassalos, D. (2001). "Benchmark Study on the Capsizing of a Damaged Ro-Ro Passenger Ship in Waves", Final Report to the ITTC Specialist Committee on the Prediction of Extreme Motions & Capsizing.
- Jasionowski, A., & Vassalos, D. (2001). Numerical Modelling of Damage Ship Stability in Waves. *Proceedings of the 5th International Workshop on Stability and Operational Safety of Ships*, (p. 9). Trieste, Italy.
- Journee, J., Vermeer, H., & Vredeveltdt, A. (1997). Systematic Model Experiments of Flooding of Two Ro-Ro Vessels. *Proceedings of the 6th International Conference on Stability of Ships and Ocean Vehicles*, (pp. 22-27). Varna, Bulgaria.

- Khaddaj-Mallat, C., Rousset, J., & Ferrant, P. (2009). On Factors Affecting the Transient and Progressive Flooding Stages of Damaged Ro-Ro Vessels. *10th International Conference on Stability of Ships and Ocean Vehicles*, (pp. 295-306). St Petersburg, Russian Federation.
- King, J. (1998). Origins of the theory of ship stability. *The Royal Institute of Naval Architects*.
- Kitamura, O. (1997). Comparative study on collision resistance of side structure. *Marine Technology and SNAME News*, Vol 34.
- Kitamura, O. (2001). FEM approach to simulate of collision and grounding damage. *Proceedings of the second international conference on collision and grounding of the ships*. Copenhagen, Denmark.
- Klanac, A. (2011). *Design Methods for Safe Ship Structures*. Aalto, Finland: Aalto University.
- Klanac, A., Ehlers, S., Tabri, K., Rudan, S., & Broekhuijsen, J. (2005). Qualitative design assessment of crashworthy structures. *Proceedings of the International Maritime Association of Mediterranean*, (pp. 461-469). Lisbon, Portugal.
- Kulovaara, H. (2015). Safety & Stability through Innovation in Cruise Ship Design. *Proceedings of the 12th International Conference on the Stability of Ships and Ocean Vehicles*, (pp. 3-14). Glasgow, UK.
- Lancaster, J. (1997). *Engineering Catastrophes: Causes and Effects of Major Accidents*. Abington: Woodhead Publishing.
- Lehmann, E., & Peschmann, J. (2002). Energy absorption by the steel structure of ships in the event of collision. *Marine Structures*, Vol. 15, 429-441.
- Letizia, L. (1996). *Damage Survivability of Passenger Ships in a Seaway*, PhD thesis. University of Strathclyde.
- Lloyds Register Foundation. (2018). *Insight Report on Safety in the Passenger Ferry Industry - A Global Safety Challenge*. LR.
- Ludolphy, J., & Boon, B. (2000). Collision resistant side shell structures for ships. *Proceedings of the Int Maritime Design Conference*. Kyongju, South Korea.
- Lützen, M. (2001). Ship collision damage, Doctoral thesis. *Technical University of Denmark, Department of Mechanical Engineering*.
- Maritime UK. (2016). *The UK's Global Maritime Professional Services: Contribution and Trends*. London: The City of London Corporation.
- McDermott, J. F., & R. G. Kline, E. L. (1974). Tanker structural analysis for minor collisions. *SNAME Transactions*, Vol. 82, 382-414.
- Meng, Q., Weng, J., & Suyi, L. (2014). Analysis with Automatic Identification System Data of Vessel Traffic Characteristics in the Singapore Strait. *Transport Research Record: Journal of the Transportation Research Board*, No. 2426, 33-43.
- Minorsky, V. (1959). An analysis of ship collision with reference to protection of nuclear power ships. *Journal of Ship Research*, 208-214.
- Misra, S. (2016). *Design Principles of Ship and Marine Structures*. Taylor and Francis Group.

- Naar, H., Kujala, P., Simonsen, B., & Ludolphy, H. (2002). Comparison of the crashworthiness of various bottom and side structures. *Marine Structures, Vol 15*, 443-460.
- NEREUS. (1999-2002). "First-Principles Design for Damage Resistance against Capsize". *EC Project CONTRACT No. G3RD-CT 1999-00029*.
- Paik, J. (2007). Practical techniques for finite element modeling to simulate structural crashworthiness in ship collisions and grounding Ships and Offshore Structures. *Ships and Offshore Structures*, 69-80.
- Paik, J. (2020). *Advanced Structural Safety Studies*. Springer.
- Papanikolaou, A., Hamann, R., Lee, B. S., Mains, C., Olufsen, O., Vassalos, D., & Zaraphonitis, G. (2013). GOALDS—Goal Based Damage Ship Stability and safety standard. *Accident Analysis & Prevention*, 353-365.
- Papanikolaou, A., Zaraphonitis, G., & Vassalos, D. (2010). GOALDS - Goal Based Damage Stability. *Proceedings of the 11th International Ship Stability Workshop*. Wageningen, The Netherlands: STAB.
- Papanikolaou, A., Zaraphonitis, G., Spanos, D., Boulougouris, E., & Eliopoulou, E. (2000). Investigation into the Capsizing of Damaged Ro-Ro Passenger Ships in Waves. *Proceedings of the 7th International Conference on Stability of Ships and Ocean*, (pp. 351-362). Launceston, Tasmania, Australia.
- Pedersen, P. T., & Zhang, S. (2000). Absorbed energy in ship collisions and grounding: Revising Minorsky's empirical method. *Journal of Ship Research*, 140-154.
- R. Ball, C. C. (1994). Establishing the fundamentals for a surface ship survivability design discipline. *Naval Engineering Journal*, 106(1), 71-74.
- R. Pusia, A. M. (2012). Design Customisation and Optimisation through Effective Design Space Exploration. *International Marine Design Conference IMDC*. Glasgow, UK.
- R. Van't Veer, J. d. (2004). Large Passenger Ship Safety: Time-to-Flood Simulations. *Marine Technology and SNAME News, Vol 41, No.2*, 82-88.
- Rahola, J. (1939). The Judging of the Stability of Ships and the Determination of the Minimum Amount of Stability. *Doctoral Thesis, The University of Finland*.
- ROROPROB. (1999-2002). "Probabilistic Rules-Based Optimal Design for Ro-Ro Passenger Ships". *EU FP5 RTD Project G3RD-CT-2000-00030*.
- ROROPROB. (1999-2002). Probabilistic Rules-Based Optimal Design for Ro-Ro Passenger Ships". *EU FP5 RTD Project G3RD-CT-2000-00030*.
- Ruponen, P. (2007). *Progressive Flooding of a Damaged Passenger Ship - Doctoral Dissertation*. Espoo, Finland: Helsinki University of Technology.
- Ruponen, P., & Routi, A. (2011). *FLOODSTAND D2.2b Guidelines and criteria on leakage occurrence modelling*. NAPA.
- Rusaas, S. (1996). A New Damage Stability Framework Based Upon Probabilistic Methods. *Intl Seminar on the Safety of Passenger Ro-Ro Vessels, Presenting the Results of the Northwest European Research & Development Project* (pp. 21-24). London: RINA.

- S McCartan, T. T. (2015). Design-Driven Innovation: A New Design Meaning for Superyachts as a Less Egocentric User Experience. *Marine Design Conference*. London, UK: The Royal Institution of Naval Architects.
- SAFEDOR. (2005-2009). Design, Operation and Regulation for Safety. *Integrated Project, FP6_2 Contract TIP4-CT-2005-516278*.
- SAFEMODE. (2019-2022). Strengthening synergies between Aviation and maritime in the area of human Factors towards achieving more Efficient and resilient MODE of transportation. *EU H2020, Grant agreement ID: 814961*.
- SAFEPASS. (2018-2020). Next generation of life Saving appliances and systems for saFE and swift evacuation operations on high capacity PASSenger ships in extreme scenarios and conditions 815146 - SafePASS. *H2020-MG-2018-2019-2020/H2020-MG-2018*.
- Sames, P. C. (2009). Introduction to Risk-Based Approaches in the Maritime Industry. In A. D. Papanikolaou, *Risk-Based Ship Design* (pp. 1-15). Berlin: Springer.
- Spouge, J. (1989). The safety of Ro-Ro Passenger Ferries. *Transactions of the Royal Institution of Naval Architects*, 27-32.
- Spouge, J. R. (1986). The technical investigation of the sinking of the Ro-Ro ferry European Gateway. *Transactions of the Royal Institute of Naval Architects*, 128, 49-72.
- Storheim, M., & Amdahl, J. (2014). Design of offshore structures against accidental ship collisions. *Marine Structures, Vol. 37*, 135-172.
- T. E. Svensen, D. V. (1998). Safety of Passenger/RoRo Vessels: Lessons Learnt from the NWE R&D Project. *Journal of Marine Technology, Vol. 35, No.4*, 191-200.
- Tobias King, C. V. (2016). Stability barrier management for large passenger ships. *Ocean Engineering*, 342-358.
- Turan, O., & Vassalos, D. (1994). A realistic approach to assessing the damage survivability of passenger ships. *Transactions of Society of Naval Architects and Marine Engineers, Vol 102*, (pp. 367-394).
- Tuzcu, C. (2003). A Performance-Based Assessment of the Survival of Damaged Ships: Final Outcome of the EU Research Project HARDER. *Marine Technology, 40(4)*, 288-295.
- Tuzcu, C., & Tagg, R. (2002). A Performance-based Assessment of the Survival of Damaged Ships - Final Outcome of the EU Research Project HARDER. *Proceedings of the 6th International Ship Stability Workshop*. New York, USA.
- UNCTAD. (2017). *Structure, Ownership and Registration of the World Fleet*. United Nations Conference on Trade and Development.
- USCG, D. (2012). *Code of Federal Regulations, Subchapter S - Subdivision and Stability*. United States Government Printing Office.
- Vassalos, D. (1999). Shaping ship safety: the face of the future. *Marine Technology, Vol. 36, No.2*, 61-74.

- Vassalos, D. (2004). A risk-based approach to probabilistic damage stability. *Proceedings of the 7th International Workshop on the Stability and Operational Safety of Ships*, (pp. 1-12). Shanghai, China.
- Vassalos, D. (2008). Chapter 2: Risk-Based Ship Design - Methods, Tools and Applications. In A. Papanikolaou, *Risk-Based Ship Design* (pp. 17-98). Springer.
- Vassalos, D. (2012). Design for Safety, Risk-Based Design, Life-Cycle Risk Management. *The 11th International Marine Design Conference* (p. Keynote Address). Glasgow, UK: IMDC.
- Vassalos, D. (2013). Damage stability and survivability – ‘nailing’ passenger ship safety problems. *Ships and Offshore Structures*.
- Vassalos, D. (2016). Damage survivability of cruise ships - Evidence and conjecture. *Ocean Engineering*, 89-97.
- Vassalos, D. (2016). Damage Survivability of Cruise Ships – Evidence and Conjecture. *Ocean Engineering Vol.121*, 89-978.
- Vassalos, D., & Guarin, L. (2009). Designing for Damage Stability and Survivability - Contemporary Developments and Implementation. *1st International Ship Design and Naval Engineering Congress*, (pp. 25-27). Cartagena Colombia.
- Vassalos, D., & Jasionowski, A. (2011). Chapter 6: SOLAS 2009 – Raising the Alarm . In M. Neves, *Contemporary Ideas on Ship Stability and Capsizing in Waves*. Springer.
- Vassalos, D., & Jasionowski, A. (2011). SOLAS 2009 - Raising the Alarm. In *Contemporary Ideas on Ship Stability* (p. Chapter 6). Springer.
- Vassalos, D., & Letizia, L. (1995). Formulation of a non-linear mathematical model for a damaged ship subjected to flooding. *Proceedings of Sevastianov Symposium*. Kliningrad, Russia.
- Vassalos, D., & Papanikolaou, A. (2002). Stockholm Agreement - Past, Present and Future. *Journal of Marine Technology*, Vol. 39, No.3, 137-158.
- Vassalos, D., & Papanikolaou, A. (2018). A holistic view of Design for Safety. *Proceedings of the 7th International Maritime Safety Conference on Design for Safety*. Kobe, Japan.
- Vassalos, D., & Paterson, D. (2020). If you doubt the value of safety, try an accident. *Damaged Ship V Conference*. London, UK: RINA.
- Vassalos, D., & Turan, O. (1992). *Development of Survival Criteria for Ro-Ro Passenger Ships - A Theoretical Approach, Final Report on the SOT Damage Stability Programme*. Glasgow, UK: University of Strathclyde.
- Vassalos, D., Atzampos, G., Cichowicz, J., & Paterson, D. (2018). Life-Cycle Flooding Risk Management of Passenger Ships. *13th International Conference on the Stability of Ships and Ocean Vehicles*, (pp. 648-662). Kobe, Japan.
- Vassalos, D., Ikeda, Y., Jasionowski, A., & Kuroda, T. (2004). Transient Flooding on Large Passenger Ships. *Proceedings of the 7th International Ship Stability Workshop*. Shanghai, China.
- Vassalos, D., Jasionowski, A., & Guarin, L. (2005). Passenger Ship Safety - Science Paving the Way. *Proceedings of the 8th International Ship Stability Workshop*. Istanbul, Turkey.

- Vassalos, D., Jasionowski, A., & Guarin, L. (2005). Passenger Ship Safety - Science Paving the Way. *Proceedings of the 8th International Ship Stability Workshop*. Istanbul, Turkey.
- Vassalos, D., Jasionowski, A., York, A., & Tsaklakis, N. (2008). SOLAS '90, Stockholm Agreement, SOLAS 2009 – The False Theory of Oranges and Lemons. *Proceedings of the 10th International Stability Workshop*. Daejeon, Korea.
- Vassalos, D., Paterson, D., & Boulougouris, E. (2019). Water, Water Everywhere: Can High Expansion Foam Significantly Reduce Vessel Flooding Risk? *Marine Technology*, 42-49.
- Vassalos, D., Turan, O., & Pawlowski, M. (1997). Dynamic Stability Assessment of Damaged Passenger/Ro-Ro Ships and Proposal of Rational Survival Criteria. *Marine Technology*, Vol. 34, 241-266.
- Vassalos, D., York, A., Jasionowski, A., Kanerva, M., & Scott, A. (2006). Harmonised Damage Stability Regulations. *Proceedings of the 9th International Conference on Stability of Ships and Ocean Vehicles*. Rio de Janeiro, Brazil.
- Vie, R. (2014). The Design and Construction of a Modern Cruise Vessel. *IMAREST President's Day Lecture*.
- Vredeveltdt, A. W., & Journee, J. M. (1991). Roll motions of ships due to sudden water ingress, calculations and experiments. *RINA International Conference on Ro-Ro Safety and Vulnerability*. London, UK.
- Wang, B., & H. C. Yu, R. B. (2008). Ship and ice collision modeling and strength evaluation of LNG ship structure. *ASME, 27th International Conference on Offshore Mechanics and Arctic Engineering*.
- Wendel, K. (1960). Die Wahrscheinlichkeit des Uberstehens von Verletzungen. *Schiffstechnik*, Vol.7, No.36, 47-61.
- Wendel, K. (1968). Subdivision of Ships. *Proceedings, 1968 Diamond Jubilee International Meeting – 75th Anniversary* (p. Paper 12). New York, USA: SNAME.
- Wierzbicki, T., & Abramowicz, W. (1983). On the crushing mechanics of thin-walled structures. *Journal of Applied Mechanics*, 727-734.
- Wilson, P. (2018). *Basic Naval Architecture*. Springer.
- Woisin, G. (1979). Design against collision. *Proceedings of the International Symposium on Advances in Marine Technology*, 309-336.
- Womack, J. (2002). Small Commercial Fishing Vessel Stability Analysis Where Are We Now? Where Are We Going? *Proceedings of the 6th International Ship Stability Workshop*. New York, USA.
- Zaraphonitis, G., Papanikolaou, A., & Spanos, D. (1997). On a 3D Mathematical Model of the Damage Stability of Ships in Waves. *Proceedings of the 6th International Conference on Stability of Ships and Ocean Vehicles*, (pp. 233-239). Varna, Bulgaria.

Appendix A: Interpretation of Results

This Appendix provides information on how the results presented in the following Appendices should be interpreted.

Maximum values:

Maximum roll angle – maximum (in terms of magnitude) roll angle recorded during the simulations, in degrees

Maximum average heel over 3-minutes interval – maximum (in terms of magnitude) average heel recorded during any 3-minutes interval, in degrees (time of the maximum heel plotted on the graph corresponds to the beginning of the interval)

Maximum floodwater mass – maximum amount of floodwater recorded during the simulations, in metric tons

Final average values

Final average value – average of a specific quantity (sinkage, heel, pitch, floodwater mass, upper envelope of the floodwater mass) over the final 180 seconds of the simulations

The final envelope of floodwater mass is a curve constructed to detect progressive flooding. The curve is defined as shown here

$$m_{flev}(t_i) = \max \{m_{flev}(t_{i-1}), m_{fl}(t_i)\} \quad \text{Eq. A-1}$$

Where m_{fl} is a time history of floodwater accumulation and m_{flev} is the upper envelope.

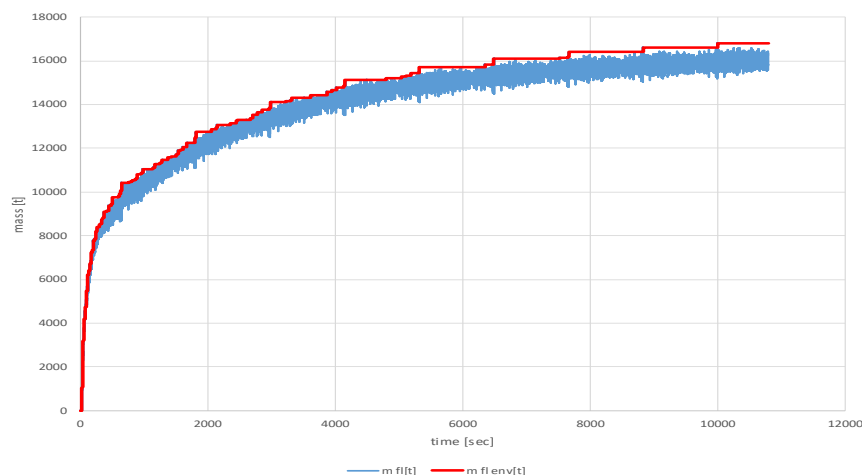


Figure A-1: Sample time history of floodwater accumulation and its upper envelope as defined by equation (Eq. A-1)

Final rates of changes

Final rate of change – the slope of the regression line obtained during the final 180 seconds of time history of the specific quantity (sinkage, heel, pitch, floodwater mass, upper envelope of the floodwater mass).

Final rates of change are linear trends that may help to identify cases, which might capsize/sink for longer simulation times.

Appendix B: R1 Simulation Results

This appendix provides detailed simulation results pertaining to the RoPax case study presented within Chapter 7. Here, details are provided in relation to the vessel floating position, motions and floodwater accumulation in each simulated case. Furthermore, these are viewed in relation to the maximum values recorded over the duration of each simulation which are followed by values recorded during the final stage.

Maximum Values

Here, the peak values realised within each simulated case are presented with respect to roll angle, average heel recorded over 3 minutes, and the maximum floodwater accumulated.

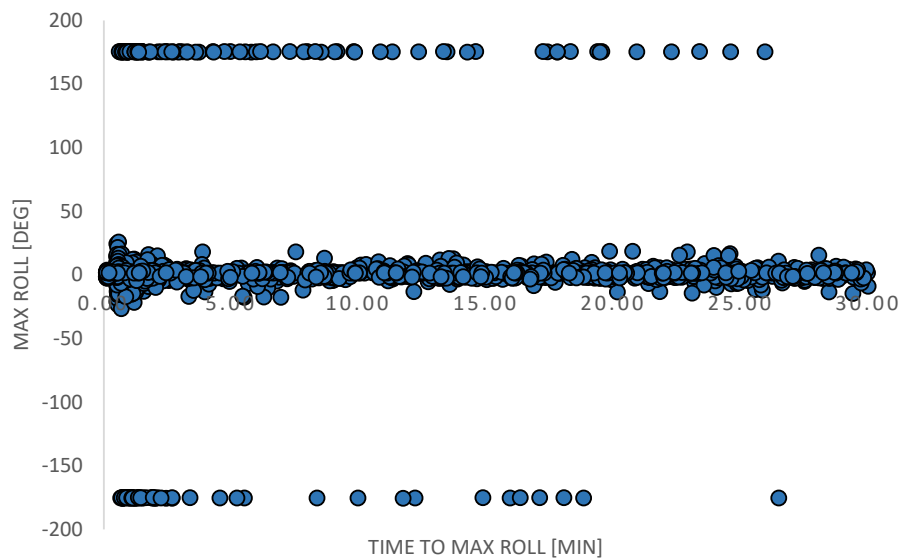


Figure B1: Occurrence of maximum roll angles

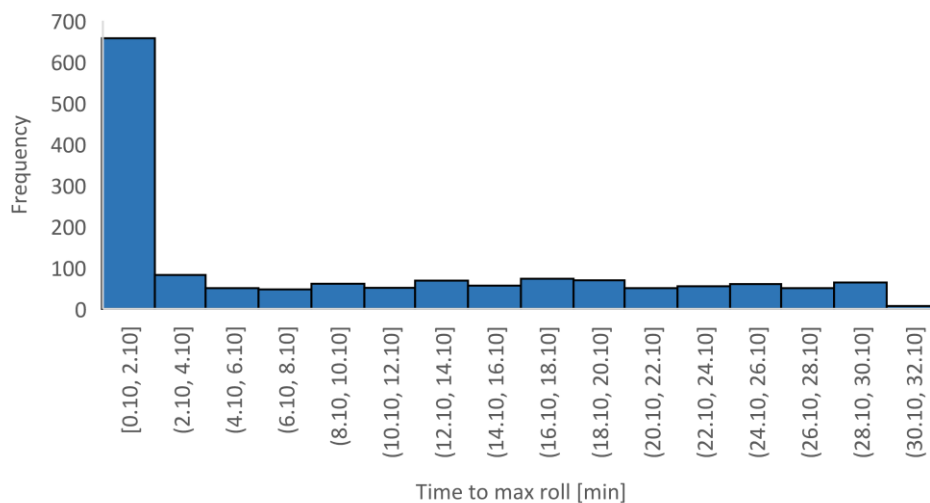


Figure B2: Distribution of times of occurrence of maximum roll angles

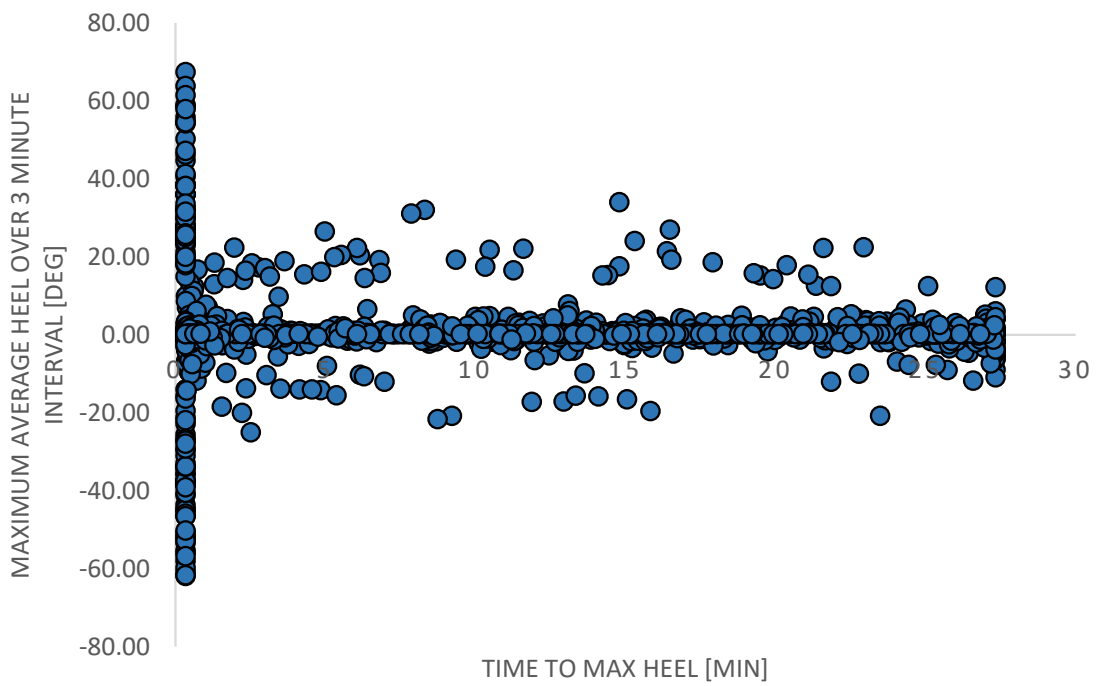


Figure B3: Occurrence of maximum 3-minute averages of heel angle

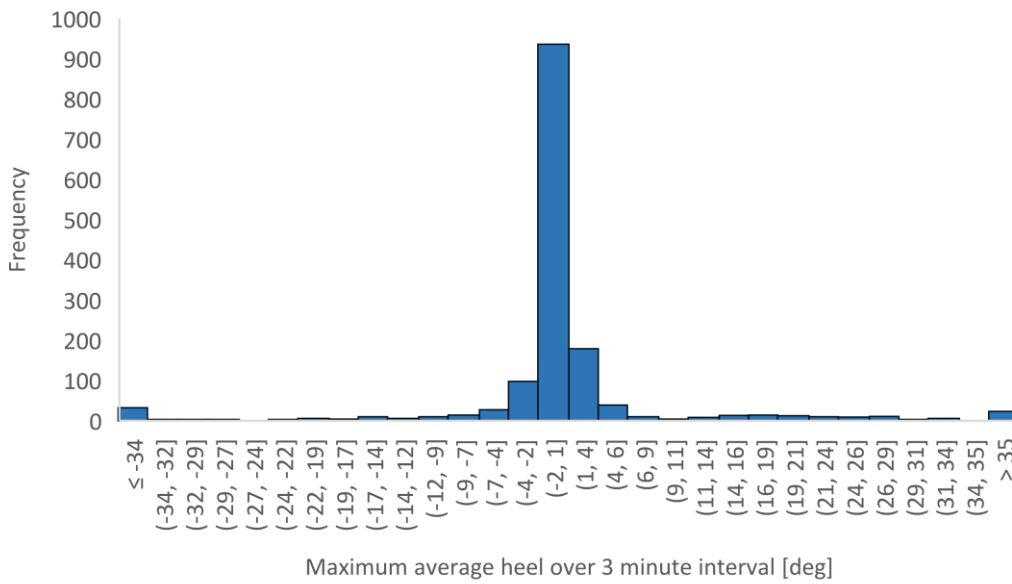


Figure B4: Distribution of maximum 3-minute averages of heel angles

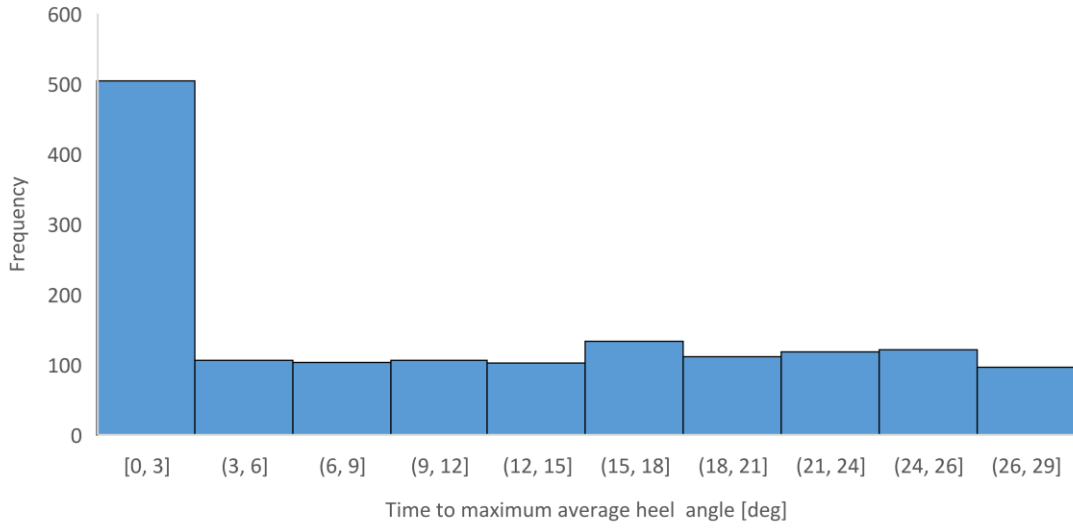


Figure B5: Distribution of time of occurrence of maximum 3-minute averages of heel angles

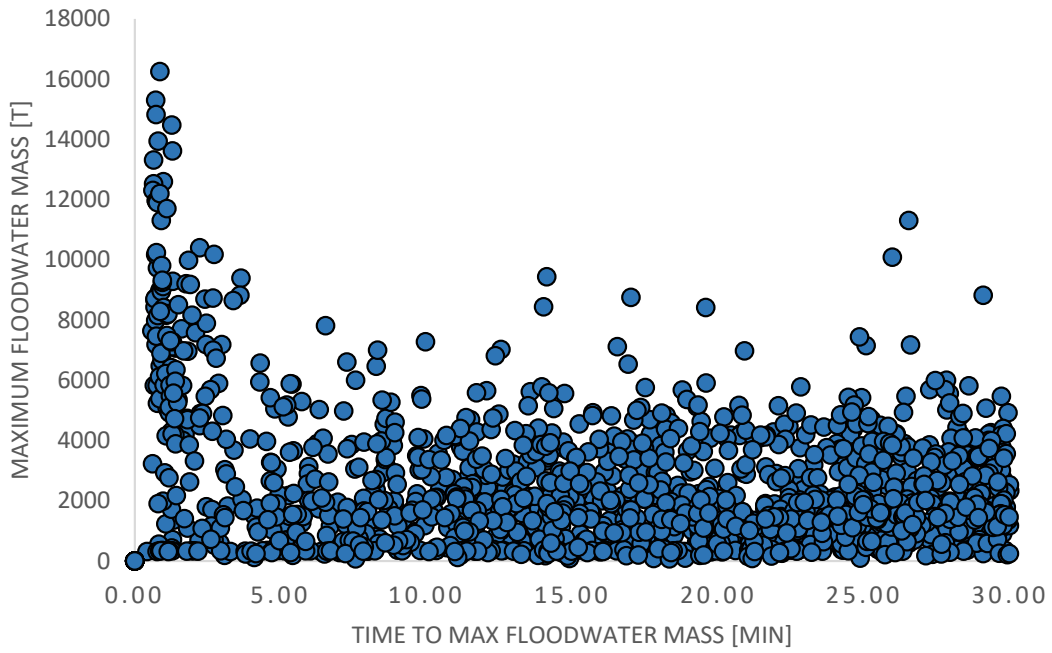


Figure B6: Occurrence of maximum amount of floodwater mass

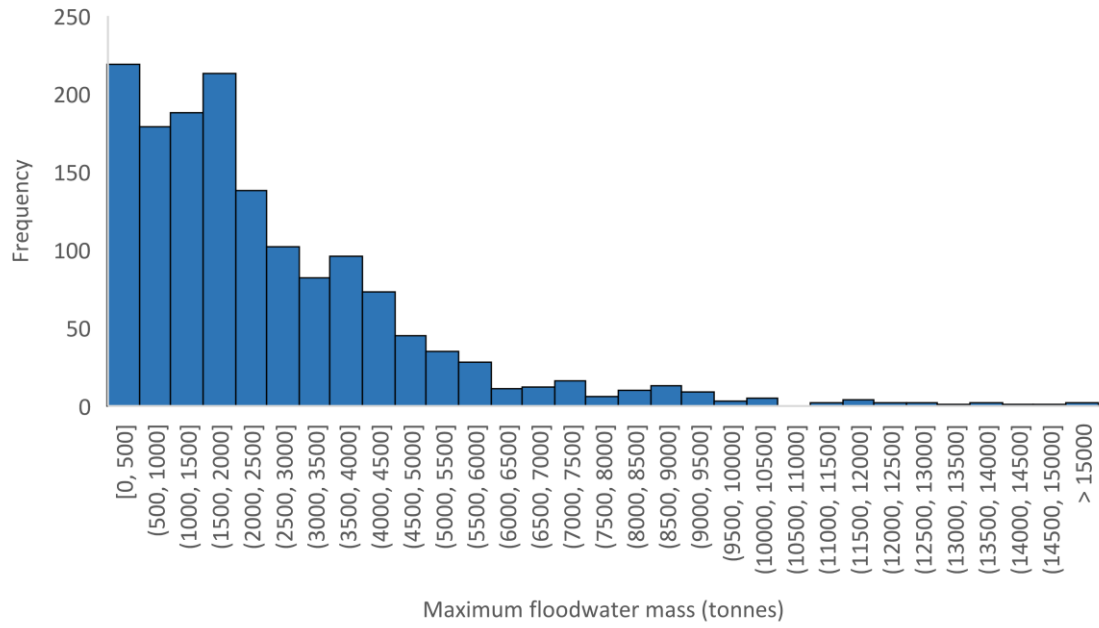


Figure B7: Distribution of maximum amount of floodwater mass

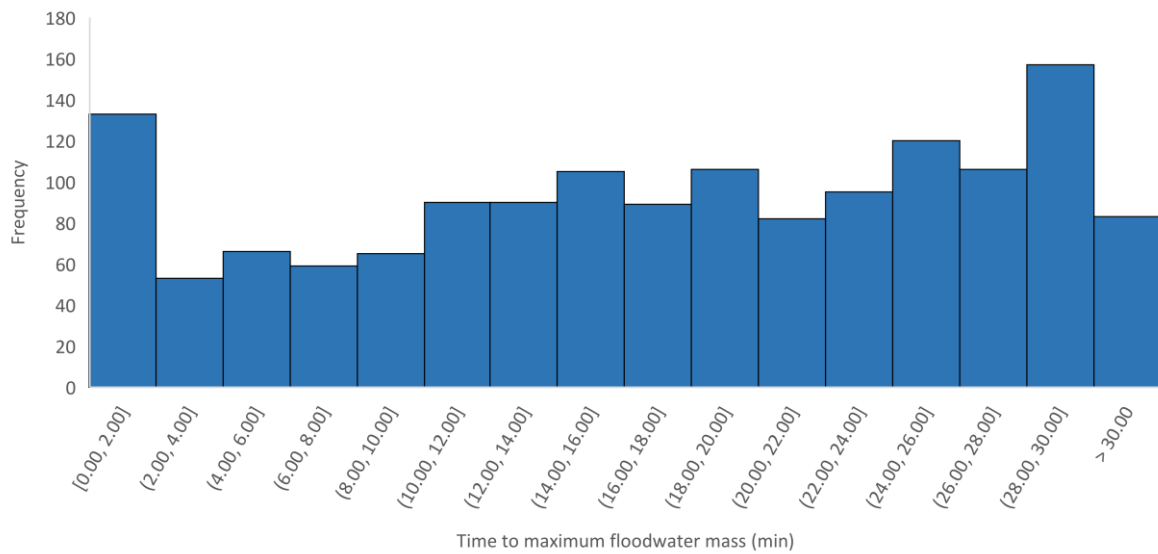


Figure B8: Distribution of time of occurrence of maximum amount of floodwater mass

Final Values

Within this section, values recorded during the final stage of flooding are presented in relation to average heel, average trim and sinkage.

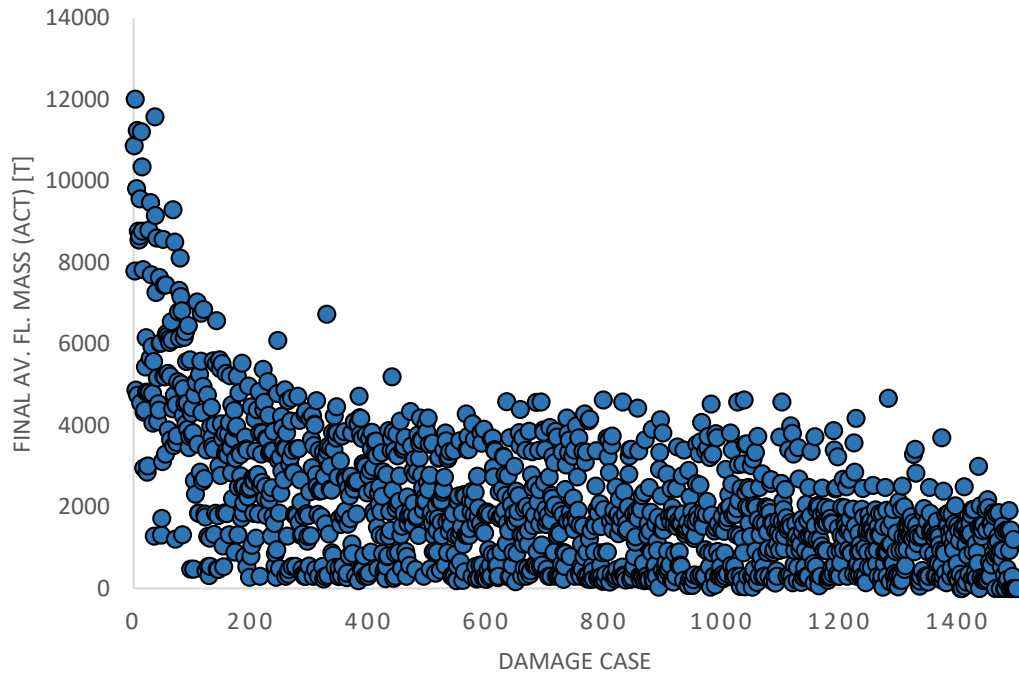


Figure B9: Final 3-minute average of floodwater mass

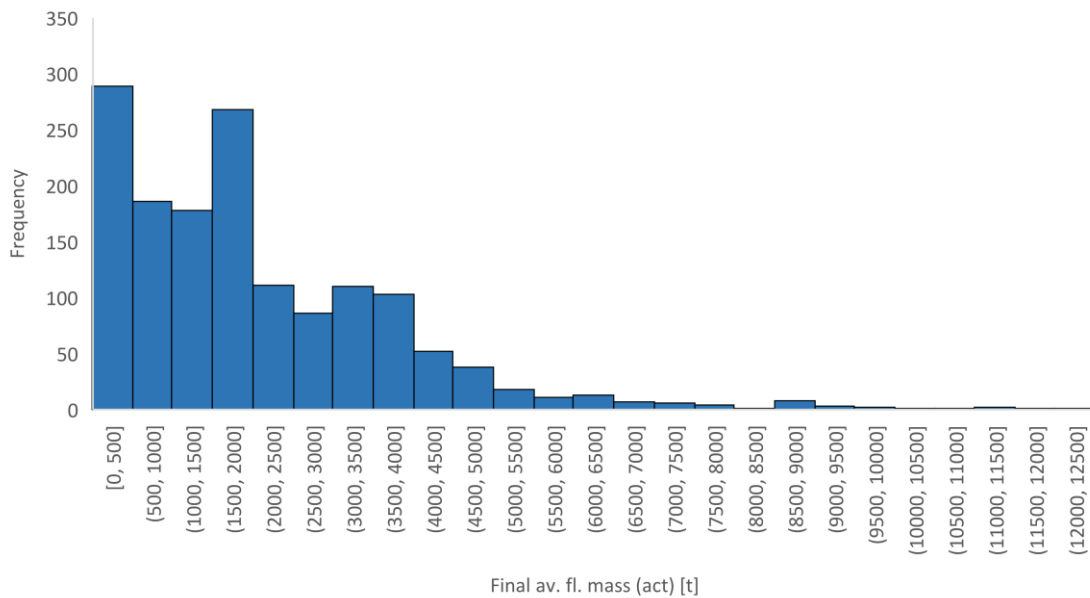


Figure B10: Distribution of final 3-minute average of floodwater mass

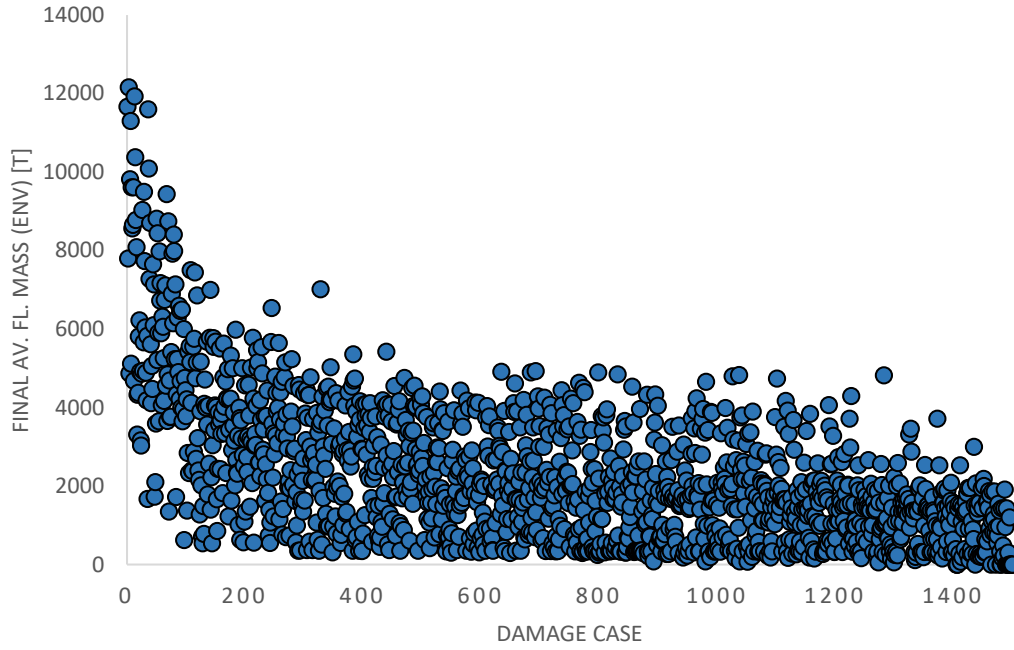


Figure B11: Final 3-minute average of upper envelope of floodwater mass

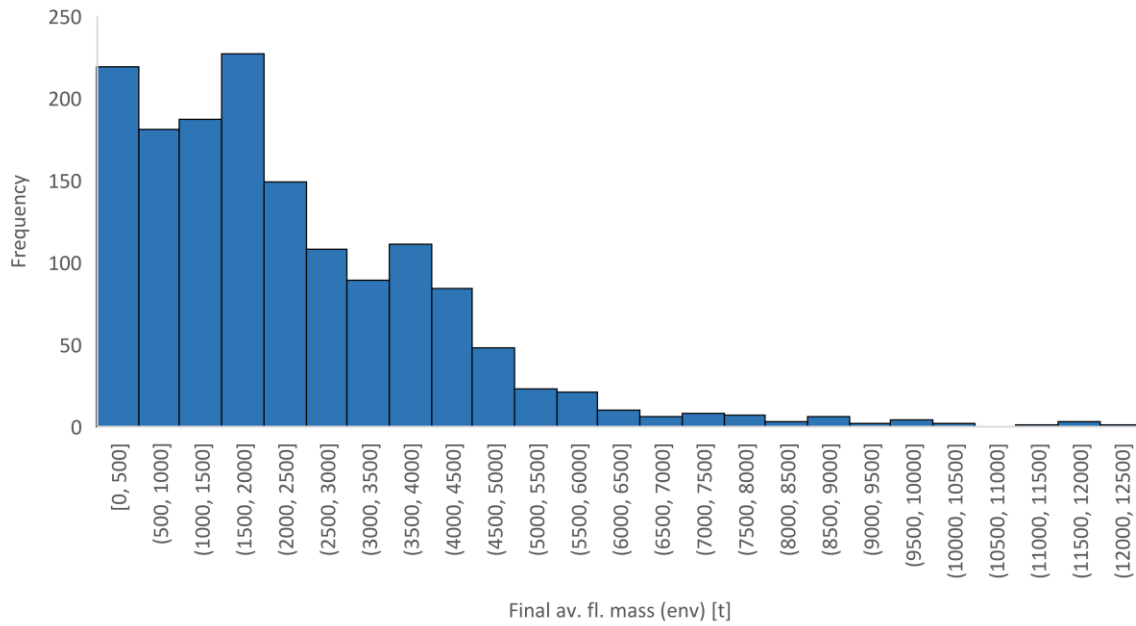


Figure B12: Distribution of final 3-minute average of upper envelope of floodwater mass

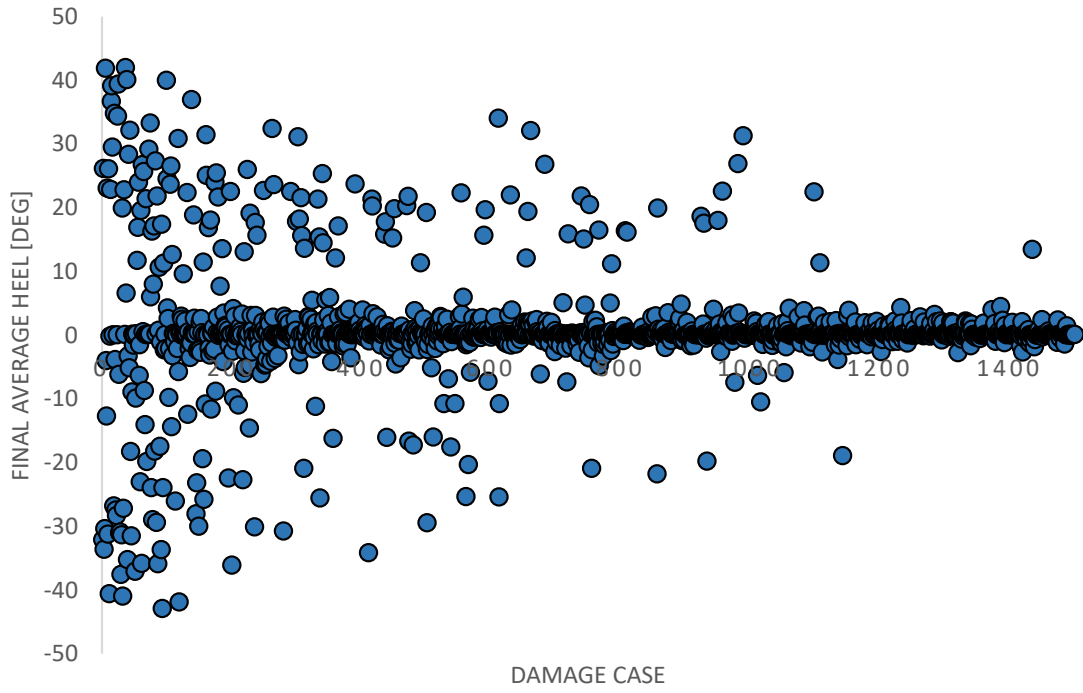


Figure B13: Final 3-minute average of heel

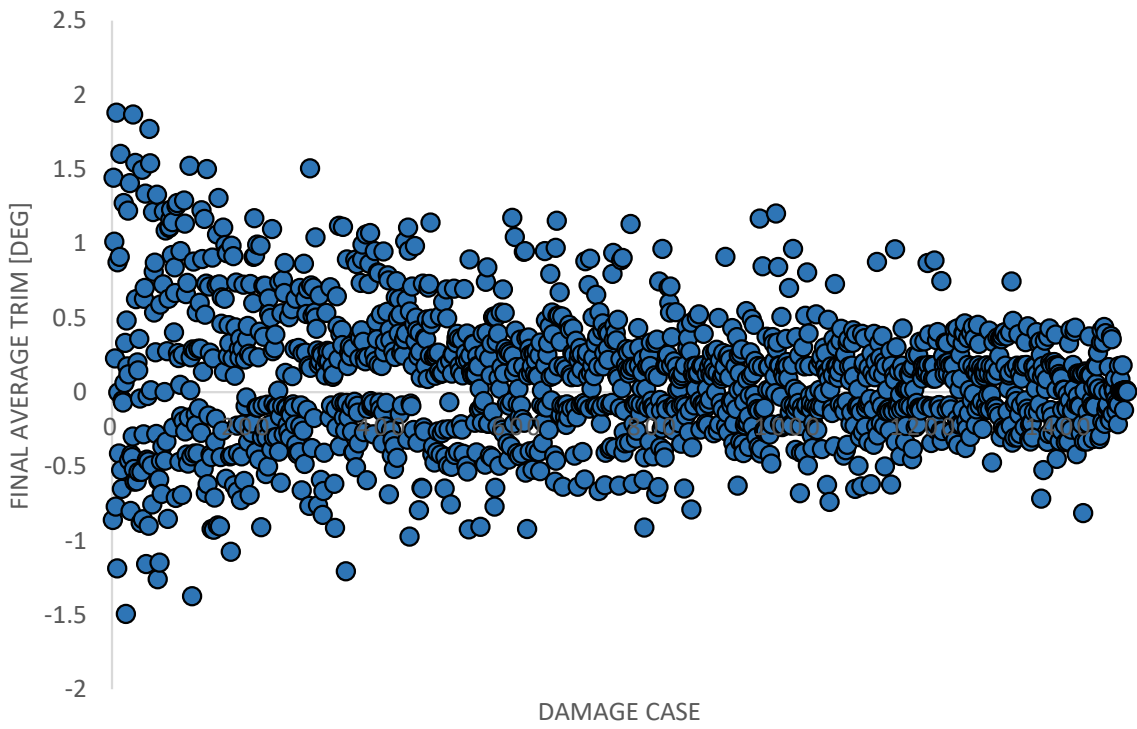


Figure B14: Final 3-minute average trim

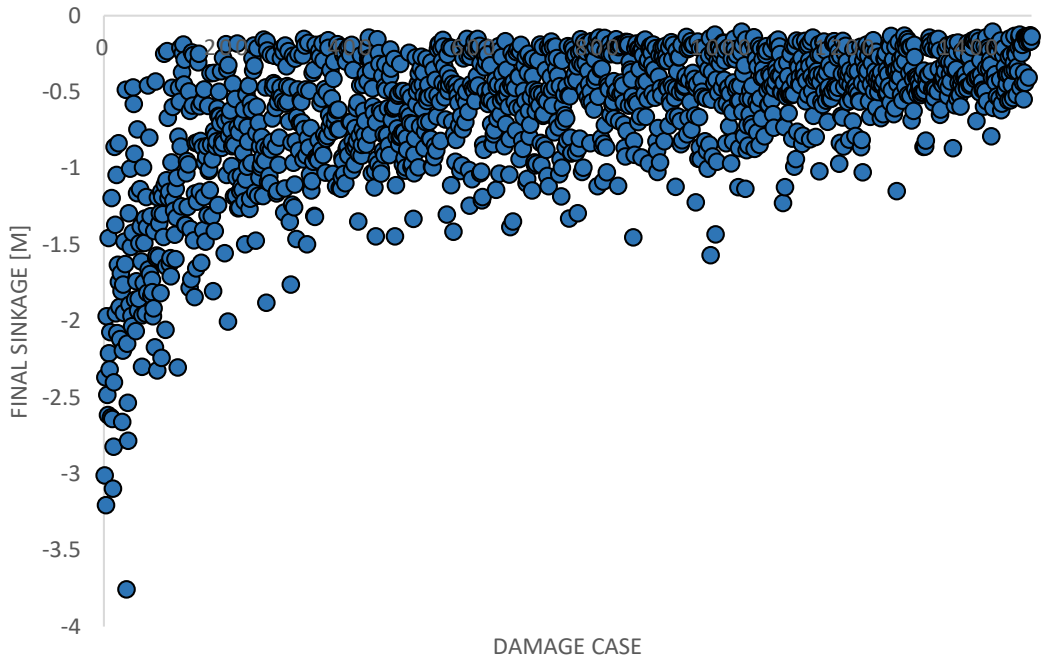


Figure B15: Final 3-minute average sinkage

Final Rates of Change

Here, the rate of change in important properties relating to the floating position of the vessel and floodwater mass accumulation are provided in relation to the final stages of the simulation.

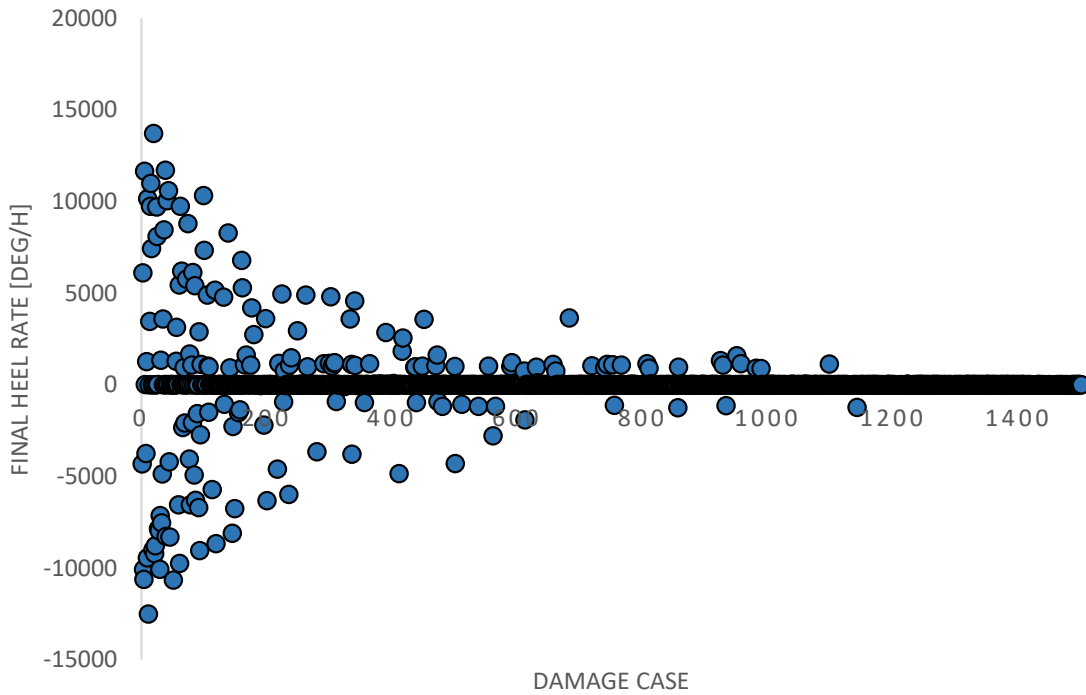


Figure B16: Final rate of change of heel

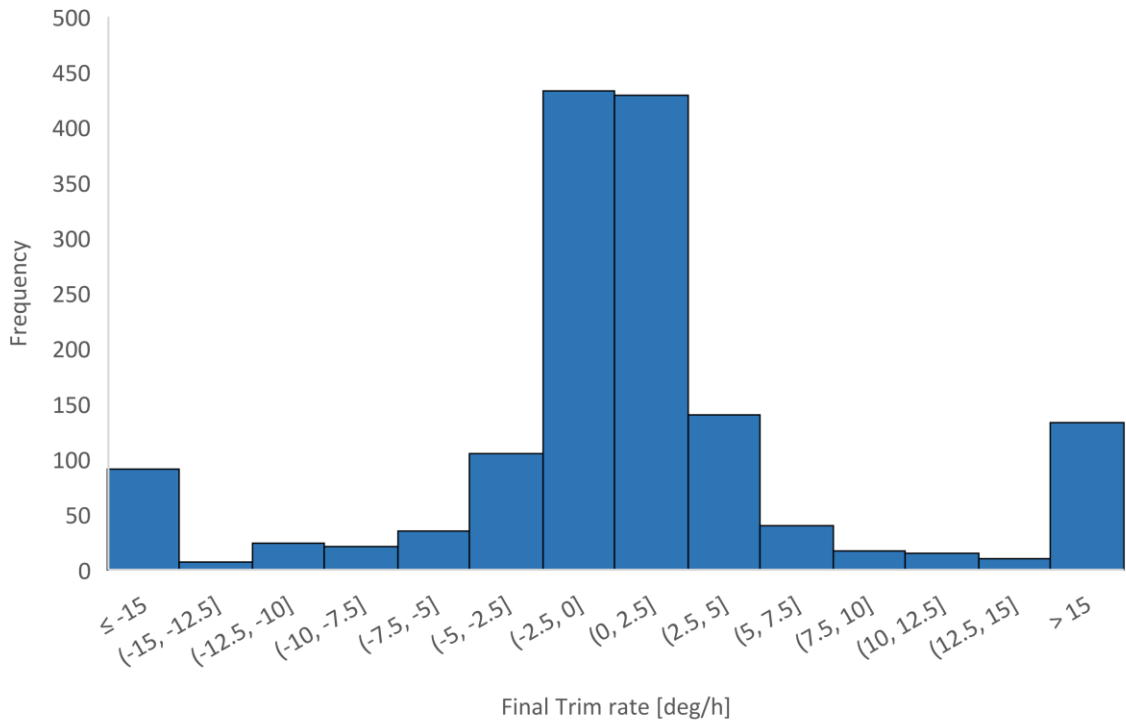


Figure B17: Distribution of final rates of change of heel angle

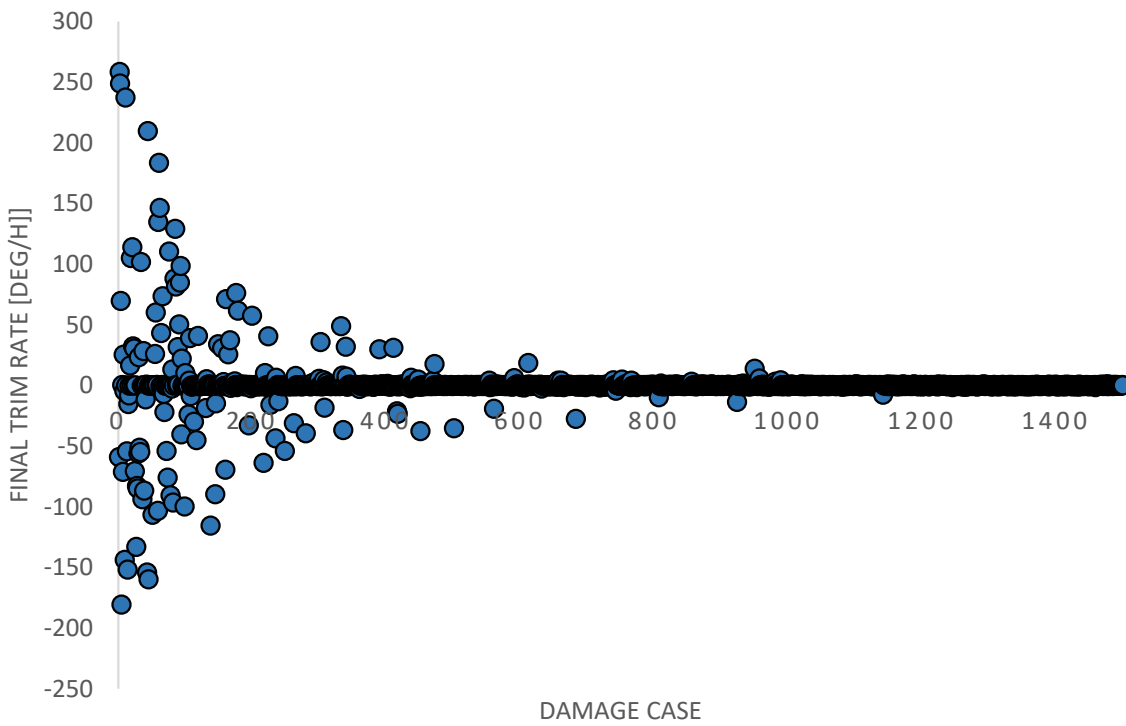


Figure B18: Final rate of change of trim

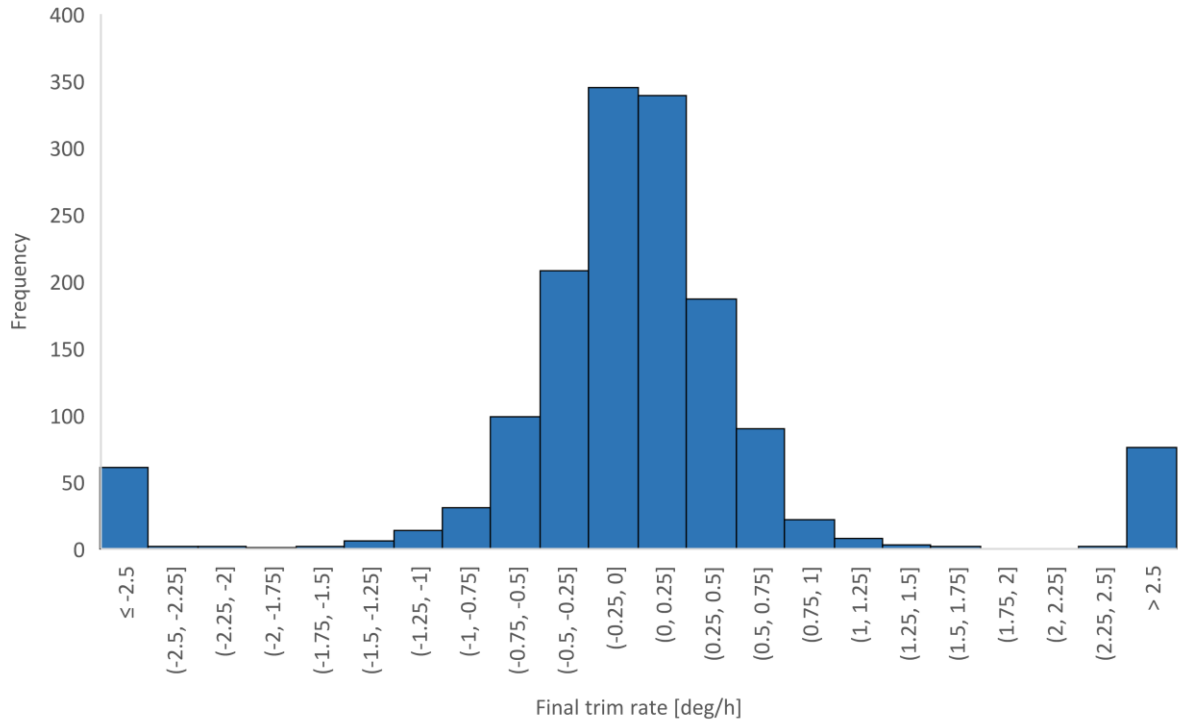


Figure B19: Distribution of final rates of change of trim angle

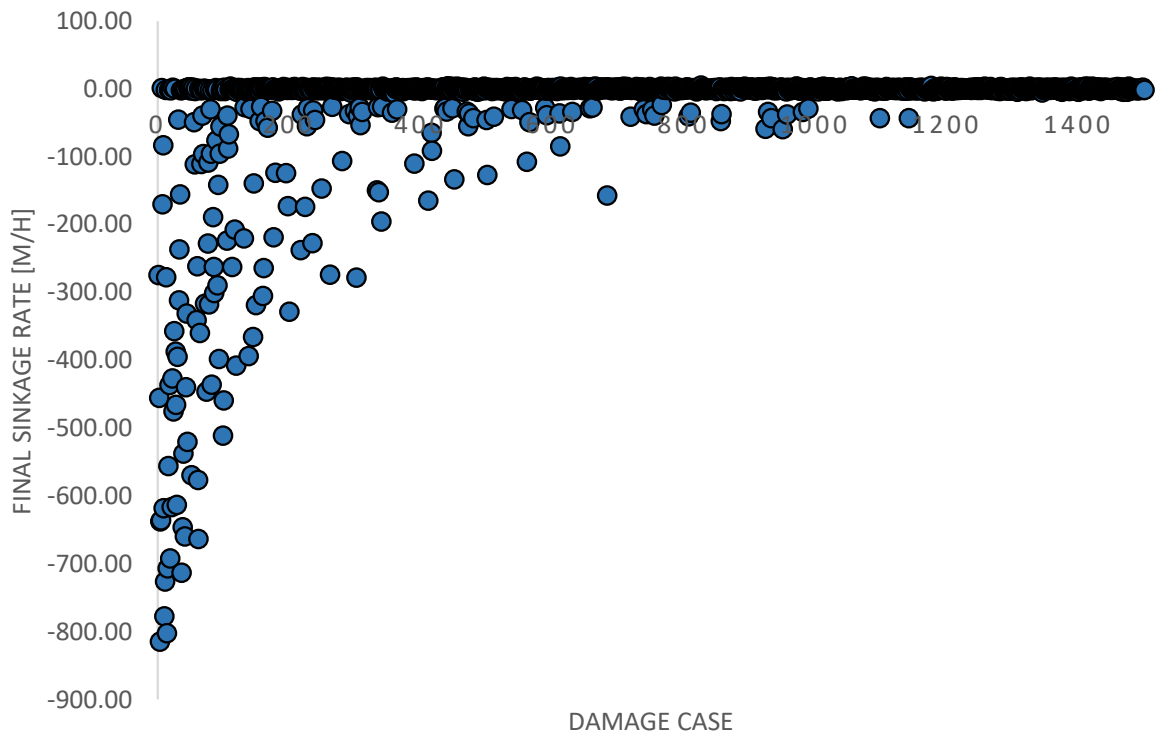


Figure B20: Final rate of change of sinkage

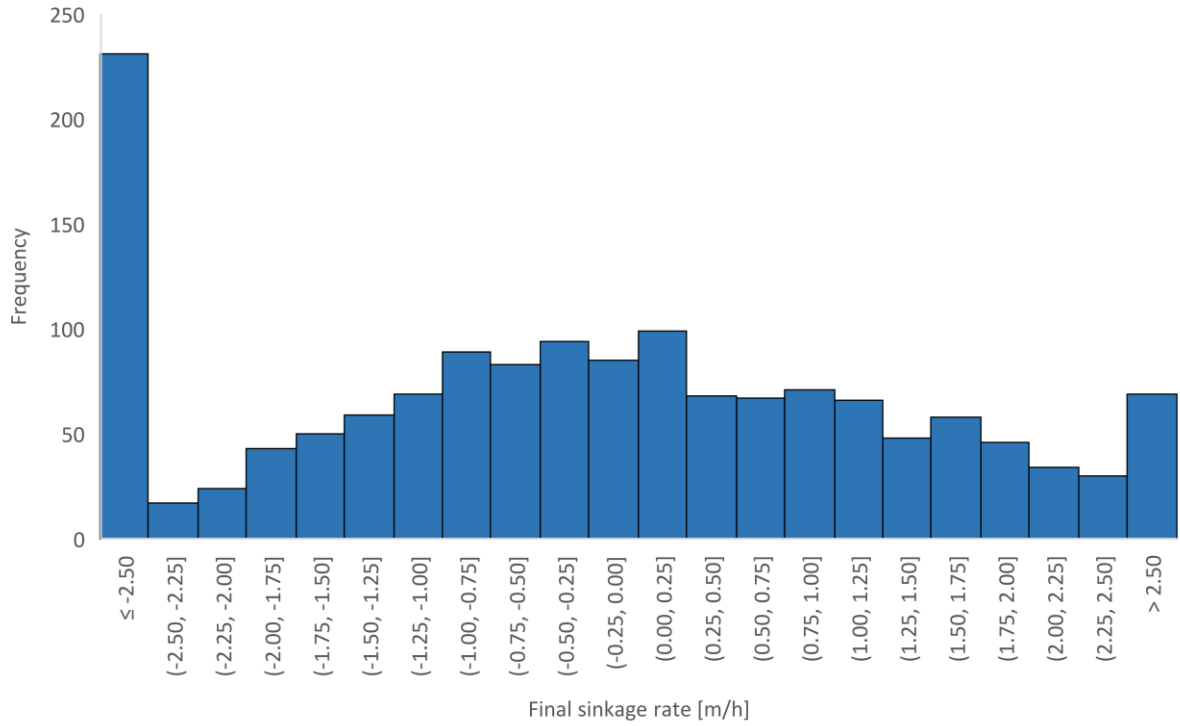


Figure B21: Distribution of final rates of change of sinkage

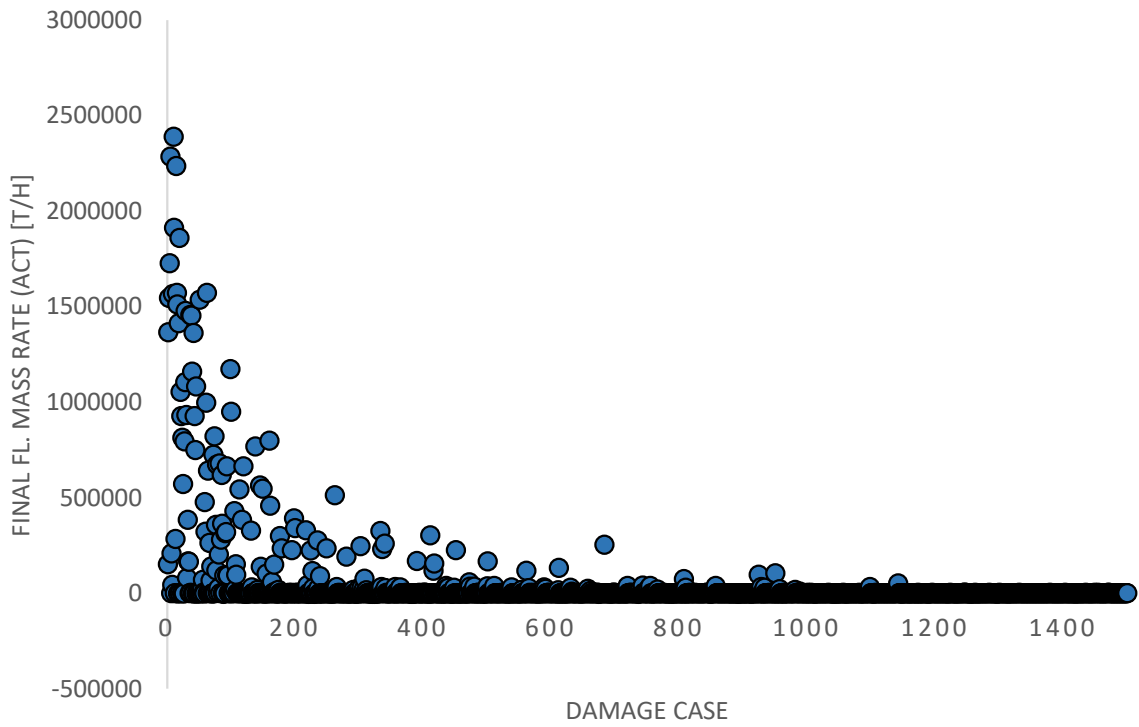


Figure B22: Final rate of change of floodwater mass

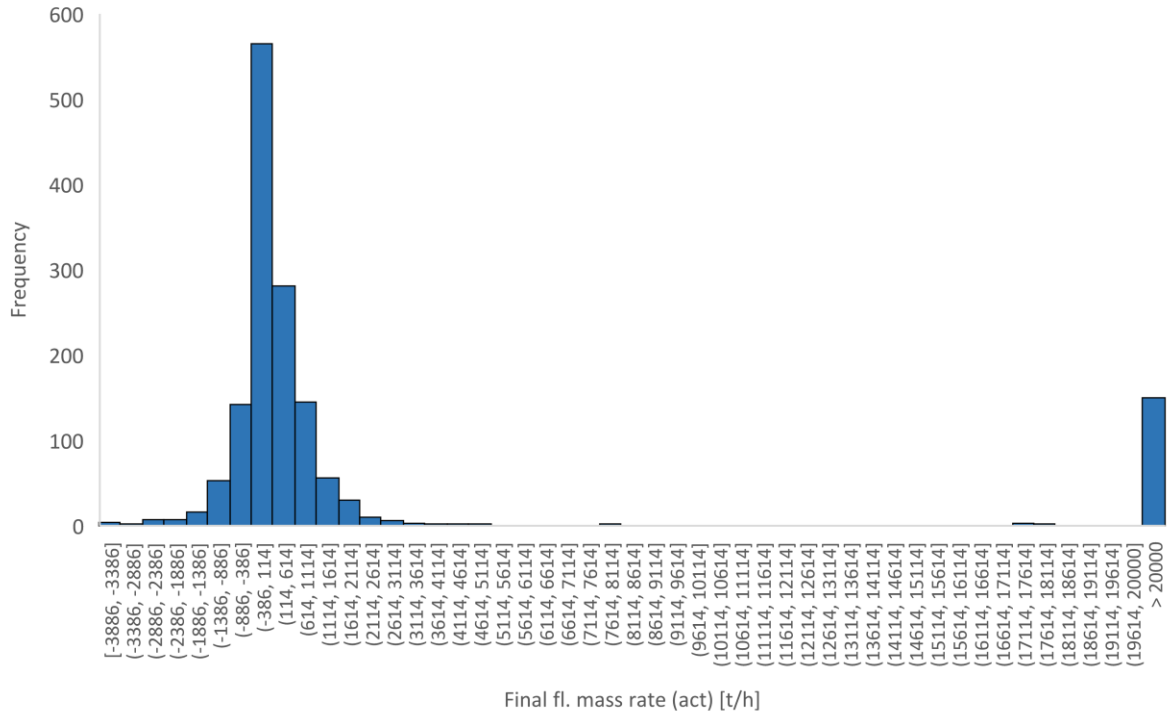


Figure B23: Distribution of final rates of change of floodwater mass

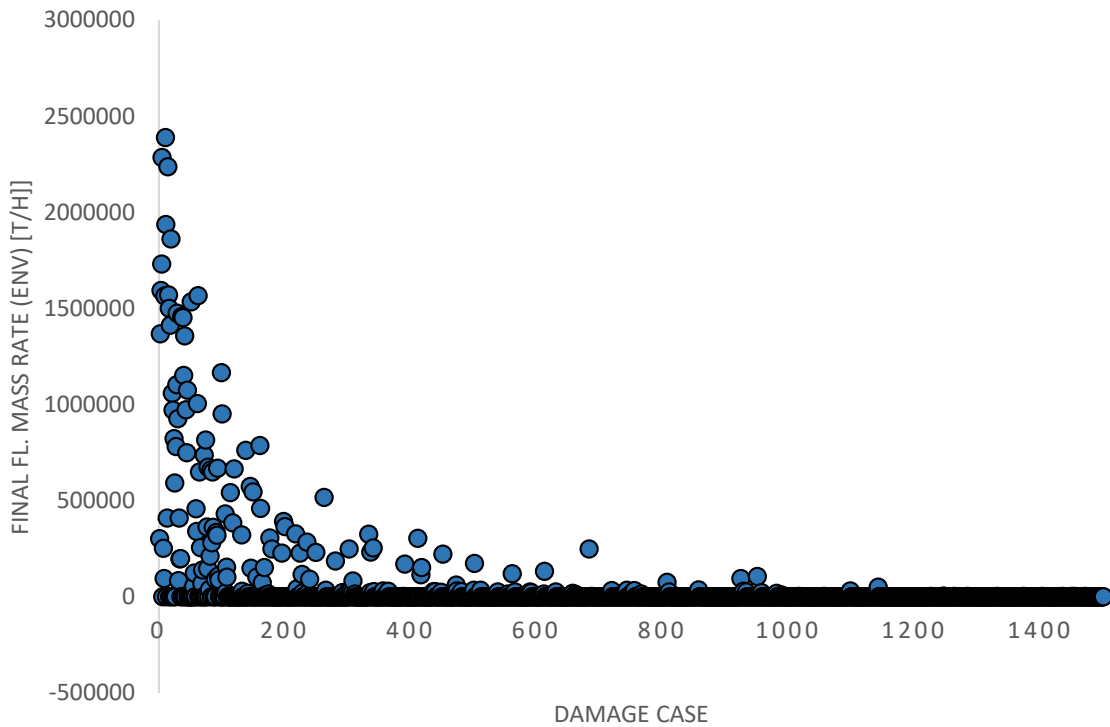


Figure B24: Final rate of change of upper envelope of floodwater mass

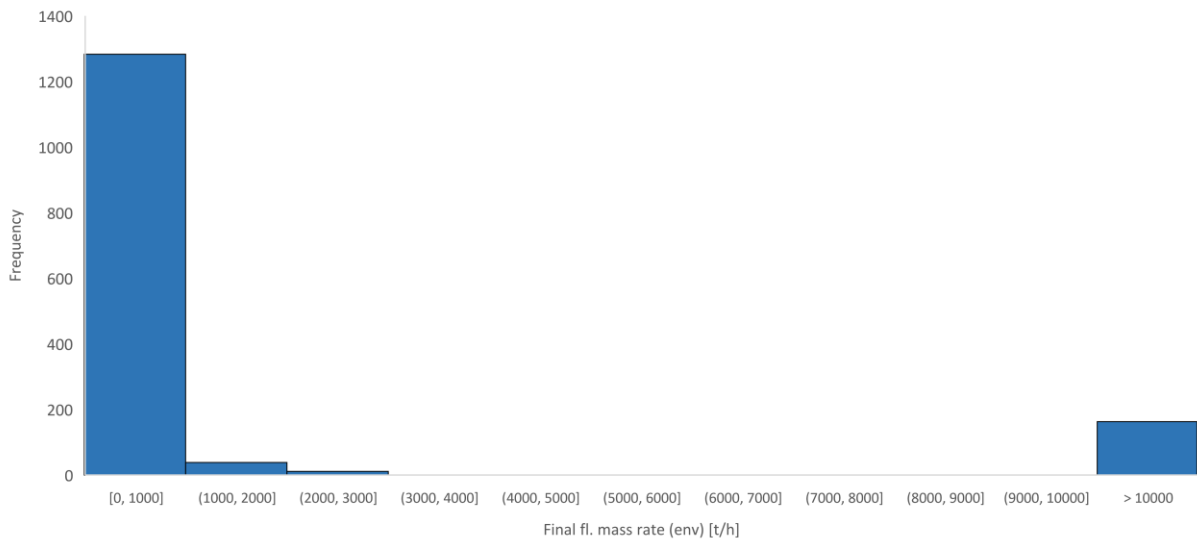


Figure B25: Distribution of final rates of change of upper envelope of floodwater mass

Appendix C: CS1 Simulation Results

This appendix provides detailed simulation results pertaining to the cruise vessel case study presented within Chapter 8. Here, details are provided in relation to the vessel floating position, motions and floodwater accumulation in each simulated case. Furthermore, these are viewed in relation to the maximum values recorded over the duration of each simulation which are followed by values recorded during the final stage.

Maximum Values

Here, the peak values realised within each simulated case are presented with respect to roll angle, average heel recorded over 3 minutes, and the maximum floodwater accumulated.

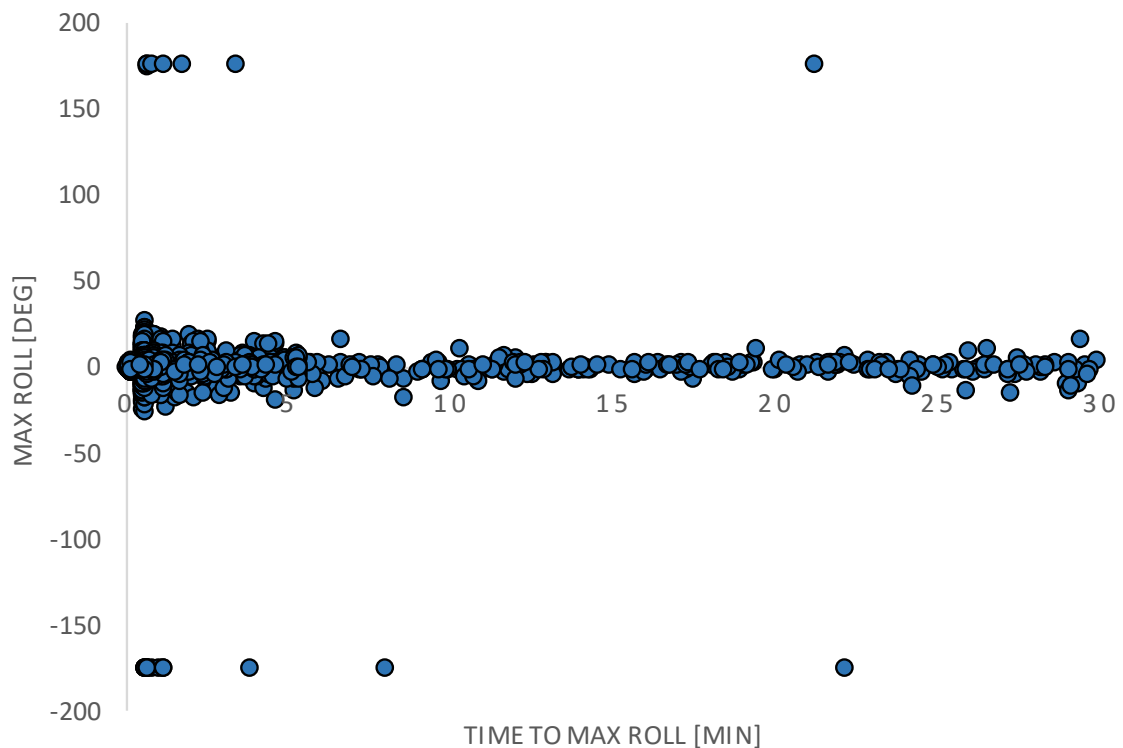


Figure C1: Occurrence of maximum roll angles

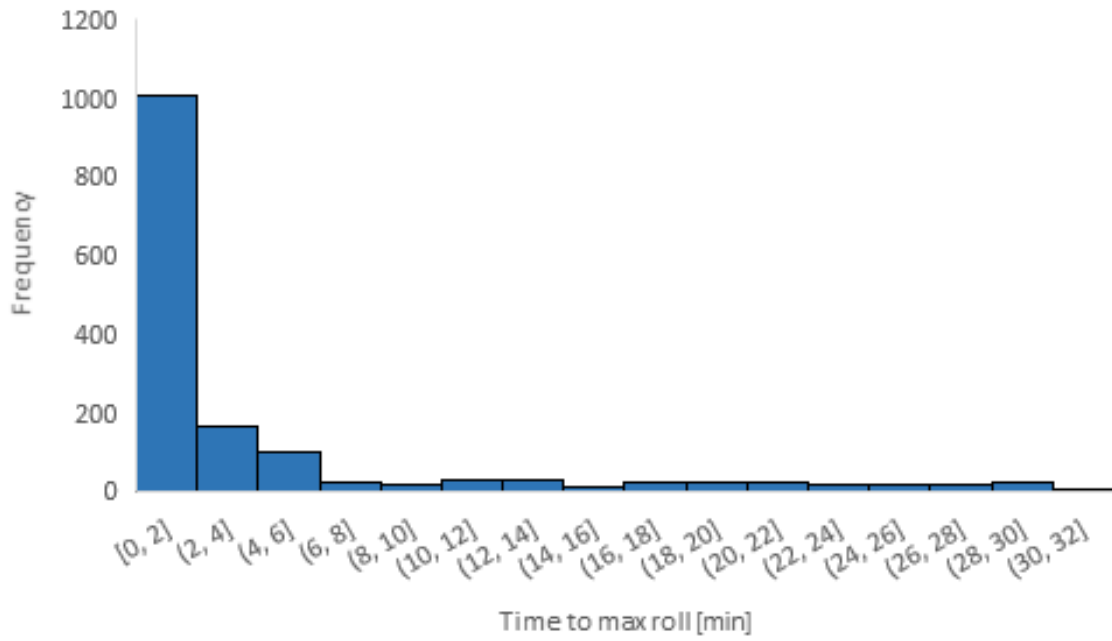


Figure C2: Distribution of times of occurrence of maximum roll angles

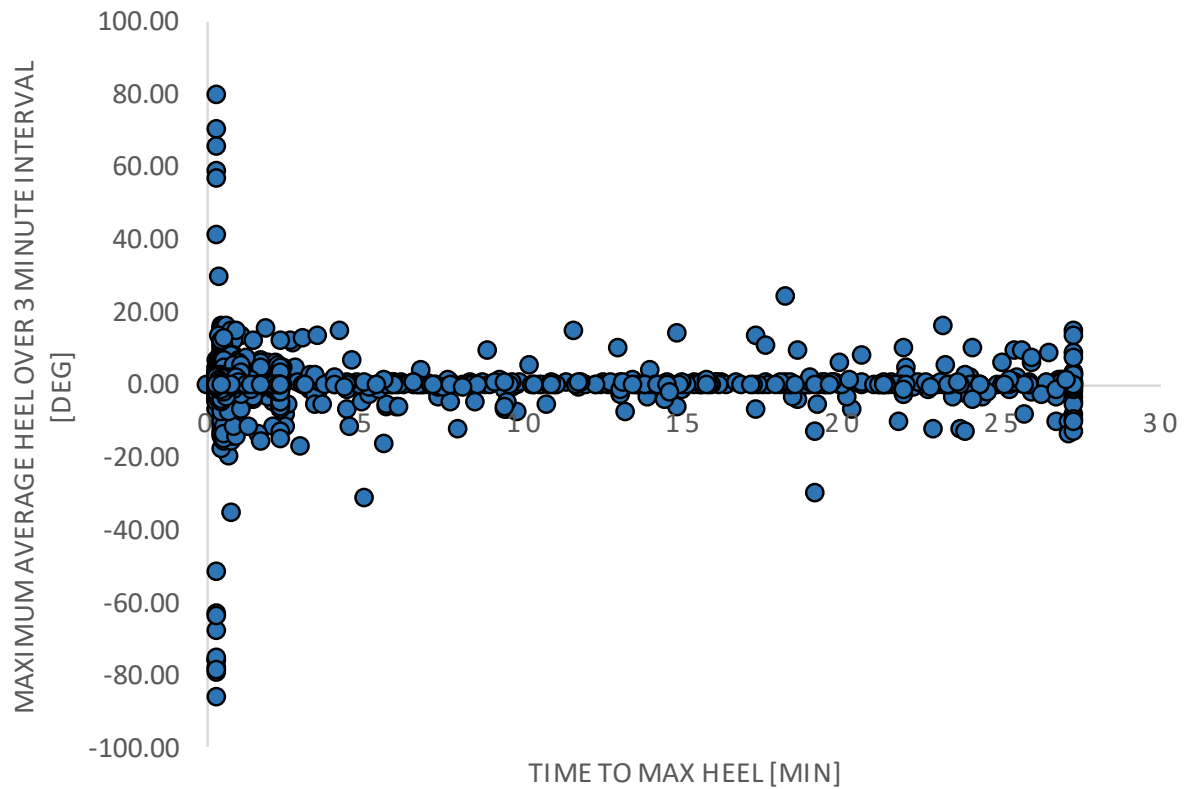


Figure C3: Occurrence of maximum 3-minute averages of heel angle

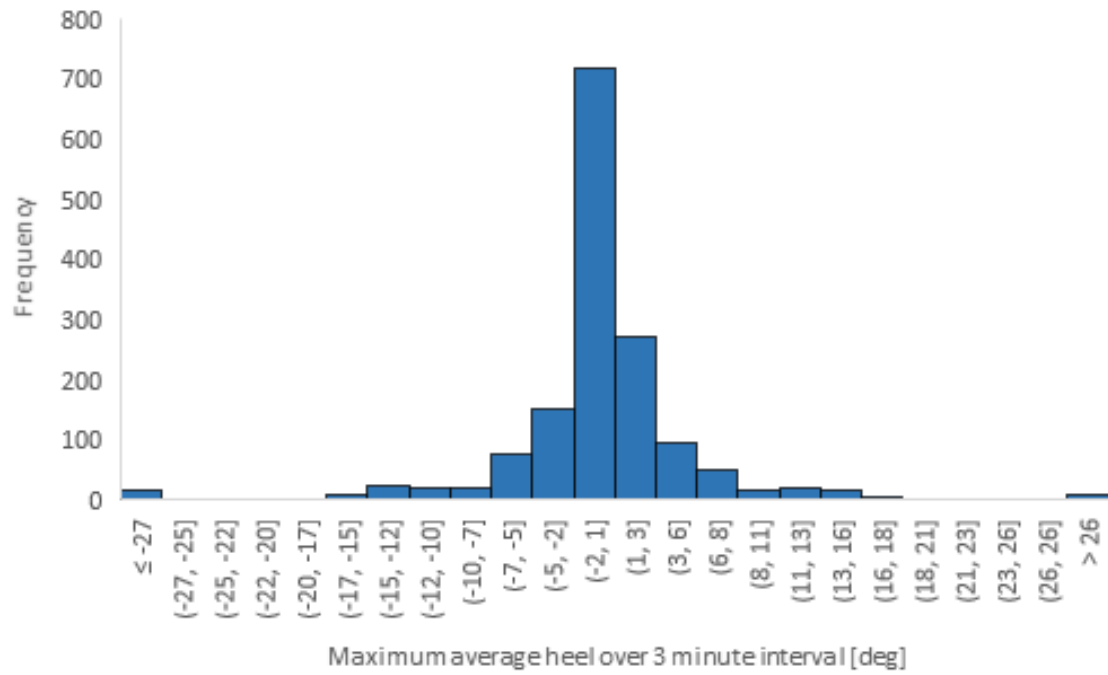


Figure C4: Distribution of maximum 3-minute averages of heel angles

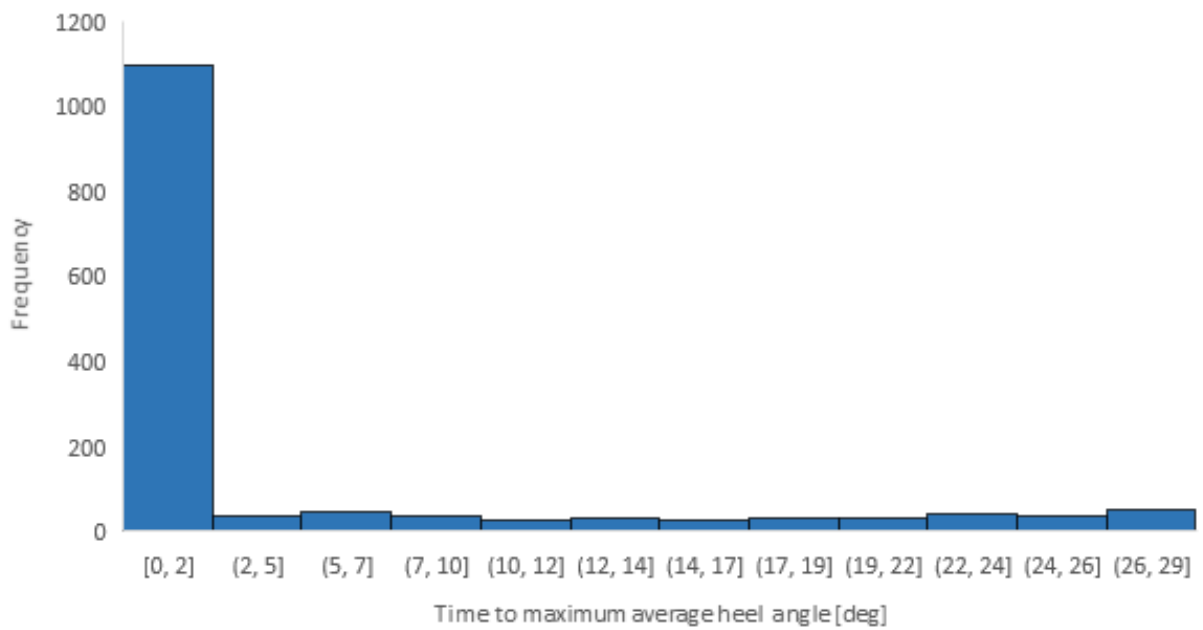


Figure C5: Distribution of time of occurrence of maximum 3-minute averages of heel angles

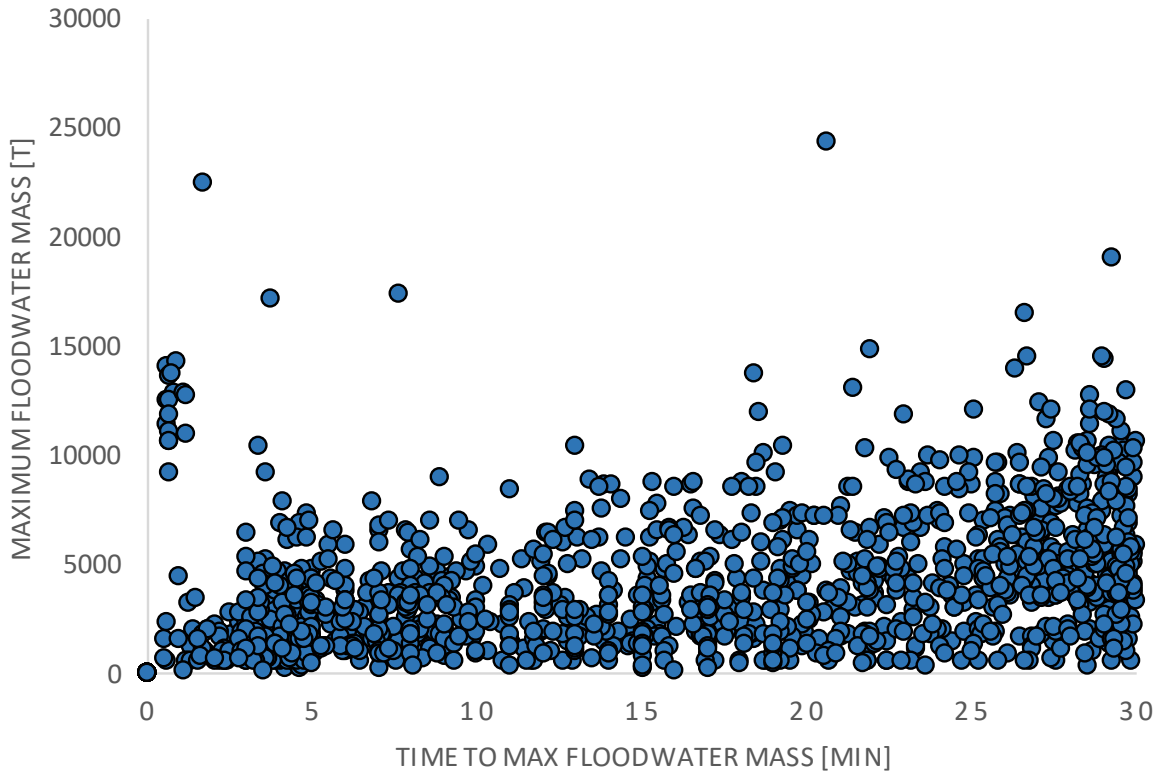


Figure C6: Occurrence of maximum amount of floodwater mass

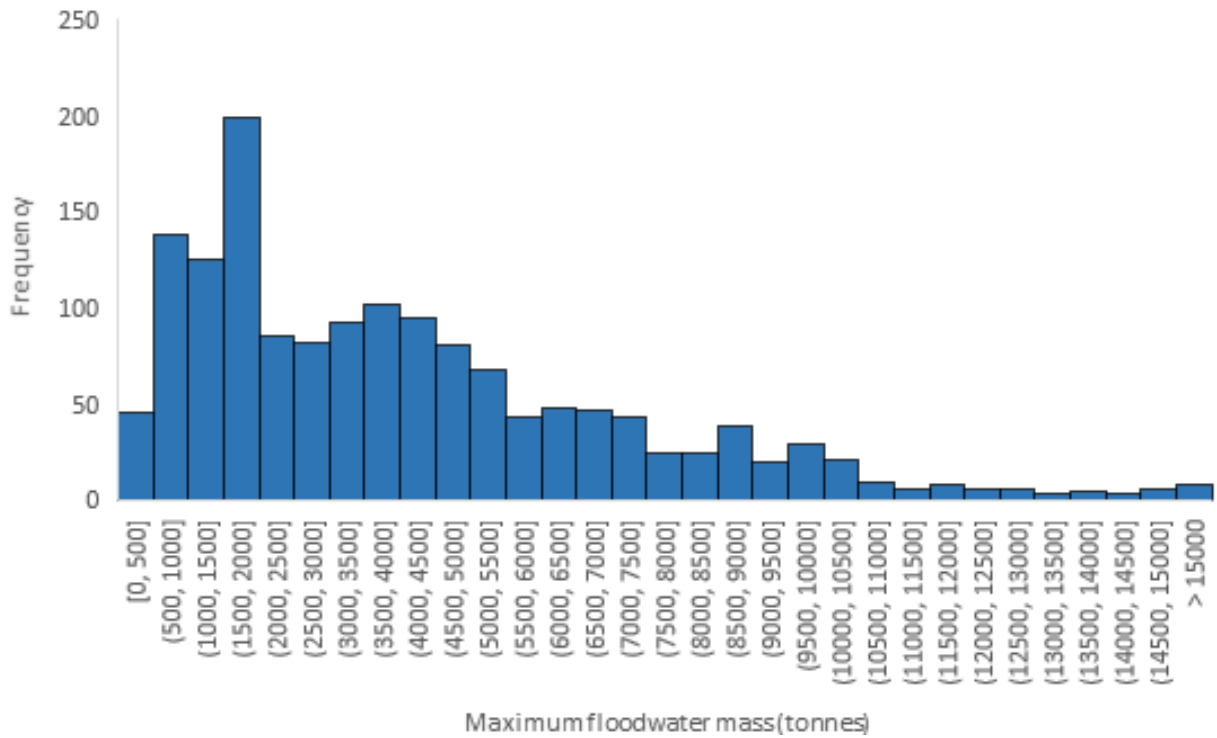


Figure C7: Distribution of maximum amount of floodwater mass

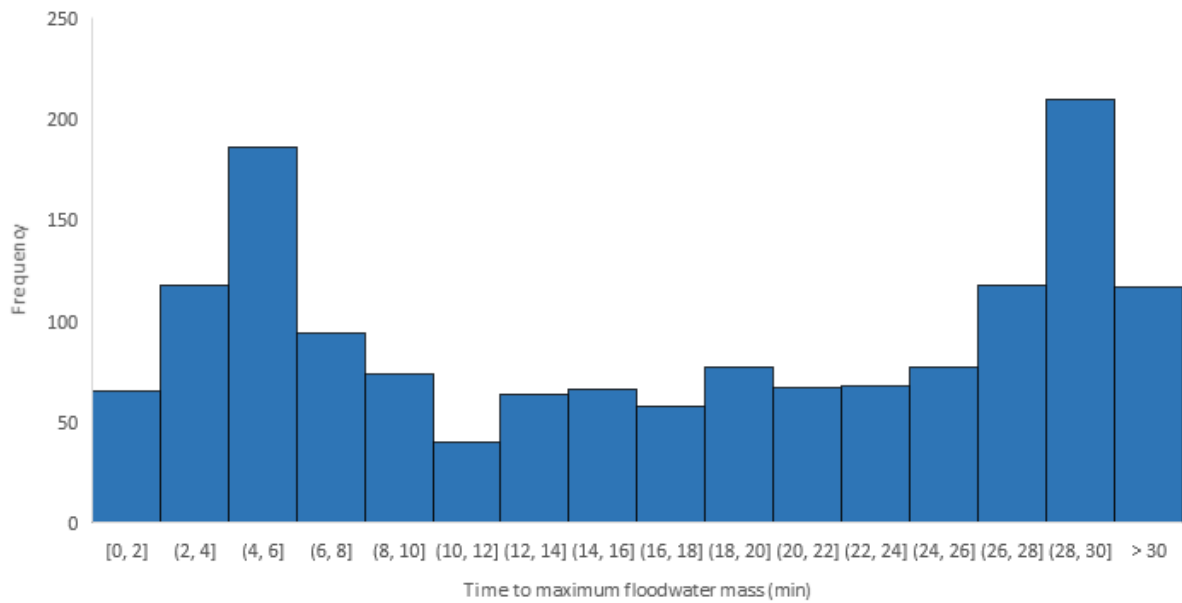


Figure C8: Distribution of time of occurrence of maximum amount of floodwater mass

Final Values

Within this section, values recorded during the final stage of flooding are presented in relation to average heel, average trim and sinkage

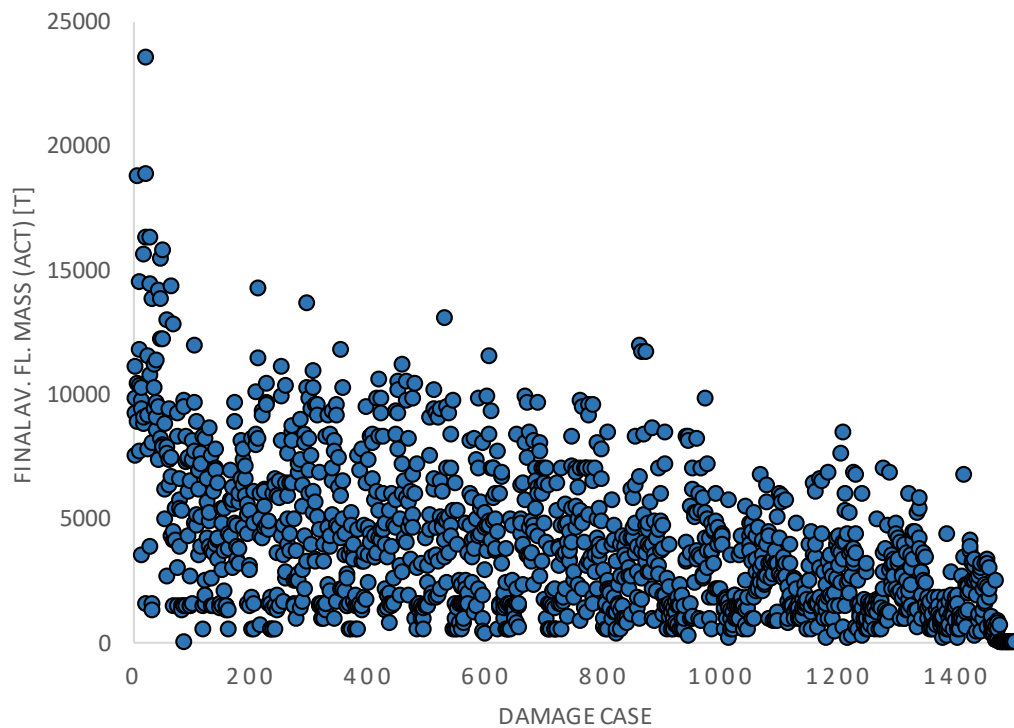


Figure C9: Final 3-minute average of floodwater mass

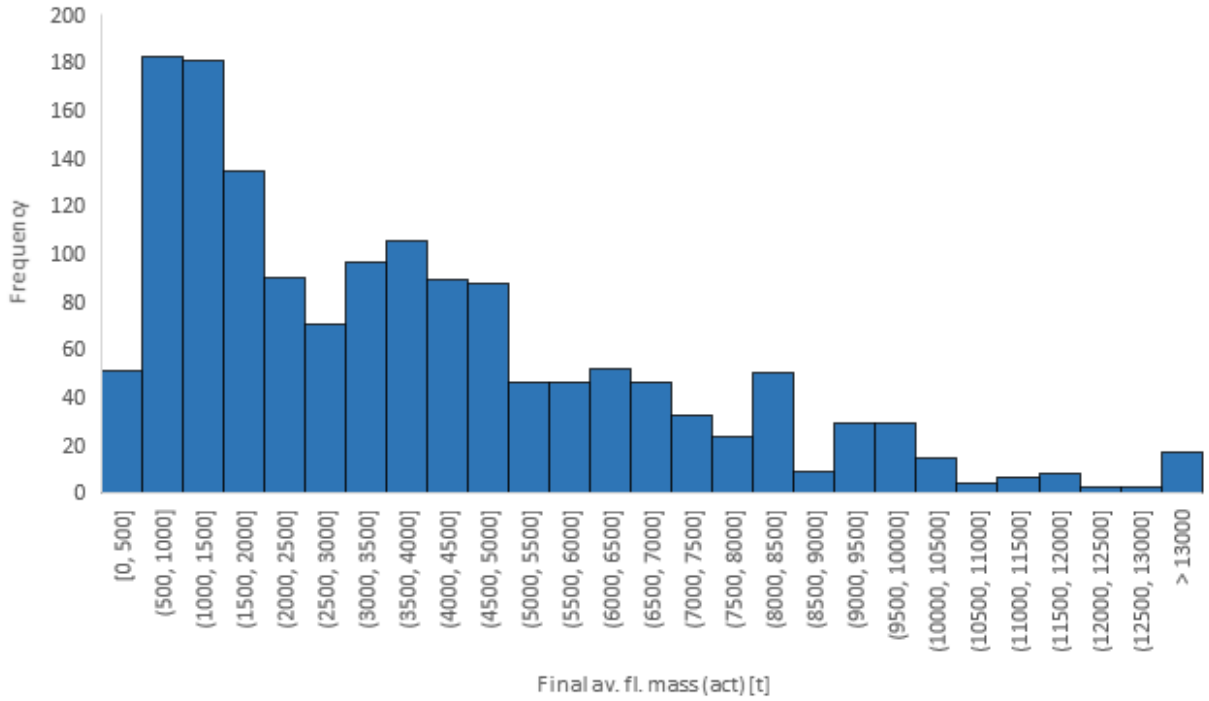


Figure C10: Distribution of final 3-minute average of floodwater mass

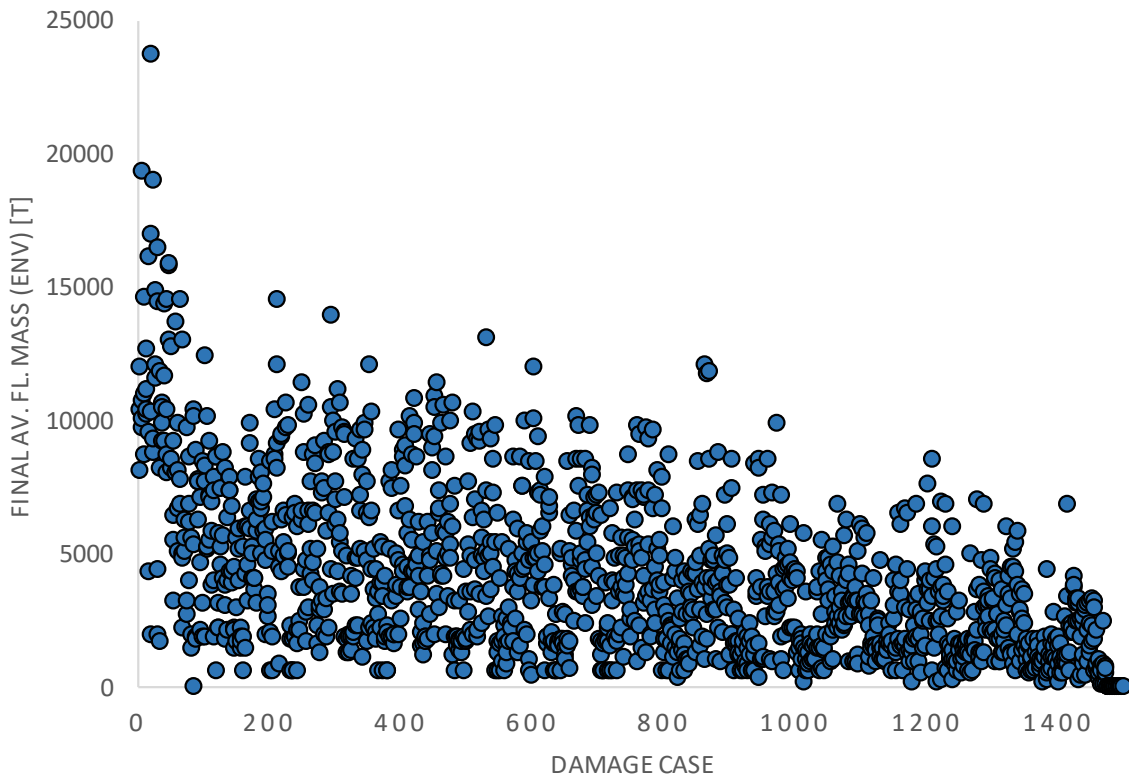


Figure C11: Final 3-minute average of upper envelope of floodwater mass

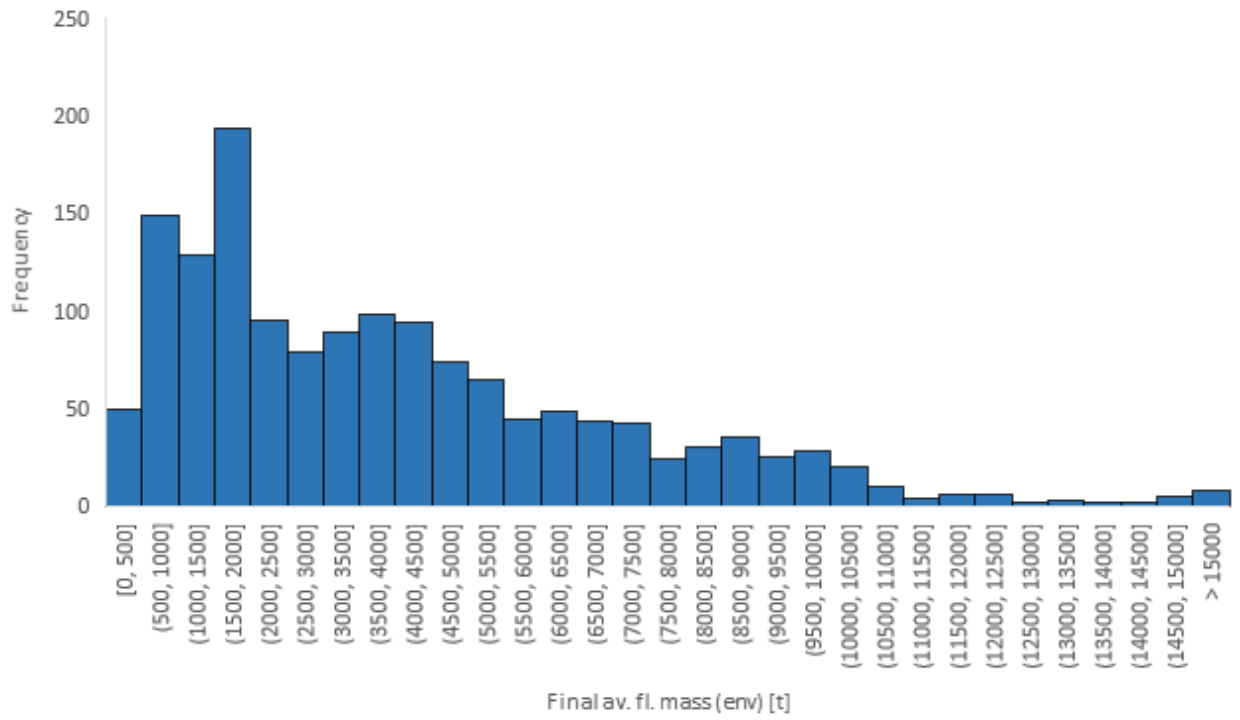


Figure C12: Distribution of final 3-minute average of upper envelope of floodwater mass

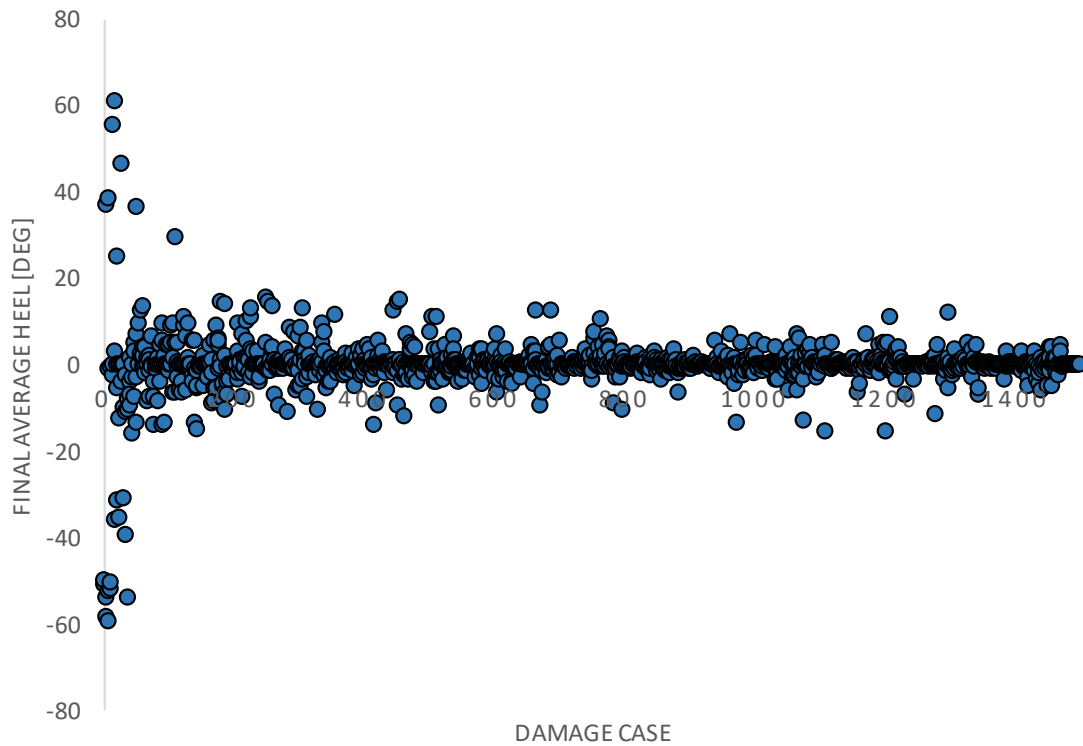


Figure C13: Final 3-minute average of heel

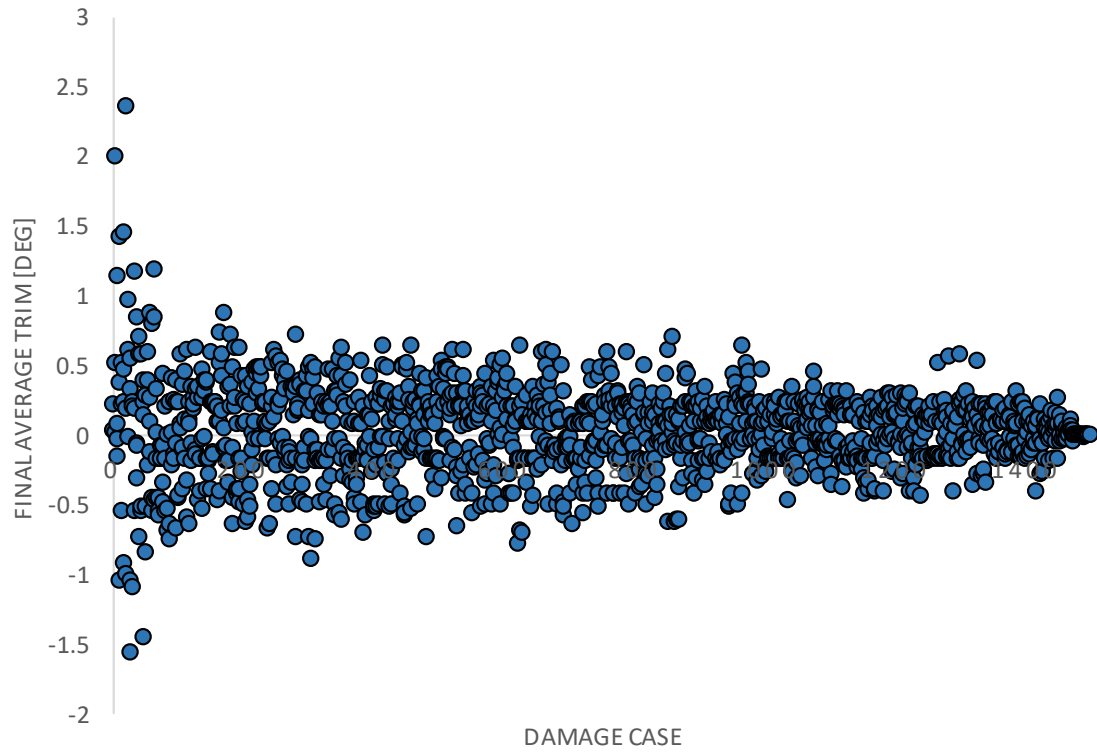


Figure C14: Final 3-minute average trim

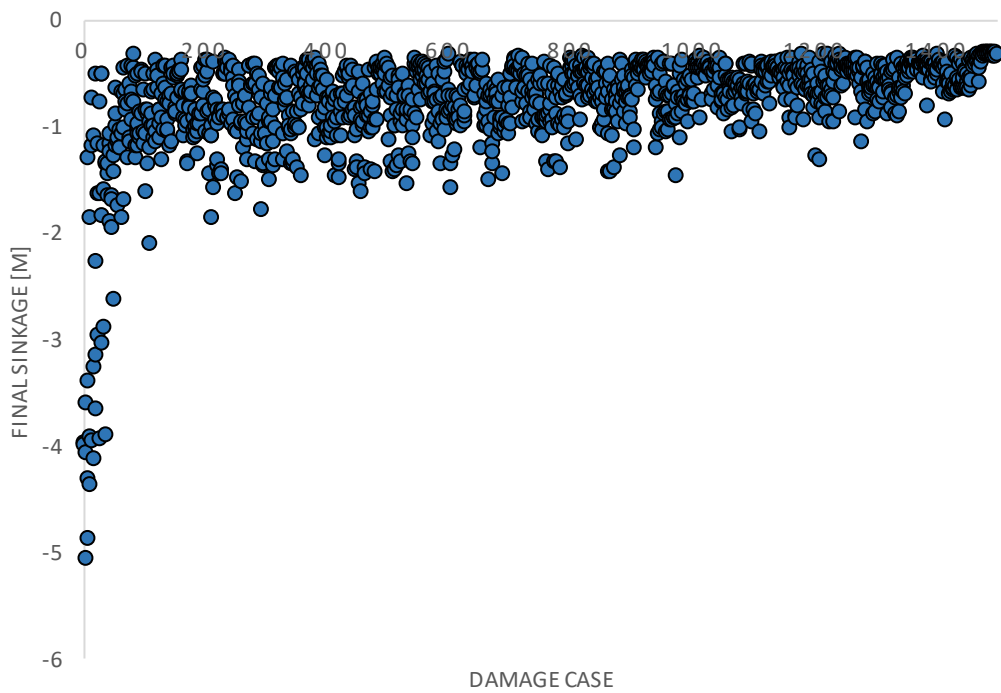


Figure C15: Final 3-minute average sinkage

Final Rates of Change

Here, the rate of change in important properties relating to the floating position of the vessel and floodwater mass accumulation are provided in relation to the final stages of the simulation.

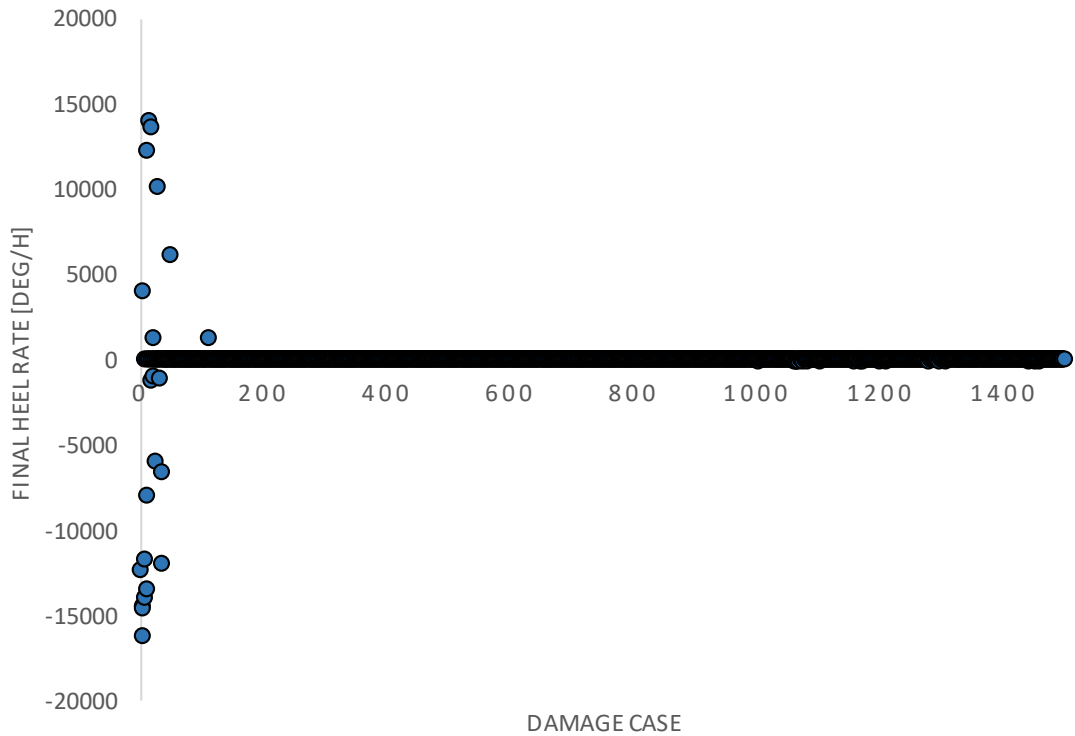


Figure C16: Final rate of change of heel

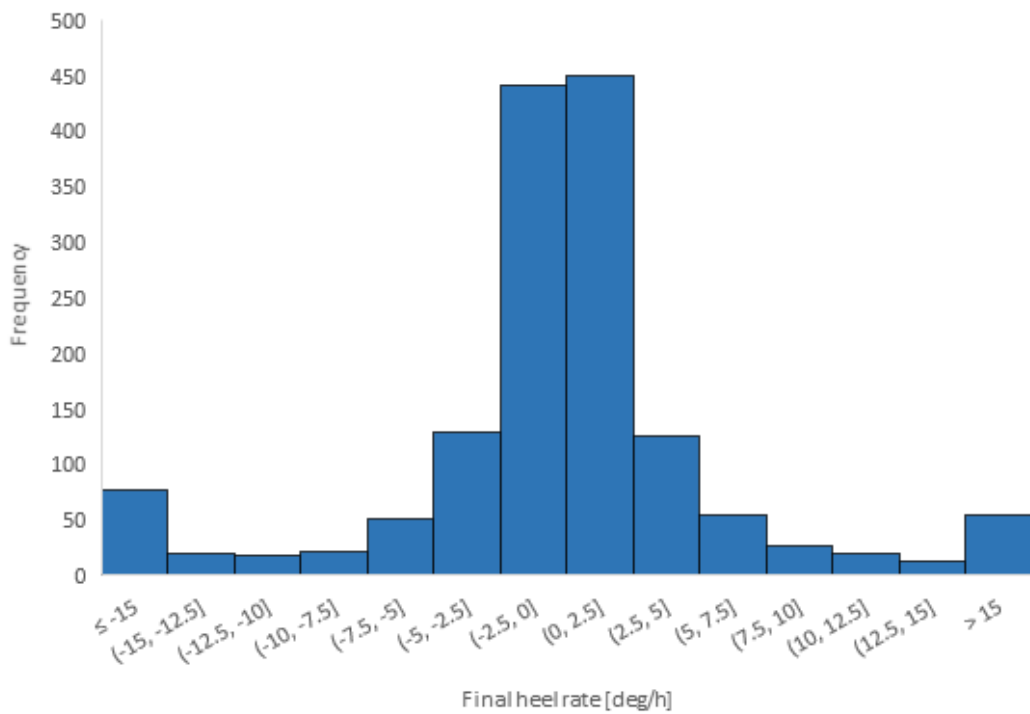


Figure C17: Distribution of final rates of change of heel angle

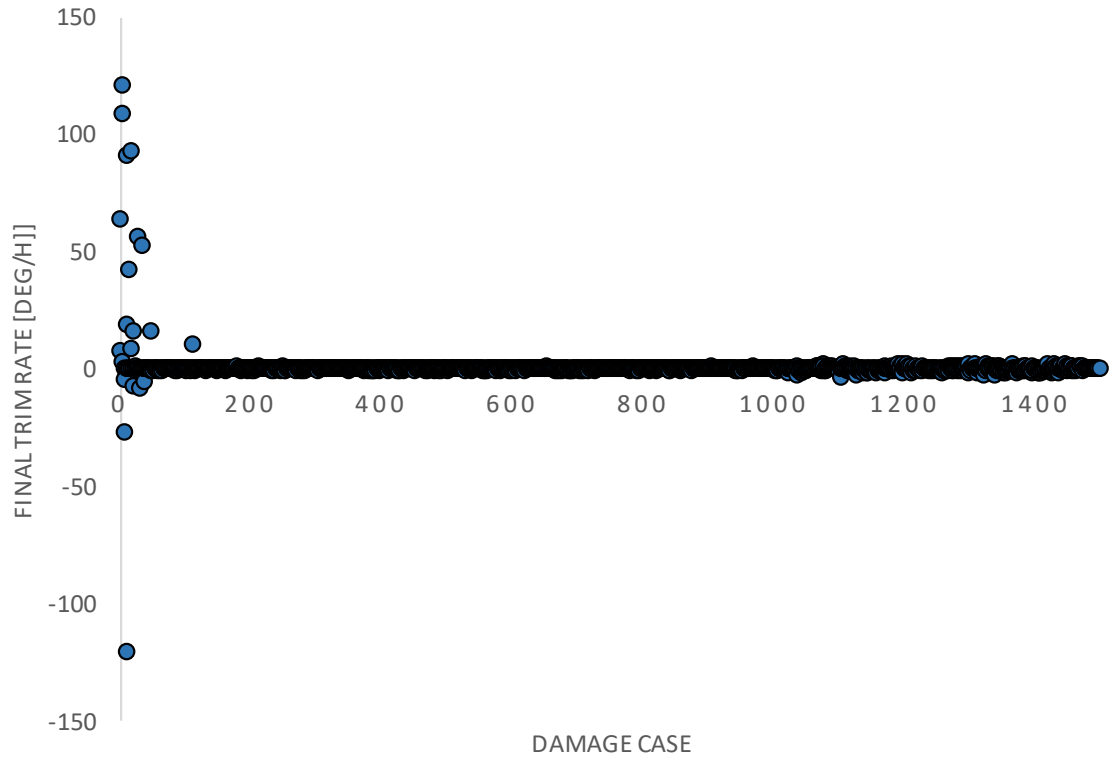


Figure C18: Final rate of change of trim

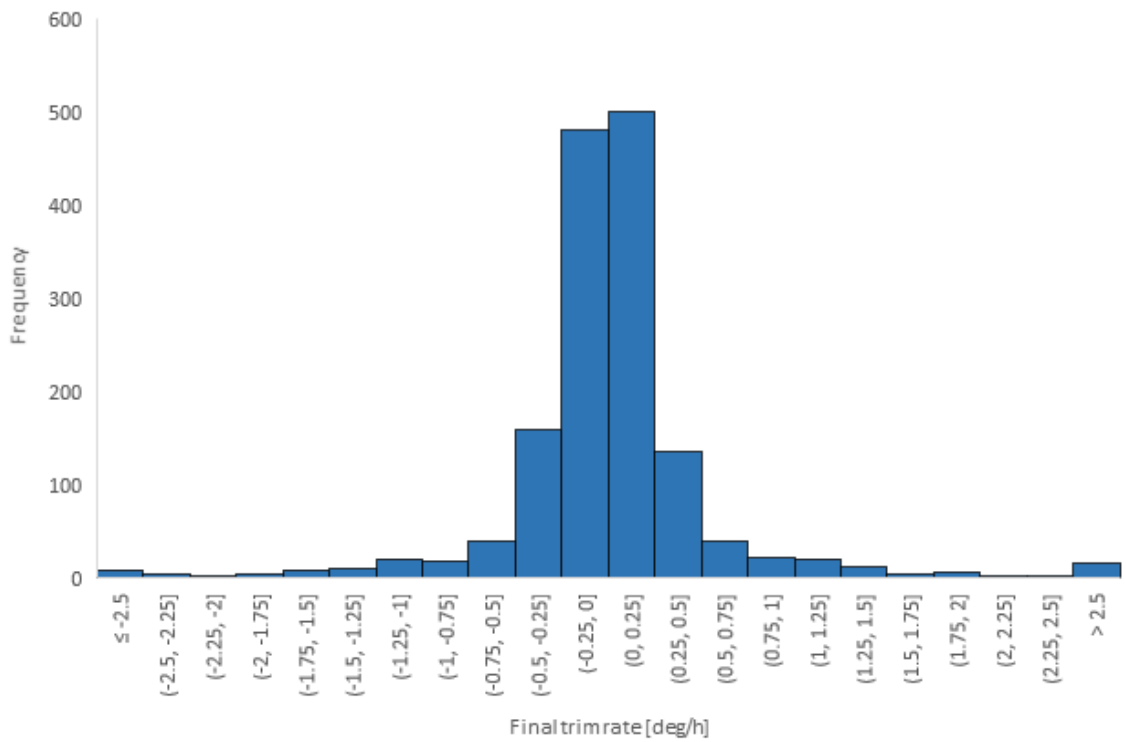


Figure C19: Distribution of final rates of change of trim angle

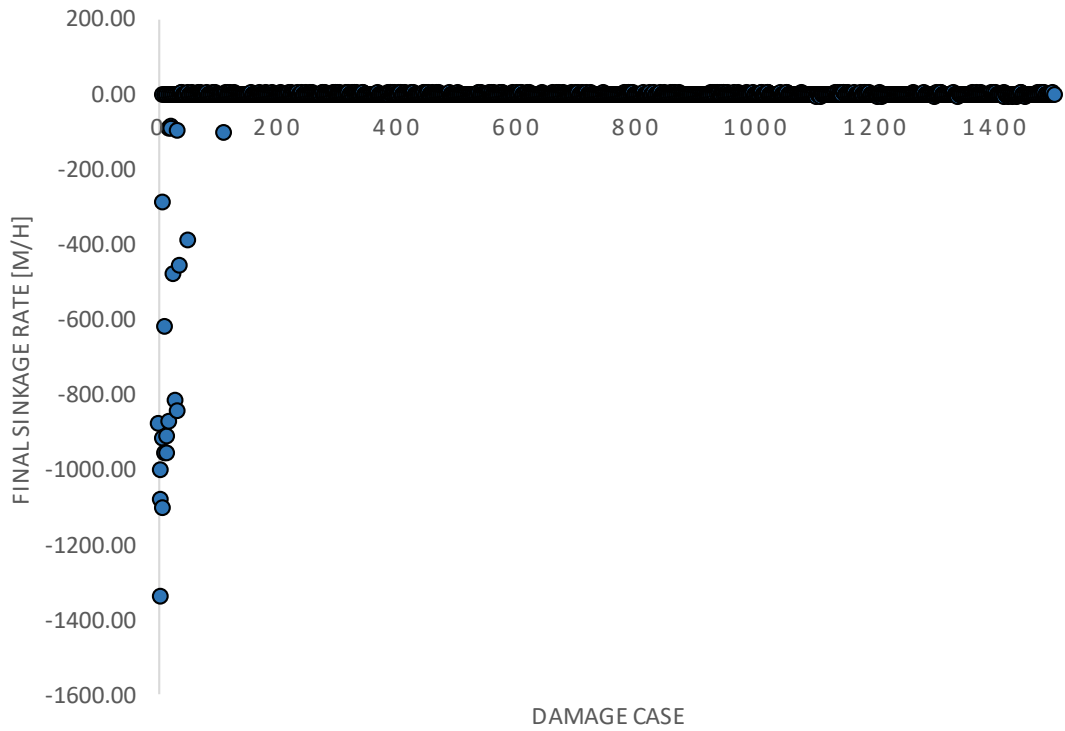


Figure C20: Final rate of change of sinkage

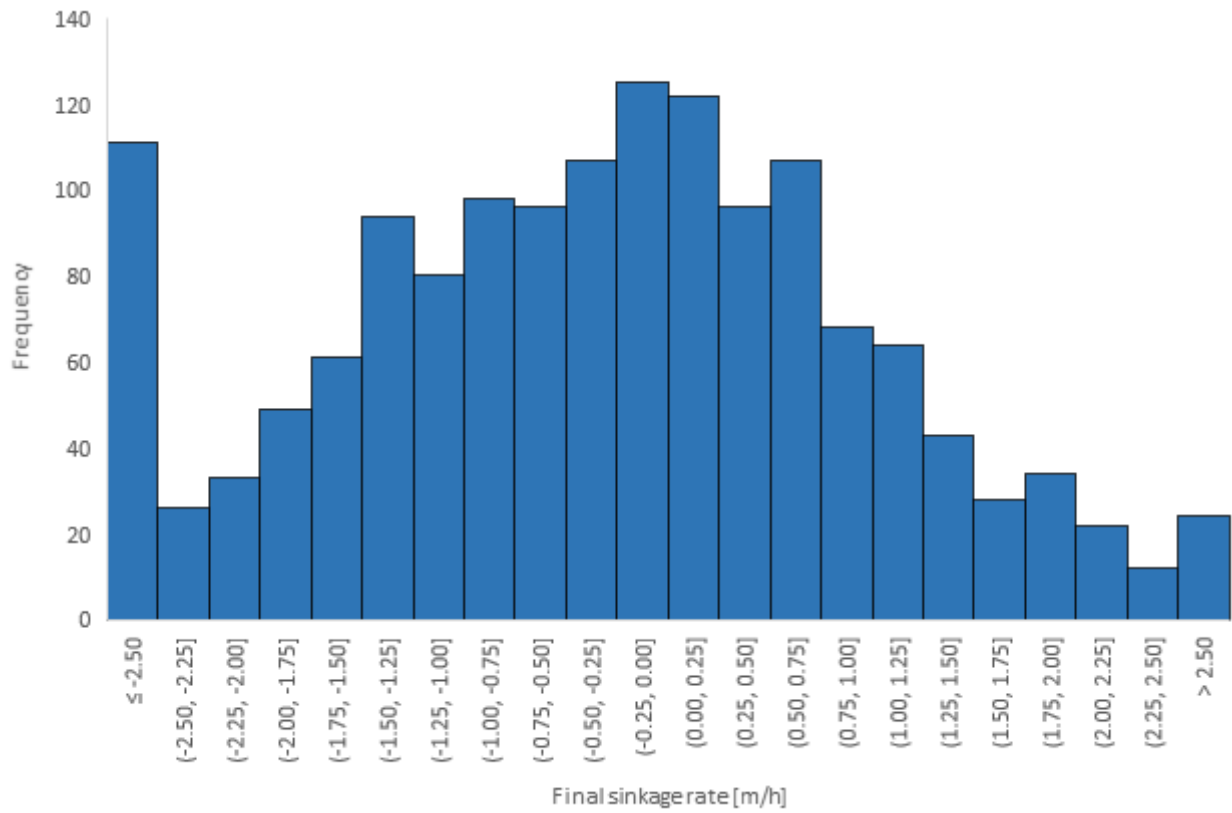


Figure C21: Distribution of final rates of change of sinkage

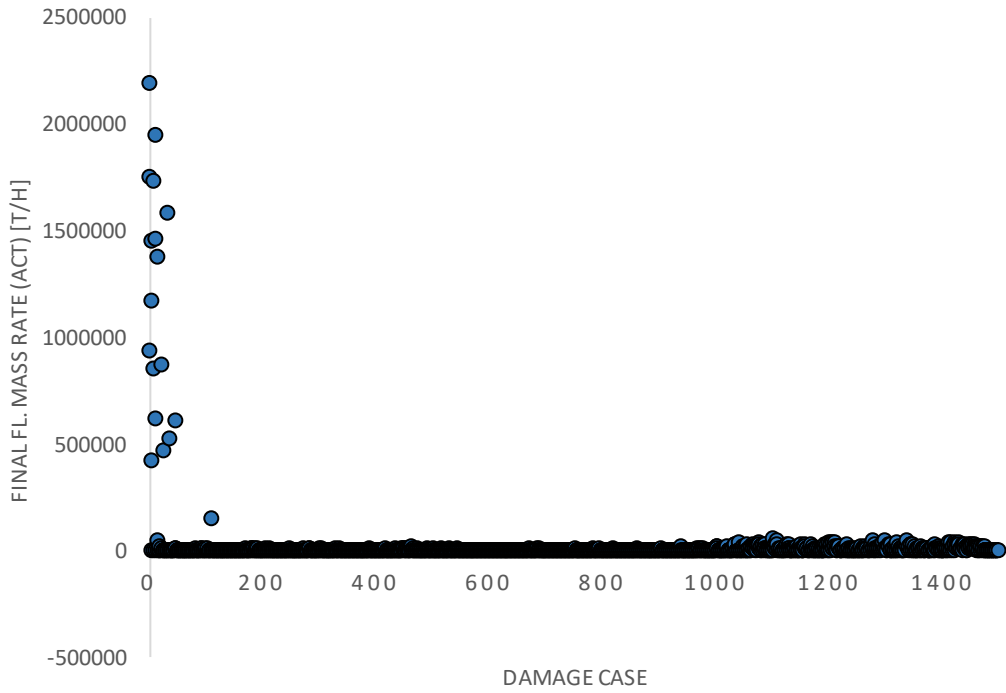


Figure C22: Final rate of change of floodwater mass

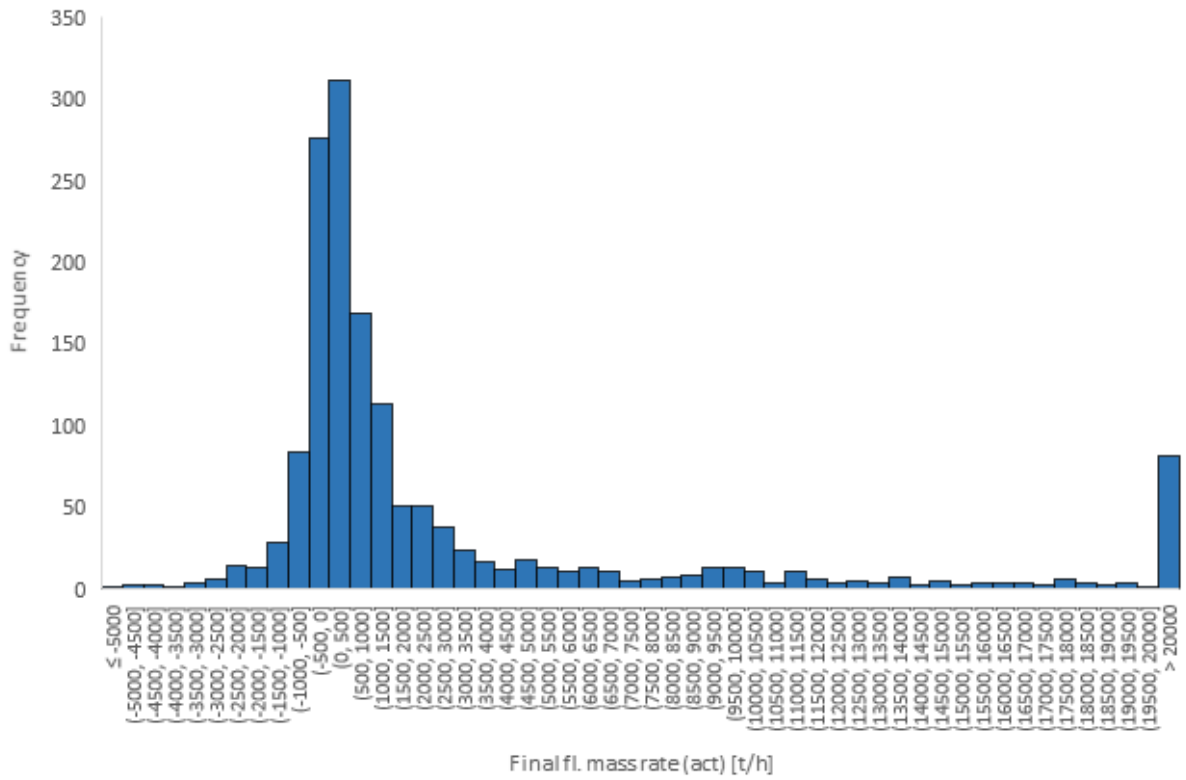


Figure C23: Distribution of final rates of change of floodwater mass

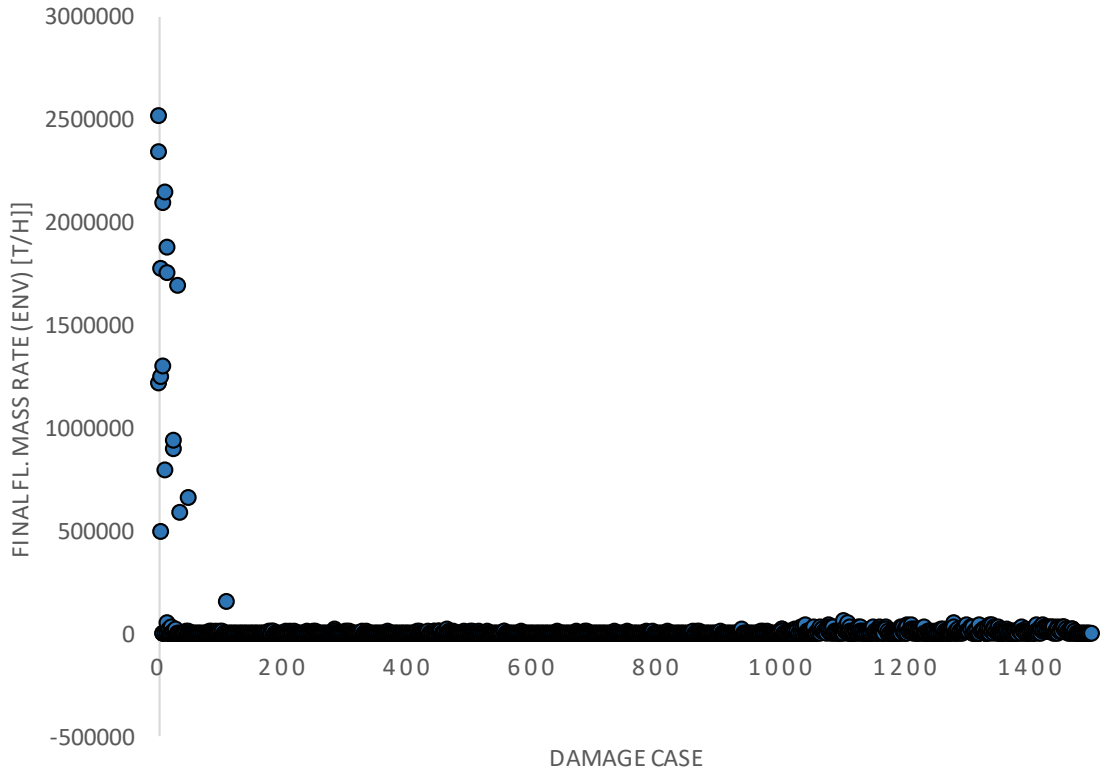


Figure C24: Final rate of change of upper envelope of floodwater mass

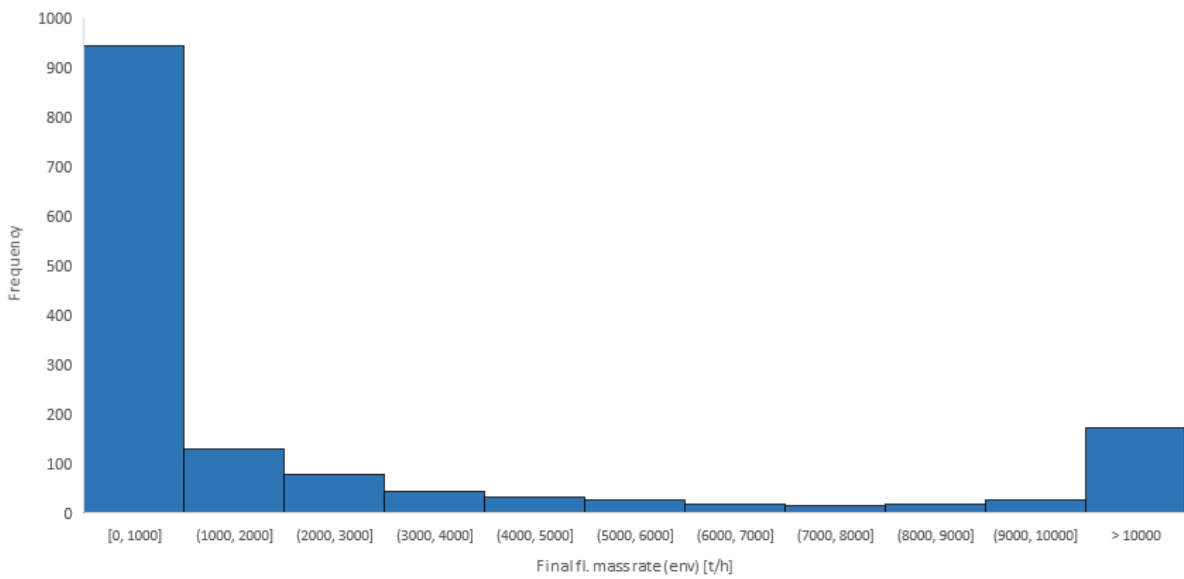


Figure C25: Distribution of final rates of change of upper envelope of floodwater mass

Appendix D: CS2 simulation results (SOLAS 2009 assumptions)

This appendix provides detailed simulation results pertaining to the new build cruise vessel case study presented within Chapter 9. Specifically, the results presented here are those in relation to the assessment conducted in line with SOLAS 2009 assumption. Here, details are provided in relation to the vessel floating position, motions and floodwater accumulation in each simulated case. Furthermore, these are viewed in relation to the maximum values recorded over the duration of each simulation which are followed by values recorded during the final stage.

Maximum Values

Here, the peak values realised within each simulated case are presented with respect to roll angle, average heel recorded over 3 minutes, and the maximum floodwater accumulated.

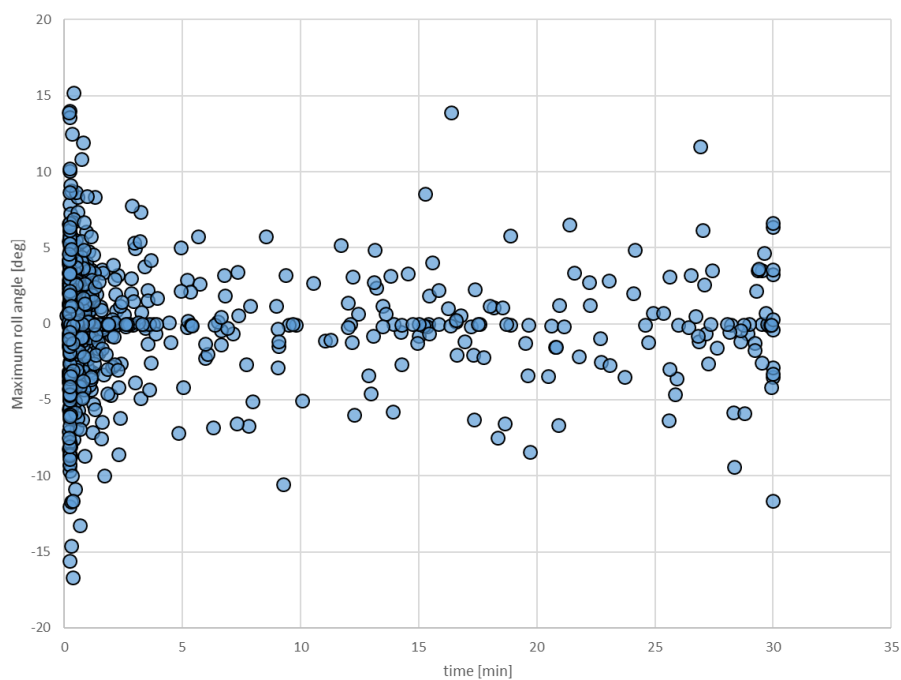


Figure D1: Occurrence of maximum roll angles

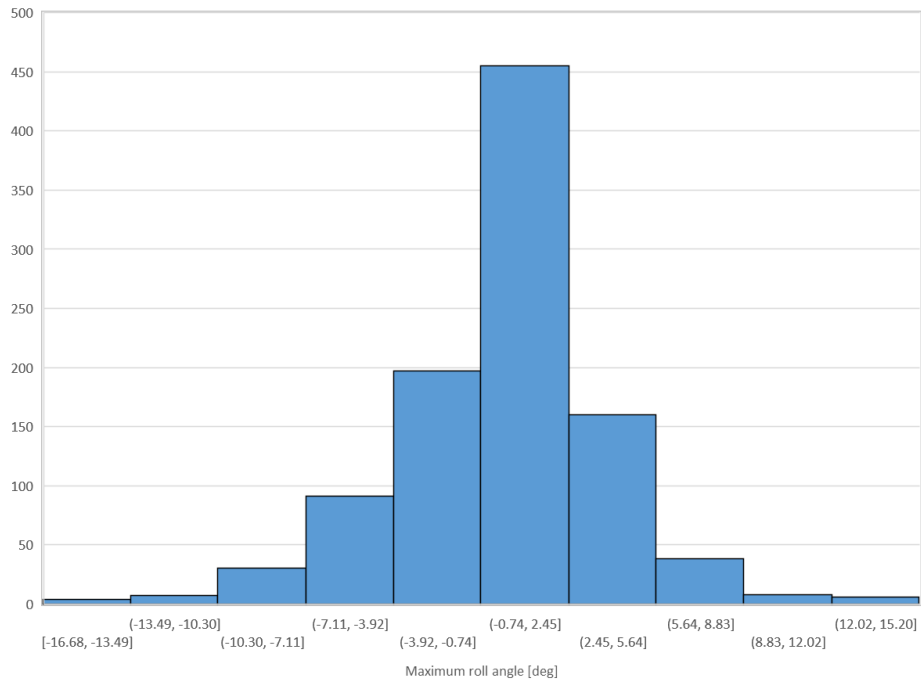


Figure D2: Distribution of magnitudes for maximum roll angles

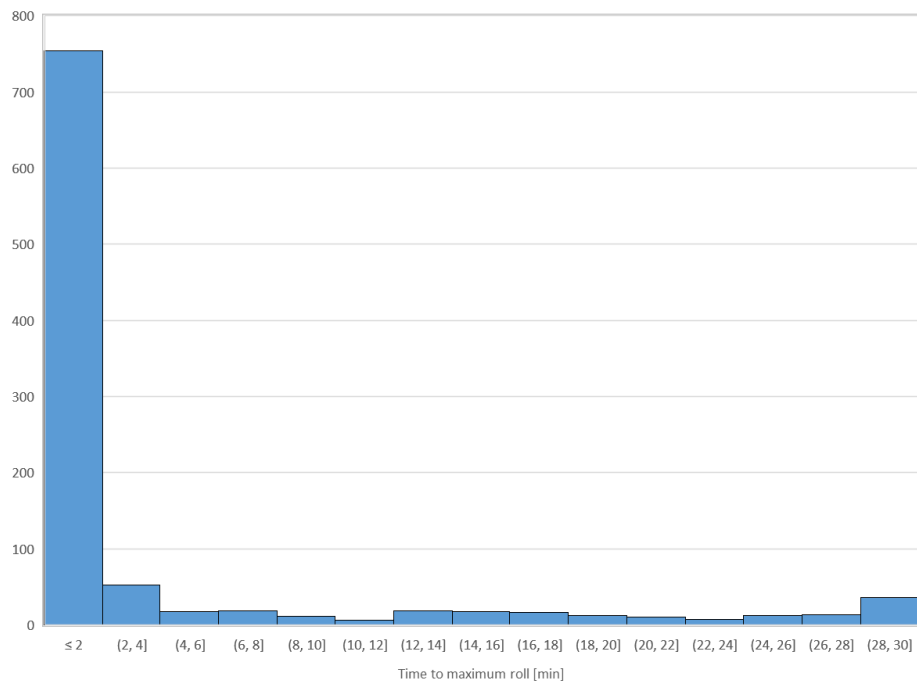


Figure D3: Distribution of times of occurrence of maximum roll angles

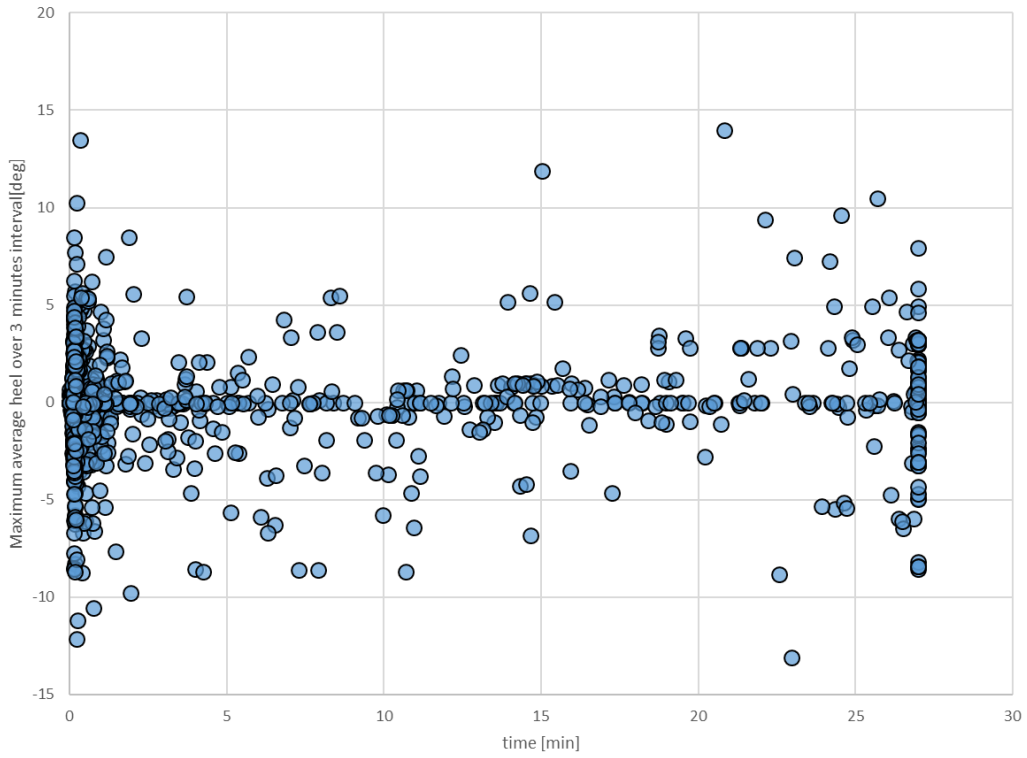


Figure D4: Occurrence of maximum 3-minute averages of heel angles

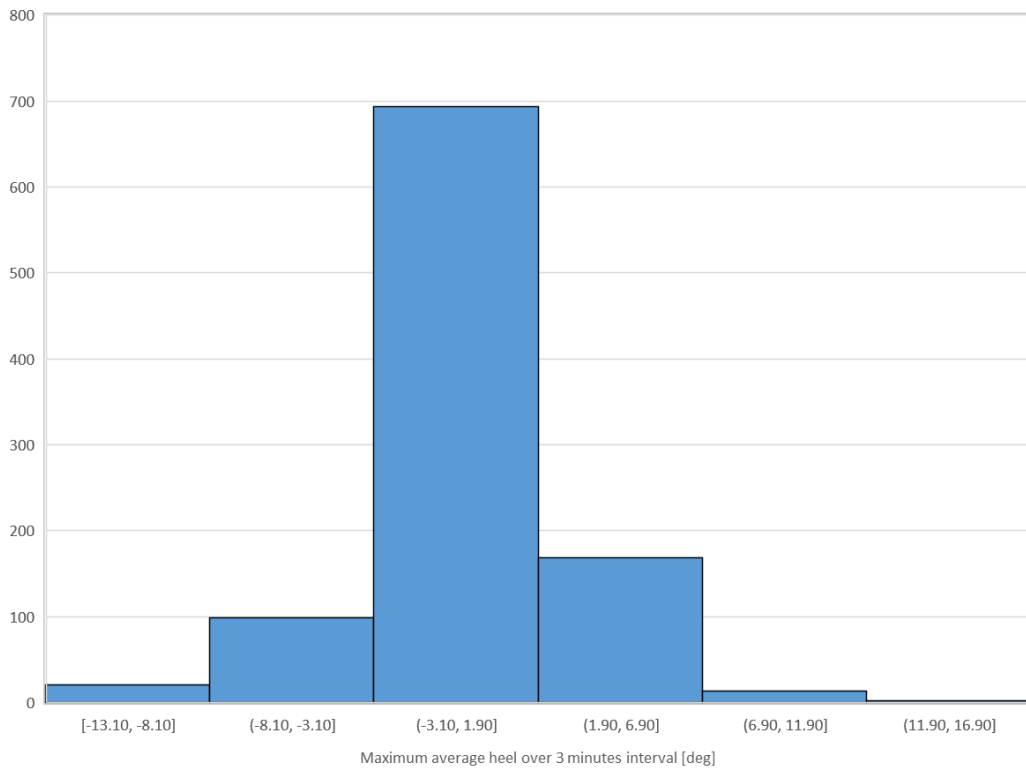


Figure D5: Distribution of maximum 3-minute averages of heel angles

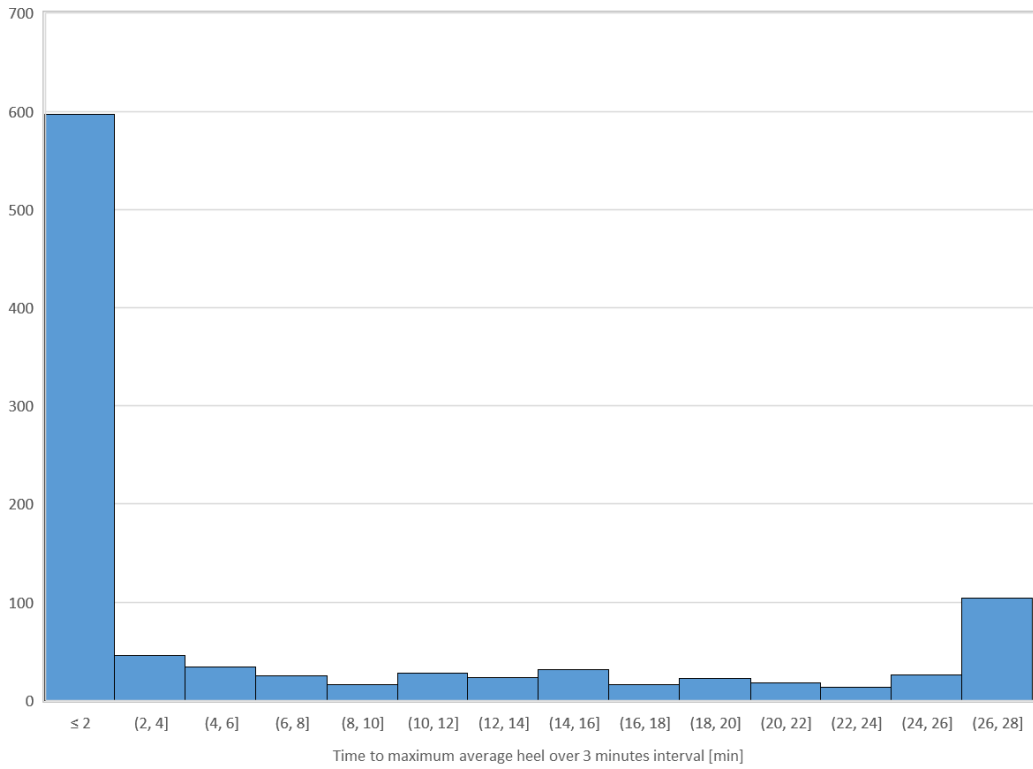


Figure D6: Distribution of time of occurrences of maximum 3-minute averages of heel angles

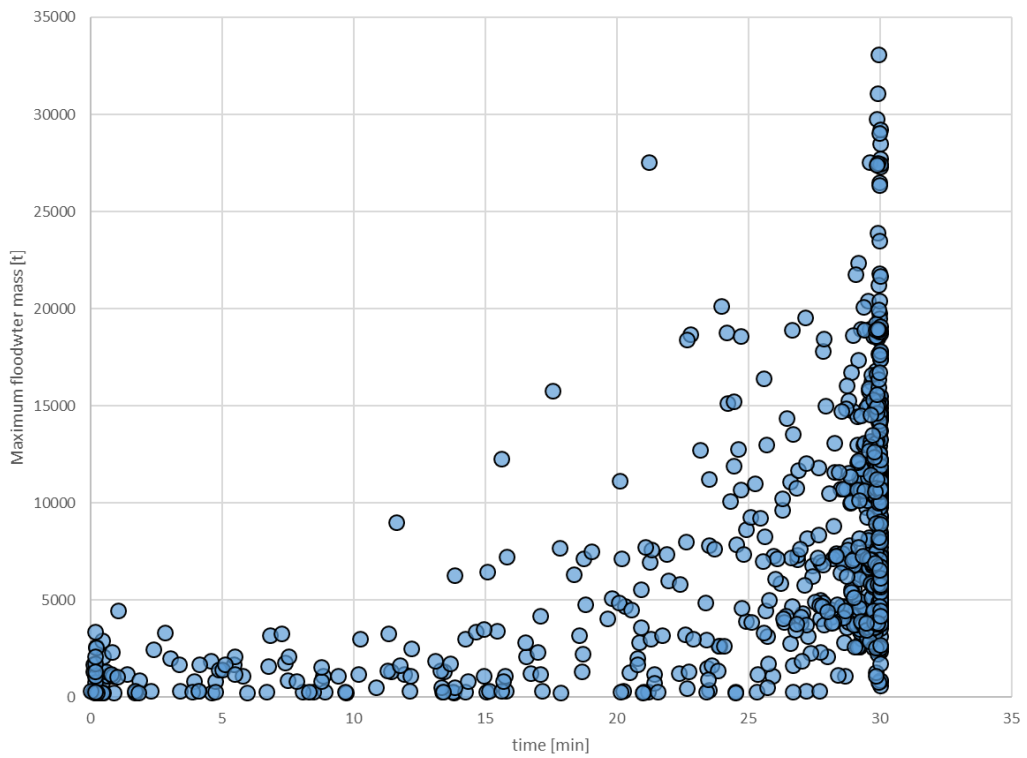


Figure D7: Occurrence of maximum amount of floodwater mass

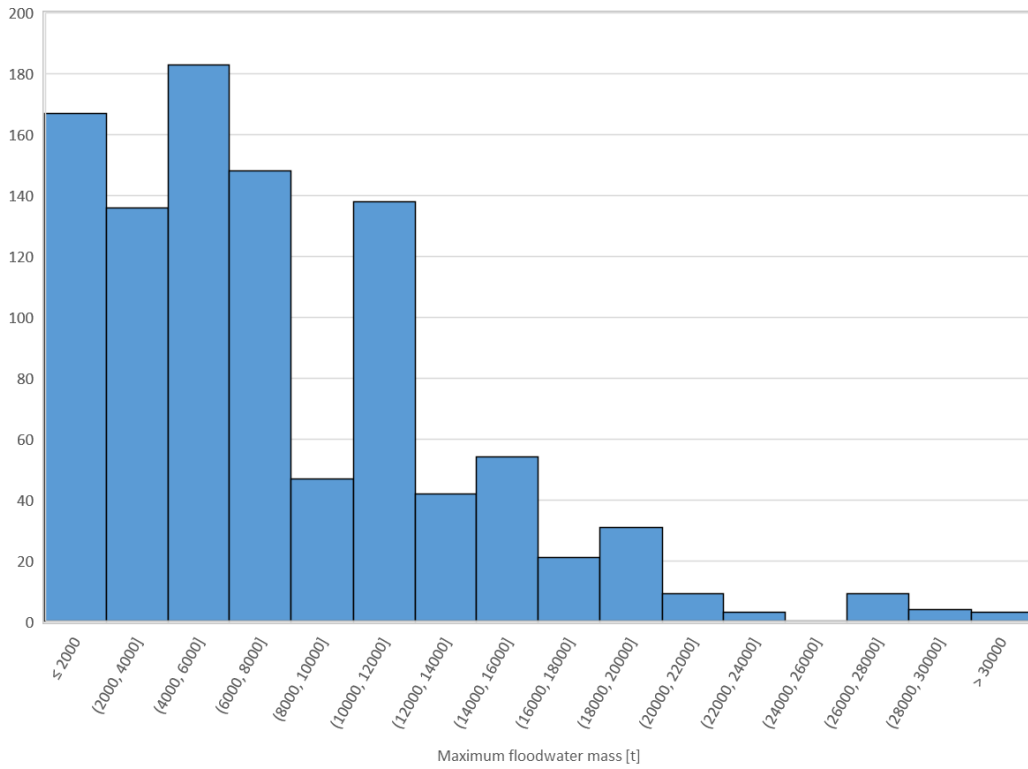


Figure D8: Distribution of maximum amount of floodwater mass

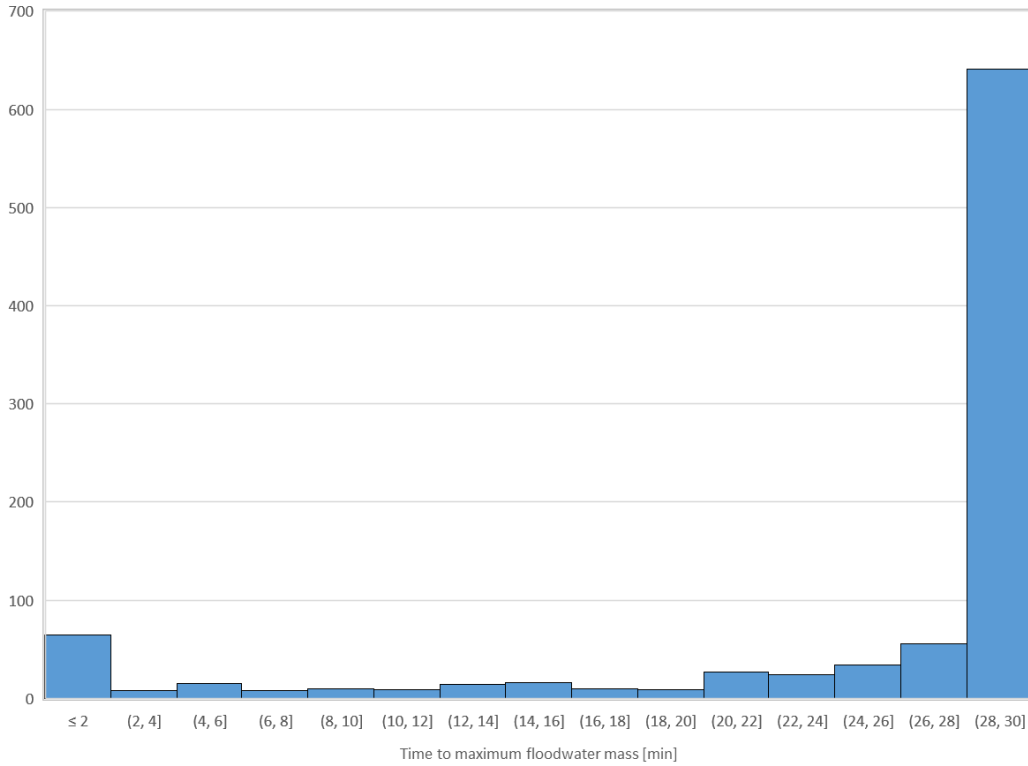


Figure D9: Distribution of time occurrence of maximum amount of floodwater mass

Final values

Within this section, values recorded during the final stage of flooding are presented in relation to average heel, average trim and sinkage

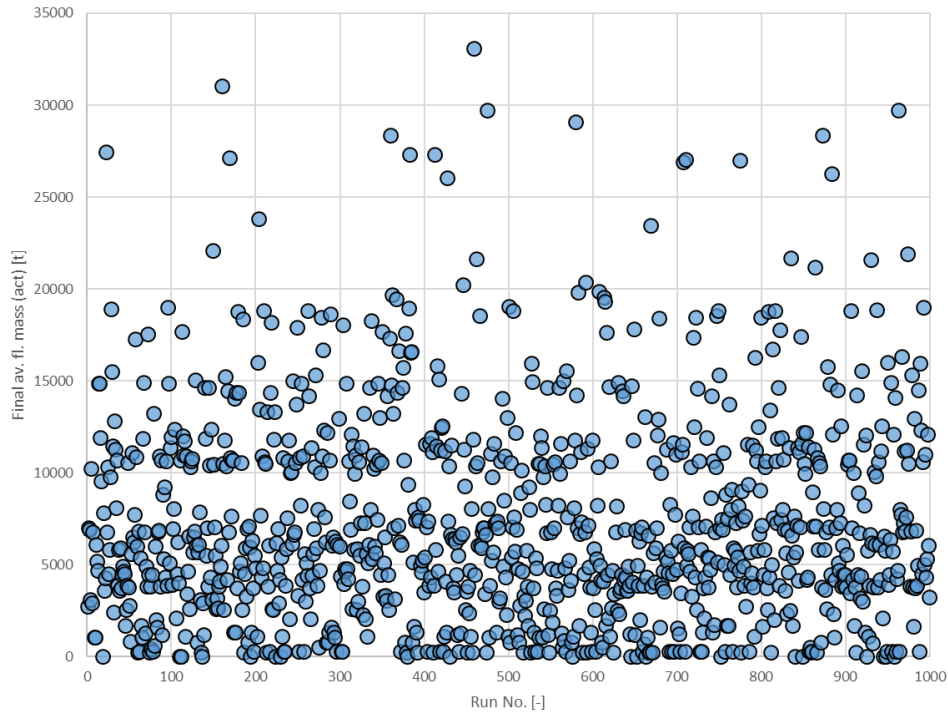


Figure D10: Final 3-minute average of floodwater mass

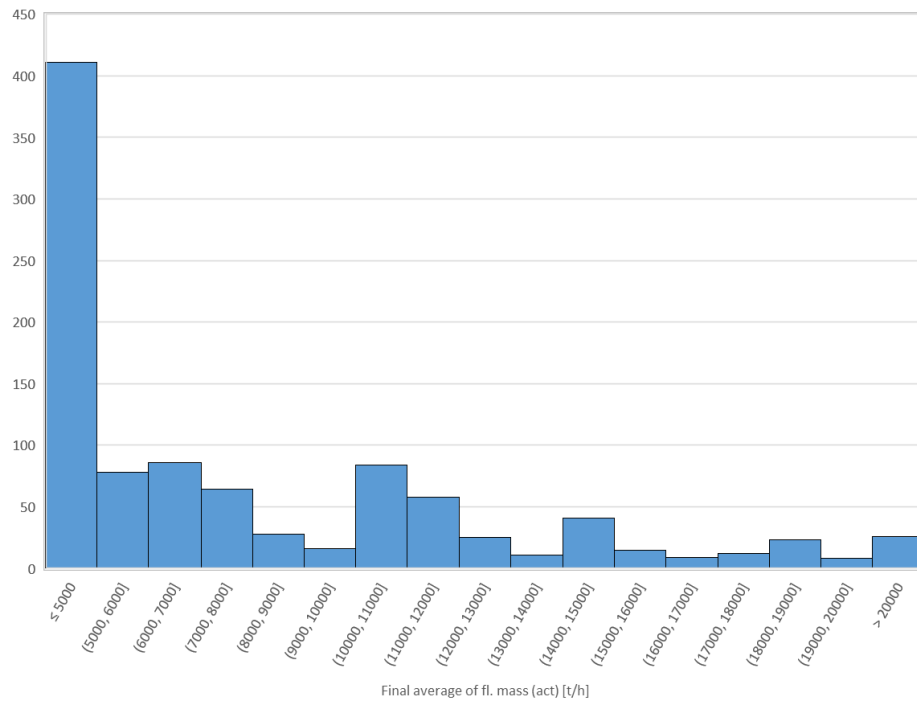


Figure D12: Distribution of final 3-minute average of floodwater mass

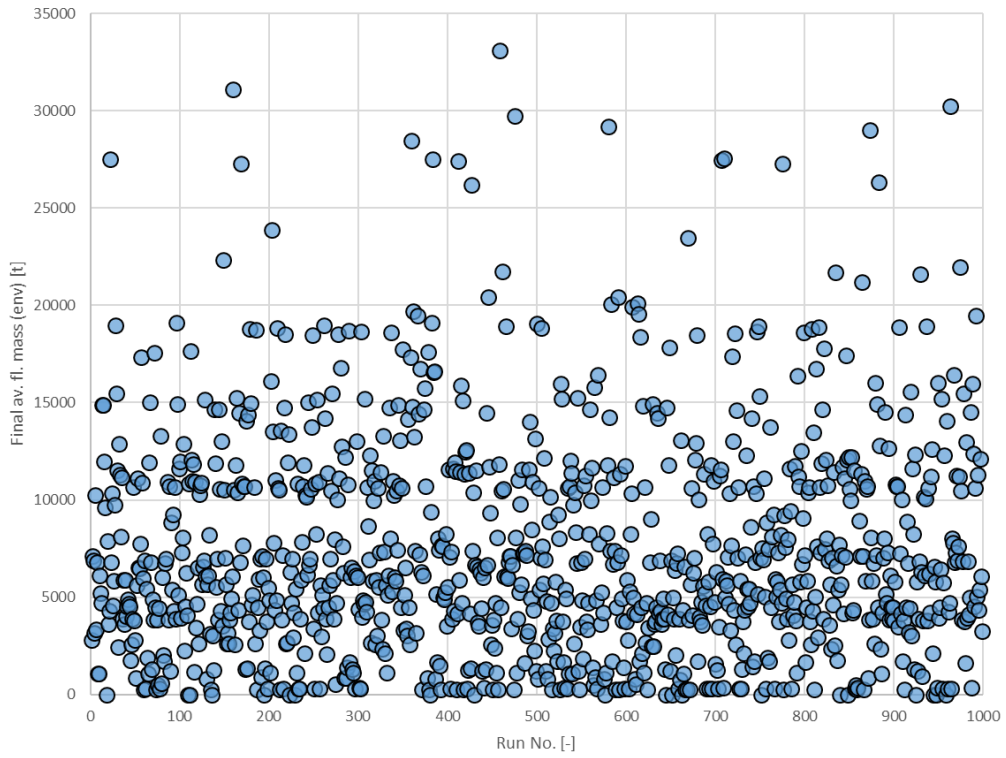


Figure D13: Final 3-minute average of upper envelope of floodwater mass

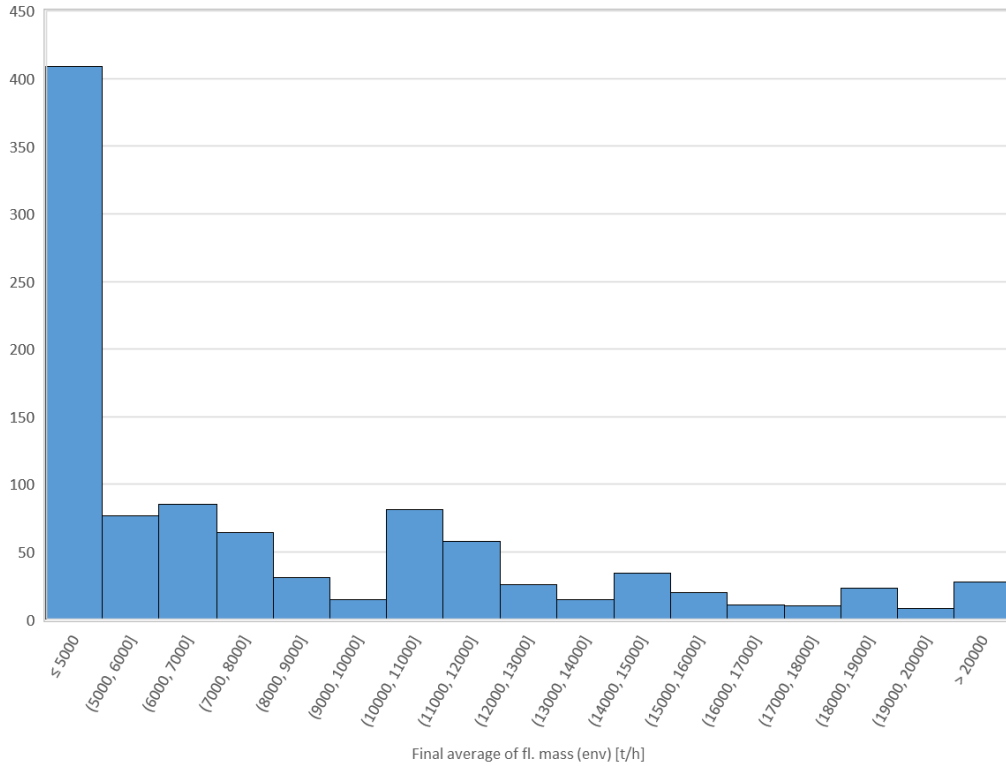


Figure D14: Distribution of final 3-minute average of upper envelope of floodwater

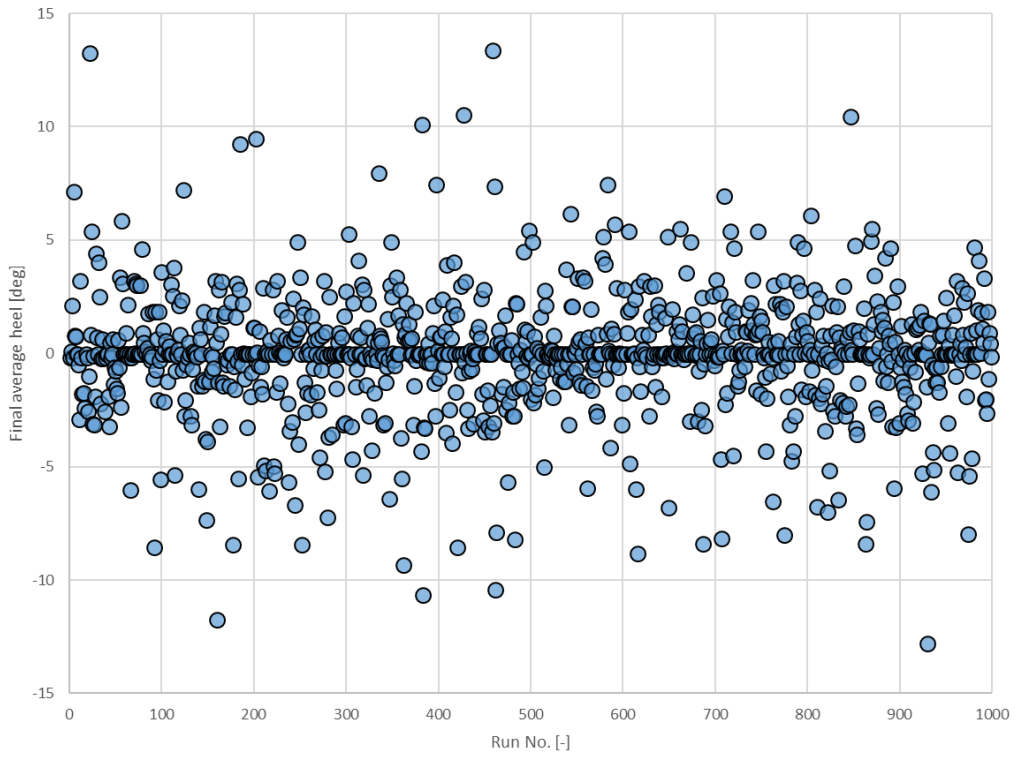


Figure D15: Final 3-minutes average of heel

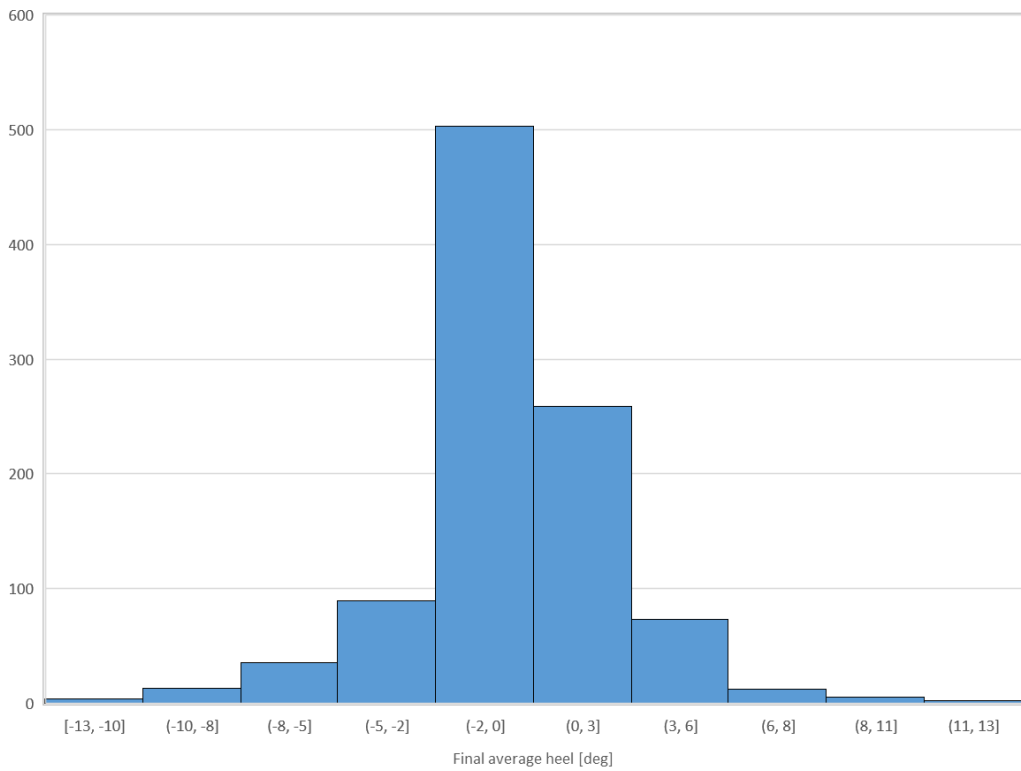


Figure D16: Distribution of final 3-minute average heel

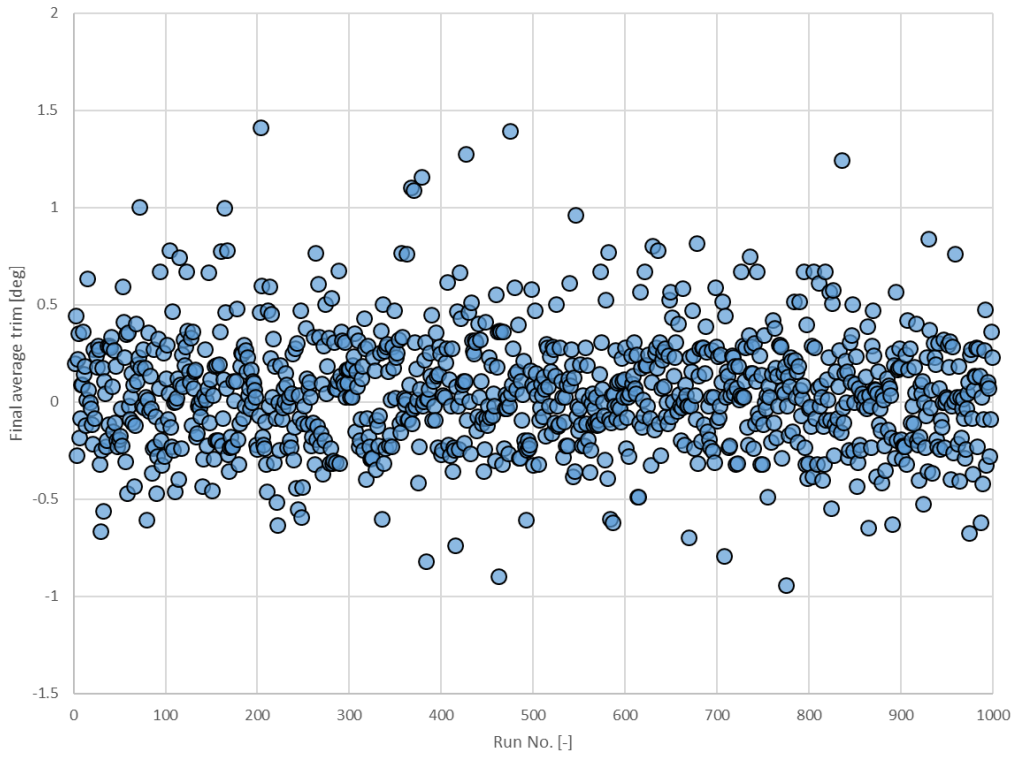


Figure D17: Final 3-minute average trim

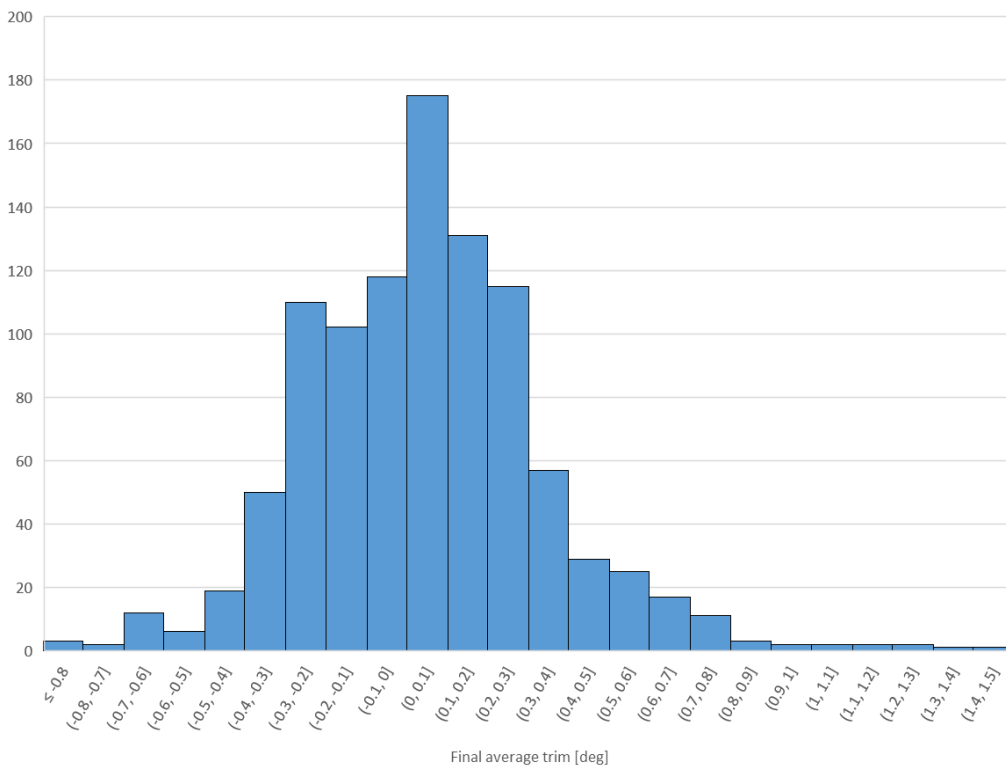


Figure D18: Distribution of final 3-minute average trim

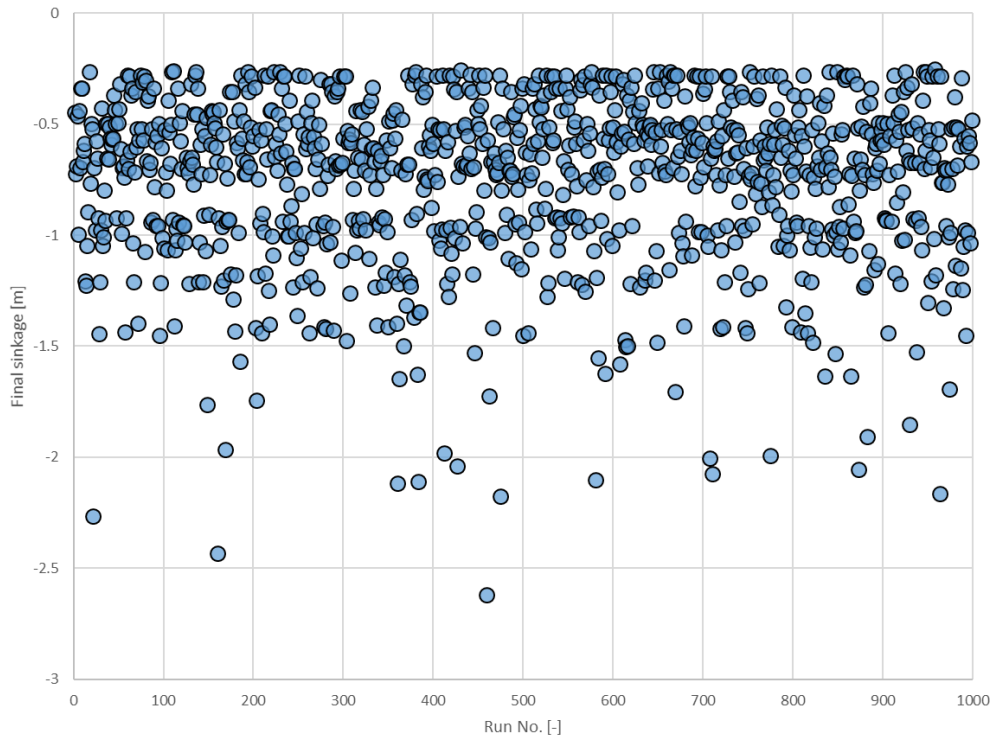


Figure D19: Final 3-minute average sinkage

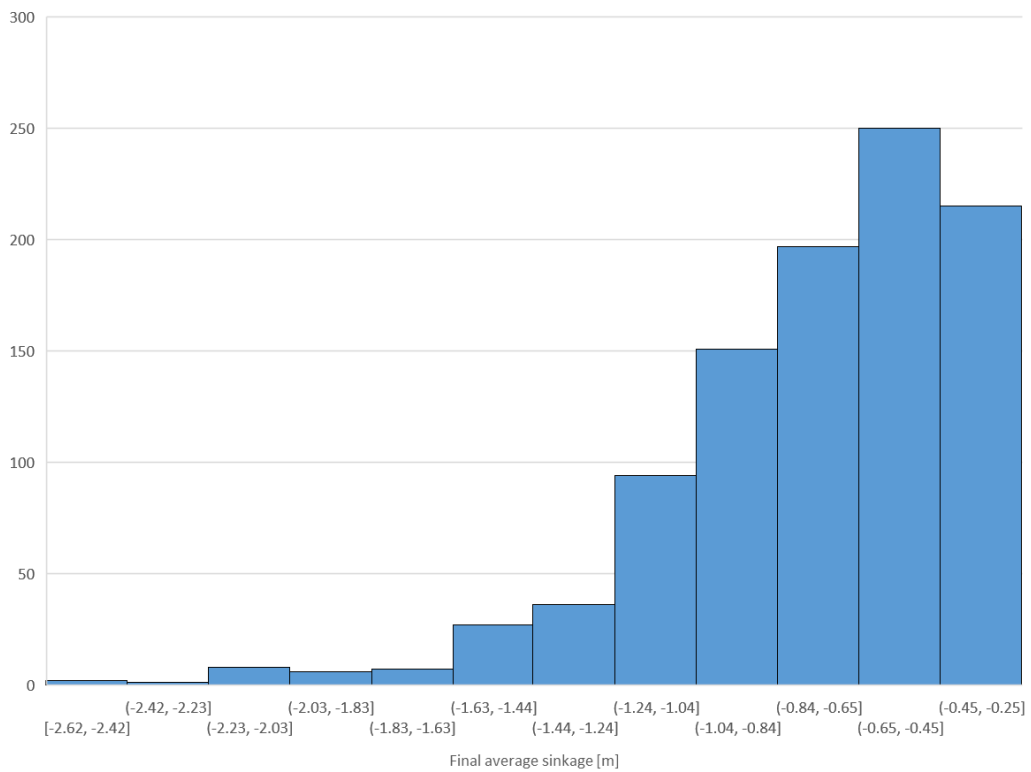


Figure D20: Distribution of final 3-minute average sinkage

Final rates of change

Here, the rate of change in important properties relating to the floating position of the vessel and floodwater mass accumulation are provided in relation to the final stages of the simulation.

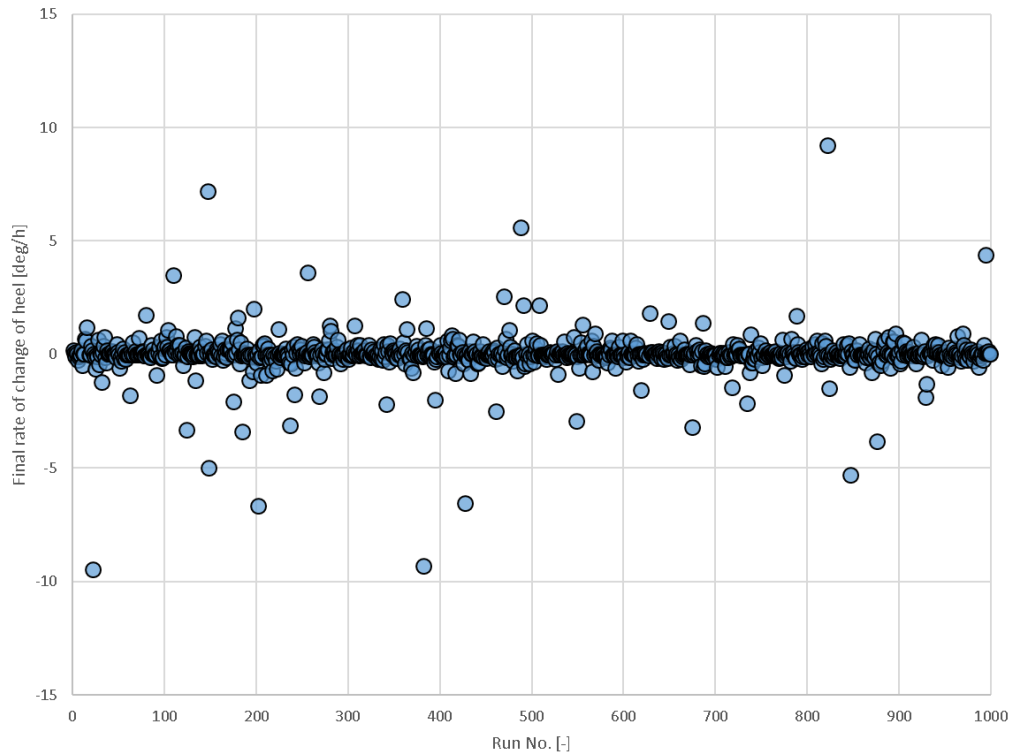


Figure D21: Final rate of change of heel angle

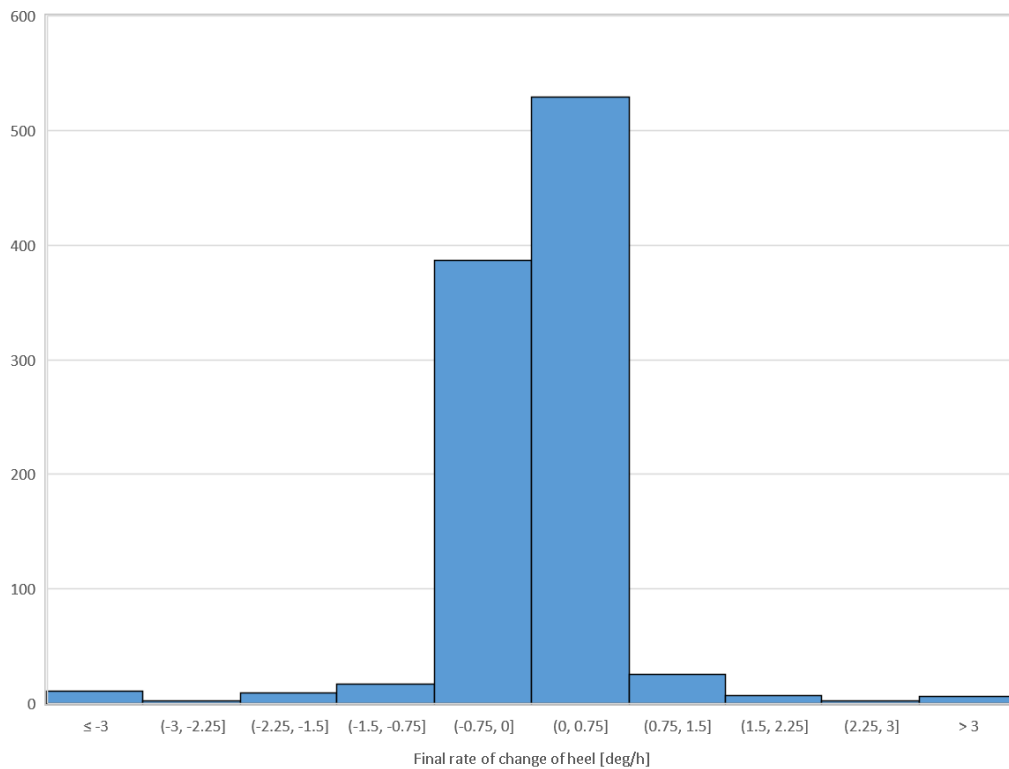


Figure D22: Distribution of final rates of change of heel angle

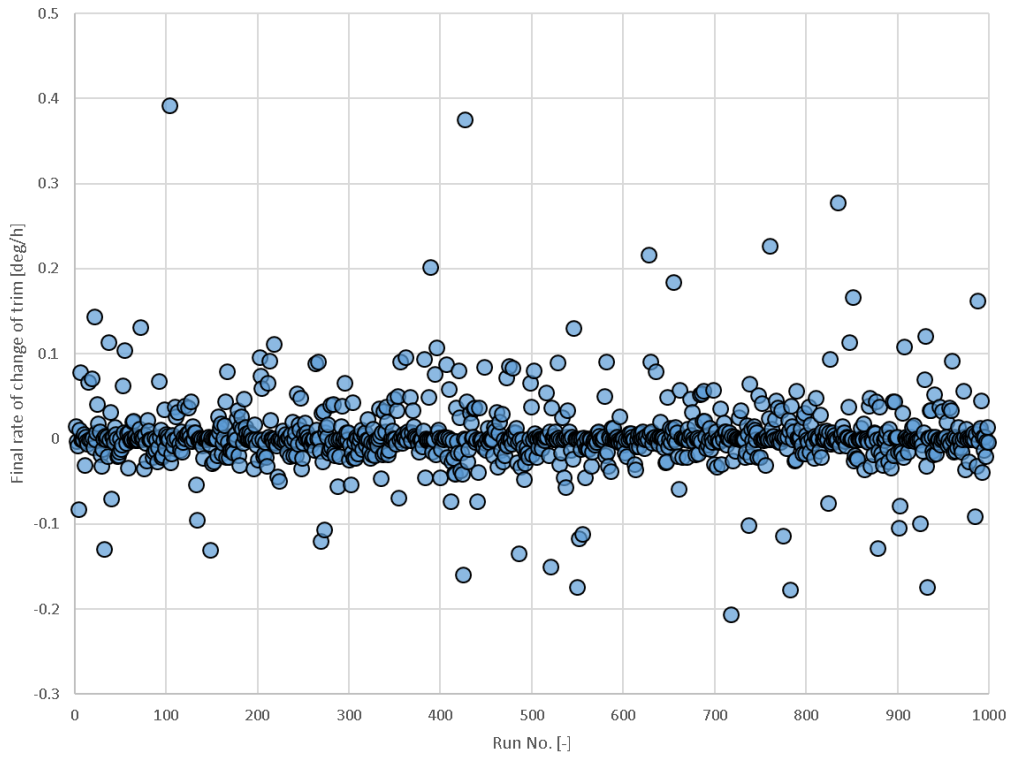


Figure D23: Final rates of change of trim

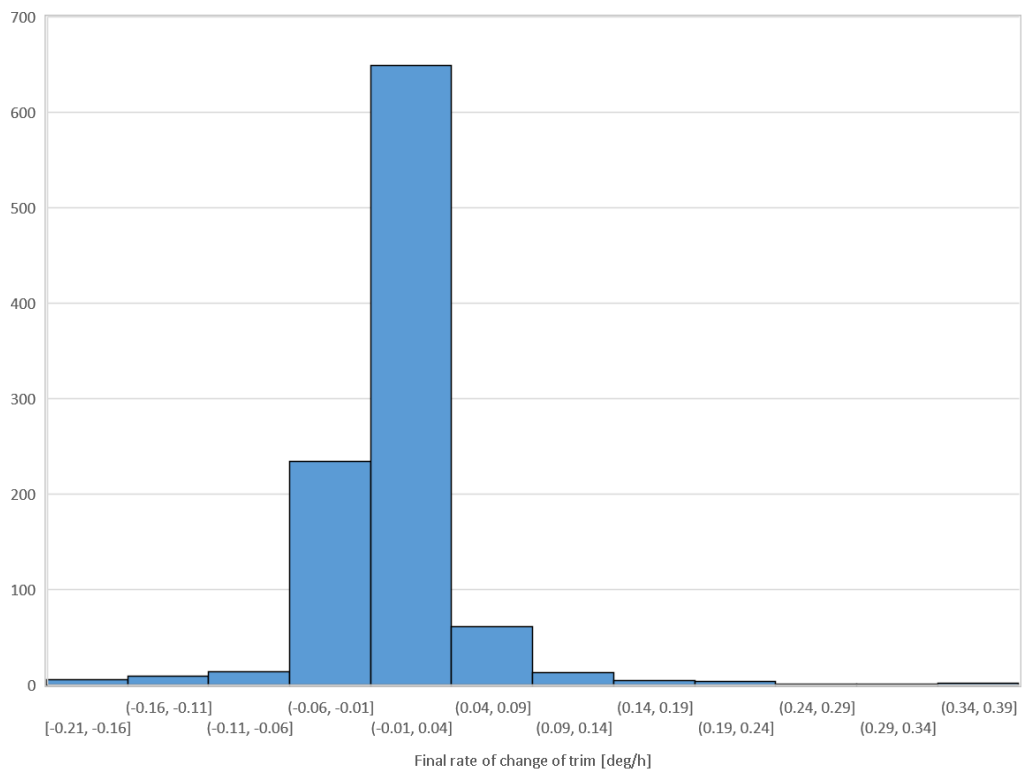


Figure D24: Distribution of final rates of change of trim

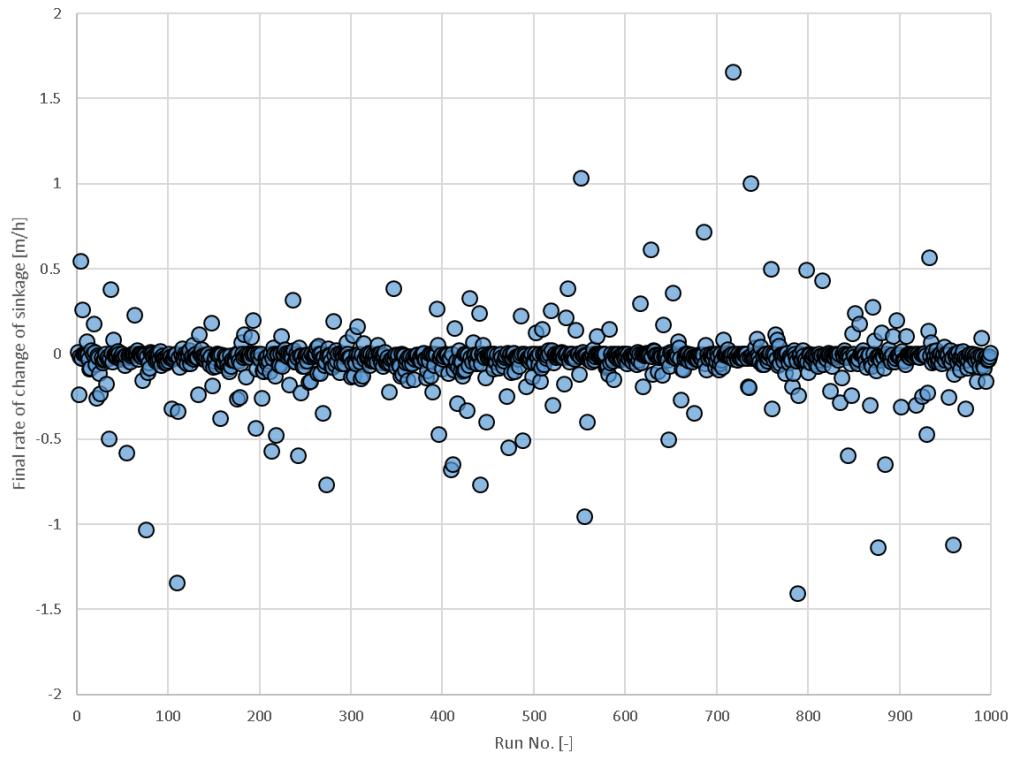


Figure D25: Final rates of change of sinkage

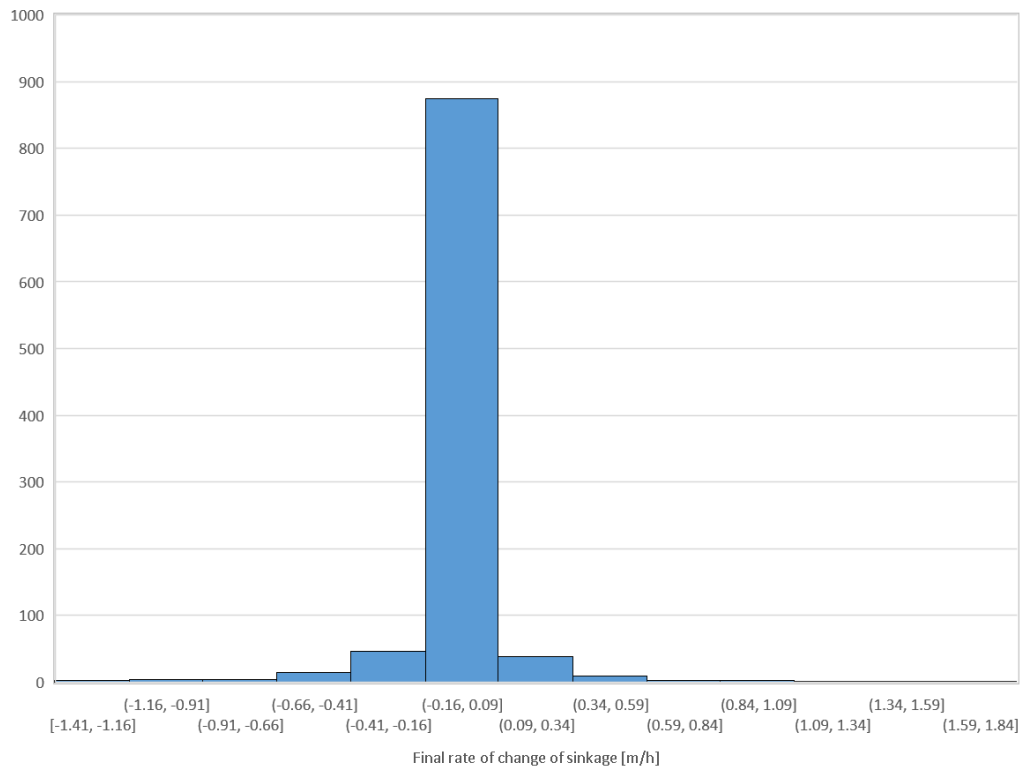


Figure D26: Distribution of final rates of change of sinkage

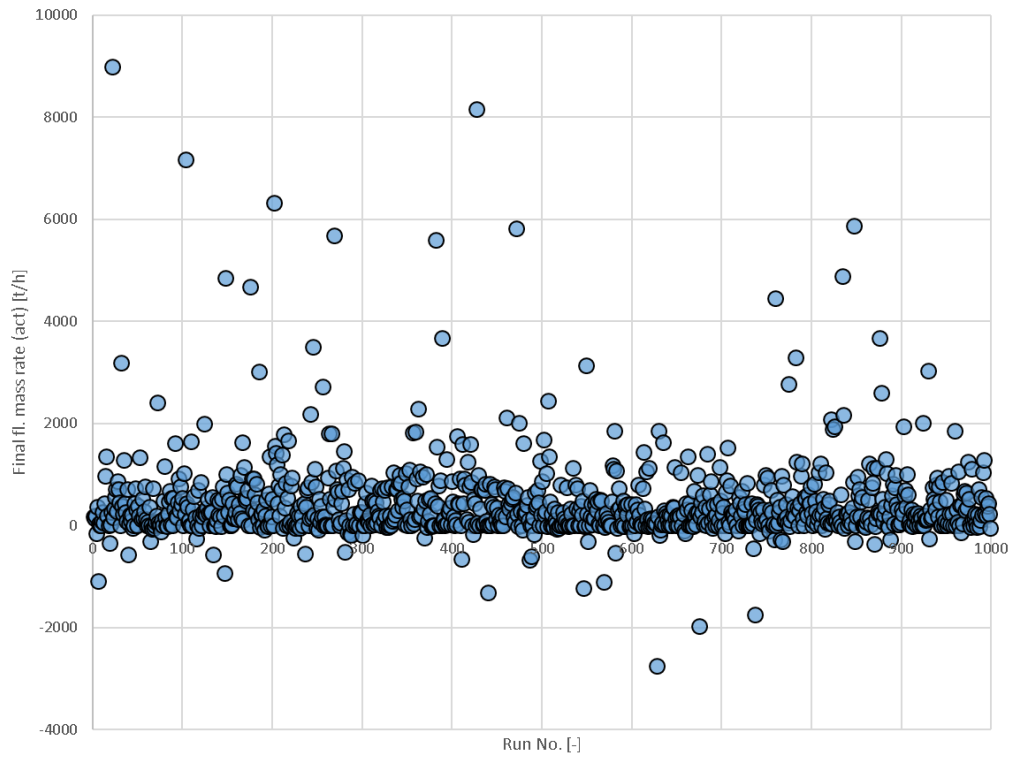


Figure D27: Final rates of change of floodwater mass

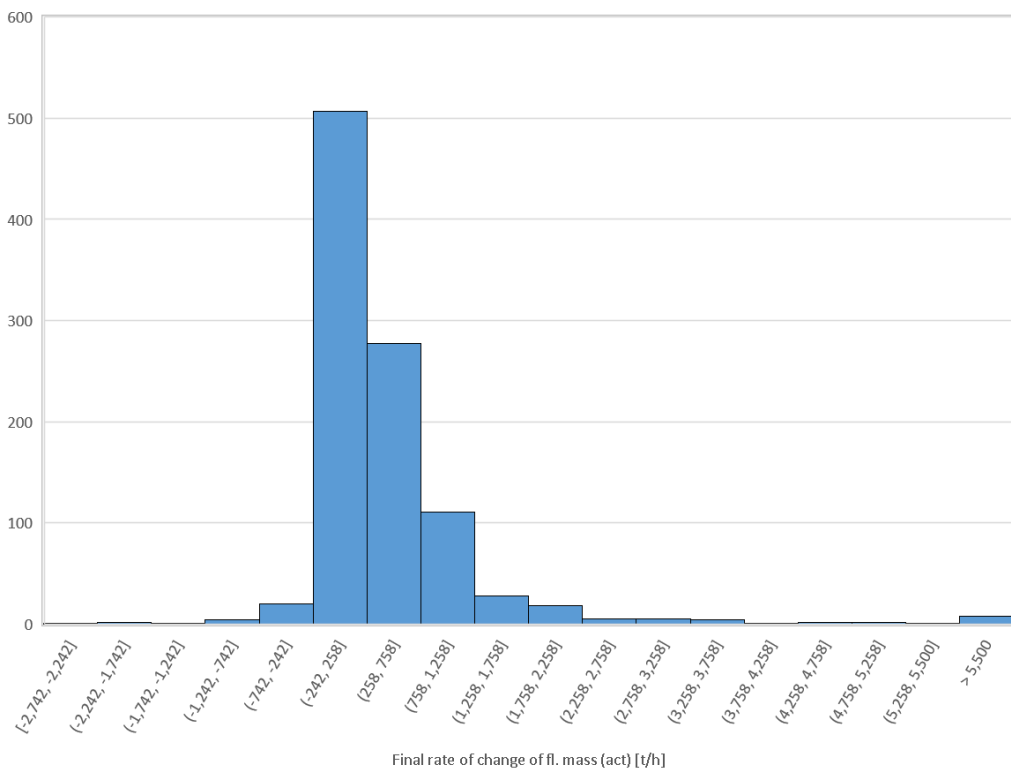


Figure D28: Distribution of final rates of change of floodwater mass

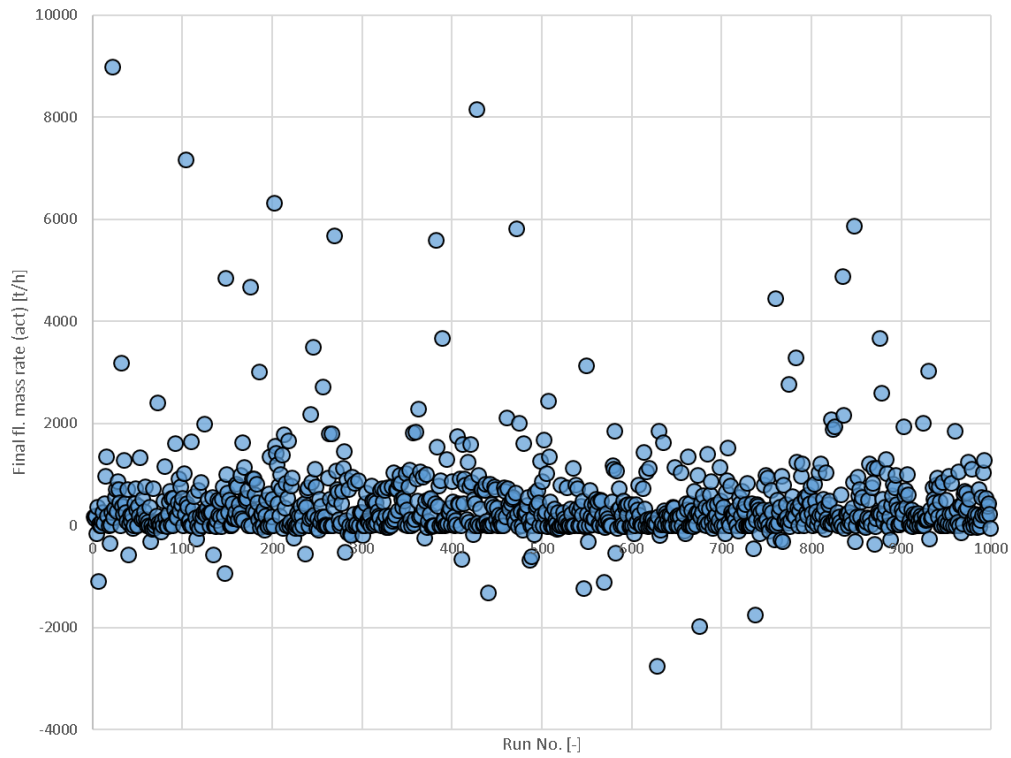


Figure D29: Final rates of change of upper envelope of floodwater mass

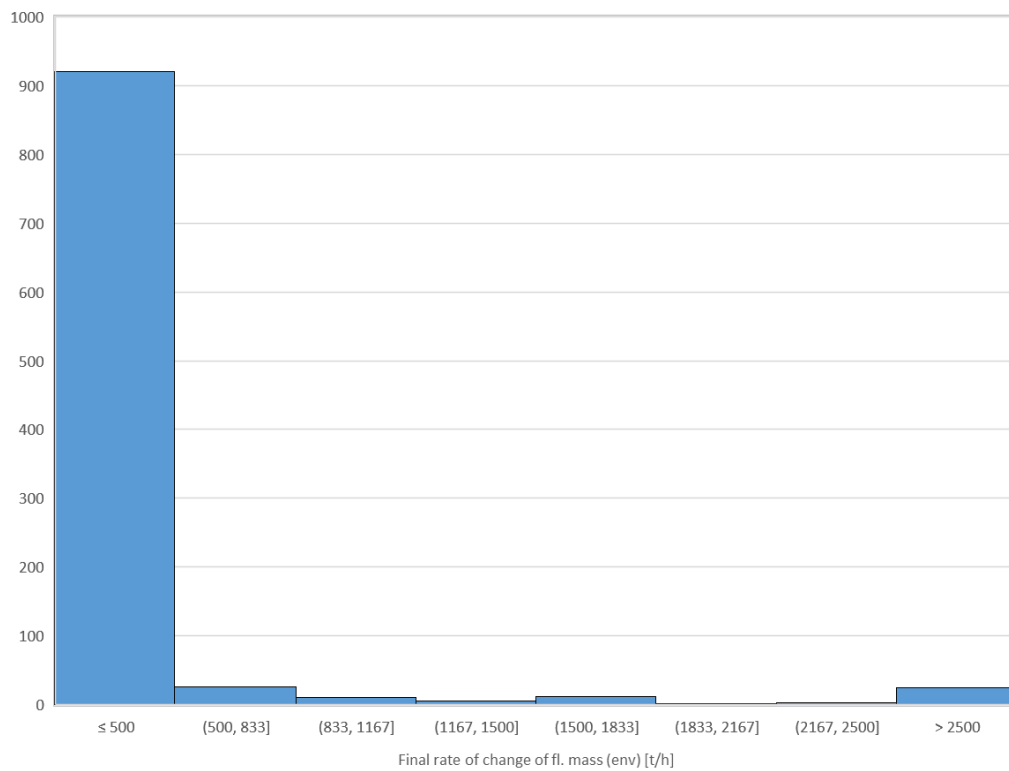


Figure D30: Distribution final rates of change of upper envelope of floodwater mass

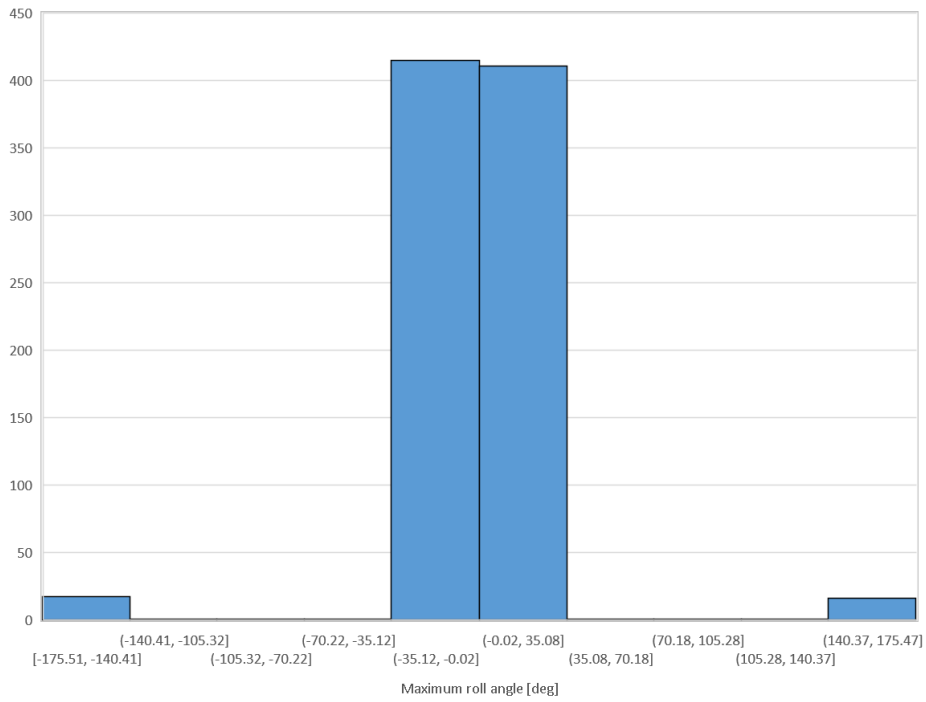


Figure E2: Distribution of magnitudes for maximum roll angles

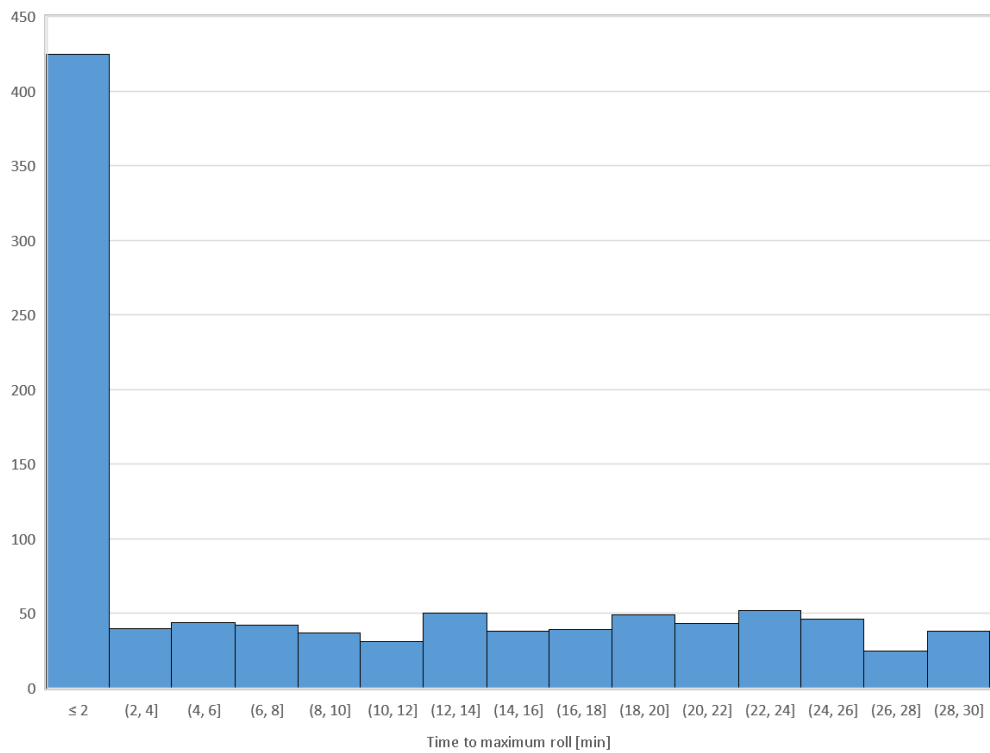


Figure E3: Distribution of times of occurrence of maximum roll angles

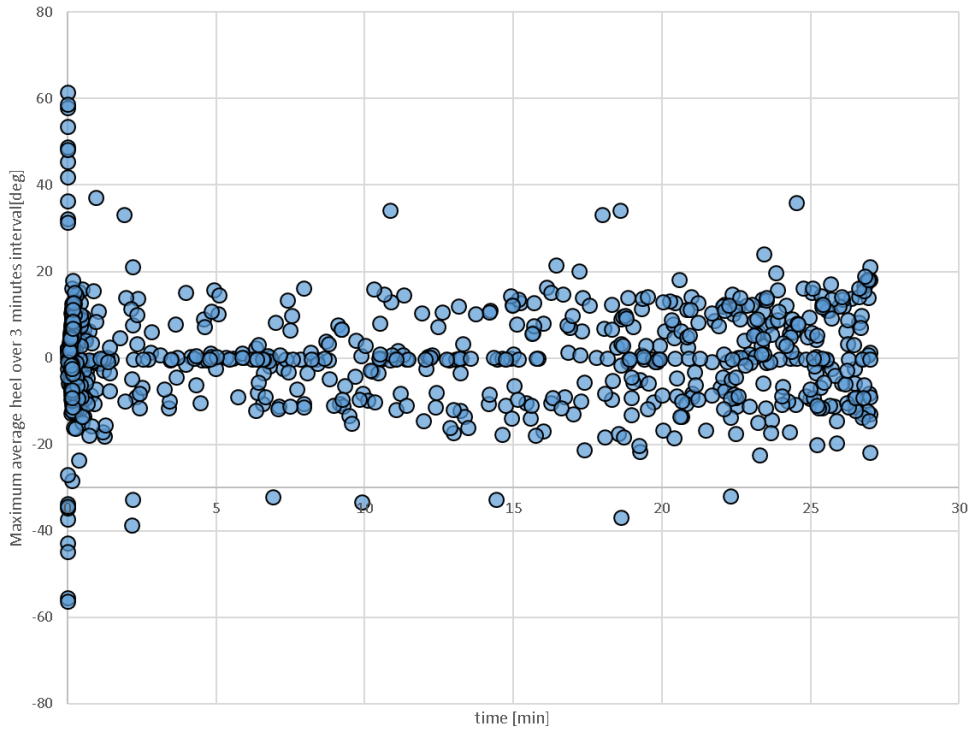


Figure E4: Occurrence of maximum 3-minute averages of heel angles

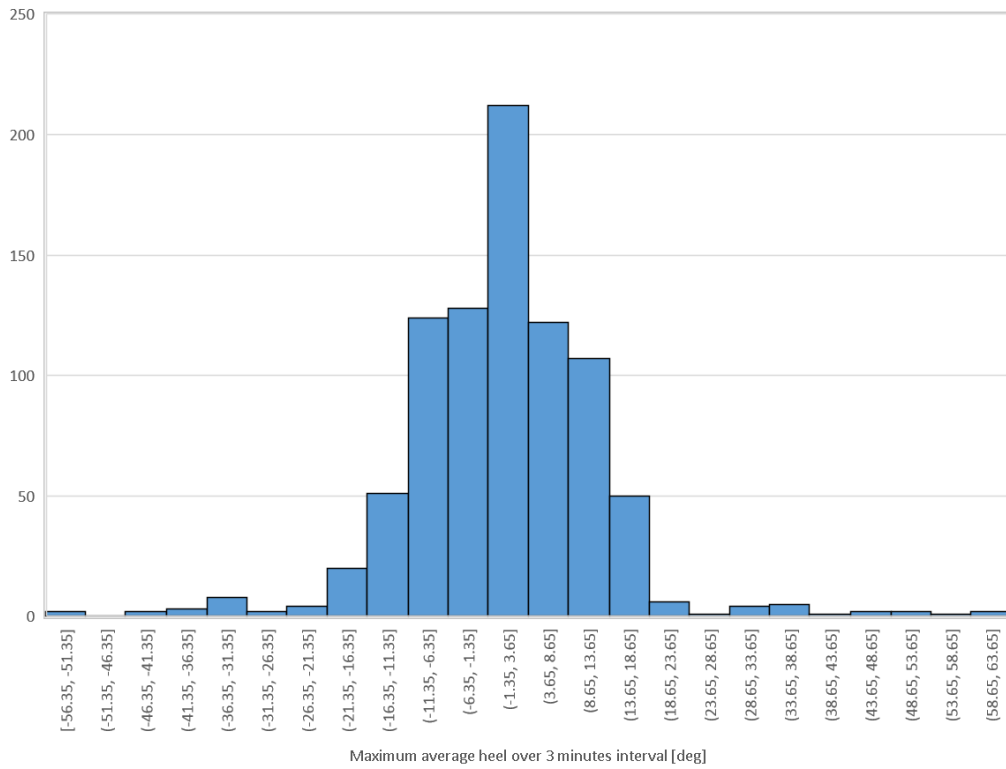


Figure E5: Distribution of maximum 3-minute averages of heel angles

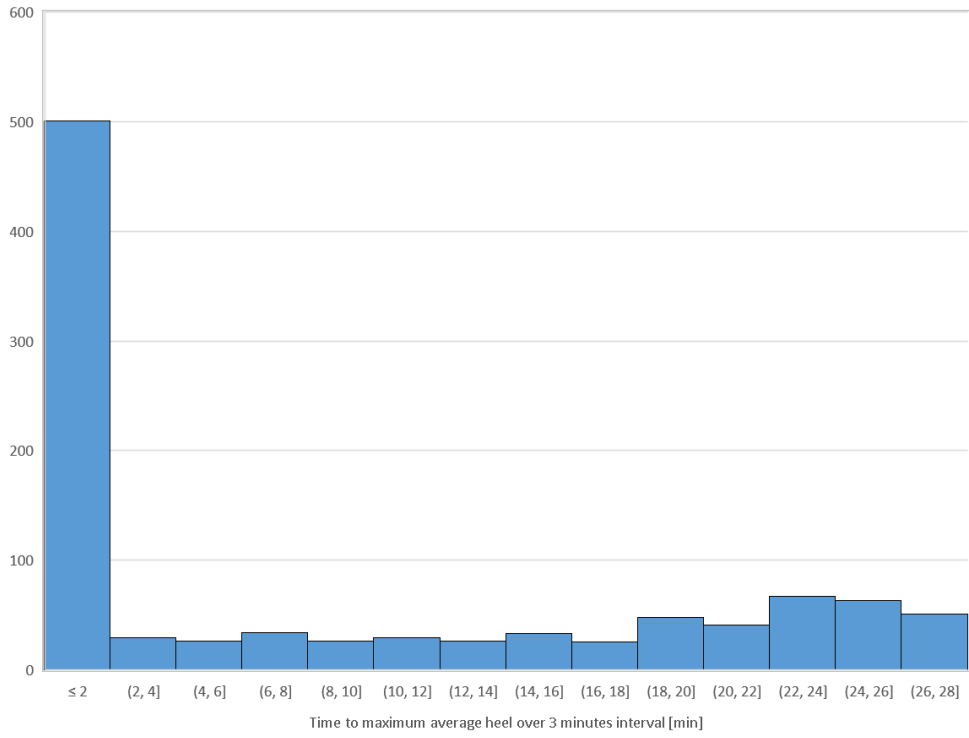


Figure E6: Distribution of time of occurrences of maximum 3-minute averages of heel angles

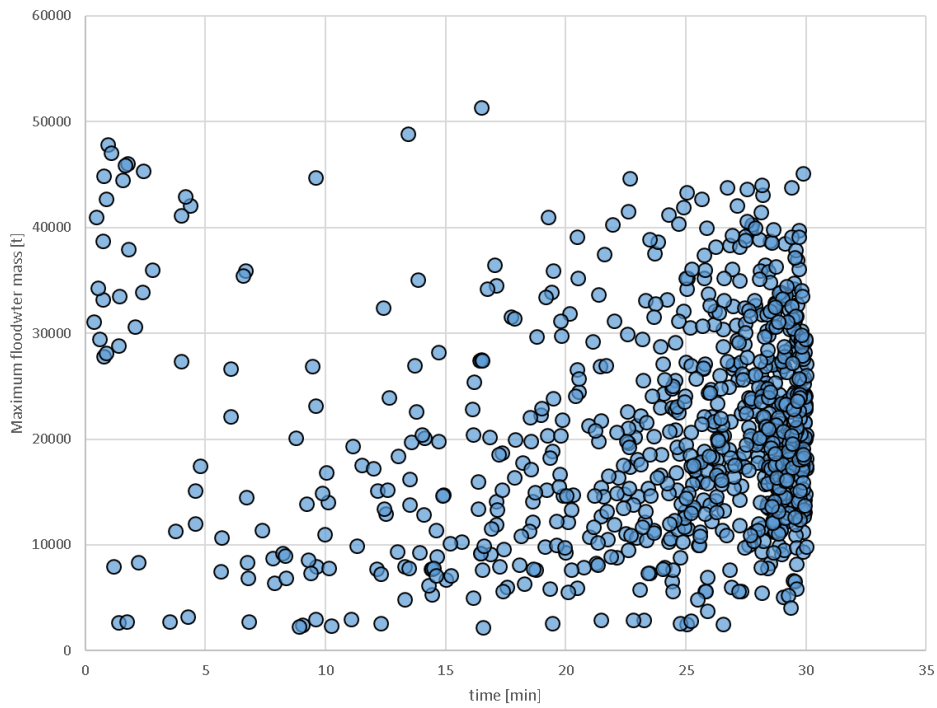


Figure E7: Occurrence of maximum amount of floodwater mass

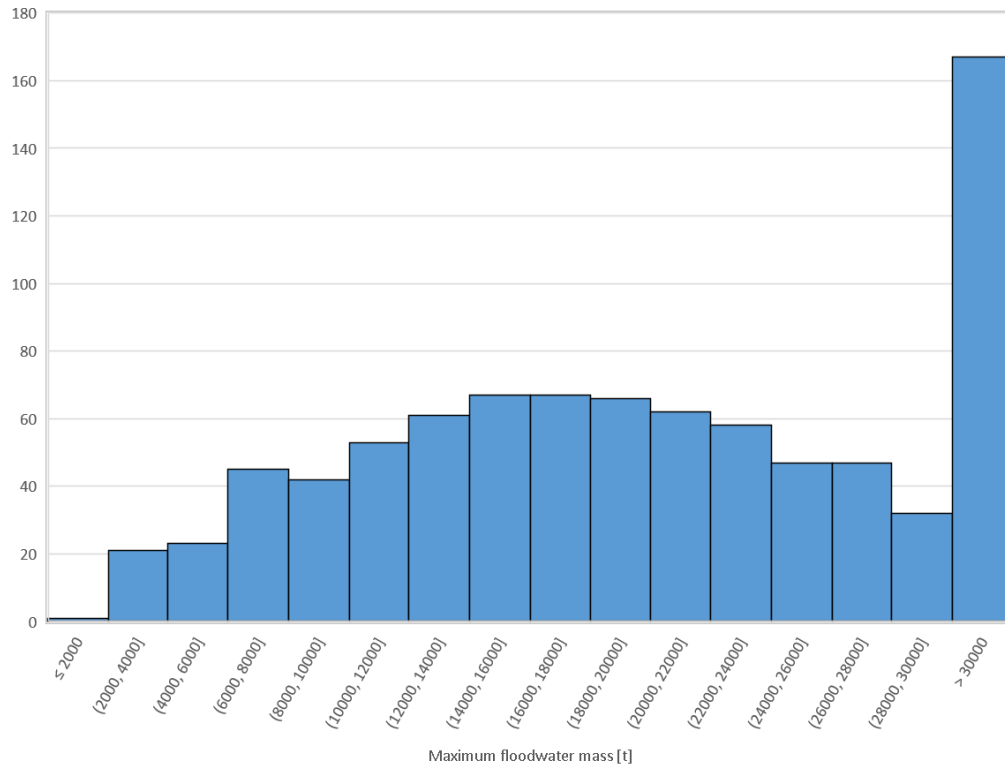


Figure E8: Distribution of maximum amount of floodwater mass

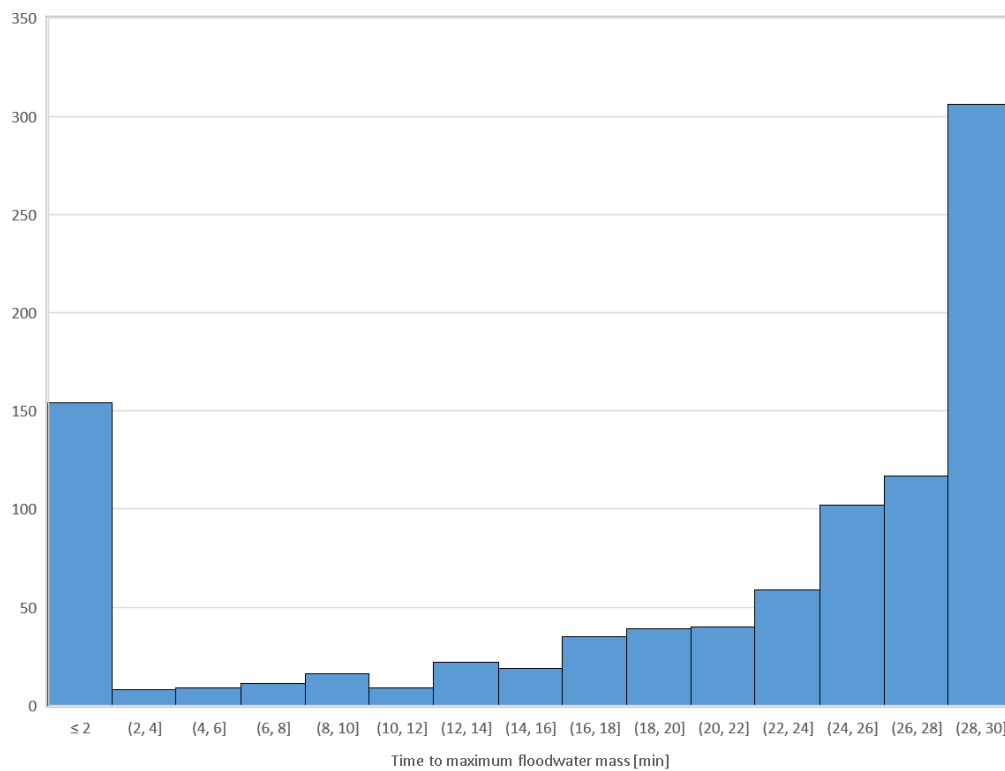


Figure E9: Distribution of time occurrence of maximum amount of floodwater mass

Final values

Within this section, values recorded during the final stage of flooding are presented in relation to average heel, average trim and sinkage

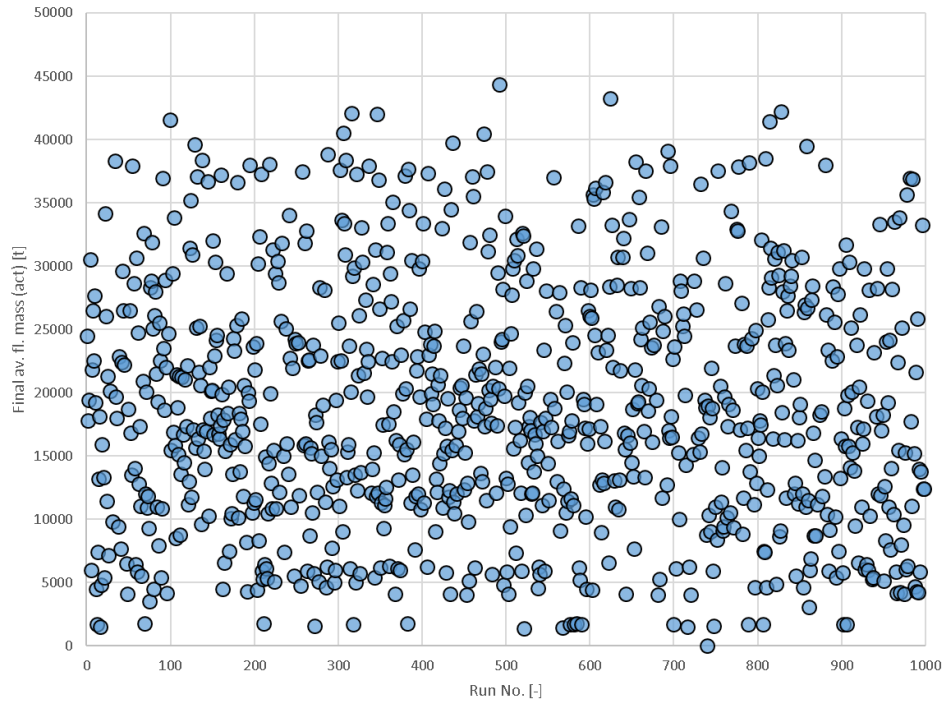


Figure E10: Final 3-minute average of floodwater mass

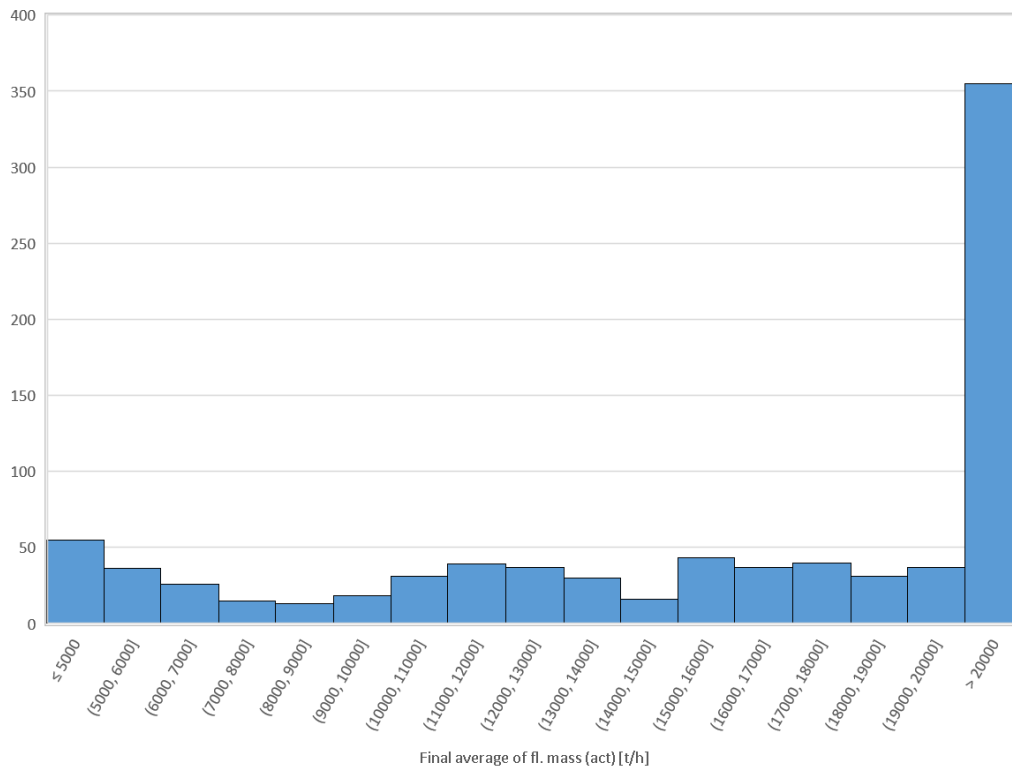


Figure E11: Distribution of final 3-minute average of floodwater mass

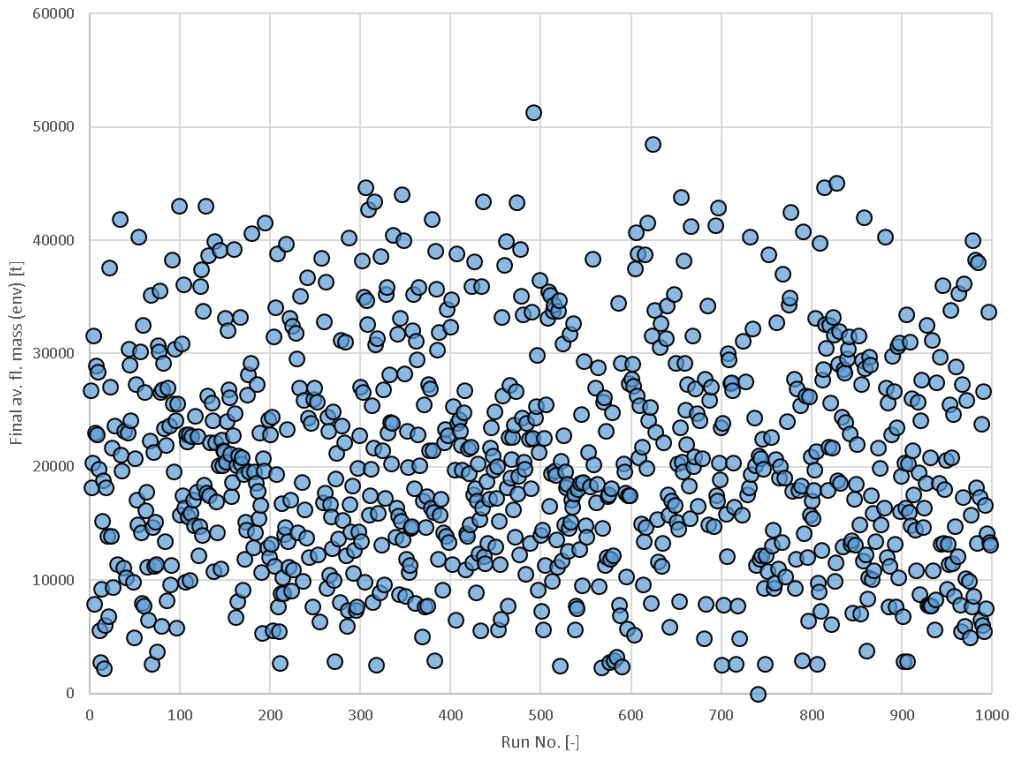


Figure E12: Final 3-minute average of upper envelope of floodwater mass

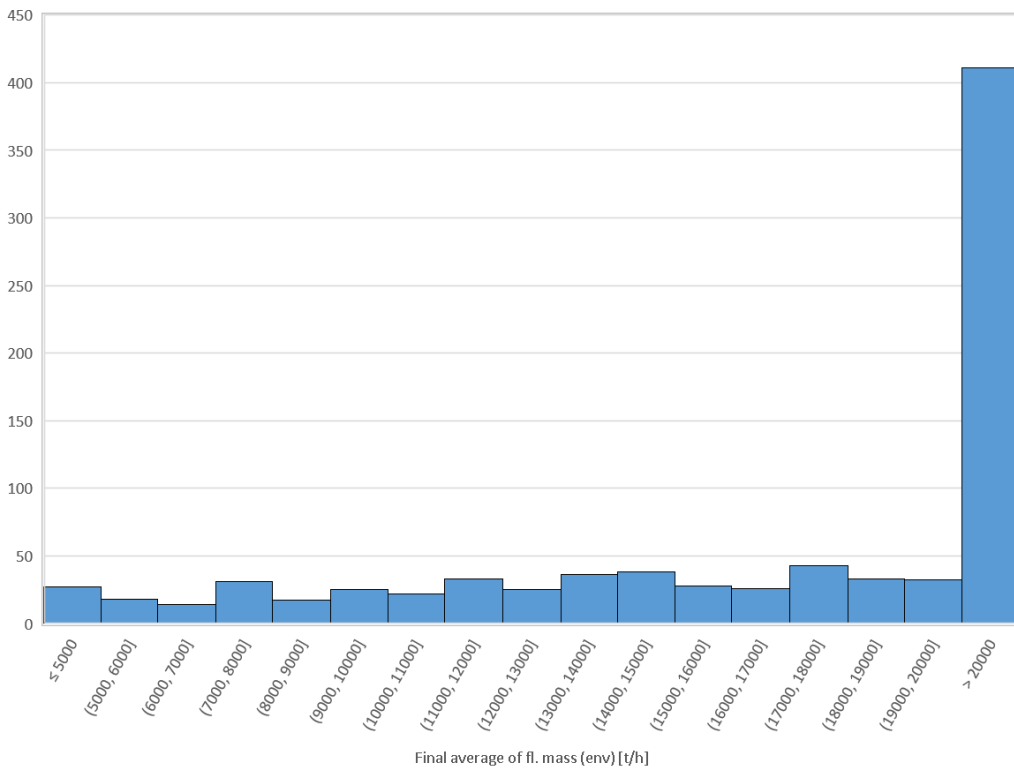


Figure E13: Distribution of final 3-minute average of upper envelope of floodwater

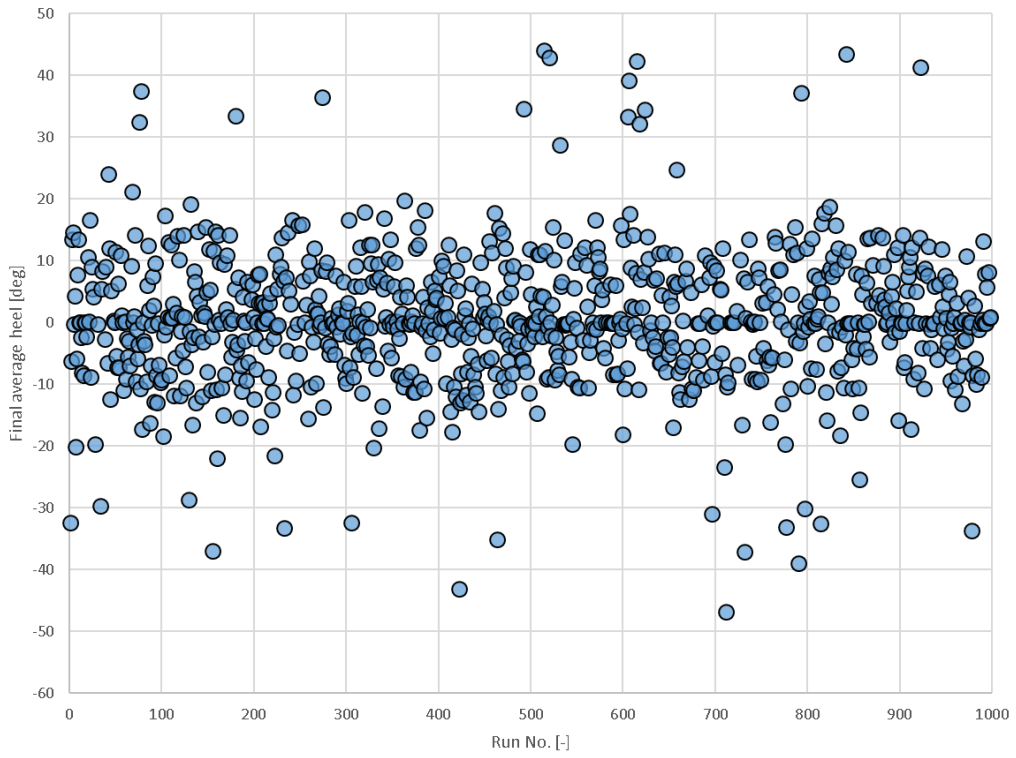


Figure E14: Final 3-minutes average of heel

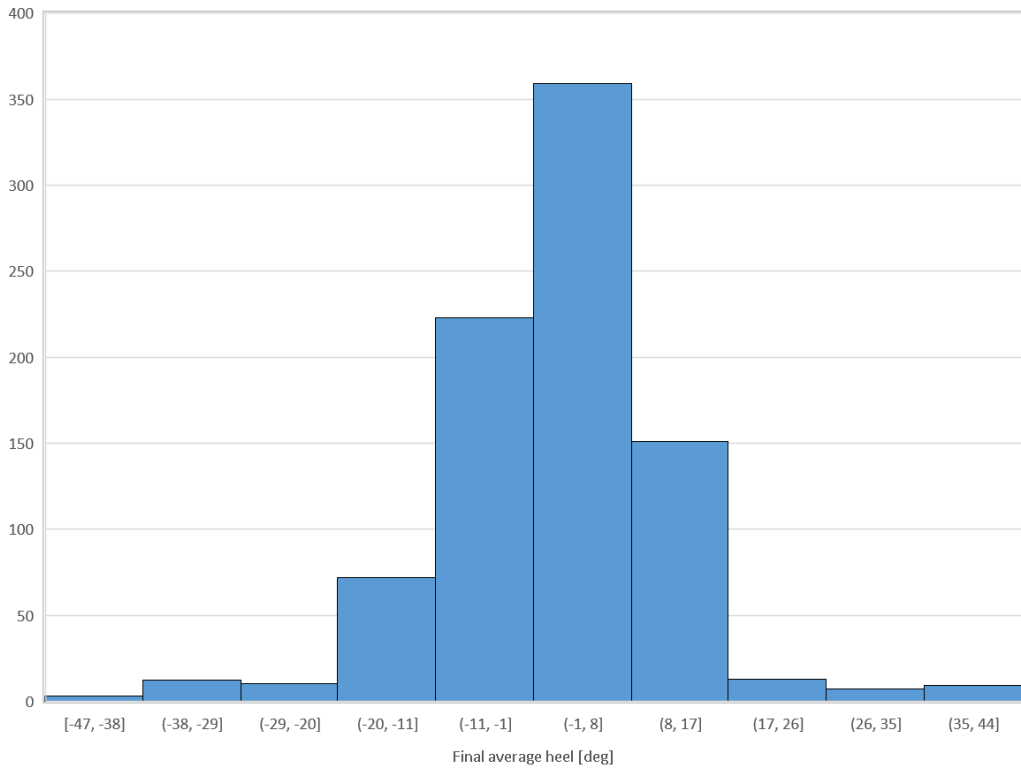


Figure E15: Distribution of final 3-minute average heel

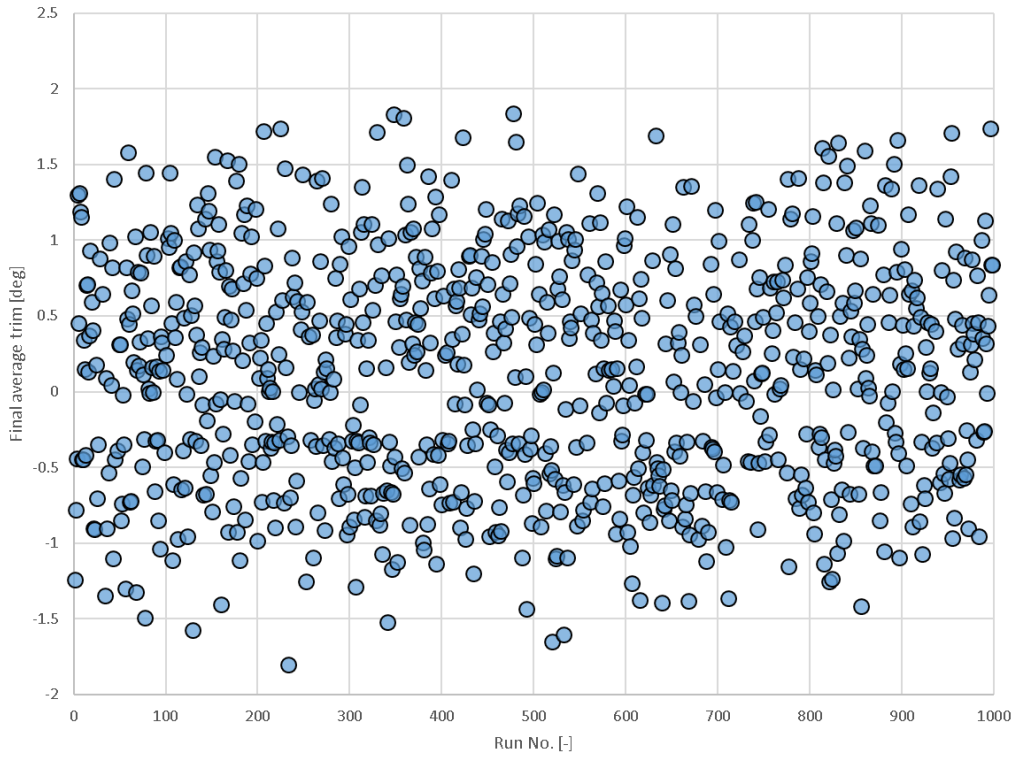


Figure E16: Final 3-minute average trim

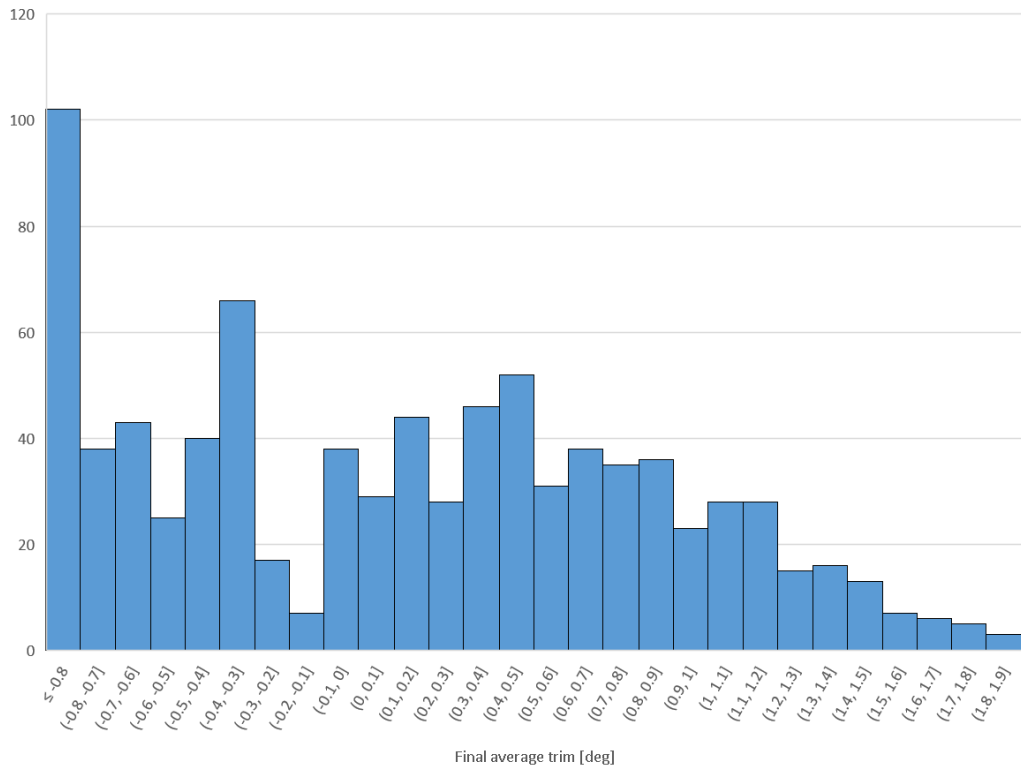


Figure E17: Distribution of final 3-minute average trim

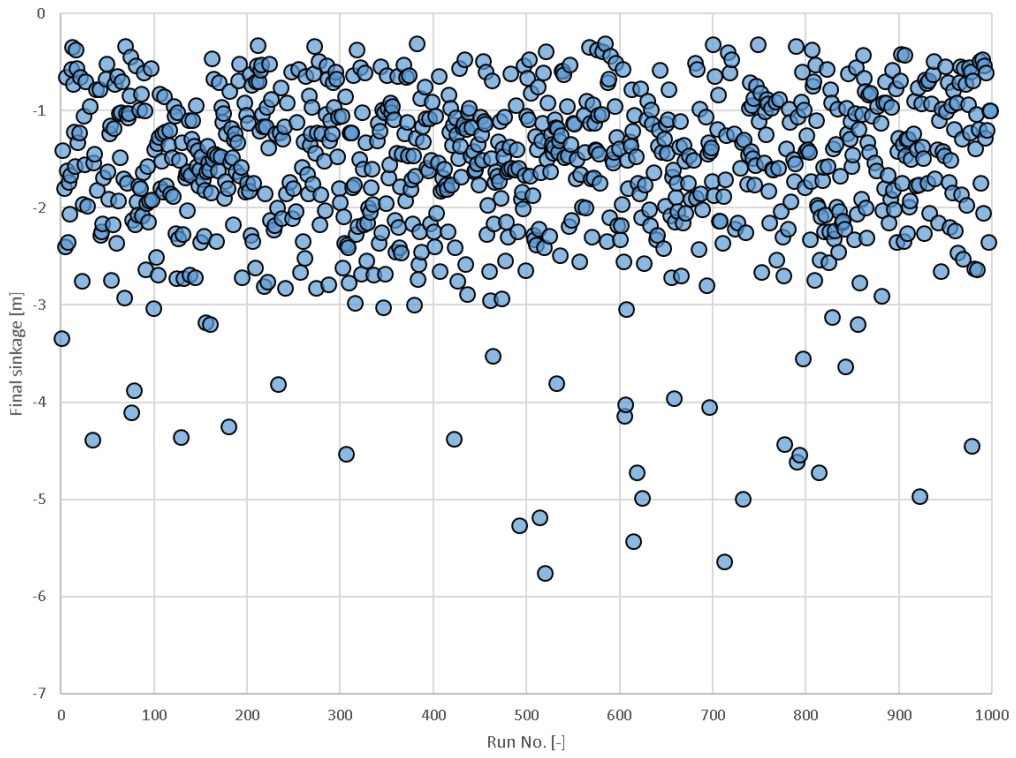


Figure E18: Final 3-minute average sinkage

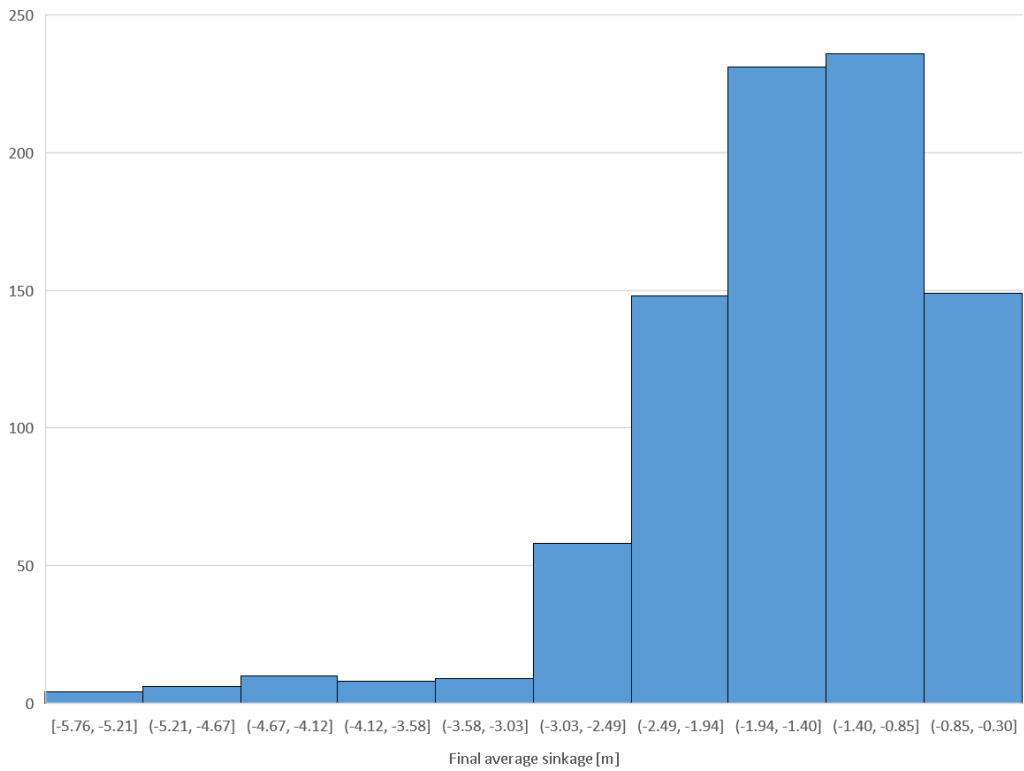


Figure E19: Distribution of final 3-minute average sinkage

Final rates of change

Here, the rate of change in important properties relating to the floating position of the vessel and floodwater mass accumulation are provided in relation to the final stages of the simulation.

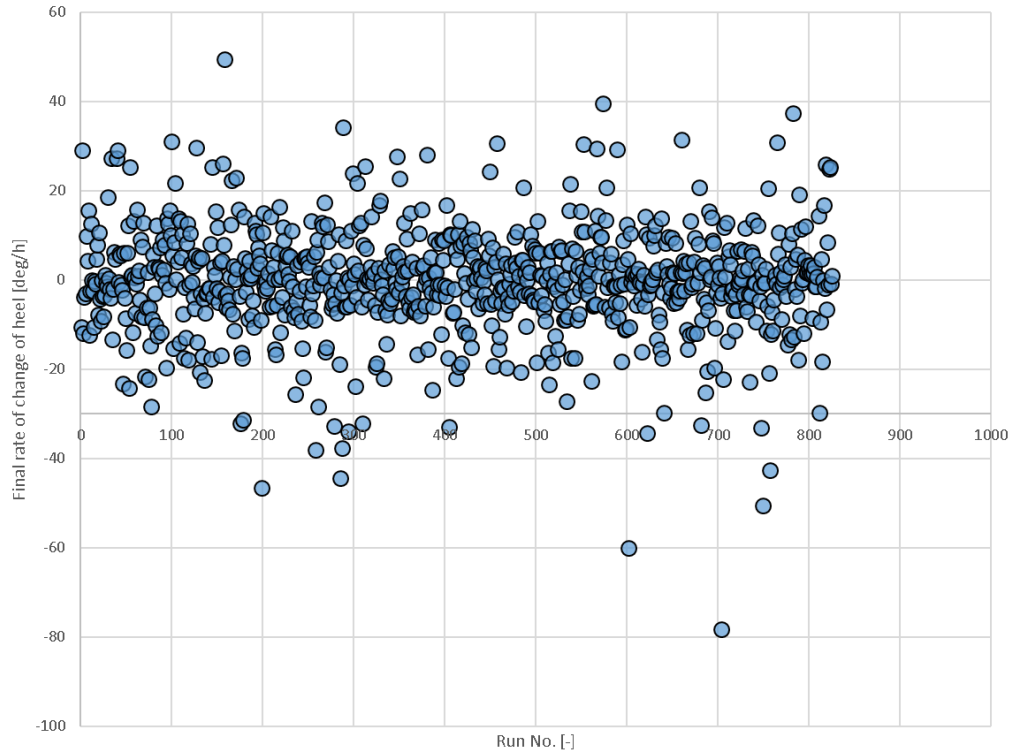


Figure E20: Final rate of change of heel angle

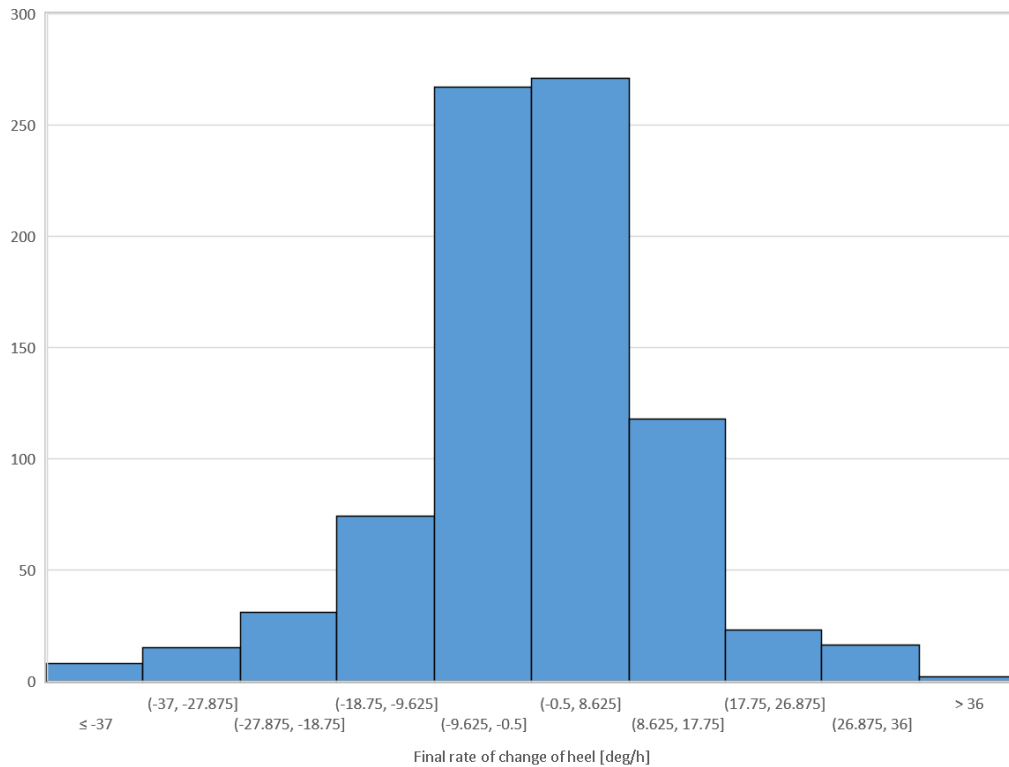


Figure E21: Distribution of final rates of change of heel angle

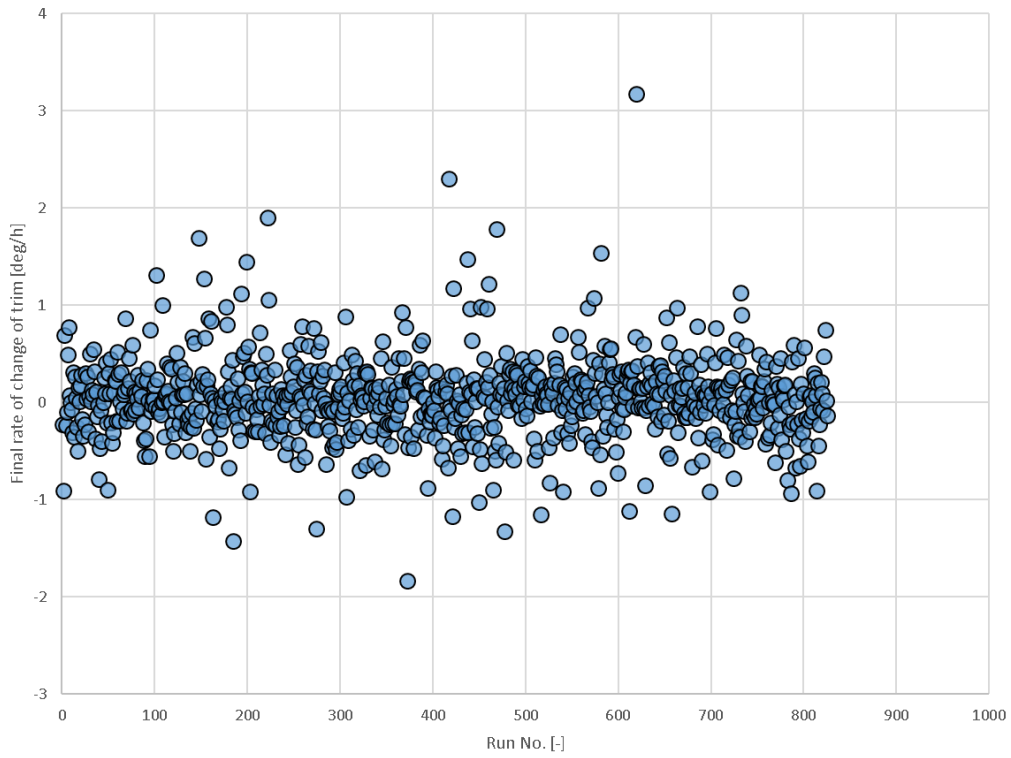


Figure E22: Final rates of change of trim

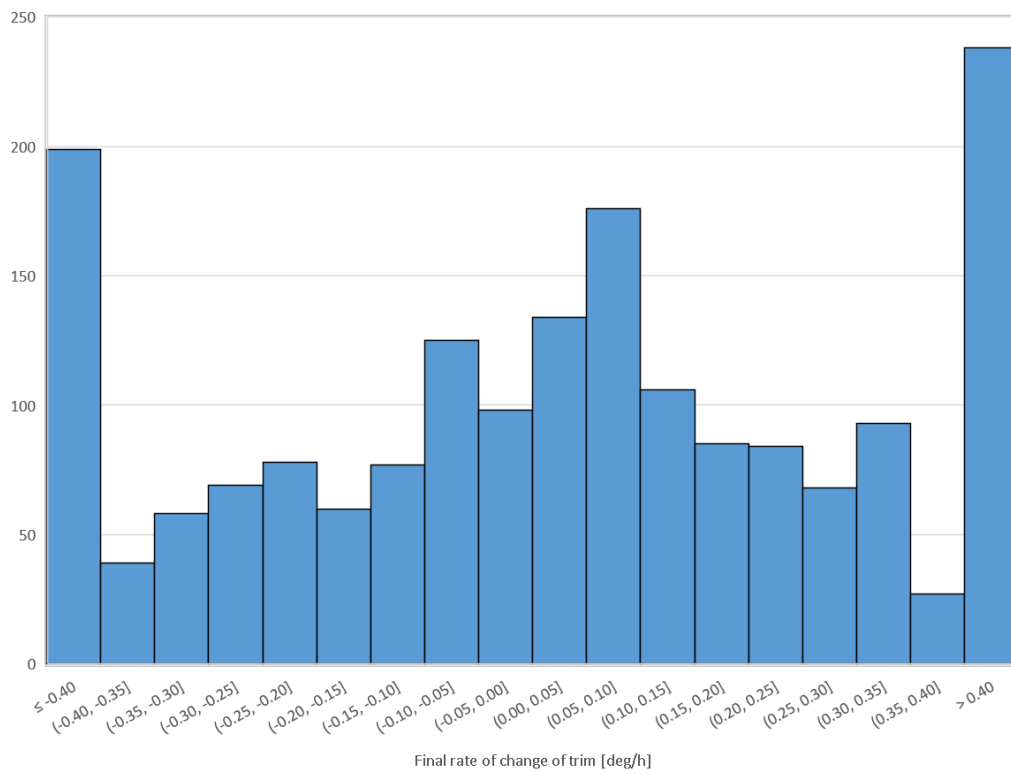


Figure E23: Distribution of final rates of change of trim

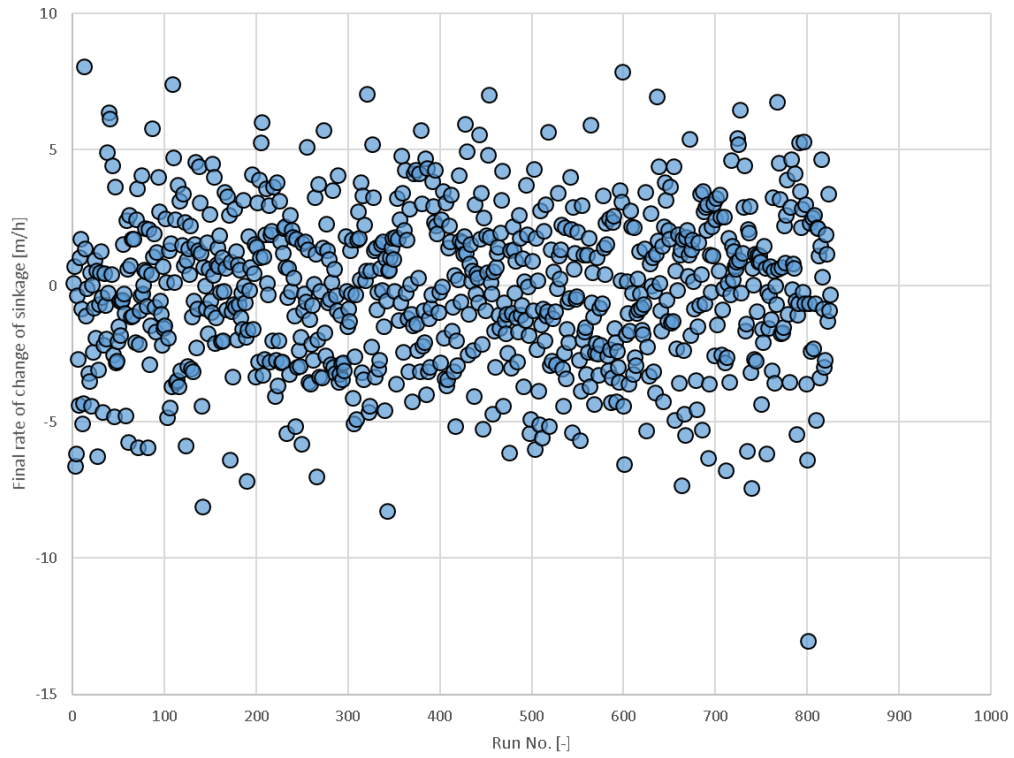


Figure E24: Final rates of change of sinkage

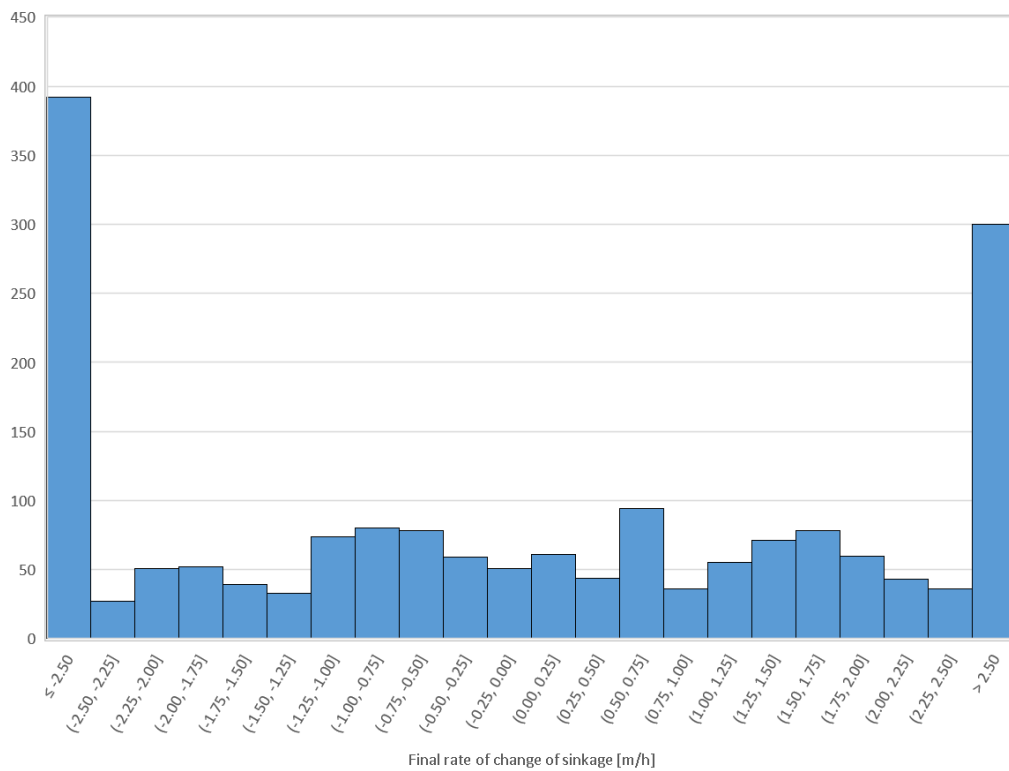


Figure E25: Distribution of final rates of change of sinkage

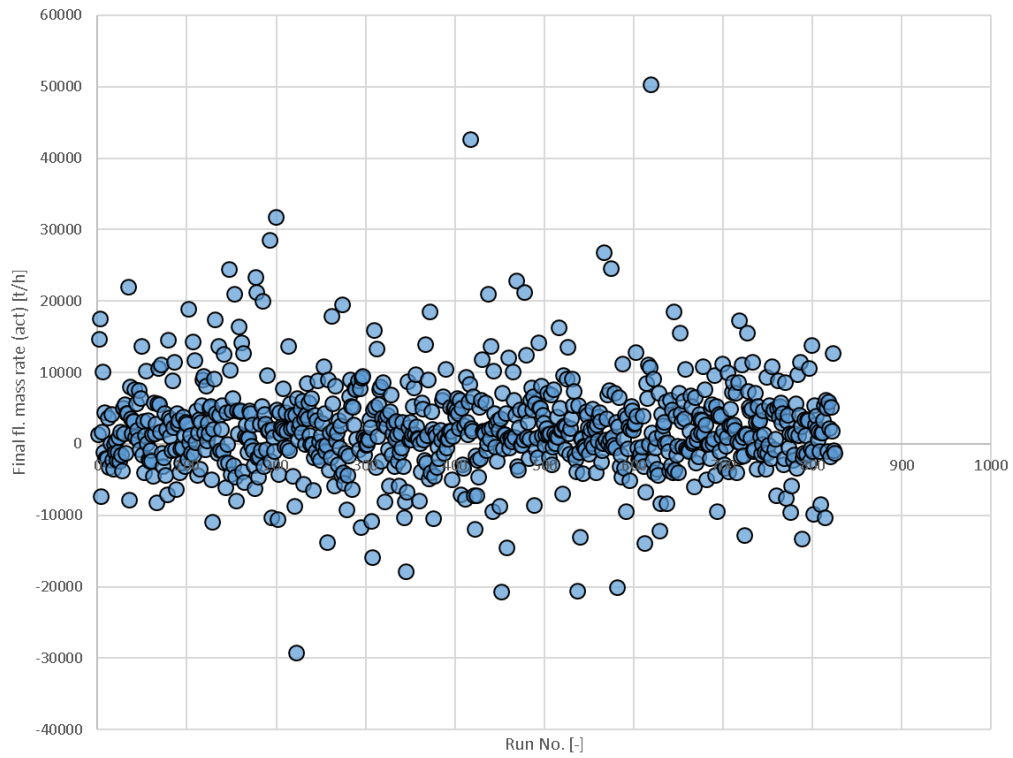


Figure E26: Final rates of change of floodwater mass

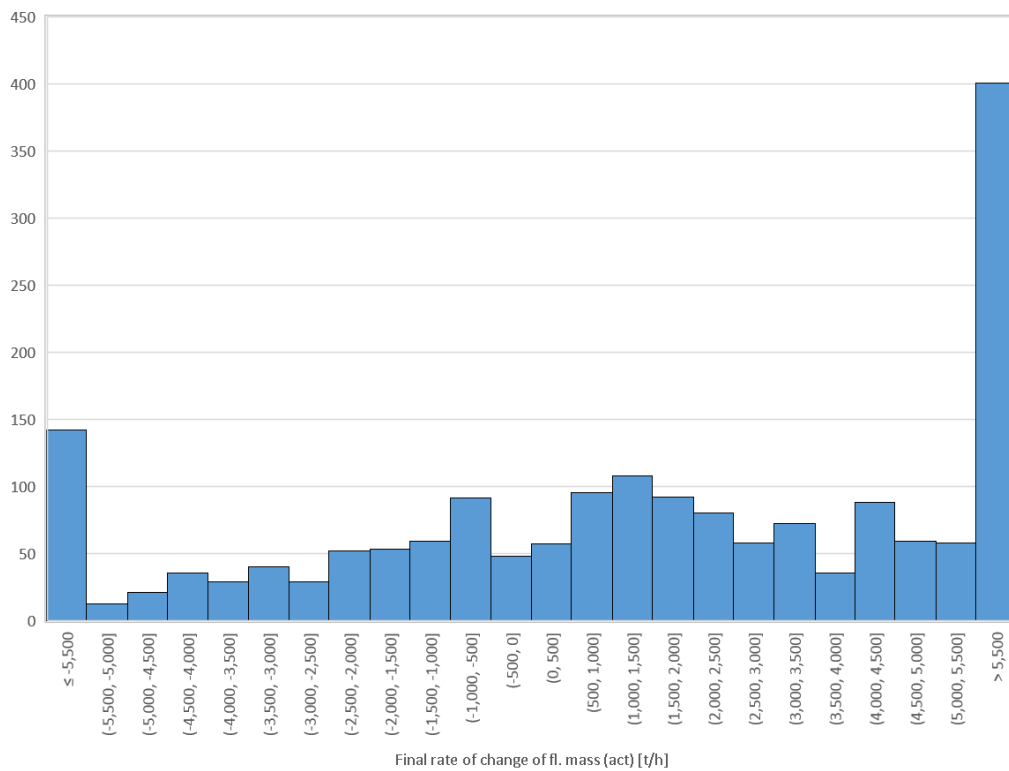


Figure E27: Distribution of final rates of change of floodwater mass

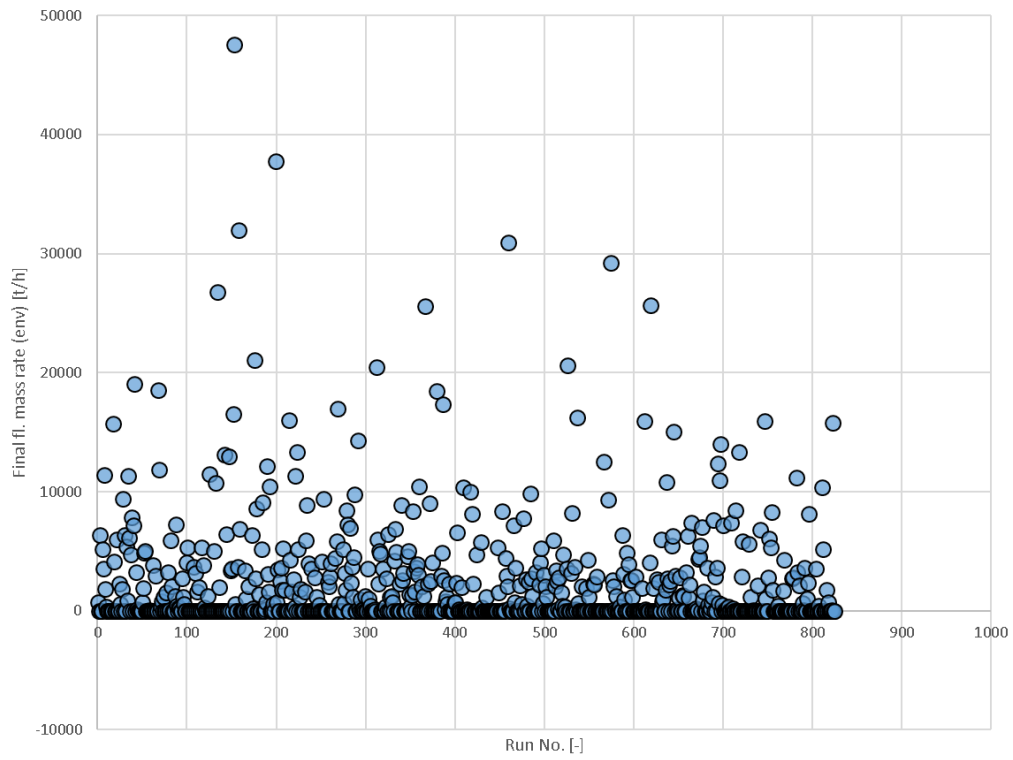


Figure E28: Final rates of change of upper envelope of floodwater mass

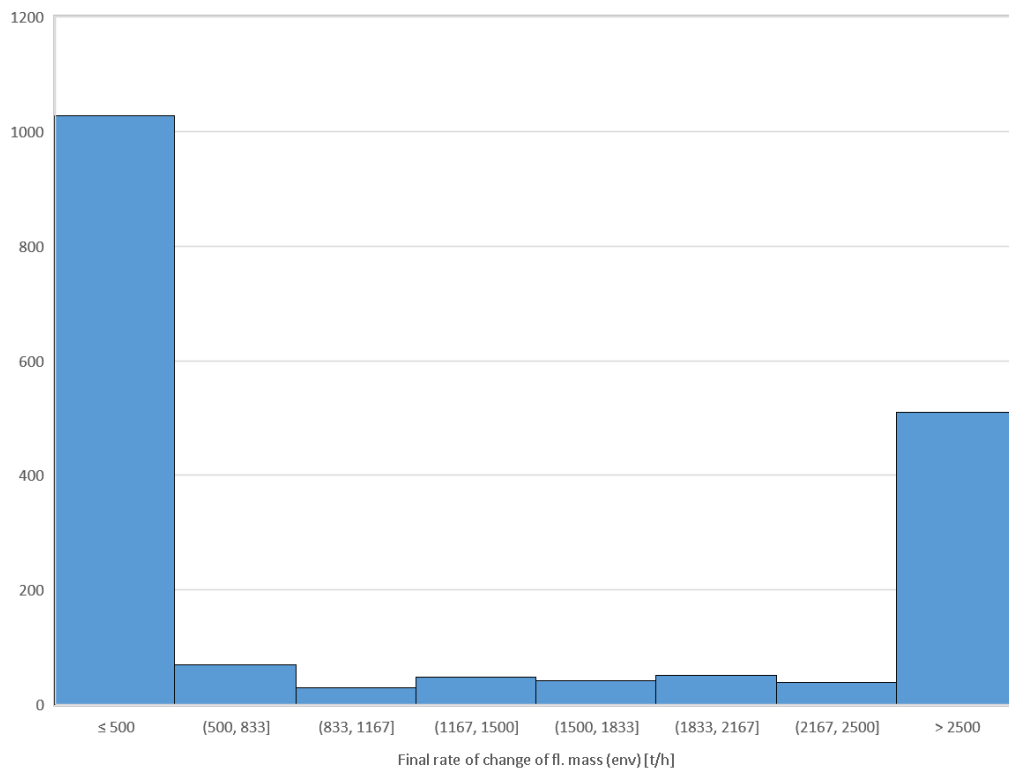


Figure E29: Distribution final rates of change of upper envelope of floodwater mass